

• ESOPHAGEAL CANCER •

Downregulation of retinoic acid receptor-*b*₂ expression is linked to aberrant methylation in esophageal squamous cell carcinoma cell lines

Zhong-Min Liu, Fang Ding, Ming-Zhou Guo, Li-Yong Zhang, Min Wu, Zhi-Hua Liu

Zhong-Min Liu, Fang Ding, Li-Yong Zhang, Min Wu, Zhi-Hua Liu, National Laboratory of Molecular Oncology, Cancer Institute, Peking Union Medical College and Chinese Academy of Medical Sciences, Beijing, China

Ming-Zhou Guo, Division of Tumor Biology, Department of Oncology, The Sidney Kimmel Comprehensive Cancer Center at Johns Hopkins, Baltimore, MD, USA

Supported by China Key Program on Basic Research, G1998051021, the Chinese Hi-tech R&D program, 2001AA231041, and National Science Foundation of China, 30170519

Correspondence to: Zhi-Hua Liu, Professor, National Laboratory of Molecular Oncology, Cancer Institute, Peking Union Medical College and Chinese Academy of Medical Sciences, Beijing 100021, China. liuzh@pubem.cicams.ac.cn

Telephone: +86-10-67723789 **Fax:** +86-10-67723789

Received: 2003-12-10 **Accepted:** 2004-01-08

Abstract

AIM: To study the role of hypermethylation in the loss of retinoic acid receptor *b*₂ (*RARB*₂) in esophageal squamous cell carcinoma (ESCC).

METHODS: The role of hypermethylation in *RARB*₂ gene silencing in 6 ESCC cell lines was determined by methylation-specific PCR (MSP), and its methylation status was compared with *RARB*₂ mRNA expression by RT-PCR. The MSP results were confirmed by bisulfite sequencing of *RARB*₂ promoter regions.

RESULTS: Methylation was detected in 4 of the 6 cell lines, and the expression of *RARB*₂ was markedly downregulated in 3 of the 4 methylated cell lines. The expression of *RARB*₂ was restored in one *RARB*₂-downregulated cell line with the partial demethylation of promoter region of *RARB*₂ after 5-aza-2'-deoxycytidine (5-aza-dc) treatment.

CONCLUSION: The methylation of the 5' region may play an important role in the downregulation of *RARB*₂ in some ESCC cell lines, suggesting that multiple mechanisms contribute to the loss of *RARB*₂ expression in ESCC cell lines. This study may have clinical applications for treatment and prevention of ESCC.

Liu ZM, Ding F, Guo MZ, Zhang LY, Wu M, Liu ZH. Downregulation of retinoic acid receptor-*b*₂ expression is linked to aberrant methylation in esophageal squamous cell carcinoma cell lines. *World J Gastroenterol* 2004; 10(6): 771-775
<http://www.wjgnet.com/1007-9327/10/771.asp>

INTRODUCTION

Retinoids, the important factors in modulating cell growth, differentiation, apoptosis and suppressing carcinogenesis *in vitro* and *in vivo*, are a group of natural and synthetic vitamin

A analogs. In many animal models, such as cancers of skin, lung, prostate and esophagus, retinoids could suppress or reverse epithelial carcinogenesis^[1]. The effects of retinoids are mainly mediated through two classes of nuclear receptors: the retinoic acid receptors (RARs) and retinoid X receptors (RXRs) which belong to a steroid/thyroid hormone-receptor superfamily. Each of them is composed of 3 subtypes (α , β and γ), of which *RARB* is expressed as three isoforms: *b1*, *b2* and *b4*^[2]. Most human cells express *RARB2* as the major isoform. Many studies have confirmed that altered expression or function of the retinoid receptors may be related to malignant transformation of human cells^[3,4].

RARB2 was decreased in many tumors, including lung carcinoma, breast cancer and esophageal cancers^[5-7]. A study of esophageal cancer demonstrated that loss of *RARB* expression was an early event associated with esophageal carcinogenesis and the status of squamous differentiation^[6], however the mechanisms underlying the inactivation of *RARB2* expression in cancer, especially the esophageal cancer, have not been well known yet. In breast cancer, no mutation or polymorphism was detected within the *BRARE* promoter, which was located in the promoter regions of target genes, and the lack of correlation between *RARB2* expression and LOH at chromosome 3p24 was demonstrated in esophageal cancer^[8,9]. The *RARB2* promoter was characterized by an island, which was located in the 5' -untranslated region, and increasing data showed that aberrant methylation of the CpG islands in tumors was associated with transcriptional repression of tumor suppressor genes, such as *p16* in esophageal cancer^[10]. To clarify the epigenetic mechanism of *RARB2* loss or reduction in ESCC cell lines, we analyzed the methylation status of the *RARB2* promoter region by MSP assay and bisulfite sequencing. Our results indicated that downregulation of *RARB2* expression was associated with the aberrant methylation of the CpG islands in some ESCC cell lines, but not in others.

MATERIALS AND METHODS

Reagents and chemicals

5-aza-dc (Sigma, St. Louis, MO) was dissolved in pure ethanol at a stock concentration of 2 mM, and stored in aliquots at -70 °C.

ESCC cell cultures and treatments

Six cell lines were used in this study: KYSE180, KYSE410, KYSE450, KYSE510, COLO680N, and TE12 were purchased from DSMZ (Deutsche Sammlung von Mikroorganismen und Zellkulturen GmbH). Each of the cell lines was cultured in either 90% RPMI 1640 medium (Invitrogen, Carlsbad, CA) or 45% RPMI 1640/45% Ham's F-12 medium (Invitrogen) with 100 mL/L fetal bovine serum at 37 °C containing 50 mL/LCO₂. In the demethylation experiment, the cells with lower *RARB*₂ expression were treated with 5-aza-dc at a final concentration of 5 μ mol/L for 96 h. The growth medium with or without the drug was changed every 24 h.

DNA preparation

The esophageal cell cultures were digested with trypsin-EDTA before collection. Genomic DNA from cell lines was extracted by proteinase-K digestion and phenol/chloroform extraction as described previously^[11]. DNA was dissolved in TE buffer and stored at -20 °C.

RNA isolation and semi-quantitative RT-PCR

Total RNAs were isolated from ESCC cell lines with Trizol reagent (Invitrogen) according to the manufactures' instructions. RNA quality was assessed with agarose gel electrophoresis and spectrophotometric analysis. Ten µg of total RNA of each sample was treated with 2 µL DNase I (10 units/µL, Promega, Madison, WI), 1 µL LRNasin (40 units/µL, Promega) at 37 °C for 15 min to remove contaminated DNA. First strand cDNA was reversely transcribed from 5 µg of total RNAs using SuperScript™ first-strand synthesis system for RT-PCR II kit (Invitrogen) at 42 °C for 80 min and 0.5-1 µL aliquots of the cDNA was then subjected to RT-PCR. The primers used for the amplification of *RARB2* were as follows: sense 5' - ATCGATGCCAATACTGTCTGA-3', antisense 5' - GACTCGATGGTCAGCACTG-3'^[8]. As, *GAPDH* was used as an internal control to ensure quality and quantity of cDNA for each RT-PCR. A product with 241 bp was generated, and PCR products were analyzed on 20g/L agarose gels. The PCR assay for each sample was repeated at least twice.

Methylation-specific PCR

Bisulfite modification of genomic DNA from primary esophageal cancer cell lines was carried out essentially as described previously^[12]. Briefly, 2 µg of genomic DNA was denatured with freshly prepared NaOH (final concentration 0.3 mol/L) for 15 min in a 37 °C water bath, 30 µL of freshly prepared 10 mmol/L hydroquinone (Sigma) and 520 µL of freshly prepared 3.6 mol/L sodium bisulfite (Sigma) at pH 5 were added and mixed. The samples were then incubated under mineral oil for 16 h at 50 °C. The modified DNA was purified with a Wizard DNA clean-up system (Promega). After purification, the samples were treated with NaOH (0.3 M) for 15 min at 37 °C. The DNA was ethanol-precipitated and re-suspended in water for MSP analysis.

The bisulfite-induced changes affecting unmethylated (U) and methylated (M) alleles were detected by nested PCR. The primers for the first round PCR were as follows: sense 5' - AAGTGAGTTGTTTAGAGGTAGGAGGG3', and antisense 5' - CCTATAATTAATCCAAATAATCATTTACC-3'^[13]. The amplification was performed under the following modified conditions: pre-denaturation at 95 °C for 5 min; 35 amplification cycles (denature at 95 °C for 15 s; annealing at 53 °C for 15 s; and extension at 72 °C for 30 s) and final extension at 72 °C for 5 min for the first round of PCR. The PCR products were diluted (1:10 dilution) and used in the second round of PCR with the primers: forward 5' -TTGAGAATGTGAGTGATTTGA-3', reverse 5' -AACCAATCCAACCAAAACAA-3' for the unmethylated sequence; and forward 5' -TCGAGAACGCG-AGCGATTTCG-3', reverse 5' -GACCAATCCAACCGAAA-CGA-3' for the methylated sequences^[14]. The amplification was performed under following conditions: pre-denaturation at 95 °C for 5 min; 35 amplification cycles (denature at 95 °C for 15 s; annealing at 52 °C for 15 s; and extension at 72 °C for 15 s for U-primers) and pre-denaturation at 95 °C for 5 min; 20 amplification cycles (denature at 95 °C for 15 s; annealing at 62 °C for 15 s; and extension at 72 °C for 15 s M-primers). DNA from normal lymphocytes was used as negative control for methylated alleles, and placental DNA treated *in vitro* with SssI methyltransferase (New England Biolabs, Beverly, MA) was used as positive control for methylated genes. The product of

146 bp was generated, and the PCR products were analyzed on 25g/L agarose gels and photographed. The controls without DNA were performed in each set of PCR, and MSP assay for each sample was repeated at least twice.

Bisulfite sequencing

The PCR products amplified with primers specific either for the methylated or for the unmethylated DNA were purified and cloned into the pMD-T vector (Takara, Dalian, China) according to the manufacture's protocol. Recombinants were transformed into *Escherichia coli*. Plasmid DNA was isolated and integrated PCR fragments were verified by enzyme digestion and PCR. The cloned PCR fragments were further analyzed by automated sequencing (Bioasia, Shanghai, China).

RESULTS

Expression of *RARB2* in ESCC cell lines

The expression of the *RARB2* mRNA was detected in the six ESCC cell lines by RT-PCR. Figure 1 shows representative examples of RT-PCR and MSP results. Markedly downregulation of *RARB2* expression was observed in the cell lines KYSE410, KYSE510 and COLO680N as shown in Figure 1A.

Methylation analysis of the *RARB2* promoter region

Using MSP method, both the methylated and unmethylated alleles were found in the four cell lines except KYSE180 and TE12 in which only the unmethylated alleles were present (Figure 1B). The quantitation of the unmethylated or the methylated products varied in different cell lines. To confirm the reliability of the nested MSP method, PCR products amplified with primers specific either for the methylated (cell lines KYSE410) or for the unmethylated (cell line KYSE180) DNA were cloned and sequenced. Bisulfite sequencing of 4 individual clones of PCR products from cell line KYSE180 revealed no methylation of CpGs within the promoter region, whereas the methylated products showed dense methylation within the CpG islands in cell line KYSE410 (Figure 2).

Association between *RARB2* promoter methylation and downregulation of its expression in ESCC cell lines

The reduction of *RARB2* mRNA expression was observed in three of the four cell lines that had partially methylated alleles, however the another one cell line showed strong *RARB2* gene expression, which suggesting that the aberrant methylation might play other roles except leading to gene silencing.

Restoration of *RARB2* expression after 5-aza-dc treatment

To confirm whether *RARB2* promoter methylation could be further linked to downregulation of its expression, the cancer cell lines which showed evidently decreased expression of *RARB2* and cell line KYSE180 without methylated alleles were treated with the demethylating agent (5-aza-dc). To determine the effects of demethylating agent, we analyzed the methylation status in KYSE410 cells after 5-aza-dc treatment, and partial demethylation was detected by MSP as shown in Figure 3A. In addition, the MSP product was still observed after treatment because 5-aza-dc only inhibited methylation of newly synthesized DNA. The level of *RARB2* mRNA was not changed in cell line KYSE180 before and after demethylating treatment. Among the three cell lines where *RARB2* genes were methylated, the treatment led to up-regulation of *RARB2* mRNA expression only in cell line KYSE410 (Figure 3B). The other two cell lines showed no detectable re-expression of *RARB2* mRNA after 5-aza-dc treatment (data not shown). These data indicated that *RARB2* promoter methylation was closely associated with downregulation of *RARB2* expression in some ESCC cell lines.

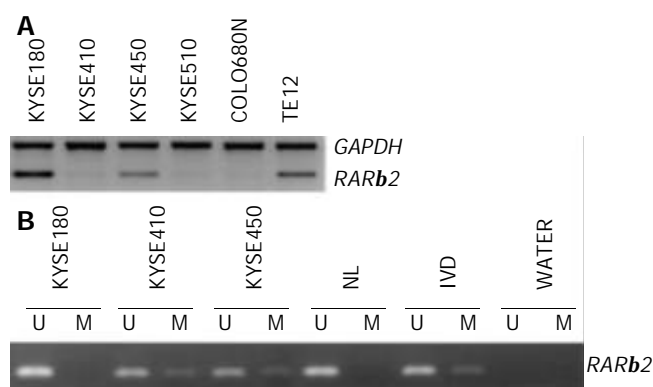


Figure 1 *RARB2* expression and methylation in ESCC cell lines. A: RT-PCR analysis of *RARB2* expression, *GAPDH* was used as internal control. B: MSP analysis of *RARB2* promoter methylation status, (U) lanes and (M) lanes represent amplification of unmethylated and methylated alleles, respectively. *In vitro* methylated DNA (IVD) and normal human peripheral lymphocytes (NL) serve as positive and negative methylation controls, respectively.

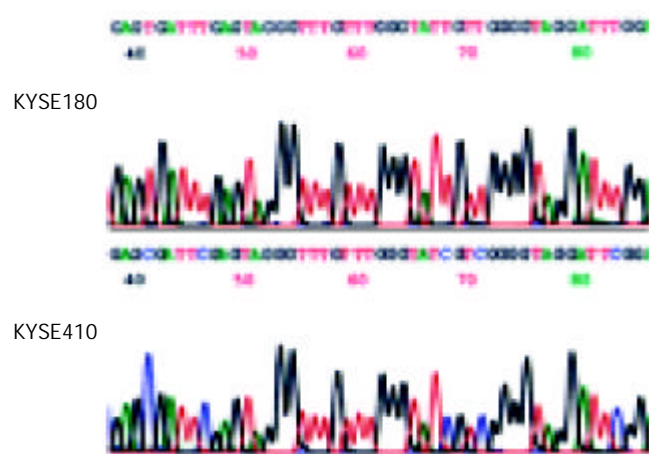


Figure 2 Sodium bisulfite sequencing of *RARB2* in the cell lines that were found to include only unmethylated alleles (cell line KYSE180) or partial methylated alleles (cell line KYSE410) by MSP.

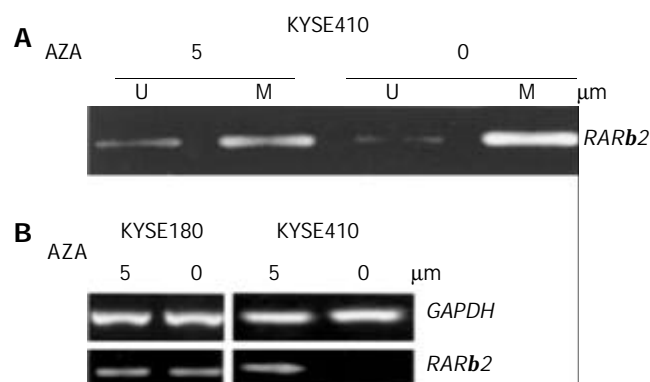


Figure 3 Treatment with the indicated concentrations of 5-aza-dc induced demethylation and *RARB2* mRNA expression in ESCC cell lines. A: MSP analysis shows partial demethylation of the *RARB2* promoter region after 5-aza-dc treatment. B: RT-PCR analysis of *RARB2* mRNA expression before and after 5-aza-dc treatment in cell lines that were found to have either positive (cell line KYSE180) or reduced (cell line KYSE410) baseline *RARB2* expression, *GAPDH* was used as internal control.

DISCUSSION

There were two major *RARB2* antineoplastic mechanisms in breast cancer cell lines, which were RA-dependent and RA-independent apoptosis^[15,16], however little was known how *RARB2* performed its anticancer activity. A growing evidence indicated that *RARB2* was required for the growth inhibitory action of RA. In *RARB2*-negative cancer cells, RA-induced growth inhibition and decreased tumorigenicity could be restored by expression of *RARB2*; on the contrary, in *RARB2*-positive cancer cells, RA effects could be abolished by inhibition of *RARB2* expression^[17-19]. Another study indicated that not only expression but also up-regulation of *RARB* was linked to retinoid sensitivity in esophageal cancer cell lines^[20], and our previous study also suggested that RA resistance in EC109 cells paralleled with the loss of *RARB2* inducibility^[21]. A clinical trial using N-4-(ethoxycarbonyl) retinamide, a synthetic retinoid, demonstrated that cancer incidence among the treatment groups with severe esophageal dysplasia was decreased by 43.2% compared with the placebo group^[22], whereas this was not the case for recent clinical trials of 13-cis retinoic acid in the treatment of advanced esophageal cancer patients, for which an explanation was that the loss of *RARB* expression could lead to the resistance to treatment with 13-cis RA in esophageal cancer^[23,24]. Recent study suggested that hypermethylation of *RARB* might play an important role in the early stage of esophageal squamous cell carcinogenesis^[25]. However, the mechanisms of *RARB2* suppression remained largely unknown in esophageal cancer.

Genetic and epigenetic mechanisms may be involved in progressive decrease in *RARB2* mRNA expression during esophageal carcinogenesis. *RARB* was localized on chromosome 3p24, and LOH occurred frequently on chromosome arm 3p in many cancers, including esophageal cancer^[2]. However, no correlation was observed between the expression of *RARB* and the LOH on chromosome 3p24 in ESCC; moreover, no mutations or other genetic alterations were found in different cell lines without *RARB2* mRNA expression^[9,26,27]. Thus, other mechanisms for *RARB2* suppression should be considered. DNA methylation, which led to the inactivation of all kinds of essential genes, such as *HLA class I*, *E-cadherin*, *FHIT* and *p16*, was an important mechanism for gene silencing or suppressing in ESCC^[10,28-30]. In addition, Arapshian *et al.*^[31] concluded that methylation of the RARE region might be particularly important in *RARB2* suppression. Data presented in this report demonstrated that epigenetic silencing of the *RARB2* gene promoter might be an important event, and that downregulation of *RARB2* expression was closely associated with *RARB2* gene promoter methylation in some ESCC cell lines. In our study, of the three *RARB2*-downregulated cell lines, only the one poorly differentiated cell line showed evidently re-expression of *RARB2* with the partial demethylation of its promoter region, indicating that repression was, at least in part, mediated by methylation in the poorly differentiated cell lines, and multiple mechanisms were involved in the gene silencing in the other two cell lines. Our results suggested that a relationship between methylation status and decreased *RARB2* expression only existed in some differentiated ESCC cell lines or ESCC. Previous study has demonstrated that for breast carcinoma a relationship between methylation status and decreased *RARB2* expression in breast cancer was found only in invasive grade II lesions^[13]. There was mounting evidence that suggested epigenetic modifications might be a mechanism responsible for the lack of *RARB2* expression in many epithelial cancers or cancer cell lines, such as breast cancer, colon cancer and prostate cancer^[8,13,32,33]. Taken together the further analysis of the cytogenetic data of the cell lines, we found that there was

no deletion in 3p in the cell line exhibiting re-expression of *RARB2*. We therefore speculate that methylation may be at least one of the major mechanisms resulting in loss of *RARB2* expression in such cell lines. It has been reported that in ESCC cell lines without any structural alteration, hypermethylation at CpG sites was the important mechanism for transcription inactivation of the *FHIT* gene^[30]. Given that the *RARB2* gene is recognized as a putative tumor suppressor gene, restoration of its function may have implications for both cancer therapy and prevention.

Notely, demethylation could only lead to the restoration of *RARB2* expression in 1/3 ESCC cell lines without 3p deletion, but not in the other cell lines with 3p deletion, indicating that there were other mechanisms, such as deletion, involved in the loss of *RARB2* expression in ESCC cell lines. It was reported that differential function of coactivators and corepressors might determine the level of *RARB* induction that might mediate retinoid action in colon cancer cells^[34]. In lung cancer cell lines, loss of *RARB* gene expression was linked to aberrant histone H3 acetylation, so the aberrant acetylation status might have effects on *RARB2* expression^[35]. In addition, orphan receptor COUP-TF have been identified to play a key role in modulating *RARB* expression and retinoid sensitivity in cancer cells^[36]. Thus, multiple mechanisms may contribute to the loss of *RARB2*.

In conclusion, this study not only shows a high frequency of methylation of *RARB2* promoter region but also provides the first evidence that downregulation of *RARB2* is closely associated with DNA methylation in ESCC cell lines. These findings will be helpful to further understand the mechanisms underlying tumor progression in ESCC, and subsequently improve the prevention and treatment.

REFERENCES

- 1 **Evans TR**, Kaye SB. Retinoids: present role and future potential. *Br J Cancer* 1999; **80**: 1-8
- 2 **Chambon P**. A decade of molecular biology of retinoic acid receptors. *FASEB J* 1996; **10**: 940-954
- 3 **Collins SJ**, Robertson KA, Mueller L. Retinoic acid-induced granulocytic differentiation of HL-60 myeloid leukemia cells is mediated directly through the retinoic acid receptor (RAR- α). *Mol Cell Biol* 1990; **10**: 2154-2163
- 4 **Xu XC**, Lotan R. Aberrant expression and function of retinoic acid receptors in cancer. In Nau H, Blaner WS, editors. *Handbook of experimental pharmacology: retinoids*. Berlin: Springer-Verlag 1999: p323-324
- 5 **Picard E**, Seguin C, Monhoven N, Rochette-Egly C, Siat J, Borrelly J, Martinet Y, Martinet N, Vignaud JM. Expression of retinoic acid receptor genes and proteins in non-small-cell lung cancer. *J Natl Cancer Inst* 1999; **91**: 1059-1066
- 6 **Qiu H**, Zhang W, El-Naggar AK, Lippman SM, Lin P, Lotan R, Xu XC. Loss of retinoic acid receptor-beta expression is an early event during esophageal carcinogenesis. *Am J Pathol* 1999; **155**: 1519-1523
- 7 **Xu XC**, Sneige N, Liu X, Nandagiri R, Lee JJ, Lukmanji F, Hortobagyi G, Lippman SM, Dhingra K, Lotan R. Progressive decrease in nuclear retinoic acid receptor beta messenger RNA level during breast carcinogenesis. *Cancer Res* 1997; **57**: 4992-4996
- 8 **Yang Q**, Mori I, Shan L, Nakamura M, Nakamura Y, Utsunomiya H, Yoshimura G, Suzuma T, Tamaki T, Umemura T, Sakurai T, Kakudo K. Biallelic inactivation of retinoic acid receptor beta2 gene by epigenetic change in breast cancer. *Am J Pathol* 2001; **158**: 299-303
- 9 **Qiu H**, Lotan R, Lippman SM, Xu XC. Lack of correlation between expression of retinoic acid receptor-beta and loss of heterozygosity on chromosome band 3p24 in esophageal cancer. *Genes Chromosomes Cancer* 2000; **28**: 196-202
- 10 **Tanaka H**, Shimada Y, Imamura M, Shibagaki I, Ishizaki K. Multiple types of aberrations in the p16 (INK4a) and the p15 (INK4b) genes in 30 esophageal squamous-cell-carcinoma cell lines. *Int J Cancer* 1997; **70**: 437-442
- 11 **Sambrook J**, Fritsch EF, Maniatis T. Molecular cloning: a laboratory manual. Cold Spring Harbor Laboratory Press, NY (1989)
- 12 **Herman JG**, Graff JR, Myohanen S, Nelkin BD, Baylin SB. Methylation-specific PCR: a novel PCR assay for methylation status of CpG islands. *Proc Natl Acad Sci U S A* 1996; **93**: 9821-9826
- 13 **Widschwendter M**, Berger J, Hermann M, Muller HM, Amberger A, Zeschnigk M, Widschwendter A, Abendstein B, Zeimet AG, Daxenbichler G, Marth C. Methylation and silencing of the retinoic acid receptor-beta2 gene in breast cancer. *J Natl Cancer Inst* 2000; **92**: 826-832
- 14 **Ivanova T**, Petrenko A, Gritsko T, Vinokourov S, Eshilev E, Kobzeva V, Kisseljov F, Kisseljova N. Methylation and silencing of the retinoic acid receptor-beta 2 gene in cervical cancer. *BMC Cancer* 2002; **2**: 4
- 15 **Lin F**, Xiao D, Kolluri SK, Zhang X. Unique anti-activator protein-1 activity of retinoic acid receptor beta. *Cancer Res* 2000; **60**: 3271-3280
- 16 **Liu Y**, Lee MO, Wang HG, Li Y, Hashimoto Y, Klaus M, Reed JC, Zhang X. Retinoic acid receptor beta mediates the growth-inhibitory effect of retinoic acid by promoting apoptosis in human breast cancer cells. *Mol Cell Biol* 1996; **16**: 1138-1149
- 17 **Faria TN**, Mendelsohn C, Chambon P, Gudas LJ. The targeted disruption of both alleles of RARbeta(2) in F9 cells results in the loss of retinoic acid-associated growth arrest. *J Biol Chem* 1999; **274**: 26783-26788
- 18 **Houle B**, Rochette-Egly C, Bradley WE. Tumor-suppressive effect of the retinoic acid receptor beta in human epidermoid lung cancer cells. *Proc Natl Acad Sci U S A* 1993; **90**: 985-989
- 19 **Si SP**, Lee X, Tsou HC, Buchsbaum R, Tibaduiza E, Peacocke M. RAR beta 2-mediated growth inhibition in HeLa cells. *Exp Cell Res* 1996; **223**: 102-111
- 20 **Xu XC**, Liu X, Tahara E, Lippman SM, Lotan R. Expression and up-regulation of retinoic acid receptor-beta is associated with retinoid sensitivity and colony formation in esophageal cancer cell lines. *Cancer Res* 1999; **59**: 2477-2483
- 21 **Liu G**, Wu M, Levi G, Ferrari N. Inhibition of cancer cell growth by all-trans retinoic acid and its analog N-(4-hydroxyphenyl) retinamide: a possible mechanism of action via regulation of retinoid receptors expression. *Int J Cancer* 1998; **78**: 248-254
- 22 **Han J**. Highlights of the cancer chemoprevention studies in China. *Prev Med* 1993; **22**: 712-722
- 23 **Roth AD**, Morant R, Alberto P. High dose etretinate and interferon-alpha-a phase I study in squamous cell carcinomas and transitional cell carcinomas. *Acta Oncol* 1999; **38**: 613-617
- 24 **Slabber CF**, Falkson G, Burger W, Schoeman L. 13-Cis-retinoic acid and interferon alpha-2a in patients with advanced esophageal cancer: a phase II trial. *Invest New Drugs* 1996; **14**: 391-394
- 25 **Kuroki T**, Trapasso F, Yendamuri S, Matsuyama A, Alder H, Mori M, Croce CM. Allele loss and promoter hypermethylation of VHL, RAR-beta, RASSF1A, and FHIT tumor suppressor genes on chromosome 3p in esophageal squamous cell carcinoma. *Cancer Res* 2003; **63**: 3724-3728
- 26 **Bartsch D**, Boye B, Baust C, zur Hausen H, Schwarz E. Retinoic acid-mediated repression of human papillomavirus 18 transcription and different ligand regulation of the retinoic acid receptor beta gene in non-tumorigenic and tumorigenic HeLa hybrid cells. *EMBO J* 1992; **11**: 2283-2291
- 27 **Hu L**, Crowe DL, Rheinwald JG, Chambon P, Gudas LJ. Abnormal expression of retinoic acid receptors and keratin 19 by human oral and epidermal squamous cell carcinoma cell lines. *Cancer Res* 1991; **51**: 3972-3981
- 28 **Nie Y**, Yang G, Song Y, Zhao X, So C, Liao J, Wang LD, Yang CS. DNA hypermethylation is a mechanism for loss of expression of the HLA class I genes in human esophageal squamous cell carcinomas. *Carcinogenesis* 2001; **22**: 1615-1623

- 29 **Si HX**, Tsao SW, Lam KY, Srivastava G, Liu Y, Wong YC, Shen ZY, Cheung AL. E-cadherin expression is commonly downregulated by CpG island hypermethylation in esophageal carcinoma cells. *Cancer Lett* 2001; **173**: 71-78
- 30 **Tanaka H**, Shimada Y, Harada H, Shinoda M, Hatoooka S, Imamura M, Ishizaki K. Methylation of the 5' CpG island of the FHIT gene is closely associated with transcriptional inactivation in esophageal squamous cell carcinomas. *Cancer Res* 1998; **58**: 3429-3434
- 31 **Arapshian A**, Kuppumbatti YS, Mira-y-Lopez R. Methylation of conserved CpG sites neighboring the beta retinoic acid response element may mediate retinoic acid receptor beta gene silencing in MCF-7 breast cancer cells. *Oncogene* 2000; **19**: 4066-4070
- 32 **Cote S**, Sinnett D, Momparler RL. Demethylation by 5-aza-2'-deoxycytidine of specific 5-methylcytosine sites in the promoter region of the retinoic acid receptor beta gene in human colon carcinoma cells. *Anticancer Drugs* 1998; **9**: 743-750
- 33 **Nakayama T**, Watanabe M, Yamanaka M, Hirokawa Y, Suzuki H, Ito H, Yatani R, Shiraishi T. The role of epigenetic modifications in retinoic acid receptor beta2 gene expression in human prostate cancers. *Lab Invest* 2001; **81**: 1049-1057
- 34 **Lee MO**, Kang HJ. Role of coactivators and corepressors in the induction of the *RAR* beta gene in human colon cancer cells. *Biol Pharm Bull* 2002; **25**: 1298-1302
- 35 **Suh YA**, Lee HY, Virmani A, Wong J, Mann KK, Miller WH Jr, Gazdar A, Kurie JM. Loss of retinoic acid receptor beta gene expression is linked to aberrant histone H3 acetylation in lung cancer cell lines. *Cancer Res* 2002; **62**: 3945-3949
- 36 **Lin B**, Chen GQ, Xiao D, Kolluri SK, Cao X, Su H, Zhang XK. Orphan receptor COUP-TF is required for induction of retinoic acid receptor beta, growth inhibition, and apoptosis by retinoic acid in cancer cells. *Mol Cell Biol* 2000; **20**: 957-970

Edited by Gupta MK **Proofread by** Xu FM

Expression of heparanase gene, CD44v6, MMP-7 and *nm23* protein and their relationship with the invasion and metastasis of gastric carcinomas

Jun-Qiang Chen, Wen-Hua Zhan, Yu-Long He, Jun-Sheng Peng, Jian-Ping Wang, Shi-Rong Cai, Jin-Ping Ma

Jun-Qiang Chen, Wen-Hua Zhan, Yu-Long He, Jun-Sheng Peng, Jian-Ping Wang, Shi-Rong Cai, Jin-Ping Ma, Department of Gastrointestinal Surgery, The First Affiliated Hospital, Sun Yat-sen University, Guangzhou 510080, Guangdong Province, China
Supported by the National Natural Science Foundation of China, No. 30271276

Correspondence to: Dr. Wen-Hua Zhan, Department of Gastrointestinal Surgery, the First Affiliated Hospital, Sun Yat-sen University, Guangzhou 510080, Guangdong Province, China. wzwk@gzsums.edu.cn
Telephone: +86-20-87755766 Ext 8211 **Fax:** +86-20-87335945
Received: 2003-11-17 **Accepted:** 2003-12-16

Abstract

AIM: To explore the expression of heparanase gene, CD44v6, MMP-7 and *nm23* proteins in human gastric carcinoma as well as their relationship with the clinicopathological factors.

METHODS: Reverse transcription polymerase chain reaction (RT-PCR) was used to measure the expressions of heparanase mRNA in 43 human gastric carcinomas and 10 adjacent normal gastric tissues. Streptavidin-peroxidase (S-P) two step method was used to measure the immunohistochemical expression of CD44v6, MMP-7 and *nm23* protein in 43 human gastric carcinomas.

RESULTS: The expression of heparanase gene was positive in 29 cases of gastric cancer with a positive rate of 67.4%, which was significantly higher than those in adjacent normal gastric tissues ($P < 0.05$). The heparanase mRNA expression was significantly related to advanced stage of disease, serosal infiltration, lymph node metastasis and size of tumors ($P < 0.05$), but not related to tumor location, gross and histological types of the cancer, peritoneal dissemination and liver metastasis ($P > 0.05$). The positive rate of CD44v6, *nm23* and MMP-7 proteins was 76.7%, 37.2% and 60.5%, respectively. The CD44v6 protein expression was significantly related to serosal infiltration, lymph node metastasis and TNM stage of disease ($P < 0.05$). The *nm23* protein expression was significantly related to the tumor gross appearance, lymph node and peritoneal metastasis ($P < 0.05$). The MMP-7 protein expression was significantly related to serosal infiltration and TNM stage of disease ($P < 0.05$). In an attempt to measure the association between these agents, we found that the expression of heparanase mRNA had significantly negative correlation with the expression of CD44v6 and MMP-7 protein ($P < 0.05$), the expression of MMP-7 protein had significantly positive correlation with the expression of CD44v6 protein ($r = 0.568$, $P < 0.05$), the expression of MMP-7 protein had no correlation with the expression of *nm23* protein ($P > 0.05$), and the expression of *nm23* protein had no correlation with the expression of CD44v6 protein ($P > 0.05$).

CONCLUSION: Despite their different mechanisms of action, heparanase, CD44v6 and *nm23* may play important roles in the invasive infiltration and lymph node metastasis

in gastric carcinomas. Instead of metastatic spreading, MMP-7 may be just related to the invasion of gastric carcinomas. However, co-detection of these factors may be important to predict metastatic spreading in such patients.

Chen JQ, Zhan WH, He YL, Peng JS, Wang JP, Cai SR, Ma JP. Expression of heparanase gene, CD44v6, MMP-7 and *nm23* protein and their relationship with the invasion and metastasis of gastric carcinomas. *World J Gastroenterol* 2004; 10(6): 776-782
<http://www.wjgnet.com/1007-9327/10/776.asp>

INTRODUCTION

Invasion and metastasis of gastric carcinomas involve many processes including adherence, degradation, motility, and angiogenesis and escaping from immune surveillance. However, the penetration through the barrier formed by the basement membrane (BM) and extracellular matrix (ECM) is critical for invasion and metastasis of cancerous cells. This barrier is mainly composed of structural proteins and glycosaminoglycans. The former mainly includes collagen, laminin and fibronectin, whereas the latter chiefly consists of heparan sulfate proteoglycans (HSPGs) which is formed by a core protein and several covalent-binding heparan sulfate (HS) side chains. In the past decade, the damage of structural proteins has been considered to be a critical step for tumors' invasion and metastasis^[1-3]. Previous researches mostly focused on property of some enzymes such as matrix metalloproteinases (MMPs) which use structural proteins as substrates. However, we should never neglect the effect of hydrolytic enzymes which use HSPGs as substrates, as well as their roles in degrading the BM and ECM. Heparanase is an endoglycosidase cloned out by Vlodavsky *et al* in 1999, which degrades the HS chain of HSPGs^[1,2]. Recently, protein or messenger RNA (mRNA) expression of heparanase has been identified in various cancer cells, and the overexpression of heparanase protein or mRNA in tumour cells has been reported to correlate with the metastatic potential of tumour cells *in vitro* and *in vivo* as well as with poor prognosis^[4-7]. However its role in gastric carcinomas is still not clearly clarified. In the present study, the expression of heparanase mRNA in gastric carcinomas and its correlation with clinicopathological features were investigated.

nm23, a metastasis suppressor gene, was reported to be associated with the tumor invasion and metastasis^[8,9]. CD44v6, a highly glycosylated cell surface protein, was reported to be involved in cell-cell and cell-matrix interactions and thought to take part in cell motility, tumor growth, and invasion^[10]. MMP-7, a member of matrix metalloproteinases family, was reported to play an important role in the degradation of connective tissue which is associated with the development of tumor metastases^[11]. However, their roles in gastric carcinomas have not been clearly illustrated. In current study, CD44v6, *nm23* and MMP-7 protein expression in gastric carcinomas and their relationship with each other were also investigated.

MATERIALS AND METHODS

Patients

Between Oct 2002 and May 2003, 43 patients with gastric carcinoma underwent radical gastrectomy (D2 or D3), as subtotal or total gastrectomy in the Department of Gastrointestinal Surgery at the First Affiliated Hospital of Sun Yat-sen University. The age and sex of the patients, as well as the location, macroscopic type, histological grade, stage and depth of the invasion of the tumor, histological lymph node metastasis, and type of surgical procedures were retrieved from the patients' records. Pathological diagnosis and classifications were done according to the UICC standard published in 1997. Histological grouping based on UICC TNM classification was confirmed by histological examination.

mRNA extraction

The gastric tissues were obtained from those duly informed patients whose consents were obtained for the use of their subsequent resected tissues. The present study conformed to regulations of the Ethic Committee of the First Affiliated Hospital of Sun Yat-sen University. Tissue samples of approximately 1 g were collected immediately after each gastrectomy. Non-cancerous gastric tissues were obtained from regions distant from the tumours. Half of the both cancerous and non-cancerous tissues were fixed in 40g/L buffered formaldehyde and embedded in paraffin. Sections (4 mm thick) were prepared with haematoxylin-eosin staining for histopathological diagnosis and with immunohistochemical staining. The other half of the tissues was stored in RNAlater (Sigma, USA) at 4 °C overnight, then transferred to a clean freezing tube and stored at -80 °C for mRNA extraction. Before starting the study, histopathological examination had confirmed that no cancerous cells had contaminated the non-cancerous gastric tissues. Total RNA from tissues was isolated using RNeasy Mini Kits (Qiagen, USA) according to the manufacturer's protocol. Complementary DNA (cDNA) was synthesized from 2 µg of total RNA in a 25 µL reaction mixture. The 25 µL reaction mixture contained 2 µg RNA solution, 1 µL oligo d(T)18 (0.5 µg/µL), 1 µL M-MLV reverse transcriptase (Promega, USA), 1 µL RNasin ribonuclease inhibitor (Promega, USA) and 2 µL dNTP. The integrity of RNA was checked electrophoretically and quantified spectrophotometrically.

Real-time reverse transcription^[6,12,13]

The following primers such as forward primer 5'-TTC GAT CCC AAG AAG GAA TCA AC-3' and reverse primer 5'-GTA GTG ATG CCA TGT AAC TGA ATC-3' were used for heparanase. The PCR reaction was run for 40 cycles under the following conditions: denaturation at 94 °C for 3 min, denaturation at 94 °C for another 30 s, annealing at 50 °C for 30 s and extension at 72 °C for 1 min with an extra 10-min extension for the last cycle. We determined the nucleotide sequence of this PCR product and confirmed that it was identical to the expected fragment of cDNA of heparanase. Glyceraldehyde-3-phosphate dehydrogenase (GAPDH) transcripts were monitored as a control to quantify the transcripts of the genes in each sample. GAPDH-specific sequences were amplified using the forward primer 5'-CAG GGG GGG AGC CAA AAG-3', reverse primer 5'-GGC AGT GGG GAC ACG GAA-3', which yielded a 378-bp product. After completion of these amplification cycles, 10 µL of each PCR product was electrophoresed at 50-80V for 30-40 minutes on a 10g/L agarose gel in Tris boric acid EDTA buffer together with 100 bp DNA ladder marker (TaKaRa Biotechnology(Dalian) Co.,Ltd) and was stained with ethidium bromide.

Immunohistochemistry

Streptavidin-peroxidase (S-P) two step method was used for

the immunohistochemical detection of CD44v6, *nm23* and MMP-7 proteins. Immunohistochemical detection of CD44v6, *nm23* and MMP-7 was performed with monoclonal antibodies (Maixin Biological, Fuzhou, China) against CD44v6, MMP-7 and *nm23*/NDP kinase.

The sections were first washed for 3 min with phosphate buffered saline (PBS) 3 times and then blocked with a solution of 30mL/L hydrogen peroxide in ethanol for 10 min at room temperature. After that they were immersed in 30mL/L normal horse serum for 10 min also at room temperature. Primary antibodies to CD44v6, *nm23* and MMP-7 were incubated for 1 h at room temperature. The ultrasensitive S-P kit (Maixin Biological, Fuzhou, China) was used to detect the resulting immune complex. The procedures of blocking, linkage, and labeling of binding reaction were carried out according to manufacturer's instructions. The peroxidase activity was visualized by DAB kit (Maixin Biological, Fuzhou, China), the sections were finally counterstained with hematoxylin and the negative control was processed by incubation with non-immune rabbit IgG in substitution for the primary antibody.

To evaluate the expression of CD44v6, only cell membrane staining equivalent to normal control was considered positive, while for *nm23* and MMP-7, only cytoplasmic staining equivalent to normal control was considered positive. Slides were examined and scored by two pathologists ignorant of the clinical details. Those slides exhibiting diffuse immunostaining or presenting more than 50% of tumor cells were classified as (++), more than 10% but less than 50% as (+) and those with immunoreactivity less than 10% were classified as (-). (+) and (++) were combined together as positive cases for statistical analysis.

Statistics

Statistical analyses were done with the SPSS 10.0 for Windows program. Frequency tables were analyzed with the Pearson Chi-square test or Fisher's exact test. The relationships between heparanase and *nm23* and CD44v6 and MMP-7 in gastric tumor tissues were evaluated statistically using the Kendall rank correlation test. Statistical differences with *P* values less than 0.05 by two-tailed tests were considered significant.

RESULTS

Clinical findings

The subjects included 26 men and 17 women. Their average age at the time of surgery was 58.5±13.4 years (ranging from 29 to 86 years). Ten cases of gastric cancer located at the upper third of the stomach, 7 at the middle third and 26 at the lower third. Of these 43 patients, 3 had peritoneal metastasis, 2 had liver metastasis, 35 had serosal invasion, and 27 had lymph node metastasis. Histopathological diagnoses of the patients were made according to the guidelines for classification of the primary gastric cancer. Thirty patients were classified as adenocarcinoma, 5 as mucinous carcinoma and 8 as signet-ring cell carcinoma. For histological differentiation, 4 were well differentiated, 10 were moderate differentiated and 29 were poorly differentiated. For TNM staging, 6 patients belonged to stage I, 8 belonged to stage II, 13 belonged to stage III, and 16 belonged to stage IV. None of the patients had received preoperative chemotherapy.

Relationship between heparanase gene expression and clinicopathological features in gastric carcinomas

The expression of heparanase mRNA was positive in 29 cases of gastric cancer with a positive rate of 67.4%. While its expression rate in the 10 cases of non-cancerous gastric tissues

was 10.0% (1 case). The difference was statistically significant ($P<0.05$) (Figure 1).

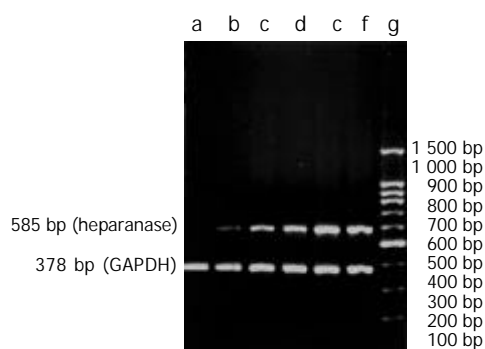


Figure 1 Expression of heparanase mRNA in gastric carcinomas. a: non-cancerous tissue, b-f: cancerous tissue, g: marker (100 bp DNA ladder marker).

From Table 1, we could find that the mRNA expression of heparanase was not correlated with tumor location, gross appearance, histological characteristics, peritoneal dissemination and liver metastasis ($P>0.05$). It was correlated with tumor size, serosal infiltration, lymph node metastasis, distant metastasis and TNM staging of gastric carcinomas ($P<0.05$). In 14 cases of negative expression of heparanase mRNA, only 5 cases had lymph node metastasis. However, in 29 cases of positive expression of heparanase mRNA, twenty-two had lymph node metastasis, among which N₁ was in 11 cases, N₂ in 3 cases and N₃ in 8 cases. The difference between these two groups was statistically significant ($P<0.05$).

Relationship between CD44v6, nm23 and mmp-7 protein expression and clinicopathological features in gastric carcinomas

The expression of CD44v6 protein was positive in 33 cases of gastric cancer with a positive rate of 76.7% and the intensity of its immunoreactivity in cancer tissue was scored as (+) in 27

Table 1 Relationship between clinicopathological features and heparanase mRNA expression and CD44v6, nm23 and MMP-7 protein expression in primary gastric carcinomas

Clinicopathological features	Number of patients											
	Heparanase			CD44v6			nm23			MMP-7		
	(+)	(-)	<i>P</i> value	(+)	(-)	<i>P</i> value	(+)	(-)	<i>P</i> value	(+)	(-)	<i>P</i> value
Gender			0.307			0.481			0.280			0.415
Female	13	4		12	5		8	9		9	8	
Male	16	10		21	5		8	18		17	9	
Tumor location			0.216			0.346			0.903			0.804
Upper third	9	1		9	1		4	6		6	4	
Middle third	4	3		6	1		3	4		5	2	
Lower third	16	10		18	8		9	17		15	11	
Gross type			0.242			0.325			0.025			0.121
Borrmann I	1	0		1	0		0	1		1	0	
Borrmann II	4	5		5	4		7	2		5	4	
Borrmann III	21	9		25	5		9	21		20	10	
Borrmann IV	3	0		2	1		0	3		0	3	
Histologic type			0.671			0.297			0.444			0.325
Adenocarcinoma	19	11		23	7		13	17		20	10	
Mucinous carcinoma	4	1		5	0		1	4		3	2	
Signet-ring cell carcinoma	6	2		5	3		2	6		3	5	
Peritoneal metastasis			0.539			1.000			0.045			0.266
Absent	26	14		30	10		13	27		23	17	
Present	3	0		3	0		3	0		3	0	
Liver metastasis			1.000			1.000			0.133			0.511
Absent	27	14		31	10		14	27		24	17	
Present	2	0		2	0		2	0		2	0	
Histologic differentiation			1.000			0.704			0.888			0.101
Well/moderate	9	5		10	4		5	9		6	8	
Poorly	20	9		23	6		11	18		20	9	
Serosal invasion			0.009			0.010			0.101			0.042
Absent	2	6		3	5		5	3		2	6	
Present	27	8		30	5		11	24		24	11	
Lymph node metastasis			0.018			0.024			0.008			0.084
Absent	7	9		9	7		10	6		7	9	
Present	22	5		24	3		6	21		19	8	
Distant metastasis			0.039			0.656			0.125			1.000
Absent	21	14		26	9		11	24		21	14	
Present	8	0		7	1		5	3		5	3	
TNM stage			0.001			0.001			0.228			0.021
I-II	4	10		6	8		7	7		5	9	
III-IV	25	4		27	2		9	20		21	8	

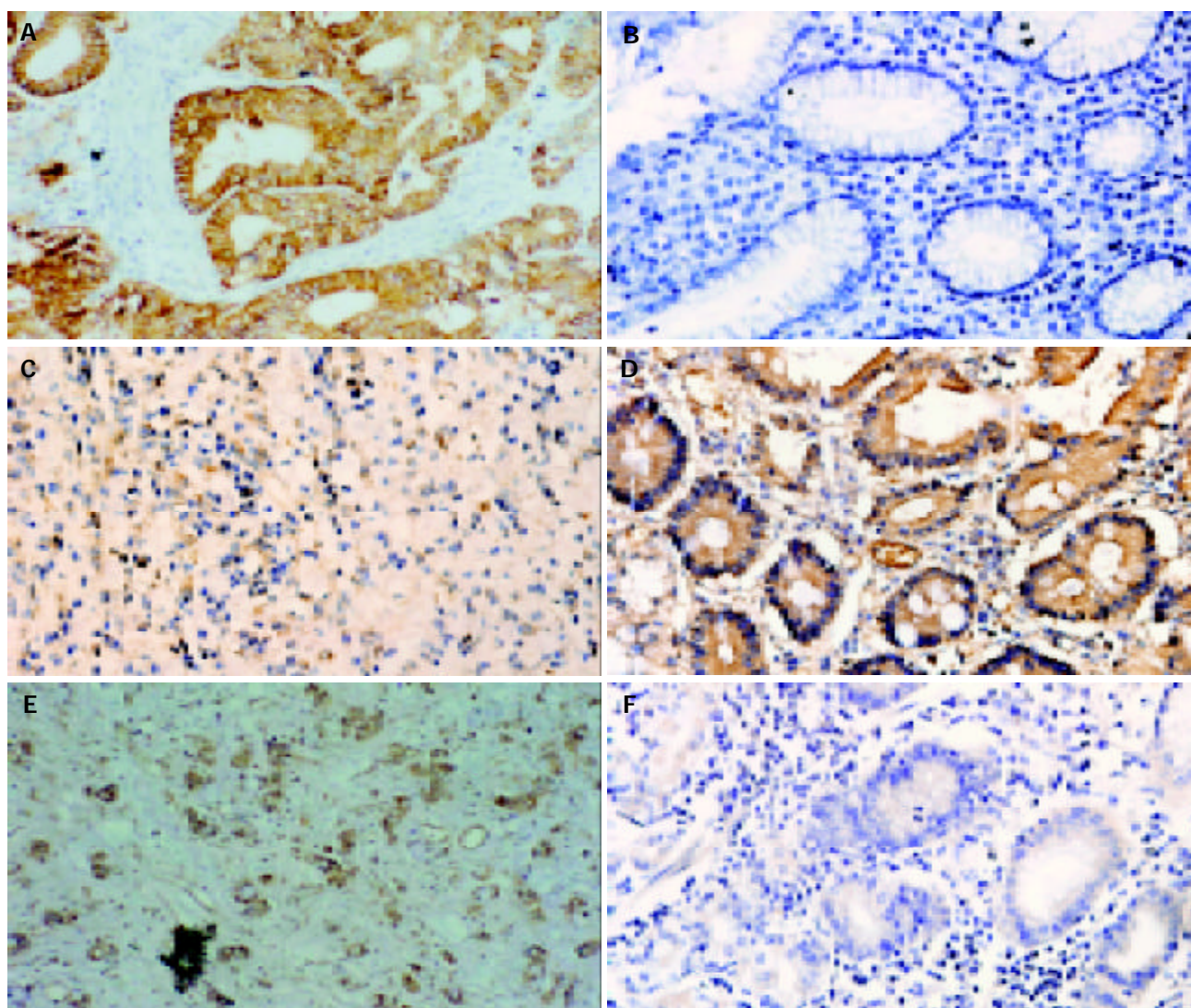


Figure 2 Expression of CD44v6, *nm23* and MMP-7 protein in gastric carcinomas and non-cancerous gastric tissues. A: gastric carcinoma stained for CD44v6($\times 400$), B: non-cancerous gastric tissue stained for CD44v6($\times 400$), C: gastric carcinoma stained for *nm23* ($\times 400$), D: non-cancerous gastric tissue stained for *nm23* ($\times 400$), E: gastric carcinoma stained for MMP-7 ($\times 400$), F: non-cancerous gastric tissue stained for MMP-7 ($\times 400$).

patients and (++) in 6 patients. The expression of *nm23* protein was positive in 16 cases of gastric cancer with a positive rate of 37.2% and the intensity of its immunoreactivity in cancer tissue was scored as (+) in 10 patients and (++) in 6 patients. The expression of MMP-7 protein was positive in 26 cases of gastric cancer with a positive rate of 60.5% and the intensity of its immunoreactivity in cancer tissue was scored as (+) in 20 patients and (++) in 6 patients (Figure 2).

The expression of CD44v6 protein was significantly correlated with lymph node metastasis, TNM staging and serosal infiltration ($P < 0.05$). The expression of *nm23* protein was significantly correlated with the tumor gross appearance, peritoneal metastasis and lymph node metastasis ($P < 0.05$). The expression of MMP-7 protein was significantly correlated with serosal invasion and TNM staging (Table 1).

Correlation between heparanase mRNA expression and CD44v6, *nm23* and MMP-7 protein expression

The expression of heparanase mRNA had significant negative correlation with the expression of CD44v6 and MMP-7 protein ($P < 0.05$) (Table 2). The expression of MMP-7 protein had significant positive correlation with the expression of CD44v6 protein ($\gamma = 0.568$, $P < 0.01$). The expression of MMP-7 protein had no correlation with the expression of *nm23* protein ($P > 0.05$).

The expression of *nm23* protein had no correlation with the expression of CD44v6 protein ($P > 0.05$).

Table 2 Correlation between the expression of heparanase mRNA and the expression of CD44v6, *nm23* and MMP-7 protein

Items	Number of cases	Heparanase (+)	Correlation coefficient	P value
CD44v6			-0.440	0.004
(-)	10	3		
(+)	33	26		
<i>Nm23</i>			-0.021	0.889
(-)	27	18		
(+)	16	11		
MMP-7			-0.352	0.023
(-)	17	8		
(+)	26	21		

DISCUSSION

In normal human tissues, heparanase mRNA is chiefly distributed in placenta and lymphatic tissues. Contrarily in the connective tissues and most of the epithelial cell, its expression is rare or even absent^[1-3]. Vlodavsky *et al.*^[1] confirmed that

heparanase could promote the metastasis of tumor by gene transfection experiments. They transfected non-metastatic Eb cells with a full-length human heparanase cDNA using a pcDNA3 expression plasmid. As a result, the transfected cells expressed high levels of heparanase mRNA and high heparanase activity. Ninety percent of the DBA/2 mice injected with heparanase-transfected Eb cells died by d 34, whereas 60% of the mice inoculated with mock-transfected cells were alive at that time. The livers of mice inoculated with heparanase-transfected cells were infiltrated with numerous Eb lymphoma cells. In contrast, metastatic lesions could not be detected by gross examination in the liver of the mice with mock-transfected and control Eb cells. Few or no lymphoma cells infiltrated the liver tissue. Furthermore, transient transfection of the heparanase gene into B16-F1 mouse melanoma cells with low metastatic potential followed by intravenous inoculation resulted in a 400-500% increase in lung metastases. All these implied that heparanase might play an important role in tumor invasion and metastasis.

In the present study, the positive rate of heparanase mRNA expression in gastric carcinomas (67.4%) was significantly higher than that of non-cancerous gastric tissues (10%) ($P < 0.05$). Heparanase mRNA tended to express more in those patients with serosal invasion, lymph node metastasis, advanced stage of diseases, distant metastasis and larger size of tumors ($P < 0.05$). The results indicated that heparanase mRNA was closely related with the clinicopathological features that reflected the invasion and metastatic potential and prognosis. Up to now, invasion depth, lymph node metastasis or distant metastasis and TNM stage were considered to be the prognostic factors for gastric carcinomas^[14,15]. That heparanase mRNA expression statistically related with these factors implied that the invasion and metastasis induced by heparanase might indicate a poor prognosis of the gastric carcinomas. This needs to be confirmed by further survival analysis.

According to the researches on other kinds of carcinomas, the mechanisms by which heparanase accelerates invasion and metastasis can be summarized as the following two points. First, heparanase is responsible for degrading HSPGs side chain HS which is the chief component of the BM and ECM but not degraded by MMPs. Second, the degradation of HSPGs by heparanase leads to the release of various growth factors and cytokines trapped in HSPGs which regulate the angiogenesis, tissue repair, inflammation and lipid metabolism^[12,16,17]. In our study, we observed that heparanase mRNA expression often occurred in patients with serosal infiltration and advanced stage of disease, which might imply the important role of heparanase in damaging and penetrating the BM in gastric carcinomas.

The metastasis in gastric carcinomas occurs not only through lymphatic and hematogenous ways but also by direct infiltration. It is still unknown of the definite roles of heparanase in the metastasis of gastric carcinomas. We found none of the patients with liver metastasis expressed heparanase mRNA, while those with lymph node metastasis were significantly related with the expression of heparanase mRNA ($P < 0.05$). We supposed that heparanase was involved in lymphatic metastasis of gastric carcinomas instead of hematogenous metastasis. To draw a further conclusion, larger sample investigations on gastric carcinoma are needed, since the cases with liver metastasis in our study were few. However, Endo *et al.*^[12] found there was no correlation between heparanase expression and lymph node metastasis in gastric carcinomas. In their study, 65%(20/31) patients with positive expression of heparanase mRNA had venous metastasis, compared with 47%(15/32) in negative mRNA expression. They thought heparanase was involved in hematogenous metastasis of gastric carcinomas instead of lymphatic metastasis.

The *nm23* was the first identified metastasis suppressor

gene. In 1988, Steeg *et al.*^[18] discovered murine *nm23* cDNA by using differential colony hybridization between murine K-1735 melanoma cell lines that varied in metastatic potential *in vivo*. They found that the *nm23* mRNA levels of two low metastatic potential cell lines were quantitatively higher than that of five related but highly metastatic cell lines. Later, the examination of protein levels exhibited a similar pattern^[19]. This discovery aroused much interest in the role of *nm23* in progression of carcinomas. Up to now, eight members of the human *nm23* family have been reported and are found in multiple subcellular compartments. Homologs in other species are known as nucleoside diphosphate kinases (NDP kinase or ndpk) or, in *Drosophila*, as abnormal wing discs (awd)^[20]. Two highly homologous genes have been described so far, both located at the long arm of chromosome 17, coding for the 18.5 and 17 kD proteins *nm23-H1* and *nm23-H2*, respectively. The *nm23-H1* and *nm23-H2* gene products have been shown to be identical to human nucleoside diphosphate (NDP) kinases A and B^[19]. *nm23* has been considered as an antimetastatic gene for most malignancies, but the role of *nm23* gene in gastric carcinomas is still not completely known.

In our study, we found that *nm23* had a significant association with lymph node metastasis and peritoneal dissemination. In 27 patients with lymph node metastasis 21 were *nm23* negative, while in 16 patients without lymph node metastasis only 6 were *nm23* negative. The difference was statistically significant ($P < 0.01$). In 40 patients without peritoneal metastasis, 27 were *nm23* negative, but in 3 patients with peritoneal metastasis all were *nm23* positive. The difference was also statistically significant ($P < 0.05$). It indicates that *nm23* suppresses lymphatic metastasis and peritoneal metastasis in gastric carcinomas. Our study also demonstrated that decreased expression of *nm23* was related to tumor's gross type. Other researches showed similar results and proposed *nm23* was related to 5 year survival of the patients^[21]. However Yoo *et al.*^[22] found there was no significant difference in 5-year survival rates between patients with *nm23*-positive and *nm23*-negative tumors ($P > 0.05$) and denied *nm23* to be a predictor of outcome of patients with gastric carcinomas.

CD44 is a highly glycosylated cell surface protein. In normal tissues, CD44 is expressed in a variety of epithelial and mesenchymal cells, as well as in blood cells and glial cells of the central nervous system^[10,23]. Tremendous interest in CD44 was generated when Gunthert and colleagues conferred metastatic potential on a non-metastatic cell line by transfecting a variant of CD44^[23,24]. CD44 has two isoforms, one has been termed CD44 standard (CD44s) and the other CD44 variant (CD44v). The mRNA of CD44s contains no variant exons, while CD44v may contain one or more variant regions, such as CD44v6 or CD44v3-v7. CD44v6 now is considered to be involved in cell-cell and cell-matrix interactions and take part in cell motility, tumour growth, invasion and metastasis^[10,23,25].

Our results demonstrated that CD44v6 was significantly related to lymph node metastasis, serosal invasion and TNM stage. Twenty-four out of 27 patients with lymph node metastases were CD44v6 positive, while 9 out of 16 patients without lymph node metastasis were CD44v6 positive. The difference was statistically significant ($P < 0.05$). Twenty-seven out of 29 stage III and IV patients were CD44v6 positive but only 6 out of 14 stage I and II patients were CD44v6 positive. Their difference was also statistically significant ($P < 0.05$). These indicated that CD44v6 might be a useful predictor of lymph node metastasis in gastric carcinomas. Joo *et al.*^[26,27] obtained almost the same results as ours. But Yamaguchi *et al.*^[28] tended to consider CD44v6 protein to have an important role in hematogenous metastasis of gastric carcinomas.

MMPs are a family of zinc-dependent endoproteinases whose enzymatic activity is directed against components of

the ECM. Up to now, 24 different vertebrate MMPs have been identified, of which 23 are found in humans. On the basis of substrate specificity, sequence similarity, and domain organization, vertebrate MMPs can be divided into six groups: collagenases; gelatinases; stromelysins; membrane-type MMPs; matrilysins and other MMPs. MMP-7 is also called matrilysin^[29,30]. The mechanism of MMP-7 in gastric carcinomas is still unclear. Our study demonstrated that only serosal invasion and advanced stage of disease were closely related to MMP-7 protein expression and it had no correlation with other clinicopathological features. In 26 MMP-7 positive cases, 24 cases had serosal invasion while for 17 MMP-7 negative cases, only 11 cases had serosal invasion ($P < 0.05$). Yonemura *et al.*^[31] found MMP-7 had not only significant positive correlation with serosal involvement but also with lymph node metastasis, poor differentiation and peritoneal dissemination. Patients with MMP-7-positive tumor had significantly poorer survival and more frequently died of peritoneal recurrence than did those with MMP-7-negative tumors. So MMP-7 was considered to be a good indicator of peritoneal dissemination. This was confirmed later by the study using MMP-7-specific antisense oligonucleotide which could inhibit peritoneal dissemination in human gastric cancer^[32]. However, our study did not show any correlation between MMP-7 expression and peritoneal metastasis.

According to the studies on other kinds of carcinomas, MMPs facilitate tumor cell invasion and metastasis by at least three distinct mechanisms. First, proteinase removes physical barriers to invasion through degradation of ECM macromolecules such as collagens, laminins, and proteoglycans. Second, MMPs have the ability to modulate cell adhesion. Finally, MMPs may act on ECM components or other proteins to unknown hidden biologic activities^[11]. Liu *et al.*^[33] investigated immunohistochemically MMP-7 expression in 214 gastric carcinomas and found MMP-7-positive tumor cells were preferentially found in deeply invading nests, especially at the invasive front. The mean MMP-7 labeling index (LI) at the invasive front was significantly higher in tumors invading or penetrating the muscularis propria and in stages II - IV than within the submucosal layer and in stage I, respectively ($P < 0.001$). Our study also showed serosal invasion and advanced stage of disease were closely related to MMP-7 protein expression. Liu *et al.*^[34] also found Ki-67 antigen, an indicator of cell proliferation, was absent in MMP-7 positive tumor cells and vice versa and concluded that MMP-7 expression was related inversely with proliferative activity of tumor cells. So it could be deduced that MMP-7 might participate in the penetration of BM and ECM in gastric carcinomas instead of promoting cell proliferation. Recently, two studies demonstrated that MMP-7 upregulation was closely related with the *H. pylori* cag pathogenicity island and this implied a certain role of MMP-7 in carcinogenesis of gastric carcinomas^[35,36].

Invasion and metastasis of gastric carcinomas are a multistep process. As far as we know, the relationship between heparanase, CD44v6, *nm23* and MMP-7 has not been reported. In our study, we found the expression of heparanase mRNA had significant negative correlation with the expression of CD44v6 and MMP-7 protein. Although heparanase and MMPs both acted on BM and ECM, their substrates were different. Heparanase mainly used HS as substrate while MMPs mainly used structural proteins as substrates. This might account for the negative correlation between the expression of heparanase mRNA and MMP-7 protein. But what exactly caused this is worthy of further studying. That the expression of MMP-7 protein had significant positive correlation with the expression of CD44v6 protein further confirmed that MMPs have the ability to modulate cell adhesion. Why there was no correlation

between the expression of MMP-7 and *nm23* protein? Might it be caused by their different mechanisms? Further studies will be needed to elucidate their relationship in tumors.

REFERENCES

- 1 **Vlodavsky I**, Friedmann Y, Elkin M, Aingorn H, Atzmon R, Ishai-Michaeli R, Bitan M, Pappo O, Peretz T, Michal I, Spector L, Pecker I. Mammalian heparanase: gene cloning, expression and function in tumor progression and metastasis. *Nat Med* 1999; **5**: 793-802
- 2 **Hulett MD**, Freeman C, Hamdorf BJ, Baker RT, Harris MJ, Parish CR. Cloning of mammalian heparanase, an important enzyme in tumor invasion and metastasis. *Nat Med* 1999; **5**: 803-809
- 3 **Parish CR**, Freeman C, Hulett MD. Heparanase: a key enzyme involved in cell invasion. *Biochim Biophys Acta* 2001; **1471**: 99-108
- 4 **Kuniyasu H**, Chihara Y, Kubozoe T, Takahashi T. Co-expression of CD44v3 and heparanase is correlated with metastasis of human colon cancer. *Int J Mol Med* 2002; **10**: 333-337
- 5 **Kim AW**, Xu X, Hollinger EF, Gattuso P, Godellas CV, Prinz RA. Human heparanase-1 gene expression in pancreatic adenocarcinoma. *J Gastrointest Surg* 2002; **6**: 167-172
- 6 **Rohloff J**, Zinke J, Schoppmeyer K, Tannapfel A, Witzigmann H, Mossner J, Wittekind C, Caca K. Heparanase expression is a prognostic indicator for postoperative survival in pancreatic adenocarcinoma. *Br J Cancer* 2002; **86**: 1270-1275
- 7 **Uno F**, Fujiwara T, Takata Y, Ohtani S, Katsuda K, Takaoka M, Ohkawa T, Naomoto Y, Nakajima M, Tanaka N. Antisense-mediated suppression of human heparanase gene expression inhibits pleural dissemination of human cancer cells. *Cancer Res* 2001; **61**: 7855-7860
- 8 **Ouatas T**, Salerno M, Palmieri D, Steeg PS. Basic and translational advances in cancer metastasis: Nm23. *J Bioenerg Biomembr* 2003; **35**: 73-79
- 9 **Wang YK**, Ji XL, Ma NX. nm23 expression in gastric carcinoma and its relationship with lymphoproliferation. *World J Gastroenterol* 1999; **5**: 87-89
- 10 **Jothy S**. CD44 and its partners in metastasis. *Clin Exp Metastasis* 2003; **20**: 195-201
- 11 **Kleiner DE**, Stetler-Stevenson WG. Matrix metalloproteinases and metastasis. *Cancer Chemother Pharmacol* 1999; **43**(Suppl): S42-51
- 12 **Endo K**, Maejara U, Baba H, Tokunaga E, Koga T, Ikeda Y, Toh Y, Kohno S, Okamura T, Nakajima M, Sugimachi K. Heparanase gene expression and metastatic potential in human gastric cancer. *Anticancer Res* 2001; **21**: 3365-3369
- 13 **El-Assal ON**, Yamanoi A, Ono T, Kohno H, Nagasue N. The clinicopathological significance of heparanase and basic fibroblast growth factor expressions in hepatocellular carcinoma. *Clin Cancer Res* 2001; **7**: 1299-1305
- 14 **Shiraishi N**, Inomata M, Osawa N, Yasuda K, Adachi Y, Kitano S. Early and late recurrence after gastrectomy for gastric carcinoma. Univariate and multivariate analysis. *Cancer* 2000; **89**: 255-261
- 15 **Borie F**, Millat B, Fingerhut A, Hay JM, Fagniez PL, Saxce B. Lymphatic involvement in early gastric cancer: prevalence and prognosis in France. *Arch Surg* 2000; **135**: 1218-1223
- 16 **Marchetti D**, Li J, Shen R. Astrocytes contribute to the brain-metastatic specificity of melanoma cells by producing heparanase. *Cancer Res* 2000; **60**: 4767-4770
- 17 **Myler HA**, West JL. Heparanase and platelet factor-4 induce smooth muscle cell proliferation and migration via bFGF release from the ECM. *J Biochem* 2002; **131**: 913-922
- 18 **Steeg PS**, Bevilacqua G, Kopper L, Thorgerisson UP, Talmadge JE, Liotta LA, Sobel ME. Evidence for a novel gene associated with low tumor metastatic potential. *J Natl Cancer Inst* 1988; **80**: 200-204
- 19 **Salerno M**, Ouatas T, Palmieri D, Steeg PS. Inhibition of signal transduction by the nm23 metastasis suppressor: possible mechanisms. *Clin Exp Metastasis* 2003; **20**: 3-10
- 20 **Lacombe ML**, Milon L, Munier A, Mehus JG, Lambeth DO. The human nm23/nucleoside diphosphate kinases. *J Bioenerg Biomembr* 2000; **32**: 247-258
- 21 **Nesi G**, Palli D, Pernice LM, Saieva C, Paglierani M, Kroning

- KC, Catarzi S, Rubio CA, Amorosi A. Expression of nm23 gene in gastric cancer is associated with a poor 5-year survival. *Anticancer Res* 2001; **21**: 3643-3649
- 22 **Yoo CH**, Noh SH, Kim H, Lee HY, Min JS. Prognostic significance of CD44 and nm23 expression in patients with stage II and stage IIIA gastric carcinoma. *J Surg Oncol* 1999; **71**: 22-28
- 23 **Ponta H**, Sherman L, Herrlich PA. CD44: from adhesion molecules to signalling regulators. *Nat Rev Mol Cell Biol* 2003; **4**: 33-45
- 24 **Gunthert U**, Hofmann M, Rudy W, Reber S, Zoller M, Haussmann I, Matzku S, Wenzel A, Ponta H, Herrlich P. A new variant of glycoprotein in CD44 confers metastatic potential to rat carcinoma cells. *Cell* 1991; **65**: 13-24
- 25 **Zhang JC**, Wang ZR, Cheng YJ, Yang DZ, Shi JS, Liang AL, Liu NN, Wang XM. Expression of proliferating cell nuclear antigen and CD44 variant exon 6 in primary tumors and corresponding lymph node metastases of colorectal carcinoma with Dukes' stage C or D. *World J Gastroenterol* 2003; **9**: 1482-1486
- 26 **Joo M**, Lee HK, Kang YK. Expression of E-cadherin, beta-catenin, CD44s and CD44v6 in gastric adenocarcinoma: relationship with lymph node metastasis. *Anticancer Res* 2003; **23**: 1581-1588
- 27 **Xin Y**, Grace A, Gallagher MM, Curran BT, Leader MB, Kay EW. CD44v6 in gastric carcinoma: a marker of tumor progression. *Appl Immunohistochem Mol Morphol* 2001; **9**: 138-142
- 28 **Yamaguchi A**, Goi T, Yu J, Hirose Y, Ishida M, Iida A, Kimura T, Takeuchi K, Katayama K, Hirose K. Expression of CD44v6 in advanced gastric cancer and its relationship to hematogenous metastasis and long-term prognosis. *J Surg Oncol* 2002; **79**: 230-235
- 29 **Visse R**, Nagase H. Matrix metalloproteinases and tissue inhibitors of metalloproteinases: structure, function, and biochemistry. *Circ Res* 2003; **92**: 827-839
- 30 **Stamenkovic I**. Matrix metalloproteinases in tumor invasion and metastasis. *Semin Cancer Biol* 2000; **10**: 415-433
- 31 **Yonemura Y**, Endou Y, Fujita H, Fushida S, Bandou E, Taniguchi K, Miwa K, Sugiyama K, Sasaki T. Role of MMP-7 in the formation of peritoneal dissemination in gastric cancer. *Gastric Cancer* 2000; **3**: 63-70
- 32 **Yonemura Y**, Endo Y, Fujita H, Kimura K, Sugiyama K, Momiyama N, Shimada H, Sasaki T. Inhibition of peritoneal dissemination in human gastric cancer by MMP-7-specific antisense oligonucleotide. *J Exp Clin Cancer Res* 2001; **20**: 205-212
- 33 **Liu XP**, Kawauchi S, Oga A, Tsushimi K, Tsushimi M, Furuya T, Sasaki K. Prognostic significance of matrix metalloproteinase-7 (MMP-7) expression at the invasive front in gastric carcinoma. *Jpn J Cancer Res* 2002; **93**: 291-295
- 34 **Liu XP**, Oga A, Suehiro Y, Furuya T, Kawauchi S, Sasaki K. Inverse relationship between matrilysin expression and proliferative activity of cells in advanced gastric carcinoma. *Hum Pathol* 2002; **33**: 741-747
- 35 **Bebb JR**, Letley DP, Thomas RJ, Aviles F, Collins HM, Watson SA, Hand NM, Zaitoun A, Atherton JC. *Helicobacter pylori* upregulates matrilysin (MMP-7) in epithelial cells *in vivo* and *in vitro* in a Cag dependent manner. *Gut* 2003; **52**: 1408-1413
- 36 **Crawford HC**, Krishna US, Israel DA, Matrisian LM, Washington MK, Peek RM Jr. *Helicobacter pylori* strain-selective induction of matrix metalloproteinase-7 *in vitro* and within gastric mucosa. *Gastroenterology* 2003; **125**: 1125-1136

Edited by Zhu LH Proofread by Xu FM

Expression of vascular endothelial growth factor C and chemokine receptor CCR7 in gastric carcinoma and their values in predicting lymph node metastasis

Chao Yan, Zheng-Gang Zhu, Ying-Yan Yu, Jun Ji, Yi Zhang, Yu-Bao Ji, Min Yan, Jun Chen, Bing-Ya Liu, Hao-Ran Yin, Yan-Zhen Lin

Chao Yan, Zheng-Gang Zhu, Ying-Yan Yu, Jun Ji, Yi Zhang, Yu-Bao Ji, Min Yan, Jun Chen, Bing-Ya Liu, Hao-Ran Yin, Yan-Zhen Lin, Department of General Surgery, Ruijin Hospital, Shanghai Second Medical University, Shanghai Institute of Digestive Surgery, Shanghai 200025, China

Correspondence to: Dr. Zheng-Gang Zhu, Shanghai Institute of Digestive Surgery, Ruijin Hospital, Shanghai Second Medical University, 197 Ruijin Road II, Shanghai 200025, China. digsurg@online.sh.cn

Telephone: +86-21-64373909 **Fax:** +86-21-64373909

Received: 2003-10-20 **Accepted:** 2003-12-08

Abstract

AIM: To study the expression of vascular endothelial growth factor C (VEGF-C) and chemokine receptor CCR7 in gastric carcinoma and to investigate their associations with lymph node metastasis of gastric carcinoma and their values in predicting lymph node metastasis.

METHODS: The expression of VEGF-C and CCR7 in gastric carcinoma tissues obtained from 118 patients who underwent curative gastrectomy was examined by immunohistochemistry. Among these patients, 39 patients underwent multi-slice spiral CT (MSCT) examination.

RESULTS: VEGF-C and CCR7 were positively expressed in 52.5 and 53.4% of patients. VEGF-C expression was more frequently found in tumors with lymph node metastasis than those without it ($P<0.001$). VEGF-C expression was also closely related to lymphatic invasion ($P<0.001$), vascular invasion ($P<0.01$), and TNM stage ($P<0.001$). However, there was no significant correlation between VEGF-C expression and age at surgery, gender, tumor size, tumor location, Lauren classification, and depth of invasion. CCR7 expression was significantly higher in patients with lymph node metastasis compared with those without lymph node metastasis ($P<0.001$) and was also associated with tumor size ($P<0.01$), depth of invasion ($P<0.001$), lymphatic invasion ($P<0.001$), and TNM stage ($P<0.001$). However, the presence of CCR7 had no correlation to age at surgery, gender, tumor location, Lauren classification, and vascular invasion. Among the 39 patients who underwent MSCT examination, only CCR7 expression was related to lymph node metastasis determined by MSCT ($P<0.05$). In the current retrospective study, the sensitivity, specificity, positive predictive value (PPV), negative predictive value (NPV), and accuracy of VEGF-C and CCR7 expression in the diagnosis of lymph node metastasis for patients with gastric carcinoma were 73.8%, 70.2%, 72.6%, 71.4% and 72.0%, and 82.0%, 77.2%, 79.4%, 80.0% and 79.7%, respectively. After subdivision according to the combination of VEGF-C and CCR7 expression, receiver operating characteristic (ROC) analysis showed that the accuracy of the combined examination of VEGF-C and CCR7 expression in predicting

lymph node metastasis was relatively high (area under ROC curve [Az]=0.83).

CONCLUSION: The expression of VEGF-C and CCR7 is related to lymph node metastasis of gastric carcinoma and both of them may become new targets for the treatment of gastric carcinoma. Furthermore, the combined examination of VEGF-C and CCR7 expression in endoscopic biopsy specimens may be useful in predicting lymph node metastasis of gastric carcinoma and deciding the extent of surgical lymph node resection.

Yan C, Zhu ZG, Yu YY, Ji J, Zhang Y, Ji YB, Yan M, Chen J, Liu BY, Yin HR, Lin YZ. Expression of vascular endothelial growth factor C and chemokine receptor CCR7 in gastric carcinoma and their values in predicting lymph node metastasis. *World J Gastroenterol* 2004; 10(6): 783-790

<http://www.wjgnet.com/1007-9327/10/783.asp>

INTRODUCTION

Lymph node metastasis is an important prognostic factor for patients with gastric carcinoma^[1-4]. In spite of this, the function of intratumor lymphatic vessels in lymph node metastasis of gastric carcinoma is unclear. Recently, the molecular pathway that signals for lymphangiogenesis and relatively specific markers for lymphatic endothelium have been described allowing analyses of tumor lymphangiogenesis to be performed^[5-8]. Many experimental studies indicated that lymphangiogenic factors (VEGF-C and VEGF-D) could stimulate lymphangiogenesis in tumors by binding to their receptors (VEGFR-3) on the lymphatic endothelial cells and inducing proliferation and growth of new lymphatic capillaries, then enhance the incidence of lymph node metastasis in animal models^[9-12]. A recent study by Orlandini *et al.*^[13] demonstrated that β -catenin was a negative regulator of VEGF-D mRNA stability, therefore VEGF-D expression might only be responsible for the nodal metastatic behavior in tumors that have lost or reduced expression of β -catenin. In addition, there was apparent discrepancy of VEGF-D expression in tumors reported by different authors^[14-18]. Thus, here we only investigate the role of VEGF-C in promoting lymph node metastasis in gastric carcinoma.

It has long been unclear as to why particular cancers preferentially metastasize to certain sites. However, a recent report by Muller *et al.*^[19] provided evidence for preferential homing of breast cancer to metastatic sites. The findings indicated that the chemokine receptors CXCR4 and CCR7 were found on breast cancer cells and their ligands were highly expressed at sites associated with breast cancer metastases. In addition, both CCL19 and CCL21 (chemokines, ligands of CCR7) are highly expressed in lymph nodes, therefore the migration of tumor cells positive for CCR7 towards lymph nodes may share many similarities with leukocyte trafficking,

which is critically regulated by chemokines and their receptors^[20]. A recent study by Takanami *et al.*^[20] has demonstrated that CCR7 was related to the development of lymph node metastasis in nonsmall cell lung cancers. Here, we aim to explore the association of CCR7 expression with lymph node metastasis in gastric carcinoma. Furthermore, activation of lymphatics by VEGF-C may promote production of chemoattractants such as CCL21 by lymphatic endothelial cells and thereby facilitate tumor cell positive for CCR7 expression entry into lymphatics^[21], so the other aim of this study is to investigate the value of the combined examination of VEGF-C and CCR7 expression in predicting lymph node metastasis of gastric carcinoma.

MATERIALS AND METHODS

Patients and tumor samples

One hundred and eighteen patients, who had undergone curative gastrectomy for gastric carcinoma between 2001 and 2002 in the Department of General Surgery, Ruijin Hospital affiliated to Shanghai Second Medical University, Shanghai, China, were enrolled in this study. All of the resected primary tumors and regional lymph nodes were histologically examined by hematoxylin and eosin staining according to the TNM classification. Among these patients, 39 cases preoperatively underwent MSCT examination by using the method previously reported^[22].

Immunohistochemical staining

Formalin-fixed and paraffin-embedded sections of tumor tissue obtained from resected stomach were cut 4 μ m thick, dewaxed in xylene and rehydrated in graded alcohol, then immersed in 30 mL/L hydrogen peroxide in methanol for 30 min to inhibit endogenous peroxidase activity. The sections were boiled in EDTA (0.01 mol/L, pH 8.0) for 20 min for antigen retrieval. After being rinsed in phosphate-buffered saline (PBS), the sections for CCR7 staining were treated sequentially with avidin and biotin (Biotin blocking system) (Dako) to block the endogenous biotin-like molecules. Then, all sections were incubated with normal goat serum for 10 min for blocking nonspecific reaction. The sections were then incubated with primary antibody at 37 °C in humid chambers for 1 h. The rabbit anti-human VEGF-C polyclonal antibody (Zymed) was at a 1:100 dilution, and the mouse anti-human CCR7 monoclonal antibody (BD PharMingen) was at a 1:300 dilution. After washing 3 times with PBS, the sections for CCR7 staining were then incubated for 10 min at room temperature with biotinylated secondary antibody (goat anti-mouse IgM) and streptavidin conjugated to horseradish peroxidase, respectively, whereas the sections for VEGF-C staining were reacted with EnVision plus (Dako) for 30 min at room temperature. After being rinsed 3 times with PBS, the sections were incubated with 3, 3'-diaminobenzidine tetrahydrochloride (DAB) (Dako), then rinsed with distilled water, counterstained with haematoxylin, dehydrated with alcohol and xylene, and mounted routinely. Negative controls were performed in all cases by omitting the first antibody.

Evaluation of immunohistochemical staining

Two pathologists evaluated and interpreted the results of immunohistochemical staining, without knowledge of the clinical data of each patient. The immunohistochemical expression of VEGF-C was defined as positive if distinct staining was observed in at least 30% of tumor cells^[23]. CCR7 expression in the cancer tissue was classified as positive if more than 10% tumor cells were immunoreactive. Very faint or equivocal immunoreaction was ignored.

Evaluation of lymph node status by MSCT

Two radiologists prospectively analyzed the CT images. Lymph nodes were considered involved when the short-axis diameter was more than 6 mm for the perigastric lymph nodes and more than 8 mm for the extraperigastric lymph nodes^[24]. The preoperative N staging obtained by MSCT was compared with the pathological findings according to the TNM classification (UICC).

Statistical analysis

Statistical analyses were performed using the χ^2 test and ROC analysis. $P < 0.05$ was considered statistically significant. All the statistical analyses were performed using SAS 6.04 software.

RESULTS

Expression of VEGF-C and CCR7 in gastric carcinoma and adjacent normal mucosa

In adjacent normal gastric mucosa, no or faint cytoplasmic staining of VEGF-C was seen in the parietal cells, but almost all epithelial cells were negative. Moderate to strong staining of VEGF-C protein was identified in the cytoplasm of immunoreactive cancer cells (Figure 1). Furthermore, in a few cases, some stromal cells were also positive for VEGF-C. The percentage of patients positive for VEGF-C was 52.5% (62/118). In adjacent normal gastric mucosa, no or very weak staining of CCR7 was also found, whereas moderate to strong staining of CCR7 was found mainly in cell membrane and/or cytoplasm of immunoreactive cancer cells as well as a few lymphocytes (Figure 2). The percentage of patients positive for CCR7 was 53.4% (63/118). Among these samples, there were 2 specimens with 1 metastatic lymph node adjacent to the primary tumor. It turned out that not only the primary tumors but also the metastatic lymph nodes were positive for both VEGF-C and CCR7 expression in both cases (Figures 3 and 4).

Association of VEGF-C and CCR7 expression with clinicopathological features

The correlation between VEGF-C and CCR7 expression and clinicopathological factors is summarized in Table 1. VEGF-C expression was more frequently found in tumors with lymph node metastasis than those without it ($P < 0.001$). VEGF-C expression was also closely related to lymphatic invasion ($P < 0.001$), vascular invasion ($P < 0.01$), and TNM stage ($P < 0.001$). However, there was no significant correlation between VEGF-C expression and age at surgery, gender, tumor size, tumor location, Lauren classification, and depth of invasion. The CCR7 expression was significantly higher in patients with lymph node metastasis compared with those without lymph node metastasis ($P < 0.001$) and was also associated with tumor size ($P < 0.01$), depth of invasion ($P < 0.001$), lymphatic invasion ($P < 0.001$), and TNM stage ($P < 0.001$). However, the presence of CCR7 had no correlation to age at surgery, gender, tumor location, Lauren classification, and vascular invasion.

Relationship between expression of VEGF-C and CCR7 and lymph node metastasis of gastric carcinoma determined by MSCT

As shown in Table 2, among the 39 patients who underwent MSCT examination, CCR7 expression was related to lymph node metastasis determined by MSCT ($P < 0.05$), whereas there was no significant correlation between VEGF-C expression and lymph node metastasis determined by MSCT (Figures 5-7). However, both VEGF-C and CCR7 expression were closely

related to lymph node metastasis determined by pathological examination ($P < 0.01$). In addition, the accuracy of MSCT in determining the N stage was 69.2% (27/39) (Table 3). Findings at MSCT were concordant with pathological findings in 15 of 20 N_0 tumors (75.0%), 5 of 10 N_1 tumors (50.0%), and 7 of 9 N_2 tumors (77.8%), respectively. The sensitivity, specificity, PPV, NPV, and accuracy of MSCT in predicting lymph node metastasis were 84.2% (16/19), 75.0% (15/20), 76.2% (16/21), 83.3% (15/18), and 79.5% (31/39). However, the sensitivity, specificity, PPV, NPV, and accuracy of VEGF-C and CCR7 expression in the diagnosis of lymph node metastasis for patients with gastric carcinoma were 68.4% (13/19), 75.0% (15/20), 72.2% (13/18), 71.4% (15/21) and 71.8% (28/39), and 73.7% (14/19), 75.0% (15/20), 73.7% (14/19), 75.0% (15/20) and 74.4% (29/39), respectively (Table 2).

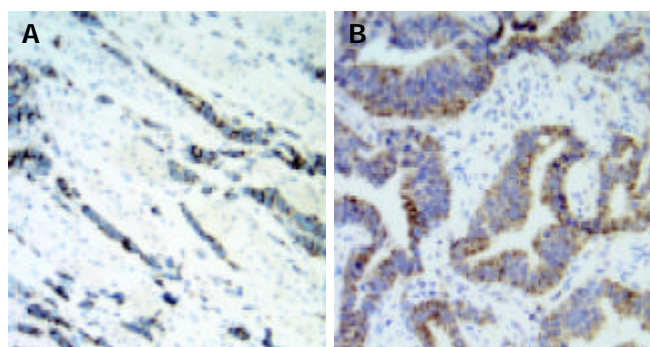


Figure 1 Expression of VEGF-C was observed mainly in the cytoplasm of gastric carcinoma cells (original magnification $\times 200$). A: diffuse gastric carcinoma; B: intestinal gastric carcinoma.

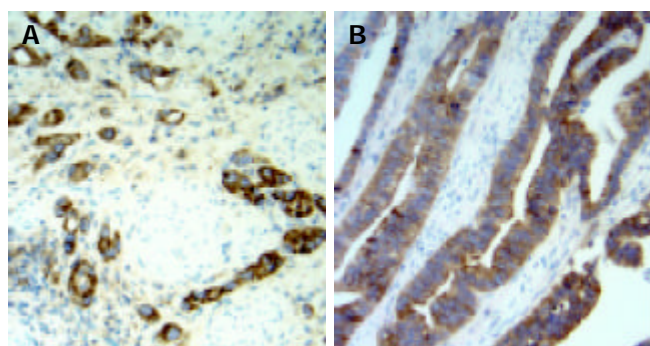


Figure 2 Expression of CCR7 was observed mainly in the cytoplasm and membrane of gastric carcinoma cells (original magnification $\times 200$). A: diffuse gastric carcinoma; B: intestinal gastric carcinoma.



Figure 3 Expression of VEGF-C was observed mainly in gastric carcinoma cells in metastatic lymph node (original magnification $\times 400$).

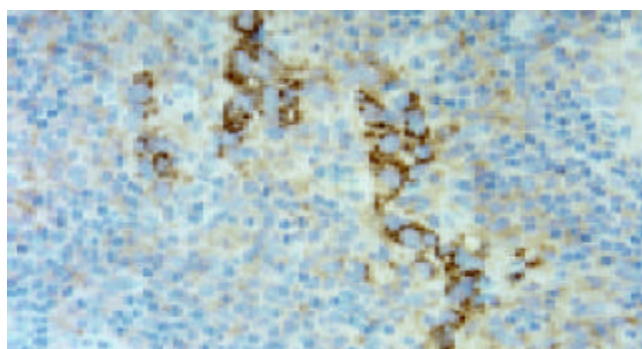


Figure 4 Expression of CCR7 was observed mainly in gastric carcinoma cells in metastatic lymph node (original magnification $\times 400$).

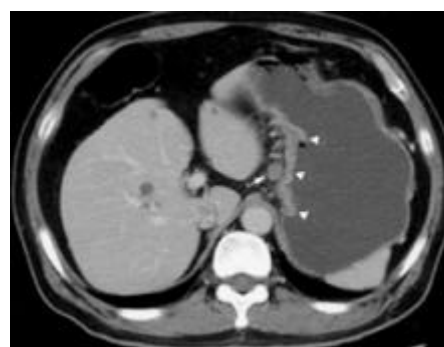


Figure 5 CT scan shows a metastatic lymph node (confirmed by pathologic examination) (arrow) 10 mm in short-axis diameter, which is adjacent to the primary lesion of gastric carcinoma (arrowhead).

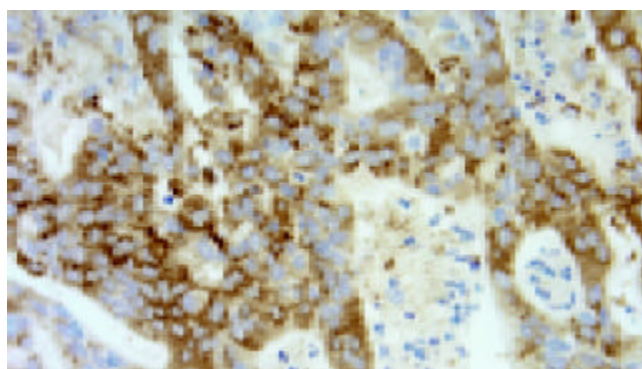


Figure 6 The same patient as Figure 5, expression of CCR7 was observed in the cytoplasm and membrane of gastric carcinoma cells (original magnification $\times 400$).

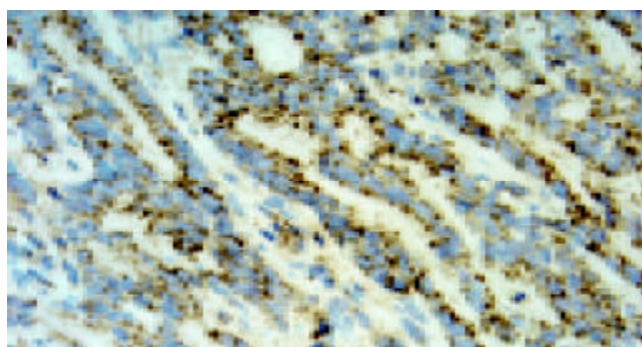


Figure 7 The same patient as Figure 5, expression of VEGF-C was observed in the cytoplasm of gastric carcinoma cells (original magnification $\times 400$).

Table 1 Relationship between expression of VEGF-C and CCR7 and clinicopathologic parameters in patients with gastric carcinoma

	No. of patients	Expression of VEGF-C		P value	Expression of CCR7		P value
		Positive	Negative		Positive	Negative	
Age				NS*			NS
<61 years	46	21	25		23	23	
≥61 years	72	41	31		40	32	
Gender				NS			NS
Male	71	38	33		39	32	
Female	47	24	23		24	23	
Tumor size				NS			<0.01
<5 cm	53	23	30		21	32	
≥5 cm	65	39	26		42	23	
Tumor location				NS			NS
Lower third (L)	81	40	41		44	37	
Middle third (M)	21	12	9		11	10	
Upper third (U)	16	10	6		8	8	
Lauren classification				NS			NS
Intestinal	53	24	29		25	28	
Diffuse	53	30	23		32	21	
Mixed	12	8	4		6	6	
Depth of invasion				NS			<0.001
T1/2	24	9	15		5	19	
T3/4	94	53	41		58	36	
Lymph node metastasis				<0.001			<0.001
Positive	61	45	16		50	11	
Negative	57	17	40		13	44	
Lymphatic invasion				<0.001			<0.001
Positive	68	48	20		51	17	
Negative	50	14	36		12	38	
Vascular invasion				<0.01			NS
Positive	35	25	10		20	15	
Negative	83	37	46		43	40	
Stage				<0.001			<0.001
I, II	55	19	36		13	42	
III, IV	63	43	20		50	13	

*NS, not significant.

Table 2 Correlation between expression of VEGF-C and CCR7 and lymph node metastasis determined by MSCT and pathological examination

	No. of patients	Expression of VEGF-C		P value	Expression of CCR7		P value
		Positive	Negative		Positive	Negative	
Lymph node metastasis ¹				NS ³			<0.05
Positive	21	12	9		14	7	
Negative	18	6	12		5	13	
Lymph node metastasis ²				<0.01			<0.01
Positive	19	13	6		14	5	
Negative	20	5	15		5	15	

¹Lymph node metastasis determined by MSCT; ²Lymph node metastasis determined by pathological examination; ³NS, not significant.**Table 3** Comparison of MSCT and pathological diagnosis of N stage

Pathologic N stage	No. of patients	N stage determined by MSCT		
		N ₀	N ₁	N ₂
N ₀	20	15 ¹	2	3
N ₁	10	2	5 ¹	3
N ₂	9	1	1	7 ¹

¹MSCT findings were concordant with pathological findings.**Table 4** Relationship between expression of VEGF-C and CCR7 after the subdivision and lymph node metastasis

Lymph node metastasis	No. of patients	Expression of VEGF-C and CCR7			
		CCR7(+) and VEGF-C(+)	CCR7(+) and VEGF-C(-)	CCR7(-) and VEGF-C(+)	CCR7(-) and VEGF-C(-)
Positive	61	41	9	4	7
Negative	57	7	6	10	34

Value of the combined examination of VEGF-C and CCR7 expression in predicting lymph node metastasis

As shown in Table 1, in the current retrospective study, the sensitivity, specificity, PPV, NPV, and accuracy of VEGF-C and CCR7 expression in the diagnosis of lymph node metastasis for patients with gastric carcinoma were 73.8% (45/61), 70.2% (40/57), 72.6% (45/62), 71.4% (40/56) and 72.0% (85/118), and 82.0% (50/61), 77.2% (44/57), 79.4% (50/63), 80.0% (44/55) and 79.7% (94/118), respectively. To further investigate the value of the combined examination of VEGF-C and CCR7 expression in predicting lymph node metastasis, we divided patients into four groups: group A, CCR7(+) and VEGF-C(+); group B, CCR7(+) and VEGF-C(-); group C, CCR7(-) and VEGF-C(+); group D, CCR7(-) and VEGF-C(-). In groups A, B, C, and D, the percentage of patients with lymph node metastasis was 85.4% (41/48), 60.0% (9/15), 28.6% (4/14), and 17.1% (7/41), respectively (Table 4). In addition, ROC analysis showed that the accuracy of the combined examination of VEGF-C and CCR7 expression in predicting lymph node metastasis was relatively high (area under ROC curve [Az]=0.83) (Figure 8). When the patients with positive expression of both VEGF-C and CCR7 were regarded as those with lymph node metastasis, the PPV in the diagnosis of lymph node metastasis reached to 85.4% (41/48). In addition, when the patients with negative expression of both VEGF-C and CCR7 were regarded as those without lymph node metastasis, the NPV reached to 82.9% (34/41).

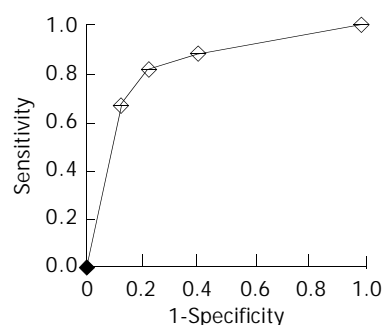


Figure 8 ROC curve generated from the combination of VEGF-C and CCR7 expression shows area under curve to be 0.83.

DISCUSSION

Tumor cells can disseminate within the body by a number of mechanisms, such as direct invasion of surrounding tissues, lymphatic spread and hematogenous spread. The role of angiogenesis involving blood vessels in facilitating the growth and hematogenic spread of solid tumors has been well established. The ability of tumor cells to induce angiogenesis is considered a prerequisite for tumor growth, invasion, and successful metastasis, and the angiogenic switch is recognized as one of the key events in tumorigenesis^[25-30]. In contrast, studies of the lymphatic system have been hindered by the lack of specific markers for tumor-associated lymphatic vessels and growth factors that control lymphatic development and lymphatic vessel growth (lymphangiogenesis), although the importance of the lymphatic system as a pathway for lymph node metastasis has been well recognized. In the past few years, with the identification of proteins such as hyaluronan receptor LYVE-1^[31], prox-1^[7], podoplanin^[32], and desmoplakin^[33] specifically expressed on lymphatic vessels and the discovery of molecules (VEGF-C and VEGF-D) that can drive lymphatic vessel growth, occurrence of tumor lymphangiogenesis and its correlation with lymph node metastasis has been proved in animal models and clinicopathological studies.

Nine recently reported animal studies have provided the first direct *in vivo* evidence that tumours are able not only to induce lymphangiogenesis but also to enhance lymph node metastasis^[8-12,34-37]. Yanai *et al.*^[37] constructed a VEGF-C transfectant (AZ-VEGF-C) from the AZ521 human gastric carcinoma cell line, which ordinarily shows little nodal metastatic potential and little VEGF-C expression. They orthotopically implanted transfected tumor cells into the stomachs of nude mice. The number of mice developing lymph node metastases and the number of lymph node metastases per mouse with nodal metastases were higher than with implants of mock-transfected control cells. In addition, the number of vessels stained for VEGFR-3 in tumors and surrounding tissues was higher for AZ-VEGF-C than for controls. Furthermore, recent studies in human head and neck cancer^[38,39] and melanoma^[40] have demonstrated the existence of proliferating intratumoral lymphatic vessels. Clinical studies using the RT-PCR, *in situ* hybridization, and/or immunohistochemistry have revealed significant associations between lymph node metastasis and VEGF-C or VEGF-D expression in human primary tumors of the breast, colon, rectum, prostate, testis, esophagus, stomach, thyroid, lung, pleura, head-and-neck squamous cells, uterine cervix, and endometrium^[41]. Because of the reasons above-mentioned, we only investigated the VEGF-C expression in gastric carcinoma.

The findings of the current study demonstrated a positive correlation of VEGF-C expression with both lymph node metastasis and lymphatic invasion in gastric carcinoma. Our results were consistent with those of previous reports^[23,42-47]. A study by Yanai *et al.*^[37] indicated that VEGF-C was a specific lymphangiogenic growth factor with an important role in lymph node metastasis of gastric carcinoma in an animal model. In addition, the studies by Yonemura *et al.*^[42,43] showed that VEGF-C mRNA level was closely related to VEGFR-3 mRNA level and the number of VEGFR-3-positive lymphatic vessels in human gastric carcinoma. Thus, VEGF-C may stimulate lymphangiogenesis in gastric carcinoma by binding to their receptors (VEGFR-3) on the lymphatic endothelial cells and inducing proliferation and growth of new lymphatic capillaries, then enhance the incidence of lymph node metastasis in gastric carcinoma. However, our present study showed that VEGF-C expression was closely related to lymph node metastasis determined by pathological examination, but not by MSCT examination, although the accuracy of MSCT in the diagnosis of the lymph node metastasis for 39 patients with gastric carcinoma reached to 79.5%. Nevertheless, Hashimoto *et al.*^[48] demonstrated that VEGF-C mRNA expression was correlated with lymph node metastasis diagnosed by magnetic resonance (MR) imaging in cervical cancer. So further study must be made. Furthermore, our present study showed that the VEGF-C expression was correlated with vascular invasion in gastric carcinoma. Other investigators^[42,45] also found a positive correlation between VEGF-C expression and vascular invasion in gastric carcinoma. In addition, a study by Amioka *et al.*^[23] showed that VEGF-C expression in tumor cells was closely related to the microvessel density (MVD) in gastric carcinoma. As we all know, VEGF-C is a ligand for VEGFR-2 and VEGFR-3. VEGFR-2 is mainly expressed on vascular endothelial cells. However, VEGF-C displays greater affinity for VEGFR-3 than VEGFR-2, and only the mature 21-kDa form of VEGF-C can bind to VEGFR-2^[36]. As a result, VEGF-C may also be correlated with angiogenesis in gastric carcinoma, but the activity of tumor angiogenesis by VEGF-C may be weak. Further study is needed to investigate the biological effect of VEGF-C on angiogenesis in gastric carcinoma.

Chemokines are chemoattractant cytokines that bind to specific G-protein-coupled receptors on target cells; these target cells follow chemokine concentration gradients into selected

tissues. Through their interactions with target cells, these small proteins induce cytoskeletal rearrangement and directional migration. Chemokines are involved in physiologic and pathologic regulation of leukocyte trafficking^[41]. Recent studies showed that chemokine receptor CCR7 was expressed in the tumor cells of breast cancer^[19], nonsmall cell lung cancer^[20], esophageal squamous cell carcinoma^[49], and gastric carcinoma^[50]. In addition, both CCL21 and CCL19 (chemokines, ligands of CCR7) show most abundant expression in lymph nodes. CCL21 is expressed in the high endothelial venules of lymph nodes and in the T-cell zone of lymph nodes. CCL19 is expressed predominantly by stromal cells within the T-cell zones of lymph nodes^[19]. Previous studies showed that lymphatic endothelial cells also produced CCL21^[51, 52]. *In vitro* experiments showed that actin polymerization and pseudopodia formation, which were needed for the invasion of malignant cells into tissues and for efficient metastasis, could be induced by CCL21 and CCL19 in tumor cells with CCR7 expression^[19, 49, 50]. Thus, the migration of tumor cells positive for CCR7 towards lymph nodes may share many similarities with leukocyte trafficking. In addition, CCR7 may help retain tumor cells in the lymph nodes where the CCR7 ligands are rich.

Wiley *et al.*^[53] examined the role of CCR7 in regional lymph node metastasis in a murine melanoma model. They transduced a murine melanoma cell line, B16, with CCR7 and, surprisingly, transduction with this single gene was sufficient to substantially increase the metastasis to draining lymph nodes of B16 cells, which otherwise have a low propensity to spread, and metastasis was completely blocked by adding neutralizing anti-CCL21 antibodies. In the model used by Wiley *et al.*, transduced cells were injected subcutaneously, thus mimicking lymphgenic metastasis of melanoma cells from the skin. Of interest, intravenous application of CCR7-transduced B16 melanoma cells did not show increased spread of the tumor cells to lung or peripheral lymph nodes. In clinicopathologic studies, a positive correlation of CCR7 expression with lymphatic invasion and lymph node metastasis has been found in nonsmall cell lung cancer^[20], esophageal squamous cell carcinoma^[49], and gastric carcinoma^[50]. Here we investigate the role of chemokine receptor CCR7 in directional migration of gastric carcinoma cells towards lymph nodes.

The findings of the current study demonstrated that the CCR7 expression in the cytoplasm and / or member of gastric carcinoma cells was closely correlated with lymphatic invasion, lymph node metastasis, and TNM stage, but was not correlated with vascular invasion. Our findings were consistent with those reported by Mashino *et al.*^[50]. In addition, the study by Mashino *et al.*^[50] showed that CCR7 expression was closely related to histological classification, whereas the current study showed that there was no significant correlation between CCR7 expression and Lauren classification. The main reason for this discrepancy was that there was no significant correlation between Lauren classification and lymph node metastasis among the 118 patients, although the incidence of lymph node metastasis in diffuse gastric carcinoma (50.9%) was higher than that in intestinal gastric carcinoma (45.3%). Furthermore, the current study showed that the CCR7 expression was closely correlated with lymph node metastasis determined not only by pathological examination but also by MSCT examination.

Many factors affect prognosis in patients with gastric carcinoma, including tumor size, lymph node metastasis, depth of tumor invasion, distant metastasis, histological classification, and surgery performed. Of these, lymph node metastasis is one of the most important factors. Therefore, preoperative evaluation of lymph node status is essential. With the development of endoscopic or laparoscopic resection of small, localized gastric carcinoma, the pretherapeutic evaluation of

lymph node metastasis has become more important. For preoperative N staging, endoscopic ultrasonography (EUS), CT, and MR imaging have been used^[4, 54-58]. However, the paraaortic and celiac regions are often beyond the scope of the EUS^[55], and comparative studies demonstrated that the accuracy of CT in N staging was higher than that of MR imaging^[57, 58]. Therefore, among these three methods, CT may be superior to EUS and MR imaging in predicting lymph node status for patients with gastric carcinoma. In the current study, the accuracy of MSCT in N staging was 69.2%. Notably, the accuracy of MSCT in predicting lymph node metastasis reached to 79.5%, and the sensitivity and specificity was 84.2% and 75.0%, respectively. However, although spiral CT could detect lymph nodes small than 5 mm and the sensitivity for detecting metastasis-positive nodes was remarkably higher than that for detecting metastasis-negative nodes^[59], both overstaging and downstaging still existed because lymph node size was not a reliable indicator for lymph node metastasis of gastric carcinoma^[60]. Furthermore, Maruyama computer program can also be used to predict lymph node metastasis for patients with gastric carcinoma. Analysis of eight prognostic parameters such as gender, age, macroscopic type, location, position, diameter, histological classification, and depth of invasion using this computer program can gain the information on the expected frequency of metastasis in the 16 lymph node stations of each patient with gastric carcinoma^[61, 62]. However, to date, the prospective study for evaluating the accuracy of this computer program has not been reported. Two retrospective studies^[61, 62] showed that the accuracy of Maruyama computer program in predicting lymph node metastasis was relatively high, but the specificity was too low. In addition, only clinicopathologic parameters were included in this computer program, whereas the molecular biologic features of gastric carcinoma were neglected.

Recently, a study using the microarray technology showed that lymph node metastasis of gastric carcinoma could be precisely predicted from the view of molecular biologic features. In this study, investigators developed an equation to achieve a scoring parameter for the prediction of lymph node metastasis on the basis of 12 genes with statistically significant differences in expression between node-positive and node-negative tumors. In the prospective study, the lymph node status of all nine test cases was correctly predicted^[63]. In the current retrospective study, the sensitivity, specificity, PPV, NPV, and accuracy of VEGF-C and CCR7 expression in the diagnosis of lymph node metastasis for patients with gastric carcinoma were 73.8%, 70.2%, 72.6%, 71.4% and 72.0%, and 82.0%, 77.2%, 79.4%, 80.0% and 79.7%, respectively. Especially when the combined examination of VEGF-C and CCR7 expression was performed, the PPV and NPV reached to 85.4% and 82.9%, respectively. However, the PPV and NPV of MSCT in predicting lymph node metastasis was only 76.2% and 83.3%, respectively, among 39 patients. In addition, successful lymph node metastasis requires a complex series of related steps, such as detachment of cancer cells, invasion into the lymphatic vessels, transfer within the lymphatic vessels, embedding in the lymph nodes and proliferation in the lymph nodes. Therefore, lymphangiogenesis and directional migration of gastric carcinoma cells towards lymph nodes may only be two main steps involved in lymph node metastasis. Thus, we hypothesize that an equation established on the basis of many factors involved in the metastasis-associated steps can predict the lymph node status for patients with gastric carcinoma more accurately, especially when it is combined with Maruyama computer program and MSCT.

In conclusion, the current study demonstrates that expression of VEGF-C and CCR7 is related to lymph node metastasis of gastric carcinoma and both of them may become

new targets for the treatment of gastric carcinoma. Furthermore, the combined examination of VEGF-C and CCR7 expression in endoscopic biopsy specimens may be useful in predicting lymph node metastasis of gastric carcinoma and deciding the extent of surgical lymph node resection.

REFERENCES

- Zheng HC**, Li YL, Sun JM, Yang XF, Li XH, Jiang WG, Zhang YC, Xin Y. Growth, invasion, metastasis, differentiation, angiogenesis and apoptosis of gastric cancer regulated by expression of PTEN encoding products. *World J Gastroenterol* 2003; **9**: 1662-1666
- Ding YB**, Chen GY, Xia JG, Zang XW, Yang HY, Yang L. Association of VCAM-1 overexpression with oncogenesis, tumor angiogenesis and metastasis of gastric carcinoma. *World J Gastroenterol* 2003; **9**: 1409-1414
- Zhou YN**, Xu CP, Han B, Li M, Qiao L, Fang DC, Yang JM. Expression of E-cadherin and beta-catenin in gastric carcinoma and its correlation with the clinicopathological features and patient survival. *World J Gastroenterol* 2002; **8**: 987-993
- Yan C**, Zhu ZG, Zhu Q, Yan M, Chen J, Liu BY, Yin HR, Lin YZ. A preliminary study of endoscopic ultrasonography in the pre-operative staging of early gastric carcinoma. *Zhonghua Zhongliu Zazhi* 2003; **25**: 390-393
- Joukov V**, Pajusola K, Kaipainen A, Chilov D, Lahtinen I, Kukk E, Saksela O, Kalkkinen N, Alitalo K. A novel vascular endothelial growth factor, VEGF-C, is a ligand for the Flt4 (VEGFR-3) and KDR (VEGFR-2) receptor tyrosine kinases. *EMBO J* 1996; **15**: 290-298
- Achen MG**, Jeltsch M, Kukk E, Makinen T, Vitali A, Wilks AF, Alitalo K, Stacker SA. Vascular endothelial growth factor D (VEGF-D) is a ligand for the tyrosine kinase VEGF receptor 2 (Flk1) and VEGF receptor 3 (Flt4). *Proc Natl Acad Sci U S A* 1998; **95**: 548-553
- Wigle JT**, Harvey N, Detmar M, Lagutina I, Grosveld G, Gunn MD, Jackson DG, Oliver G. An essential role for Prox1 in the induction of the lymphatic endothelial cell phenotype. *EMBO J* 2002; **21**: 1505-1513
- Padera TP**, Kadambi A, di Tomaso E, Carreira CM, Brown EB, Boucher Y, Choi NC, Mathisen D, Wain J, Mark EJ, Munn LL, Jain RK. Lymphatic metastasis in the absence of functional intratumor lymphatics. *Science* 2002; **296**: 1883-1886
- Karpanen T**, Egeblad M, Karkkainen MJ, Kubo H, Yla-Herttuala S, Jaattela M, Alitalo K. Vascular endothelial growth factor C promotes tumor lymphangiogenesis and intralymphatic tumor growth. *Cancer Res* 2001; **61**: 1786-1790
- Mattila MM**, Ruohola JK, Karpanen T, Jackson DG, Alitalo K, Harkonen PL. VEGF-C induced lymphangiogenesis is associated with lymph node metastasis in orthotopic MCF-7 tumors. *Int J Cancer* 2002; **98**: 946-951
- Stacker SA**, Caesar C, Baldwin ME, Thornton GE, Williams RA, Prevo R, Jackson DG, Nishikawa S, Kubo H, Achen MG. VEGF-D promotes the metastatic spread of tumor cells via the lymphatics. *Nat Med* 2001; **7**: 151-152
- Skobe M**, Hawighorst T, Jackson DG, Prevo R, Janes L, Velasco P, Riccardi L, Alitalo K, Claffey K, Detmar M. Induction of tumor lymphangiogenesis by VEGF-C promotes breast cancer metastasis. *Nat Med* 2001; **7**: 192-198
- Orlandini M**, Semboloni S, Oliviero S. Beta-catenin inversely regulates VEGF-D mRNA stability. *J Biol Chem* 2003; **278**: 44650-44656
- Funaki H**, Nishimura G, Harada S, Ninomiya I, Terada I, Fushida S, Tani T, Fujimura T, Kayahara M, Shimizu K, Ohta T, Miwa K. Expression of vascular endothelial growth factor D is associated with lymph node metastasis in human colorectal carcinoma. *Oncology* 2003; **64**: 416-422
- Kawakami M**, Furuhashi T, Kimura Y, Yamaguchi K, Hata F, Sasaki K, Hirata K. Expression analysis of vascular endothelial growth factors and their relationships to lymph node metastasis in human colorectal cancer. *J Exp Clin Cancer Res* 2003; **22**: 229-237
- White JD**, Hewett PW, Kosuge D, McCulloch T, Enholm BC, Carmichael J, Murray JC. Vascular endothelial growth factor -D expression is an independent prognostic marker for survival in colorectal carcinoma. *Cancer Res* 2002; **62**: 1669-1675
- Hanrahan V**, Currie MJ, Gunningham SP, Morrin HR, Scott PA, Robinson BA, Fox SB. The angiogenic switch for vascular endothelial growth factor (VEGF)-A, VEGF-B, VEGF-C, and VEGF-D in the adenoma-carcinoma sequence during colorectal cancer progression. *J Pathol* 2003; **200**: 183-194
- Yokoyama Y**, Charnock-Jones DS, Licence D, Yanaihara A, Hastings JM, Holland CM, Emoto M, Sakamoto A, Sakamoto T, Maruyama H, Sato S, Mizunuma H, Smith SK. Expression of vascular endothelial growth factor (VEGF)-D and its receptor, VEGF receptor 3, as a prognostic factor in endometrial carcinoma. *Clin Cancer Res* 2003; **9**: 1361-1369
- Muller A**, Homey B, Soto H, Ge N, Catron D, Buchanan ME, McClanahan T, Murphy E, Yuan W, Wagner SN, Barrera JL, Mohar A, Verastegui E, Zlotnik A. Involvement of chemokine receptors in breast cancer metastasis. *Nature* 2001; **410**: 50-56
- Takanami I**. Overexpression of CCR7 mRNA in nonsmall cell lung cancer: correlation with lymph node metastasis. *Int J Cancer* 2003; **105**: 186-189
- Cassella M**, Skobe M. Lymphatic vessel activation in cancer. *Ann NY Acad Sci* 2002; **979**: 120-130
- Takao M**, Fukuda T, Iwanaga S, Hayashi K, Kusano H, Okudaira S. Gastric cancer: evaluation of triphasic spiral CT and radiologic-pathologic correlation. *J Comput Assist Tomogr* 1998; **22**: 288-294
- Amioka T**, Kitadai Y, Tanaka S, Haruma K, Yoshihara M, Yasui W, Chayama K. Vascular endothelial growth factor-C expression predicts lymph node metastasis of human gastric carcinomas invading the submucosa. *Eur J Cancer* 2002; **38**: 1413-1419
- D'Elia F**, Zingarelli A, Palli D, Grani M. Hydro-dynamic CT pre-operative staging of gastric cancer: correlation with pathological findings. A prospective study of 107 cases. *Eur Radiol* 2000; **10**: 1877-1885
- Wang ZQ**, Li JS, Lu GM, Zhang XH, Chen ZQ, Meng K. Correlation of CT enhancement, tumor angiogenesis and pathologic grading of pancreatic carcinoma. *World J Gastroenterol* 2003; **9**: 2100-2104
- Du JR**, Jiang Y, Zhang YM, Fu H. Vascular endothelial growth factor and microvascular density in esophageal and gastric carcinomas. *World J Gastroenterol* 2003; **9**: 1604-1606
- Shi H**, Xu JM, Hu NZ, Xie HJ. Prognostic significance of expression of cyclooxygenase-2 and vascular endothelial growth factor in human gastric carcinoma. *World J Gastroenterol* 2003; **9**: 1421-1426
- Xiong B**, Sun TJ, Yuan HY, Hu MB, Hu WD, Cheng FL. Cyclooxygenase-2 expression and angiogenesis in colorectal cancer. *World J Gastroenterol* 2003; **9**: 1237-1240
- Zheng S**, Han MY, Xiao ZX, Peng JP, Dong Q. Clinical significance of vascular endothelial growth factor expression and neovascularization in colorectal carcinoma. *World J Gastroenterol* 2003; **9**: 1227-1230
- Gupta MK**, Qin RY. Mechanism and its regulation of tumor-induced angiogenesis. *World J Gastroenterol* 2003; **9**: 1144-1155
- Banerji S**, Ni J, Wang SX, Clasper S, Su J, Tammi R, Jones M, Jackson DG. LYVE-1, a new homologue of the CD44 glycoprotein, is a lymph-specific receptor for hyaluronan. *J Cell Biol* 1999; **144**: 789-801
- Sedivy R**, Beck-Mannagetta J, Haverkamp C, Battistutti W, Honigschnabl S. Expression of vascular endothelial growth factor-C correlates with the lymphatic microvessel density and the nodal status in oral squamous cell cancer. *J Oral Pathol Med* 2003; **32**: 455-460
- Ebata N**, Nodasaka Y, Sawa Y, Yamaoka Y, Makino S, Totsuka Y, Yoshida S. Desmoplakin as a specific marker of lymphatic vessels. *Microvasc Res* 2001; **61**: 40-48
- Mandriota SJ**, Jussila L, Jeltsch M, Compagni A, Baetens D, Prevo R, Banerji S, Huarte J, Montesano R, Jackson DG, Orci L, Alitalo K, Christofori G, Pepper MS. Vascular endothelial growth factor-C-mediated lymphangiogenesis promotes tumor metastasis. *EMBO J* 2001; **20**: 672-682
- He Y**, Kozaki K, Karpanen T, Koshikawa K, Yla-Herttuala S, Takahashi T, Alitalo K. Suppression of tumor lymphangiogenesis and lymph node metastasis by blocking vascular endothelial growth factor receptor 3 signaling. *J Natl Cancer Inst* 2002; **94**: 819-825
- Skobe M**, Hamberg LM, Hawighorst T, Schirner M, Wolf GL, Alitalo K, Detmar M. Concurrent induction of lymphangiogenesis,

- angiogenesis, and macrophage recruitment by vascular endothelial growth factor-C in melanoma. *Am J Pathol* 2001; **159**: 893-903
- 37 **Yanai Y**, Furuhashi T, Kimura Y, Yamaguchi K, Yasoshima T, Mitaka T, Mochizuki Y, Hirata K. Vascular endothelial growth factor C promotes human gastric carcinoma lymph node metastasis in mice. *J Exp Clin Cancer Res* 2001; **20**: 419-428
- 38 **Beasley NJ**, Prevo R, Banerji S, Leek RD, Moore J, van Trappen P, Cox G, Harris AL, Jackson DG. Intratumoral lymphangiogenesis and lymph node metastasis in head and neck cancer. *Cancer Res* 2002; **62**: 1315-1320
- 39 **Maula SM**, Luukkkaa M, Grenman R, Jackson D, Jalkanen S, Ristamaki R. Intratumoral lymphatics are essential for the metastatic spread and prognosis in squamous cell carcinomas of the head and neck region. *Cancer Res* 2003; **63**: 1920-1926
- 40 **Straume O**, Jackson DG, Akslen LA. Independent prognostic impact of lymphatic vessel density and presence of low-grade lymphangiogenesis in cutaneous melanoma. *Clin Cancer Res* 2003; **9**: 250-256
- 41 **Nathanson SD**. Insights into the mechanisms of lymph node metastasis. *Cancer* 2003; **98**: 413-423
- 42 **Yonemura Y**, Endo Y, Fujita H, Fushida S, Ninomiya I, Bandou E, Taniguchi K, Miwa K, Ohoyama S, Sugiyama K, Sasaki T. Role of vascular endothelial growth factor C expression in the development of lymph node metastasis in gastric cancer. *Clin Cancer Res* 1999; **5**: 1823-1829
- 43 **Yonemura Y**, Fushida S, Bando E, Kinoshita K, Miwa K, Endo Y, Sugiyama K, Partanen T, Yamamoto H, Sasaki T. Lymphangiogenesis and the vascular endothelial growth factor receptor (VEGFR)-3 in gastric cancer. *Eur J Cancer* 2001; **37**: 918-923
- 44 **Kabashima A**, Maehara Y, Kakeji Y, Sugimachi K. Overexpression of vascular endothelial growth factor C is related to lymphogenous metastasis in early gastric carcinoma. *Oncology* 2001; **60**: 146-150
- 45 **Ichikura T**, Tomimatsu S, Ohkura E, Mochizuki H. Prognostic significance of the expression of vascular endothelial growth factor (VEGF) and VEGF-C in gastric carcinoma. *J Surg Oncol* 2001; **78**: 132-137
- 46 **Takahashi A**, Kono K, Itakura J, Amemiya H, Feng Tang R, Iizuka H, Fujii H, Matsumoto Y. Correlation of vascular endothelial growth factor-C expression with tumor-infiltrating dendritic cells in gastric cancer. *Oncology* 2002; **62**: 121-127
- 47 **Ishikawa M**, Kitayama J, Kazama S, Nagawa H. Expression of vascular endothelial growth factor C and D (VEGF-C and -D) is an important risk factor for lymphatic metastasis in undifferentiated early gastric carcinoma. *Jpn J Clin Oncol* 2003; **33**: 21-27
- 48 **Hashimoto I**, Kodama J, Seki N, Hongo A, Yoshinouchi M, Okuda H, Kudo T. Vascular endothelial growth factor-C expression and its relationship to pelvic lymph node status in invasive cervical cancer. *Br J Cancer* 2001; **85**: 93-97
- 49 **Ding Y**, Shimada Y, Maeda M, Kawabe A, Kaganai J, Komoto I, Hashimoto Y, Miyake M, Hashida H, Imamura M. Association of CC chemokine receptor 7 with lymph node metastasis of esophageal squamous cell carcinoma. *Clin Cancer Res* 2003; **9**: 3406-3412
- 50 **Mashino K**, Sadanaga N, Yamaguchi H, Tanaka F, Ohta M, Shibuta K, Inoue H, Mori M. Expression of chemokine receptor CCR7 is associated with lymph node metastasis of gastric carcinoma. *Cancer Res* 2002; **62**: 2937-2941
- 51 **Gunn MD**, Tangemann K, Tam C, Cyster JG, Rosen SD, Williams LT. A chemokine expressed in lymphoid high endothelial venules promotes the adhesion and chemotaxis of naive T lymphocytes. *Proc Natl Acad Sci USA* 1998; **95**: 258-263
- 52 **Saeki H**, Moore AM, Brown MJ, Hwang ST. Cutting edge: secondary lymphoid-tissue chemokine (SLC) and CC chemokine receptor 7 (CCR7) participate in the emigration pathway of mature dendritic cells from the skin to regional lymph nodes. *J Immunol* 1999; **162**: 2472-2475
- 53 **Wiley HE**, Gonzalez EB, Maki W, Wu MT, Hwang ST. Expression of CC chemokine receptor-7 and regional lymph node metastasis of B16 murine melanoma. *J Natl Cancer Inst* 2001; **93**: 1638-1643
- 54 **Xi WD**, Zhao C, Ren GS. Endoscopic ultrasonography in preoperative staging of gastric cancer: determination of tumor invasion depth, nodal involvement and surgical resectability. *World J Gastroenterol* 2003; **9**: 254-257
- 55 **Willis S**, Truong S, Gribnitz S, Fass J, Schumpelick V. Endoscopic ultrasonography in the preoperative staging of gastric cancer: accuracy and impact on surgical therapy. *Surg Endosc* 2000; **14**: 951-954
- 56 **Chen F**, Ni YC, Zheng KE, Ju SH, Sun J, Ou XL, Xu MH, Zhang H, Marchal G. Spiral CT in gastric carcinoma: Comparison with barium study, fiberoptic gastroscopy and histopathology. *World J Gastroenterol* 2003; **9**: 1404-1408
- 57 **Kim AY**, Han JK, Seong CK, Kim TK, Choi BI. MRI in staging advanced gastric cancer: is it useful compared with spiral CT? *J Comput Assist Tomogr* 2000; **24**: 389-394
- 58 **Sohn KM**, Lee JM, Lee SY, Ahn BY, Park SM, Kim KM. Comparing MR imaging and CT in the staging of gastric carcinoma. *Am J Roentgenol* 2000; **174**: 1551-1557
- 59 **Fukuya T**, Honda H, Hayashi T, Kaneko K, Tateshi Y, Ro T, Maehara Y, Tanaka M, Tsuneyoshi M, Masuda K. Lymph-node metastases: efficacy for detection with helical CT in patients with gastric cancer. *Radiology* 1995; **197**: 705-711
- 60 **Monig SP**, Zirbes TK, Schroder W, Baldus SE, Lindemann DG, Dienes HP, Holscher AH. Staging of gastric cancer: correlation of lymph node size and metastatic infiltration. *Am J Roentgenol* 1999; **173**: 365-367
- 61 **Bollschweiler E**, Boettcher K, Hoelscher AH, Sasako M, Kinoshita T, Maruyama K, Siewert JR. Preoperative assessment of lymph node metastases in patients with gastric cancer: evaluation of the Maruyama computer program. *Br J Surg* 1992; **79**: 156-160
- 62 **Guadagni S**, de Manzoni G, Catarci M, Valenti M, Amicucci G, De Bernardinis G, Cordiano C, Carboni M, Maruyama K. Evaluation of the Maruyama computer program accuracy for preoperative estimation of lymph node metastases from gastric cancer. *World J Surg* 2000; **24**: 1550-1558
- 63 **Hasegawa S**, Furukawa Y, Li M, Satoh S, Kato T, Watanabe T, Katagiri T, Tsunoda T, Yamaoka Y, Nakamura Y. Genome-wide analysis of gene expression in intestinal-type gastric cancers using a complementary DNA microarray representing 23040 genes. *Cancer Res* 2002; **62**: 7012-7017

Edited by Zhang JZ Proofread by Xu FM

Coexpression of cholecystokinin-B/gastrin receptor and gastrin gene in human gastric tissues and gastric cancer cell line

Jian-Jiang Zhou, Man-Ling Chen, Qun-Zhou Zhang, Jian-Kun Hu, Wen-Ling Wang

Jian-Jiang Zhou, Man-Ling Chen, Department of Biochemistry and Molecular Biology, School of Basic Medical Sciences, Sichuan University, Chengdu 610041, Sichuan Province, China

Qun-Zhou Zhang, Oral & Maxillofacial Department, Charles R. Drew University of Medicine and Science, Los Angeles, CA 90059, USA

Jian-Kun Hu, Department of Surgery, West China Medical School, Sichuan University, Chengdu 610041, Sichuan Province, China

Wen-Ling Wang, Department of Oncology, Affiliated Hospital of Guiyang Medical College, Guiyang 550001, Guizhou Province, China

Correspondence to: Professor Man-Ling Chen, Department of Biochemistry and Molecular Biology, School of Basic Medical Sciences, West China Medical Center, Sichuan University, Chengdu 610041, Sichuan Province, China. zjjdjb@hotmail.com

Telephone: +86-28-85501254

Received: 2003-08-11 **Accepted:** 2003-10-22

Abstract

AIM: To compare the expression patterns of cholecystokinin-B (CCK-B)/gastrin receptor genes in matched human gastric carcinoma and adjacent non-neoplastic mucosa of patients with gastric cancer, inflammatory gastric mucosa from patients with gastritis, normal stomachs from 2 autopsied patients and a gastric carcinoma cell line (SGC-7901), and to explore their relationship with progression to malignancy of human gastric carcinomas.

METHODS: RT-PCR and sequencing were employed to detect the mRNA expression levels of CCK-B receptor and gastrin gene in specimens from 30 patients with gastric carcinoma and healthy bordering non-cancerous mucosa, 10 gastritis patients and normal stomachs from 2 autopsied patients as well as SGC-7901. The results were semi-quantified by normalizing it to the mRNA level of β -actin gene using Lab Image software. The sequences were analyzed by BLAST program.

RESULTS: CCK-B receptor transcripts were detected in all of human gastric tissues in this study, including normal, inflammatory and malignant tissues and SGC-7901. However, the expression levels of CCK-B receptor in normal gastric tissues were higher than those in other groups ($P < 0.05$), and its expressions did not correlate with the differentiation and metastasis of gastric cancer ($P > 0.05$). On the other hand, gastrin mRNA was detected in SGC-7901 and in specimens obtained from gastric cancer patients (22/30) but not in other gastric tissues, and its expression was highly correlated with the metastases of gastric cancer ($P < 0.05$).

CONCLUSION: Human gastric carcinomas and gastric cancer cell line SGC-7901 cells coexpress CCK-B receptor and gastrin mRNA. Gastrin/CCK-B receptor autocrine or paracrine pathway may possibly play an important role in the progression of gastric cancer.

Zhou JJ, Chen ML, Zhang QZ, Hu JK, Wang WL. Coexpression of cholecystokinin-B/gastrin receptor and gastrin gene in human gastric tissues and gastric cancer cell line. *World J Gastroenterol* 2004; 10(6): 791-794

<http://www.wjgnet.com/1007-9327/10/791.asp>

INTRODUCTION

Human beings have developed highly efficient cell-cell communication to integrate and coordinate the proliferation of individual cell types, among which growth factors and hormones play a pivotal role. Gastrointestinal peptides, including gastrin and cholecystokinin (CCK), are a structurally diverse group of molecular messengers that play an important role in the control of appetite and hormonal secretion. Gastrin is secreted by gastrin (G) cells located in the antral part of the stomach, and identified as the circulating hormone responsible for stimulation of acid secretion from the parietal cells. It stimulates gastric enterochromaffin-like (ECL) cells to release histamine, which in turn increases acid secretion via histamine H_2 -receptors in parietal cells^[1-3]. Recently, it has been demonstrated that gastrin plays a significant role in the proliferation and differentiation of gastric and intestinal epithelial cells^[4-6].

Previous studies have shown that hormones and receptors are key molecules in regulating cell growth, differentiation and apoptosis^[7]. Cholecystokinin-B (CCK-B)/gastrin receptor belongs to the seven transmembrane G-protein-coupled receptor superfamily and is mainly expressed in parietal cells and ECL cells of gastrointestinal tract. It has been reported that CCK-B receptor on the basolateral cell membrane domain was immunoreactive and showed high-affinity binding sites for gastrin^[8]. It has been widely accepted that gastrin, a trophic factor, promotes growth of cancer cells both *in vitro* and *in vivo* through CCK-B receptors, and that expressions of gastrin gene and CCK-B receptor are closely related to the development, progression and invasion of cancer cells, in particular, colorectal and pancreatic cancers^[9,10]. Taken together, we propose that gastrin/CCK-B receptors may play an important role in the development and progression of gastric cancers. To test this viewpoint, we detected the levels of gastrin and CCK-B mRNA transcripts in human gastric cancer cell line SGC-7901 and in gastric tissues including gastric cancers and their corresponding normal mucosa tissues, gastritis and normal autopsied stomach specimens.

MATERIALS AND METHODS

Gastric tissues

Thirty gastric cancer specimens (including 12 moderate and 18 low differentiation adenocarcinomas, 22 with and 8 without local lymph node metastases) and surrounding non-tumour mucosa surgically resected from gastric corpus were confirmed histopathologically. Two normal autopsied gastric mucosa specimens were authorized by the Pathology Department of West China Medical School of Sichuan University. Ten gastritis specimens from gastroscopic examination were histopathologically confirmed by Pathology Department of Guiyang Medical College. Tissue samples were immediately stored in RNA protection solution (Omega).

Cell culture

SGC-7901 cells were cultured in RPMI 1640 medium supplemented with 100 mL/L newborn calf serum, 100 units/mL penicillin, and 100 μ g/mL streptomycin in a humidified environment of 50 mL/L CO_2 in air at 37 °C.

Table 1 PCR primers

Gene	Primers	Sequences	Base pairs	GenBank accession number
CCK-B/gas- trin receptor	Sense (545-566)	5'-CGGACTACTCATGGTGCCCTAC-3'	316	L08112.1
	Antisense (861-842)	5'-GCCAACCGCGCCAGTCTCAG-3'		
Gastrin	Sense (166-189)	5'-TAGGTACAGGGGCCAACA-3'	266	NM-000805
	Antisense (431-413)	5'-GGGGACAGGGCTGAAGTG-3'		
β -actin	Sense (320-340)	5'-TGGAGAAAATCTGGCACCAC-3'	190	BC016045
	Antisense (509-489)	5'-GAGGCGTACAGGGATAGCAC-3'		

CCK-B: cholecystokinin-B.

Reverse transcription

Total RNA was extracted from gastric samples or 10^6 cells using TRIzol (Invitrogen) reagent according to the manufacturer's recommendations. Five microgramme of total RNA was used as a template for the first-strand cDNA synthesis when the reaction mixture consisted of 120 units of MMLV (Maloney murine leukemia virus) reverse transcriptase, 5 μ mol/L random hexamer oligonucleotide primer, 10 mmol/L dithioerythritol, 2 mmol/L dNTP, and 1 \times first-strand buffer in a total volume of 20 μ L. RNA was denatured at 65 $^{\circ}$ C for 15 min and immediately chilled on ice, and then incubated for 10 min at room temperature before reverse transcriptase was added. The reverse transcription was performed for 60 min at 37 $^{\circ}$ C and terminated by heating to 95 $^{\circ}$ C for 10 min.

PCR analysis of CCK-B receptor and gastrin

The primers used for PCR amplification in the study are listed in Table 1. Two microliter of reverse transcripts was amplified by PCR in a total volume of 50 μ L containing 0.1 μ mol/L oligonucleotide primers for CCK-B receptor or gastrin and β -actin, respectively, 250 μ mol/L dNTP, 2 mmol/L $MgCl_2$, and 1 \times PCR buffer. cDNAs were denatured for 5 min at 95 $^{\circ}$ C before 2.5 units *Taq* DNA polymerase was added. The conditions of touch-down PCR were at 94 $^{\circ}$ C for 45 s, at 68-62 $^{\circ}$ C for 1 min for CCK-B receptor or at 60-55 $^{\circ}$ C for 1 min for gastrin with decreasing 1 $^{\circ}$ C per cycle at beginning, and at 72 $^{\circ}$ C for 1 min for 35 cycles. PCR products were visualized by agarose gel electrophoresis and ethidium bromide staining.

Semi-quantitative analysis of CCK-B/gastrin receptor gene expression

PCR was performed simultaneously by adding the specific primers for both CCK-B/gastrin receptor and β -actin in a single reaction system after reverse transcription. PCR products were separated by 15 g/L agarose gel and the results of electrophoresis were photographed. The level of CCK-B/gastrin receptor mRNA expression vs β -actin was semi-quantified by Lab image software and the data were expressed as mean \pm SD and followed statistical analysis through one-way ANOVA, Student-Newman-Keuls multiple comparisons and independent-samples *t* test by SPSS 10.0. Statistical significance was assumed when $P < 0.05$.

Sequencing

The PCR products of CCK-B/gastrin receptor amplified from the gastric tissues were separately purified by a gel extraction kit, and sequenced by an ABI sequencing machine. The sequences were compared with the GenBank database using BLAST analysis.

RESULTS

Expression of CCK-B receptor gene in human gastric tissues and SGC-7901 cells

CCK-B receptor expression was indicated by the presence of

a 316-bp PCR product, and the gastrin gene expression yielded a 266-bp PCR product while the β -actin mRNA as an internal control revealed a 190-bp product on agarose gel. Figure 1 shows the expression of CCK-B/gastrin receptor detected in all specimens taken from normal, inflammatory, cancerous gastric tissues and SGC-7901 cells.

Then, all of the samples were further divided into three groups including normal (surrounding healthy and autopsied gastric tissues, $n=32$), inflammatory ($n=10$) and malignant groups ($n=30$) which were subdivided into the local lymph node metastases ($n=22$) and non-metastases ($n=8$) groups, or moderate (12) and low (18) differentiation adenocarcinoma groups. Data were analyzed by one-way ANOVA. As shown in Figure 2, the expression level of CCK-B receptor mRNA in surrounding healthy gastric tissues is significantly higher than that in neoplastic and inflammatory tissues ($P < 0.05$) while there are neither significant differences between metastases and non-metastases groups nor between groups with different differentiations ($P > 0.05$).

Gastrin gene expression in human gastric cancer tissues and SGC-7901 cells

Gastrin mRNA was detected on both SGC-7901 cells and gastric cancer specimens (22/30), among which 86.4% (19/22) with local lymph node metastases, and 10.0% (3/30) without metastases. The positive expression rate of gastrin mRNA in metastatic cases was significantly higher than that in lymph node metastasis-negative cases ($P < 0.05$). Gastrin mRNA was detected in 9 out of 12 gastric adenocarcinoma specimens with moderate differentiation and in 13 out of 18 cancerous specimens with poor differentiation. Statistical analyses showed no significant difference between the poor and moderate differentiation groups ($P > 0.05$). Surprisingly, gastrin mRNA transcripts were detected neither in normal gastric tissues nor in inflammatory ones (Figure 1).

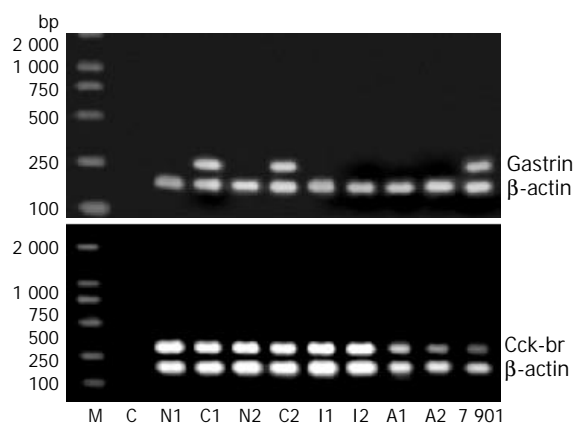


Figure 1 Expression of CCK-B receptor (below) and gastrin (above) mRNA in human gastric tissues and gastric cancer cell line. Total RNA extracted from matched tumor (C1, C2) and non-neoplastic (N1, N2) gastric tissues of patients with gastric

cancer, inflammatory gastric mucosa (I1 and I2) from patients with gastritis, normal stomachs from two autopsied patients (A1, A2) and SGC-7901 cells (7901) were analyzed by RT-PCR. The second lane (C) corresponds to the negative control (H₂O). The results are representatives of all specimens. Cck-br and gastrin stand for cholecystokinin B receptor and gastrin gene, respectively. β -actin: β -actin gene. M: marker (bp).

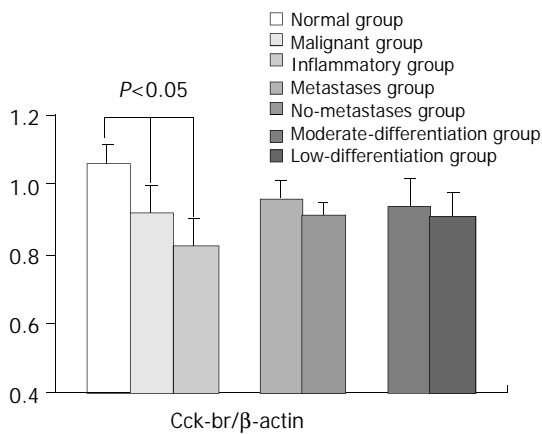


Figure 2 Semi-quantitative analysis of CCK-B receptor expression in human gastric tissues. The expression levels of CCK-B receptors were higher in normal group than in malignant and inflammatory groups, but there was no significant difference compared with other groups. Cck-br/ β -actin: ratio of the intensities of the bands of CCK-B receptor vs β -actin on agarose gel. The results are expressed as mean \pm SD in every group.

Confirmation of CCK-B receptor and gastrin genes from samples

The gene sequence identities of CCK-B receptor/gastrin amplified from four different gastric tissues were 100% and 96%, respectively, as compared with CCK-B receptor/gastrin gene sequences from GenBank (Figure 3).

DISCUSSION

CCK-B receptor is widely distributed throughout the human gastrointestinal tract, pancreas, lung and some neuroendocrine tissues. It mediates the normal physiological function of gastrin. Gastrin has proliferative effects on various malignancies including gastric, colorectal, pancreatic, medullary thyroid cancers, small cell lung cancer as well as tumors of the central and peripheral nervous systems through CCK-B receptors^[11-17].

Coexpression of gastrin gene and CCK-B receptor in cancer tissues *in vivo* or cell lines *in vitro* may suggest the existence of autocrine or paracrine pathways, through which gastrin exerts its physiological or pathological effects. All of the gastric

specimens tested expressed CCK-B receptor mRNA, but only gastric cancer samples (22/30) expressed gastrin transcript and the expression levels of gastrin mRNA were closely correlated with the progression and metastasis of malignant tumors. However, there was no correlation between the expression level of gastrin mRNA and the grade of tumor differentiation. Taken together, our results suggested that the existence of an autocrine or paracrine pathway of gastrin/CCK-B receptors might play an important role in the pathogenesis, especially in the progression, of gastric carcinomas.

SGC-7901 cells were originated from metastatic lymph nodes of a Chinese patient with gastric cancer in 1981. Coexpression of CCK-B receptor and gastrin gene in this cell line provided further evidences that the gastrin/CCK-B autocrine loop might be involved in the development of human gastric cancer. This autocrine loop has also been proved to be functional in human colorectal^[9], pancreatic^[18] and lung^[19,20] carcinomas.

Using semi-quantitative method, we demonstrated that the expression levels of CCK-B receptor mRNA in normal gastric tissues were higher than those in gastric cancer and gastritis, and its expression did not correlate with the grade of differentiation and metastases of gastric cancers. Henwood's group^[21] reported that a significantly increased expression of CCK-B receptor protein was seen along the pathway from normal gastric tissues, gastritis to gastric adenocarcinoma by immunohistochemistry. Other malignant tumors also showed the inconsistency with a published paper^[22].

Recent insights into CCK receptors have improved our understanding of new receptor isoforms including CCK-C receptor, intron 4-containing splice variant of CCK-B receptor and glycine-extended gastrin receptor besides classic CCK-A and CCK-B receptor subtypes^[23-25]. These new receptor subtypes have been found to present in many human malignancies and cell lines and to have a functional role in mediating gastrin's proliferative effects on malignancies^[26,27].

Apart from CCK receptor heterogeneity, post-translational processing of pro-gastrin is known to increase glycine-extended gastrin and progastrin other than the amidated forms known to be biologically active. Although extended forms have limited biological activities in the stimulation of gastric acid secretion, it has been found that they exist in many cancers and cultured cell lines and have amidated gastrin-independent trophic activities^[28-32]. Unfortunately, to date, no specific receptors have been characterized and no specific antagonists are available, making it difficult to study their potential effects on the pathogenesis of carcinomas.

In conclusion, the coexpression of gastrin gene and CCK-B receptors in SGC-7901 cells and gastric carcinoma tissue suggests that a functional autocrine loop exists and may play an important role in the pathogenesis and progression of human

Cck-br	92	tactgctgcttctgctcttgttcttcatcccggtgtggttatggccgtg	141
L08112.1	659	tactgctgcttctgctcttgttcttcatcccggtgtggttatggccgtg	708
Gastrin	138	agaagaagaagcctatggcatggatggacttcggccgccgagtgctgag	187
NM_000805	312	agaagaagaagcctatgg-atggatggacttcggccgccgagtgctgag	359

Figure 3 Sequence analyses of CCK-B receptor/gastrin mRNA from samples. L08112.1: Human brain CCK-B/gastrin receptor gene from GenBank. NM_000805: Homo sapiens gastrin gene from GenBank. Cck-br and gastrin: CCK-B receptor and gastrin gene sequences from specimens, respectively. The results showed are representatives of four samples.

gastric carcinomas. However, human tumor cells can express different CCK-B receptor subtypes and different bioactive forms of gastrin amidated and non-amidated, and that complex networks may exist among these components. More studies are needed for their roles in the development of human gastric carcinomas.

REFERENCES

- Dockray GJ.** Gastrin and gastric epithelial physiology. *J Physiol* 1999; **518**(Pt 2): 315-324
- Sun FP, Song YG.** G and D cells in rat antral mucosa: An immunoelectron microscopic study. *World J Gastroenterol* 2003; **9**: 2768-2771
- Li YY.** Mechanisms for regulation of gastrin and somatostatin release from isolated rat stomach during gastric distention. *World J Gastroenterol* 2003; **9**: 129-133
- Rozengurt E, Walsh JH.** Gastrin, CCK, Signaling, and Cancer. *Annu Rev Physiol* 2001; **63**: 49-76
- Zhang ZL, Chen WW.** Proliferation of intestinal crypt cells by gastrin-induced ornithine decarboxylase. *World J Gastroenterol* 2002; **8**: 183-187
- Wang Z, Chen WW, Li RL, Wen B, Sun JB.** Effect of gastrin on differentiation of rat intestinal epithelial cells *in vitro*. *World J Gastroenterol* 2003; **9**: 1786-1790
- Konturek PC, Kania J, Kukharsky V, Ocker S, Hahn EG, Konturek SJ.** Influence of gastrin on the expression of cyclooxygenase-2, hepatocyte growth factor and apoptosis-related proteins in gastric epithelial cells. *J Physiol Pharmacol* 2003; **54**: 17-32
- Kulaksiz H, Arnold R, Goke B, Maronde E, Meyer M, Fahrenholz F, Forssmann WG, Eissele R.** Expression and cell-specific localization of the cholecystokinin B/gastrin receptor in the human stomach. *Cell Tissue Res* 2000; **299**: 289-298
- Watson SA, Morris TM, McWilliams DF, Harris J, Evans S, Smith A, Clarke PA.** Potential role of endocrine gastrin in the colonic adenoma carcinoma sequence. *Br J Cancer* 2002; **87**: 567-573
- Clerc P, Leung-Theung-Long S, Wang TC, Dockray GJ, Bouisson M, Delisle MB, Vaysse N, Pradayrol L, Fourmy D, Dufresne M.** Expression of CCK2 receptors in the murine pancreas: proliferation, transdifferentiation of acinar cells, and neoplasia. *Gastroenterology* 2002; **122**: 428-437
- Pagliocca A, Wroblewski LE, Ashcroft FJ, Noble PJ, Dockray GJ, Varro A.** Stimulation of the gastrin-cholecystokinin(B) receptor promotes branching morphogenesis in gastric AGS cells. *Am J Physiol Gastrointest Liver Physiol* 2002; **283**: G292-299
- Xie B, He SW, Wang XD.** Effect of gastrin on protein kinase C and its subtype in human colon cancer cell line SW480. *World J Gastroenterol* 2000; **6**: 304-306
- Yen TW, Sandgren EP, Liggitt HD, Palmiter RD, Zhou W, Hinds TR, Grippo PJ, McDonald JM, Robinson LM, Bell RH Jr.** The gastrin receptor promotes pancreatic growth in transgenic mice. *Pancreas* 2002; **24**: 121-129
- Lefranc F, Chaboteaux C, Belot N, Brotchi J, Salmon I, Kiss R.** Determination of RNA expression for cholecystokinin/gastrin receptors (CCKA, CCKB and CCKC) in human tumors of the central and peripheral nervous system. *Int J Oncol* 2003; **22**: 213-219
- Blaker M, de Weerth A, Tometten M, Schulz M, Hoppner W, Arlt D, Hoang-Vu C, Dralle H, Terpe H, Jonas L, von Schrenck T.** Expression of the cholecystokinin 2-receptor in normal human thyroid gland and medullary thyroid carcinoma. *Eur J Endocrinol* 2002; **146**: 89-96
- Moody TW, Jensen RT.** CI-988 inhibits growth of small cell lung cancer cells. *J Pharmacol Exp Ther* 2001; **299**: 1154-1160
- Wang XJ, Ma QJ, Lai DN, Li CJ, Li JM, Wu YZ, Wang Q.** Gastrin receptor antagonist combined with cytosine deaminase suicide gene therapy enhances killing of colorectal carcinoma. *Shijie Huaren Xiaohua Zazhi* 2003; **11**: 1385-1388
- Reubi JC, Waser B, Gugger M, Friess H, Kleeff J, Kaye H, Buchler MW, Laissue JA.** Distribution of CCK1 and CCK2 receptors in normal and diseased human pancreatic tissue. *Gastroenterology* 2003; **125**: 98-106
- Rozengurt E.** Autocrine loops, signal transduction, and cell cycle abnormalities in the molecular biology of lung cancer. *Curr Opin Oncol* 1999; **11**: 116-122
- Cong B, Li SJ, Ling YL, Yao YX, Gu ZY, Wang JX, You HY.** Expression and cell-specific localization of cholecystokinin receptors in rat lung. *World J Gastroenterol* 2003; **9**: 1273-1277
- Henwood M, Clarke PA, Smith AM, Watson SA.** Expression of gastrin in developing gastric adenocarcinoma. *Br J Surg* 2001; **88**: 564-568
- Baldwin GS, Shulkes A.** Gastrin, gastrin receptors and colorectal carcinoma. *Gut* 1998; **42**: 581-584
- He SW, Shen KQ, He YJ, Xie B, Zhao YM.** Regulatory effect and mechanism of gastrin and its antagonists on colorectal carcinoma. *World J Gastroenterol* 1999; **5**: 408-416
- Seva C, Dickinson CJ, Yamada T.** Growth-promoting effects of glycine-extended progastrin. *Science* 1994; **265**: 410-412
- Hellmich MR, Rui XL, Hellmich HL, Fleming RY, Evers BM, Townsend CM.** Human colorectal cancers express a constitutively active cholecystokinin-B/gastrin receptor that stimulates cell growth. *J Biol Chem* 2000; **275**: 32122-32128
- Gales C, Sanchez D, Poirot M, Pyronnet S, Buscail L, Cussac D, Pradayrol L, Fourmy D, Silvente-Poirot S.** High tumorigenic potential of a constitutively active mutant of the cholecystokinin 2 receptor. *Oncogene* 2003; **22**: 6081-6089
- Ding WQ, Kuntz SM, Miller LJ.** A misspliced form of the cholecystokinin-B/gastrin receptor in pancreatic carcinoma: role of reduced cellular U2AF35 and a suboptimal 3-splicing site leading to retention of the fourth intron. *Cancer Res* 2002; **62**: 947-952
- Smith JS, Verderame MF, McLaughlin P, Martenisi M, Ballard E, Zagon I.** Characterization of the CCK-C(cancer) receptor in human pancreatic cancer. *Int J Mol Med* 2002; **10**: 689-694
- Konturek PC, Bielanski W, Konturek SJ, Hartwich A, Pierzchalski P, Gonciarz M, Marlicz K, Starzynska T, Zuchowicz M, Darasz Z, Gotze JP, Rehfeld J, Hahn EG.** Progastrin and cyclooxygenase-2 in colorectal cancer. *Dig Dis Sci* 2002; **47**: 1984-1991
- Kermorgant S, Lehy T.** Glycine-extended gastrin promotes the invasiveness of human colon cancer cells. *Biochem Biophys Res Commun* 2001; **285**: 136-141
- Kelly A, Hollande F, Shulkes A, Baldwin GS.** Expression of progastrin-derived peptides and gastrin receptors in a panel of gastrointestinal carcinoma cell lines. *J Gastroenterol Hepatol* 1998; **13**: 208-214
- Jensen RT.** Involvement of cholecystokinin/gastrin-related peptides and their receptors in clinical gastrointestinal disorders. *Pharmacol Toxicol* 2002; **91**: 333-350

Edited by Chen WW and Wang XL Proofread by Xu FM

Effect of mitogen-activated protein kinase signal transduction pathway on multidrug resistance induced by vincristine in gastric cancer cell line MGC803

Bo Chen, Feng Jin, Ping Lu, Xiang-Lan Lu, Ping-Ping Wang, Yun-Peng Liu, Fan Yao, Shu-Bao Wang

Bo Chen, Feng Jin, Ping Lu, Fan Yao, Shu-Bao Wang, Department of Surgical Oncology, the First Affiliated Hospital, China Medical University, Shenyang 110001, Liaoning Province, China

Xiang-Lan Lu, Ping-Ping Wang, Institute of Hematology, the First Affiliated Hospital, China Medical University, Shenyang 110001, Liaoning Province, China

Yun-Peng Liu, Department of Medical Oncology, the First Affiliated Hospital, China Medical University, Shenyang 110001, Liaoning Province, China

Correspondence to: Bo Chen, Department of Surgical Oncology, the First Affiliated Hospital, China Medical University, Shenyang 110001, Liaoning Province, China. chbyxl@163.com

Telephone: +86-24-23256666 to 6227

Received: 2003-08-28 **Accepted:** 2003-11-06

Abstract

AIM: To investigate the correlation between mitogen-activated protein kinase (MAPK) signal transduction pathway and multidrug resistance (MDR) in MGC803 cells.

METHODS: Western blot was used to analyze the expression of MDR associated gene in transient vincristine (VCR) induced MGC803 cells, which were treated with or without the specific inhibitor of MAPK, PD098059. Morphologic analysis of the cells treated by VCR with or without PD098059 was determined by Wright-Giemsa staining. The cell cycle analysis was performed by using flow cytometric assay and the drug sensitivity of MGC803 cells which were exposed to VCR with or without PD098059 was tested by using MTT assay.

RESULTS: Transient exposure to VCR induced P-gp but not MRP1 or GST- π expression in MGC803 cells and the expression of P-gp was inhibited by PD098059. Apoptotic bodies were found in the cells treated with VCR or VCR+PD098059. FCM results indicated that more MGC803 cells showed apoptotic phenotype when treated by VCR and PD098059 (rate: 31.23%) than treated by VCR only (rate: 18.42%) ($P < 0.05$). The IC_{50} ($284 \pm 13.2 \mu\text{g/L}$) of MGC803 cells pretreated with VCR was 2.24-fold as that of negative control group ($127 \pm 17.6 \mu\text{g/L}$) and 1.48-fold as that of the group treated with PD098059 ($191 \pm 27.9 \mu\text{g/L}$).

CONCLUSION: This study shows that the expression of P-gp can be induced by transient exposure to VCR and this induction can be prevented by PD098059, which can block the activity of MAPK. MAPK signal transduction pathway may play some roles in modulating MDR1 expression in gastric cancer.

Chen B, Jin F, Lu P, Lu XL, Wang PP, Liu YP, Yao F, Wang SB. Effect of mitogen-activated protein kinase signal transduction pathway on multidrug resistance induced by vincristine in gastric cancer cell line MGC803. *World J Gastroenterol* 2004; 10(6): 795-799

<http://www.wjgnet.com/1007-9327/10/795.asp>

INTRODUCTION

Multidrug resistance (MDR) is a major factor in the failure of many forms of chemotherapy^[1-4]. Several different molecular mechanisms will switch on in MDR cells, the most investigated mechanisms with known clinical significance are: (1) activation of transmembrane proteins effluxing different chemical substance from the cells, including mainly P-glycoprotein (P-gp) encoded by MDR1 and multidrug resistance related protein (MRP); (2) activation of the enzymes of the glutathione detoxification system (especially GST- π); (3) alteration of the genes and proteins involved in the control of apoptosis (especially p53 and Bcl-2)^[5-14]. MDR associated genes are expressed in a large proportion of human tumors, and its expression in several different forms of cancer was shown to be associated with a lack of response to combination chemotherapy. MDR1 expression is usually low or undetectable prior to treatment, but it is frequently increased during the progression of the disease and, most noticeably, after chemotherapy^[15-20]. The increased expression of MDR1 mRNA can be found in some drug-sensitive cancer cells by transient exposure to different chemotherapeutic drugs^[21-24].

The signal transduction pathway of the mitogen-activated protein kinase (MAPK) plays a critical role in cell proliferation, differentiation and apoptosis. The ERK1/2 (Ras/Raf-1/MEK1/2/ERK1/2) signal transduction pathway is a subfamily of MAPK. The expression of MDR and the activation of MAPK are increased in cancer cells after treatment with various therapeutic drugs. The selective inhibitor of MEK1/2, PD098058, has been shown to significantly reverse the drug resistance of drug resistant cell line L1210/VCR^[25]. The mechanism is unclear. Whether MAPK plays a role in MDR, and whether the alteration of MEK can regulate the expression of MDR need to be elucidated.

Our study was to observe the expressions of associated genes of MDR of human gastric cancer cell line MGC803 by their transient exposure to vincristine (VCR) and the effect on MDR by the specific inhibitor of MEK1/2, PD098059.

MATERIALS AND METHODS

Reagents

Human gastric cancer cell line MGC803 was obtained from Tumor Research Institute (China Medical University, Shenyang). RPMI1640 medium was the product of Gibco (USA). Chemical drug vincristine was purchased from Hualian Co. (Shanghai, China). PD098059 was the product of Promega (USA). Rabbit anti-human P-gp, MRP1, GST- π polyclonal antibody were products of Oncogen (USA). Alkaline phosphatase-conjugated goat anti-rabbit IgG was purchased from Zhongshan Co. (Beijing).

Morphological analysis of cells

After treated with VCR ($20 \mu\text{g/L}$) or VCR ($20 \mu\text{g/L}$)+PD098059 ($10 \mu\text{mol/L}$) for 24 h, 48 h, MGC803 cells were analyzed by wright-Giemsa staining, and the morphology of cells was examined under optic microscope.

Cell cycle analysis

MGC803 cells ($1 \times 10^8/L$) were seeded into 12-well plates and cultured in 1 mL RPIM medium. After cultured for 4 h, cells were treated with VCR (20 $\mu g/L$), PD098059 (10 $\mu mol/L$) or VCR (20 $\mu g/L$) + PD098059 (10 $\mu mol/L$) for 24 h, 48 h, 96 h. Cells were harvested and washed with ice-cold PBS twice, centrifuged (120 $\times g$, 5 min) and supplemented with ice-cold 70 mL/L ethanol overnight. Cells were treated with RNase (200 mg/L) at 37 °C for 1 h after washed with ice-cold PBS twice, then centrifuged (120 g, 5 min), treated with PI (20 mg/L) for 30 min in dark room at 4 °C. Cell cycle was analyzed by flow cytometer and CELLQuest software.

MTT assay of drug sensitivity

Cells ($1 \times 10^8/L$) pretreated with VCR (20 $\mu g/L$) for 72 h were plated into 96-well plates and cultured in 100 μL RPMI medium. After cultured for 4 h, cells were divided into two groups: one group was treated with various concentrations of VCR (1 $\mu g/L$, 10 $\mu g/L$, 100 $\mu g/L$, 1 000 $\mu g/L$), the other group was treated with a fixed concentration of PD098059 (10 $\mu mol/L$) and various concentration of VCR (1 $\mu g/L$, 10 $\mu g/L$, 100 $\mu g/L$, 1 000 $\mu g/L$). The untreated MGC803 was treated with various concentration of VCR (1 $\mu g/L$, 10 $\mu g/L$, 100 $\mu g/L$, 1 000 $\mu g/L$) as negative control group. After treated for 72 h, 20 μL of 5 g/L MTT [3-(4,4-dimethylthiazol-2-yl)2,5-diphenylterazolium bromide] in PBS was added to each well, incubated for 4 h at 37 °C and the formed formazan crystals were dissolved in 100 μL of DMSO. The absorbance was recorded at 570 nm on a microplate reader (BIORAD). Drug sensitivity is expressed as IC_{50} for cells, which the concentration of drugs that caused a 50% reduction in the at 570 nm relative to untreated cells (controls).

Western blot analysis

MGC803 cells were harvested after treated with VCR (20 $\mu g/L$) or VCR (20 $\mu g/L$) + PD098059 (10 $\mu mol/L$) for 24, 48, 72 h. A total of 2×10^7 cells were lysed in 200 μL RIPA buffer containing phenylmethylsulfonyl fluoride (PMSF, 100 mg/L), Aprotinin (2 mg/L), 50 mmol/L TrisCl pH 7.4, 150 mmol/L NaCl, 1 g/L SDS, 10 g/L Triton-100, 1 mmol/L EDTA pH 8.0. Protein samples were sonicated on ice, lysed for 40 min at 4 °C, then centrifuged (15 400 g, 20 min) at 4 °C. The supernatant was transferred to a new tip on ice and then the amount of the protein calculated. Protein samples were separated by sodium dodecyl sulfate polyacrylamide gel electrophoresis (SDSPAGE), transferred to a PVDF membrane. The membrane was incubated in a blocking solution containing 50 g/L fat free milk powder for 1 h, then probed with rabbit anti-human P-gp polyclonal antibody overnight, and incubated with alkaline phosphatase-conjugated goat anti-rabbit IgG for 2 h. The membrane was then stained by blue tetrazolium (NBT) and 5'-bromo-4-chloro-3-indolylphosphate (BCIP) solution. The integrated density value (IDV) was analyzed by Fluorchem software.

Statistical analysis

Data were analyzed by chi square test. $P < 0.05$ was considered as significant.

RESULTS

Apoptosis of cells treated with VCR and PD098059

The apoptotic bodies were observed in the MGC803 cells after treated with VCR (20 $\mu g/L$) or VCR (20 $\mu g/L$) + PD098059 (10 $\mu mol/L$) for 48 h (Figure 1A, B, C).

The apoptosis of MGC803 cells was detected by flow cytometric analysis. The rate of apoptotic cells treated with VCR for 72 h was 18.41%, and that treated with VCR and

PD098059 for 72 h was 35.61%. There was a significant difference between them ($P < 0.05$). The apoptotic rates of MGC803 cells untreated and treated with PD098059 only were 8.46% and 6.26%. There was no significant difference between them ($P > 0.05$) (Figure 2).

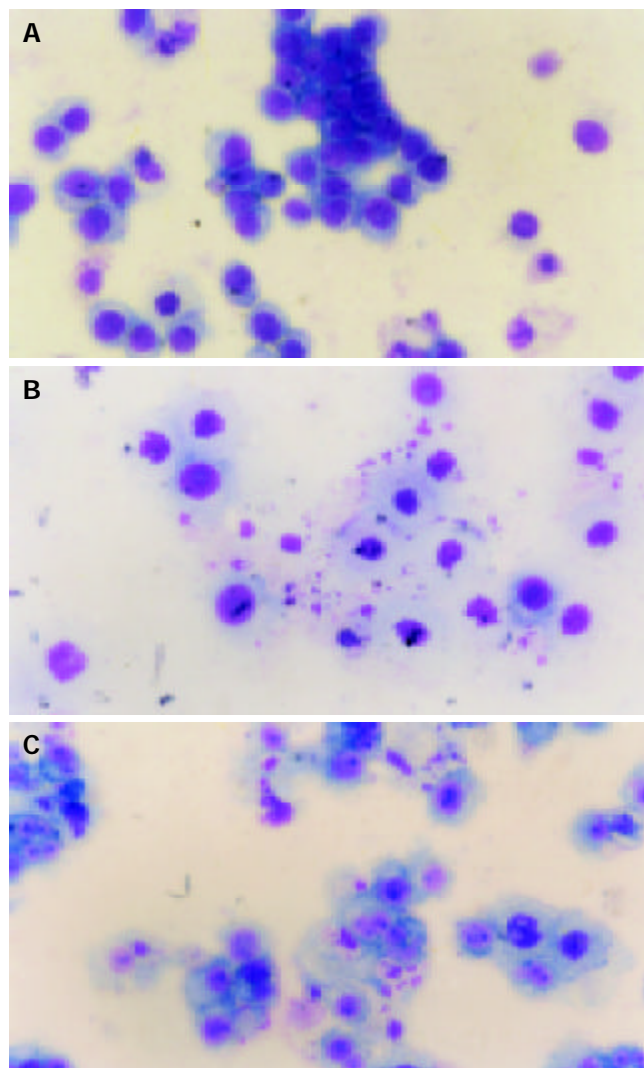


Figure 1 A: Untreated MGC803 Cells (apoptotic bodies could not be found), B: MGC803 cells treated with VCR 48 h (apoptotic bodies could be found), C: MGC803 cells treated with VCR+PD098059 48 h (apoptotic bodies could be found).

Drug sensitivity of cells treated with VCR and PD098059

The IC_{50} of MGC803 pretreated with VCR for 72 h followed by treatment with various concentrations of VCR was $284 \pm 13.2 \mu g/L$. It was 2.24-fold as that of negative control group ($127 \pm 17.6 \mu g/L$), and 1.48-fold as those of cells treated with various concentrations of VCR ($191 \pm 27.9 \mu g/L$). And, the concentration of PD098059 was fixed. It showed that the drug-resistance of MGC803 pretreated with VCR was increased and PD098059 could reverse the drug resistance induced by VCR partially.

Expression of MDR1, MRP1 and GST-p

Western blot was used to detect the expression of MDR associated genes. The expression of P-gp in MGC803 cells gradually increased after treated with VCR for 24-72 h (Table 1, Figure 3). But the expression of MRP1 and GST- π did not increase significantly (Table 1, Figure 3). The expression of P-gp was inhibited when MGC803 cells were treated with VCR and PD098059 for 24-72 h (Table 1, Figure 3).

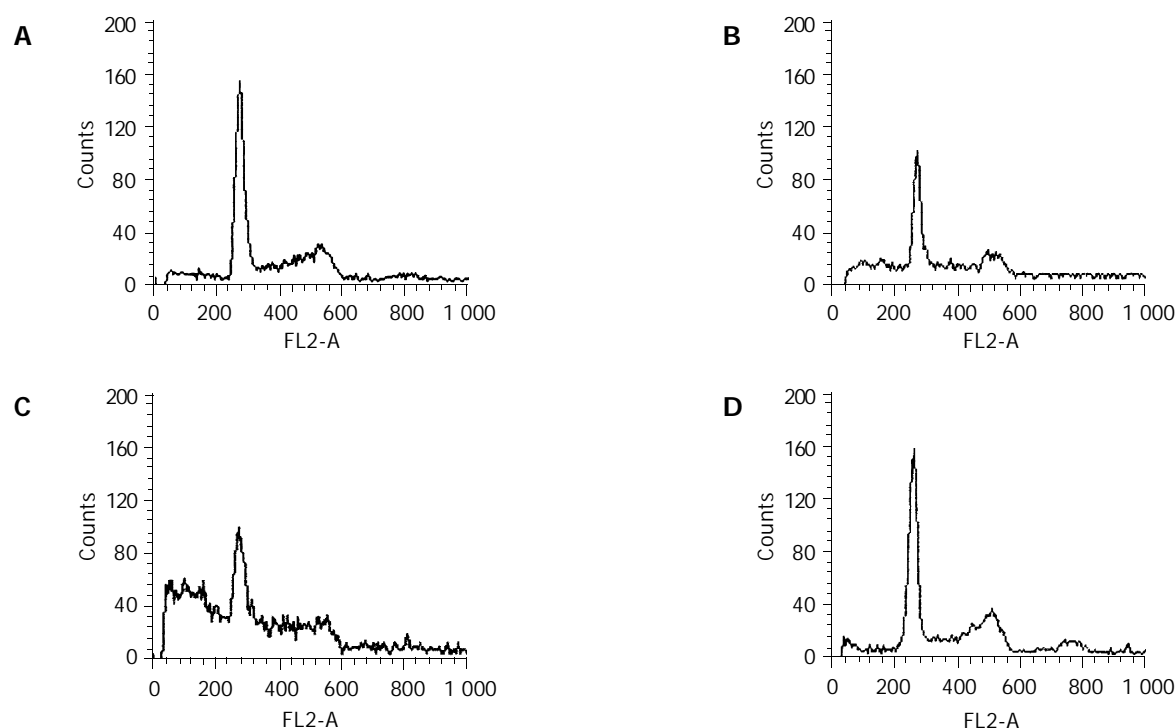


Figure 2 Cell cycle analysis of MGC803. A: Untreated MGC803 cells at 72 h (G_0G_1 : 48.20%; G_2M : 28.18%, S: 14.16%, apoptosis: 8.46%), B: MGC803 cells treated with VCR (20 ng/mL) after 72 h (G_0G_1 : 37.62%; G_2M : 20.05%, S: 24.92%, apoptosis: 18.41%), C: MGC803 cells treated with VCR (20 ng/mL) +PD098059 (10 nmol/mL) after 72 h (G_0G_1 : 32.53%; G_2M : 13.91%, S: 18.95%, apoptosis: 35.61%), D: MGC803 cells treated with PD098059 (10 nmol/mL) only after 72 h (G_0G_1 : 49.27%; G_2M : 27.56%, S: 16.91%, apoptosis: 6.26%).

Table 1 IDV of expression of MDR associated gene

Group	VCR (MDR1)	VCR (MRP1)	VCR (GST- π)	VCR+PD098059 (MDR1)
Untreated MGC803 cells	116 \pm 7.5	38 \pm 14.5	122 \pm 16	54 \pm 9.5
Positive control	192 \pm 8.6	64 \pm 13.2	144 \pm 21	105 \pm 9.5
24 h	159 \pm 9.5	34 \pm 9.3	123 \pm 19.5	63 \pm 16.7
48 h	172 \pm 7.6	30 \pm 11.5	110 \pm 15.6	64 \pm 21.1
72 h	196 \pm 15.1	33 \pm 15.5	110 \pm 13.6	58 \pm 9.5



Figure 3 The expression of associated gene of MDR in MGC803 cells treated with VCR or VCR+PD098059 24h-72 h. A: The expression of MDR1 of MGC803 cells treated with VCR increased. B,C: The expression of MRP1 and GST- π of MGC803 cells treated with VCR did not increase. D: The expression of MDR1 was inhibited when MGC803 cells treated with VCR and PD098059. E: The protein level of β -actin was detected to assess the loading amount in each well in SDS-PAGE. Lane 1, untreated cells; Lane 2, positive control cells; Lane 3, cells treated for 24 h; Lane 4, cells treated 48 h; Lane 5, cells treated for 72 h.

DISCUSSION

Different tumors are different in sensitivity to chemotherapeutic drugs, and drug resistance can be induced by chemotherapy. The failure of cancer chemotherapy is mainly due to the overexpression of associated genes of MDR. Cytotoxic drug resistant cell lines have been induced after long-term exposure to gradient concentrations of cytotoxic drugs. Whether the expression of MDR could be induced by transient exposure to chemotherapeutic drugs has aroused. Chaudhary *et al* have found that the expressions of MDR1 mRNA in drug sensitive leukemia cell line K562 increased by short-term exposure to different chemotherapeutic drugs^[21]. Schondorf *et al* also found that MDR1-mRNA was detectable in each cell line when short-term cultures of 6 established ovarian cancer cell lines were exposed to one of three anticancer drugs at concentrations equivalent to the clinically achievable plasma peak concentration. The method described here was easy to perform and could be of striking value in predicting the development of tumor chemoresistance^[24]. Our results of western blot showed that the expression of P-gp in MGC803 cells increased significantly but the expressions of MRP1 and GST- π did not increase after induction by VCR for 72 h and the MTT assay showed that the drug resistance of MGC803 cells pretreated with VCR was 2.24-fold as that of untreated MGC803 cells. It suggested that the expression of MDR1 in MGC803 cells could be induced after transient exposure to VCR.

Mitogen-activated protein kinases (MAPKs), found in all eukaryotes, are common participants in signal transduction pathway from the membrane to the nucleus, and play an important role in cell proliferation, differentiation and apoptosis^[26-28]. The mammalian MAPK family includes ERK1/2, JNK/SAPKs, ERK4 and *etc.* ERK1/2 is the most important subgroup among them. ERK1/2 signal transduction pathways contain at least three protein kinases. They are Raf-1, MAPK/ERK kinases1/2(MEK1/2) and ERK1/2. Raf-1 is activated by Ras, then phosphorylates two residues, either serine or threonine, to activate MEK1/2^[29,30]. MEK1/2 activates ERK1/ERK2 by

phosphorylating a tyrosine and a threonine residues^[31].

Signal transduction pathways play critical roles in pathogenesis and progress of tumor. The activation of MAPK and expression of MDR can be induced by anti-cancer drugs^[32]. But the relation between them is not clear. Kisucka *et al* found PD098059 significantly reduced the survival of murine vincristine resistant L1210/VCR cells with a decrease of LC₅₀ to vincristine from 2.65 mmol/L to 0.67 mmol/L. The result of the study demonstrated that the inhibitor of MEK1/2 signaling pathway was a reversal agent of VCR resistance in L1210/VCR cells, but the precise mechanism of PD098059 in modulation of MDR is not resolved yet, and the role of ERK-mediated phosphorylation cascade could be considered^[25]. Ding *et al* found that PD098059 re-sensitized the Taxol resistant human ovarian cancer cell line A1847/TX at least 20-fold, but when MDR1 cDNA was stably expressed in the wild-type cell line to generate a highly Taxol-resistant sub-line, 1847/MDR5, MAPK kinases again became activated. This result demonstrated that the increased activity of the signaling pathway in the Taxol-resistant lines was directly attributable to MDR1 overexpression and was not due to the effects of Taxol itself, and that MAPK regulated the expression of MDR1^[33]. It has been found that the expression of MDR1 can block apoptosis induced by the Fas ligand cascade. Expression of MDR1 resulted in a decrease in the rate of production of active caspase 3, a key effector caspase in the apoptotic cascade, upon Fas ligation^[11]. The ERK1/2 pathway has also been shown to inhibit caspase-3 activation^[34]. Another possibility is that MDR1 may have additional physiological functions, for instance, MDR1 induces novel Na⁺ and Cl⁻ dependent pathway for transmembrane H⁺ efflux that results in intracellular alkalization^[35]. Apoptosis induced by chemotherapeutic drugs is prevented by intracellular acidification and the induction of apoptotic events such as DNA laddering can be inhibited by increasing the intracellular pH in this manner. In a recent study, Wittstein *et al* demonstrated that inhibition of the ERK1/2 pathway using PD098059 resulted in re-alkalinisation of vascular endothelial cells in perfusion experiments^[36]. Thus alterations in cellular pH may provide the stimulus for a variety of signaling pathways and responses mediated by both MDR and ERK1/2. The relation between MAPK and MDR1 is not clear yet. MAPK signal pathway may combine with other different mechanisms to modulate the expression of MDR1. Our study showed that PD098059 could reduce the drug resistance and enhance the killing action of VCR, and rates of apoptosis of MGC803 cells which were treated with VCR only increased from 18.41% to 35.61% when treated with PD098059 and VCR. It showed that PD098059 could reverse the drug resistance partially by reducing the IC₅₀ of MGC803 cells pretreated by VCR from (287±13.2) µg/L to (191±27.9) µg/L. At the same time, the expression of P-gp was inhibited by PD098059. It was suggested that when MGC803 cells were treated with VCR, the stimulation may be transduced by activation of MAPK signaling pathway to MDR1 gene and the expression of MDR1 increased. As a result, VCR was transported out of cells and multidrug resistance developed. The inhibitor of MEK1/2, PD098059 could reduce the expression of mdr1 and drug resistance of cells exposed to VCR by blocking the ERK1/2 signal transduction pathway. The precise mechanism between MDR1 and MAPK signal transduction pathway needs further study.

REFERENCES

- Zhang LJ, Chen KN, Xu GW, Xing HP, Shi XT. Congenital expression of mdr-1 gene in tissues of carcinoma and its relation with pathomorphology and prognosis. *World J Gastroenterol* 1999; **5**: 53-56
- Thottassery JV, Zambetti GP, Arimori K, Schuetz EG, Schuetz JD. p53-dependent regulation of MDR1 gene expression causes selective resistance to chemotherapeutic agents. *Proc Natl Acad Sci U S A* 1997; **94**: 11037-11042
- Nagata J, Kijima H, Hatanaka H, Asai S, Miyachi H, Abe Y, Yamazaki H, Nakamura M, Watanabe N, Mine T, Kondo T, Scanlon KJ, Ueyama Y. Reversal of drug resistance using hammerhead ribozymes against multidrug resistance-associated protein and multidrug resistance 1 gene. *Int J Oncol* 2002; **21**: 1021-1026
- Lage H, Perlitz C, Abele R, Tampe R, Dietel M, Schadendorf D, Sinha P. Enhanced expression of human ABC-transporter tap is associated with cellular resistance to mitoxantrone. *FEBS Lett* 2001; **503**: 179-184
- Zhan M, Yu D, Lang A, Li L, Pollock RE. Wild type p53 sensitizes soft tissue sarcoma cells to doxorubicin by down-regulating multidrug resistance-1 expression. *Cancer* 2001; **92**: 1556-1566
- Liu B, Staren E, Iwamura T, Appert H, Howard J. Effects of Taxotere on invasive potential and multidrug resistance phenotype in pancreatic carcinoma cell line SUIT-2. *World J Gastroenterol* 2001; **7**: 143-148
- Stavrovskaya AA. Cellular mechanisms of multidrug resistance of tumor cells. *Biochemistry* 2000; **65**: 95-106
- van Brussel JP, van Steenbrugge GJ, Romijn JC, Schroder FH, Mickisch GH. Chemosensitivity of prostate cancer cell lines and expression of multidrug resistance-related proteins. *Eur J Cancer* 1999; **35**: 664-671
- Ruefli AA, Smyth MJ, Johnstone RW. HMBA induces activation of a caspase-independent cell death pathway to overcome P-glycoprotein-mediated multidrug resistance. *Blood* 2000; **95**: 2378-2385
- Bohacova V, Kvackajova J, Barancik M, Drobná Z, Breier A. Glutathione S-transferase does not play a role in multidrug resistance of L1210/VCR cell line. *Physiol Res* 2000; **49**: 447-453
- Smyth MJ, Krasovskis E, Sutton VR, Johnstone RW. The drug efflux protein, P-glycoprotein, additionally protects drug-resistant tumor cells from multiple forms of caspase-dependent apoptosis. *Proc Natl Acad Sci U S A* 1998; **95**: 7024-7029
- Naito S, Yokomizo A, Koga H. Mechanisms of drug resistance in chemotherapy for urogenital carcinoma. *Int J Urol* 1999; **6**: 427-439
- Warr JR, Bamford A, Quinn DM. The preferential induction of apoptosis in multidrug-resistance KB cells by 5-fluorouracil. *Cancer Lett* 2002; **175**: 39-44
- Roepe PD. PH and multidrug resistance. *Novartis Found Symp* 2001; **240**: 232-247
- Holzmayr TA, Hilsenbeck S, Von Hoff DD, Roninson IB. Clinical correlates of MDR1 (P-glycoprotein) gene expression in ovarian and small-cell lung carcinomas. *J Natl Cancer Inst* 1992; **84**: 1486-1491
- Chan HS, Thorner PS, Haddad G, Ling V. Immunohistochemical detection of P-glycoprotein: Prognostic correlation in soft tissue sarcoma of childhood. *J Clin Oncol* 1990; **8**: 689-704
- Tseng CP, Cheng AJ, Chang JT, Tseng CH, Wang HM, Liao CT, Chen IH, Tseng KC. Quantitative analysis of multidrug-resistance mdr1 gene expression in head and neck cancer by real-time RT-PCR. *Jpn J Cancer Res* 2002; **93**: 1230-1236
- Schondorf T, Kurbacher CM, Gohring UJ, Benz C, Becker M, Sartorius J, Kolhagen H, Mallman P, Neumann R. Induction of MDR1-gene expression by antineoplastic agents in ovarian cancer cell lines. *Anticancer Res* 2002; **22**: 2199-2203
- Kato A, Miyazaki M, Ambiru S, Yoshitomi H, Ito H, Nakagawa K, Shimizu H, Yokosuka O, Nakajima N. Multidrug resistance gene (MDR-1) expression as a useful prognostic factor in patients with human hepatocellular carcinoma after surgical resection. *J Surg Oncol* 2001; **78**: 110-115
- Sonneveld P. Multidrug resistance in haematological malignancies. *J Intern Med* 2000; **247**: 521-534
- Chaudhary PM, Roninson IB. Induction of multidrug resistance in human cells by transient exposure to different chemotherapeutic drugs. *J Natl Cancer Inst* 1993; **85**: 632-639
- Zhang P, Wang D, Zheng G. Induction of multidrug resistance in Tca8113 cells by transient exposure to different chemotherapeutic drugs. *Huaxi Kouqiang Yixue Zazhi* 2003; **21**: 70-73
- Brugger D, Brischwein K, Liu C, Bader P, Niethammer D, Gekeler V, Beck JF. Induction of drug resistance and protein kinase C genes in A2780 ovarian cancer cells after incubation with antine-

- oplastic agents at sublethal concentrations. *Anticancer Res* 2002; **22**: 4229-4232
- 24 **Schondorf T**, Neumann R, Benz C, Becker M, Riffelmann M, Gohring UJ, Sartorius J, von Konig CH, Breidenbach M, Valter MM, Hoopmann M, Di Nicolantonio F, Kurbacher CM. Cisplatin, doxorubicin and paclitaxel induce *mdr1* gene transcription in ovarian cancer cell lines. *Recent Results Cancer Res* 2003; **161**: 111-116
 - 25 **Kisucka J**, Barancik M, Bohacova V, Breier A. Reversal effect of specific inhibitors of extracellular-signal regulated protein kinase pathway on P-glycoprotein mediated vincristine resistance of L1210 cells. *Gen Physiol Biophys* 2001; **20**: 439-444
 - 26 **Lewis TS**, Shapiro PS, Ahn NG. Signal transduction through MAP kinase cascades. *Adv Cancer Res* 1998; **74**: 49-139
 - 27 **Karin M**. Mitogen-activated protein kinase cascades as regulators of stress responses. *Ann N Y Acad Sci* 1998; **851**: 139-146
 - 28 **Evans DR**, Hemmings BA. Signal transduction. What goes up must come down. *Nature* 1998; **394**: 23-24
 - 29 **Chen J**, Fujii K, Zhang L, Roberts T, Fu H. Raf-1 promotes cell survival by antagonizing apoptosis signal-regulating kinase 1 through a MEK-ERK independent mechanism. *Proc Natl Acad Sci U S A* 2001; **98**: 7783-7788
 - 30 **Busca R**, Abbe P, Mantoux F, Aberdam E, Peyssonnaud C, Eyche A, Ortonne JP, Ballotti R. Ras mediates the cAMP-dependent activation of extracellular signal-regulated kinases (ERKs) in melanocytes. *EMBO J* 2000; **19**: 2900-2910
 - 31 **Payne DM**, Rossomando AJ, Martino P, Erickson AK, Her JH, Shabanowitz J, Hunt DF, Weber MJ, Sturgill TW. Identification of the regulatory phosphorylation sites in pp42/mitogen-activated protein kinase (MAP kinase). *EMBO J* 1991; **10**: 885-892
 - 32 **Dent P**, Jarvis WD, Birrer MJ, Fisher PB, Schmidt-Ullrich RK, Grant S. The roles of signaling by the p42/p44 mitogen-activated protein (MAP) kinase pathway; a potential route to radio- and chemo-sensitization of tumor cells resulting in the induction of apoptosis and loss of clonogenicity. *Leukemia* 1998; **12**: 1843-1850
 - 33 **Ding S**, Chamberlain M, McLaren A, Goh L, Duncan I, Wolf CR. Cross-talk between signalling pathways and the multidrug resistant protein MDR-1. *Br J Cancer* 2001; **85**: 1175-1184
 - 34 **Kim MS**, So HS, Park JS, Lee KM, Moon BS, Lee HS, Kim TY, Moon SK, Park R. Hwansodan protects PC12 cells against serum-deprivation-induced apoptosis via a mechanism involving Ras and mitogen-activated protein (MAP) kinase pathway. *Gen Pharmacol* 2000; **34**: 227-235
 - 35 **Fritz F**, Howard EM, Hoffman MM, Roepe PD. Evidence for altered ion transport in *Saccharomyces cerevisiae* overexpressing human MDR1 protein. *Biochemistry* 1999; **38**: 4214-4226
 - 36 **Wittstein IS**, Qiu W, Ziegelstein RC, Hu Q, Kass DA. Opposite effects of pressurized steady versus pulsatile perfusion on vascular endothelial cell cytosolic pH: role of tyrosine kinase and mitogen-activated protein kinase signaling. *Circ Res* 2000; **86**: 1230-1236

Edited by Zhu LH Proofread by Xu FM

Mitochondrial microsatellite instability in gastric cancer and its precancerous lesions

Xian-Long Ling, Dian-Chun Fang, Rong-Quan Wang, Shi-Ming Yang, Li Fang

Xian-Long Ling, Dian-Chun Fang, Rong-Quan Wang, Shi-Ming Yang, Li Fang, Department of Gastroenterology, Southwest Hospital, Third Military Medical University, Chongqing 400038, China

Supported by the National Natural Science Foundation of China, No. 30070043, and Scientific Research Project of Chinese PLA during the 10th Five-year plan period, No. 01Z075

Correspondence to: Dian-Chun Fang, M.D., Ph.D. Southwest Hospital, Third Military Medical University, Chongqing 400038, China. fangdianchun@hotmail.com

Telephone: +86-23-68754624 **Fax:** +86-23-68754124

Received: 2003-08-26 **Accepted:** 2003-09-18

Abstract

AIM: To evaluate the role of mitochondrial microsatellite instability (mtMSI) in gastric carcinogenesis.

METHODS: MtMSI was measured with PCR-single strand conformation polymorphism (PCR-SSCP) in 68 cases of advanced gastric cancer, 40 cases of chronic gastritis, 30 cases of intestinal metaplasia and 20 cases of dysplasia.

RESULTS: MtMSI was observed in 12.5% (5 of 40) of chronic gastritis, 20.0% (6 of 30) of intestinal metaplasia, 25.0% (5 of 20) of dysplasia and 38.2% (26 of 68) of gastric cancer. These findings showed a sequential accumulation of mtMSI in the histological progression from chronic gastritis to gastric cancer. An association of mtMSI with intestinal histological type and distal location was found ($P=0.001$ and $P=0.002$), whereas no significant correlation was found between mtMSI and age at diagnosis, sex, tumor size, depth of invasion, lymph node spread and clinical stages ($P>0.05$).

CONCLUSION: MtMSI may play an early and important role in the gastric carcinogenesis pathway, especially in the intestinal type and distal gastric cancer.

Ling XL, Fang DC, Wang RQ, Yang SM, Fang L. Mitochondrial microsatellite instability in gastric cancer and its precancerous lesions. *World J Gastroenterol* 2004; 10(6): 800-803

http://www.wjgnet.com/1007-9327/10/800.asp

INTRODUCTION

The mechanisms of carcinogenesis in the gastric mucosa remain unclear. Genetic instability is strongly involved in neoplastic transformation and progression^[1-7]. In gastrointestinal carcinomas, such genetic instability may be classified into two different forms in which hypermutability occurs either due to chromosomal instability or due to microsatellite instability (MSI)^[8-11]. MSI represents an important form of genomic instability associated with defective DNA mismatch repair in tumors. Although the MSI in nuclear DNA (nMSI) of gastric cancer has been established, little attention was paid to the MSI in mitochondrial DNA (mtMSI) in this cancer. In the present study, we analysed the mtMSI in gastric cancer and its premalignant lesions to elucidate whether

mtMSI led to the progression from chronic gastritis to gastric cancer, via intestinal metaplasia and dysplasia.

MATERIALS AND METHODS

Tissue samples

Forty cases of chronic gastritis, 30 cases of intestinal metaplasia and 20 cases of dysplasia obtained from patients undergoing upper endoscopy for dyspepsia and 68 cases of surgically resected gastric cancer tissues were studied. Tissues from non-tumor or non-inflammatory gastric mucosa, showing no dysplasia or metaplasia, were used as a control in analysis of mtMSI. Hematoxylin-eosin (HE) staining was used for the histopathological diagnosis, evaluation and grading of gastritis, atrophy, intestinal metaplasia, dysplasia and cancer. Genomic DNA was isolated by standard proteinase-K digestion and phenol-chloroform extraction protocols. None of the patients with gastric cancer included in the present series had received chemotherapy or radiation therapy before operation.

mtMSI detection

PCR-single strand conformation polymorphism (PCR-SSCP) was performed to amplify the microsatellite sequence of mtDNA using published primers^[18]. The primer consisted of 2 D-loop regions and 5 coding regions (Table 1). The reaction conditions and procedures were similar to those reported by Hebano *et al*^[12].

Each PCR was digested by appropriate restriction enzymes and electrophoresed at 300 V at 22 °C for 2 h on a 75g/L polyacrylamide gel containing 50 mmol/L boric acid, 1 mmol/L EDTA and 25g/L glycerol. After silver staining, PCR products that showed mobility shifts were directly sequenced using an appropriate internal primer and analyzed using the 373A automated DNA sequencer (Perkin Elmer Cetus). All analyses were repeated twice to rule out PCR artifacts.

Table 1 Sequences of primer for PCR analysis

Repeat sequence	mtDNA region	Position	Annealing (°C)	Primer (5'-3')
(C) _n	270-425	D-loop	58	TCCACACAGACATCAATAACA AAAGTGCATACCGCCAAAAG
(CA) _n	467-556	D-loop	55	CCCATACTACTAATCTCATCAA TTTGTTGGTTCGGGGTATG
(C) ₆	3 529-3 617	ND1	55	CCGACCTTAGCTCTCACCAT AATAGGAGGCTAGGTTGAG
(A) ₇	4 555-4 644	ND2	55	CCTGAGTAGGCCTAGAAATAAA ACTTGATGGCAGCTTCTGTG
(T) ₇	9 431-9 526	COIII	55	CCAAAAAGGCCTTCGATACG GCTAGGCTGGAGTGTAATA
(C) ₆ and (A) ₈	12 360-12 465	ND5	55	CACCCTAACCCCTGACTTCC GGTGGATGCGACAATGGATT
(CCT) ₃ and (AGC) ₃	12 940-13 032	ND5	55	GCCCTTCTAAACGCTAATCC TCAGGGGTGGAGACCTAATT

Statistical analysis

Chi-square test with Yates' correction was used. A P value <0.05 was considered statistically significant.

RESULTS

Sixty-eight gastric cancer samples and 90 benign gastric mucosal lesions were screened for mtMSI at seven repeat sites using the PCR-RFLP method. Figure 1 exhibits a representative mobility-shift band compared with normal counterpart. mtMSI was observed in 26 out of 68 cases (38.2%) of gastric cancer, 5 out of 40 cases (12.5%) of chronic gastritis, 6 out of 30 cases (20%) of intestinal metaplasia, and 5 out of 20 cases (25.0%) of dysplasia (Table 2).

The clinicopathological characteristics of mtMSI-positive cases were compared with those of cases that were mtMSI-negative (Table 3). An association of mtMSI with intestinal histological type and distal location was found ($P=0.001$ and $P=0.002$), whereas no significant correlation was found between mtMSI and age at diagnosis, sex, tumor size, depth of invasion, lymph node spread and clinical stages ($P>0.05$).

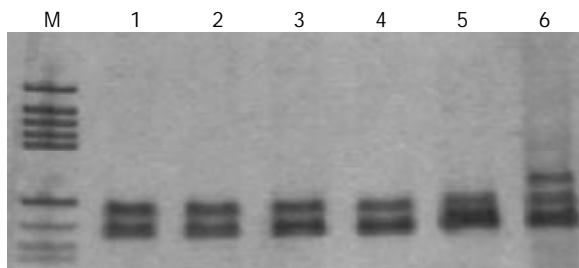


Figure 1 Detection of mitochondrial DNA microsatellite instability in gastric cancer by PCR-single strand conformation polymorphism. Lane 6 indicates conformational variants associated with mitochondrial DNA microsatellite instability.

Table 2 mtMSI in gastric cancer and its precursor

	<i>n</i>	mtMSI(%)
Chronic gastritis	40	5(12.5)
Intestinal metaplasia	30	6(20.0)
Dysplasia	20	5(25.0)
Gastric cancer	68	26(38.2)

Table 3 Characteristics of 68 gastric cancer patients

Characteristic	<i>n</i>	mtMSI-positive	tMSI-negative
Age			
<40 years	15	5	10
>40 years	53	21	32
Sex			
Male	42	15	27
Female	26	11	15
Size			
<5 cm	38	14	24
>5 cm	30	12	18
Histological type			
Intestinal	41	22 ^b	19
Diffuse	27	4	23
Tumor location			
Distal	45	23 ^c	22
Proximal	23	3	20
Invasion			
Within the wall	33	12	21
Invading serosa	35	14	21
Lymph node spread			
Absent	30	11	19
Present	38	15	23

^b $P=0.001$ vs the groups of diffuse type and ^c $P=0.002$ vs the groups of proximal location.

DISCUSSION

Carcinogenesis is a long-term, multistep process driven by multiple genetic and epigenetic changes in susceptible cells, which gain a selective growth advantage and undergo clonal expansion. Genetic instability is an important factor in the rapid accumulation of these genetic changes. Much attention has been directed to the genetic events in nDNA, such as activation of oncogenes, inactivation of tumor suppressor genes, and defects of mismatched DNA repair genes^[13,14]. However, several aspects in the process of carcinogenesis are still unclear. It has been shown that somatic mutations in mtDNA were detected in various human tumors^[15-18]. In addition, microsatellite instability has also been shown in mtDNA of colorectal and gastric carcinomas^[18-20]. Further studies demonstrated that repeated mononucleotide alteration, missense mutation, and small deletion in NADH dehydrogenase genes and alteration in polycytidine (C)_n tract in the D-loop region of mtDNA could occur in colorectal carcinomas^[18]. These results imply that mtMSI of colorectal carcinomas may likely result from certain deficiencies in DNA repair. Therefore, it has been proposed that somatic mutations and mtMSI play a role in tumorigenesis and development of cancer^[21,22]. To study the role of mtMSI in gastric carcinogenesis, we analyzed 68 cases of gastric cancer using seven microsatellite markers known to be altered in gastrointestinal carcinomas. MtMSI was found in 38.2% of patients with gastric cancer, implying that mtMSI may play an important role in the occurrence of a part of gastric cancers.

The majority of gastric carcinomas, particularly the "intestinal" type, which is most common in populations at high risk, were preceded by a precancerous stage, characterized by the following sequential steps, namely chronic gastritis, intestinal metaplasia, and dysplasia^[23,24]. Although numerous cytogenetic and molecular genetic studies have been performed on gastric adenocarcinomas, fundamental data pertaining to precursor lesions which could substantially clarify our understanding of the tumorigenesis in gastric mucosa are not available. This is the first study to examine the frequency of mtMSI in intestinal metaplasia and dysplasia, two premalignant lesions of gastric cancer in individuals without gastric cancer. If mtMSI plays an early and significant role in gastric carcinogenesis, one might expect to find mtMSI in metaplastic and dysplasia tissues before the development of cancer. In this study, mtMSI was detected in 12.5% of chronic gastritis, 20.0% of intestinal metaplasia, and 38.2% of gastric cancer tissues examined. These findings showed a sequential accumulation of mtMSI in the histological progression from chronic gastritis to cancer via intestinal metaplasia and dysplasia, suggesting an early and important role of mtMSI in the gastric carcinogenesis pathway, and they may define a subset of individuals susceptible to gastric cancer.

Cancers from different mutational pathways are thought to have different clinical features. nMSI+ gastric cancer was characterized by older age, antral location, intestinal type, lower prevalence of lymph node metastasis, and a lower pTNM stage^[25,26]. However, the clinicopathologic characteristics of mtMSI+ gastric cancers remain unclear. In the current study, we did not find an obvious relationship between mtMSI and tumor size, depth of invasion, node metastasis or clinical stages, indicating a limited role of mtMSI in predicting the prognosis of gastric carcinomas. Gastric carcinomas can be divided into "intestinal" type and "diffuse" type. A distinct genetic pathway has been found in gastric carcinogenesis of different histological subtypes and their tumor progression^[27-29]. Increased beta-catenin mRNA levels and mutational alterations of APC and beta-catenin gene were present in intestinal type gastric cancer^[30,31], whereas epigenetic inactivation of E-cadherin via promoter hypermethylation might be an early critical event

in the development of undifferentiated tumors^[32-35]. In this study, a marked difference in mtMSI was noted in gastric cancer. MtMSI was much more frequent in intestinal-type gastric cancers as compared with diffuse-type gastric cancer, suggesting that mtMSI is a predisposing event in intestinal type of gastric cancer. In contrast to mtMSI-negative gastric cancer, mtMSI-positive gastric tumors tended to exhibit a predominant distal location, similar to nMSI-positive gastric tumors.

The mechanisms underlying mtMSI in gastric mucosa remain unclear. In gastric mucosa, reactive oxygen species (ROS) are commonly released in inflamed gastric mucosa as a result of infection with *Helicobacter pylori* (*H. pylori*), especially CagA+ strains, and they might be responsible for mtMSI-positive gastric cancer^[36-38]. Mitochondrial genome was particularly susceptible to oxidative damage and mutation because of the high rate of ROS generation and inefficient DNA repair system in the organelle^[39,40]. ROS and defective DNA repair were the two causes of increased damage proposed to explain mtMSI in *H. pylori*-associated gastric cancer^[41-43]. A possibly important role of *H. pylori* in the development of mtMSI-positive gastric cancer needed to be further studied.

Although gastric cancer is a common disease, molecular markers for its early diagnosis are lacking. Mitochondrial DNA mutations occurred in a wide variety of cancers and might be useful in the detection of cancer^[44]. Indeed, some authors have implied that mitochondrial genome instability is so common and the enrichment of mutations in cancer is so significant that some mutations probably confer a selective or replicative advantage to those cells that have acquired such mutations^[21]. Others have suggested that mtDNA mutations may enhance the toxicity of anti-cancer treatments^[45-48]. Thus, the existence of mtDNA mutations in cancer may impact diagnosis and treatment and may be important in understanding the progression of some cancers. Given the early involvement of mtMSI in the multistep gastric carcinogenesis model, detection of mtMSI could serve as a surrogate marker for the risk of gastric cancer development^[49]. It might help to identify high-risk patient, by determining mtMSI of preneoplastic lesions, such that close monitoring or potential intervention can be performed. Because the majority of patients with intestinal metaplasia and dysplasia will not progress to cancer and only a proportion of these patients harbor mtMSI, it is conceivable that patients with intestinal metaplasia and dysplasia displaying mtMSI are at greater risk of developing gastric cancer than those without mtMSI.

In conclusion, a high frequency of mtMSI can be found in gastric cancer and its premalignant lesions. Taking into consideration of the progressive increase in mtMSI frequency from premalignant to malignant lesions, our results suggest the early involvement and continuous accumulation of mtMSI in gastric cells that have entered the multistep gastric carcinogenesis pathway. The role of mtMSI in premalignant gastric lesions as a surrogate marker of the risk of gastric cancer development warrants further investigation.

REFERENCES

- Lengauer C, Kinzler KW, Vogelstein B. Genetic instability in colorectal cancers. *Nature* 1997; **386**:623-627
- Thibodeau SN, Bren G, Schaid D. Microsatellite instability in cancer of the proximal colon. *Science* 1993; **260**: 816-819
- Ionov Y, Peinado MA, Malkhosyan S, Shibata D, Perucho M. Ubiquitous somatic mutations in simple repeated sequences reveal a new mechanism for colonic carcinogenesis. *Nature* 1993; **363**: 558-561
- Vogelstein B, Fearon ER, Hamilton SR, Kern SE, Preisinger AC, Leppert M, Nakamura Y, White R, Smits AM, Bos JL. Genetic alterations during colorectal-tumor development. *N Engl J Med* 1988; **319**: 525-532
- Fearon ER, Vogelstein B. A genetic model for colorectal tumorigenesis. *Cell* 1990; **61**: 759-767
- Jen J, Kim H, Piantadosi S, Liu ZF, Levitt RC, Sistonen P, Kinzler KW, Vogelstein B, Hamilton SR. Allelic loss of chromosome 18q and prognosis in colorectal cancer. *N Engl J Med* 1994; **331**: 213-221
- White RL. Tumor suppressing pathways. *Cell* 1998; **92**: 591-592
- Fang DC, Jass JR, Wang DX, Zhou XD, Luo YH, Young J. Infrequent loss of heterozygosity of APC/MCC and DCC genes in gastric cancer showing DNA microsatellite instability. *J Clin Pathol* 1999; **52**: 504-508
- Fang DC, Yang SM, Zhou XD, Wang DX, Luo YH. Telomere erosion is independent of microsatellite instability but related to loss of heterozygosity in gastric cancer. *World J Gastroenterol* 2001; **7**: 522-526
- Martins C, Kedda MA, Kew MC. Characterization of six tumor suppressor genes and microsatellite instability in hepatocellular carcinoma in southern African blacks. *World J Gastroenterol* 1999; **5**: 470-476
- Wu BP, Zhang YL, Zhou DY, Gao CF, Lai ZS. Microsatellite instability, MMR gene expression and proliferation kinetics in colorectal cancer with familial predisposition. *World J Gastroenterol* 2000; **6**: 902-905
- Habano W, Nakamura S, Sugai T. Microsatellite instability in the mitochondrial DNA of colorectal carcinomas: evidence for mismatch repair systems in mitochondrial genome. *Oncogene* 1998; **17**: 1931-1937
- Fang DC, Wang RQ, Yang SM, Yang JM, Liu HF, Peng GY, Xiao TL, Luo YH. Mutation and methylation of hMLH1 in gastric carcinomas with microsatellite instability. *World J Gastroenterol* 2003; **9**: 655-659
- Fang DC, Luo YH, Yang SM, Li XA, Ling XL, Fang L. Mutation analysis of APC gene in gastric cancer with microsatellite instability. *World J Gastroenterol* 2002; **8**: 787-791
- Fliiss MS, Usadel H, Caballero OL, Wu L, Buta MR, Eleff SM, Jen J, Sidransky D. Facile detection of mitochondrial DNA mutations in tumors and bodily fluids. *Science* 2000; **287**: 2017-2019
- Richard SM, Bailliet G, Paez GL, Bianchi MS, Peltomaki P, Bianchi NO. Nuclear and mitochondrial genome instability in human breast cancer. *Cancer Res* 2000; **60**: 4231-4237
- Yeh JJ, Lunetta KL, van Orsouw NJ, Moore FD Jr, Mutter GL, Vij J, Dahia PL, Eng C. Somatic mitochondrial DNA (mtDNA) mutations in papillary thyroid carcinomas and differential mtDNA sequence variants in cases with thyroid tumours. *Oncogene* 2000; **19**: 2060-2066
- Habano W, Sugai T, Yoshida T, Nakamura S. Mitochondrial gene mutation, but not large-scale deletion, is a feature of colorectal carcinomas with mitochondrial microsatellite instability. *Int J Cancer* 1999; **83**: 625-629
- Habano W, Sugai T, Nakamura SI, Uesugi N, Yoshida T, Sasou S. Microsatellite instability and mutation of mitochondrial and nuclear DNA in gastric carcinoma. *Gastroenterology* 2000; **118**: 835-841
- Maximo V, Soares P, Seruca R, Rocha AS, Castro P, Sobrinho-Simoes M. Microsatellite instability, mitochondrial DNA large deletions, and mitochondrial DNA mutations in gastric carcinoma. *Genes Chromosomes Cancer* 2001; **32**: 136-143
- Hochhauser D. Relevance of mitochondrial DNA in cancer. *Lancet* 2000; **356**: 181-182
- Liu MR, Pan KF, Li ZF, Wang Y, Deng DJ, Zhang L, Lu YY. Rapid screening mitochondrial DNA mutation by using denaturing high-performance liquid chromatography. *World J Gastroenterol* 2002; **8**: 426-430
- Correa P, Shiao YH. Phenotypic and genotypic events in gastric carcinogenesis. *Cancer Res* 1994; **54**(7 Suppl): 1941s-1943s
- Leung WK, Kim JJ, Kim JG, Graham DY, Sepulveda AR. Microsatellite instability in gastric intestinal metaplasia in patients with and without gastric cancer. *Am J Pathol* 2000; **156**: 537-543
- Wu MS, Lee CW, Shun CT, Wang HP, Lee WJ, Chang MC, Sheu JC, Lin JT. Distinct clinicopathologic and genetic profiles in sporadic gastric cancer with different mutator phenotypes. *Genes Chromosomes Cancer* 2000; **27**: 403-411
- Wu MS, Chang MC, Huang SP, Tseng CC, Sheu JC, Lin YW, Shun CT, Lin MT, Lin JT. Correlation of histologic subtypes and replication error phenotype with comparative genomic hybrid-

- ization in gastric cancer. *Genes Chromosomes Cancer* 2001; **30**: 80-86
- 27 **Wu MS**, Shun CT, Wang HP, Sheu JC, Lee WJ, Wang TH, Lin JT. Genetic alterations in gastric cancer: relation to histological subtypes, tumor stage, and *Helicobacter pylori* infection. *Gastroenterology* 1997; **112**: 1457-1465
 - 28 **Endoh Y**, Sakata K, Tamura G, Ohmura K, Ajioka Y, Watanabe H, Motoyama T. Cellular phenotypes of differentiated-type adenocarcinomas and precancerous lesions of the stomach are dependent on the genetic pathways. *J Pathol* 2000; **191**: 257-263
 - 29 **Ohmura K**, Tamura G, Endoh Y, Sakata K, Takahashi T, Motoyama T. Microsatellite alterations in differentiated-type adenocarcinomas and precancerous lesions of the stomach with special reference to cellular phenotype. *Hum Pathol* 2000; **31**: 1031-1035
 - 30 **Ebert MP**, Fei G, Kahmann S, Muller O, Yu J, Sung JJ, Malfertheiner P. Increased beta-catenin mRNA levels and mutational alterations of the APC and beta-catenin gene are present in intestinal-type gastric cancer. *Carcinogenesis* 2002; **23**: 87-91
 - 31 **Park WS**, Oh RR, Park JY, Lee SH, Shin MS, Kim YS, Kim SY, Lee HK, Kim PJ, Oh ST, Yoo NJ, Lee JY. Frequent somatic mutations of the beta-catenin gene in intestinal-type gastric cancer. *Cancer Res* 1999; **59**: 4257-4260
 - 32 **Tamura G**, Sato K, Akiyama S, Tsuchiya T, Endoh Y, Usuba O, Kimura W, Nishizuka S, Motoyama T. Molecular characterization of undifferentiated-type gastric carcinoma. *Lab Invest* 2001; **81**: 593-598
 - 33 **Becker KF**, Atkinson MJ, Reich U, Becker I, Nekarda H, Siewert JR, Hofler H. E-cadherin gene mutations provide clues to diffuse type gastric carcinomas. *Cancer Res* 1994; **54**: 3845-3852
 - 34 **Ascano JJ**, Frierson H Jr, Moskaluk CA, Harper JC, Roviello F, Jackson CE, El-Rifai W, Vindigni C, Tosi P, Powell SM. Inactivation of the E-cadherin gene in sporadic diffuse-type gastric cancer. *Mod Pathol* 2001; **14**: 942-949
 - 35 **Machado JC**, Oliveira C, Carvalho R, Soares P, Berx G, Caldas C, Seruca R, Carneiro F, Sobrinho-Simoes M. E-cadherin gene (CDH1) promoter methylation as the second hit in sporadic diffuse gastric carcinoma. *Oncogene* 2001; **20**: 1525-1528
 - 36 **Wu AH**, Crabtree JE, Bernstein L, Hawtin P, Cockburn M, Tseng CC, Forman D. Role of *Helicobacter pylori* CagA+ strains and risk of adenocarcinoma of the stomach and esophagus. *Int J Cancer* 2003; **103**: 815-821
 - 37 **Farinati F**, Cardin R, Degan P, Rugge M, Mario FD, Bonvicini P, Naccarato R. Oxidative DNA damage accumulation in gastric carcinogenesis. *Gut* 1998; **42**: 351-356
 - 38 **Drake IM**, Mapstone NP, Schorah CJ, White KL, Chalmers DM, Dixon MF, Axon AT. Reactive oxygen species activity and lipid peroxidation in *Helicobacter pylori* associated gastritis: relation to gastric mucosal ascorbic acid concentrations and effect of *H pylori* eradication. *Gut* 1998; **42**: 768-771
 - 39 **Yakes FM**, Van Houten B. Mitochondrial DNA damage is more extensive and persists longer than nuclear DNA damage in human cells following oxidative stress. *Proc Natl Acad Sci U S A* 1997; **94**: 514-519
 - 40 **Li JM**, Cai Q, Zhou H, Xiao GX. Effects of hydrogen peroxide on mitochondrial gene expression of intestinal epithelial cells. *World J Gastroenterol* 2002; **8**: 1117-1122
 - 41 **Bagchi D**, McGinn TR, Ye X, Bagchi M, Krohn RL, Chatterjee A, Stohs SJ. *Helicobacter pylori*-induced oxidative stress and DNA damage in a primary culture of human gastric mucosal cells. *Dig Dis Sci* 2002; **47**: 1405-1412
 - 42 **Shimoyama T**, Fukuda S, Liu Q, Nakaji S, Fukuda Y, Sugawara K. Production of chemokines and reactive oxygen species by human neutrophils stimulated by *Helicobacter pylori*. *Helicobacter* 2002; **7**: 170-174
 - 43 **Bohr VA**, Stevnsner T, de Souza-Pinto NC. Mitochondrial DNA repair of oxidative damage in mammalian cells. *Gene* 2002; **286**: 127-134
 - 44 **Bianchi NO**, Bianchi MS, Richard SM. Mitochondrial genome instability in human cancers. *Mutat Res* 2001; **488**: 9-23
 - 45 **Shen ZY**, Shen J, Li QS, Chen CY, Chen JY, Zeng Y. Morphological and functional changes of mitochondria in apoptotic esophageal carcinoma cells induced by arsenic trioxide. *World J Gastroenterol* 2002; **8**: 31-35
 - 46 **Peters U**, Preisler-Adams S, Lanvers-Kaminsky C, Jurgens H, Lamprecht-Dinnesen A. Sequence variations of mitochondrial DNA and individual sensitivity to the ototoxic effect of cisplatin. *Anticancer Res* 2003; **23**: 1249-1255
 - 47 **Carew JS**, Zhou Y, Albitar M, Carew JD, Keating MJ, Huang P. Mitochondrial DNA mutations in primary leukemia cells after chemotherapy: clinical significance and therapeutic implications. *Leukemia* 2003; **17**: 1437-1447
 - 48 **Wardell TM**, Ferguson E, Chinnery PF, Borthwick GM, Taylor RW, Jackson G, Craft A, Lightowlers RN, Howell N, Turnbull DM. Changes in the human mitochondrial genome after treatment of malignant disease. *Mutat Res* 2003; **525**: 19-27
 - 49 **Hiyama T**, Tanaka S, Shima H, Kose K, Kitadai Y, Ito M, Sumii M, Yoshihara M, Shimamoto F, Haruma K, Chayama K. Somatic mutation of mitochondrial DNA in *Helicobacter pylori*-associated chronic gastritis in patients with and without gastric cancer. *Int J Mol Med* 2003; **12**: 169-174

Edited by Zhang JZ and Wang XL Proofread by Xu FM

Detection of micrometastasis of gastric carcinoma in peripheral blood circulation

Xi-Mei Chen, Guo-Yu Chen, Zhi-Rong Wang, Feng-Shang Zhu, Xiao-Lei Wang, Xia Zhang

Xi-Mei Chen, Guo-Yu Chen, Zhi-Rong Wang, Feng-Shang Zhu, Xiao-Lei Wang, Xia Zhang, Department of Gastroenterology, Tongji Hospital of Tongji University, Shanghai 200065, China
Correspondence to: Dr. Guo-Yu Chen, Department of Endoscopy, Tongji Hospital of Tongji University, 200065, Shanghai, China. cguoyu@yahoo.com.cn
Telephone: +86-21-56051080-2102
Received: 2003-07-17 **Accepted:** 2003-08-25

Abstract

AIM: To detect the micrometastasis of gastric carcinoma in peripheral blood circulation using immunomagnetic beads sorting technique and RT-PCR technique, and to discuss its significance and the difference between the two methods.

METHODS: Density gradient centrifugation was used to isolate mononuclear cells from peripheral blood, immunomagnetic beads sorting technique and RT-PCR technique were used to detect the disseminated carcinoma cells. HE, immunocytochemical and immunofluorescence staining were also used to identify the characteristics of the cells separated with immunomagnetic beads sorting technique.

RESULTS: Cells expressing cytokeratin were separated and enriched from the peripheral blood specimens of patients suffering from gastric carcinoma or chronic gastritis. After HE staining, two kinds of cells with little cytoplasm were found. Majority of these cells had small and round nuclei, even chromatin and the thickness of nuclear membrane was normal. Immunohistochemical staining indicated that there were CD34 and CD45 expression on the cell membrane of this kind of cells and these cells also showed expressed human telomerase reverse transcriptase by immunofluorescence staining, but the expression of carcinoembryonic antigen was absent. So, these cells might hematopoiesis precursors. Another kind of cells had larger and abnormal nuclei with thicker nuclear membranes. Massed chromatin and poly-nucleoli were found in the nuclei. These cells expressed human telomerase reverse transcriptase and carcinoembryonic antigen, but CD34 and CD45 were not found on the cell membrane. So, these cells were considered as gastric carcinoma cells escaping from the original focuses and existing in the peripheral blood circulation. Carcinoma cells were found in 25 of 60(41.7%) specimens of peripheral blood from patients with gastric carcinoma, while there were no such cells separated from the blood specimens of chronic gastritis patients. The difference of positive rates of disseminated carcinoma cells between two groups was markedly significant ($P < 0.005$). The expressions of CK20 mRNA in peripheral blood specimens were examined with RT-PCR. CK20 mRNA was detected from 32 of 60(53.3%) peripheral blood specimens in the group of gastric carcinoma patients, while none of the specimens from patients suffering from chronic gastritis had CK20 mRNA. Significant difference was also found between two groups ($P < 0.005$). Statistic analyses also showed that there was a significant difference

between the positive rates of two methods in detecting the disseminated carcinoma cells from the peripheral blood circulation of gastric carcinoma patients ($P < 0.05$).

CONCLUSION: The results demonstrated that there were disseminated carcinoma cells in the peripheral blood circulation of some patients with gastric carcinoma. Disseminated carcinoma cells can be detected from the peripheral blood samples with immunomagnetic beads sorting technique and RT-PCR technique. The positive rate of RT-PCR technique is higher than that of immunomagnetic beads sorting technique in detecting micrometastasis.

Chen XM, Chen GY, Wang ZR, Zhu FS, Wang XL, Zhang X. Detection of micrometastasis of gastric carcinoma in peripheral blood circulation. *World J Gastroenterol* 2004; 10(6): 804-808
<http://www.wjgnet.com/1007-9327/10/804.asp>

INTRODUCTION

Gastric carcinoma is one of the most common causes of cancer mortality in China and is responsible for approximately 160 000 deaths annually. The disease is often advanced at first presentation, and only 30-40% patients undergoing surgery have a curative resection. Metastasis and relapse are the common reasons leading to death of patients^[1-6]. During the development of malignant neoplasm of non-hematopoietic system, a few of tumor cells escape from the original focus and disseminated into the lymph system, blood circulation, bone marrow, liver, kidney and other organs, which is called micrometastasis. It cannot be detected by any routine biochemical and histopathological assays or any graphical methods such as X-ray, CT, MRI, etc.^[7-11]. At the same time, the patients have not any obvious symptoms. Minute focus would grow rapidly and develop to metastasis and relapse. So, to develop an efficient diagnostic method for the detection of micrometastasis is of great clinical significance^[12-14]. In this study, immunomagnetic beads sorting technique and RT-PCR technique were used to detect the micrometastatic carcinoma cells in peripheral blood circulation of patients suffering from gastric carcinoma; HE staining was utilized to observe the cells' morphology changes; immunocytochemical staining and immunofluorescence staining were also used to identify the characteristics of the cells separated by immunomagnetic beads sorting technique. The significance of the micrometastatic carcinoma cell detection and the difference between the two methods were also discussed.

MATERIALS AND METHODS

Specimens

Eighty specimens of peripheral blood from sixty advanced gastric cancer patients and twenty chronic gastritis patients were collected from the Department of Endoscopy of the Tongji Hospital of Tongji University. The final diagnoses of these patients were determined pathologically. The blood specimens were anti-coagulated with heparin (5 U/mL).

Separation of mononuclear cells

We carefully layered a maximum of diluted whole blood with Hank's solution over 10 mL Ficoll-Paque and centrifuged for 25 min at 2 400 r/min at room temperature, aspirated the mononuclear cells located at the plasm-Ficoll-Paque interface. We then washed the mononuclear cells once by 10 mL Hank's solution and centrifuged them at 600 r/min for 10 min.

Immunomagnetic beads separation

MACS carcinoma cell enrichment and detection kits were purchased from Miltenyi Biotech, the beads were coated with cytokeratin7 (CK7) and cytokeratin 8 (CK8). The mononuclear cells were diluted with 10 mL Dilution-Buffer and 1.3 mL MACS CellPerm Solution for 5 min. After incubated with 1.3 mL MACS CellFix solution for 30 min, the solution was centrifuged at 2 000 rpm for 10 min. Then, the sediment was mixed with 7.5 mL MACS CellStain solution and centrifuged, these two procedures were repeated again. The sediment acquired was incubated with 50 μ L MACS CellStain solution, 50 μ L FcR blocking reagent and 50 μ L MACS cytokeratin microbeads for 45 min, and after that, the mixture was centrifuged at 2 000 rpm for 5 min. The sediment was diluted with 500 μ L dilution buffer and flew through the MACS column in magnetic field. The column was washed with 500 μ L Dilution Buffer apart from magnetic field. The solution obtained included CK⁺ cells and was smeared on slides. The slides were fixed with acetone and stained with HE.

Immunocytochemical detection of CD34 and CD45 expressions in CK⁺ cells

Immunohistochemical detection of CD34 and CD45 expressions was performed through a two-step procedure and the kits were purchased from Immunotech Co.

Immunofluorescence detection for hTERT and CEA expression in CK⁺ cells

Immunofluorescence detection of human telomerase reverse transcriptase (hTERT) and carcinoembryonic antigen (CEA) expression was operated through two-step procedure and the kits were purchased from Sigma Co.

RT-PCR

Total RNA was extracted with Trizol (Gibco. Co) and resuspended in sterile RNase-free water for storage at -70 °C. RT-PCR analysis was performed as follows. RNA was incubated at 60 °C for 10 min and chilled to 4 °C immediately before being reverse transcribed. Reverse transcription of 1 μ g total RNA using antisense primers was performed in a volume of 20 μ L for 40 min at 65 °C, containing 200 U MMLV reverse transcriptase, 1 \times buffer RT, 1 MU/L RNasin, 2.0 mmol/L dNTP and 0.2 μ mol/L oligo (dT) as a primer (All primers were synthesized by Life Technology, Shanghai). The primers of CK20 and β -actin were as follows: CK20 (485 bp) upstream primer: 5' AAG GCT CTG GGA GGT GCG TCT C3', downstream primer: 5' CAG TGT TGC CCA GAT GCT TGT G3'; β -actin (317 bp) upstream primer: 5' ATC ATG TTT GAG ACC A3', downstream primer: 5' CAT CTC TTG CTC GAA GTC CA3' [15]. The samples were heated to 94 °C for 5 min to terminate the reverse transcription reaction. The amplification reaction mixture consisted of 10 \times buffer 5 μ L, 0.2 mmol/L dATP, dGTP, dCTP and dTTP respectively, 2.5 U TaqDNA polymerase, and 0.2 μ mol/L each of sense and antisense primers including CK20 and β -actin respectively in a final volume of 50 μ L. The reaction mixture was first heated at 94 °C for 5 min and amplification was carried out for 35 cycles at 94 °C for 1 min, at 58 °C for 1 min, at 72 °C for 1 min, followed by an incubation at 72 °C for 10 min. A volume of

10 μ L RT-PCR products was added in 20 g/L agarose gel containing 0.5 mg/L EB and visualized with UV illumination after electrophoresis.

Statistic analysis

Experimental results were analyzed with Chi-square tests and $P < 0.05$ was accepted as the level of significance.

RESULTS

Detection of micrometastasis by immunomagnetic sorting technique

After immunomagnetic separation, CK⁺ cells were separated in all of the peripheral blood specimens from gastric carcinoma and chronic gastritis patients. There were two kinds of cells on the slides after HE staining. Because of the application of CellPerm solution, the cytoplasm of these cells decreased obviously. One kind of these cells had small and round nuclei, even chromatin and the thickness of nuclear membrane was normal. The other kind of cells had larger nuclei, which had abnormal forms and thicker membrane. Massed chromatin and more than one nuclei could also be found in this kind of cells.

Immunocytochemical and immunofluorescence staining

Immunohistochemical staining showed that there were CD34 (Figure 1) and CD45 (Figure 2) expressions on the cell membranes of the first kind of cells and these cells also had positive expressions of hTERT (Figure 3) after immunofluorescence staining, but the expression of CEA was negative. So this kind of cells might be hematopoiesis precursors (Figure 4)^[17-20]. The other kind of cells had positive hTERT and CEA (Figure 5) expressions after immunohistochemical staining, but expression of CD34 and CD45 was absent. According to the morphology and the outcome of immunohistochemical and immunofluorescence staining, these cells were considered as the disseminated carcinoma cells escaped from the primary neoplasm focus (Figure 6)^[17,21-23]. The first kind of cells was found on all slides, while the other kind of cells was only found on the slides from some gastric carcinoma patients (25/60), the positive rate was about 41.7% (Table 1). There was a significant difference between two groups ($P < 0.005$).

Detection of micrometastasis by RT-PCR technique

CK20 mRNA was detected in 32 blood specimens from gastric carcinoma patients; the positive rate was 53.3% (Figure 7). While no CK20 mRNA was detected from the blood specimens of patients with chronic gastritis. There was a significant difference between these positive rates ($P < 0.005$, Table 2).

Table 1 Comparison of tumor cells detected with immunomagnetic beads technique

Patients	+	-	Total	%
Gastric carcinoma	25	35	60	41.7
Chronic gastritis	0	20	20	0.0
Total	25	55	80	41.7

$\chi^2=10.26$, $P < 0.005$.

Table 2 Comparison of tumor cells detected with RT-PCR

Patients	+	-	Total	%
Gastric carcinoma	32	28	60	53.3
Chronic gastritis	0	20	20	0.0
Total	32	48	80	53.3

$\chi^2=15.63$, $P < 0.005$.



Figure 1 Immunohistochemical staining showed that there was CD34 expression on the membranes of the cells, these cells had small and round nuclei, even chromatin and the thickness of nuclear membrane was normal (amplification $\times 1\,000$).



Figure 2 Immunohistochemical staining showed that there was CD45 expression on the membranes of the cells, these cells had small and round nuclei, even chromatin and the thickness of nuclear membrane was normal (amplification $\times 1\,000$).

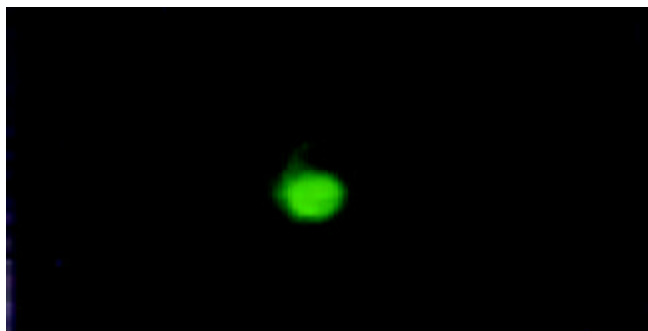


Figure 3 Immunofluorescence staining the cells, which had small and round nuclei, even chromatin and the thickness of nuclear membrane was normal (amplification $\times 200$), had positive expressions of hTERT.

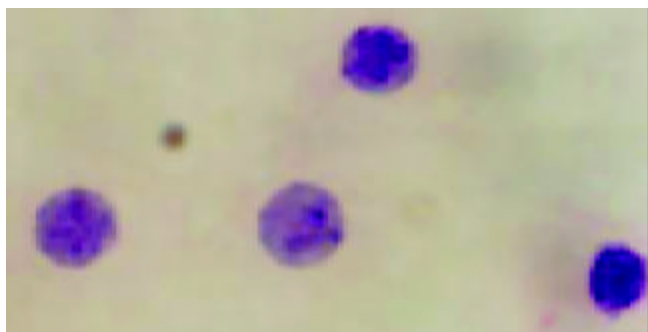


Figure 4 The cells, which had small and round nuclei, even chromatin and the thickness of nuclear membrane was normal (HE staining, amplification $\times 1\,000$), might be hematopoiesis precursors.

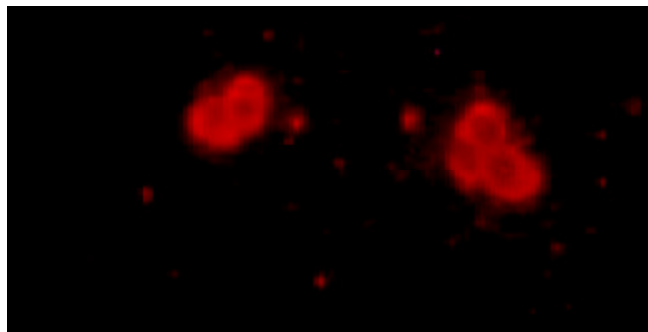


Figure 5 The cells, which had larger nuclei, abnormal forms and thicker membrane, and massed chromatin and more than one nuclei could also be found in this kind of cells, had positive expression of CEA (Immunofluorescence staining, amplification $\times 200$).

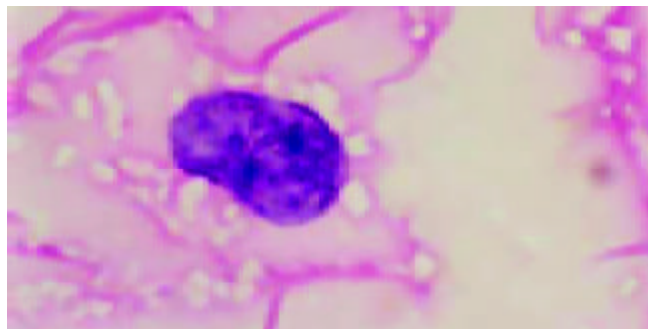


Figure 6 The cells, which had larger nuclei, abnormal forms and thicker membrane, and massed chromatin and more than one nuclei could also be found in this kind of cells, had positive expressions of CEA and hTERT, and negative expressions of CD34 and CD45, were considered as the disseminated carcinoma cells escaped from the primary neoplasm focus (HE staining, amplification $\times 1\,000$).

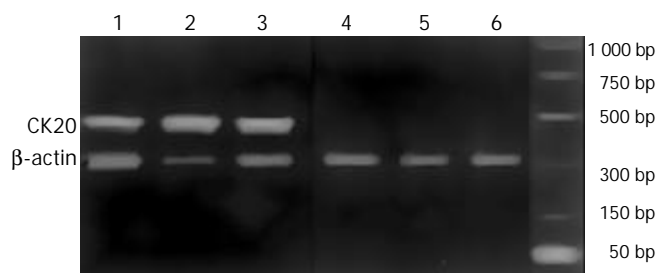


Figure 7 RT-PCR for CK20 and β -actin. M: Marker; Lanes1-4 blood from gastric cancer; Lanes5-6 blood from chronic gastritis.

Difference between positive rates of these two methods

Statistic analysis indicated that the difference between the positive rates of these two methods which were used to detect the disseminated carcinoma cells was significant ($P < 0.05$, Table 3), that is to say the positive rate of RT-PCR was higher than that of immunomagnetic bead separation technique.

Table 3 Comparison of positive rates between two methods

RT-PCR	Immunomagnetic bead separation		Total
	+	-	
+	25	7	32
-	0	28	28
Total	25	35	60

$\chi^2 = 5.14$, $P < 0.05$.

DISCUSSION

The first reporter of micrometastasis is Ashworth who claimed that he had found cells similar to tumor cells from the peripheral blood circulation of a carcinoma patient in 1869. After that more than twenty methods have been used to detect micrometastasis on about 5 000 patients. But the latest researches indicated that those so called tumor cells were components of hematopoietic tissues, especially prokaryotic cells^[24,25].

In this study, immunomagnetic beads sorting technique and RT-PCR technique were used to detect the micrometastatic gastric carcinoma cells from peripheral blood circulation and the difference of these two methods was also discussed. There are many components in peripheral blood. It has been found that tumor cells had the similar density with mononuclear cells and they located in the same layer after density gradient centrifugation^[26,27]. So we removed about 90% hemocytes from blood specimens with Ficoll's solution and mononuclear cells mixed with carcinoma cells were enriched. Because gastric carcinoma is derived from epithelial tissue, so carcinoma cells could express CK, a particular component of epithelial tissue^[28,29]. To separate micrometastatic gastric carcinoma cells expressing CK, immunomagnetic beads coated with anti-CK7 and anti-CK8 antibodies were used to incubate or those mononuclear cells that had been reacted with MACS CellPerm. Anti-CK7 and anti-CK8 antibodies combined with CK in the plasma of carcinoma cells by antigen-antibody reaction. So, the cells expressing CK combined with magnetic beads and detained in the magnetic field. To define the origin and characteristics of these cells, HE, immunocytochemical and immunofluorescence staining were performed. Two kinds of cells were separated after staining. Majority of these cells had small and round nuclei, and their chromatins were even. These cells' nuclear membranes had normal thickness and expressed CD34 and CD45. They also expressed hTERT, but no CEA. Normally, CD34 and CD45 in hematopoiesis precursors, could also express hTERT^[30-32]. So, these cells might be hematopoietic precursors. Minority of these cells had larger and abnormal forms of nuclei that had thicker nuclear membrane. Massive chromatins could be observed in these cells. These cells expressed hTERT and CEA, but the expressions of CD34 and CD45 were absent on the membrane of cells. Usually, hTERT and CEA could be found in tumor cells and CEA was a marker of carcinoma derived from digestive tract^[33-35], so these cells were gastric carcinoma cells escaped from the primary focuses and existed in peripheral blood circulation. This kind of cells was detected from 25 of 60 patients suffering from gastric carcinoma, while no cells were acquired from chronic gastritis patients.

CK is a component of cell skeleton and distributes in cells deriving from ectoderm. CK20, a member of this family has been found to have a stricter selectivity to epithelial tissue^[28,36]. CK8 and CK9 mRNA could be detected in blood circulation with nested RT-PCR in healthy subjects, but CK20 mRNA could not be detected^[37]. In this study, anti-CK7 and anti-CK8 but not anti-CK20 antibodies were coated on the beads, this should take responsibility for the separation of those hematopoietic precursors in the process of immunomagnetic beads sorting. If the immunomagnetic beads were coated with CK20, cells derived from epithelial tissue would be separated from hemocytes. These cells should be gastric carcinoma cells escaped from primary gastric carcinoma focus. Traditional methods for detecting disseminated tumor cells such as cell morphology, flowcytometer and cytogenetics were not so sensitive^[38-40]. It has been found that immunomagnetic beads sorting technique has a high sensitivity to 1/10⁵^[41], but it has a complicated procedure and a high cost and is not so practical in clinical application. In recent years, convenient RT-PCR was invented and it has a high efficiency in detecting the

micrometastasis of peripheral blood circulation, bone marrow, lymph tract and peritoneal cavity. It could detect one tumor cell diluted with one-milliliter body fluid or one gram tissue and it has been presently regarded as the most effective method to detect the disseminated carcinoma cells^[42].

In this study, RT-PCR was also used to detect micrometastatic gastric carcinoma cells. According to the researches of Soeth and Burchill^[15,37], CK20 was selected as the target gene for amplification. Because of the RNase existing in blood circulation, mRNA free to live cells would be decomposed rapidly. This means that there were live cells expressing CK20 mRNA existing in blood specimens when CK20 mRNA was detected from the peripheral blood circulation of patients. On the other hand, hemocytes came from mesoderm and there were no epithelial cells in blood circulation. So, when CK20 was amplified from blood circulation, there must be tumor cells in the specimen. If the specimen was extracted from a gastric carcinoma patient, the tumor cells might be gastric carcinoma cells. In this study, CK20 mRNA was detected from 32 of 60 specimens extracted from gastric carcinoma patients, but not from patients with chronic gastritis. This also confirmed that there were carcinoma cells in the peripheral blood circulation of gastric carcinoma patients.

Statistical analysis also indicated that the positive rate of detection of disseminated carcinoma cells with RT-PCR technique was higher than that with immunomagnetic beads sorting technique. This might be related with the high sensitivity of RT-PCR, which cell morphology and immunocytochemistry could not possess^[43,44]. On the other hand, it is cheaper in detecting disseminated carcinoma cells with RT-PCR than immunomagnetic beads sorting technique, so it is more worthy of clinical practice. Immunomagnetic beads sorting technique could directly separate micrometastatic carcinoma cells with high behaviors of metastasis. Those tumor cells separated with immunomagnetic beads sorting technique could be cultured and the characteristics of the cells could be determined, so it is more valuable for further research^[45].

In conclusion, our results indicate that there are micrometastatic carcinoma cells in the peripheral blood circulation of patients suffering from gastric carcinoma. Immunomagnetic beads sorting technique and RT-PCR technique can detect the disseminated carcinoma cells in the peripheral blood circulation. RT-PCR technique has a higher positive rate and a lower cost than immunomagnetic beads sorting technique, so it is worthy of clinical practice. Immunomagnetic beads sorting technique can directly separate carcinoma cells, so this method is more valuable for research work.

REFERENCES

- Zhou Y**, Gao SS, Li YX, Fan ZM, Zhao X, Qi YJ, Wei JP, Zou JX, Liu G, Jiao LH, Bai YM, Wang LD. Tumor suppressor gene p16 and Rb expression in gastric cardia precancerous lesions from subjects at a high incidence area in northern China. *World J Gastroenterol* 2002; **8**: 423-425
- Cai L**, Yu SZ, Zhan ZF. Cytochrome p450 2E1 genetic polymorphism and gastric cancer in Changle, Fujian Province. *World J Gastroenterol* 2001; **7**: 792-795
- Su M**, Lu SM, Tian DP, Zhao H, Li XY, Li DR, Zheng ZC. Relationship between ABO blood groups and carcinoma of esophagus and cardia in Chaoshan inhabitants of China. *World J Gastroenterol* 2001; **7**: 657-661
- Cai L**, Yu SZ, Zhang ZF. Glutathione S-transferases M1, T1 genotypes and the risk of gastric cancer: A case-control study. *World J Gastroenterol* 2001; **7**: 506-509
- Xin Y**, Li XL, Wang YP, Zhang SM, Zheng HC, Wu DY, Zhang YC. Relationship between phenotypes of cell function differentiation and pathobiological behavior of gastric carcinomas. *World J Gastroenterol* 2001; **7**: 53-59
- Wang RT**, Wang T, Chen K, Wang JY, Zhang JP, Lin SR, Zhu

- YM, Zhang WM, Cao YX, Zhu CW, Yu H, Cong YJ, Zheng S, Wu BQ. *Helicobacter pylori* infection and gastric cancer: evidence from a retrospective cohort study and nested case-control study in China. *World J Gastroenterol* 2002; **8**: 1103-1107
- 7 **Yin T**, Ji XL, Shen MS. Relationship between lymph node sinuses with blood and lymphatic metastasis of gastric cancer. *World J Gastroenterol* 2003; **9**: 40-43
 - 8 **Zhou YN**, Xu CP, Han B, Li M, Qiao L, Fang DC, Yang JM. Expression of E-cadherin and beta-catenin in gastric carcinoma and its correlation with the clinicopathological features and patient survival. *World J Gastroenterol* 2002; **8**: 987-993
 - 9 **Culp LA**, Lin W, Kleinman NR, O' Connor KL, Lechner R. Earliest steps in primary tumor formation and micrometastasis resolved with histochemical markers of gene-tagged tumor cells. *J Histochem Cytochem* 1998; **46**: 557-568
 - 10 **Funke I**, Schraut W. Meta-analyses of studies on bone marrow micrometastases: an independent prognostic impact remains to be substantiated. *J Clin Oncol* 1998; **16**: 557-566
 - 11 **Timar J**, Csuka O, Orosz Z, Jeney A, Kopper L. Molecular pathology of tumor metastasis. *Pathol Oncol Res* 2002; **8**: 204-219
 - 12 **Schleiermacher G**, Peter M, Oberlin O, Philip T, Rubie H, Mechinaud F, Sommelet-Olive D, Landman-Parker J, Bours D, Michon J, Delattre O. Increased risk of systemic relapses associated with bone marrow micrometastasis and circulating tumor cells in localized ewing tumor. *J Clin Oncol* 2003; **21**: 85-91
 - 13 **Kakeji Y**, Maehara Y, Shibahara K, Hasuda S, Tokunaga E, Oki E, Sugimachi K. Clinical significance of micrometastasis in bone marrow of patients with gastric cancer and its relation to angiogenesis. *Gastric Cancer* 1999; **2**: 46-51
 - 14 **Zhao A**, Li J, Sun W. Detection and significance of lymph node micrometastases in patients with histologically node-negative gastric carcinoma. *Zhonghua Zhongliu Zazhi* 2000; **22**: 222-224
 - 15 **Soeth E**, Roder C, Juhl H, Kruger U, Kremer B, Kalthoff H. The detection of disseminated tumor cells in bone marrow from colorectal-cancer patients by a cytokeratin-20-specific nested reverse-transcriptase-polymerase-chain reaction is related to the stage of disease. *Int J Cancer* 1996; **69**: 278-282
 - 16 **Van der Velde-Zimmermann D**, Roijers JF, Bouwens-Rombouts A, De Weger RA, De Graaf PW, Tilanus MG, Van den Tweel JG. Molecular test for the detection of tumor cells in blood and sentinel nodes of melanoma patients. *Am J Pathol* 1996; **149**: 759-764
 - 17 **Cima F**, Matozzo V, Marin MG, Ballarin L. Haemocytes of the clam *Tapes philippinarum* (Adams & Reeve, 1850): morphofunctional characterisation. *Fish Shellfish Immunol* 2000; **10**: 677-693
 - 18 **Kruger W**, Datta C, Badbaran A, Togel F, Gutensohn K, Carrero I, Kroger N, Janicke F, Zander AR. Immunomagnetic tumor cell selection-implications for the detection of disseminated cancer cells. *Transfusion* 2000; **40**: 1489-1493
 - 19 **Xing J**, Zhan WB, Zhou L. Endoenzymes associated with haemocyte types in the scallop (*Chlamys farreri*). *Fish Shellfish Immunol* 2002; **13**: 271-278
 - 20 **Anggraeni MS**, Owens L. The haemocytic origin of lymphoid organ spheroid cells in the penaeid prawn *Penaeus monodon*. *Dis Aquat Organ* 2000; **40**: 85-92
 - 21 **Oertel J**, Huhn D. Immunocytochemical methods in haematology and oncology. *J Cancer Res Clin Oncol* 2000; **126**: 425-440
 - 22 **Hu XC**, Wang Y, Shi DR, Loo TY, Chow LW. Immunomagnetic tumor cell enrichment is promising in detecting circulating breast cancer cells. *Oncology* 2003; **64**: 160-165
 - 23 **Benez A**, Geiselhart A, Handgretinger R, Schiebel U, Fierlbeck G. Detection of circulating melanoma cells by immunomagnetic cell sorting. *J Clin Lab Anal* 1999; **13**: 229-233
 - 24 **Noack F**, Schmitt M, Bauer J, Helmecke D, Kruger W, Thorban S, Sandherr M, Kuhn W, Graeff H, Harbeck N. A new approach to phenotyping disseminated tumor cells: methodological advances and clinical implications. *Int J Biol Markers* 2000; **15**: 100-104
 - 25 **Woitats RP**, Petersen U, Moshage D, Brackmann HH, Matz B, Sauerbruch T, Spengler U. HCV-specific cytokine induction in monocytes of patients with different outcomes of hepatitis C. *World J Gastroenterol* 2002; **8**: 562-566
 - 26 **Meier V**, Mihm S, Braun Wietzke P, Ramadori G. HCV-RNA positivity in peripheral blood mononuclear cells of patients with chronic HCV infection: does it really mean viral replication? *World J Gastroenterol* 2001; **7**: 228-234
 - 27 **Su Q**, Fu Y, Liu YF, Zhang W, Liu J, Wang CM. Laminin induces the expression of cytokeratin 19 in hepatocellular carcinoma cells growing in culture. *World J Gastroenterol* 2003; **9**: 921-929
 - 28 **Natsugoe S**, Nakashima S, Matsumoto M, Nakajo A, Miyazono F, Kijima F, Ishigami S, Aridome K, Hokita S, Baba M, Takao S, Aikou T. Para-aortic lymph node micrometastasis and tumor cell microinvolvement in advanced gastric carcinoma. *Gastric Cancer* 1999; **2**: 179-185
 - 29 **Song ZJ**, Gong P, Wu YE. Relationship between the expression of iNOS, VEGF, tumor angiogenesis and gastric cancer. *World J Gastroenterol* 2002; **8**: 591-595
 - 30 **Li HX**, Chang XM, Song ZJ, He SX. Correlation between expression of cyclooxygenase-2 and angiogenesis in human gastric adenocarcinoma. *World J Gastroenterol* 2003; **9**: 674-677
 - 31 **Yao XX**, Yin L, Sun ZC. The expression of hTERT mRNA and cellular immunity in gastric cancer and precancerosis. *World J Gastroenterol* 2002; **8**: 586-590
 - 32 **Shen ZY**, Xu LY, Li EM, Cai WJ, Chen MH, Shen J, Zeng Y. Telomere and telomerase in the initial stage of immortalization of esophageal epithelial cell. *World J Gastroenterol* 2002; **8**: 357-362
 - 33 **Hu JK**, Chen ZX, Zhou ZG, Zhang B, Tian J, Chen JP, Wang L, Wang CH, Chen HY, Li YP. Intravenous chemotherapy for resected gastric cancer: meta-analysis of randomized controlled trials. *World J Gastroenterol* 2002; **8**: 1023-1028
 - 34 **Cui JH**, Krueger U, Henne-Bruns D, Kremer B, Kalthoff H. Orthotopic transplantation model of human gastrointestinal cancer and detection of micrometastases. *World J Gastroenterol* 2001; **7**: 381-386
 - 35 **Chausovsky G**, Luchansky M, Figer A, Shapira J, Gottfried M, Novis B, Bogelman G, Zemer R, Zimlichman S, Klein A. Expression of cytokeratin 20 in the blood of patients with disseminated carcinoma of the pancreas, colon, stomach, and lung. *Cancer* 1999; **86**: 2398-2405
 - 36 **Burchill SA**, Selby PJ. Molecular detection of low-level disease in patients with cancer. *J Pathol* 2000; **190**: 6-14
 - 37 **Huang MS**, Wang TJ, Liang CL, Huang HM, Yang IC, Yi-Jan H, Hsiao M. Establishment of fluorescent lung carcinoma metastasis model and its real-time microscopic detection in SCID mice. *Clin Exp Metastasis* 2002; **19**: 359-368
 - 38 **Su LD**, Lowe L, Bradford CR, Yahanda AI, Johnson TM, Sondak VK. Immunostaining for cytokeratin 20 improves detection of micrometastatic Merkel cell carcinoma in sentinel lymph nodes. *J Am Acad Dermatol* 2002; **46**: 661-666
 - 39 **Leers MP**, Schoffelen RH, Hoop JG, Theunissen PH, Oosterhuis JW, vd Bijl H, Rahmy A, Tan W, Nap M. Multiparameter flow cytometry as a tool for the detection of micrometastatic tumour cells in the sentinel lymph node procedure of patients with breast cancer. *J Clin Pathol* 2002; **55**: 359-366
 - 40 **Burkhardt O**, Merker HJ. Phagocytosis of immunobeads by CD8 positive lymphocytes during magnetic cell sorting. *Ann Anat* 2002; **184**: 55-60
 - 41 **Sakakura C**, Hagiwara A, Shirasu M, Yasuoka R, Fujita Y, Nakanishi M, Aragane H, Masuda K, Shimomura K, Abe T, Yamagishi H. Polymerase chain reaction for detection of carcinoembryonic antigen-expressing tumor cells on milky spots of the greater omentum in gastric cancer patients: a pilot study. *Int J Cancer* 2001; **95**: 286-289
 - 42 **Okada Y**, Fujiwara Y, Yamamoto H, Sugita Y, Yasuda T, Doki Y, Tamura S, Yano M, Shiozaki H, Matsuura N, Monden M. Genetic detection of lymph node micrometastases in patients with gastric carcinoma by multiple-marker reverse transcriptase-polymerase chain reaction assay. *Cancer* 2001; **92**: 2056-2064
 - 43 **Lin JC**, Chen KY, Wang WY, Jan JS, Liang WM, Wei YH. Evaluation of cytokeratin-19 mRNA as a tumor marker in the peripheral blood of nasopharyngeal carcinoma patients receiving concurrent chemoradiotherapy. *Int J Cancer* 2002; **97**: 548-553
 - 44 **Ghossein RA**, Osman I, Bhattacharya S, Ferrara J, Fazzari M, Cordon-cardo C, Scher HI. Detection of prostatic specific membrane antigen messenger RNA using immuno bead reverse transcriptase polymerase chain reaction. *Diagn Mol Pathol* 1999; **8**: 59-65
 - 45 **Luers GH**, Hartig R, Mohr H, Hausmann M, Fahimi HD, Cremer C, Volkl A. Immuno-isolation of highly purified peroxisomes using magnetic beads and continuous immunomagnetic sorting. *Electrophoresis* 1998; **19**: 1205-1210

Effects of PI3K and p42/p44 MAPK on overexpression of vascular endothelial growth factor in hepatocellular carcinoma

Geng-Wen Huang, Lian-Yue Yang, Wei-Qun Lu

Geng-Wen Huang, Lian-Yue Yang, Wei-Qun Lu, Department of Surgery and Liver Cancer Laboratory, Xiangya Hospital, Central South University, Changsha 410008, Hunan Province, China

Supported by the grant from National Key Technologies R and D Program, No.2001BA703B04 and the grant from Hunan Province Developing Planning Committee, No.2001-907

Correspondence to: Lian-Yue Yang, MD. Department of Surgery and Liver Cancer Laboratory, Xiangya Hospital, Central South University, Changsha 410008, Hunan Province, China. lianyueyang@hotmail.com

Telephone: +86-731-4327326

Received: 2003-11-18 **Accepted:** 2003-12-08

Abstract

AIM: To study the relationship between hypoxia or epidermal growth factor (EGF) and the overexpression of vascular endothelial growth factor (VEGF) in hepatocellular carcinoma (HCC) and the signal transduction pathway of the transcription of VEGF in hepatoma cells.

METHODS: Cobalt chloride and recombinant human EGF were used to stimulate the hepatoma cell lines HepG₂. VEGF mRNA was detected by using of semi-quantitative polymerase chain reaction (RT-PCR). Specific inhibitors of phosphatidylinositol 3-kinase (PI3K) and p42/p44 mitogen activated protein kinase (MAPK) were used to observe the effects of the two kinases on the regulation of the transcription of VEGF in hepatoma cells.

RESULTS: The expression of VEGF mRNA in HepG₂ cells cultured in serum-free medium was 0.117. However, 100 μ mol/L cobalt chloride for 24 h increased the expression of VEGF mRNA and VEGF mRNA increased gradually with the increase of the concentration and duration of cobalt chloride. Also, 25 ng/mL recombinant human EGF stimulated the expression of VEGF in HepG₂ cells and the expression increased with the increase of EGF concentration. 5 μ mol/L LY294002 inhibited the expression of VEGF stimulated by cobalt chloride or recombinant human EGF and the inhibition decreased step by step with increase of the concentration of LY294002. But even 20 μ mol/L LY294002 could not completely block the expression of VEGF. In contrast, PD98059 had no inhibitory effects on the transcription of VEGF stimulated by cobalt chloride or recombinant human EGF.

CONCLUSION: The overexpression of VEGF in HCC could be promoted by hypoxia and EGF expression in HCC. The signal transduction pathway of VEGF transcription in HepG₂ cells may be through PI3K pathway, but not through p42/p44 MAPK pathway.

Huang GW, Yang LY, Lu WQ. Effects of PI3K and p42/p44 MAPK on overexpression of vascular endothelial growth factor in hepatocellular carcinoma. *World J Gastroenterol* 2004; 10 (6): 809-812

<http://www.wjgnet.com/1007-9327/10/809.asp>

INTRODUCTION

Hepatocellular carcinoma (HCC) is one of the most common cancers in China. Owing to the improvement of surgical technique and early diagnostic methods, the resection rate of HCC has increased. However, the postoperative relapse rate remains high, which has become one of the main obstacles to the therapy of HCC. The mechanisms leading to the relapse are still unclear. Much effort has been done to make it clear. Recently, neovascularization, commonly observed in HCC, has been suggested to play important roles in the relapse of HCC^[1-3]. Vascular endothelial growth factor (VEGF) is one of the most potent proangiogenic agents to date. It is confirmed that there is overexpression of VEGF in HCC tissue. However, the mechanisms of VEGF overexpression in HCC are still unclear.

Phosphatidylinositol 3-kinase (PI3K) is a kind of lipid kinase which generates specific inositol lipids that are implicated in many cellular processes, such as cell growth, proliferation, survival, differentiation and cytoskeletal changes^[4,5]. MAP kinases are a family of serine/threonine kinases activated through a signaling pathway triggered by numerous agonists such as growth factors, hormones, lymphokines, extracellular matrix components, tumor promoters and stress factors^[6]. It has become clear that MAPKs regulate almost all cellular processes, from gene expression to cell death. Recently, both PI3K and p42/p44MAPK pathways have been both found to play important roles in the regulation of angiogenesis^[7-9].

The objective of the current study was to investigate the mechanisms leading to the overexpression of VEGF in HCC *in vitro* and the possible roles of PI3K and p42/p44 MAPK in the regulation of VEGF transcription in hepatoma cells.

MATERIALS AND METHODS

Cell culture

The HepG₂ cells (a hepatocellular carcinoma cell line), provided by the Center of Cell Culture in Xiangya Medical College, were cultured in DMEM supplemented with 100 mL/L fetal bovine serum (FBS) and incubated at 37 °C in a 50 mL/L CO₂ atmosphere. The cells were cultured overnight in DMEM without FBS before intervention.

Reagents

Hypoxia-inducer cobalt chloride (Sigma) and recombinant human epidermal growth factor (rhEGF, Promega) were used to stimulate the cells. Before stimulation, LY294002 (Promega) and PD98059 (Promega) were used to pretreat the cells to test the function of PI3K and p42/p44 MAPK, respectively.

Treatment procedures and drugs

Seven groups included: 1. no stimulation group (NS); 2. cobalt chloride group (CC), 100-400 μ mol/Lcobalt chloride stimulated the cells for 3-24 h; 3. EGF group (EGF), 25-200 ng/mL rhEGF stimulated the cells for 24 h; 4. cobalt chloride plus LY294002 group (CCL), 5-20 μ mol/LLY294002 stimulated the cells 30 min before cobalt chloride treatment; 5. EGF plus LY294002 group

(EL), 5-20 $\mu\text{mol/L}$ LY294002 stimulated the cells 30 min before rhEGF stimulation; 6. cobalt chloride plus PD98059 group (CCP), 25-100 $\mu\text{mol/L}$ PD98059 stimulated the cells 30 min before cobalt chloride treatment; 7. EGF plus PD98059 group (EP), 25-100 $\mu\text{mol/L}$ PD98059 stimulated the cells 30 min before rhEGF treatment.

Reverse transcription-polymerase chain reaction (RT-PCR)

After incubation for a given duration, the cells were harvested and the total RNA was extracted by using the TRIZOL Reagent (GIBCO BRL, USA). One microgram of RNA was reversely transcribed into cDNA in 20 μL reverse transcriptional system containing 50 mmol/L Tris-HCl, 75 mmol/L KCl, 3 mmol/L MgCl_2 , 0.5 μg oligo-dT primer, 0.5 mmol/L deoxynucleotide triphosphate (dNTP), 20U RNasin and 200 U murine Moloney leukemia virus (M-MLV) reverse transcriptase (Promega Corp., Madison, WI), at 37 $^{\circ}\text{C}$ for 1 h. After reverse transcription, 5 μL of product was added to PCR buffer containing 10 mmol/L Tris-HCl, 1.5 mmol/L MgCl_2 , 50 mmol/L KCl, 1 g/L Triton-X-100, 0.2 $\mu\text{mol/L}$ forward primer, 0.2 $\mu\text{mol/L}$ reverse primer, 200 $\mu\text{mol/L}$ dNTP and 2.5U DNA polymerase (SANGON, SHANGHAI). The PCR was performed in a DNA thermal cycler (Perkin Elmer, USA) with a program of denaturing at 94 $^{\circ}\text{C}$ for 5 min; denaturing at 94 $^{\circ}\text{C}$ for 30 s, annealing at 55 $^{\circ}\text{C}$ for 30 s, extension at 72 $^{\circ}\text{C}$ for 1 min, the amplification was carried out for 30 cycles. The reaction was stopped in a final extension at 72 $^{\circ}\text{C}$ for 5 min. The forward and reverse primers for human VEGF and beta actin were purchased from SANGON (SHANGHAI) and their nucleotide sequences were listed below: VEGF: forward primer: 5'-TTGCTGCTCTACCTCCAC-3'; reverse primer: 5'-AATGCTTTCTCCGCTCTG-3' beta actin: forward primer: 5'-ACACTGTGCCCATCTAGGAGG-3'; reverse primer: 5'-AGGGGCCGGACTCGTCATACT-3'. The sizes of PCR products were: 417 bp for VEGF, 680 bp for beta actin, respectively.

PCR products were loaded on a 20 g/L agarose gel with ethidium bromide, and band intensity was quantified by photo image analyzer (Stratagene Eagleeye II). The ratio of band intensity of the sample to the internal standard was calculated in the four reactions that contained significant amounts of both sample and standard, which stood for the amount of expression of VEGF mRNA.

Immunocytochemistry

The cells were fixed in cool acetone and sections were stained for VEGF based on streptavidin-biotin-horseradish peroxidase complex formation mentioned before^[10]. In brief, the slides were treated with target retrieval solution. Monoclonal anti-VEGF antibody JH121 (200 $\mu\text{g/mL}$, NEOMARKERS, USA) was used at a dilution of 1:50. The peroxidase reaction was developed using diaminobenzidine and slides were washed. Nuclei were lightly counterstained with hematoxylin. Negative controls were performed using PBS instead of the monoclonal antibody. Two investigators independently evaluated the results of immunocytochemistry.

Statistical analysis

ANOVA was used appropriately. For the test, a P value of less than 0.05 was considered as significant. All statistics were calculated through SPSS 10.0 software.

RESULTS

The effects of cobalt chloride and rhEGF on the expression of VEGF mRNA in HepG₂ cells

The amount of expression of VEGF mRNA in HepG₂ cells cultured in DMEM without FBS was 0.117. With the increase

of the concentration of cobalt chloride, the expression of VEGF mRNA increased ($P < 0.05$) (Figure 1). And also with the increase of the duration of cobalt chloride stimulation, the expression of VEGF mRNA also increased. rhEGF also stimulated the expression of VEGF mRNA in HepG₂ cells in a dependant manner of concentration and duration (Figure 2).

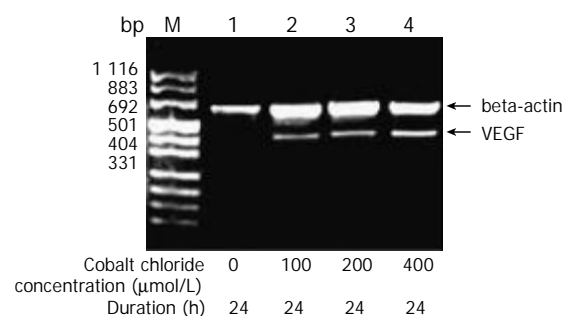


Figure 1 Cobalt chloride stimulated the expression of VEGF mRNA in HepG₂ cells in a concentration-dependant manner.

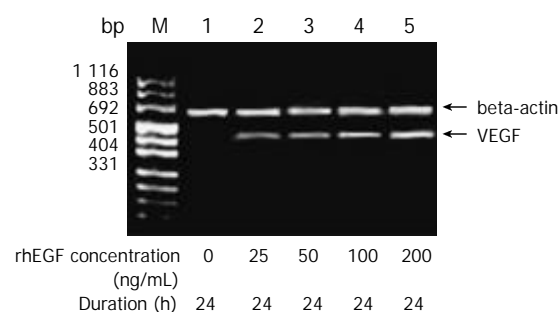


Figure 2 rhEGF stimulated the expression of VEGF mRNA in HepG₂ cells in a concentration-dependant manner.

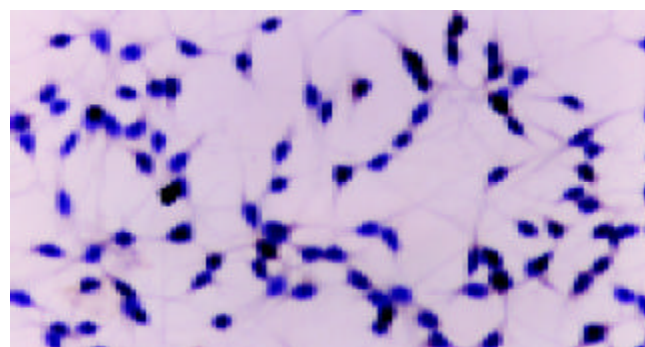


Figure 3 Negative expression of VEGF protein in HepG₂ cells cultured in DMEM without serum. Immunocytochemistry $\times 400$.

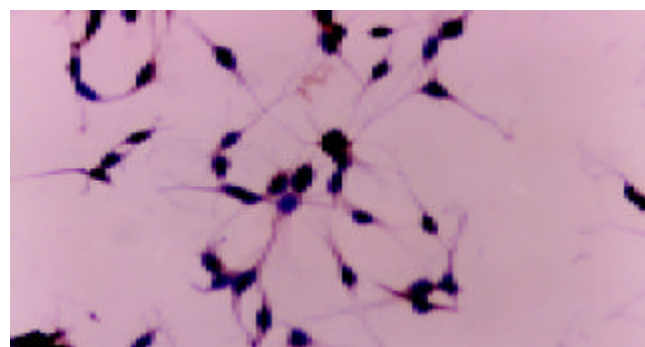


Figure 4 Expression of VEGF protein in HepG₂ cells stimulated by cobalt chloride (400 $\mu\text{mol/L}$, 24 h) immunocytochemistry $\times 400$.

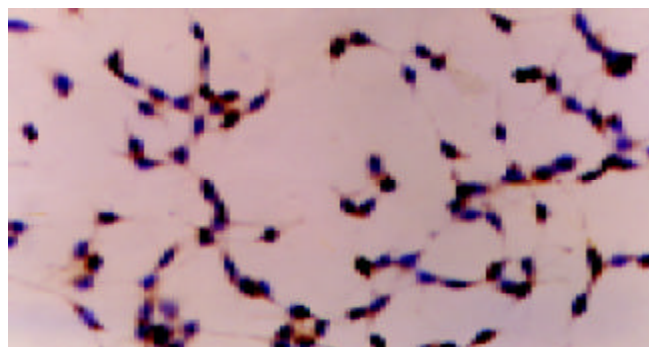


Figure 5 Expression of VEGF protein in HepG₂ cells stimulated by rhEGF(25 ng/mL, 24 h) immunocytochemistry ×400.

The effects of cobalt chloride and rhEGF on the expression of VEGF protein in HepG₂ cells

There was no positive staining in HepG₂ cells cultured in DMEM without FBS. Cobalt chloride or rhEGF stimulated the expression of VEGF protein in the cytoplasm of HepG₂ cells (Figure 3-5), which demonstrated the results of RT-PCR.

Effects of LY294002 or PD98059 on VEGF transcription stimulated by cobalt chloride or rhEGF in HepG₂ cells

A 5 μmol/L LY294002 inhibited the expression of VEGF stimulated by cobalt chloride or recombinant human EGF and the inhibition decreased step by step with increase of the concentration of LY294002 ($P < 0.05$). But even 20 μmol/L LY294002 did not completely block the expression of VEGF mRNA (Figure 6). In contrast, PD98059 had no inhibitory effects on the transcription of VEGF stimulated by cobalt chloride or recombinant human EGF ($P > 0.05$) (Figure 7).

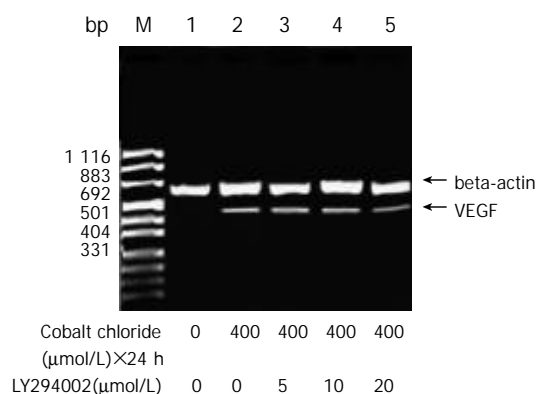


Figure 6 LY294002 inhibited the expression of VEGF mRNA in HepG₂ cells stimulated by cobalt chloride.

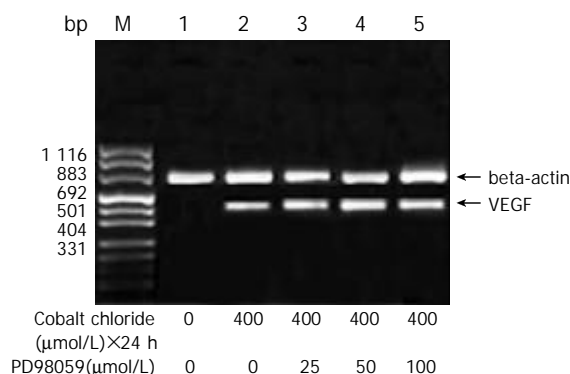


Figure 7 PD98059 had no effect on the expression of VEGF mRNA in HepG₂ cells stimulated by cobalt chloride.

DISCUSSION

Neovascularization was essential for tumour growth and metastasis^[1-3]. The mechanisms underlying the neovascularization in malignancies have been the “hot spot” in the cancer research. VEGF is one of the growth factors proven to be specific and critical for blood vessel formation. In clinical experiment, we have demonstrated that there is VEGF overexpression in HCC and the level of VEGF expression in HCC is correlated not only with microvessel invasion of cancer cells, but also with the survival^[11]. So it is very important to make clear the mechanisms and signal transduction pathways that control the VEGF expression in HCC. This would help us find new targets to prevent the neovascularization in HCC so as to preclude the relapse and metastasis of HCC.

Hypoxia, one of the fundamental characteristics of the tumour microenvironment, was demonstrated to be involved in the progression and metastasis of malignancy^[12-16]. In the current study, we have shown that hypoxia-inducer cobalt chloride could induce the expression of VEGF in HepG₂ cells in a concentration and duration-dependant manner. We have also shown that rhEGF could stimulate the expression of VEGF in HepG₂ cells in the same manner. As a result, we could draw a conclusion that both hypoxia and EGF might be the fundamental stimulators of VEGF overexpression in HepG₂ cells.

Phosphatidylinositol 3-kinase (PI3K) was a kind of lipid kinase^[17-21]. The lipid product of PI3K, phosphatidylinositol-3,4,5-trisphosphate (PIP₃), recruited a subset of signaling proteins with pleckstrin homology (PH) domains to the membrane, where they were activated. These proteins included protein serine-threonine kinases (Akt and PDK1), protein tyrosine kinases (Tec family), exchange factors for GTP-binding proteins (Grp1 and Rac exchange factors), and adaptor proteins (GAB-1). Ultimately, these proteins initiated complex sets of events that controlled protein synthesis, actin polymerization, cell survival, and cell cycle entry.

Recently, PI3K has been demonstrated to be involved in the regulation of the transcription of VEGF in certain types of cells. Overexpression of VEGF mRNA has been found in endothelial cells in which the PI3K pathway has been activated^[22]. LY294002, the specific inhibitor of PI3K, could inhibit the expression of VEGF in endothelial cells. In addition, PI3K was found to be involved in the regulation of VEGF transcription in cancer cells. In the prostate cancer cell line, LY294002 could completely block the expression of VEGF^[23]. Maity *et al* also demonstrated PI3K was essential in the regulation of VEGF transcription in glioma cell line U87MG^[24]. In the current study, we have shown that LY294002 inhibit VEGF transcription stimulated by cobalt chloride or rhEGF in a concentration and duration dependant manner. To our knowledge we demonstrated for the first time that PI3K was involved in the regulation of the signal transduction pathway of VEGF transcription in the hepatoma cells. At the same time, we observed that even 20 μmol/L LY294002 could not block the VEGF mRNA expression completely, which was likened to the results of Zhong^[23] and Maity^[24]. So there was PI3K-independent pathway in the regulation of VEGF transcription in HepG₂ cells.

MAPKs were important signal transducing enzymes, unique to eukaryotes, that were involved in many facets of cellular regulation, such as gene expression, cellular proliferation and programmed cell death^[25-27]. Recently, MAPKs has been shown to be involved in the regulation of neovascularization. Rak *et al* have shown that in the Ras-transforming mouse fibroblast cell line 3T3RAS, VEGF expression was not blocked by LY294002, but by PD98059, the specific inhibitor of p42/p44 MAPK^[28]. This result suggested that p42/p44 MAPK was involved in the regulation of VEGF transcription in 3T3RAS cells. In the current study, we did not observe PD98059 could

preclude VEGF transcription in HepG₂ cells, which indicated p42/p44 MAPK was not involved in the regulation of VEGF transcription in HepG₂ cells.

In conclusion, hypoxia and EGF were two stimulators to the VEGF overexpression in hepatoma cells. VEGF transcription might be regulated by PI3K pathway and other PI3K-independent pathway, but not by p42/p44 MAPK pathway.

REFERENCES

- Folkman J.** Seminars in medicine of the beth israsl hospital, bos clinical applications of research on angiogenesis. *N Eng J Med* 1995; **333**: 1757-1763
- Carmeliet P, Jain RK.** Angiogenesis in cancer and other diseases. *Nature* 2000; **407**: 249-257
- Yancopoulos GD, Davis S, Gale NW, Rudge JS, Wiegand SJ, Holash J.** Vascular-specific growth factors and blood vessel formation. *Nature* 2000; **407**: 242-248
- Sotsios Y, Ward SG.** Phosphoinositide 3-kinase: a key biochemical signal for cell migration in response to chemokines. *Immunol Rev* 2000; **177**: 217-235
- Roymans D, Slegers H.** Phosphatidylinositol 3-kinases in tumor progression. *Eur J Biochem* 2001; **268**: 487-498
- Chang L, Karin M.** Mammalian MAP kinase signalling cascades. *Nature* 2001; **410**: 37-40
- Dimmeler S, Zeiher AM.** Akt takes center stage in angiogenesis signaling. *Circ Res* 2000; **86**: 4-5
- Jiang BH, Zheng JZ, Aoki M, Vogt PK.** Phosphatidylinositol 3-kinase signaling mediates angiogenesis and expression of vascular endothelial growth factor in endothelial cells. *Proc Natl Acad Sci U S A* 2000; **97**: 1749-1753
- Berra E, Milanini J, Richard DE, Le Gall M, Vinals F, Gothie E, Roux D, Pages G, Pouyssegur J.** Signaling angiogenesis via p42/p44 MAP kinase and hypoxia. *Biochem Pharmacol* 2000; **60**: 1171-1178
- Huang GW, Yang LY.** Metallothionein expression in hepatocellular carcinoma. *World J Gastroenterol* 2002; **8**: 650-653
- Huang GW, Yang LY, Lu XS, Liu HL, Yang JQ, Yang ZL.** Expression of hypoxia-inducible factor 1 alpha in hepatocellular carcinoma and the impact on neovascularization. *Zhonghua Xiaohua Zazhi* 2002; **22**: 627-628
- Huang GW, Yang LY.** Molecular mechanisms of hypoxia-induced malignant transformation. *Shijie Huaren Xiaohua Zazhi* 2001; **9**: 1300-1304
- Huang GW, Yang LY.** Hypoxic signal transduction pathway in malignancy. *Shijie Huaren Xiaohua Zazhi* 2002; **10**: 1441-1444
- Sutherland RM.** Tumor hypoxia and gene expression-implications for malignant progression and therapy. *Acta Oncol* 1998; **37**: 567-574
- Dachs GU, Tozer GM.** Hypoxia modulated gene expression: angiogenesis, metastasis and therapeutic exploitation. *Eur J Cancer* 2000; **36**: 1649-1660
- Wykoff CC, Beasley NJ, Watson PH, Turner KJ, Pastorek J, Sibtain A, Wilson GD, Turley H, Talks KL, Maxwell PH, Pugh CW, Ratcliffe PJ, Harris AL.** Hypoxia-inducible expression of tumor-associated carbonic anhydrases. *Cancer Res* 2000; **60**: 7075-7083
- Cantley LC.** The phosphoinositide 3-kinase pathway. *Science* 2002; **296**: 1655-1657
- Dhawan P, Singh AB, Ellis DL, Richmond A.** Constitutive activation of Akt/protein kinase B in melanoma leads to up-regulation of nuclear factor-kappaB and tumor progression. *Cancer Res* 2002; **62**: 7335-7342
- Romieu-Mourez R, Landesman-Bollag E, Seldin DC, Sonenshein GE.** Protein kinase CK2 promotes aberrant activation of nuclear factor-kappaB, transformed phenotype, and survival of breast cancer cells. *Cancer Res* 2002; **62**: 6770-6778
- Narita Y, Nagane M, Mishima K, Huang HJ, Furnari FB, Cavenee WK.** Mutant epidermal growth factor receptor signaling down-regulates p27 through activation of the phosphatidylinositol 3-kinase/Akt pathway in glioblastomas. *Cancer Res* 2002; **62**: 6764-6769
- Neri LM, Borgatti P, Capitani S, Martelli AM.** The nuclear phosphoinositide 3-kinase/AKT pathway: a new second messenger system. *Biochim Biophys Acta* 2002; **1584**: 73-80
- Wang D, Huang HJ, Kazlarskas A, Cavenee WK.** Induction of vascular endothelial growth factor expression in endothelial cells by platelet-derived growth factor through the activation of phosphatidylinositol 3-kinase. *Cancer Res* 1999; **59**: 1464-1472
- Zhong H, Chiles K, Feldser D, Laughner E, Hanrahan C, Georgescu MM, Simons JW, Semenza GL.** Modulation of hypoxia-inducible factor 1α expression by the epidermal growth factor/phosphatidylinositol 3-kinase/PTEN/AKT/FRAP pathway in human prostate cancer cells: implications for tumor angiogenesis and therapeutics. *Cancer Res* 2000; **60**: 1541-1545
- Maity A, Pore N, Lee J, Solomon D, O'Rourke DM.** Epidermal growth factor receptor transcriptionally up-regulates vascular endothelial growth factor expression in human glioblastoma cells via a pathway involving phosphatidylinositol 3'-kinase and distinct from that induced by hypoxia. *Cancer Res* 2000; **60**: 5879-5886
- Johnson GL, Lapadat R.** Mitogen-activated protein kinase pathways mediated by ERK, JNK, and p38 protein kinases. *Science* 2002; **298**: 1911-1912
- Chen G, Goeddel DV.** TNF-R1 signaling: a beautiful pathway. *Science* 2002; **296**: 1634-1635
- Ling MT, Wang X, Ouyang XS, Lee TK, Fan TY, Xu K, Tsao SW, Wong YC.** Activation of MAPK signaling pathway is essential for Id-1 induced serum independent prostate cancer cell growth. *Oncogene* 2002; **21**: 8498-8505
- Rak J, Mitsuhashi Y, Sheehan C, Tamir A, Vilorio-Petit A, Filmus J, Mansour SJ, Ahn NG, Kerbel RS.** Oncogenes and tumor angiogenesis: differential modes of vascular endothelial growth factor up-regulation in ras-transformed epithelial cells and fibroblasts. *Cancer Res* 2000; **60**: 490-498

Edited by Hu DK and Xu FM

Vascular endothelial growth factor antisense oligodeoxynucleotides with lipiodol in arterial embolization of liver cancer in rats

Han-Ping Wu, Gan-Sheng Feng, Hui-Min Liang, Chuan-Sheng Zheng, Xin Li

Han-Ping Wu, Gan-Sheng Feng, Hui-Min Liang, Chuan-Sheng Zheng, Xin Li, Department of Interventional Radiology, Union Hospital, Tongji Medical College, Huazhong University of Science and Technology, Wuhan 430022, Hubei Province, China

Supported by the National Natural Science Foundation of China, No. 39770839

Correspondence to: Dr. Han-Ping Wu, Department of Interventional Radiology, Union Hospital, Tongji Medical College, Huazhong University of Science and Technology, Wuhan 430022, Hubei Province, China. shhwhp@public.wh.hb.cn

Telephone: +86-27-85726432 **Fax:** +86-27-85727002

Received: 2003-07-17 **Accepted:** 2003-07-30

Abstract

AIM: Transcatheter arterial embolization (TAE) of the hepatic artery has been accepted as an effective treatment for unresectable hepatocellular carcinoma (HCC). However, embolized vessel recanalization and collateral circulation formation are the main factors of HCC growth and recurrence and metastasis after TAE. Vascular endothelial growth factor (VEGF) plays an important role in tumor angiogenesis. This study was to explore the inhibitory effect of VEGF antisense oligodeoxynucleotides (ODNs) on VEGF expression in cultured Walker-256 cells and to observe the anti-tumor effect of intra-arterial infusion of antisense ODNs mixed with lipiodol on rat liver cancer.

METHODS: VEGF antisense ODNs and sense ODNs were added to the media of non-serum cultured Walker-256 cells. Forty-eight hours later, VEGF concentrations of supernatants were detected by ELISA. Endothelial cell line ECV-304 cells were cultured in the supernatants. Seventy-two hours later, growth of ECV-304 cells was analyzed by MTT method. Thirty Walker-256 cell implanted rat liver tumor models were divided into 3 groups. 0.2 mL lipiodol (LP group, $n=10$), 3OD antisense ODNs mixed with 0.2 mL lipiodol (LP+ODNs group, $n=10$) and 0.2 mL normal saline (control group, $n=10$) were infused into the hepatic artery. Volumes of tumors were measured by MRI before and 7 d after the treatment. VEGF mRNA in cancerous and peri-cancerous tissues was detected by RT-PCR. Microvessel density (MVD) and VEGF expression were observed by immunohistochemistry.

RESULTS: Antisense ODNs inhibited Walker-256 cells' VEGF expression. The tumor growth rate was significantly lower in LP+ODNs group than that in LP and control groups ($140.1\pm33.8\%$, $177.9\pm64.9\%$ and $403.9\pm69.4\%$ respectively, $F=60.019$, $P<0.01$). VEGF mRNAs in cancerous and peri-cancerous tissues were expressed highest in LP group and lowest in LP+ODNs group. The VEGF positive rates showed no significant difference among LP, control and LP+ODNs groups (90%, 70% and 50%, $H=3.731$, $P>0.05$). The MVD in LP+ODNs group (53.1 ± 18.4) was significantly less than that in control group (73.2 ± 20.4) and LP group (80.3 ± 18.5) ($F=5.44$, $P<0.05$).

CONCLUSION: VEGF antisense ODNs can inhibit VEGF

expression of Walker-256 cells. It may be an antiangiogenesis therapy agent for malignant tumors. VEGF antisense ODNs mixed with lipiodol embolizing liver cancer is better in inhibiting liver cancer growth, VEGF expression and microvessel density than lipiodol alone.

Wu HP, Feng GS, Liang HM, Zheng CS, Li X. Vascular endothelial growth factor antisense oligodeoxynucleotides with lipiodol in arterial embolization of liver cancer in rats. *World J Gastroenterol* 2004; 10(6): 813-818

<http://www.wjgnet.com/1007-9327/10/813.asp>

INTRODUCTION

Hepatocellular carcinoma (HCC) is one of the most common malignant tumors in human beings^[1,2]. In China, HCC is responsible for 130 000 deaths every year and the second cause of cancer deaths^[3]. Surgical resection is still the only potentially curative treatment for HCC, particularly for small HCC^[3,4]. To date, the resection rate for HCC is unfortunately less than 30%^[3,5,6]. Since HCC's blood supply is derived almost exclusively from hepatic arteries, transcatheter arterial embolization (TAE) of the hepatic artery has been accepted as an effective treatment for unresectable HCC^[5-10]. Although embolic materials and technique have been improved during the last decade, the outcome of TAE is not satisfactory. It hardly leads to tumor necrosis totally. The 3-year survival rate is about 14-35%^[11-14]. Recanalization of the embolized vessel and collateral circulation formation, which are related with tumor angiogenesis, are the main factors of HCC growth, recurrence and metastasis after TAE^[15,16]. In TAE, HCC cells undergo coagulative necrosis, a pathologic feature of anoxia. Anoxia and hypoxic liver injury are caused by the absolute and relative deficiency of oxygen, respectively. It is well known that hypoxia tension is a key factor of the gene expression of angiogenic factors such as VEGF, acidic and basic fibroblast growth factors (FGF), platelet derived growth factor (PDGF). These factors could promote tumor angiogenesis, growth, recurrence and metastasis^[17,18]. It is possible that in addition to elimination of cancer cells, TAE may play a role in enhancing some cells' malignant potency and ability to escape anoxia and ischemia after treatment.

VEGF is a key mediator of pathological angiogenesis. Many researchers found that it overexpressed in many solid tumor tissues including HCC, and was associated with tumor growth, recurrence, metastasis and patient's prognosis^[19-23]. It has been reported that preoperative TAE enhanced VEGF expression in both HCC cells and non-carcinoma liver cells. Antisense RNA could inhibit and block gene expression effectively^[24-26]. In this study, we devised antisense ODNs specific to VEGF mRNA, and observed their inhibitory effects on VEGF expression in Walker-256 cell lines *in vitro*, and the anti-tumor effect of them mixed with lipiodol arterial embolization on Walker-256 cell transplanted rat liver cancer models.

MATERIALS AND METHODS

Cell culture

Walker 256 carcinosarcoma cells were purchased from China

Center for Type Culture Collection. After recovery, the cells were inoculated in the abdominal cavity of male pathogen-free Wistar rats, weighing 100-120 g (supplied by Department of Experimental Animal, Tongji Medical College). Three days later, cancerous ascites was aspirated and cultured in RPMI-1640 containing 50 mL/L fetal calf serum (FCS) (Gibco, Grand Island, NY) and equilibrated with 950 mL/L air and 50 mL/L CO₂. Cells were passaged every 2 d. The cells at passage 3 were used for experiments.

Oligodeoxynucleotides (ODNs)

Phosphorothioate ODNs were synthesized by Shanghai Sangon Biological Engineering Technology and Service Co., LTD. The sequences of ODNs were designed as follows: antisense ODNs: 5'-GCA GTA GCT GCG CTG ATA GCG C-3', complementary to the linkage area of VEGF exon 2 and exon 3; sense ODNs: 5'-GCA CTA TCA GCG CAG CTA CTG C-3', equivalent to the linkage area of VEGF exon 2 and exon 3.

Cell proliferation studies

Walker-256 carcinosarcoma cells were planted into a 24-well plate at 1×10^5 /well (1 mL/well) and cultured in non-serum medium. Ten μ L of 0.25, 0.5, 1.0, 2.0 μ mol/L antisense ODNs and sense ODNs was added to the media every 24 h. Ten μ L of non-serum medium was added to the blank control wells. Forty-eight hours later, the supernatant fluids were collected. The concentration of VEGF was measured by ELISA. Two hundred μ L of supernatant fluids was added triplicate to a 96-well plate to culture ECV-304 cells (endothelial cell line, purchased from China Center for Type Culture Collection, 1×10^4 /well), equilibrated with 950 mL/L air and 50 mL/L CO₂. Seventy-two hours later, ECV-304 cells were collected. MTT method was used to detect the growth of ECV-304 cells.

Tumor model and treatment schedule

Walker-256 carcinosarcoma cells were inoculated subcutaneously in the right flank of rats with 10^7 tumor cells in approximately 0.1 mL of cell suspension. Tumors were palpable 7 d after transplantation. Fresh tumor tissues were isolated and cut into 1 mm³ size. Following midline laparotomy, the Walker 256 carcinosarcoma tissue pieces were implanted into the left hepatic lobe of rats. Seven days later, after anesthesia and laparotomy, the gastroduodenal artery was retrograde catheterized with a Portex PE10 tube (inner diameter 0.28 mm, external diameter 0.61 mm, Neolab, Germany) under a binocular operative microscope (Suzhou Medical Instruments Factory, Jiangsu, China) and infused embolic materials to perform TAE. The common hepatic artery and right hepatic artery were temporarily ligated during infusion. Thirty tumor-bearing rats were randomly divided into 3 groups, 10 rats each. LP group: the hepatic arteries were embolized with 0.2 mL lipiodol (Lipiodol Ultra-Fluid; Andre Guerbet, Aulnay-Sous-Bois, France), LP+ODNs group: the hepatic arteries were embolized with 3OD antisense ODNs mixed with 0.2 mL lipiodol, control group: 0.2 mL normal saline was infused into hepatic arteries. Then the gastroduodenal artery was ligated and the abdominal cavity was closed.

MR scans were performed on 1.5-Tesla system (Magnetom Vision, Siemens, Germany) supplemented by a cervical coil before and 7 d after TAE. T1-weighted (TR/TE, 450/12 ms) and T2-weighted (TR/TE, 2800/96 ms) transverse SE images (slice thickness 2 mm) were acquired using acquisition times of 7:25 and 6:16 min, respectively. Tumor volume was determined from MR measurements of the largest and smallest diameters and calculated according to the following formula: Tumor volume (mm³, V) = largest diameter (mm) \times [smallest diameter (mm)]²/2. The tumor growth rate = $V_{\text{post}}/V_{\text{pre}} \times 100\%$.

The rats were sacrificed 7 d after TAE. Liver cancerous and peri-cancerous tissues were dissected. Some of them were frozen at -70 °C for RNA isolation. The reminders were fixed in 40g/L formaldehyde, dehydrated and embedded in paraffin. Five- μ m sections were stained with hematoxylin-eosin for light microscopy and measurement of the degree of tumor necrosis.

RNA isolation and RT-PCR analysis

Total RNA was extracted from liver cancerous and peri-cancerous tissues using the TRIzol reagent (Gibco). Reverse transcription of 5 μ g total RNA was performed in a volume of 20 μ L for 60 min at 37 °C, containing AMV 5U, Oligo dT 0.050 μ g, RNasin 20 U, 10 mmol/L dNTP 2 μ L. The samples were heated to 95 °C for 5 min to terminate the reverse transcription reaction. By using a Perkin-Elmer DNA thermocycler 2 400 (Perkin-Elmer, Norwalk, CT), 2 μ L cDNA mixture obtained from the reverse transcription reaction was then amplified for VEGF and G₃PDH. G₃PDH was used as a housekeeping gene and amplified with VEGF as control. The amplification reaction mixture consisted of 10 \times buffer 2.5 μ L, 5 mmol/L dNTP 0.5 μ L, 25 mmol/L MgCl₂ 1.5 μ L, 10 pmol/L each of sense and antisense primers, Taqase 5U. The reaction mixture was first heated at 95 °C for 5 min and amplification was carried out for 35 cycles at 94 °C for 30 s, at 60 °C for 30 s, and at 72 °C for 30 s, followed by incubation for 10 min at 72 °C. The PCR primers used were: VEGF, sense 5'-GAA GTG GTG AAG TTC ATG GAT GTC-3' and antisense 5'-CGA TCG TTC TGT ATC AGT CTT TCC-3'; G₃PDH, sense 5'-TCC CTC AAG ATT GTC AGC AA-3' and antisense 5'-AGA TCC ACA ACG GAT ACA TT-3'. The length of PCR products for VEGF and G₃PDH was 394 bp and 309 bp. PCR products were checked with 15 g/L agarose gel electrophoresis stained with ethidium bromide.

Immunohistochemical analysis

Five micron paraffin-embedded tissue sections were deparaffinized and rehydrated. Rabbit anti-mouse vWF, VEGF monoclonal antibody and SABC kit were provided by Beijing Zhongshan Biological Technology Co., Ltd. Immunohistochemical studies were performed by SABC methods according to the manufacturer's instructions. VEGF staining was evaluated semiquantitatively on the basis of the percentage of positive cells, and classified as follows: diffusely positive (+++) when positive cells accounted for more than 50% of the total cells, moderately positive (++) when positive cells were 16-50%, weakly positive (+) when positive cells accounted for 5-15%, and negative (-) when positive cells accounted for less than 5%. For MVD determination, 5 areas were randomly selected and counted at a magnification of 200. Briefly, the stained sections were screened at a magnification of 40 under a light microscope to identify 3 regions of the section with the highest microvessel density. Microvessels were counted in these areas at a magnification of 200, and the average number of microvessels was recorded.

Statistical analysis

Experimental results were analyzed with analysis of variance (ANOVA) and Kruskal-Wallis rank test. The difference between 2 groups was analyzed by SNK-*q* and Dunn test respectively. Statistical significance was determined at $P < 0.05$.

RESULTS

VEGF concentration in supernatant of walker-256 cells

After incubated with walker-256 cells for 48 h, antisense ODNs decreased the concentration of VEGF in the supernatant of walker-256 cells in a dose-dependent manner, whereas no significant changes were seen in sense ODNs (Table 1).

Table 1 Concentration of VEGF in supernatant of Walker-256 cells (pg/ml)(mean±SD)

Group	0.25 µmol/L	0.5 µmol/L	1.0 µmol/L	2.0 µmol/L
Antisense ODNs	84.2±2.2	79.2±2.6	74.4±2.1	65.2±2.0
Sense ODNs	89.2±1.9	90.4±2.6	88.2±1.9	88.6±2.5
Control	90.2±1.9	90.8±1.8	89.4±2.1	90.4±1.7
F values	7.877	23.132	49.906	133.636
P values	0.021 ¹	0.002 ¹	0.000 ¹	0.000 ¹

¹SNK-q test: The difference between sense ODNs and control groups was not statistically significant.

Cell proliferation study

The supernatants of Walker-256 cells that were incubated with antisense ODNs could inhibit the growth of ECV-304 cells in a dose-dependent manner. No significant effects were seen in those incubated with sense ODNs (Table 2).

Table 2 Inhibitory effect of supernatants of Walker-256 cells cultured with ODNs on ECV-304 proliferation (OD) (mean±SD)

Group	0.25 µmol/L	0.5 µmol/L	1.0 µmol/L	2.0 µmol/L
Antisense ODNs	0.339±0.012	0.332±0.006	0.327±0.008	0.321±0.019
Sense ODNs	0.345±0.021	0.348±0.014	0.336±0.022	0.359±0.014
Control	0.357±0.010	0.359±0.008	0.356±0.005	0.360±0.009
F values	2.477	5.573	12.931	7.296
P values	0.164	0.043 ¹	0.007 ¹	0.025 ¹

¹SNK-q test: The difference between sense ODNs and control groups was not statistically significant.

Tumor growth and histopathological findings

Seven days after implantation, the tumor was located in the left lobe of liver as a solitary mass. There was no statistical difference between the volumes of tumors in control group, LP group and LP+ODNs group (212.3±117.5 mm³, 174.6±106.5 mm³, 173.9±91.8 mm³ respectively) before TAE treatment. Seven days after the treatment, all tumors grew. The volumes and growth rates in LP group (286.0±186.4 mm³, 177.9±64.9%, respectively) and LP+ODNs group (337.6±98.1 mm³, 140.1±33.8%, respectively) were significantly less than those in control group (823.3±426.1 mm³, 403.9±69.4%, respectively, *P*<0.01) (Table 3).

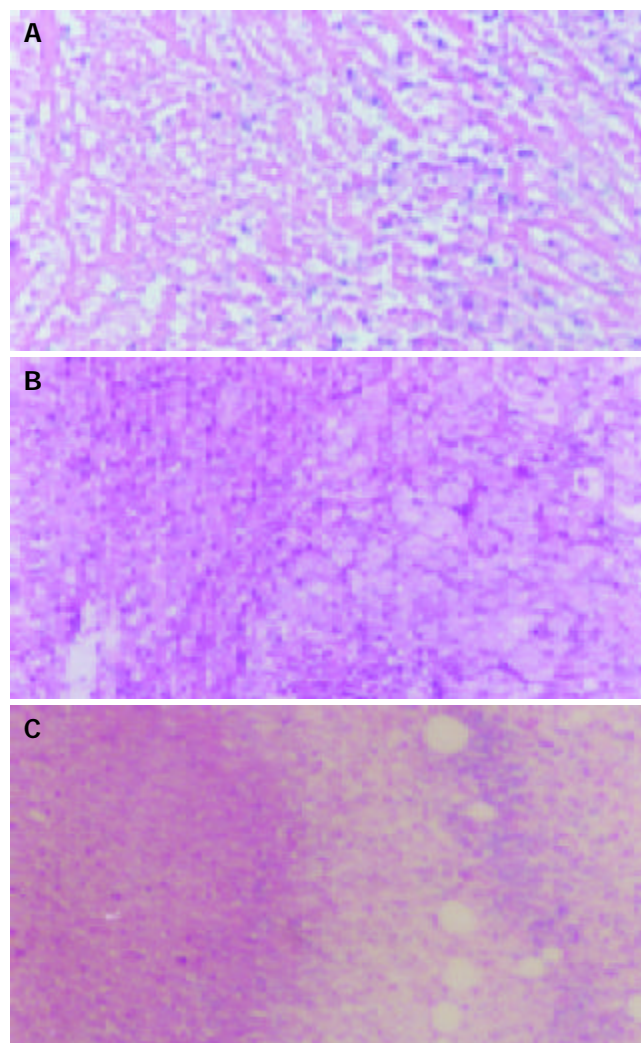
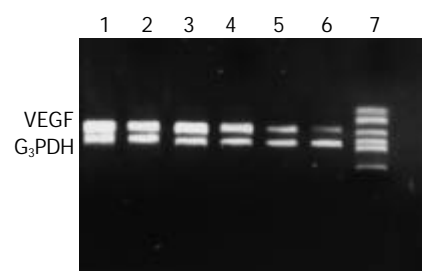
Table 3 Volumes and growth rates of transplanted liver tumors (mean±SD)

Group	Volume of pre-TAE(mm ³)	Volume of post-TAE(mm ³)	Growth rate (%)
Control	212.3±117.5	823.3±426.1	403.9±69.4
LP	174.6±106.5	286.0±186.4	177.9±64.9
LP+ODNs	173.9±91.8	337.6±98.1	140.1±33.8
F values	0.432	14.319	60.019
P values	0.653	0.000 ¹	0.000

¹SNK-q test: The difference between antisense LP and LP+ODNs groups was not statistically significant.

Hematoxylin-eosin (H & E) stained sections of the liver specimens showed a poorly differentiated carcinoma, which was spherical or ovoid in shape. Tumor cells arranged in irregular nests and signs of malignancy including hyperchromatosis, polymorphism and numerous mitoses were detected. The mass had a sharp demarcation from the surrounding normal hepatic parenchyma, its capsules were thin and composed of collagen fibers, which were caused by the

compression of the tumor. The tumor showed inhomogeneous signs of hypervascularization consisting mainly of small arteries and capillaries. Seven days after therapy, spotty and scattered necrosis were seen in all cases of control group (Figure 1A). Satellite nodules could be seen in some tumors. In LP group, the necrotic area was increased. Many patched necrotic zones were seen in tumor tissues (Figure 1B). In LP+ODNs group, the tumor necrotic area was much wider. It showed a big area of central necrosis. The residual tumors could be seen only in the margin of tumor (Figure 1C).

**Figure 1** Pathological changes of tumor tissues 7 d after TAE. A: Control group showing spotty and scattered necrosis. B: LP group showing many patched necrotic zones. C: LP+ODNs group showing big areas of central necrosis. Hematoxylin-eosin ×40.**Figure 2** RT-PCR analysis of VEGF mRNA level in cancerous and peri-cancerous tissues using G₃PDH as internal control. Control group: 1 tumor, 2 peri-tumor. LP group: 3 tumor, 4 peri-tumor. LP+ODNs group: 5 tumor, 6 peri-tumor, 7 marker.

RT-PCR analysis of VEGF mRNA expression

VEGF mRNA expression was detected in cancerous and peri-cancerous tissues. The expression level in cancerous tissue was higher than that in peri-cancerous tissues. The VEGF mRNA levels in cancerous and peri-cancerous tissues in LP group were higher than those in control group, and those in LP+ODNs group were lower than those in control and LP groups (Figure 2).

Table 4 Expression of VEGF and MVD by immunohistochemical staining ($n=10$)

Group	MVD (mean \pm SD)	VEGF				Positive rate (%)
		+++	++	+	-	
Control	73.2 \pm 20.4	3	2	2	3	70
LP	80.3 \pm 18.5	3	4	2	1	90
LP+ODNs	53.1 \pm 18.4	1	2	2	5	50
Test values	$F=5.440$	$H=3.731$				
P values	0.010 ¹	0.1545				

¹SNK- q test: The difference between LP and control groups was not statistically significant.

Immunohistochemical analysis of VEGF protein expression and MVD

VEGF immunoreactivity was observed mainly in the cytoplasm of tumor cells, and also frequently in hepatic cells in peri-cancerous tissues. The distribution of strong VEGF-staining zones and microvessels was mainly in the survival nidui and margins of the tumor. The positive rate of VEGF in LP group, control group and LP+ODNs group was 90%, 70% and 50% respectively, and the difference was not statistically significant

($P=0.065$) (Table 4, Figure 3). The MVD in LP+ODNs group (53.1 \pm 18.4) was significantly less than that in control group (73.2 \pm 20.4) and LP group (80.3 \pm 18.5). Although the MVD in control group and LP group showed no significant difference, but abundant tumor vessels were seen in residual nidui in LP group (Table 4, Figure 4).

DISCUSSION

Many authors have reported the effects of TAE on VEGF expression of HCC. An *et al*^[27] found that preoperative TAE enhanced VEGF expression in both HCC cells and non-carcinoma liver cells. Kobayashi *et al*^[28] reported that the frequency of Bcl-2 positive cells was higher in HCCs undergone TAE than that in HCCs not undergone TAE, and the immunohistochemical staining intensity for VEGF was higher in Bcl-2 positive than in Bcl-2 negative area. Suzuki *et al*^[29] reported that the serum levels of VEGF in HCC patients increased significantly 7 d after TAE. Guo *et al*^[30] reported that blockage of hepatic arterial blood supply resulted in decreased blood perfusion and increased expression of metastasis-associated genes VEGF and MMP-1 of transplanted liver cancer in rats. The results in this study showed that VEGF mRNA and protein had an increasing tendency after TAE. These findings suggested that TAE could enhance the expression of VEGF in HCC cells. The rationale is based on the following points: TAE was hard to lead to total tumor necrosis and to make the tumor tissue anoxia further. Hypoxia induced transcription of VEGF mRNA was mediated by the binding of hypoxia-inducible factor 1 (HIF-1) to an HIF-1 binding site located in the VEGF promoter^[31-33]. VEGF plays an important role in each stage of tumor angiogenesis. The overexpression of VEGF in cancerous and peri-cancerous tissues of HCC could certainly promote tumor

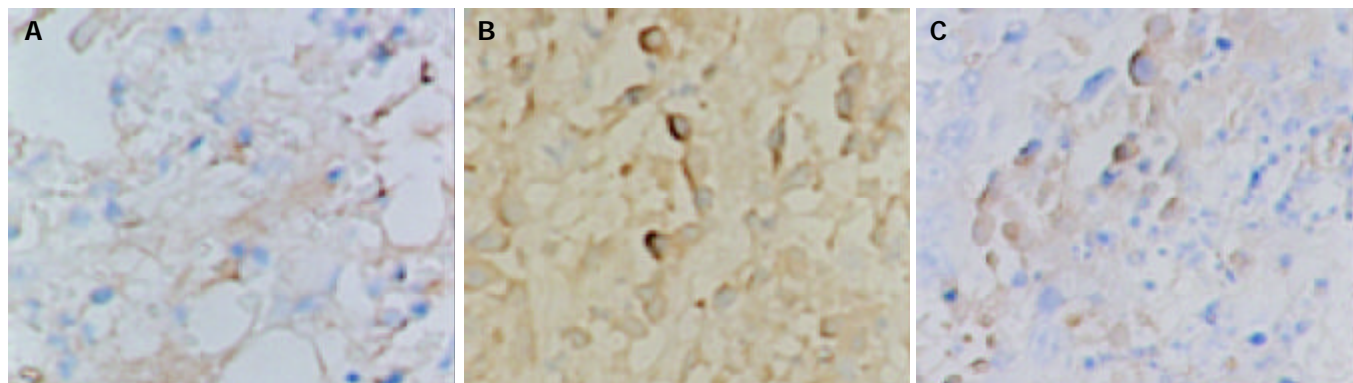


Figure 3 Immunohistochemical staining of VEGF in tumor tissues 7 d after TAE, showing strong expression in LP group and low expression in LP+ODNs group. A: Control group, B: LP group, C: LP+ODNs group. SABC $\times 200$.

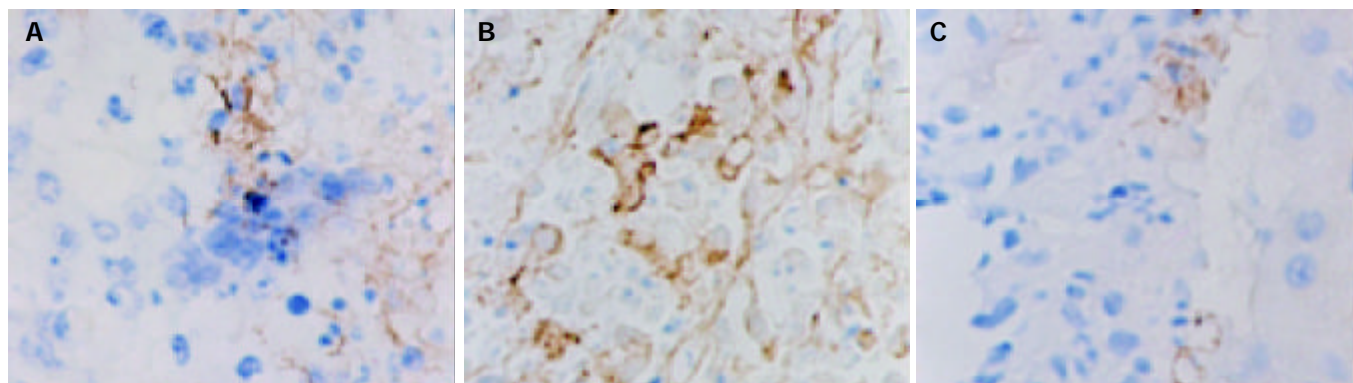


Figure 4 Immunohistochemical staining of vWF in tumor tissues 7 d after TAE, showing plenty of microvessels in LP group and a few microvessels in LP+ODNs group. A: Control group, B: LP group, C: LP+ODNs group. SABC $\times 200$.

angiogenesis and collateral vessels formation, and enhance the possibility of recurrence and metastasis^[34-37]. In this study, although we found that the MVD in LP group was higher than that in control group, but the difference was not significant and abundant tumor vessels were seen in residual nidui in LP group. It must be due to tumor angiogenesis enhancement caused by VEGF overexpression after TAE. In clinical setting, we also found that the collateral vessels were increased with the time of increased TAE. These vessels are very small and hard to catheterize, resulting in the embolized HCC tissue receiving blood and escaping from anoxia stress. Some HCC vessels not embolized completely would grow acceleratedly and were prone to recurrence and metastasis. So it is very important to reduce VEGF expression and collateral vessel formation after TAE.

Antisense ODNs have shown great efficacy in selective inhibition of gene expression. They are designed and synthesized artificially, and can enter cells directly to hybridize with complementary mRNA and decrease protein expression. They have been used as an important tool to inhibit the expression of oncogenes and/or growth factors and some of them have been used as drugs in tumor gene therapies^[38-41]. In this study, antisense ODNs were designed to complement the region between exon 2 and exon 3 of VEGF gene. They could inhibit 4 kinds of VEGF molecules' expression^[42,43]. To enforce their stability, ODNs were modified by phosphorothioate. Our previous study showed fluorescence labeled ODNs could transfect Walker-256 cells and keep in them for about 48 h (in press). The *in vitro* experimental results in this study showed that VEGF antisense ODNs could decrease VEGF expression of cultured Walker-256 cells in a dose-dependent manner. Similar effect has been reported on other tumor cell lines^[41, 44-46]. In *in vivo* study, we also found that VEGF antisense ODNs could inhibit VEGF expression of liver tumor tissues after TAE, reduce tumor MVD and growth rate in walker-256 cell transplanted rat liver cancer models. These imply that VEGF antisense ODNs could be used as an antiangiogenesis agent to inhibit HCC's overexpression and collateral vessel formation after TAE.

Intravenous injection is the routine means for phosphothioate ODNs in clinical administration. However, intravenous infusion is not an ideal route for VEGF antisense ODNs in HCC treatment. First, it has a very short lifetime after injection into animal bodies. To enhance the target cell transfection rate and therapeutic effect, it is needed to increase the dose of antisense ODNs. A higher dose of ODNs may result in more side effects such as dose-dependent hypotension, complement activation, and transient prolongation of thromboplastin time^[47-50]. Second, systemic administration of VEGF antisense ODNs might inhibit physiological angiogenesis, such as wound healing, menstruation. In this study, we mixed antisense ODNs with lipiodol and used them as an embolic agent in liver tumor TAE therapy. To infuse the agents into the left hepatic artery (the tumor was planted in the left lobe of the rat liver) and to make each tumor receive the same amount of agents, we catheterized the gastroduodenal artery retrograde and ligated the common hepatic artery and right hepatic artery temporarily during infusion. The results showed that antisense ODNs mixed with lipiodol was better in inhibiting tumor growth rate, VEGF expression and MVD than lipiodol alone. These indicated that antisense ODNs used in combination with lipiodol and transcatheter artery embolization were the ideal route in HCC treatment. The rationale is based on the following points. The blood supply of HCC is mainly from hepatic artery. ODNs hepatic artery infusion could increase the concentration in tumor tissue and reduce the dosage and systemic side-effects. When injected to the hepatic artery, lipiodol could stay in tumor tissue for a long time (several months), and could even be

absorbed by tumor cells^[51,52]. When mixed with lipiodol, the latter could act as a carrier, ODNs would give off slowly from it. It would prolong the contact time of ODNs and tumor cells, which is very important to increase the transfect rate. Our previous *in vivo* experimental study showed that fluorescence labeled ODNs could stay in tumor tissue for about 6 d when used in combination with lipiodol hepatic artery embolization on Walker-256 cell transplanted rat liver cancer models (in press). This is why the long-term inhibitory effect on VEGF expression and MVD was achieved in this study.

In conclusion, TAE can increase the formation of microvessels in residual tumor tissues. VEGF plays an important role in liver cancer angiogenesis and collateral vascular formation after TAE treatment. VEGF antisense ODNs are able to inhibit tumor cells' VEGF expression. VEGF antisense ODNs can inhibit the residual tumor angiogenesis and growth and reduce the possibility of metastasis and recurrence. The combination of TAE and VEGF antisense ODNs will be a hopeful strategy for HCC treatment.

REFERENCES

- 1 **Pisani P**, Parkin DM, Bray FI, Ferlay J. Estimates of the world-wide mortality from 25 cancers in 1990. *Int J Cancer* 1999; **83**: 18-29
- 2 **Akriviadis EA**, Llovet JM, Efremidis SC, Shouval D, Canelo R, Ringes B, Meyers WC. Hepatocellular carcinoma. *Br J Surg* 1998; **85**: 1319-1331
- 3 **Tang ZY**. Hepatocellular carcinoma-cause, treatment and metastasis. *World J Gastroenterol* 2001; **7**: 445-454
- 4 **Yuen MF**, Cheng CC, Laufer JJ, Lam SK, Ooi CG, Lai CL. Early detection of hepatocellular carcinoma increases the chance of treatment: Hong Kong experience. *Hepatology* 2000; **31**: 330-335
- 5 **Acunas B**, Rozanes I. Hepatocellular carcinoma: treatment with transcatheter arterial chemoembolization. *Eur J Radiol* 1999; **32**: 86-89
- 6 **Rose DM**, Chapman WC, Brockenbrough AT, Wright JK, Rose AT, Meranze S, Mazer M, Blair T, Blanke CD, Debelak JP, Pinson CW. Transcatheter arterial chemoembolization as primary treatment for hepatocellular carcinoma. *Am J Surg* 1999; **177**: 405-410
- 7 **Zangos S**, Gille T, Eichler K, Engelmann K, Woitaschek D, Balzer JO, Mack MG, Thalhammer A, Vogl TJ. Transarterial chemoembolization in hepatocellular carcinomas: technique, indications, results. *Radiologe* 2001; **41**: 906-914
- 8 **Livraghi T**. Treatment of hepatocellular carcinoma by interventional methods. *Eur Radiol* 2001; **11**: 2207-2219
- 9 **Poon RT**, Ngan H, Lo CM, Liu CL, Fan ST, Wong J. Transarterial chemoembolization for inoperable hepatocellular carcinoma and postresection intrahepatic recurrence. *J Surg Oncol* 2000; **73**: 109-114
- 10 **Camma C**, Schepis F, Orlando A, Albanese M, Shahied L, Trevisani F, Andreone P, Craxi A, Cottone M. Transarterial chemoembolization for unresectable hepatocellular carcinoma: meta-analysis of randomized controlled trials. *Radiology* 2002; **224**: 47-54
- 11 **Loewe C**, Cejna M, Schoder M, Thurnher MM, Lammer J, Thurnher SA. Arterial embolization of unresectable hepatocellular carcinoma with use of cyanoacrylate and lipiodol. *J Vasc Interv Radiol* 2002; **13**: 61-69
- 12 **Zheng C**, Feng G, Liang H. Bletilla striata as a vascular embolizing agent in interventional treatment of primary hepatic carcinoma. *Chin Med J* 1998; **111**: 1060-1063
- 13 **Li X**, Hu G, Liu P. Segmental embolization by ethanol iodized oil emulsion for hepatocellular carcinoma. *J Tongji Med Univ* 1999; **19**: 135-140
- 14 **Li L**, Wu PH, Li JQ, Zhang WZ, Lin HG, Zhang YQ. Segmental transcatheter arterial embolization for primary hepatocellular carcinoma. *World J Gastroenterol* 1998; **4**: 511-512
- 15 **Tian JM**, Wang F, Ye H, Wang ZT, Sun F, Liu Q, Yang JJ, Cheng D. Classification study of arterial blood supply of hepatic cancer: regular, variant and parasitic blood supply. *Linchuang Fangshexue Zazhi* 1997; **16**: 40-43
- 16 **Li HP**, Cao J, Wang XY, Luo JQ. Effect of hepatic artery

- chemoembolization in patients with primary liver carcinoma and analysis of factors affecting the prognosis. *Linchuang Fangshexue Zazhi* 2001; **20**: 66-69
- 17 **Carmeliet P**, Jain RK. Angiogenesis in cancer and other disease. *Nature* 2000; **407**: 249-257
- 18 **Battegay EJ**. Angiogenesis: mechanistic insights, neovascular diseases, and therapeutic prospects. *J Mol Med* 1995; **73**: 333-346
- 19 **Ferrara N**. Role of vascular endothelial growth factor in the regulation of angiogenesis. *Kidney Int* 1999; **56**: 794-814
- 20 **Ferrara N**. Molecular and biological properties of vascular endothelial growth factor. *J Mol Med* 1999; **77**: 527-543
- 21 **Zheng S**, Han MY, Xiao ZX, Peng JP, Dong Q. Clinical significance of vascular endothelial growth factor expression and neovascularization in colorectal carcinoma. *World J Gastroenterol* 2003; **9**: 1227-1230
- 22 **Tao HQ**, Qin LF, Lin YZ, Wang RN. Expression of vascular endothelial growth factor and its prognostic significance in gastric carcinoma. *China Natl J New Gastroenterol* 1996; **2**: 128-130
- 23 **Jiang YF**, Yang ZH, Hu JQ. Recurrence or metastasis of HCC: predictors, early detection and experimental antiangiogenic therapy. *World J Gastroenterol* 2000; **6**: 61-65
- 24 **Narayanan R**, Akhtar S. Antisense therapy. *Curr Opin Oncol* 1996; **8**: 509-515
- 25 **Gu ZP**, Wang YI, Li JG, Zhou YA. VEGF₁₆₅ antisense RNA suppresses oncogenic properties of human esophageal squamous cell carcinoma. *World J Gastroenterol* 2002; **8**: 44-48
- 26 **Tang YC**, Li Y, Qian GX. Reduction of tumorigenicity of SMMC-7721 hepatoma cells by vascular endothelial growth factor antisense gene therapy. *World J Gastroenterol* 2001; **7**: 22-27
- 27 **An FQ**, Matsuda M, Fujii H. Expression of vascular endothelial growth factor in surgical specimens of hepatocellular carcinoma. *J Cancer Res Clin Oncol* 2000; **126**: 153-160
- 28 **Kobayashi N**, Ishii M, Ueno Y, Kisara N, Chida N, Iwasaki T, Toyota T. Co-expression of Bcl-2 protein and vascular endothelial growth factor in hepatocellular carcinomas treated by chemoembolization. *Liver* 1999; **19**: 25-31
- 29 **Suzuki H**, Mori M, Kawaguchi C, Adachi M, Miura S, Ishii H. Serum vascular endothelial growth factor in the course of transcatheter arterial embolization of hepatocellular carcinoma. *Int J Oncol* 1999; **14**: 1087-1090
- 30 **Guo WJ**, Li J, Ling WL, Bai YR, Zhang WZ, Cheng YF, Gu WH, Zhuang JY. Influence of hepatic arterial blockage on blood perfusion and VEGF, MMP-1 expression of implanted liver cancer in rats. *World J Gastroenterol* 2002; **8**: 476-479
- 31 **Nomura M**, Yamagishi S, Harada S, Hayashi Y, Yamashita T, Yamashita J, Yamamoto H. Possible participation of autocrine and paracrine vascular endothelial growth factors in hypoxia-induced proliferation of endothelial cells and pericytes. *J Biol Chem* 1995; **270**: 28316-28324
- 32 **Sivridis E**, Giatromanolaki A, Gatter KC, Harris AL, Koukourakis MI. Tumor and Angiogenesis Research Group. Association of hypoxia-inducible factors 1alpha and 2alpha with activated angiogenic pathways and prognosis in patients with endometrial carcinoma. *Cancer* 2002; **95**: 1055-1063
- 33 **Buchler P**, Reber HA, Buchler M, Shrinkante S, Buchler MW, Friess H, Semenza GL, Hines OJ. Hypoxia-inducible factor 1 regulates vascular endothelial growth factor expression in human pancreatic cancer. *Pancreas* 2003; **26**: 56-64
- 34 **Carmeliet P**, Collen D. Vascular development and disorders: molecular analysis and pathogenic insights. *Kidney Int* 1998; **53**: 1519-1549
- 35 **Poon RT**, Ng IO, Lau C, Zhu LX, Yu WC, Lo CM, Fan ST, Wong J. Serum vascular endothelial growth factor predicts venous invasion in hepatocellular carcinoma: a prospective study. *Ann Surg* 2001; **233**: 227-235
- 36 **Qin LX**, Tang ZY. The prognostic molecular markers in hepatocellular carcinoma. *World J Gastroenterol* 2002; **8**: 385-392
- 37 **Meng C**, Chen X. Association of VEGF, uPA, ICAM-1 and PCNA expression with metastasis and recurrence in hepatocellular carcinoma. *Zhonghua Waike Zazhi* 2002; **40**: 673-675
- 38 **Oza AM**, Elit L, Swenerton K, Faught W, Ghatage P, Carey M, McIntosh L, Dorr A, Holmlund JT, Eisenhauer E. Phase II study of CGP 69846A (ISIS 5132) in recurrent epithelial ovarian cancer: an NCIC clinical trials group study (NCIC IND.116). *Gynecol Oncol* 2003; **89**: 129-133
- 39 **Taylor AH**, al-Azzawi F, Pringle JH, Bell SC. Inhibition of endometrial carcinoma cell growth using antisense estrogen receptor oligodeoxyribonucleotides. *Anticancer Res* 2002; **22**: 3993-4003
- 40 **Yacyshyn BR**, Barish C, Goff J, Dalke D, Gaspari M, Yu R, Tami J, Dorr FA, Sewell KL. Dose ranging pharmacokinetic trial of high-dose alicaforsen (intercellular adhesion molecule-1 antisense oligodeoxynucleotide) (ISIS 2302) in active Crohn's disease. *Aliment Pharmacol Ther* 2002; **16**: 1761-1770
- 41 **Robinson GS**, Pierce EA, Rook SL, Foley E, Webb R, Smith LE. Oligodeoxynucleotides inhibit retinal neovascularization in a murine model of proliferative retinopathy. *Proc Natl Acad Sci U S A* 1996; **93**: 4851-4856
- 42 **Tischer E**, Mitchell R, Hartman T, Silva M, Gospodarowicz D, Fiddes JC, Abraham JA. The human gene for vascular endothelial growth factor: Multiple protein forms are encoded through alternative exon splicing. *J Biol Chem* 1991; **266**: 11947-11954
- 43 **Park JE**, Keller GA, Ferrara N. The vascular endothelial growth factor (VEGF) isoforms: differential deposition into the sub-epithelial extracellular matrix and bioactivity of extracellular matrix-bound VEGF. *Mol Biol Cell* 1993; **4**: 1317-1326
- 44 **Dong F**, Jin YX. Inhibition of angiogenesis with antisense ODN of VEGF. *Chin J Oncol* 1997; **19**: 264-266
- 45 **Chen YF**, Sun HW, Zou Q, Zou SQ. Inhibition of growth of human cholangiocarcinoma in nude mice by vascular endothelial growth factor antisense phosphorothioate oligodeoxynucleotides. *Zhonghua Shiyan Waike Zazhi* 2000; **17**: 22-23
- 46 **Shi W**, Siemann DW. Inhibition of renal cell carcinoma angiogenesis and growth by antisense oligonucleotides targeting vascular endothelial growth factor. *Br J Cancer* 2002; **87**: 119-126
- 47 **Iversen PL**, Copple BL, Tewary HK. Pharmacology and toxicology of phosphorothioate oligonucleotides in the mouse, rat, monkey and man. *Toxicol Lett* 1995; **82**: 425-430
- 48 **Leeds JM**, Henry SP, Bistner S, Scherrill S, Williams K, Levin AA. Pharmacokinetics of an antisense oligonucleotide injected intravitreally in monkeys. *Drug Metab Dispos* 1998; **26**: 670-675
- 49 **Tolcher AW**, Reyno L, Venner PM, Ernst SD, Moore M, Geary RS, Chi K, Hall S, Walsh W, Dorr A, Eisenhauer E. A randomized phase II and pharmacokinetic study of the antisense oligonucleotides ISIS 3521 and ISIS 5132 in patients with hormone-refractory prostate cancer. *Clin Cancer Res* 2002; **8**: 2530-2535
- 50 **Webb MS**, Tortora N, Cremese M, Kozłowska H, Blaquiére M, Devine DV, Kornbrust DJ. Toxicity and toxicokinetics of a phosphorothioate oligonucleotide against the c-myc oncogene in cynomolgus monkeys. *Antisense Nucleic Acid Drug Dev* 2001; **11**: 155-163
- 51 **Han GH**, Guo QL, Huang GS, Guo YL. Distribution of lipiodol in hepatocellular carcinoma after hepatic arterial injection and its significance. *Zhonghua Fangshexue Zazhi* 1993; **27**: 828-831
- 52 **Kan Z**, Sato M, Ivancev K, Uchida B, Hedgpeth P, Lunderquist A, Rosch J, Yamada R. Distribution and effect of iodized poppyseed oil in the liver after hepatic artery embolization: experimental study in several animal species. *Radiology* 1993; **186**: 861-866

Alpha-fetoprotein stimulated the expression of some oncogenes in human hepatocellular carcinoma Bel 7402 cells

Meng-Sen Li, Ping-Feng Li, Qian Chen, Guo-Guang Du, Gang Li

Meng-Sen Li, Qian Chen, Department of Biochemistry, Hainan Medical College, Haikou 571101, China

Ping-Feng Li, Guo-Guang Du, Gang Li, Department of Biochemistry and Molecular Biology, Health Science Center, Peking University, Beijing 100083, China

Supported by the National Natural Science Foundation of China, No. 30260117, Natural Science Foundation of Hainan Province, No. 30315 and the Nursery Foundation of Hainan Medical College, No. 200202

Correspondence to: Dr. Meng-Sen Li, Department of Biochemistry, Hainan Medical College, Haikou 571101, China. mengsenli@163.com

Telephone: +86-898-66893779

Received: 2003-09-18 **Accepted:** 2003-11-15

Abstract

AIM: To investigate the molecular mechanism of alpha-fetoprotein (AFP) on regulating the proliferation of human hepatocellular carcinoma cells.

METHODS: Alpha-fetoprotein purified from human umbilical blood was added to cultured human hepatocellular carcinoma Bel 7402 cells *in vitro* for various treatment periods. The expression of *c-fos*, *c-jun*, and *N-ras* mRNA involved in proliferation and differentiation of cells was analyzed by Northern blot, and the expression of mutative p53 and p21^{ras} proteins was determined by Western blot.

RESULTS: The results showed that AFP (20 mg/L) stimulated mRNA expression of these oncogenes in Bel 7402 cells. The expression of *c-fos* mRNA increased by 51.1%, 60.9%, 96.0%, and 25.5% at 2, 6, 12, and 24 h, respectively. The expression of *c-jun* and *N-ras* mRNA reached to the maximum which increased by 81.3% and 59.9% as compared with the control after 6 h and 24 h incubation with AFP, respectively. Western blot assay also demonstrated that AFP promoted the expression of mutative p53 and p21^{ras} proteins, and the increased rate of those proteins was 13.0%, 39.9%, and 70.9%, as well as 35.2%, 102.6%, and 46.8% at 6, 12, and 24 h, respectively, as compared with the control. Both human serum albumin (the same dosage as AFP) and monoclonal anti-AFP antibody failed to stimulate the expression of these oncogenes, but anti-AFP antibody could block the functions of AFP.

CONCLUSION: The data indicate that AFP can stimulate the expression of some oncogenes to enhance the proliferation of human hepatocellular carcinoma Bel 7402 cells.

Li MS, Li PF, Chen Q, Du GG, Li G. Alpha-fetoprotein stimulated the expression of some oncogenes in human hepatocellular carcinoma Bel 7402 cells. *World J Gastroenterol* 2004; 10(6): 819-824

<http://www.wjgnet.com/1007-9327/10/819.asp>

INTRODUCTION

Alpha-fetoprotein is the major serum protein in human

embryos, and is synthesized by embryonic liver and yolk sac. During the embryonic growth course, AFP expresses much more (3 g/L), and falls to the adult level (0.02×10^{-3} g/L) after one-year birth. Although many investigations for the function of AFP had been carried out, the biological role of AFP is still a riddle so far. Because the composition and the sequence of the amino acid residues of AFP were very similar to those of human serum albumin, thus, people always think that the function of AFP just like human serum albumin, which functions to transport materials and stabilize blood colloid osmotic pressure in the life course of the fetus. However, the concentration of serum AFP increases apparently with liver cancer or liver optimum regeneration in humans. AFP always accompanies with the growth of liver cells, and it is possible that AFP may be related to the proliferation of tumor or fetal cells. Some investigations had showed that AFP could be individually synergy with other growth factors to promote the growth of many tumor or normal cells^[1-6]. Alpha-fetoprotein (MW 69 ku) is a kind of biomacromolecules, and it is impossible to directly permeate the cells to regulate cell proliferation. We previously found that AFP could enhance growth of human hepatocellular carcinoma Bel 7402 and NIH3T3 cells, and there were two typical receptors of AFP existed on the membranes of these cells^[7,8]. However, it has not been reported in former investigations how AFP influences the expression of oncogenes which are mediated by AFP receptors to regulate growth of human hepatocellular carcinoma cells. This study used human hepatocellular carcinoma Bel 7402 cell line, which is closely related to AFP, to observe mRNA expression of the oncogene *c-fos*, *c-jun*, and *N-ras*, and protein expression of mutative p53 and p21^{ras}, which are correlated with cell proliferation, after treated with AFP. Additionally, the study explored some molecular mechanisms for AFP-mediated growth of human hepatocellular carcinoma cells.

MATERIALS AND METHODS

Materials

Human hepatocellular carcinoma Bel 7402 cells, crude AFP, and monoclonal anti-AFP antibody were provided by Endocrine Research Group of the Department of Biochemistry and Molecular Biology, Health Science Center, Peking University; RPMI 1640 medium was purchased from GIBCO; Fetal calf serum (FCS) was from the Blood Research Institute of Chinese Medicine Science Academy (Tianjin, China); Human serum albumin (HSA) and MOPS were purchased from Sigma Company; Diethyl pyrocarbonate (DEPC), sodium dodecyl sulfate (SDS), agarose, and Tris were obtained from Bio-Rad Company; Total RNA extraction kit was purchased from Promega Company; α -³²P-dCTP was bought from YaHui Biology Engineer Company (Beijing, China); *N-ras*, *c-fos*, *c-jun*, and β -actin cDNA probes were from the Department of Endocrinology, Northwestern University (Chicago); Random primer labeling kit was the product of Takara company (Japan); Salmon sperm DNA, fraction V of bovine serum albumin (BSA), and Ficoll-400 were bought from the Jingke Chemical

Reagents Company (Beijing, China); Monoclonal antibodies for mutative p53 and p21^{ras} were from NEOMARKERS Company.

Methods

Purification of human AFP Human AFP was prepared by the method as described elsewhere^[9]. Briefly, human cord blood AFP was precipitated by ammonium sulfate and passed through an anti-AFP antibody affinity chromatography column. The AFP-positive fractions were collected and concentrated. The purity of prepared AFP was 92.7% determined by SDS-polyacrylamide gel electrophoresis (SDS-PAGE). The protein was stored at -80 °C until analysis.

Cells culture Human hepatocellular carcinoma Bel 7402 cells (1.5×10⁴/mL) were cultured in RPMI 1640 medium supplemented with 100 mL/L FCS at 37 °C in a humidified atmosphere of 50 mL/L CO₂. The cultured medium was changed after 24 h.

RNA isolation and Northern blot analysis The cells were treated with AFP (20 mg/L), HSA (20 mg/L), anti-AFP antibody (40 mg/L), or AFP (20 mg/L) + anti-AFP antibody (40 mg/L) for 2, 6, 12, and 24 h, respectively. Total cellular RNA was isolated from Bel 7402 cells using a TRIzol reagent kit (Promega, Madison, WI) according to the manufacturer's protocol. Then, RNA was quantitated by the absorbance at 260 nm, and RNA (10-20 µg/lane) was fractionated by electrophoresis through 10 g/L formaldehyde agarose gel. The fractionated RNA was transferred in 20×SSC buffer to the nitrocellulose membrane (Millipore Corporation, Bedford, MA) using the standard procedure^[10]. These membranes were hybridized with α-³²P labeled probe, and washed using the standard protocol. The membranes were then exposed to the X-ray film at -80 °C.

Purification of protein and Western blot analysis The cells were treated with AFP (20 mg/L), HSA (20 mg/L), anti-AFP antibody (40 mg/L), or AFP (20 mg/L) + anti-AFP antibody (40 mg/L) for 6, 12, and 24 h, respectively. After washed three times with PBS (pH 7.4, 0.15 mol/L), the cells were lysed in 10 µL of lysis buffer containing 2 mL/L Triton X-100, 500 mmol/L NaCl, 500 mmol/L sucrose, 1 mmol/L EDTA, 0.15 mmol/L spermine, 0.5 mmol/L spermidine, 10 mmol/L HEPES (pH 8.0), 200 µmol/L phenylmethylsulfonyl fluoride, 2 mg/L leupeptin, 2 mg/L pepstatin, 24 000 IU/L aprotinin, and 7 mmol/L β-mercaptoethanol. Proteins (40 µg) were subjected to SDS-PAGE, and transferred to the PVDF membrane for immunodetection. The SDS-PAGE molecular weight markers (Bio-Rad) verified the correct location of the visualized bands. The membranes were blocked with 50 mL/L nonfat milk in PBS-Tween, probed with anti-p53 or anti-p21 antibody, and followed by secondary antibody (goat anti-mouse IgG-alkaline phosphatase). Immunoreactive proteins were detected using a color develop system (NBT/BCIP) by the standard procedure^[10].

RESULTS

Expression of *c-fos* mRNA

Northern blot analysis demonstrated the overexpression of *c-fos* mRNA in Bel 7402 cells after treated with AFP for 2, 6, and 12 h. The data showed that AFP (20 mg/L) treated for 2 h significantly increased the expression of *c-fos* mRNA in Bel 7402 cells by 51.1% compared with the control group. The expression of *c-fos* mRNA continuously increased by 60.9% and 96.0% when treated with AFP for 6 h and 12 h, respectively, and declined thereafter to 25.5% increase at 24 h, compared with control group (Figure 1). However, HSA at the same dosage (20 mg/L) as AFP and anti-AFP antibody (40 mg/L)

had no significant influence on the expression of *c-fos* mRNA in Bel 7402 cells. Anti-AFP antibody partially blocked an increase in the expression of *c-fos* mRNA by AFP (Figure 2).

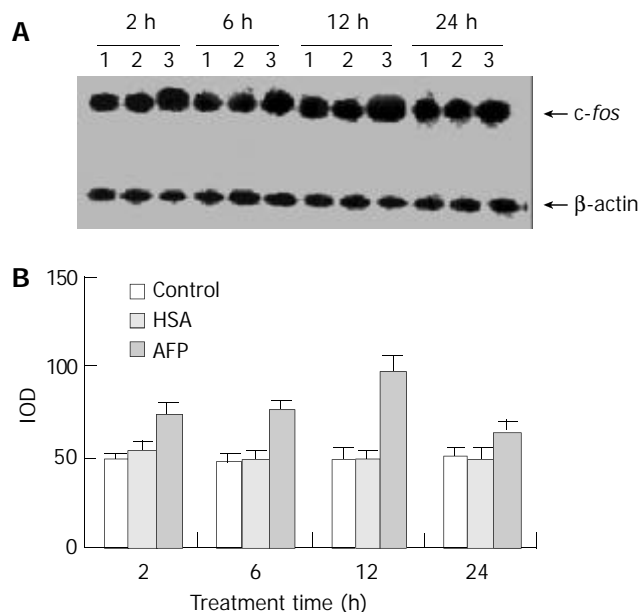


Figure 1 Effects of AFP (20 mg/L) or HSA (20 mg/L) on the expression of *c-fos* mRNA in human hepatocellular carcinoma Bel 7402 cells analyzed by Northern blot. The cells were incubated with AFP or HSA for 2, 6, 12, and 24 h, respectively. A: Autoradiogram of Northern blot. Lane 1: control group; Lane 2: HSA treated group; Lane 3: AFP treated group. B: Densitometric intensity of absorbance (IOD) of *c-fos* mRNA expression in Bel 7402 cells. The data were selected from 3 independent experiments.

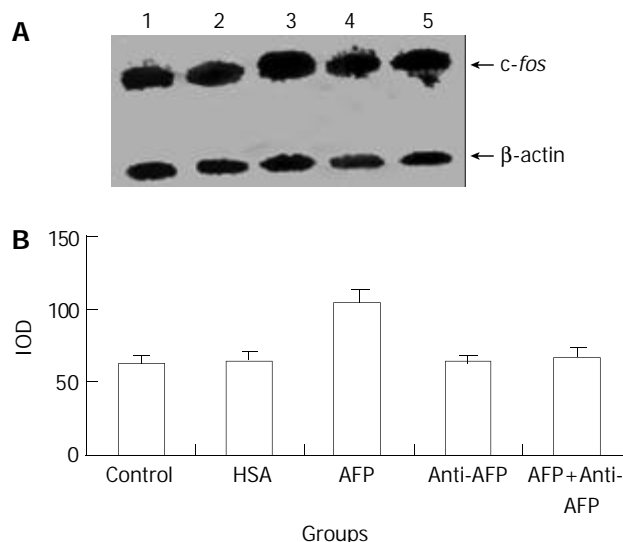


Figure 2 Effects of AFP (20 mg/L), HSA (20 mg/L), anti-AFP antibody (40 mg/L), and AFP (20 mg/L) + anti-AFP antibody (40 mg/L) on *c-fos* mRNA expression in human hepatocellular carcinoma Bel 7402 cells analyzed by Northern blot after 2 h treatment. A: Autoradiogram of Northern blot. Lane 1: control group; Lane 2: HSA treated group; Lane 3: AFP treated group; Lane 4: anti-AFP antibody treated group; Lane 5: AFP + anti-AFP antibody treated group. B: Densitometric intensity of absorbance (IOD) of *c-fos* mRNA expression in Bel 7402 cells. The data were selected from 3 independent experiments.

Expression of *c-jun* mRNA

AFP (20 mg/L) had no significant influence on the expression

of *c-jun* mRNA in human hepatocellular carcinoma cells when treated for 2 h, but when treated for 6 h the expression of *c-jun* mRNA increased obviously, the increase rate was 81.3%, but when treated for 24 h, increased rate fell to 14.6% as compared with the control group (Figure 3). However, HSA (20 mg/L) at the same dosage as AFP and anti-AFP antibody (40 mg/L) had no significant influence on the expression of *c-jun* mRNA in Bel 7402 cells. Anti-AFP antibody partially inhibited an increase in the expression of *c-jun* mRNA by AFP (Figure 4).

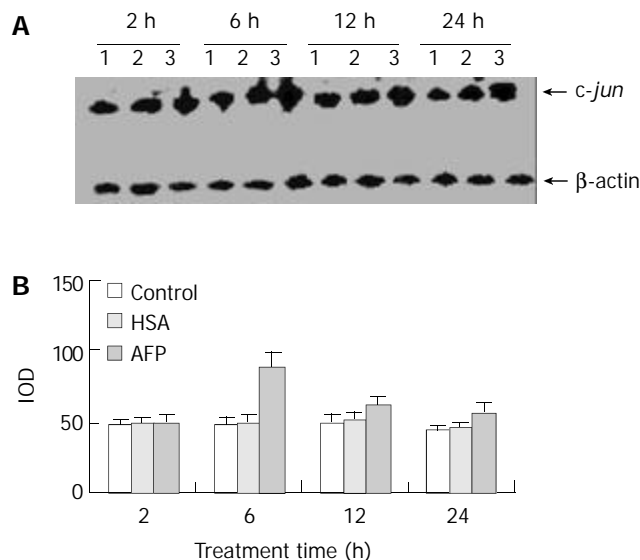


Figure 3 Effects of AFP (20 mg/L) or HSA (20 mg/L) on the expression of *c-jun* mRNA in human hepatocellular carcinoma Bel 7402 cells analyzed by Northern blot. The cells were incubated with AFP or HSA for 2, 6, 12, and 24 h, respectively. A: Autoradiogram of Northern blot. Lane 1: control group; Lane 2: HSA treated group; Lane 3: AFP treated group. B: Densitometric intensity of absorbance (IOD) of *c-jun* mRNA expression in Bel 7402 cells. The data were selected from 3 similar experiments.

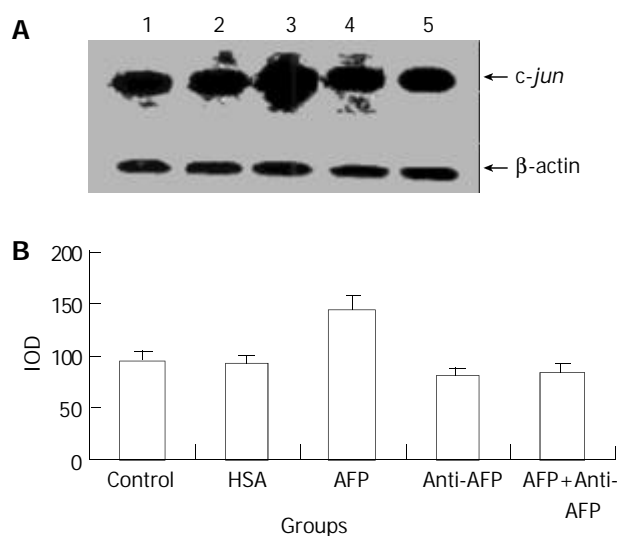


Figure 4 Effects of AFP (20 mg/L), HSA (20 mg/L), anti-AFP antibody (40 mg/L), and AFP (20 mg/L) + anti-AFP antibody (40 mg/L) on the expression of *c-jun* mRNA in human hepatocellular carcinoma Bel 7402 cells analyzed by Northern blot after 6 h treatment. A: Autoradiogram of Northern blot. Lane 1: control group; Lane 2: HSA treated group; Lane 3: AFP treated group; Lane 4: anti-AFP antibody treated group; Lane 5: AFP + anti-AFP antibody treated group. B: Densitometric

intensity of absorbance (IOD) of *c-jun* mRNA expression in Bel 7402 cells. The data were selected from 3 independent experiments.

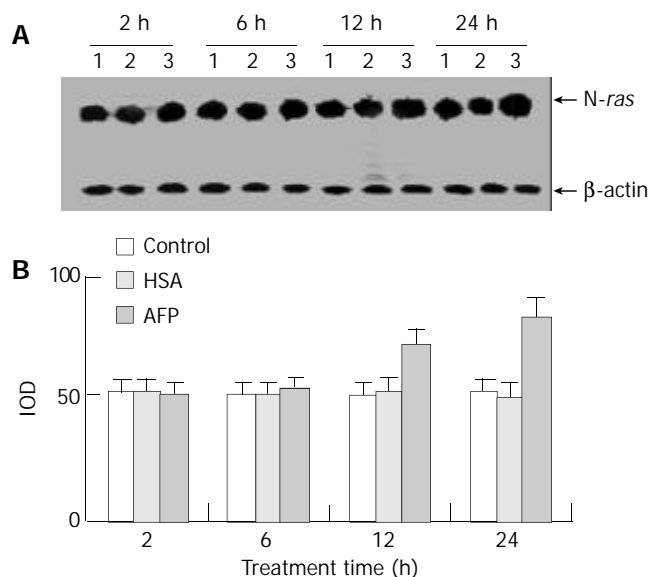


Figure 5 The effects of AFP (20 mg/L) or HSA (20 mg/L) on the expression *N-ras* mRNA in human hepatocellular carcinoma Bel 7402 cells analyzed by Northern blot. The cells were incubated with AFP or HSA for 2, 6, 12, and 24 h, respectively. A: Autoradiogram of Northern blot. Lane 1: control group; Lane 2: HSA treated group; Lane 3: AFP treated group. B: Densitometric intensity of absorbance (IOD) of *N-ras* mRNA expression in Bel 7402 cells. The data were selected from 3 similar experiments.

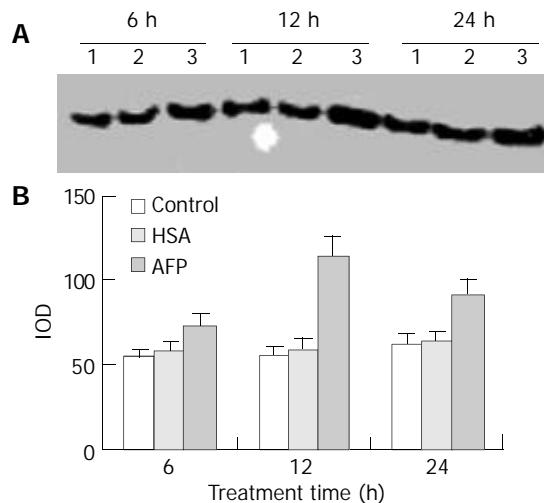


Figure 6 Effects of AFP (20 mg/L) or HSA (20 mg/L) on the expression of p21^{ras} in Bel 7402 cells analyzed by Western blot. The cells were incubated with AFP or HSA for 6, 12, and 24 h, respectively. A: Western blot analysis. Lane 1: control group; Lane 2: HSA treated group; Lane 3: AFP treated group. B: Densitometric intensity of absorbance (IOD) of p21^{ras} protein. The data were selected from 3 similar experiments.

Expression of *N-ras* mRNA

Northern blot analysis showed that AFP (20 mg/L) had no significant influence on the expression of *N-ras* mRNA in Bel 7402 cells when treated for 2 h and 6 h, but *N-ras* mRNA was overexpressed when treated with AFP (20 mg/L) for 12 h and 24 h. The increased ratios were 22.6% (12 h) and 59.9% (24 h), respectively, compared with the control group, and HSA (20 mg/L) did not significantly affect the expression of *N-ras* mRNA (Figure 5).

Expression of p21^{ras} protein

Western blot analysis demonstrated that AFP significantly enhanced the expression of p21^{ras} protein in Bel 7402 cells by 35.2%, 102.6%, and 46.8% at 6, 12, and 24 h, respectively, compared with the control group. However, HSA (20 mg/L) did not influence the expression of p21^{ras} protein (Figure 6).

Expression of mutative p53 protein

The data showed that AFP significantly influenced the expression of mutative p53 protein in Bel 7402 cells by 13.4%, 39.9%, and 70.6% at 6, 12, and 24 h, respectively, compared with the control group. However, HSA (20 mg/L) did not affect the expression of mutative p53 protein (Figure 7).

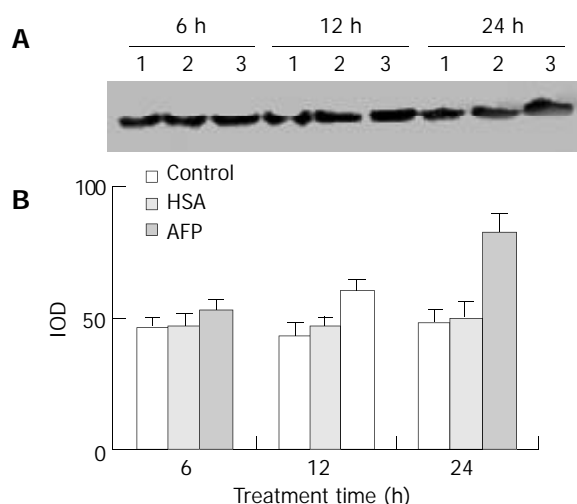


Figure 7 Effects of AFP (20 mg/L) or HSA (20 mg/L) on the expression of mutative p53 protein in Bel 7402 cells analyzed by Western blot. The cells were treated with AFP or HSA for 6, 12, and 24 h, respectively. A: Western blot analysis. Lane 1: control group; Lane 2: HSA treated group; Lane 3: AFP treated group. B: Densitometric intensity of absorbance (IOD) of p53 protein. The data were selected from 3 similar experiments.

DISCUSSION

Many investigations have shown that AFP receptors exist on the membrane of various tumor cells^[5,7,8,11-13], and play an important role in regulating growth of the cells^[7,8,14]. The receptor may mediate intercellular signal transduction which influences the expression of genes related to proliferation, and the expression of these genes is the most direct factor that controls cell cycle. Our results showed that AFP stimulated the expression of *c-fos*, *c-jun*, and *N-ras* mRNA in hepatocellular carcinoma Bel 7402 cells. Both *c-fos* and *c-jun* have the characteristics of early response genes. When treated with AFP, the two oncogenes in Bel 7402 cells express promptly, thereafter the expression of these oncogenes dramatically declines. Previous researches had showed that AFP promoted the proliferation^[1-6] and some oncogene expression of many tumor cells^[15,16]. Cell growth was regulated by various factors, in which, some oncogene coding proteins have an important function in modulating growth and differentiation of the cells. *c-fos* and *c-jun* are the immediate early genes (IEG) with the characteristics of early response gene. When Bel 7402 cells were treated with AFP, the expression of these oncogenes had the characteristics of dynamics, which was independent on the translation of RNA. Additionally, IEG coding regulated-proteins can control the expression of some later response genes through the activation of nuclear transcription factors. Furthermore, *c-Fos* and *c-Jun* proteins can interact with each other to form a heterodimer (*Fos-Jun*) called AP-1 (activator

protein-1). The dimer has leucine zipper structure, which has stronger binding affinity to DNA, and is the third messenger of signal transduction. The AP-1 protein is a nuclear transcription factor, which can regulate gene transcription by binding to a gene transcription-regulated element, and can increase transcriptional activation of downstream target genes. A previous study showed that the transcriptional properties of AP-1 depended on the site of cAMP-response elements to influence the expression of growth-related genes in hepatocellular carcinoma^[17]. Therefore, we thought that AFP regulated cell cycle of Bel 7402 cells, which was related to the expression of early-response genes. Our result also showed that AFP promoted the expression of *N-ras* in Bel 7402 cells. The *N-ras* gene is closely related to cell proliferation, and p21^{ras}, the *N-ras* coding protein, is an important intermediate of tyrosine-protein kinase (TPK) signal pathway in the cells to regulate growth-related gene expression. Therefore, we suggested that AFP could affect signal transduction to regulate growth of Bel 7402 cells probably through stimulating the expression of *N-ras*.

The wild type p53 is a very important tumor suppressor gene to inhibit proliferation of tumor cells. Some studies had showed that hepatocellular carcinoma was closely related to abnormal expression of p53 gene^[18,19]. Additionally, p53 and beta-catenin mutation rates were inversely correlated in hepatocellular carcinoma^[20]. The inactivation of p53 was an important cause of aberrant accumulation of beta-catenin, which was involved in both cell-cell interactions and wnt pathway-dependent cell fate determination in many cancer cells^[20]. A previous study found that p53 mutation was correlated significantly with invasiveness including vascular permeation of hepatocellular carcinoma cells, and p53 mutation in the primary lesion was useful as an indicator of the biological behavior of recurrent hepatocellular carcinoma^[21]. It showed that mutative p53 protein played a critical role in cell proliferation of hepatocellular carcinoma. The p53 gene could influence AFP expression to regulate the biological behavior of tumor cells^[22,23]. Our data had showed that AFP could enhance the expression of mutative p53 protein. When p53 gene is mutated, it can not suppress the growth of tumor cells, on the contrary, it possesses the functions of oncogenes. There are two types of mutative p53 genes in tumor cells, one of the mutative p53 genes can restrain the growth-suppressing activity of wild type p53 gene, then display apparently its negative regulation; the other type of mutative p53 genes can cooperate with *ras* gene to actuate cell transformation, and then become a dominant oncogene, which promotes the growth of tumor cells. Because *Ras* protein is an important intermediate in TPK signal transduction pathway, we analyzed the expression of *N-ras* mRNA, and then further detected its protein in this study. The results showed that AFP promoted the expression of p21^{ras} protein in Bel 7402 cells. The functions of p21^{ras} protein are similar to those of guanylate binding protein, and it can phosphorylate the intermediate in the downstream of TPK signal pathway to activate mitogen-activated protein kinase (MAPK) and to participate in intercellular signal transduction. The p21^{ras} protein can transduce the signal from TPK to threonine/serine protein kinase chain through Ras-Raf-MAPK signal pathway. These responses further activate some transcription factors which promote gene expression to enhance the growth of various cells. Our results demonstrated that AFP increased the expression of p21^{ras}. Therefore, we speculated that AFP affected the expression of p53 and p21^{ras} proteins through AFP receptor-mediated signal transduction pathway to accelerate the proliferation of Bel 7402 cells. Similar to the findings in this study, our previous study found that AFP enhanced the growth of HeLa and NIH3T3 cells through stimulating the expression of some oncogenes^[8,15,16], suggesting

that AFP might unselectively regulate proliferation of tumor cells in different tissues and species.

The mechanism for growth-promoting activity of AFP is still unclear. It has been known for a long time that AFP has the ability to transport the substances essential for cell proliferation to enter the cells. Studies have indicated that AFP is an important protein in the embryos to regulate growth of the fetus^[24], and required for female fertility, but not essential for embryonic development^[25]. Up to date, it is not clear whether the biological function of AFP is involved in regulating cell proliferation. Some studies indicated that AFP inhibited immune response to promote the growth of tumor cells *in vivo*^[26,27]. Escaping from the surveillance of immune system was the primary cause for malignant growth of tumor cells. Hepatocellular carcinoma cells can escape from the surveillance of immune system through altering the expression of tumor necrosis factor-related apoptosis-inducing ligand (TRAIL) receptors^[28], which can sustain the growth of tumor cells *in vivo*. However, our *in vitro* study could not establish the immune response without immune factors to affect the expression of the oncogenes in Bel 7402 cells. Therefore, it could not explain that AFP inhibited immune response to affect cell growth. Because AFP is a macromolecule, it is impossible to enter the cells through the cell membrane directly. Although AFP can transport some substances required for cell proliferation, it is not enough to completely support cell proliferation. Many studies found that AFP receptors existed on the membrane surface of various tumor cells, and mediated signal transduction to regulate the expression of the genes. The expression of these genes was the ultimate determination factor in regulating cell growth. Our results showed that AFP had the ability to stimulate the expression of the oncogenes *c-fos*, *c-jun*, and *N-ras* in Bel 7402 cells, and the response of these genes to AFP was various. Both the expression of *c-fos* and *c-jun* responded early, whereas the expression of *N-ras* and mutative p53 gene responded thereafter. Some oncogenes such as p53 and ras are important prognostic molecular markers in human hepatocellular carcinoma^[29]. According to previous studies^[5,7,8] and our results, we considered that the action of AFP was via TPK signal transduction pathway to stimulate the expression of some oncogenes which could regulate the growth of tumor cells. Many investigations had showed that the expression of some oncogenes was up-regulated in hepatocellular carcinoma, and some factors such as integrin gene, p28/gankyrin, and HLA class I could influence cell proliferation of hepatocellular carcinoma^[30-32]. However, some studies had shown that treatment of tumor cells *in vitro* with high dosage of AFP (1-10 $\mu\text{mol/L}$) significantly suppressed the growth of tumor cells, because AFP positively regulated cytochrome c-mediated caspase activation, apoptosome complex formation, and low-dose cytochrome c-mediated signals^[33,34]. The mechanisms for how AFP regulates the expression of these genes and signal transduction, and why it is not essential for embryonic development^[24], although it promotes the growth of some tumor cells^[1-8] remain to be studied.

A previous study showed that AFP could coordinate other growth factors existed in HSA and serum to promote the growth of porcine granulosa cells, and AFP could function to modulate growth factor-mediated cell proliferation during development and neoplasia^[4]. To further verify the up-regulation of these oncogenes was mediated by AFP, this study used HSA as a negative control due to similar amino acid sequences of AFP as HSA. The results showed that HSA or anti-AFP antibody did not stimulate the expression of these genes in Bel 7402 cells, but anti-AFP antibody efficiently blocked the function of AFP, which can be explained that AFP specifically stimulated the expression of these oncogenes in human hepatocellular carcinoma Bel 7402 cells.

REFERENCES

- 1 **Dudich E**, Semonkova L, Gorbatova E, Dudich I, Khromykh L, Tatulov E, Grechko G, Sukhikh G. Growth-regulative activity of human alpha-fetoprotein for different types of tumor and normal cells. *Tumour Biol* 1998; **19**: 30-40
- 2 **Wang XW**, Xie H. Alpha-fetoprotein enhances the proliferation of human hepatoma cells *in vitro*. *Life Sci* 1999; **64**: 17-23
- 3 **Wang XW**, Xu B. Stimulation of tumor-cell growth by alpha-fetoprotein. *Int J Cancer* 1998; **75**: 596-599
- 4 **Keel BA**, Eddy KB, Cho S, May JV. Synergistic action of purified alpha-fetoprotein and growth factors on the proliferation of porcine granulosa cells in monolayer culture. *Endocrinology* 1991; **129**: 217-225
- 5 **Li MS**, Li PF, Zhou AR, Li G, Du GG. Growth factor like activity of alpha-fetoprotein in human hepatoma cell line, Bel7402 and HeLa cell (abstract). *Endo 2000 the Endocrine Society 82nd Annual Meeting, Toronto, Canada* 2000: 143
- 6 **Nunez EA**. Biological role of alpha-fetoprotein in the endocrinological field: data and hypothesis. *Tumour Biol* 1994; **15**: 63-72
- 7 **Li MS**, Li PF, He SP, Du GG, Li G. The promoting molecular mechanism of alpha-fetoprotein on the growth of human hepatoma Bel7402 cell line. *World J Gastroenterol* 2002; **8**: 469-475
- 8 **Li MS**, Li PF, Yang FY, He SF, Du GG, Li G. The intracellular mechanism of alpha-fetoprotein promoting the proliferation of NIH 3T3 cells. *Cell Res* 2002; **12**: 151-156
- 9 **Yamada T**, Kakinoki M, Totsuka K, Ashida Y, Nishizono K, Tsuchiya R, Kobayashi K. Purification of canine alpha-fetoprotein and alpha-fetoprotein values in dogs. *Vet Immunol Immunopathol* 1995; **47**: 25-33
- 10 **Sambrook J**, Fritsch EF, Maniatis T. Molecular cloning: A laboratory manual, 2nd ed. New York: Cold Spring Harbor Laboratory Press 1989: 888-897
- 11 **Esteban C**, Geuskens M, Uriel J. Activation of an alpha-fetoprotein (AFP)/receptor autocrine loop in HT-29 human colon carcinoma cells. *Int J Cancer* 1991; **49**: 425-430
- 12 **Villacampa MJ**, Moro R, Naval J, Faily-Crepin C, Lempreave F, Uriel J. Alpha-fetoprotein receptors in a human breast cancer cell line. *Biochem Biophys Res Commun* 1984; **122**: 1322-1327
- 13 **Naval J**, Villacampa MJ, Goguel AF, Uriel J. Cell-type-specific receptor for alpha-fetoprotein in mouse T-lymphoma cell line. *Proc Natl Acad Sci U S A* 1985; **82**: 3301-3305
- 14 **Laderoute MP**, Pilarski LM. The inhibition of apoptosis by alpha-fetoprotein (AFP) and the role of AFP receptors in anti-cellular senescence. *Anticancer Res* 1994; **14**(6B): 2429-2438
- 15 **Li MS**, Li PF, Du GG, Li G. The enhancement effects of alpha-fetoprotein on the expression on *N-ras* and p53 and p21^{ras} in HeLa cells. *Chin J Biochem Mol Biol* 2002; **18**: 750-754
- 16 **Li MS**, Li PF, Li G, Du GG. Enhancement of proliferation of HeLa cells by the α -fetoprotein. *Shengwu Huaxue Yu Shengwu Wuli Xuebao* 2002; **34**: 769-774
- 17 **Guberman AS**, Scassa ME, Giono LE, Varone CL, Canepa ET. Inhibitory effect of AP-1 complex on 5-aminolevulinate synthase gene expression through sequestration of cAMP-response element protein (CRE)-binding protein (CBP) coactivator. *J Biol Chem* 2003; **278**: 2317-2326
- 18 **Caruso ML**, Valentini AM. Overexpression of p53 in a large series of patients with hepatocellular carcinoma: a clinicopathological correlation. *Anticancer Res* 1999; **19**(5B): 3853-3856
- 19 **Zhang XW**, Xu B. Differential regulation of P53, c-Myc, Bcl-2, Bax and AFP protein expression, and caspase activity during 10-hydroxycamptothecin-induced apoptosis in Hep G2 cells. *Anticancer Drugs* 2000; **11**: 747-756
- 20 **Cagatay T**, Ozturk M. P53 mutation as a source of aberrant beta-catenin accumulation in cancer cells. *Oncogene* 2002; **21**: 7971-7980
- 21 **Sheen IS**, Jeng KS, Wu JY. Is p53 gene mutation an indicator of the biological behaviors of recurrence of hepatocellular carcinoma? *World J Gastroenterol* 2003; **9**: 1202-1207
- 22 **Ogden SK**, Lee KC, Wernke-Dollries K, Stratton SA, Aronow B, Barton MC. p53 targets chromatin structure alteration to repress alpha-fetoprotein gene expression. *J Biol Chem* 2001; **276**: 42057-42062
- 23 **Lee KC**, Crowe AJ, Barton MC. p53-mediated repression of alpha-fetoprotein gene expression by specific DNA binding. *Mol*

- Cell Biol* 1999; **19**: 1279-1288
- 24 **Mazure NM**, Chauvet C, Bois-Joyeux B, Bernard MA, Nacer-Cherif H, Danan JL. Repression of alpha-fetoprotein gene expression under hypoxic conditions in human hepatoma cells: characterization of a negative hypoxia response element that mediates opposite effects of hypoxia inducible factor-1 and c-Myc. *Cancer Res* 2002; **62**: 1158-1165
- 25 **Gabant P**, Forrester L, Nichols J, Van Reeth T, De Mees C, Pajack B, Watt A, Smitz A, Alexandre H, Szpirer C, Szpirer J. Alpha-fetoprotein, the major fetal serum protein, is not essential for embryonic development but is required for female fertility. *Proc Natl Acad Sci U S A* 2002; **99**: 12865-12870
- 26 **Semeniuk DJ**, Boismenu R, Tam J, Weissenhofer W, Murgita RA. Evidence that immunosuppression is an intrinsic property of the alpha-fetoprotein molecule. *Adv Exp Med Biol* 1995; **383**: 255-269
- 27 **Gotsman I**, Israeli D, Alper R, Rabbani E, Engelhardt D, Ilan Y. Induction of immune tolerance toward tumor-associated enables growth of human hepatoma in mice. *Int J Cancer* 2002; **97**: 52-57
- 28 **Chen XP**, He SQ, Wang HP, Zhao YZ, Zhang WG. Expression of TNF-related apoptosis-inducing Ligand receptors and anti-tumor effects of TNF-related apoptosis-inducing Ligand in human hepatocellular carcinoma. *World J Gastroenterol* 2003; **9**: 2433-2440
- 29 **Qin LX**, Tang ZY. The prognostic molecular markers in hepatocellular carcinoma. *World J Gastroenterol* 2002; **8**: 385-392
- 30 **Liu LX**, Jiang HC, Liu ZH, Zhou J, Zhang WH, Zhu AL, Wang XQ, Wu M. Intergrin gene expression profiles of human hepatocellular carcinoma. *World J Gastroenterol* 2002; **8**: 631-637
- 31 **Fu XY**, Wang HY, Tan L, Liu SQ, Cao HF, Wu MC. Overexpression of p28/gankyrin in human hepatocellular carcinoma and its clinical significance. *World J Gastroenterol* 2002; **8**: 638-643
- 32 **Huang J**, Cai MY, Wei DP. HLA class I expression in primary hepatocellular carcinoma. *World J Gastroenterol* 2002; **8**: 654-657
- 33 **Dudich E**, Semenkova L, Dudich I, Gorbatova E, Tochtamisheva N, Tatulov E, Nikolaeva M, Sukhikh G. Alpha-fetoprotein causes apoptosis in tumor cells via a pathway independent of CD95, TNFR1 and TNFR2 through activation of caspase-3-like proteases. *Eur J Biochem* 1999; **266**: 750-761
- 34 **Semenkova L**, Dudich E, Dudich I, Tokhtamisheva N, Tatulov E, Okruzhnov Y, Garcia-Foncillas J, Palop-Cubillo JA, Korpela T. Alpha-fetoprotein positively regulates cytochrome c-mediated caspase activation and apoptosome complex formation. *Eur J Biochem* 2003; **270**: 4388-4399

Edited by Chao JCJ Proofread by Xu FM

Comparison of long-term effects between intra-arterially delivered ethanol and Gelfoam for the treatment of severe arterioportal shunt in patients with hepatocellular carcinoma

Ming-Sheng Huang, Qu Lin, Zai-Bo Jiang, Kang-Shun Zhu, Shou-Hai Guan, Zheng-Ran Li, Hong Shan

Ming-Sheng Huang, Zai-Bo Jiang, Kang-Shun Zhu, Shou-Hai Guan, Zheng-Ran Li, Hong Shan, Department of Radiology, The 3rd Affiliated Hospital of Sun Yat-sen University, Guangzhou 51000, Guangdong Province, China

Qu Lin, Department of Internal Medicine, The 3rd Affiliated Hospital of Sun Yat-sen University, Guangzhou 51000, Guangdong Province, China

Correspondence to: Professor Hong Shan, Department of Radiology, The 3rd Affiliated Hospital of Sun Yat-sen University, 600 Tianhe Road Guangzhou, 510630 China. gzshsums@public.guangzhou.gd.cn

Telephone: +86-20-85516867-2316 **Fax:** +86-20-87580725

Received: 2003-11-12 **Accepted:** 2003-12-16

Abstract

AIM: To evaluate long-term effect of ethanol embolization for the treatment of hepatocellular carcinoma (HCC) with severe hepatic arterioportal shunt (APS), compared with Gelfoam embolization.

METHODS: Sixty-four patients (ethanol group) and 33 patients (Gelfoam group) with HCC and APS were respectively treated with ethanol and Gelfoam for APS before the routine interventional treatment for the tumor. Frequency of recanalization of shunt, complete occlusion of the shunt, side effects, complications, and survival rates were analyzed between the two groups.

RESULTS: The occlusion rate of APS after initial treatment in ethanol group was 70.3%(45/64), and recanalization rate of 1 month after embolization was 17.8%(8/45), and complete occlusion rate was 82.8%(53/64). Those in Gelfoam group were 63.6%(21/33), 85.7%(18/21), and 18.2%(6/33). There were significant differences in recanalization rate and complete occlusion rate between the two groups ($P<0.05$). The survival rates in ethanol group were 78% at 6 months, 49% at 12 months, 25% at 24 months, whereas those in Gelfoam group were 58% at 6 months, 23% at 12 months, 15% at 24 months. The ethanol group showed significantly better survival than Gelfoam group ($P<0.05$). In the ethanol group, there was a significant prolongation of survival in patients with monofocal HCC ($P<0.05$) and Child class A ($P<0.05$). There were no significant differences in survival rate in the Gelfoam group with regard to the number of tumor and Child class ($P>0.05$). The incidence rate of abdominal pain during procedure in ethanol group was 82.8%. There was no significant difference in postembolization syndromes between two groups. Procedure-related hepatic failure did not occur in ethanol group.

CONCLUSION: Ethanol embolization for patients with HCC and severe APS is efficacious and safe, and may contribute to prolongation of the life span versus Gelfoam embolization.

Huang MS, Lin Q, Jiang ZB, Zhu KS, Guan SH, Li ZR, Shan H. Comparison of long-term effects between intra-arterially

delivered ethanol and Gelfoam for the treatment of severe arterioportal shunt in patients with hepatocellular carcinoma. *World J Gastroenterol* 2004; 10(6): 825-829

<http://www.wjgnet.com/1007-9327/10/825.asp>

INTRODUCTION

Hepatocellular carcinoma is frequently associated with arterioportal shunts. Kido and Ngan *et al*^[1,2] reported that APS in HCC occurred in 60%, and Okuda *et al*^[3] reported that severe APS of main or right or left portal veins occurred in 30% of patients with HCC. Severe APS led to life threatening conditions (*e.g.*, esophageal varices, ascites and hepatic encephalopathy) as a result of portal regurgitation or portal hypertension^[4-7]. To improve portal hypertension caused by severe APS in patients with HCC, APS needs to be treated. To date, Gelfoam and steel coil are the most commonly used embolic materials^[8-10]. However, any long-term effect of embolization of APS with steel coil or Gelfoam on survival have not been proved, although they produced a good short-term effect as reported^[8-10]. It has been a hot issue how to choose an ideal embolic material to occlude APS. In this study, we used ethanol as the embolic material to treat the APS before the routine interventional treatment for 64 patients. The purpose of this study was to evaluate the long-term effect of the transcatheter arterial embolization (TAE) of APS with new embolic material in patients with HCC and APS, in comparison with the most commonly used material: Gelfoam.

MATERIALS AND METHODS

Patients

Among 596 patients with HCC treated with transcatheter arterial chemoembolization (TACE) or transcatheter arterial infusion chemotherapy (TAI) at the 3rd Affiliated Hospital of Sun Yat-sen University from February 1999 to March 2003, 161(27%) patients with severe APS were identified by digital subtraction angiography (DSA). We excluded patients with Child class C disease and patients who underwent the treatment of surgical resection, percutaneous local ethanol injection, microwave coagulation, or systemic chemotherapy throughout the study period. According to the exclusive criteria, 64 of 161 patients were excluded from this study. Ninety-seven patients were enrolled in our study (78 men and 19 women, ranging from 21 to 78 years of age; mean age, 57.9). All the patients were treated with TAI or TACE after undergoing embolization of APS.

Written informed consent was obtained from the patients involved in this study. We divided the patients into 2 groups: ethanol group, in which APS was treated with ethanol for 64 patients from April 2000 to March 2003, and Gelfoam group, in which APS was treated with gelatin sponge particles for 33 patients from February 1999 to March 2000. The clinical characteristics of two therapeutic groups were illustrated in Table 1. Although this was a retrospective nonrandomized

study, there were no significant differences between two groups in background factors (Table 1).

Table 1 Clinicopathologic characteristics of patients with HCC and APS

Characteristics	Ethanol group (n=64)	Gelfoam group (n=33)	P value
Age (y)	56.4±21.4	52.3±26.6	0.42
Sex (M/F)	52/12	25/7	0.72
Child classification			
Child class A	35(55%)	20(61%)	
Child class B	29(45%)	13(39%)	0.56
Serum total bilirubin (mg/ml)	1.6±1.5	2.0±1.8	0.31
Serum albumin (g/dl)	3.6±0.8	3.4±1.1	0.30
Number of tumors			
1	15(23%)	11(33%)	
2-3	19(30%)	8(24%)	
≥4, diffuse	30(47%)	14(43%)	0.32

Treatments

Firstly, arteriography of hepatic common artery was performed to visualize the arterial vascularization of the liver and to identify the location, severity and direction of vessels of APS. Secondly, a 3-F microcatheter was superselectively inserted into the dominant artery of APS through a 5-F catheter. The embolic material was injected to occlude APS. All diagnostic studies and treatments of APS were performed during the same procedure.

Ethanol group: 2-3 mL absolute ethanol was injected slowly and gently at the rate of about 1 mL/min after 2 mL 10g/L lidocaine was injected through catheter. About 5-10 min later, a repeated DSA was performed to evaluate the occlusive extent of APS. If persistence of APS was shown, another 2-3 mL ethanol was injected repeatedly until the occlusion of APS was confirmed with angiography.

Gelfoam group: Gelatin sponge particles (size, 1 mm×1 mm×1 mm) were mixed with contrast media (Iopamilon, Schering, Berlin, Germany) and were injected with 1-mL tuberculin syringe under fluoroscopic monitoring until a slow flow or stasis of APS was demonstrated. Then arteriography was done again to confirm the occlusion of APS. If APS could not be occluded with Gelatin sponge particles (size, 1 mm×1 mm×1 mm) and microcatheter, a 4F Röscher hepatic catheter or 4F cobra catheter would replace the 3-F microcatheter and be inserted into or by the way of the feeding artery of shunt. Then several large pieces of Gelfoam (beyond 1×1×1 mm) were used to occlude the shunt.

After embolization of APS, the routine interventional therapy was done for the tumor, as reported^[11-15]. After catheter was inserted into feeding artery of tumour, pirarubicin (THP)/lipiodol(LPD) emulsion was injected through catheter for the patients without tumour thrombus in main portal vein. THP/LPD was prepared with the following procedure. THP (60-80 mg) was dissolved in 3-10 mL of 50 g/L glucose and then mixed with 3-10 mL LPD at a 1:1 ratio repeating approximately 10 times. Then gelatin sponges embolization of feeding artery was performed. We only injected pirarubicin (60-80 mg) which was dissolved in 100 mL of 50g/L glucose for the patients with tumour thrombus in main portal vein.

Criteria for evaluating embolic effect

Recanalization of APS was defined as APS was shown again at arterial phase of DSA 1 month postprocedure in the patients who had the complete occlusion of shunt after initial treatment. Complete occlusion of APS was defined as APS was not demonstrated in DSA for 2 times consecutively.

Follow-up protocol

All patients were followed up by means of spiral CT scan of liver and laboratory tests such as concentrations of α -fetoprotein, liver function before and after treatment. Change of APS was evaluated with DSA which was performed 1 and 2 mo after initial treatment. Then all patients should be followed up every 2-3 mo. When elevation of tumor markers (α -fetoprotein), persistence of APS or recurrence of tumor were observed, patients were readmitted for angiography and treatment as before.

Statistical analysis

The cumulative proportional survival rates were calculated according to the Kaplan-Meier method. The starting point was defined as the day of initial treatment. The significance of differences between background clinical characteristics of the patients groups (ethanol and Gelfoam) was assessed with the χ^2 test and Student's *t* test. The significance of difference in survival rates between patients was evaluated by the generalized Wilcoxon test. Values of $P < 0.05$ were considered significant.

RESULTS

Results of occlusion of APS

In the ethanol group, APS was occluded completely at the initial treatment in 45(70.3%) patients. Among them, recanalization of APS 1 month post-procedure was shown in 8(17.8%). There were 30(46.9%) patients with APS 1 month after initial treatment, which included incomplete occlusion of APS in the initial treatment, recanalizational and newly occurred APS. Of them APSs were occluded completely after a second treatment in 16 patients. The rate of complete occlusion of APS in ethanol group was 82.8%(53/64) totally (Figures 1A-F).

In the Gelfoam group, 21(63.6%) patients had the complete occlusion of APS in the initial treatment. Recanalization of APS occurred in 18(85.7%) patients of them 1 mo after initial treatment. Thirty (90.6%) patients were with APS 1 mo after initial treatment, which consisted of incomplete occlusion of APS in the initial treatment, recanalization and newly occurred APS. In 3 patients of them, APS were occluded completely after another treatment. The complete occlusion rate of APS in Gelfoam group was 18.2%(6/33) totally.

The recanalization rate of APS in ethanol group was lower than that in Gelfoam group ($\chi^2=24.91$, $P < 0.05$), and the complete occlusion rate of APS in ethanol group was higher than that in Gelfoam group ($\chi^2=32.06$, $P < 0.05$).

Survival

The survival rate in the ethanol group were 78% at 6 mo, 49% at 12 mo, and 25% at 24 mo. The median survival was 11 mo. By comparison, the survival rates in the Gelfoam group were 58% at 6 mo, 29% at 12 mo, 15% at 24 mo, and the median survival was 7 mo. The survival rates in the ethanol group were significantly higher than those in the Gelfoam group ($P < 0.05$) (Figure 2).

In the ethanol group, the survival rates of patients with single HCC nodule were 92% at 6 mo, 70% at 12 mo, and 55% at 24 mo. The survival rates of patients with two or three HCC nodules were 73% at 6 mo, 55% at 12 mo and 22% at 24 mo. The survival rates of patients with multiple HCC nodules or diffuse HCC were 68% at 6 mo, 33% at 12 mo and 15% at 24 mo. The survival rates of patients with monofocal HCC were significantly higher than those of patients with multifocal HCC ($P < 0.05$) (Figure 3). The survival rates of patients of Child class A were 91% at 6 mo, 60% at 12 mo, and 38% at 24 mo. The survival rates of patients of Child class B were 62% at 6 mo, 35% at 12 mo and 13% at 24 mo. The survival rates of patients of Child class A were higher than those of patients of Child class B ($P < 0.05$) (Figure 4).

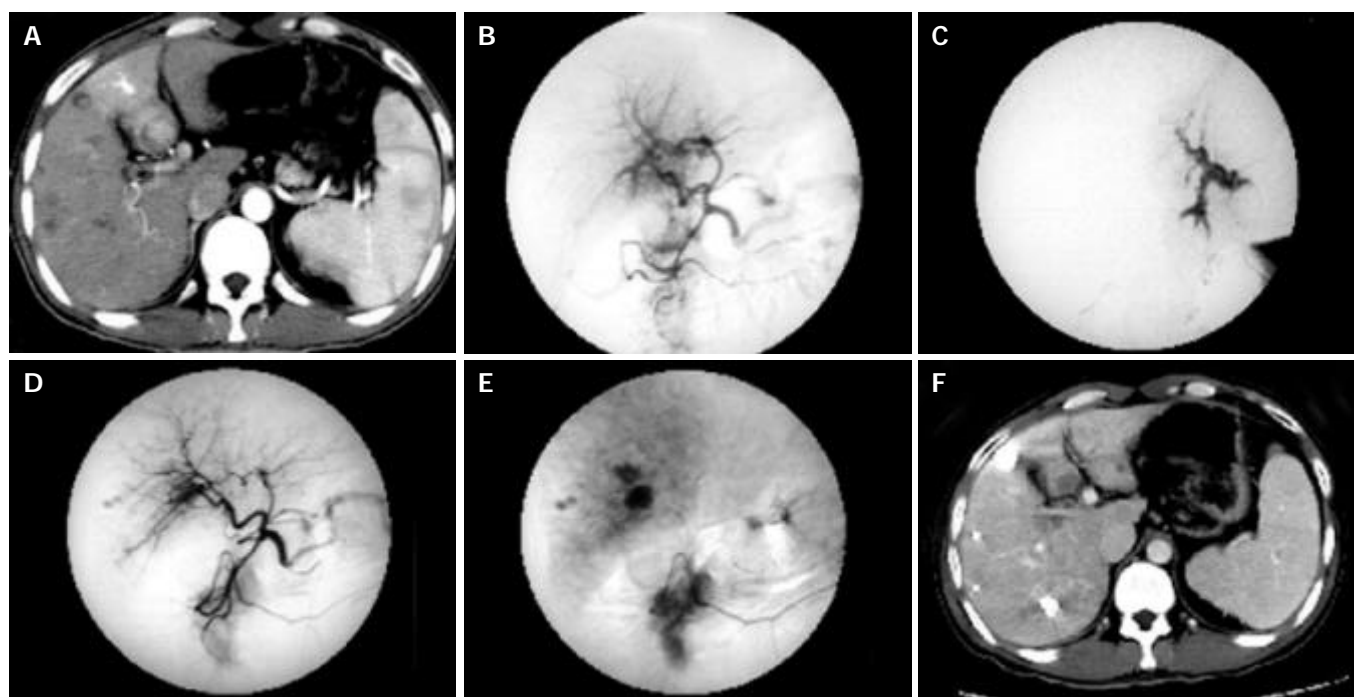


Figure 1 Multiple HCC nodules in a 34-year-old patient. A: CT image obtained during the arterial phase showed the predominant enhancement of the medial segment of left lobe and the enhancement of left portal branches, which represent APS. B: Hepatic arteriogram demonstrated the arterioportal shunt. C: The microcatheter was inserted into the feeding artery of APS. DSA showed the strong or fast blood flow of APS. D-E: Hepatic arteriogram showed that the arterioportal shunt was no longer visible after embolization with a microcoil and ethanol. F: Follow-up CT scan showed lipiodol accumulation in multiple HCC nodules, and liver necrosis was not seen in the distribution of the hepatic artery which had been treated with ethanol.

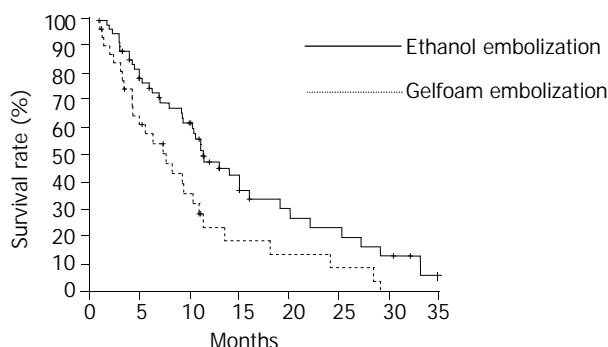


Figure 2 Cumulative survival curves for patients with HCC and APS in two therapeutic groups are shown. The survival rates for patients in the ethanol group were significantly higher than those in the Gelfoam group ($P < 0.05$).

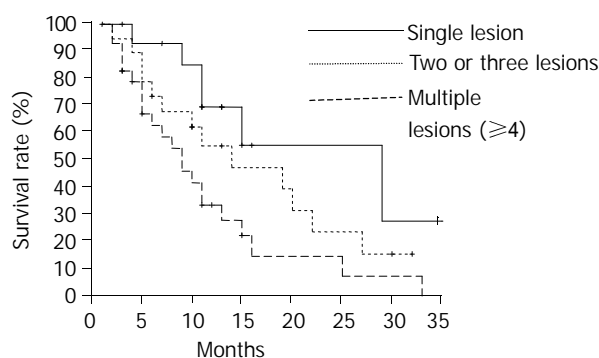


Figure 3 Cumulative survival curves for patients with HCC and APS in relation to number of tumors are shown in ethanol group. The survival rates of patients with monofocal HCC and APS were significantly higher than those of patients with multifocal HCC and APS (single lesion vs two or three lesions, $P < 0.05$; two or three lesions vs four or more lesions, $P < 0.05$).

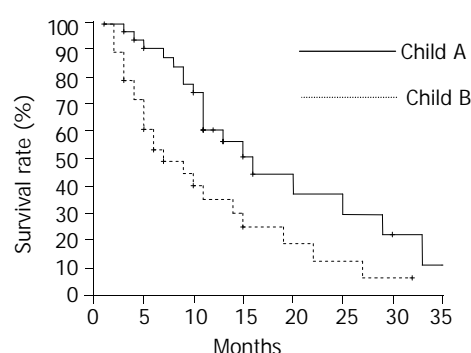


Figure 4 Cumulative survival curves for patients with HCC and APS according to the Child class were shown in ethanol group. The survival rates of patients of Child class A were higher than those of Child class B ($P < 0.05$).

In the Gelfoam group, the survival rates of patients with single HCC nodule were 62% at 6 mo, 38% at 12 mo, and 19% at 24 mo. The survival rates of patients with two or three HCC nodules were 61% at 6 mo, 26% at 12 mo and 12% at 24 mo. The survival rates of patients with multiple HCC nodules or diffuse HCC were 60% at 6 mo, 28% at 12 mo and 0 at 24 mo. The survival rates of patients of Child class A were 60% at 6 mo, 25% at 12 mo, and 18% at 24 mo. The survival rates of patients of Child class B were 68% at 6 mo, 30% at 12 mo and 15% at 24 mo. There were no significant differences in survival rates with regard to the number of tumor, and Child class ($P > 0.05$).

Side effects and complications

In the ethanol group, a short-period intense abdominal pain occurred in 53 (82.8%) patients during the process of ethanol injection, and mild abdominal pain in 9 (14.1%) patients, and indolence in 2 (3.1%) patients. Postembolization syndromes (such as nausea, vomiting, fever, and abdominal pain) occurred

in 50(78.1%) patients in ethanol group, and 30(90.9%) patients in Gelfoam group. There was no significant difference between the 2 groups ($\chi^2=1.66$, $P>0.05$). No patient died of procedure-related hepatic failure. In ethanol group, all feeding artery remained patent in the follow-up DSA arteriograms, and liver necrosis in the distribution of the hepatic artery which had been treated with ethanol was not seen in all patients according to the follow-up CT scans.

DISCUSSION

Hepatocellular carcinoma is frequently associated with arterioportal shunts. In our series, severe APSs were verified in 27% of patients with HCC by DSA. Severe APS leads to or aggravates portal hypertension which leads to life-threatening conditions such as esophageal varices, refractory ascites, refractory diarrhea and hepatic encephalopathy^[4-7,16,17]. Additionally, severe APSs have an influence on the performance of TAI or TACE for the treatment of HCC^[18]. The persistence of APS may possibly result in the poor prognosis of HCC. For the reasons as above, severe APS needs to be treated effectively.

Many embolic materials have been used to treat APS in patients with HCC^[8,9,19-23]. Of those Gelfoam and steel coil were the most commonly used. Clark^[9] and Tarazov^[8] reported that Gelfoam and steel coil emboli for the treatment of APS could not prolong the survival of patients with HCC, although they had a good short-term effect on the control of gastric bleeding and ascites. Those effects may be attributable to certain actions of those embolic materials. Firstly, Gelfoam embolization was likely to result in inadvertent embolization, and cause the occlusion of feeding artery of tumor, which would influence the procedure of TAI or TACE for the treatment of tumor. Secondly, the recanalization of APS occurred easily as a result of the development of collateral vessels and the absorption of Gelfoam two to four weeks after embolization. In our study, the recanalization rate of APS was 85.7% 1 month after embolization with Gelfoam. Similarly, the embolization with steel coil also produced the recanalization of APS as a result of the development of collateral anastomoses^[8].

Ethanol is a liquid embolic agent that causes immediate vascular sclerosis and occlusion by a combination of direct toxic effect on the vascular wall and clumping of damaged erythrocytes and denatured proteins^[24-26]. It has been used widely in the treatment of renal cell carcinoma, esophageal varices, and arteriovenous malformations^[24-35]. Similar to the treatment of arteriovenous malformation, injecting ethanol into APS results in clot formation, denudes the endothelium and causes embolization by penetrating into the capillaries. As an embolic material, ethanol is superior to Gelfoam in the treatment of APS. First, ethanol can pass to and occlude the capillaries and veins of shunt, and does not lead to the occlusion of feeding artery of tumor. Thus it produces a more complete occlusion of APS than Gelfoam. Second, ethanol is a kind of long-acting embolic material, and it rarely develops the collateral anastomoses after embolization with ethanol. It has a low recanalization rate of APS. Third, ethanol also has a direct tumoricidal effect. Our results showed the recanalization rate of APS 1 month after embolization with ethanol was 17.8%, and complete occlusion rate was 82.8%, which were better than those of Gelfoam group ($P<0.05$).

Furuse *et al*^[10] reported that the survival rate of patients with HCC and APS after steel coil embolization were 45% at 6 mo, 12% at 12 mo, and 6% at 2 yr, and it could not prolong the survival of patient with HCC after the treatment of APS. However, Liu *et al*^[36] reported that the survivals of HCC patients without APS were higher than those of patients with APS. It indicated that the persistence of APS was an important

prognostic factor. In our study, the complete occlusion rate of shunt in ethanol group was higher than that in Gelfoam group ($P<0.05$). The survival rate of patients in the ethanol group was 78% at 6 mo, 49% at 12 mo, 25% at 24 mo, which were higher than those of Gelfoam group ($P<0.05$). Our results suggest that the embolization of APS with ethanol provides a survival advantage over that with gelfoam in patient with HCC. In addition, there was a significant prolongation of survival in patients with monofocal HCC and Child class A in ethanol group ($P<0.05$). However, there were no significant differences in survival rates in Gelfoam group with regard to the differences in the number of tumor and Child class ($P>0.05$). It was suggested that the survival rate was also related to the stage and invasive extent of tumor, and general state of patients. On the other hand, the persistence of severe APS was the important factor which influenced the survival of patient with HCC and APS.

The most common complication of embolization of APS with ethanol was abdominal pain caused by destruction of the vascular endothelium when ethanol was injected^[24,25]. The incidence was 82.8% in our study. It could be alleviated immediately when we stopped injecting ethanol. There was no severe complication related to ethanol embolization. In our study, liver necrosis was not seen in the distribution of the hepatic artery which had been treated with ethanol in the follow-up CT scans. The postembolization syndromes were related to the specific treatment of tumor, and there was no significant difference between the two groups.

In conclusion, ethanol embolization for patients with HCC and severe APS is efficacious and safe, and may contribute to prolongation of the life span versus Gelfoam embolization.

ACKNOWLEDGMENTS

We thank David A. Kumpe, MD, from the Health Sciences Center, University of Colorado Derver, USA, for his assistance in revising the manuscript.

REFERENCES

- 1 Kido C, Sasaki T, Kaneko M. Angiography of primary liver cancer. *Am J Roentgenol Radium Ther Nacl Med* 1971; **113**: 70-81
- 2 Ngan H, Peh WC. Arteriovenous shunting in hepatocellular carcinoma: its prevalence and clinical significance. *Clin Radiol* 1997; **52**: 36-40
- 3 Okuda K, Musha H, Yamasaki T, Kubo Y, Shimokawa Y, Nagasaki Y, Sawa Y, Jinnouchi S, Kaneko T, Obata H, Hisamitsu T, Motoike Y, Okazaki N, Kojiro M, Sakamoto K, Nakashima T. Angiographic demonstration of intrahepatic arterio-portal anastomoses in hepatocellular carcinoma. *Radiology* 1977; **122**: 53-58
- 4 Lazaridis KN, Kamath PS. Images in hepatology. Arterio-portal fistula causing recurrent variceal bleeding. *J Hepatol* 1998; **29**: 142
- 5 Choi BI, Lee KH, Han JK, Lee JM. Hepatic arterioportal shunts: dynamic CT and MR features. *Korean J Radiol* 2002; **3**: 1-15
- 6 Yu JS, Rofsky NM. Magnetic resonance imaging of arterioportal shunts in the liver. *Top Magn Reson Imaging* 2002; **13**: 165-176
- 7 Okuyama M, Fujiwara Y, Hayakawa T, Shiba M, Watanabe T, Tomimaga K, Tamori A, Oshitani N, Higuchi K, Matsumoto T, Nakamura K, Wakasa K, Hirohashi K, Ashida S, Shuin T, Arakawa T. Esophagogastric varices due to arterioportal shunt in a serous cystadenoma of the pancreas in von Hippel-Lindau disease. *Dig Dis Sci* 2003; **48**: 1948-1954
- 8 Tarazov PG. Intrahepatic arterioportal fistulae: role of transcatheter embolization. *Cardiovasc Intervent Radiol* 1993; **16**: 368-373
- 9 Clark RA, Frey RT, Colley DP, Eiseman WR. Transcatheter embolization of hepatic arteriovenous fistulas for control of hemobilia. *Gastrointest Radiol* 1981; **6**: 353-356
- 10 Furuse J, Iwasaki M, Yoshino M, Konishi M, Kawano N, Kinoshita T, Ryu M, Satake M, Moriyama N. Hepatocellular car-

- cinoma with portal vein tumor thrombus: embolization of arterioportal shunts. *Radiology* 1997; **204**: 787-790
- 11 **Ueno K**, Miyazono N, Inoue H, Nishida H, Kanetsuki I, Nakajo M. Transcatheter arterial chemoembolization therapy using iodized oil for patients with unresectable hepatocellular carcinoma: evaluation of three kinds of regimens and analysis of prognostic factors. *Cancer* 2000; **88**: 1574-1581
 - 12 **Favoulet P**, Cercueil JP, Faure P, Osmak L, Isambert N, Beltramo JL, Cognet F, Krause D, Bedenne L, Chauffert B. Increased cytotoxicity and stability of Lipiodol-pirarubicin emulsion compared to classical doxorubicin-Lipiodol: potential advantage for chemoembolization of unresectable hepatocellular carcinoma. *Anticancer Drugs* 2001; **12**: 801-806
 - 13 **Fan J**, Wu ZQ, Tang ZY, Zhou J, Qiu SJ, Ma ZC, Zhou XD, Ye SL. Multimodality treatment in hepatocellular carcinoma patients with tumor thrombi in portal vein. *World J Gastroenterol* 2001; **7**: 28-32
 - 14 **Chen MS**, Li JQ, Zhang YQ, Lu LX, Zhang WZ, Yuan YF, Guo YP, Lin XJ, Li GH. High-dose iodized oil transcatheter arterial chemoembolization for patients with large hepatocellular carcinoma. *World J Gastroenterol* 2002; **8**: 74-78
 - 15 **Lin SC**, Shih SC, Kao CR, Chou SY. Transcatheter arterial embolization treatment in patients with hepatocellular carcinoma and risk of pulmonary metastasis. *World J Gastroenterol* 2003; **9**: 1208-1211
 - 16 **Morse SS**, Sniderman KW, Galloway S, Rapoport S, Ross GR, Glickman MG. Hepatoma, arterioportal shunting, and hyperkinetic portal hypertension: therapeutic embolization. *Radiology* 1985; **155**: 77-82
 - 17 **Velazquez RF**, Rodriguez M, Navascues CA, Linares A, Perez R, Sotorrios NG, Martinez I, Rodrigo L. Prospective analysis of risk factors for hepatocellular carcinoma in patients with liver cirrhosis. *Hepatology* 2003; **37**: 520-527
 - 18 **Ueno K**, Miyazono N, Inoue H, Nishida H, Kanetsuki I, Nakajo M. Transcatheter arterial chemoembolization therapy using iodized oil for patients with unresectable hepatocellular carcinoma: evaluation of three kinds of regimens and analysis of prognostic factors. *Cancer* 2000; **88**: 1574-1581
 - 19 **Applbaum YN**, Renner JW. Steel coil embolization of hepatoportal fistulae. *Cardiovasc Intervent Radiol* 1987; **10**: 75-79
 - 20 **Yamagami T**, Nakamura T, Nishimura T. Portal hypertension secondary to spontaneous arterio-portal venous fistulas: transcatheter arterial embolization with n-butyl cyanoacrylate and microcoils. *Cardiovasc Intervent Radiol* 2000; **23**: 400-402
 - 21 **Orons PD**, Zajko AB, Jungrels CA. Arterioportal fistula causing portal hypertension and variceal bleeding: treatment with a detachable balloon. *J Vasc Interv Radiol* 1994; **5**: 373-376
 - 22 **Raghuram L**, Korah IP, Jaya V, Athyal RP, Thomas A, Thomas G. Coil embolization of a solitary congenital intrahepatic hepatoportal fistula. *Abdom Imaging* 2001; **26**: 194-196
 - 23 **Akpek S**, Ilgit ET, Cekirge S, Yucel C. High-flow arterioportal fistula: treatment with detachable balloon occlusion. *Abdom Imaging* 2001; **26**: 277-280
 - 24 **Guan SH**, Shan H, Jiang ZB, Huang MS, Zhu KS, Li ZR, Meng XC. Transmicrocatheter local injection of ethanol to treat hepatocellular carcinoma with high flow arteriovenous shunts. *Zhonghua Fangshexue Zazhi* 2002; **36**: 997-1000
 - 25 **Luo PF**, Chen XM, Zhang LM, Zhou ZJ, Fu L, Wei ZH. The management of arteriovenous shunting in hepatocellular carcinoma. *Zhonghua Fangshexue Zazhi* 2002; **36**: 114-117
 - 26 **Wang SP**, Xu WD, Huo F, Chen GZ. The clinical significance of intrahepatic arteriovenous shunt in patients with hepatic carcinoma. *Zhonghua Putong Waikexue Zazhi* 2003; **18**: 84-86
 - 27 **Lee BB**, Bergan JJ. Advanced management of congenital vascular malformations: a multidisciplinary approach. *Cardiovasc Surg* 2002; **10**: 523-533
 - 28 **De Baere T**, Lagrange C, Kuoch V, Morice P, Court B, Roche A. Transcatheter ethanol renal ablation in 20 patients with persistent urine leaks: an alternative to surgical nephrectomy. *J Urol* 2000; **164**: 1148-1152
 - 29 **Lee W**, Kim TS, Chung JW, Han JK, Kim SH, Park JH. Renal angiomyolipoma: embolotherapy with a mixture of alcohol and iodized oil. *J Vasc Interv Radiol* 1998; **9**: 255-261
 - 30 **Shimamura T**, Nakajima Y, Une Y, Namieno T, Ogasawara K, Yamashita K, Haneda T, Nakanishi K, Kimura J, Matsushita M, Sato N, Uchino J. Efficacy and safety of preoperative percutaneous transhepatic portal embolization with absolute ethanol: a clinical study. *Surgery* 1997; **121**: 135-141
 - 31 **Saitoh H**, Hayakawa K, Nishimura K, Kubo S, Hida S. Long-term results of ethanol embolization of renal cell carcinoma. *Radiat Med* 1997; **15**: 99-102
 - 32 **Gong GQ**, Wang XL, Wang JH, Yan ZP, Cheng JM, Qian S, Chen Y. Percutaneous transsplenic embolization of esophageal and gastro-fundal varices in 18 patients. *World J Gastroenterol* 2001; **7**: 880-883
 - 33 **Lu MD**, Chen JW, Xie XY, Liang LJ, Huang JF. Portal vein embolization by fine needle ethanol injection: experimental and clinical studies. *World J Gastroenterol* 1999; **5**: 506-510
 - 34 **Okano H**, Shiraki K, Inoue H, Kawakita T, Deguchi M, Sugimoto K, Sakai T, Ohmori S, Murata K, Nakano T. Long-term follow-up of patients with liver cirrhosis after endoscopic esophageal varices ligation therapy: comparison with ethanol injection therapy. *Hepatogastroenterology* 2003; **50**: 2013-2016
 - 35 **Ghoshal UC**, Dhar K, Chaudhuri S, Pal BB, Pal AK, Banerjee PK. Esophageal motility changes after endoscopic intravariceal sclerotherapy with absolute alcohol. *Dis Esophagus* 2000; **13**: 148-151
 - 36 **Liu Q**, Tian JM, Jia YC, Wang ZT, Ye H, Yang JJ, Sun F, Lin L, He J. Interventional therapies and analysis of prognostic in hepatocellular carcinoma with tumor thrombus of main portal vein. *Zhonghua Fangshexue Zazhi* 1999; **33**: 538-541

Edited by Zhu LH Proofread by Xu FM

Expression of transforming growth factor- α and hepatitis B surface antigen in human hepatocellular carcinoma tissues and its significance

Jing Zhang, Wen-Liang Wang, Qing Li, Qing Qiao

Jing Zhang, Wen-Liang Wang, Qing Li, Department of Pathology, Xijing Hospital, Fourth Military Medical University, Xi'an 710033, Shaanxi Province, China

Qing Qiao, Department of General Surgery, Tangdu Hospital, Fourth Military Medical University, Xi'an 710038, Shaanxi Province, China

Correspondence to: Jing Zhang, Department of Pathology, Xijing Hospital, Fourth Military Medical University, Xi'an 710033, Shaanxi Province, China. jzhang@fmmu.edu.cn

Telephone: +86-29-83375497 **Fax:** +86-29-83375497

Received: 2003-12-19 **Accepted:** 2004-01-08

Abstract

AIM: To evaluate the expression of transforming growth factor- α (TGF- α) and hepatitis B surface antigen (HBsAg) in human hepatocellular carcinoma (HCC) tissues and its significance.

METHODS: Seventy specimens of HCC tissues were detected by immunohistochemical method. Five specimens of normal human liver tissues were used as control.

RESULTS: The TGF- α positive expression rates in HCC and its surrounding tissues were 74.3%(52/70) and 88.1%(52/59), respectively. TGF- α positive granules were mainly in the cytoplasm and fewer existed on the karyotheca. The TGF- α positive expressing rate in well differentiated HCC was significantly higher than that in moderately and poorly differentiated HCC ($P<0.05$). The TGF- α positive expression also was observed in intrahepatic bile ducts (part of those were hyperplastic ducts). The HBsAg positive expression rates in HCC and its surrounding tissues were 21.4%(15/70) and 79.7%(47/59), respectively. HBsAg positive granules were in the cytoplasm, inclusion and on the karyotheca. There was a prominent positive correlation between TGF- α and HBsAg expression in HCC surrounding tissues ($P<0.05$, $\gamma=0.34$). TGF- α was usually existed with HBsAg in regenerated and/or dysplastic liver cells. In the five normal liver tissues, TGF- α and HBsAg were not detectable in hepatocytes and bile ducts.

CONCLUSION: Hepatitis B virus infection is closely related with hepatocarcinogenesis. The overexpression of TGF- α in the liver seems to be associated with the regeneration of hepatocytes injured by HBsAg. The continued expression of TGF- α might lead to dysplasia of liver cells and development of HCC. Furthermore, TGF- α might play a role in morphogenesis and regeneration of intrahepatic bile ducts.

Zhang J, Wang WL, Li Q, Qiao Q. Expression of transforming growth factor- α and hepatitis B surface antigen in human hepatocellular carcinoma tissues and its significance. *World J Gastroenterol* 2004; 10(6): 830-833

<http://www.wjgnet.com/1007-9327/10/830.asp>

INTRODUCTION

Hepatocellular carcinoma (HCC) is a common malignant tumor in China with poor prognosis^[1-8]. Substantial evidences have supported the concept that hepatitis B virus (HBV) infection is a causative factor for HCC^[9-12]. The idiographic mechanisms of HBV in hepatocarcinogenesis had not been clearly defined yet. Transforming growth factor- α (TGF- α) is a multi-peptide, which can promote cellular proliferation and transformation^[13-15]. The normal hepatocytes almost had no expression of TGF- α mRNA except the epitheliums of bile ducts in human normal liver tissues^[16]. It was also thought to be an autocrine regulator of normal growth and regeneration in the rat liver. There was also a close relationship between TGF- α and hepatocarcinogenesis^[17-19]. In order to find the relationship between TGF- α and HBV infection in hepatocarcinogenesis, the expression of TGF- α and HBsAg in HCC tissues was studied by immunohistochemical method. Such studies have been rarely reported in China.

MATERIALS AND METHODS

Specimens

Tissue samples were obtained from seventy cases of HCC in Xijing Hospital from January 1988 to January 1995. Among them, fifty-nine cases of HCC had surrounding tissues. Five cases of normal human liver tissues were obtained from autopsy (excluding liver disease). All specimens were fixed in 40 g/L methanal solution, embedded in wax, and cut into 5 μ m thick serial sections.

Reagents and methods

Mouse anti-human TGF- α was purchased from Santa Cruze, UAS. Mouse anti-human HBsAg and SABC kit were purchased from Wuhan Boster Co. Ltd. The expression of TGF- α and HBsAg was detected by SABC immunohistochemical method. In the control group, the primary antibody was substituted by PBS or normal mouse serum. All paraffin embedded sections were deparaffinized and rehydrated, and pretreated for 20 min at 75 °C in a microwave oven. After being treated with 1 mL/L H₂O₂ for 30 min to block the endogenous peroxidase, the sections were incubated with 20 mL/L fetal calf serum for 30 min to reduce nonspecific binding. Then the primary HBsAg and TGF- α antibodies were applied to the sections and incubated at 4 °C overnight. The sections were subsequently incubated with goat anti mouse IgG at 37 °C for 30 min, followed by incubation with SABC at 37 °C for 30 min, and stained with DAB-H₂O₂ for 5-10 min and counterstained with hematoxylin. Results estimation: the specimens with no positive cells or positive cells <10% were negative (-); with light brownish yellow cells or positive cells between 10-50% were weakly positive (\pm); with deep brownish yellow cells or positive cells >50% were positive (+).

Statistical analysis

Chi-square test was used to analyse the results. The expression of TGF- α and HBsAg were compared by analysis of coherence.

RESULTS

The expression of TGF- α and HBsAg in HCC

The TGF- α positive expression rates in HCC and its surrounding tissues were 74.3% (52/70) and 88.1% (52/59), respectively. The positive cells mainly existed diffusely and fewer existed in foci. The positive stainings were like brown-yellow granules, and were mainly located in the cytoplasm and/or fewer located on the karyotheca (Figure 1). There was a prominent difference in TGF- α distribution between HCC and its surrounding tissues ($\chi^2=3.93$, $P<0.05$). The TGF- α positive expression rate in well differentiated HCC was significantly higher than that in moderately and poorly differentiated HCC ($\chi^2=9.11$, $P<0.05$, Table 1). TGF- α positive expression also was observed in intrahepatic bile ducts (part of those were hyperplastic ducts). In the five cases of normal liver tissues, TGF- α was undetectable in hepatocytes and bile ducts.

Table 1 TGF- α expression in different HCC differentiation

Differentiation	<i>n</i>	Positive cases	Positive rate (%)
Well	15	15	100.0
Moderately	48	34	70.8
Poorly	7	3	42.9

The HBsAg positive expression rates in HCC and its surrounding tissues were 21.4% (15/70) and 79.7% (47/59), respectively. The positive cells mainly existed diffusely and fewer existed in foci. The positive stainings were like brown-yellow granules or floccules. They were located in the cytoplasm, inclusion and on the karyotheca (Figure 2). There was a prominent difference in HBsAg distribution between HCC and its surrounding tissues ($\chi^2=43.5$, $P<0.05$). HBsAg expression was negative in the five cases of normal liver tissues.

The PBS blank controls and normal mouse serum substituted controls were negative for immunohistochemical staining.

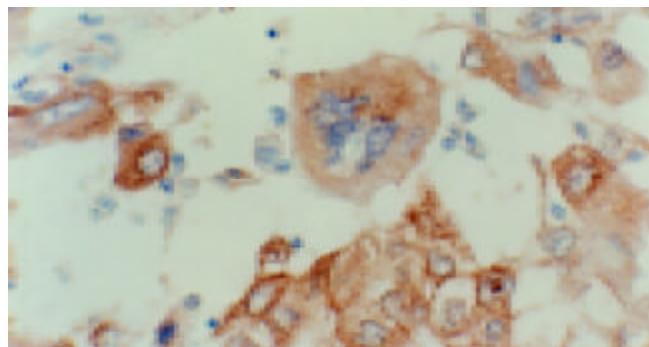


Figure 1 TGF- α positive stainings as brownish yellow granules in the cytoplasm of HCC tumor cells. SABC $\times 400$.

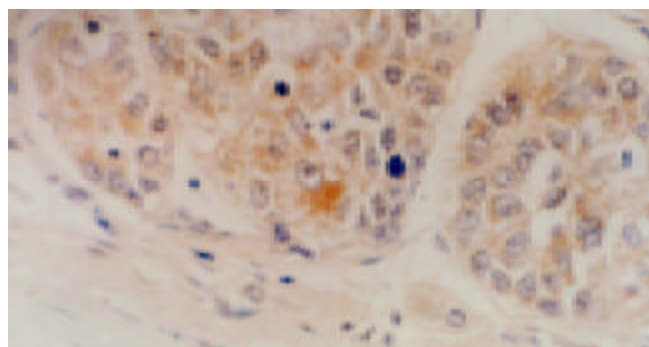


Figure 2 HBsAg positive stainings as brownish yellow granules in the cytoplasm of HCC tumor cells. SABC $\times 400$.

Relationship between TGF- α and HBsAg expression

There was not a prominent correlation between TGF- α and HBsAg expression in HCC tissues, but there was a prominent positive correlation between TGF- α and HBsAg expression in HCC surrounding tissues ($P<0.05$, $\gamma=0.34$, Table 2). TGF- α was usually existed with HBsAg in regenerated and/or dysplastic liver cells. These cells had increscent or double nucleus, prominent or anomalous nucleolus, high ratio of nucleus/ cytoplasm, *etc.* (Figures 3 and 4).

Table 2 Relation between TGF- α and HBsAg expression in HCC surrounding tissues

TGF- α	<i>n</i>	HBsAg	
		+	-
+	52	44	8
-	7	3	4
Total	59	47	12

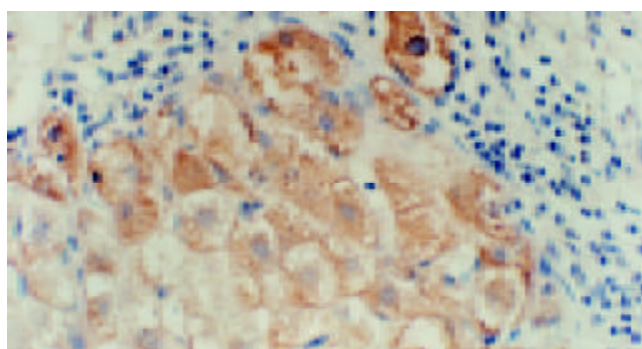


Figure 3 Location of immunohistochemical staining of TGF- α expression in regenerated and/or dysplastic liver cells. SABC $\times 400$.

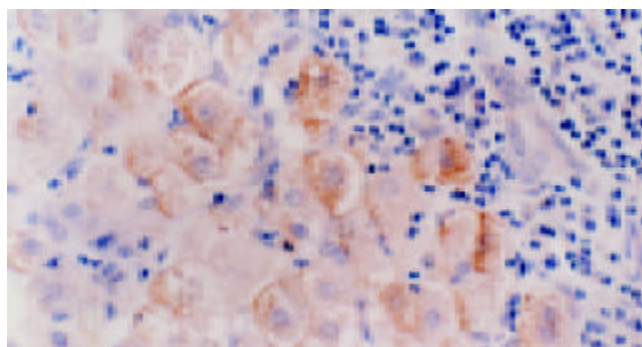


Figure 4 Location of immunohistochemical staining of HBsAg expression in regenerated and/or dysplastic liver cells. SABC $\times 400$.

DISCUSSION

TGF- α was found in culture medium of fibroblasts transformed by some retroviruses in 1970s and nominated because of its ability to transform and induce the renal fibroblasts to proliferate. It is composed of 50 amino acid residues, with a 30% to 40% amino acid homology to epidermal growth factor (EGF), and binds the EGF receptor in the cellular membrane^[20]. TGF- α was secreted by many transformed cells and involved in embryonic development. In human cancers, studies showed that TGF- α could serve as a tumor marker and as a marker for the malignant potential of a tumor^[21]. Thus far, the types of carcinomas with which abnormal TGF- α expression has been associated include liver^[22], gastrointestinal^[23], breast^[24], skin^[25], lung^[26], brain^[27] and ovarian cancers^[28]. TGF- α might play a role in the processes involved with tumor initiation and

growth. In cell lines, TGF- α has been found to be associated with autocrine and/or paracrine types of cellular growth initiation and with increased levels of oncogene expression^[29,30]. It could promote the hepatocellular proliferation, differentiation, regeneration and tumor cell growth^[31]. Transgenic mice that overexpressed TGF- α developed liver tumors between 12 and 15 months of age^[22]. In our study, we found the TGF- α expression in the HCC and its surrounding tissues was significantly higher than that of normal liver tissues. The positive rate of TGF- α expression in well differentiated HCC was higher than that in moderately and poorly differentiated HCC. These may suggest the involvement of TGF- α in cellular transformation and provide a supporting evidence for the autocrine stimulation model. Increased expression of TGF- α might be the events of human primary hepatocarcinogenesis. In the later stages of HCC, there might be the other factors responsible for decreasing expression of TGF- α . Furthermore, we also found that intrahepatic bile ducts (part of these were hyperplasia ducts) were stained positive for TGF- α , suggesting that TGF- α might play a role in morphogenesis and regeneration of intrahepatic bile ducts.

Up to now, the close relationship among hepatitis B virus, liver cirrhosis and HCC has been approved^[32], but the mechanisms have not been clearly defined yet. One hypothesis is that chronic HBV infection caused prolonged liver cellular injury, inflammation and cellular death. The hepatic regeneration after liver necrosis, along with DNA damage from genotoxic agents generated during the inflammatory response, was thought to increase the risk of HCC development^[33]. Because of HBV replication in liver cells, HBV major envelope protein, HBsAg was often overexpressed. It accumulated to toxic levels in the endoplasmic reticulum of hepatocytes. This could lead to the chronic injury of hepatocytes, inflammation and cellular death by immune reaction^[34]. In our study, we found the positive expression rate of HBsAg in the HCC surrounding tissues was higher than that of HCC tissues. There was a prominent difference in HBsAg distribution between the HCC and its surrounding tissues ($\chi^2=43.5$, $P<0.05$). This suggested HBsAg might have more closely involved in hepatic cells injury than in hepatocarcinogenesis.

TGF- α is a potent mitogen for hepatocytes. It can induce hepatocytes to proliferate. Though we did not find the correlation between TGF- α and HBsAg in the HCC tissues, we found there was a prominent positive correlation between TGF- α and HBsAg in the HCC surrounding tissues. They were usually existed in regenerated and/or dysplastic liver cells. These cells had increscent or double nucleus, prominent or anomalous nucleolus and high ratio of nucleus/cytoplasm, etc. These data suggest that TGF- α overexpression in the liver seems to be associated with the hepatocellular regeneration injured by HBsAg. HBsAg may up-regulate the expression of TGF- α . Continued overexpression of TGF- α could lead to hepatocellular proliferation and dysplasia. These might have contributed to hepatocarcinogenesis and HCC growth.

REFERENCES

- Zhao H**, Zhou KR, Yan FH. Role of multiphase scans by multirow-detector helical CT in detecting small hepatocellular carcinoma. *World J Gastroenterol* 2003; **9**: 2198-2201
- Li QL**, Wang WL, Zhang XH, Yan W. Expression of hsMAD₂ in human hepatocellular carcinoma and its significance. *Shijie Huaren Xiaohua Zazhi* 2003; **11**: 1326-1328
- Ge NL**, Ye SL, Zheng N, Sun RX, Liu YK, Tang ZY. Prevention of hepatocellular carcinoma in mice by IL-2 and B7-1 genes co-transfected liver cancer cell vaccines. *World J Gastroenterol* 2003; **9**: 2182-2185
- Wang W**, Yang LY, Yang ZL, Huang GW, Lu WQ. Expression and significance of RhoC gene in hepatocellular carcinoma. *World J Gastroenterol* 2003; **9**: 1950-1953
- Jin ZY**, Cheng RX, Zheng CL, Zheng H. Expression of PTTG and *c-myc* gene in human primary hepatocellular carcinoma. *Shijie Huaren Xiaohua Zazhi* 2003; **11**: 1677-1681
- Qian J**, Feng GS, Vogl T. Combined interventional therapies of hepatocellular carcinoma. *World J Gastroenterol* 2003; **9**: 1885-1891
- Huang J**, Cai MY, Wei DP. HLA class I expression in primary hepatocellular carcinoma. *World J Gastroenterol* 2002; **8**: 654-657
- Hsu CY**, Chu CH, Lin SC, Yang FS, Yang TL, Chang KM. Concomitant hepatocellular adenoma and adenomatous hyperplasia in a patient without cirrhosis. *World J Gastroenterol* 2003; **9**: 627-630
- Ma CH**, Sun WS, Tian PK, Gao LF, Liu SX, Wang XY, Zhang LN, Cao YL, Han LH, Liang XH. A novel HBV antisense RNA gene delivery system targeting hepatocellular carcinoma. *World J Gastroenterol* 2003; **9**: 463-467
- Shen LJ**, Zhang HX, Zhang ZJ, Li JY, Chen MQ, Yang WB, Huang R. Detection of HBV, PCNA and GST- π in hepatocellular carcinoma and chronic liver diseases. *World J Gastroenterol* 2003; **9**: 459-462
- Dai ZY**, Xu QH, Li G, Ma HH, Tang ZH, Shu X, Yao JL. Study on X gene mutation of hepatitis B virus from patients with hepatocellular carcinoma. *Shijie Huaren Xiaohua Zazhi* 2003; **11**: 1349-1352
- Tang ZY**. Hepatocellular carcinoma—cause, treatment and metastasis. *World J Gastroenterol* 2001; **7**: 445-454
- Awwad RA**, Sergina N, Yang H, Ziober B, Willson JK, Zborowska E, Humphrey LE, Fan R, Ko TC, Brattain MG, Howell GM. The role of transforming growth factor alpha in determining growth factor independence. *Cancer Res* 2003; **63**: 4731-4738
- Ciana P**, Ghisletti S, Mussi P, Eberini I, Vegeto E, Maggi A. Estrogen receptor alpha, a molecular switch converting transforming growth factor-alpha-mediated proliferation into differentiation in neuroblastoma cells. *J Biol Chem* 2003; **278**: 31737-31744
- Grasl-Kraupp B**, Schausberger E, Hufnagl K, Gerner C, Low-Baselli A, Rossmanith W, Parzefall W, Schulte-Hermann R. A novel mechanism for mitogenic signaling via pro-transforming growth factor alpha within hepatocyte nuclei. *Hepatology* 2002; **35**: 1372-1380
- Derynck R**, Goeddel DV, Ullrich A, Gutterman JU, Williams RD, Bringman TS, Berger WH. Synthesis of messenger RNAs for transforming growth factors alpha and beta and the epidermal growth factor receptor by human tumors. *Cancer Res* 1987; **47**: 707-712
- Thorgeirsson SS**, Grisham JW. Molecular pathogenesis of human hepatocellular carcinoma. *Nat Genet* 2002; **31**: 339-346
- Matsumoto T**, Takagi H, Mori M. Androgen dependency of hepatocarcinogenesis in TGFalpha transgenic mice. *Liver* 2000; **20**: 228-233
- Jo M**, Stolz DB, Esplen JE, Dorko K, Michalopoulos GK, Strom SC. Cross-talk between epidermal growth factor receptor and c-Met signal pathways in transformed cells. *J Biol Chem* 2000; **275**: 8806-8811
- Todaro GJ**, Fryling C, De Larco JE. Transforming growth factors produced by certain human tumor cells: polypeptides that interact with epidermal growth factor receptors. *Proc Natl Acad Sci U S A* 1980; **77**: 5258-5262
- Grigioni WF**. Relevance of biologic markers in colorectal carcinoma: a comparative study of a broad panel. *Cancer* 2002; **94**: 647-657
- Vail ME**, Pierce RH, Fausto N. Bcl-2 delays and alters hepatic carcinogenesis induced by transforming growth factor alpha. *Cancer Res* 2001; **61**: 594-601
- Sawhney RS**, Sharma B, Humphrey LE, Brattain MG. Integrin alpha2 and extracellular signal-regulated kinase are functionally linked in highly malignant autocrine transforming growth factor-alpha-driven colon cancer cells. *J Biol Chem* 2003; **278**: 19861-19869
- More E**, Fellner T, Doppelmayr H, Hauser-Kronberger C, Dandachi N, Obrist P, Sandhofer F, Paulweber B. Activation of the MAP kinase pathway induces chicken ovalbumin upstream promoter-transcription factor II (COUP-TFII) expression in human breast cancer cell lines. *J Endocrinol* 2003; **176**: 83-94

- 25 **Wu M**, Putti TC, Bhuiya TA. Comparative study in the expression of p53, EGFR, TGF- α , and cyclinD1 in verrucous carcinoma, verrucous hyperplasia, and squamous cell carcinoma of head and neck region. *Appl Immunohistochem Mol Morphol* 2002; **10**: 351-356
- 26 **Piyathilake CJ**, Frost AR, Manne U, Weiss H, Bell WC, Heimburger DC, Grizzle WE. Differential expression of growth factors in squamous cell carcinoma and precancerous lesions of the lung. *Clin Cancer Res* 2002; **8**: 734-744
- 27 **Zhou R**, Skalli O. Identification of cadherin-11 down-regulation as a common response of astrocytoma cells to transforming growth factor- α . *Differentiation* 2000; **66**: 165-172
- 28 **Doraiswamy V**, Parrott JA, Skinner MK. Expression and action of transforming growth factor alpha in normal ovarian surface epithelium and ovarian cancer. *Biol Reprod* 2000; **63**: 789-796
- 29 **Masuda M**, Suzui M, Lim JT, Deguchi A, Soh JW, Weinstein IB. Epigallocatechin-3-gallate decreases VEGF production in head and neck and breast carcinoma cells by inhibiting EGFR-related pathways of signal transduction. *J Exp Ther Oncol* 2002; **2**: 350-359
- 30 **Wong YC**, Wang YZ. Growth factors and epithelial-stromal interactions in prostate cancer development. *Int Rev Cytol* 2000; **199**: 65-116
- 31 **Sohda T**, Iwata K, Tsutsu N, Kamimura S, Shijo H, Sakisaka S. Increased expression of transforming growth factor- α in a patient with recurrent hepatocellular carcinoma following partial hepatectomy. *Pathology* 2001; **33**: 511-514
- 32 **Yuen MF**, Lai CL. Specific considerations in the design of hepatitis B virus clinical studies in the far East. *Methods Mol Med* 2004; **96**: 457-464
- 33 **Jakubczak JL**, Chisari FV, Merlino G. Synergy between transforming growth factor alpha and hepatitis B virus surface antigen in hepatocellular proliferation and carcinogenesis. *Cancer Res* 1997; **57**: 3606-3611
- 34 **Chisari FV**, Klopchin K, Moriyama T, Pasquinelli C, Dunsford HA, Sell S, Pinkert CA, Brinster RL, Palmiter RD. Molecular pathogenesis of hepatocellular carcinoma in hepatitis B virus transgenic mice. *Cell* 1989; **59**: 1145-1156

Edited by Gupta MK **Proofread by** Xu FM

• COLORECTAL CANCER •

Somatic mutations of APC gene in carcinomas from hereditary non-polyposis colorectal cancer patients

Jian Huang, Shu Zheng, Shen-Hang Jin, Su-Zhan Zhang

Jian Huang, Shu Zheng, Su-Zhan Zhang, Department of Oncology, Second Affiliated Hospital, Zhejiang University School of Medicine, Hangzhou 310009, Zhejiang Province, China

Shen-Hang Jin, Zhejiang University School of Medicine, Hangzhou 310009, Zhejiang Province, China

Supported by the National Natural Science Foundation of China, No. 39600055, Research for Returned Chinese Visiting Scholars from Abroad, Chinese Ministry of Education and Research of Provincial Education Ministry

Correspondence to: Dr. Jian Huang, Department of Oncology, Second Affiliated Hospital, Zhejiang University School of Medicine, Hangzhou 310009, Zhejiang Province, China. hjys@zju.edu.cn

Telephone: +86-571-87784556 **Fax:** +86-571-87784556

Received: 2003-06-16 **Accepted:** 2003-09-01

Abstract

AIM: To investigate the mutational features of adenomatous polyposis coli (APC) gene and its possible arising mechanism in hereditary non-polyposis colorectal cancers (HNPCC).

METHODS: PCR-based *In Vitro* Synthesized Protein Test (IVSP) assay and sequencing analysis were used to confirm somatic mutations of whole APC gene in 19 HNPCC cases.

RESULTS: Eleven cases with 13 mutations were determined to harbor APC mutations. The prevalence of APC mutation was 58%(11/19). The mutations consisted of 9 frameshift and 4 nonsense ones, indicating that there were more frameshift mutations (69%). The frameshift mutations all exhibited deletion or insertion of 1-2 bp and most of them (7/9) happened at simple nucleotide repeat sequences, particularly within (A)_n tracts (5/9). All point mutations presented C-to-T transitions at CpG sites.

CONCLUSION: Mutations of APC gene were detected in more than half of HNPCC, indicating that its mutation was a common molecular event and might play an important role in the tumorigenesis of HNPCC. Locations of frameshift mutations at simple nucleotide repeat sequences and point mutations at CpG sites suggested that many mutations probably derived from endogenous processes including mismatch repair (MMR) deficiency. Defective MMR might affect the nature of APC mutations in HNPCC and likely occur earlier than APC mutational inactivation in some patients.

Huang J, Zheng S, Jin SH, Zhang SZ. Somatic mutations of APC gene in carcinomas from hereditary non-polyposis colorectal cancer patients. *World J Gastroenterol* 2004; 10(6): 834-836
<http://www.wjgnet.com/1007-9327/10/834.asp>

INTRODUCTION

Familial colorectal cancer (CRC) can be mainly divided into 2 distinct classes, hereditary non-polyposis colorectal cancers (HNPCC) and familial adenomatous polyposis (FAP). HNPCC is an autosomal dominant inherited disease characterized by an increased predisposition to colorectal and some extracolonic

cancers and presents with particular clinicopathological and molecular features^[1]. Affected individuals often carry germline alterations at mismatch repair (MMR) genes, such as hMsh2, hMlh1, hPsm1 and hPsm2, which lead to microsatellite instability (MSI) and replication errors (RER). FAP is caused by the germline mutation of tumor suppressor gene APC and manifested by the development of hundreds of colorectal adenomas, some of which will inevitably undergo malignant transformations if not removed. APC mutations can be detected in both FAP and non-FAP tumors including HNPCC and sporadic colorectal ones, somatic mutation of which is a common defect in sporadic colorectal tumor and FAP, both sharing similar mutational spectra and distribution^[2,3-5]. It is accepted that adenoma-carcinoma sequence of CRC was initiated by APC mutation in majority of non-HNPCC^[2,6]. Adenoma in HNPCC featured aggressiveness and followed by an alternative and rapidly evolving pathway. There was evidence that HNPCC lacked loss of heterozygosity (LOH) of APC gene, being quite different from FAP^[7]. It showed that all adenomas from *Min* mice demonstrated LOH, had significantly less numbers of somatic APC mutations compared with those from Msh2 deficient *Min* (*Apc*^{+/+}-*Msh2*^{-/-}), which had a 2-fold higher rate of somatic *Apc* mutations (10/adenoma) than the non-neoplastic intestinal mucosa (5/sample), and did not demonstrate LOH. The results proved that somatic APC mutation rather than LOH, was a likely mechanism in the development of adenomas in *Apc*^{+/+}-*Msh2*^{-/-} mice^[8].

Studies also revealed^[9,10] that APC gene might play a role in chromosomal segregation, with mutations in APC disrupting this function and causing chromosomal (or karyotypic) instability (CIN). MSI and CIN were two different forms of genetic instability occurring in CRC. In *MI*⁺ sporadic and HNPCC tumors, defective repair of mismatched bases resulted in an increased mutation rate at the nucleotide level and consequent widespread MSI with diploidy while a large fraction of others had CIN, leading to an abnormal chromosome number (aneuploidy). In HNPCC, mutations of APC, p53 and K-ras-2 genes and LOH of tumor-suppressor genes were significantly less frequent ($P=0.03$ or 0.0006), but transforming growth factor beta type II receptor mutation was significantly more frequent ($P=0.000001$) than those in non-HNPCC^[7]. Summarized data from Jass^[11] supported that the frequency of APC mutation was significantly lower in MSI-H colorectal tumors (39%, 36/92) and HNPCC (44%, 21/48) than in MSI-L (51%, 18/35) and MSS (58%, 241/417). However, the situation was quite different for 5q LOH in MSI-H tumors (3%;1/32) and HNPCC (10%;1/10), which were significantly less than MSI-L (47%;17/49) and MSS (57%;113/199). This suggested that MSI instead of APC mutation probably conferred a growth advantage in the context of early tumorigenesis of HNPCC and MSI-H tumors. Here we focused on APC gene to analyze its mutational frequency and features in carcinomas from HNPCC, which would be helpful to understand the effect of MMR deficiency on APC mutation in the early stage of carcinogenesis.

Based on the fact that both somatic and germline mutations of APC gene were dispersed throughout the 5' half of the sequence, vast majority of which were premature ones and led to truncated proteins^[3-5]. A Coupled *In Vitro* Synthesized

Protein Test (IVSP) was therefore used to selectively and rapidly detect any mutations leading to stop codons^[12-14]. The assay was proved very efficient and only a small proportion of nontruncating APC mutations like missense mutations were reported to be missed^[15]. The study aimed at exploring the possible arising mechanism of somatic APC mutation and its role through investigating frequency and mutational features of the gene in HNPCC.

MATERIALS AND METHODS

Sample collection and DNA extraction

HNPCC was determined according to ICG criteria based on the family history^[16], fresh tumor samples of the patients were from resected and histologically verified colorectal carcinomas. Genomic DNA and RNA of tumors and matched normal-looking colonic mucosa were isolated by standard procedures. Nineteen samples were collected from paired carcinomas and adjacent normal tissues in HNPCC patients.

Determination of APC mutation

Whole APC gene with at least 15 exons (8.5Kb) was divided into 5 overlapping segments (seg.), Exon 1-14 was defined as seg. 1 and exon 15 amplified with four overlapping segments as seg. 2-5. The RT-PCR primer-pair sequence for seg. 1 and PCR primer-pairs for seg. 2-5 was similar to those reported^[12,13,15]. IVSP assay, which selectively detected truncating mutations, was used to screen mutations of whole APC gene segment by segment. All samples showing producible truncated protein bands were sequenced using Sequenase 2 (United States Biochemical) with ³⁵S-labeled dATP, dried sequence gels were exposed to XAR (Kodak) film at room temperature overnight.

Table 1 Spectra of APC mutations in carcinomas from HNPCC patients

Tumor ID	APC nt change	Codon	Target sequence
Point mutations			
T27	C>T	332	CpG
T533	C>T	1 338	CpG
K1, C×7*	C>T	1 450	CpG
Frameshift mutations			
C×7*	1 bp ins	847	TCTCaAAAAAGAT
C086*	1 bp ins	941	TCGGaAAAATTCA
K40	1 bp ins	1 454	CCTaAAAAATAAA
22	1 bp ins	1 554	GCAGaAAAAAACTAT
Cx10	1 bp ins	1 935	TTTCCCCaAGTCA
K10	1 bp del	907	TCTgGGTCT
C086*	2 bp del	1 464	AAGAGAGagAGTGG
K39	2 bp del	799	GATtaTGTT
T10	1 bp del	1 416	AGTGGcATTATA

Note: ID means tumor identification; nt stands for nucleotide; '>' for transition or transversion; each tumor with more than 2 mutations marked by *; del for deletion; ins for insertion; small letter for nucleotide frameshift.

RESULTS

Spectra of APC mutations in HNPCC are listed in Table 1. Screening for truncating APC mutations was carried out using IVSP assay in carcinomas from 19 HNPCC cases. There were altogether 11 mutated cases with 13 mutations confirmed in the study, all of which were only found in the tumor tissues, indicating the somatic nature of mutation. The prevalence of APC mutation in HNPCC was 58% (11/19). Exhibiting mutations consisted of 9 frameshift ones and 4 nonsense, indicating the existence of more frameshift mutations. All of

frameshift mutations were deletion or insertion of 1-2 bp and most of them (7/9) happened at simple nucleotide repeat sequences, particularly within (A)_n tracts (5/9). Repeat number (n) of mononucleotide A ranged from 2 to 7. All of four detected point mutations presented C-to-T transitions at CpG sites in the study. Distributions of mutations were uneven and with no hot spot but hot region. Eight (61.5%) of thirteen mutations were located in the segment 3 (codon 1099-1701) and half of them in the mutation cluster region (codon 1286-1513).

DISCUSSION

Colorectal cancer is the fourth leading cause of cancer deaths and tends to increase in China, especially in big cities like Shanghai. The basic mechanism of reducing the mortality remains elusive and poses a big challenge for clinicians and researchers.

HNPCC is one of the most common inherited cancer syndromes, accounting for approximately 4-6% of all CRCs. It is characterized by defective MMR, which results in MSI and manifests hypermutable phenotype^[17,18]. In our study, MSI was defined in all but one (T16) of HNPCC cases (data not shown).

In contrast to FAP, HNPCC was usually not associated with LOH of APC allele and therefore not develop extensive polyposis but multiple primary cancers. MMR gene responsible for HNPCC functioned as caretaker and indirectly inhibited the promotion of tumor growth, defective MMR was considered to be primary event because of its occurrence throughout the adenomas in HNPCC^[19,20]. It had been reported that CRC with and without MSI involved different genes including APC^[21]. APC gene, a FAP causing gene, was proven to be rate-limiting for tumor initiation and functioned as housekeeper of cellular proliferation. APC mutation provided cells with a selective advantage without known effect on the mutation rate, it suggested that both APC and MMR genes played an important role in the early carcinogenesis of familial CRC. Accumulating evidence actually revealed that the sequence of alteration of cancer genes in MMR deficient tumor was somewhat different from non-HNPCC^[7,21]. The study was to investigate the mutational features of housekeeping gene APC and its potential arising mechanism in carcinomas with deficiency of caretaking gene MMR, in order to evaluate the role of APC gene alteration in HNPCC.

There were 11 (58%) of the 19 HNPCC carcinomas exhibiting APC somatic mutations, which was a bit higher than that (50%) reported in a series of Japanese HNPCC adenomas^[22] and somewhat lower than that (67%) in sporadic CRC^[4,5]. The result implied that inactivation of APC gene also played an important role in the tumorigenesis of HNPCC. But there was evidence that the frequency of APC gene mutation in HNPCC was likely less than that in non-HNPCC (21% *vs* >70%; *P*<0.05)^[23].

Analysis of the spectra of APC mutations revealed that APC frameshift mutations were more frequent than point ones in HNPCC (69.3% *vs* 30.7%; *P*<0.05). As with frameshift mutations, most of them (67%) occurred in the simple repeat sequences (microsatellite) of the APC coding regions, particularly at (A)_n tracts (56%), which was consistent with the effect of mismatch repair deficiency on mutations of other target genes containing short repeated sequences in the coding regions^[24]. It suggested that MMR deficiency might be one of the important pathway leading to inactivation of its tumor suppressor ability by altering microsatellite of the APC coding regions. Animal studies further supported the notion that APC mutations in Msh6(-/-)Apc1638N mice consisted predominantly of base substitutions (93%) creating stop codons, however, in Msh3(-/-)Msh6(-/-)Apc1638N tumors, a mixture of base substitutions (46%) and frameshifts (54%) was observed, indicating that Msh3 could suppress frameshift mutations of Apc gene in Msh6(-/-)Apc1638N mice^[25]. The observation demonstrated that type of APC mutation was closely related

to the function of specific MMR gene while in *Mlh1*^{-/-} *Apc*^{1638N} animals, the prevailing mechanism of APC mutation in tumors was altered from allelic loss to intragenic mutation as a result of *Mlh1* deficiency, the observed mutations were more frameshifts (73%) than base substitutions (27%), most frameshifts were located within dinucleotide repeats^[26]. We therefore hypothesized that defective MMR might precede APC mutation in some HNPCC cases whereas for those frameshifts not showing microsatellite alterations, the initiation mechanism for these tumors was not clear yet and proposed to be similar to that for sporadic CRCs^[2,3,5,12], which meant that APC mutation, rather than genomic instability, might be the initiating event in tumorigenesis.

With respect to point mutations of APC gene, they were all non-sense mutations and with pathogenic nature because of the generation of stop codons. All these mutations in the study presented C-to-T transitions and affected Cg dinucleotides, suggesting that they probably derived from endogenous processes due to spontaneous deaminations of 5-methylcytosine. Further studies were therefore necessary to clarify the origin and relationship between endogenous and exogenous processes of APC mutations in CRC tumorigenesis.

In HNPCC cases without detected APC mutations, it was still of great importance to determine methylated status of APC gene or mutation of other genes like β -catenin, although more sensitive methods needed to be developed or used. Yamamoto reported that DNA methylation of APC was higher in HNPCC than in sporadic CRC with MSI-H (53% vs 35%)^[27]. Miyaki observed that a notable frequency of β -catenin gene mutation (43%) was found to occur in HNPCC and detected in tumors without APC mutations^[23]. These data suggested that activation of the β -catenin -Tcf signaling pathway, through either β -catenin mutation or silence (methylation) of APC, might also contribute to part of HNPCC colorectal carcinogenesis.

In conclusion, inactivation of APC gene played an important role in the tumorigenesis of HNPCC; Most of APC mutations probably derived from endogenous processes including MMR deficiency and presented some mutational features. Defective MMR might occur earlier than APC mutation in some patients with HNPCC.

REFERENCES

- 1 **Lynch HT**, Smyrk T. Hereditary nonpolyposis colorectal cancer (Lynch syndrome). An updated review. *Cancer* 1996; **78**: 1149-1167
- 2 **Powell SM**, Zilz N, Beazer-Barclay Y, Bryan TM, Hamilton SR, Thibodeau SN, Vogelstein B, Kinzler KW. APC mutations occur early during colorectal tumorigenesis. *Nature* 1992; **359**: 235-237
- 3 **Gryfe R**, Swallow C, Bapat B, Redston M, Gallinger S, Couture J. Molecular biology of colorectal cancer. *Curr Probl Cancer* 1997; **21**: 233-300
- 4 **Huang J**, Zheng S, Jin SH. APC mutation analysis in sporadic colorectal cancer. *Zhonghua Zhongliu Zazhi* 1996; **18**: 415-418
- 5 **Nagase H**, Kakamura Y. Mutations of the APC (adenomatous polyposis coli). *Hum Mutat* 1993; **2**: 425-434
- 6 **Jen J**, Powell SM, Papadopoulos N, Smith KJ, Hamilton SR, Vogelstein B, Kinzler KW. Molecular determinants of dysplasia in colorectal lesions. *Cancer Res* 1994; **54**: 5523-5526
- 7 **Konishi M**, Kikuchi-Yanoshita R, Tanaka K, Muraoka M, Onda A, Okumura Y, Kishi N, Iwama T, Mori T, Koike M, Ushio K, Chiba M, Nomizu S, Konishi F, Utsunomiya J, Miyaki M. Molecular nature of colon tumors in hereditary nonpolyposis colon cancer, familial polyposis and sporadic colon cancer. *Gastroenterology* 1996; **111**: 307-317
- 8 **Sohn KJ**, Choi M, Song J, Chan S, Medline A, Gallinger S, Kim YI. Msh2 deficiency enhances somatic Apc and p53 mutations in Apc^{+/+}-Msh2^{-/-} mice. *Carcinogenesis* 2003; **24**: 217-224
- 9 **Fodde R**, Kuipers J, Rosenberg C, Smits R, Kielman M, Gaspar C, van Es JH, Breukel C, Wiegant J, Giles RH, Clevers H. Mutations in the APC tumour suppressor gene cause chromosomal instability. *Nat Cell Biol* 2001; **3**: 433-438
- 10 **Kaplan KB**, Burds AA, Swedlow JR, Bekir SS, Sorger PK, Nathke IS. A role for the Adenomatous Polyposis Coli protein in chromosome segregation. *Nat Cell Biol* 2001; **3**: 429-432
- 11 **Jass JR**, Young J, Leggett BA. Evolution of colorectal cancer: change of pace and change of direction. *J Gastroenterol Hepatol* 2002; **17**: 17-26
- 12 **Powell SM**, Petersen GM, Krush AJ, Booker S, Jen J, Giardiello FM, Hamilton SR, Vogelstein B, Kinzler KW. Molecular diagnosis of familial adenomatous polyposis. *N Eng J Med* 1993; **329**: 1982-1987
- 13 **van der Luijt R**, Khan PM, Vasen H, van Leeuwen C, Tops C, Roest P, den Dunnen J, Fodde R. Rapid detection of translation-termination mutations at the adenomatous polyposis coli (APC) gene by direct protein truncation test. *Genomics* 1994; **20**: 1-4
- 14 **Huang J**, Zheng S, Wu JM, Cai XH. Rapid detection of APC gene mutations in colorectal tumors using IVSP assay. *Zhonghua Yixue Yichuanxue Zazhi* 1997; **14**: 134-137
- 15 **Heinimann K**, Thompson A, Locher A, Furlanetto T, Bader E, Wolf A, Meier R, Walter K, Bauerfeind P, Marra G, Muller H, Foerzler D, Dobbie Z. Nontruncating APC germ-line mutations and mismatch repair deficiency play a minor role in APC mutation-negative polyposis. *Cancer Res* 2001; **61**: 7616-7622
- 16 **Vasen HF**, Mecklin JP, Khan PM, Lynch HT. The international collaborative group on hereditary nonpolyposis colorectal cancer (ICG-HNPCC). *Dis Colon Rectum* 1991; **34**: 424-425
- 17 **Fishel R**, Kolodner RD. Identification of Mismatch repair genes and their role in the development of cancer. *Curr Opin Genet Dev* 1995; **5**: 382-395
- 18 **Loeb LA**. A mutator phenotype in cancer. *Cancer Res* 2001; **61**: 3230-3239
- 19 **Jass JR**, Iino H, Ruszkiewicz A, Painter D, Solomon MJ, Koorey DJ, Cohn D, Furlong KL, Walsh MD, Palazzo J, Edmonston TB, Fishel R, Young J, Leggett BA. Neoplastic progression occurs through mutator pathways in hyperplastic polyposis of the colorectum. *Gut* 2000; **47**: 43-49
- 20 **Iino H**, Simms L, Young J, Arnold J, Winship IM, Webb SI, Furlong KL, Leggett B, Jass JR. DNA microsatellite instability and mismatch repair protein loss in adenomas presenting in hereditary polyposis colorectal cancer. *Gut* 2000; **47**: 37-42
- 21 **Salahshor S**, Kressner U, Pahlman L, Glimelius B, Lindmark G, Lindblom A. Colorectal cancer with and without microsatellite instability involves different genes. *Genes Chromosomes Cancer* 1999; **26**: 247-252
- 22 **Yoshimitsu A**, Hiromi N, Kenji Osmar Y, Tadashi N, Yasuhito Y. β -Catenin and adenomatous polyposis coli (APC) mutations in adenomas from hereditary non-polyposis colorectal cancer patients. *Cancer Lett* 2000; **157**: 185-191
- 23 **Miyaki M**, Iijima T, Kimura J, Yasuno M, Mori T, Hayashi Y, Koike M, Shitara N, Iwama T, Kuroki T. Frequent mutation of beta-catenin and APC genes in primary colorectal tumors from patients with hereditary nonpolyposis colorectal cancer. *Cancer Res* 1999; **59**: 4506-4509
- 24 **Johannsdottir JT**, Jonasson JG, Bergthorsson JT, Amundadottir LT, Magnusson J, Egilsson V, Ingvarsson S. The effect of mismatch repair deficiency on tumorigenesis; microsatellite instability affecting genes containing short repeated sequences. *Int J Oncol* 2000; **16**: 133-139
- 25 **Kuraguchi M**, Yang K, Wong E, Avdievich E, Fan K, Kolodner RD, Lipkin M, Brown AM, Kucherlapati R, Edelmann W. The distinct spectra of tumor-associated Apc mutations in mismatch repair-deficient Apc1638N mice define the roles of MSH3 and MSH6 in DNA repair and intestinal tumorigenesis. *Cancer Res* 2001; **61**: 7934-7942
- 26 **Kuraguchi M**, Edelmann W, Yang K, Lipkin M, Kucherlapati R, Brown AM. Tumor-associated Apc mutations in *Mlh1*^{-/-} *Apc*^{1638N} mice reveal a mutational signature of *Mlh1* deficiency. *Oncogene* 2000; **19**: 5755-5763
- 27 **Yamamoto H**, Min Y, Itoh F, Imsumran A, Horiuchi S, Yoshida M, Iku S, Fukushima H, Imai K. Differential involvement of the hypermethylator phenotype in hereditary and sporadic colorectal cancers with high-frequency microsatellite instability. *Genes Chromosomes Cancer* 2002; **33**: 322-325

• VIRAL HEPATITIS •

Assessment of resin perfusion in hepatic failure *in vitro* and *in vivo*

Ying-Jie Wang, Ze-Wen Wang, Bing-Wei Luo, Hong-Ling Liu, Hong-Wei Wen

Ying-Jie Wang, Ze-Wen Wang, Bing-Wei Luo, Hong-Ling Liu, Hong-Wei Wen, Institute of Infectious Diseases, Southwest Hospital, Third Military Medical University, Chongqing 400038, China
Supported by the National Natural Science Foundation of China, No. 30027001

Correspondence to: Dr. Ying-Jie Wang, Institute of Infectious Diseases, Southwest Hospital, Third Military Medical University, Chongqing 400038, China. wangyj103@263.net

Telephone: +86-23-68754479-8062

Received: 2003-08-05 **Accepted:** 2003-09-18

Abstract

AIM: To observe the adsorbent effect of resin on endotoxin, cytokine, bilirubin in plasma of patients with hepatic failure and to determine the resin perfusion as an artificial liver support system in the treatment of hepatic failure.

METHODS: One thousand milliliters of discarded plasma was collected from each of 6 severe hepatitis patients treated with plasma exchange. The plasma was passed through a resin perfusion equipment for 1-2 h via extracorporeal circulation, and then absorbent indicators of transaminase, bilirubin, blood ammonia, endotoxin and cytokines were examined. In the meantime, study of *in vivo* resin plasma perfusion was performed on 7 severe hepatitis patients to compare the changes of endotoxin and cytokines in blood before and after perfusion.

RESULTS: The levels of total bilirubin, endotoxin, interleukin 1 β and TNF- α in plasma were significantly decreased after *in vitro* resin plasma perfusion. The levels of interleukin 1 β , TNF- α and endotoxin in blood were also evidently declined after *in vivo* resin plasma perfusion. Nevertheless, no obvious changes in IL-6, creatinine (Cr) and urea nitrogen (UN), blood ammonia and electrolytes were found both *in vitro* and *in vivo*.

CONCLUSION: Bilirubin, endotoxin and cytokines in plasma of patients with hepatic failure can be effectively adsorbed by resin *in vitro*. Most cytokines and endotoxin in plasma can also be effectively removed by resin *in vivo*. It demonstrates that resin perfusion may have good treatment efficacy on hepatic failure and can be expected to slow down the progression of hepatic failure.

Wang YJ, Wang ZW, Luo BW, Liu HL, Wen HW. Assessment of resin perfusion in hepatic failure *in vitro* and *in vivo*. *World J Gastroenterol* 2004; 10(6): 837-840
<http://www.wjgnet.com/1007-9327/10/837.asp>

INTRODUCTION

In the research field of artificial liver, blood perfusion, blood filtration, plasma exchange techniques and methods are called non-biological artificial liver^[1-3]. They are based on the mechanical mechanism of blood purification to remove toxins in body to achieve the treatment goal for hepatic failure^[4-11]. New-style resin blood perfusion is mostly used in toxicosis rescue and uremia, etc in clinic, but was rarely reported in the

treatment of hepatic failure. Since endotoxin and cytokine play a pivotal role in the pathogenesis of hepatic failure in severe hepatitis^[12-16], it has become an important issue whether resin blood perfusion can effectively remove endotoxin and cytokine in body. Therefore, we examined the effect of a non-bioartificial liver with resin plasma perfusion on the plasma endotoxin and cytokine removal in patients with severe hepatitis to determine and assess the curative effect of resin plasma perfusion in the treatment of severe hepatitis.

MATERIALS AND METHODS

Subjects

Thirteen subjects with severe viral hepatitis (female 1, male 12, aged 28 to 57 years with a mean of 41.3 years) were enrolled in this study. All subjects belonged to chronic severe hepatitis caused by HBV infection according to the diagnostic criteria described in the Viral Hepatitis Protection and Cure Guideline established on a national conference. Of these patients, 8 were in middle stage, 5 in final stage, complication of encephalopathy, spontaneous peritonitis and hepatorenal syndrome was found in 11, 5 and 3, respectively.

Experimental protocol *in vitro*

One thousand milliliters of discarded plasma was collected from each of 6 severe hepatitis patients treated with plasma exchange, and mimic blood perfusion was performed in 3 h. The resin perfusion device (Lizhu Bio-material Company, Zhuhai, China) and tubes were filled with 500 mL of 50 g/L glucose injection, then rinsed with 3 000 mL of normal saline containing 80 mg heparin from bottom to top at 50-100 mL/min. In the mean time, perfusion device was tapped by hand and rotated to exclude bubbles and particles. Plasma perfusion was performed for 1-2 h (average 1.7 h) and the velocity of plasma cycling through the perfusion device was at 80-120 mL/min. Plasma before and after circulation was collected, sealed and stored at -40 °C. All the procedures, such as plasma collection, perfusion *in vitro* and sample harvesting used aseptic technique, syringe, cycling tubes and frozen tubes were radiated by ⁶⁰Co to remove pyrogen.

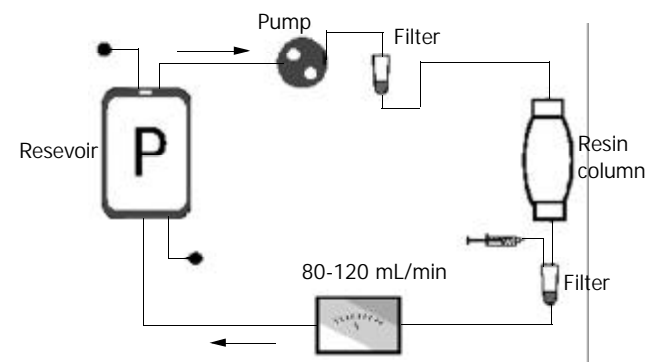


Figure 1 Schematic diagrams of resin perfusion *in vitro*.

Experimental protocol *in vivo*

Resin plasma perfusion was performed in 7 patients with severe hepatitis. Temporal artery-vein circuit was established by

insertion of femoral and pectoral venous cannulas. The patients were heparinized based on individual conditions. The first dose was 1-1.5 mg/kg, then 0.1 mg/kg each 30 min was added. The patients' blood was introduced to a plasma separator (Fresenius Medical Care, Bad Homburg, GER) at 100-120 mL/min for separation of plasma from the whole blood. The separated plasma was absorbed by the resin perfusion device, then mixed with separated blood cells, and returned to patients. The perfusion was maintained for 1-2 h (average 1.6 h) (Figure 2). The plasma before and after perfusion was collected and stored as the above methods.

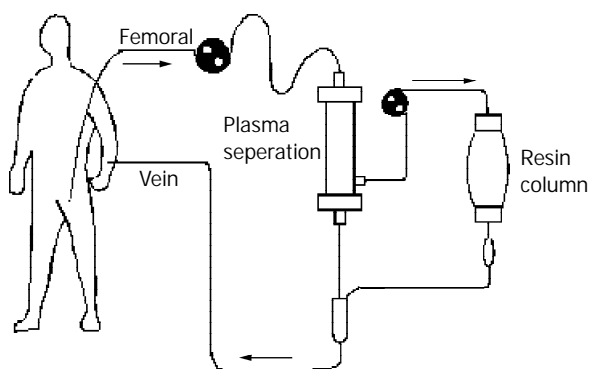


Figure 2 Circuit diagrams of plasma perfusion.

Biochemical estimations and cytokines detection

Plasma aminotransferase, total bilirubin (TB), total bile acid (TBA), electrolyte, UN and Cr were measured using a biochemical autoanalyzer (Hitach Co., Tokyo, Japan). Blood ammonia was measured by a blood ammonia detector (Shiga Co., Tokyo, Japan). Endotoxin was measured by using a limulus test kit according to the manufacturer's instructions (Yihua Medical Technology Co., Shanghai, China). The level of IL-1 β and TNF- α was measured by using a radio immunoassay (RIA) kit according to manufacturer's instructions (Department of Radio Immunoassay, PLA General Hospital Technical Development Center). IL-6 level was measured by using an ELISA kit according to manufacturer's instructions (Shengxiong Medical Technology Co., Shanghai, China).

Statistical analysis

All results were expressed as mean \pm SD. Comparisons between the groups and the same group before and after perfusion were analyzed by Student's *t* test.

RESULTS

Changes in transaminase and bilirubin

After resin perfusion device was used to absorb plasma of the patients with severe hepatitis *in vitro*, transaminase, TB and TBA were all declined with a statistically significant difference in TB, DB and IB before and after resin perfusion (*t* value was 2.081, 2.048, and 2.086 respectively, *P*<0.05).

Table 1 Comparison of transaminase, TB and TBA before and after *in vitro* resin perfusion (mean \pm SD)

	Before absorption	After absorption
ALT(IU/L)	74.17 \pm 49.68	47.83 \pm 22.33
AST(IU/L)	88.83 \pm 45.58	58.33 \pm 44.64
TB(μ mol/L)	518.8 \pm 180.27	356.13 \pm 162.87 ^a
TBA(μ mol/L)	157.17 \pm 53.53	131.67 \pm 34.95

^a*P*<0.05, vs before absorption.

TBA was markedly declined in patients with *in vivo* resin plasma perfusion with a significant difference (*P*<0.01). Nevertheless, transaminase and TB had no marked change before and after absorption (Table 2).

Table 2 Comparison of transaminase, TB, and TBA before and after *in vivo* resin perfusion (mean \pm SD)

	Before absorption	After absorption
ALT(IU/L)	270.03 \pm 355.54	288.38 \pm 314.58
AST(IU/L)	252.50 \pm 391.51	224.88 \pm 356.79
TB(μ mol/L)	519.66 \pm 209.00	460.80 \pm 165.99
TBA(μ mol/L)	194.88 \pm 47.32	166.75 \pm 48.98 ^b

^b*P*<0.01 vs before absorption.

Comparison of electrolytes and renal function

The electrolytes – K, Na, Cl, Ca, Mg, and P after absorption had no significant changes compared to those before absorption. UN and Cr were declined after absorption with no statistical significance compared to those before absorption with UN value of 6.79 \pm 4.14 mmol/L before absorption and 6.42 \pm 3.39 mmol/L after absorption, and Cr value of 135.67 \pm 30.77 μ mol/L before absorption and 121.85 \pm 20.40 μ mol/L after absorption.

Blood ammonia

After *in vitro* resin absorption, blood ammonia in plasma was not markedly decreased (98.17 \pm 20.60 μ mol/L and 91.50 \pm 18.84 μ mol/L). Similar to the result of *in vitro*, blood ammonia had no significant difference before and after *in vivo* resin plasma perfusion (48.25 \pm 8.63 μ mol/L and 46.75 \pm 9.44 μ mol/L).

Level of LPS and cytokines

The level of LPS was markedly decreased after *in vitro* absorption (*t*=6.604, *P*<0.01). The changes in TNF- α and IL-1 β had a statistical significance (*t* was 2.876 and 3.673 respectively, *P*<0.05). IL-6 had no significant change before and after *in vitro* resin absorption (Table 3).

Table 3 Level of LPS and cytokines before and after *in vitro* resin absorption (mean \pm SD)

	Before absorption	After absorption
LPS (ng/L)	60.35 \pm 8.58	32.75 \pm 10.14 ^a
TNF- α (ng/L)	1.49 \pm 1.06	1.04 \pm 0.91 ^b
IL-1 β (ng/L)	2.61 \pm 1.42	1.68 \pm 0.92 ^b
IL-6(ng/L)	100.07 \pm 10.99	87.64 \pm 12.27

^a*P*<0.05, ^b*P*<0.01 vs before absorption.

The plasma endotoxin was markedly decreased after *in vivo* resin plasma perfusion (*t*=5.233, *P*<0.001). TNF- α and IL-1 β also changed significantly (*t* value was 3.474 and 4.869 respectively, *P*<0.01) with declined levels of 16.3% and 37.1% respectively. IL-6 had no evident change before and after *in vivo* plasma perfusion (Table 4).

Table 4 Level of LPS and cytokines before and after *in vivo* resin absorption (mean \pm SD)

	Per- perfusion	Post- perfusion
LPS(ng/L)	58.64 \pm 11.03	36.13 \pm 5.24 ^a
TNF- α (ng/L)	2.28 \pm 0.89	1.69 \pm 0.76 ^a
IL-1 β (ng/L)	1.98 \pm 0.82	1.24 \pm 0.88 ^a
IL-6(ng/L)	88.41 \pm 24.96	84.85 \pm 16.55

^a *P*<0.01 vs before absorption.

DISCUSSION

Blood perfusion is a commonly used method for blood purification^[17-20]. Activated charcoal representing perfusion equipment is most widely applied in the clinical treatment for drug toxicosis, uremia and liver coma and a good result has been obtained^[21,22]. However, the shape of activated charcoal particles is irregular and their mechanical strength is inferior, thus particles are easily broken. If a broken particle directly contacts with blood, it will cause hemolysis and microvessel occlusion. Therefore, activated charcoal must be encapsulated before use. Synthetic resin is another kind of medical absorbent material with macropore high molecular polymers belonging to neutral macropore resin that absorbs substances via Vander Val gravitation. Its absorbent ability has been found to be characterized by a fast absorbent speed, high mechanical strength, relative absorbent specificity mainly absorbing the substances with a molecular weight of 500- 5 000 Da and showing an outstanding absorbent ability to those toxins which can bind to proteins closely or are highly fat-soluble^[23,24].

In the experiment of resin blood perfusion *in vitro*, we found that the resin blood perfusion device was able to effectively absorb transaminase and bilirubin but weakly affect kidney function and blood ammonia, considering that it absorbed medium molecules not small molecules. It illustrated the resin blood perfusion could improve the hepatic function in patients with severe hepatitis. In the meantime, it did not cause electrolyte imbalance and disturbance in the internal environment. Therefore, resin blood perfusion can be used as an artificial liver support system in the treatment of severe hepatitis.

Current studies considered that the pathogenesis of severe hepatitis was the superposition of virus-caused primary immunopathological damage and cytokine-induced secondary damage^[25-27]. When liver barrier function was impaired, endotoxaemia would occur. Endotoxins stimulated the mononuclear phagocyte system inside and outside the liver, and thus, enormous cytokines were released. Furthermore, this cytokine-induced secondary hepatocellular damage played an important role in the course of hepatitis. Hereby, cytokine removal was good for alleviating liver damage, reducing leukoplania and thrombocyte aggregates, maintaining internal environmental equilibrium, and sequentially slowing down or even reversing the progression of disease and improving prognosis^[28-30].

Along with the development in molecular biology, research of antagonists for various cytokines has been launched, for example, monoclonal antibody, receptor antibody, soluble antibody. However, their clinical application is not ideal. In recent years, more and more researchers have began to use blood purification to remove cytokines^[31-33]. At present, it is still disputable whether blood purification can effectively remove cytokines^[34,35]. Some researchers held that leucocytes could be activated by passing through the device during blood perfusion to cause the releasing of cytokines. In addition, it has been found the molecular weight of cytokines is relatively high, and cytokines are mostly bound to proteins in plasma, the half-life of cytokines is short and they are produced and metabolized quickly. Therefore, it would be hard to remove them via blood purification^[36].

In this study, after plasma perfusion treatment for severe hepatitis, both TNF- α and IL-1 β in plasma were significantly decreased, illustrating that plasma perfusion was an effective method for cytokine removal. The change of IL-6 was not significant, because IL-6 might be produced too fast, or it related to different absorbent efficacy of the perfusion device to various cytokines.

In conclusion, resin can effectively absorb bilirubin, LPS, TNF- α and IL-1 β *in vitro*, and LPS, TNF- α and IL-1 β can be

significantly decreased in resin plasma perfusion *in vivo*, resin perfusion has good curative effects on severe hepatitis with hepatic failure.

REFERENCES

- 1 **Dowling DJ**, Mutimer DJ. Artificial liver support in acute liver failure. *Eur J Gastroenterol Hepatol* 1999; **11**: 991-996
- 2 **Kjaergard LL**, Liu J, Als-Nielsen B, Gluud C. Artificial and bioartificial support systems for acute and acute-on-chronic liver failure: a systematic review. *JAMA* 2003; **289**: 217-222
- 3 **Stockmann HBAC**, Hiemstra CA, Marquet RL, IJzermans JNM. Extracorporeal perfusion for the treatment of acute liver failure. *Ann Surg* 2000; **231**: 460-470
- 4 **Borra M**, Galavotti D, Bellini C, Fumi L, Morsiani E, Bellini G. Advanced technology for extracorporeal liver support system devices. *Int J Artif Organs* 2002; **25**: 939-949
- 5 **Bertani H**, Gelmini R, Del Buono MG, De Maria N, Girardis M, Solfrini V, Villa E. Literature overview on artificial liver support in fulminant hepatic failure: a methodological approach. *Int J Artif Organs* 2002; **25**: 903-910
- 6 **Oda S**, Hirasawa H, Shiga H, Nakanishi K, Matsuda K, Nakamura M. Continuous hemofiltration/hemodiafiltration in critical care. *Ther Apher* 2002; **6**: 193-198
- 7 **Ash SR**, Caldwell CA, Singer GG, Lowell JA, Howard TK, Rustgi VK. Treatment of acetaminophen-induced hepatitis and fulminant hepatic failure with extracorporeal sorbent-based devices. *Adv Ren Replace Ther* 2002; **9**: 42-53
- 8 **Clemmesen JO**, Kondrup J, Nielsen LB, Larsen FS, Ott P. Effects of high-volume plasmapheresis on ammonia, urea, and amino acids in patients with acute liver failure. *Am J Gastroenterol* 2001; **96**: 1217-1223
- 9 **Steczko J**, Bax KC, Ash SR. Effect of hemodiabsorption and sorbent-based pheresis on amino acid levels in hepatic failure. *Int J Artif Organs* 2000; **23**: 375-388
- 10 **Hughes RD**. Review of methods to remove protein-bound substances in liver failure. *Int J Artif Organs* 2002; **25**: 911-917
- 11 **Di Campli C**, Zileri Dal Verme L, Andrisani MC, Armuzzi A, Candelli M, Gaspari R, Gasbarrini A. Advances in extracorporeal detoxification by MARS dialysis in patients with liver failure. *Curr Med Chem* 2003; **10**: 341-348
- 12 **Shito M**, Balis UJ, Tompkins RG, Yarmush ML, Toner M. A fulminant hepatic failure model in the rat: involvement of interleukin-1 β and tumor necrosis factor- α . *Dig Dis Sci* 2001; **46**: 1700-1708
- 13 **Galun E**, Axelrod JH. The role of cytokines in liver failure and regeneration: potential new molecular therapies. *Biochim Biophys Acta* 2002; **1592**: 345-358
- 14 **Streetz K**, Leifeld L, Grundmann D, Ramakers J, Eckert K, Spengler U, Brenner D, Manns M, Trautwein C. Tumor necrosis factor alpha in the pathogenesis of human and murine fulminant hepatic failure. *Gastroenterology* 2000; **119**: 446-460
- 15 **Yumoto E**, Higashi T, Nouse K, Nakatsukasa H, Fujiwara K, Hanafusa T, Yumoto Y, Tanimoto T, Kurimoto M, Tanaka N, Tsuji T. Serum gamma-interferon-inducing factor (IL-18) and IL-10 levels in patients with acute hepatitis and fulminant hepatic failure. *J Gastroenterol Hepatol* 2002; **17**: 285-294
- 16 **Han DW**. Intestinal endotoxemia as a pathogenetic mechanism in liver failure. *World J Gastroenterol* 2002; **8**: 961-965
- 17 **Samatskaya VV**, Lindup WE, Walther P, Maslenny VN, Yushko LA, Sidorenko AS, Nikolaev AV, Nikolaev VG. Albumin, bilirubin, and activated carbon: new edges of an old triangle. *Artif Cell Blood Substit Immobil Biotechnol* 2002; **30**: 113-126
- 18 **Nakamura T**, Ushiyama C, Suzuki Y, Inoue T, Shoji H, Shimada N, Koide H. Combination therapy with polymyxin B-immobilized fibre haemoperfusion and teicoplanin for sepsis due to methicillin-resistant *Staphylococcus aureus*. *J Hosp Infect* 2003; **53**: 58-63
- 19 **Tsuchida K**, Takemoto Y, Sugimura K, Yoshimura R, Nakatani T. Direct hemoperfusion by using Lixelle column for the treatment of systemic inflammatory response syndrome. *Int J Mol Med* 2002; **10**: 485-488
- 20 **Sechser A**, Osorio J, Freise C, Osorio RW. Artificial liver support devices for fulminant liver failure. *Clin Liver Dis* 2001; **5**: 415-430

- 21 **Ash SR.** Extracorporeal blood detoxification by sorbents in treatment of hepatic encephalopathy. *Adv Ren Replace Ther* 2002; **9**: 3-18
- 22 **Kramer L,** Gendo A, Madl C, Ferrara I, Funk G, Schenk P, Sunder-Plassmann G, Horl WH. Biocompatibility of a cuprophane charcoal-based detoxification device in cirrhotic patients with hepatic encephalopathy. *Am J Kidney Dis* 2000; **36**: 1193-1200
- 23 **Musanje L,** Darvell BW. Polymerization of resin composite restorative materials: exposure reciprocity. *Dent Mater* 2003; **19**: 531-541
- 24 **Gode F,** Pehlivan E. A comparative study of two chelating ion-exchange resins for the removal of chromium(III) from aqueous solution. *J Hazard Mater* 2003; **100**: 231-243
- 25 **Endo Y,** Shibazaki M, Yamaguchi K, Kai K, Sugawara S, Takada H, Kikuchi H, Kumagai K. Enhancement by galactosamine of lipopolysaccharide(LPS) -induced tumour necrosis factor production and lethality: its suppression by LPS pretreatment. *Br J Pharmacol* 1999; **128**: 5-12
- 26 **Masai T,** Sawa Y, Ohtake S, Nishida T, Nishimura M, Fukushima N, Yamaguchi T, Matsuda H. Hepatic dysfunction after left ventricular mechanical assist in patients with end-stage heart failure: role of inflammatory response and hepatic microcirculation. *Ann Thorac Surg* 2002; **73**: 549-555
- 27 **Rahman T,** Hodgson H. Clinical management of acute hepatic failure. *Intensive Care Med* 2001; **27**: 467-476
- 28 **Stange J,** Mitzner SR, Klammt S, Freytag J, Peszynski P, Looock J, Hickstein H, Korten G, Schmidt R, Hentschel J, Schulz M, Löhr M, Liebe S, Schareck W, Hopt UT. Liver support by extracorporeal blood purification: a clinical observation. *Liver Transpl* 2000; **6**: 603-613
- 29 **Stange J,** Mitzner SR, Risler T, Erley CM, Lauchart W, Goehl H, Klammt S, Peszynski P, Freytag J, Hickstein H, Löhr M, Liebe S, Schareck W, Hopt UT, Schmidt R. Molecular adsorbent recycling system (MARS): clinical results of a new membrane-based blood purification system for bioartificial liver support. *Artif Organs* 1999; **23**: 319-330
- 30 **Nakae H,** Yonekawa C, Wada H, Asanuma Y, Sato T, Tanaka H. Effectiveness of combining plasma exchange and continuous hemodiafiltration (combined modality therapy in a parallel circuit) in the treatment of patients with acute hepatic failure. *Ther Apher* 2001; **5**: 471-475
- 31 **Nakamura T,** Ushiyama C, Suzuki S, Shimada N, Ebihara I, Suzaki M, Takahashi T, Koide H. Effect of plasma exchange on serum tissue inhibitor of metalloproteinase 1 and cytokine concentrations in patients with fulminant hepatitis. *Blood Purif* 2000; **18**: 50-54
- 32 **Nakae H,** Asanuma Y, Tajimi K. Cytokine removal by plasma exchange with continuous hemodiafiltration in critically ill patients. *Ther Apher* 2002; **6**: 419-424
- 33 **Ho DW,** Fan ST, To J, Woo YH, Zhang Z, Lau C, Wong J. Selective plasma filtration for treatment of fulminant hepatic failure induced by D-galactosamine in a pig model. *Gut* 2002; **50**: 869-876
- 34 **Ryan CJ,** Anilkumar T, Ben-Hamida AJ, Khorsandi SE, Aslam M, Pusey CD, Gaylor JD, Courtney JM. Multisorbent plasma perfusion in fulminant hepatic failure: effects of duration and frequency of treatment in rats with grade III hepatic coma. *Artif Organs* 2001; **25**: 109-118
- 35 **Nakae H,** Yonekawa T, Narita K, Endo S. Are proinflammatory cytokine concentrations reduced by plasma exchange in patients with severe acute hepatic failure? *Res Commun Mol Pathol Pharmacol* 2001; **109**: 65-72
- 36 **Iwai H,** Nagaki M, Naito T, Ishiki Y, Murakami N, Sugihara J, Muto Y, Moriwaki H. Removal of endotoxin and cytokines by plasma exchange in patients with acute hepatic failure. *Crit Care Med* 1998; **26**: 873-876

Edited by Zhang JZ and Wang XL Proofread by Xu FM

Establishment of mice model with human viral hepatitis B

Li-Fen Gao, Wen-Sheng Sun, Chun-Hong Ma, Su-Xia Liu, Xiao-Yan Wang, Li-Ning Zhang, Ying-Lin Cao, Fa-Liang Zhu, Yu-Gang Liu

Li-Fen Gao, Wen-Sheng Sun, Chun-Hong Ma, Su-Xia Liu, Xiao-Yan Wang, Li-Ning Zhang, Ying-Lin Cao, Fa-Liang Zhu, Yu-Gang Liu, Institute of Immunology, Medical College, Shandong University, Jinan 250012, Shandong Province, China

Supported by the National Natural Science Foundation of China, No.30070341, and the National Natural Science Foundation of China for Young Scholars Abroad, No.30128023

Correspondence to: Professor Wen-Sheng Sun, Institute of Immunology, Medical College, Shandong University, Jinan 250012, Shandong Province, China. sunwenshengsws@yahoo.com

Telephone: +86-531-8382038

Received: 2003-08-26 **Accepted:** 2003-10-07

Abstract

AIM: To establish a mice model of hepatitis B by using HBV-transgenic mice, and to transfer HBV-specific cytotoxic T lymphocytes (CTL) induced from syngeneic BALB/c mice immunized by a eukaryotic expression vector containing HBV complete genome DNA.

METHODS: HBV DNA was obtained from digested pBR322-2HBV and ligated with the vector pcDNA3. Recombinant pcDNA3-HBV was identified by restriction endonuclease assay and transfected into human hepatoma cell line HepG2 with lipofectin. ELISA was used to detect the expression of HBsAg in culture supernatant, and RT-PCR to determine the existence of HBV PreS1 mRNA. BALB/c mice were immunized with pcDNA3-HBV or pcDNA3 by intramuscular injection. ELISA was used to detect the expression of HBsAb in serum. MTT assay was used to measure non-specific or specific proliferation ability and specific killing activity of spleen lymphocytes. Lymphocytes from immunized mice were transferred into HBV-transgenic mice (2.5×10^7 per mouse). Forty-eight hours later, the level of serum protein and transaminase was detected with biochemical method, liver and kidney were sectioned and stained by HE to observe the pathological changes.

RESULTS: By enzyme digestion with *Eco* RI, *Xho* I and *Hind* III, the recombinant pcDNA3-HBV was verified to contain a single copy of HBV genome, which was inserted in the positive direction. HepG2 cells transfected with the recombinant could stably express PreS1 mRNA and HBsAg. After immunized by pcDNA3-HBV for 4 weeks, HBsAb was detected in the serum of BALB/c mice. The potential of spleen lymphocytes for both non-specific and specific proliferation and the specific killing activity against target cells were enhanced. The transgenic mice in model group had no significant changes in the level of serum protein but had an obvious increase of ALT and AST. The liver had obvious pathological changes, while the kidney had no evident damage.

CONCLUSION: A eukaryotic expression vector pcDNA3-HBV containing HBV complete genome is constructed successfully. HepG2 cells transfected with the recombinant can express PreS1 mRNA and HBsAg stably. Specific cellular

immune response can be induced in mice immunized by pcDNA3-HBV. A mice model of acute hepatitis with HBV has been established.

Gao LF, Sun WS, Ma CH, Liu SX, Wang XY, Zhang LN, Cao YL, Zhu FL, Liu YG. Establishment of mice model with human viral hepatitis B. *World J Gastroenterol* 2004; 10(6): 841-846

<http://www.wjgnet.com/1007-9327/10/841.asp>

INTRODUCTION

HBV infection is a worldwide problem that affects human health severely^[1-3]. No appropriate animal model is available till now because of the strict host specificity of HBV infection. At present, HBV transgenic animals could be obtained during embryonic period, which always induce immune tolerance to dominating HBV antigens^[4-6]. In addition, it has great difference in biological characteristics between duck hepatitis B virus and HBV. So it is imperative to establish a mice model that can simulate human viral hepatitis B precisely and is convenient for wider applications.

Both clinical researches and animal experiments suggest that the pathological changes are not caused by the virus directly, but are mediated by immunity^[7,8]. HBV specific CTL induced by HBV antigens can cause immune damage to the liver to clear the viruses and recruit non-specific inflammatory cells to local infection tissue simultaneously, thus aggravating hepatic injury^[9,10]. We planned to induce HBV specific CTL by gene immunity and to establish a mice model of hepatitis B by transferring CTLs to HBV-transgenic mice.

MATERIALS AND METHODS

Animals

SPF BALB/c mice were provided by the Laboratory Animal Center of Shandong University. HBV complete genome (ayw subtype) transgenic BALB/c mice with a high level of HBsAg, HBeAg and with HBV DNA positive in peripheral blood, were purchased from Transgenic Animal Central Laboratory, 458 Hospital of PLA, China.

Cell lines

Hepatocellular carcinoma cell line HepG2 was cultured and conserved in our laboratory. HepG2.2.15 cell line carrying four whole HBV genes can not only express HBsAg and HBeAg but also produce Dane's particles of HBV. SP2/0-HBV is a mouse myeloma cell line with pcDNA3-HBV stably transfected.

Plasmids

pBR322-2HBV was a recombinant plasmid with a double copy of HBV (ayw subtype) inserted into *Eco*RI restriction site of pBR322. Mammalian cell expression vector pcDNA3 was 5.4 kb in length. It has a CMV early promoter enhancer, multiple cloning sites (MCS) and neomycin resistant gene.

Construction of recombinant pcDNA3-HBV

Alkaline lysis method was used to extract large quantity of

pBR322-2HBV and pcDNA3 DNA respectively. Precipitation with polyethylene glycol was used to purify plasmid DNA, and biometer was used for quantitative analysis. pBR322-2HBV was digested with *EcoRI* and separated by 10 g/L agarose gel electrophoresis. The gel band containing 3.2 kb DNA was cut under UV light. HBV DNA was extracted using a DNA recovery kit. pcDNA3 was also digested by *EcoRI* and a 5.4 kb fragment was recovered with the same method. Ten microliter of HBV DNA and 2 μ L of pcDNA3-HBV (mol ratio 3:1) were mixed together with 2 μ L of T4 DNA ligase, 2 μ L of buffer and 2 μ L of sterile water. The mixture was placed overnight at 4 °C, and then the reaction was terminated. Ten microliter of ligated product was transformed to competent DH5 α , which was then transferred to a LB medium plate containing 60 μ g/mL of ampicillin and incubated overnight at 37 °C.

Identification of recombinant pcDNA3-HBV

Antibiotic selection and restriction endonuclease assay were used to screen and identify positive clones. A positive clone was selected randomly and amplified for recombinant plasmid DNA. Then the recombinant DNA was digested by *EcoRI*, *XhoI* and *HindIII*, respectively. The digestion system was 20 μ L, including 1 μ L DNA, 1 μ L endonuclease, 2 μ L 10 \times buffer and 16 μ L sterile water, and incubated for 3 hours at 37 °C. The correctness of ligation was further identified by 10 g/L agarose gel electrophoresis.

pcDNA3-HBV transfected to HepG2 cell with lipofectin

HepG2 cells during logarithmic period were digested by trypsinization and diluted to 4 \times 10⁵/mL. Then the cells were plated to 24-well plates with 0.5 mL per well (cell count 2 \times 10⁵) and cultured for 24 h for transfection next day, when 80-90% of the cells were fused. One μ g purified pcDNA3-HBV plasmid DNA was transfected to the prepared HepG2 cells using lipofectin reagent. After transfection, HepG2 cells were screened by G418 resistance and routinely cultured. The culture supernatant was collected periodically to detect HBV antigens. The selected positive clone was named as HepG2.02G.

HbsAg detection

Concentration of HBsAg in culture supernatant of transfected cells was detected by ELISA. Critical value (cutoff) = 2.1 \times N, in which N is the average OD of negative control, and S is the OD of sample. The sample was positive when S/N \geq 2.1, otherwise negative.

Extraction of total RNA

HepG2.02G, HepG2.2.15, and HepG2 cells in logarithmic period were harvested, each of 1 \times 10⁶ cells, was rinsed by 0.01 mol/L PBS once and centrifuged at 1 000 rpm for 5 min. The precipitate was used for total RNA extraction according to the protocol of TRIZOL kit.

Primer design and synthesis

According to the sequence of HBV S1 (subtype ayw) described by GenBank, primers were designed to amplify HBV PreS1 gene. PCR product would be 625 bp. β -actin served as control, with a PCR product 366 bp in length. The sequences of the primers were: PreS1 forward: 5'-GCTCTAGACACCAAATGCCCTA-3', reverse: 5'-GCTCTAGAGAATCCCAGAGG-3', β -actin forward: 5'-ACACTGTGCCCATCTACGAGGGC-3', reverse: 5'-ATGATGGAGTTGAAGGTAGTT TCG TGG AT-3'. These oligonucleotide primers were synthesized by Shanghai Sangon Biological Engineering Technology and Service Co. Ltd.

Amplification of PreS1 mRNA

Reverse transcription was performed with 1 μ g of total RNA

to obtain cDNA as the template. PCR was carried out in 25 μ L volume with 1 μ L RT-PCR product, 2.5 μ L 10 \times PCR buffer, 0.3 μ L Mg²⁺, 5 nmol/L of dNTP, 3 U *Taq* polymerase and 10 nmol/L of primers (forward and reverse). The reaction conditions were pre-denatured at 94 °C for 3 min, 30 cycles (denatured at 94 °C for 1 min, annealed at 50 °C for 1 min and extended at 72 °C for 1 min), followed by a final extension at 72 °C for 5 min. Ten microliter of the PCR product then underwent 2% agarose gel electrophoresis at 70 V for 30 min. HepG2 cells were used as negative control, while HepG2.2.15 as positive.

Scheme for mice immunization with pcDNA3-HBV or pcDNA3

The purified pcDNA3-HBV DNA was diluted with sterile NS to the concentration of 1 000 μ g/mL and preserved at -20 °C. Twelve male BALB/c mice were randomly divided into 2 groups, 6 mice each. One was experimental group (Exp), which was injected 50 μ L 250 g/L sucrose intramuscularly to both sides of anterior tibial muscle, 50 μ L pcDNA3-HBV (100 μ L per mouse) was injected at the same site 20 min later. Another was the control group (Ctrl), the same quantity of pcDNA3 was injected as negative control. The immunization was intensified once 2 to 3 wk.

HbsAb detection in serum of mice immunized with pcDNA3-HBV

Blood samples were collected by cutting tails of the mice at wk 2, 4, 8 and 10, respectively. Serum was separated and HBsAb was detected by double-antibody sandwich ELISA.

Measurement of proliferation reaction of spleen lymphocytes of mice immunized by pcDNA3-HBV or pcDNA3

Mice spleen cells were prepared routinely (cell density adjusted to 5 \times 10⁶/mL) and plated to 96-well plates (100 μ L per well). The supernatant of HepG2.2.15 (containing a high level of HBsAg), PHA (eventual concentration 25 μ g/mL) or ConA (eventual concentration 10 μ g/mL) was added to 3 wells, respectively. MTT assay was performed after the cells were cultured at 37 °C for 68 h. Proliferation rate was calculated as: (OD of stimulatory - OD of non-stimulatory) / OD of non-stimulatory \times 100%.

Measurement of specific killing activity of spleen lymphocytes of mice immunized by pcDNA3-HBV or pcDNA3

Mice spleen cells were plated to 96-well plates, mixed with SP2/0-HBV cells (effector/target ratio 50:1). Control groups were designed and each group had 3 wells. MTT assay was performed after the cells were cultured for 72 h. Killing rate of CTLs was calculated as: [1 - (OD of effector and target cells - OD of effector cells) / OD of target cells] \times 100%.

Establishment of animal model

Transgenic mice were divided into 3 groups (6 mice each): Model, negative control and blank control. Mice in model or negative control group were injected with spleen lymphocytes of mice immunized by pcDNA3-HBV (HBsAb positive) or pcDNA3 respectively. Mice in blank control group were injected with NS, 0.5 mL each mouse. Spleen lymphocytes were adjusted to 5.0 \times 10⁷/mL using NS and injected to transgenic mice through caudal vein (2.5 \times 10⁷ lymphocytes, 0.5 mL per mouse).

Identification of animal model

After 48 h, the transgenic mice were killed and their venous blood was collected. Serum total protein, albumin, globulin, ALT and AST were detected. Liver and kidney were fixed with 100 g/L formaldehyde, embedded, sliced and stained with HE to observe inflammation and immune-pathological changes with a microscope.

Statistical analysis

All data were shown as mean±SD. Significant levels of differences between values were analyzed using the Chi-square test and Student's *t* test. Statistically significant *P* value was defined as <0.05.

RESULTS

Restriction digestion results of pBR322-2HBV and pcDNA3

Extracted plasmid DNA had a high purity ($OD_{260/280}=1.6-1.8$). After pBR322-2HBV was digested by *EcoRI*, 2 bands were obtained at about 4.3 kb and 3.2 kb in size (Figure 1). pcDNA3 was linear after digestion, and a band at 5.4 kb proved it was completely digested (Figure 2).

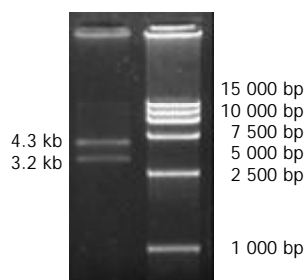


Figure 1 Enzymatic digestion of pBR322-2HBV by *EcoRI*.

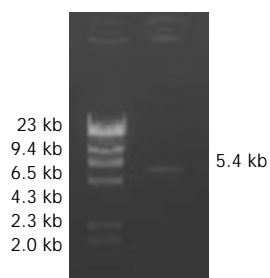


Figure 2 Enzymatic digestion of pcDNA3 by *EcoRI*.

Identification of recombinant pcDNA3-HBV

A high purity of the extracted 2 kinds of DNA was certified by electrophoresis. The recombinant pcDNA3-HBV was digested by *EcoRI* and the product underwent electrophoresis. Only a band of 5.4 kb indicated that the transformed plasmid was pcDNA3 without exogenous genes, while 2 bands at 5.4 kb and 3.2 kb indicated successful ligation (Figure 3). pcDNA3-HBV was digested by *HindIII*, and the product of 8.6 kb in size indicated that the recombinant pcDNA3-HBV contained a single HBV gene. pcDNA3-HBV was digested by *XhoI*, and the products of 3.1 kb and 5.5 kb showed that HBV was inserted at the correct direction (Figure 4).

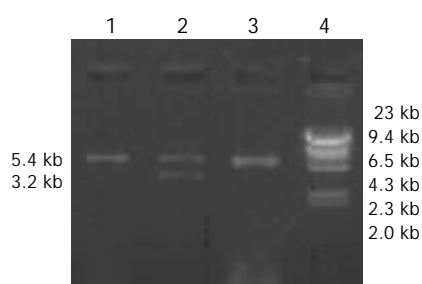


Figure 3 Analysis of ligation of HBV and pcDNA3. 1, 3: pcDNA3 vector, 2: pcDNA3-HBV (5.4 kb+3.2 kb), 4: DNA marker (λ DNA/*HindIII*).

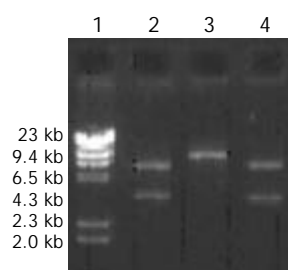


Figure 4 Digestive identification of recombinant plasmid pcDNA3-HBV. 1: DNA marker (λ DNA/*HindIII*), 2: *XhoI* digestion (3.1 kb+5.5 kb), 3: *HindIII* digestion (8.6 kb), 4: *EcoRI* digestion (5.4 kb+3.2 kb).

HBsAg expression in supernatant of HepG2.02G cell culture

HBsAg in supernatant could be detected on day 15, and expressed stably after 40 d (S/N=48).

PreS1 mRNA expression in HepG2.02G

A specific band at 625 bp demonstrated that HBV could efficiently replicate and transcript in human hepatocellular carcinoma cells, as shown in Figure 5.

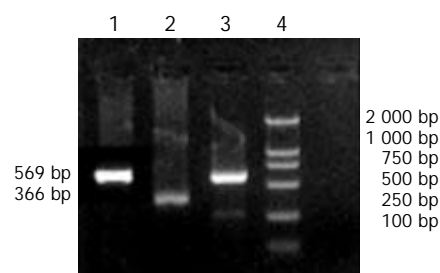


Figure 5 Expression of preS1 mRNA by RT-PCR. 1: HepG2.2.15 (positive control); 2: β -actin; 3: HepG2.02G; 4: DNA marker (DL2 000); 5: HepG2 (negative control).

HBsAb level in serum of mice immunized by pcDNA3-HBV

pcDNA3-HBV immunized mice had specific immune response at the 4th week (S/N=19). Antibody expression reached the highest level at the 8th week and this level lasted to the 10th week.

Proliferation reaction of spleen lymphocytes of mice immunized by pcDNA3-HBV or pcDNA3

As illustrated in Table 1, the non-specific proliferation ability of spleen lymphocytes of mice immunized by pcDNA3-HBV to both PHA and ConA was enhanced as compared with that of pcDNA3 ($P<0.05$), and the specific proliferation ability to supernatant of HepG2.2.15 was also promoted ($P<0.01$).

Table 1 Spleen lymphocyte proliferation of immunized mice (%)

Group	PHA (25 μ g/mL)	ConA (10 μ g/mL)	HepG2.2.15 media (1:1)
Exp	52.9±3.7	80.9±8.3	33.8±3.2
Ctrl	32.6±2.4 ^a	61.6±4.5 ^a	4.1±0.5 ^b

^a $P<0.05$ vs Exp, ^b $P<0.01$ vs Exp.

Specific killing activity of spleen lymphocytes of mice immunized by pcDNA3-HBV or pcDNA3

MTT assay showed that the killing activity of spleen lymphocytes of mice immunized by pcDNA3 against SP2/0 and SP2/0-HBV had no significant difference ($P>0.05$), but that of mice immunized by pcDNA3-HBV to SP2/0-HBV was

distinctly enhanced as compared to SP2/0 ($P<0.01$). Results are shown in Table 2.

Table 2 Specific killing activity of mice spleen lymphocytes (% , mean \pm SD)

Group	SP2/0	SP2/0-HBV
Exp	14.3 \pm 3.4 ¹	51.5 \pm 9.8 ^b
Ctrl	20.8 \pm 4.6 ²	24.5 \pm 3.7 ³

^b $P<0.01$ vs 1, 2, 3.

Identification of mice model of hepatitis B

The mice in each group had no significant changes in the level of serum protein compared with the blank control group ($P>0.05$). The serum ALT and AST of transgenic mice in blank and negative control groups were normal (0-40 U/L), while they (ALT 232 \pm 14 U/L, AST 315 \pm 21 U/L) were much higher in the model group than in the control group ($P<0.01$). The hepatic cords of mice in the blank control group had a radiated structure surrounding the central vein, the hepatic lobule had a clear structure with cells tightly connected. The hepatic cells

had large and round nuclei, with obvious nucleoli and abundant symmetrical cytoplasm. There was no inflammatory cell infiltration in the portal area with a clear structure (Figure 6A). Mice in negative control group had sporadic acidophilic changes of hepatic cells, without inflammatory cell infiltration (Figure 6B). In the model group, hepatic cells of transgenic mice had diffuse ballooning degeneration, cytoplasmic loosening, acidophilic changes, appearance of acidophilic body, spotty necrosis of hepatic tissue and obvious infiltration of inflammatory cells in the portal area (Figure 7). However, mice in the model group had no obvious inflammation and structure damage of the kidney.

DISCUSSION

The host variety of HBV infection is limited. At present, the animal models for HBV research included chimpanzee^[11], Tupaia Glis^[12] and other hepadnaviridae virus infected animals^[13]. Although duck hepatitis B virus (DHBV) has been found to be similar to HBV in mechanism of pathogenesis, ducks infected with DHBV did not develop hepatic cirrhosis and hepatocellular carcinoma because DHBV lacks X gene^[14]. Mice

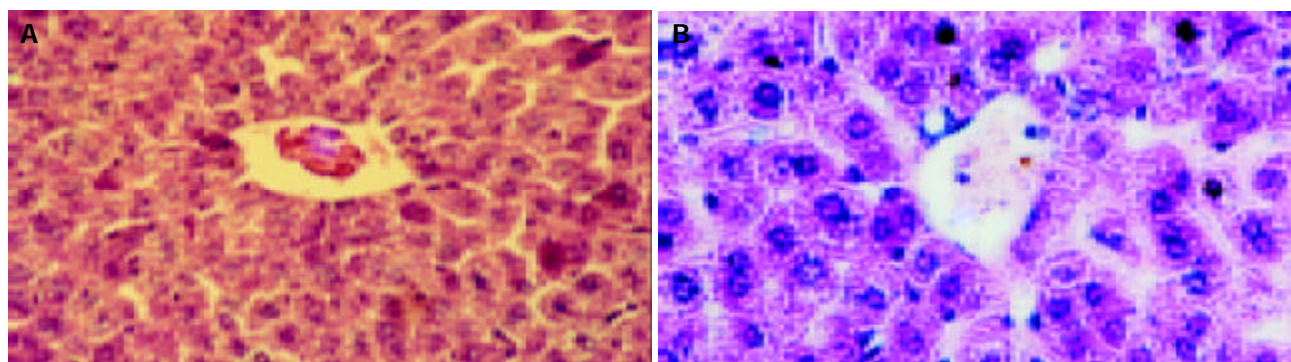


Figure 6 Liver structure of mice by HE-staining ($\times 200$). A: Liver structure of mice in blank control group, B: Liver structure of mice in negative control group.

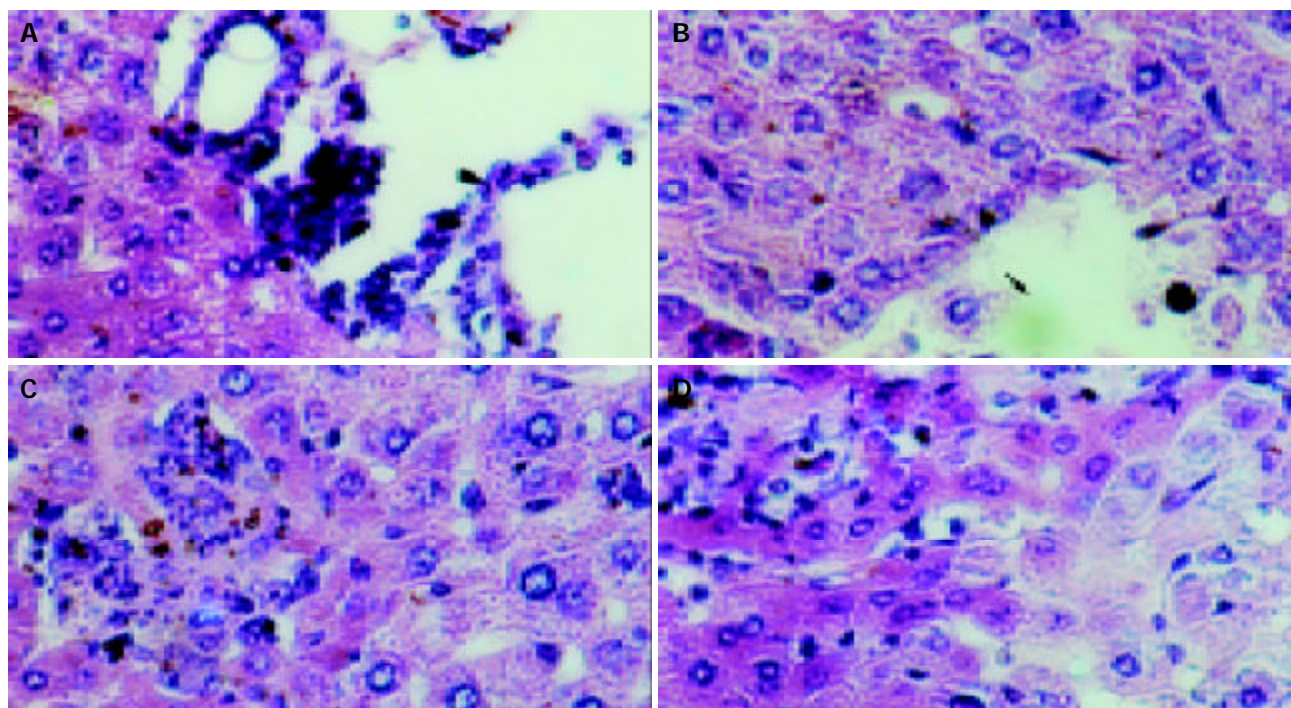


Figure 7 Pathological changes of mouse liver with acute hepatitis in model group (HE, $\times 200$). A: Infiltration of inflammatory cells in the portal area, B: Local necrosis as arrow indicated, C: Obvious infiltration of inflammatory cells and eosinophilic changes, D: Cytoplasmic loosening of liver cells.

had low susceptibility to HBV, but HBV could replicate in transgenic mice^[15]. Two research groups established the transgenic mice which could produce HBV envelopes or HBsAg particles in 1985^[16,17]. A high level of HBsAg in circulatory blood could be detected, but no hepatitis was observed in the transgenic mice. The mechanisms of HBV pathogenesis was not caused by virus directly, but closely related to T lymphocyte activation, as demonstrated both *in vitro* and *in vivo*^[18,19]. Ando *et al*^[20] induced a fulminant hepatitis mice model by transferring HBsAg-specific CTLs to HBsAg-transgenic mice, in which there was no human hepatitis B virus. To establish a mice model of human viral hepatitis B by using HBV complete genome transgenic mice with virus replication *in vivo*, we constructed a new eukaryotic expression vector containing HBV complete genome and produced HBV-specific CTLs for adoptive transfer by immunizing non-transgenic syngeneic mice with the recombinant.

HBV complete genome DNA was obtained from *EcoRI* digested pBR322-2HBV and ligated with the vector pcDNA3 which was also digested by *EcoRI*, thus constructing the recombinant pcDNA3-HBV. pcDNA3 is a eukaryotic expression vector. MCS contains the restriction sites of *EcoRI*, *XhoI* and *HindIII*. CMV promoter can express efficiently in many kinds of cells. The immunostimulatory sequences (ISS) of pcDNA3 can not only activate B lymphocytes to produce antibodies, but also stimulate lymphocytes to secrete IL-12, IFN- γ and IL-6. IL-12 and IFN- γ could foster Th1 responses and enhance cell-mediated immunity, while IL-6 could further promote B lymphocyte activation and antibody secretion and also enhance cell-mediated immunity as its primary role^[21,22]. So this vector is a better alternative for gene immunity. The recombinant was constructed by inserting the HBV complete genome to *EcoRI* sites of pcDNA3, with *HindIII* site upstream of *EcoRI* in MCS of pcDNA3 and no *HindIII* site in HBV genes. A single *XhoI* site was at 180 bp upstream of HBV gene. According to these characteristics, restriction endonuclease assay was used to verify whether pcDNA3-HBV contained a complete HBV gene with correct direction. In order to verify the expression of the recombinant in mammal cells, pcDNA3-HBV was transfected into HepG2 cells with lipofectin. Positive clones were selected by G418 resistance. A high level of HBsAg was detected in culture supernatant and HBV PreS1 mRNA expression was proved by RT-PCR. These results could demonstrate that HBV can stably replicate, transcript and express in transfected host cells.

The molecular mechanisms of hepatic cell death and viral clearance during HBV infection have not been illuminated clearly yet. Studies *in vitro* and *in vivo* indicated that hepatic injury caused by HBV infection was immunity mediated^[23-25]. It is considered at present that CTL was the dominate effector molecule during viral clearance, and CTL inducement was the precondition^[26-28]. To simulate human hepatitis after natural HBV infection, we chose HBV complete genome transgenic BALB/c mice as the experimental model. Syngeneic BALB/c mice were undertaken gene immunity by a self-constructed HBV complete genome expression vector to induce HBV specific CTLs. Mice models of viral hepatitis B were established after transgenic mice administrated CTLs with different schemes.

There were two reasons to adopt gene immunity method. First, HBV complete genome recombinant of ayw subtype was constructed because of the transgenic mice containing HBV of the same subtype, while the main component of the present gene vaccines was HBsAg with no definite subtype. Second, generally speaking, humoral immunity could be induced by protein antigens, while cell mediated immunity could be induced by gene immunization^[29-31]. There were several ways of gene transfer for gene immunity, which would influence

immune effect and even determine the type of immunity. Skeletal muscle has been found to be the exclusive tissue that can efficiently ingest and express foreign genes, especially for plasmid DNA^[32,33]. Because of its simpleness and convenience, it has become the dominant method for immunity. After immunized by pcDNA3-HBV once 2-3 wk, HBsAb was detected in the serum of BALB/c mice at the 4th wk. Pretreatment with 250g/L sucrose improved immune effect and induced HBV specific CTLs with a high activity.

The liver would have the most severe pathological changes in viral hepatitis B. The essential changes included degeneration and necrosis of hepatic cells, inflammatory cell infiltration, regeneration of hepatic cells, hyperplasia of fibrous tissue, and increase of serum transaminase^[34,35]. HBV specific CTLs produced by immunized mice were transferred into HBV-transgenic mice. Forty-eight hours later, normal serum protein content and a high level of serum AST and ALT were detected both in negative and blank control groups. The liver stained by HE in the model group showed typical pathological changes of acute viral hepatitis B, while no pathological damage was found in the negative control group. The kidney had no pathological changes in all groups. Acute hepatitis model of mice with HBV complete genome has been established successfully by the above research project, which could mimic human hepatitis B much better because of viral replication and HBV antigens expression in the model. This study would provide a new way for anti-HBV drug screening and mechanism investigation of liver injury due to HBV infection.

REFERENCES

- 1 **Ryu WS.** Molecular aspects of hepatitis B viral infection and the viral carcinogenesis. *J Biochem Mol Biol* 2003; **36**: 138-143
- 2 **Ke WM, Ye YN, Huang S.** Discriminant function for prognostic indexes and probability of death in chronic severe hepatitis B. *J Gastroenterol* 2003; **38**: 861-864
- 3 **Rabe C, Pilz T, Klostermann C, Berna M, Schild HH, Sauerbruch T, Caselmann WH.** Clinical characteristics and outcome of a cohort of 101 patients with hepatocellular carcinoma. *World J Gastroenterol* 2001; **7**: 208-215
- 4 **Wu JM, Lin JS, Chen BT, Zheng XM, Zhao HB, Liang KH.** Establishment and identification of highly expressing and replicating hepatitis B virus genome transgenic mouse models. *Zhonghua Ganzhangbing Zazhi* 2003; **11**: 338-340
- 5 **Wieland SF, Vega RG, Muller R, Evans CF, Hilbush B, Guidotti LG, Sutcliffe JG, Schultz PG, Chisari FV.** Searching for interferon-induced genes that inhibit hepatitis B virus replication in transgenic mouse hepatocytes. *J Virol* 2003; **77**: 1227-1236
- 6 **Kimura K, Kakimi K, Wieland S, Guidotti LG, Chisari FV.** Interleukin-18 inhibits hepatitis B virus replication in the livers of transgenic mice. *J Virol* 2002; **76**: 10702-10707
- 7 **Sureau C, Romet-Lemonne JL, Mullins JI, Essex M.** Production of hepatitis B virus by a differentiated human hepatoma cell line after transfection with cloned circular HBV DNA. *Cell* 1986; **47**: 37-47
- 8 **Marinos G, Torre F, Chokshi S, Hussain M, Clarke BE, Rowlands DJ, Eddleston AL, Naoumov NV, Williams R.** Induction of T-helper cell response to hepatitis B: A major factor in activation of the host immune response to the hepatitis B virus. *Hepatology* 1995; **22**: 1040-1049
- 9 **Guidotti LG.** The role of cytotoxic T cells and cytokines in the control of hepatitis B virus infection. *Vaccine* 2002; **20**: A80-82
- 10 **Liu DX.** A new hypothesis of pathogenetic mechanism of viral hepatitis B and C. *Med Hypotheses* 2001; **56**: 405-408
- 11 **Sun J, Hou JL, Xiao L, Wang ZH, Luo KX.** Analysis of three lamivudine-resistant HBV mutants with the method of restriction enzyme digestion and its application. *Zhonghua Shiyang He Linchuang Bingdu Xue Zazhi* 2003; **17**: 18-20
- 12 **Muchmore EA.** Chimpanzee models for human disease and immunobiology. *Immunol Rev* 2001; **183**: 86-93
- 13 **Cooper A, Paran N, Shaul Y.** The earliest steps in hepatitis B virus infection. *Biochim Biophys Acta* 2003; **1614**: 89-96

- 14 **Chang SF**, Netter HJ, Hildt E, Schuster R, Schaefer S, Hsu YC, Rang A, Will H. Duck hepatitis B virus expresses a regulatory HBx-like protein from a hidden open reading frame. *J Virol* 2001; **75**: 161-170
- 15 **Raney AK**, Eggers CM, Kline EF, Guidotti LG, Pontoglio M, Yaniv M, McLachlan A. Nuclear covalently closed circular viral genomic DNA in the liver of hepatocyte nuclear factor 1 alpha-null hepatitis B virus transgenic mice. *J Virol* 2001; **75**: 2900-2911
- 16 **Babinet C**, Farza H, Morello D, Hadchouel M, Pourcel C. Specific expression of hepatitis B surface antigen (HBsAg) in transgenic mice. *Science* 1985; **230**: 1160-1163
- 17 **Chisari FV**, Pinkert CA, Milich DR, Filippi P, McLachlan A, Palmiter RD, Brinster RL. A transgenic mouse model of the chronic hepatitis B surface antigen carrier state. *Science* 1985; **230**: 1157-1160
- 18 **Guidotti LG**, Matzke B, Schaller H, Chisari FV. High level -hepatitis B virus replication in transgenic mice. *J Virol* 1995; **69**: 6158-6169
- 19 **Kao JH**, Chen PJ, Lai MY, Chen DS. Basal core promoter mutations of hepatitis B virus increase the risk of hepatocellular carcinoma in hepatitis B carriers. *Gastroenterology* 2003; **124**: 327-334
- 20 **Ando K**, Moriyama T, Guidotti LG, Wirth S, Schreiber RD, Schlicht HJ, Huang SN, Chisari FV. Mechanisms of class I restricted immunopathology. A transgenic mouse model of fulminant hepatitis. *J Exp Med* 1993; **178**: 1541-1554
- 21 **Roman M**, Martin-Orozco E, Goodman JS, Nguyen MD, Sato Y, Ronaghy A, Kornbluth RS, Richman DD, Carson DA, Raz E. Immunostimulatory DNA sequences function as T-helper-1-promoting adjuvants. *Nat Med* 1997; **3**: 849-854
- 22 **Klinman DM**, Yamshchikov G, Ishigatsubo Y. Contribution of CpG motifs to the immunogenicity of DNA vaccines. *J Immunol* 1997; **158**: 3635-3639
- 23 **Moriyama T**, Guillhot S, Klopchin K, Moss B, Pinkert CA, Palmiter RD, Brinster RL, Kanagawa O, Chisari FV. Immunobiology and pathogenesis of hepatocellular injury in hepatitis B virus transgenic mice. *Science* 1990; **248**: 361-364
- 24 **Tang TJ**, Kwekkeboom J, Iaman JD, Niesters HG, Zondervan PE, De Man RA, Schalm SW, Janssen HL. The role of intrahepatic immune effector cells in inflammatory liver injury and viral control during chronic hepatitis B infection. *J Viral Hepat* 2003; **10**: 159-167
- 25 **Kasahara S**, Ando K, Saito K, Sekikawa K, Ito H, Ishikawa T, Ohnishi H, Seishima M, Kakumu S, Moriwaki H. Lack of tumor necrosis factor alpha induces impaired proliferation of hepatitis B virus-specific cytotoxic T lymphocytes. *J Virol* 2003; **77**: 2469-2476
- 26 **Sobao Y**, Sugi K, Tomiyama H, Saito S, Fujiyama S, Morimoto M, Hasuike S, Tsubouchi H, Tanaka K, Takiguchi M. Identification of hepatitis B virus-specific CTL epitopes presented by HLA-A*2402, the most common HLA class I allele in East Asia. *J Hepatol* 2001; **34**: 922-929
- 27 **Roh S**, Lee YK, Ahn BY, Kim K, Moon A. Induction of CTL responses and identification of a novel epitope of hepatitis B virus surface antigens in C57BL/6 mice immunized with recombinant vaccinia viruses. *Virus Res* 2001; **73**: 17-26
- 28 **Street M**, Herd K, Londono P, Doan T, Dougan G, Kast WM, Tindler RW. Differences in the effectiveness of delivery of B- and CTL-epitopes incorporated into the hepatitis B core antigen (HBcAg) c/e1-region. *Arch Virol* 1999; **144**: 1323-1343
- 29 **Prugnaud JL**. DNA vaccines. *Ann Pharm Fr* 2003; **61**: 219-233
- 30 **Wang J**, Murakami T, Yoshida S, Matsuoka H, Ishii A, Tanaka T, Tobita K, Ohtsuki M, Nakagawa H, Kusama M, Kobayashi E. Predominant cell-mediated immunity in the oral mucosa: gene gun-based vaccination against infectious diseases. *J Dermatol Sci* 2003; **31**: 203-210
- 31 **Isaguliant MG**, Petrakova NV, Mokhonov VV, Pokrovskaya K, Suzdaltzeva YG, Krivonos AV, Zaberezhny AD, Garaev MM, Smirnov VD, Nordenfelt E. DNA immunization efficiently targets conserved functional domains of protease and ATPase/helicase of nonstructural 3 protein (NS3) of human hepatitis C virus. *Immunol Lett* 2003; **88**: 1-13
- 32 **Wolff JA**, Malone RW, Williams P, Chong W, Acsadi G, Jani A, Felgner PL. Direct gene transfer into mouse muscle *in vivo*. *Science* 1990; **247**(4949 Pt 1): 1465-1468
- 33 **Corr M**, von Damm A, Lee DJ, Tighe H. *In vivo* priming by DNA injection occurs predominantly by antigen transfer. *J Immunol* 1999; **163**: 4721-4727
- 34 **Myers RP**, Tainturier MH, Ratziu V, Piton A, Thibault V, Imbert-Bismut F, Messous D, Charlotte F, Di Martino V, Benhamou Y, Poynard T. Prediction of liver histological lesions with biochemical markers in patients with chronic hepatitis B. *J Hepatol* 2003; **39**: 222-230
- 35 **Wang FS**. Current status and prospects of studies on human genetic alleles associated with hepatitis B virus infection. *World J Gastroenterol* 2003; **9**: 641-644

Edited by Zhang JZ and Wang XL Proofread by Xu FM

Sequence evolution of putative cytotoxic T cell epitopes in NS3 region of hepatitis C virus

Hua-Zhang Guo, Ying Yin, Wen-Liang Wang, Chuan-Shan Zhang, Tao Wang, Zhe Wang, Jing Zhang, Hong Cheng, Hai-Tao Wang

Hua-Zhang Guo, Wen-Liang Wang, Chuan-Shan Zhang, Tao Wang, Zhe Wang, Jing Zhang, Hong Cheng, Department of Pathology, Xijing Hospital, Fourth Military Medical University, Xi'an 710033, Shaanxi Province, China

Ying Yin, Department of Clinical Laboratories, Xijing Hospital, Fourth Military Medical University, Xi'an 710033, Shaanxi Province, China
Hai-Tao Wang, Institute of Microbiology and Epidemiology, Academy of Military Medical Sciences, Beijing 100071, China

Correspondence to: Wen-Liang Wang, Department of Pathology, Xijing Hospital, Fourth Military Medical University, Xi'an 710033, Shaanxi Province, China. wllwang@fmmu.edu.cn

Telephone: +86-29-3374595 **Fax:** +86-29-3284284

Received: 2003-10-20 **Accepted:** 2003-12-16

Abstract

AIM: Quasispecies of hepatitis C virus (HCV) are the foundation for rapid sequence evolution of HCV to evade immune surveillance of hosts. The consensus sequence evolution of a segment of HCV NS3 region, which encompasses putative cytotoxic T cell epitopes, was evaluated.

METHODS: Three male patients, infected with HCV through multiple transfusions, were identified from clinical symptoms and monitored by aminotransferase for 60 months. Blood samples taken at months 0, 32, and 60 were used for viral RNA extraction. A segment of HCV NS3 region was amplified from the RNA extraction by RT-PCR and subjected to subcloning and sequencing. HLA types of these three patients were determined using complement-dependent microlymphocytotoxic assay. CTL epitopes were predicted using MHC binding motifs.

RESULTS: No patient had clinical symptoms or elevation of aspartate/alanine aminotransferase. Two patients showed positive HCV PCR results at all 3 time points. The other one showed a positive HCV PCR result only at month 0. A reported HLA-A2-restricted CTL epitope had no alteration in the HLA-A2-negative carrier over 60 months. In the HLA-A2-positive individuals, all the sequences from 0 month 0 showed an amber mutation on the initial codon of the epitope. Most changes of consensus sequences in the same patient occurred on predicted cytotoxic T cell epitopes.

CONCLUSION: Amber mutation and changes of consensus sequence in HCV NS3 region may be related to viral immune escape.

Guo HZ, Yin Y, Wang WL, Zhang CS, Wang T, Wang Z, Zhang J, Cheng H, Wang HT. Sequence evolution of putative cytotoxic T cell epitopes in NS3 region of hepatitis C virus. *World J Gastroenterol* 2004; 10(6): 847-851

<http://www.wjgnet.com/1007-9327/10/847.asp>

INTRODUCTION

Hepatitis C virus (HCV) is one of the main pathogens of

transfusion-associated hepatitis. After acute transfusion-associated HCV infection, about 70-80% of the patients may progress to chronicity. Although many patients with chronic hepatitis C have no symptoms, cirrhosis may develop in 20% within 10 to 20 years after acute infection. The risk for hepatocellular carcinoma is increased in patients with chronic hepatitis C and almost exclusively in patients with cirrhosis^[1-15].

HCV is a linear, single-stranded positive-sense, 9400-nucleotide RNA virus. HCV constitutes its own genus in the family *Flaviviridae*. The HCV genome contains a single large open reading frame that codes for a virus polyprotein of approximately 3000 amino acids. Due to the high mutation rate of RNA dependent RNA polymerase, there are genotype and quasispecies diversity of HCV^[16-19]. The high mutation rate may interfere with effective immunity and cause the progression to chronicity^[20, 21].

Of the components of adaptive immunity, cytotoxic T cells play an important role in eliminating intracellular infections^[22]. They recognize body cells infected with viruses by detecting peptide fragments derived from viruses bound to MHC class I molecules on the infected body cells. Then, they kill the infected cells before viral replications complete. In this study, 3 patients with transfusion-associated hepatitis C were followed-up for 60 mo to evaluate the evolution of cytotoxic T cell epitopes in the HCV NS3 region.

MATERIALS AND METHODS

Patients

Patients C, Z and W, being 43, 48 and 49 years old Chinese males, were infected with HCV through multiple transfusions. They were followed-up for 60 mo after identification. During the follow-up period, no elevation of aspartate/alanine aminotransferase was found. Their peripheral blood was collected at mo 0 (the time of identification), 32 and 60, and stored at -70 °C. Patients C and Z were positive for HCV RNA. Patient W was positive for HCV RNA only in the blood sample taken at mo 0 and consistently negative after that.

HLA typing

HLA types of the three patients were assessed by using the Tasaki HLA class I dry tissue typing tray (One Lambda, Canoga Park, CA). Briefly, blood samples were drawn and lymphocytes were isolated immediately. After antibody and 2×10^6 lymphocytes were mixed in each well, 1 μ L of complement was added into each well to incubate at room temperature for 1 hour. After incubation, the cells were stained with eosin and fixed with formaldehyde. Positive (dead) lymphocytes appeared dark and non-refractiles with eosin dye.

RNA extraction and RT-PCR

Single step guanidine thiocyanate-chloroform method^[23] was used to extract HCV RNA from 50 μ L of plasma. RNA extracted was reverse-transcribed using random primers. Nested PCR (primers see Table 1) was used to amplify the HCV NS3 region that spanned a reported cytotoxic T cell

epitope (-KLVALGINAV-)^[24], which is HLA-A2-restricted. The first round PCR was run for 35 cycles with denaturing at 94 °C for 1 min, annealing at 53 °C for 1 min, and elongating at 72 °C for 1 min. The second round of PCR was run for 35 cycles with denaturing at 94 °C for 1 min, annealing at 60 °C for 1 min, and elongating at 72 °C for 1 min.

Cloning and sequencing of amplified segment of HCV NS3

PCR products were subcloned into M13mp19 phage. For each blood sample, 5 clones were selected and amplified. The single strand DNA produced by the M13mp19 phage was purified by QIAprep Spin 13 kit (Qiagen, Valencia, CA) and sequenced using sequence version 2.0 sequencing kit (USB, Cleveland, OH).

Sequence analysis

DNA sequences were translated and aligned. Consensus sequence was produced for every 5 clones of each blood sample. Cytotoxic T cell epitopes for each consensus sequence were predicted based on the HLA type of the patients and MHC molecule binding motifs^[25].

RESULTS

HLA types

Patient C was (A11, 30; B13, -; Bw4, -). Patient Z was [A2, 11; B60 (40), 70; Bw6, -]. Patient W was [A2, 11; B40, 55 (22); Bw6, -].

Nucleotide sequences of HCV

Five clones of NS3 sequences were ascertained for each blood sample. Since all the blood samples of patients C and Z were positive for HCV RNA, 15 sequences were obtained from each one of them. Due to the negative result of HCV RNA in the later 2 blood samples in patient W, only 5 cDNA sequences

were obtained. The GenBank accession numbers for all the sequences are in Table 2. The translated amino acid sequences are aligned in Figure 1.

Table 2 Assigned accession number for each nucleotide sequence of three patients

Time point measured	Patient W	Patient C	Patient Z
0 mo	AF051270	AF051261	AF051270
	AF051270	AF051261	AF051270
	AF051271	AF051261	AF051270
	AF051272	AF051260	AF051270
	AF051273	AF051259	AF051270
32 th mo	NA	AF051254	AF051265
		AF051255	AF051266
		AF051256	AF051267
		AF051257	AF051268
		AF051258	AF051269
60 th mo	NA	AF051253	AF051262
		AF051253	AF051262
		AF051253	AF051263
		AF051253	AF051263
		AF051253	AF051264

NA: not applicable as the sample was PCR negative for HCV RNA.

Sequence variation on reported cytotoxic T cell epitope

Our consensus sequences showed (K/*)LSSLGLNAV (*: stop codon) on the site of the reported HLA-A2-restricted cytotoxic T cell epitope^[24]. In patient C, who was not HLA-A2-restricted, all the 15 sequences were KLSSLGLNAV. In patient W, who was HLA-A2-restricted, all the 5 sequences showed a stop codon at the beginning of this peptide (four sequences showed

Table 1 Oligonucleotides used to amplify the NS3 region*

	Primer sequences	Strand	Nucleotide position in HCV genome
First round primers (5' -3')	CCCCATCAC(A/G)TACTC(C/T)ACCTA	+	4 197
	ACA(C/T)GT(A/G)TT(G/A)CAGTC(T/G)ATCAC	-	4 681
Second round primers (5' -3')	CGAGGATCCGTCCT(T/G)GACCAAGC(A/G)GAGAC	+	4 315
	GCAACTGCAGCT(G/A)G(T/A)(C/T)GG(G/T)ATGAC(A/G)GACAC	-	4 597

*Degenerate primers were used to cover the variable HCV genomes.

Table 3 Predicted CTL epitopes by MHC binding peptide motifs while incorporating persistent substitutions

Patient	HLA subtype	MHC binding peptide motif ^[38, 39]	Genome position	Predicted epitope	Time point measured
C	A11	X[MLIVSATGNCDF]XXXXXX[KRHY]	1 349	ATPPGSITVPH*	0 mo
				ATPPGSVTVPH*	32 th , 60 th mo
			1 378	KAIPIEAIR	0 mo
				KAIPIEAIK	32 th , 60 th mo
Z	A11	X[MLIVSATGNCDF]XXXXXX[KRHY]	1 381	PIEAIKGG	0 mo
				PIEAIKGG	32 th , 60 th mo
			1 347	ATATPPGSV	0 mo
				ATATPPGSI	32 th , 60 th mo
	A2	X[LMIVAT]XXXXXX[LVIAMT]	1 348	TATPPGSVT	0 mo
				TATPPGSIT	32 th , 60 th mo
			1 349	ATPPGSVTV	0 mo
				ATPPGSITV	32 th , 60 th mo

*These two peptides fitted the MHC binding motif because proline and glycine residues allowed flexibility which made the peptides accommodate to the motif by kinking in the peptide backbone^[40].

*LSSLGLNAV and one sequence showed *LSPLGLNAV). In patient Z, who was also HLA-A2-restricted, all the sequences from 0-mo showed the stop codon at the beginning of the epitope (*LSSLGLNAV), nine sequences from blood samples at mo 32 and 60 showed KLSSLGLNAV, one sequence from blood sample at mo 32 showed KLSSLGLKPV.

Sequence variation on predicted cytotoxic T cell epitopes

Using MHC binding motifs to predict cytotoxic T cell epitopes, we found that most sites which showed changes of consensus sequences between successive blood samples were on the predicted cytotoxic T cell epitopes (Table 3).

DISCUSSION

Due to errors of the RNA-dependent RNA polymerase, RNA genomes had a relatively high mutation rate^[25,26]. RNA viruses evolve as complex distributions of mutants termed viral quasispecies. These coexisting mutant genomes always have a consensus or master sequence. Despite the potentially high mutation rate and variability of RNA viruses, changes in the consensus sequence of a viral population would occur only if some selection mechanism acted on the population and caused a shift in the population equilibrium^[27]. Immune response of the host can influence the distribution between different viral variants and will consequently cause a change in the consensus

Patient W

0 mo									
	1340	1350	1360	1370	1380	1390	1400	1410	1420
Consensus	AGARLVVLATATPPGSVTVPHPNIQEVGLSNTGEIPFYGKAIP IEA IKGGRHLIFCHSKKKCDELA A *LSSLGLNAVAYYRGLD								
Clone 1								
Clone 2								
Clone 3								
Clone 4P.....								
Clone 5P.....								

Patient Z

0 mo									
	1340	1350	1360	1370	1380	1390	1400	1410	1420
Consensus	AGARLVVLATATPPGSVTVPHPNIQEVGLSNTGEIPFYGKAIP IEA IKGGRHLIFCHSKKKCDELA A *LSSLGLNAVAYYRGLD								
Clone 1								
Clone 2								
Clone 3								
Clone 4								
Clone 5								

32 th mo									
	1340	1350	1360	1370	1380	1390	1400	1410	1420
Consensus	AGARLVVLATATPPGSITVPHPNIQEVALSNTGEIPFYGKAIP IEA IRGGRHLIFCHSKKKCDELA AKLSSLGLNAVAYYRGLD								
Clone 1								
Clone 2								
Clone 3								
Clone 4P.....								
Clone 5K.....								

60 th mo									
	1340	1350	1360	1370	1380	1390	1400	1410	1420
Consensus	AGARLVVLATATPPGSITVPHPNIQEVALSNTGEIPFYGKAIP IEA IRGGRHLIFCHSKKKCDELA AKLSSLGLNAVAYYRGLD								
Clone 1								
Clone 2								
Clone 3								
Clone 4								
Clone 5KP.....								

Patient C

0 mo									
	1340	1350	1360	1370	1380	1390	1400	1410	1420
Consensus	AGARLVVLATATPPGSITVPHPNIQEVALSNTGEIPFYGKAIP IEA IKGGRHLIFCHSKKKCDELA AKLSSLGLNAVAYYRGLD								
Clone 1								
Clone 2								
Clone 3								
Clone 4R.....								
Clone 5								

32 th mo									
	1340	1350	1360	1370	1380	1390	1400	1410	1420
Consensus	AGARLVVLATATPPGSVTVPHPNIQEVALSNTGEIPFYGKAIP IEA IKGGRHLIFCHSKKKCDELA AKLSSLGLNAVAYYRGLD								
Clone 1								
Clone 2								
Clone 3								
Clone 4								
Clone 5T.....								

60 th mo									
	1340	1350	1360	1370	1380	1390	1400	1410	1420
Consensus	AGARLVVLATATPPGSVTVPHPNIQEVALSNTGEIPFYGKAIP IEA IKGGRHLIFCHSKKKCDELA AKLSSLGLNAVAYYRGLD								
Clone 1								
Clone 2								
Clone 3								
Clone 4								
Clone 5								

Figure 1 Alignment of HCV amino acid sequences from three patients. Consensus sequences were given for the 5 sequences from the same blood sample.

sequence. A cellular immune-driven selection pressure has been demonstrated by the existence of HCV escape mutants in relation to cytotoxic T cell epitopes^[28]. In the HCV-infected human, the NS3 protein seems to be fairly immunogenic. T cell activation in response to NS3 has been detected in a number of studies of patients with acute or chronic HCV infection^[24, 29]. It was proposed that a strong *in vitro* T cell reaction to NS3 correlated with clearance of acute HCV infection whereas a less vigorous, or absent, NS3-specific T cell reactivity was observed in those who progressed to chronicity^[30]. Thus, in this study, we chose a segment of HCV NS3 region as our focus on sequence evolution.

T lymphocytes recognize their antigens in context of MHC-encoded molecules, a phenomenon called MHC restriction. Our sequence segment encompassed a cytotoxic T cell epitope, which was restricted by HLA-A2 and reported by Rehmann *et al*^[24]. In patients with HLA-A2 allele, their viral consensus sequences showed stop codons at the initial part of this epitope. On the contrary, in patients without HLA-A2 allele, their viral consensus sequences did not show the stop codon. Normally, stop codons are generated by random non-sense mutations in RNA virus and they are expected to occur randomly throughout the entire coding region. Viruses with stop codon in the open reading frame have been found to be defective viruses which usually make a small fraction of the RNA virus quasispecies^[31,32]. Here, stop codons were unusually concentrated at the beginning of the reported epitope, in the sequences of patients with HLA-A2 allele, suggesting that they are specifically selected by some pressure, probably by cytotoxic T cells. We would suppose that HCV specific and HLA-A2-restricted cytotoxic T cells, which recognize and kill the infected hepatocytes to prevent replication and proliferation of the viruses, were generated in patients W and Z. Under this immune pressure, viral quasispecies in these two patients would have shifted toward a new equilibrium to avoid the immune attack. In patients W and Z, the defective viruses, which did not express the reported cytotoxic T cell epitope, dominated the viral quasispecies at month 0. This may reflect the strong immune pressure at that time. Thirty-two months later, in patient W, the viruses were cleared and the patient was recovered. In patient Z, the viruses were not cleared at month 32 or 60, suggesting that the viral quasispecies escaped from the immune pressure and survived.

Cytotoxic T cells could recognize peptides loaded on the MHC class I molecules^[33]. The solution of the crystal structure of MHC class I molecules could reveal peptide-binding groove made up by $\alpha 1$ and $\alpha 2$ domains of heavy chains^[34,35]. Naturally occurring processed peptides have been isolated from purified MHC class I molecules. Analyzing their sequences revealed the presence of simple amino acid sequence motifs that were specific to particular allelic forms of class I molecules^[36]. Based on the sequence motifs, we found that most sites, with changes of the consensus sequences, were on the putative cytotoxic T cell epitopes in the corresponding patients, implying the possible underlying immune impetus for sequence evolution.

In summary, by molecular sequencing, the quasispecies nature and sequence evolution of HCV NS3 region can be revealed. By HLA typing and epitope prediction, the non-sense mutation and changes of consensus sequences might be the result of immune pressure. This study has paved the way for further cytotoxicity assay^[37] to confirm the possible immune target sites of HCV.

REFERENCES

- National Institutes of Health Consensus Development Conference Panel statement: management of hepatitis C. *Hepatology* 1997; **26**(3 Suppl): 2S-10S
- Maier I, Wu GY. Hepatitis C and HIV co-infection: a review. *World J Gastroenterol* 2002; **8**: 577-579
- Meier V, Mihm S, Braun Wietzke P, Ramadori G. HCV-RNA positivity in peripheral blood mononuclear cells of patients with chronic HCV infection: does it really mean viral replication? *World J Gastroenterol* 2001; **7**: 228-234
- Chen MY, Huang ZQ, Chen LZ, Gao YB, Peng RY, Wang DW. Detection of hepatitis C virus NS5 protein and genome in Chinese carcinoma of the extrahepatic bile duct and its significance. *World J Gastroenterol* 2000; **6**: 800-804
- He QQ, Cheng RX, Sun Y, Feng DY, Chen ZC, Zheng H. Hepatocyte transformation and tumor development induced by hepatitis C virus NS3 c-terminal deleted protein. *World J Gastroenterol* 2003; **9**: 474-478
- Li K, Wang L, Cheng J, Lu YY, Zhang LX, Mu JS, Hong Y, Liu Y, Duan HJ, Wang G, Li L, Chen JM. Interaction between hepatitis C virus core protein and translin protein—a possible molecular mechanism for hepatocellular carcinoma and lymphoma caused by hepatitis C virus. *World J Gastroenterol* 2003; **9**: 300-303
- Worman HJ, Lin F. Molecular biology of liver disorders: the hepatitis C virus and molecular targets for drug development. *World J Gastroenterol* 2000; **6**: 465-469
- Nelson DR, Marousis CG, Davis GL, Rice CM, Wong J, Houghton M, Lau JY. The role of hepatitis C virus-specific cytotoxic T lymphocytes in chronic hepatitis C. *J Immunol* 1997; **158**: 1473-1481
- Assy N, Minuk G. A comparison between previous and present histologic assessments of chronic hepatitis C viral infections in humans. *World J Gastroenterol* 1999; **5**: 107-110
- Caselmann WH, Serwe M, Lehmann T, Ludwig J, Sproat BS, Engels JW. Design, delivery and efficacy testing of therapeutic nucleic acids used to inhibit hepatitis C virus gene expression *in vitro* and *in vivo*. *World J Gastroenterol* 2000; **6**: 626-629
- Chen LK, Hwang SJ, Tsai ST, Luo JC, Lee SD, Chang FY. Glucose intolerance in Chinese patients with chronic hepatitis C. *World J Gastroenterol* 2003; **9**: 505-508
- Fan XG, Tang FQ, Ou ZM, Zhang JX, Liu GC, Hu GL. Lymphoproliferative response to hepatitis C virus (HCV) antigens in patients with chronic HCV infection. *Shijie Huaren Xiaohua Zazhi* 1999; **7**: 1038-1040
- Song ZQ, Hao F, Zhang J, Gu CH. Detection of antibodies against hypervariable region 1 in sera from patients with hepatitis C. *Shijie Huaren Xiaohua Zazhi* 1999; **7**: 666-668
- Wu HB, Li ZW, Li Y. Clinical significance of detection of positive and negative strands of HCV RNA in peripheral blood mononuclear cells. *Shijie Huaren Xiaohua Zazhi* 1999; **7**: 220-221
- Zhou YX, Feng ZH, Jia ZS, Lian JQ, Li JG, Li WB. A study of gene immunization with recombinant expression plasmid of hepatitis C virus core antigen. *Shijie Huaren Xiaohua Zazhi* 1998; **6**: 966-968
- Major ME, Feinstone SM. The molecular virology of hepatitis C. *Hepatology* 1997; **25**: 1527-1538
- Chen S, Wang YM. Genetic evolution of structural region of hepatitis C virus in primary infection. *World J Gastroenterol* 2002; **8**: 686-693
- Flichman D, Kott V, Sookoian S, Campos R. Acute hepatitis C in a chronically HIV-infected patient: Evolution of different viral genomic regions. *World J Gastroenterol* 2003; **9**: 1496-1500
- Chen YD, Liu MY, Yu WL, Li JQ, Dai Q, Zhou ZQ, Tisminetzky SG. Mix-infections with different genotypes of HCV and with HCV plus other hepatitis viruses in patients with hepatitis C in China. *World J Gastroenterol* 2003; **9**: 984-992
- Weiner AJ, Geysen HM, Christopherson C, Hall JE, Mason TJ, Saracco G, Bonino F, Crawford K, Marion CD, Crawford KA. Evidence for immune selection of hepatitis C virus (HCV) putative envelope glycoprotein variants: potential role in chronic HCV infections. *Proc Natl Acad Sci U S A* 1992; **89**: 3468-3472
- Rehmann B, Chang KM, McHutchison JG, Kokka R, Houghton M, Chisari FV. Quantitative analysis of the peripheral blood cytotoxic T lymphocyte response in patients with chronic hepatitis C virus infection. *J Clin Invest* 1996; **98**: 1432-1440
- Li CP, Wang KX, Wang J, Pan BR. mIL-2R, T cell subsets & hepatitis C. *World J Gastroenterol* 2002; **8**: 298-300
- Chomczynski P, Sacchi N. Single-step method of RNA isolation by acid guanidinium thiocyanate-phenol-chloroform extraction.

- Anal Biochem* 1987; **162**: 156-159
- 24 **Rehermann B**, Chang KM, McHutchinson J, Kokka R, Houghton M, Rice CM, Chisari FV. Differential cytotoxic T-lymphocyte responsiveness to the hepatitis B and C viruses in chronically infected patients. *J Virol* 1996; **70**: 7092-7102
 - 25 **Guo H**, Wang W, Wang T. An application of T cell epitope prediction computer program in the study of HCV adaptive immune responses. *Disi Junyi Daxue Xuebao* 1999; **20**: 845-848
 - 26 **Huang F**, Zhao GZ, Li Y. HCV genotypes in hepatitis C patients and their clinical significances. *World J Gastroenterol* 1999; **5**: 547-549
 - 27 **Elena SF**, Miralles R, Cuevas JM, Turner PE, Moya A. The two faces of mutation: extinction and adaptation in RNA viruses. *IUBMB Life* 2000; **49**: 5-9
 - 28 **Wodarz D**. Hepatitis C virus dynamics and pathology: the role of CTL and antibody responses. *J Gen Virol* 2003; **84**(Pt 7): 1743-1750
 - 29 **Encke J**, zu Putlitz J, Geissler M, Wands JR. Genetic immunization generates cellular and humoral immune responses against the nonstructural proteins of the hepatitis C virus in a murine model. *J Immunol* 1998; **161**: 4917-4923
 - 30 **Wertheimer AM**, Miner C, Lewinsohn DM, Sasaki AW, Kaufman E, Rosen HR. Novel CD4+ and CD8+ T-cell determinants within the NS3 protein in subjects with spontaneously resolved HCV infection. *Hepatology* 2003; **37**: 577-589
 - 31 **Martell M**, Esteban JI, Quer J, Genesca J, Weiner A, Esteban R, Guardia J, Gomez J. Hepatitis C virus (HCV) circulates as a population of different but closely related genomes: quasispecies nature of HCV genome distribution. *J Virol* 1992; **66**: 3225-3229
 - 32 **Higashi Y**, Kakumu S, Yoshioka K, Wakita T, Mizokami M, Ohba K, Ito Y, Ishikawa T, Takayanagi M, Nagai Y. Dynamics of genome change in the E2/NS1 region of hepatitis C virus *in vivo*. *Virology* 1993; **197**: 659-668
 - 33 **Androlewicz MJ**. Peptide generation in the major histocompatibility complex class I antigen processing and presentation pathway. *Curr Opin Hematol* 2001; **8**: 12-16
 - 34 **Khan AR**, Baker BM, Ghosh P, Biddison WE, Wiley DC. The structure and stability of an HLA-A*0201/octameric tax peptide complex with an empty conserved peptide-N-terminal binding site. *J Immunol* 2000; **164**: 6398-6405
 - 35 **Sliz P**, Michielin O, Cerottini JC, Luescher I, Romero P, Karplus M, Wiley DC. Crystal structures of two closely related but antigenically distinct HLA-A2/melanocyte-melanoma tumor-antigen peptide complexes. *J Immunol* 2001; **167**: 3276-3284
 - 36 **Davenport MP**, Smith KJ, Barouch D, Reid SW, Bodnar WM, Willis AC, Hunt DF, Hill AV. HLA class I binding motifs derived from random peptide libraries differ at the COOH terminus from those of eluted peptides. *J Exp Med* 1997; **185**: 367-371
 - 37 **Zhou HC**, Xu DZ, Wang XP, Zhang JX, Huang Y, Yan YP, Zhu Y, Jin BQ. Identification of the epitopes on HCV core protein recognized by HLA-A2 restricted cytotoxic T lymphocytes. *World J Gastroenterol* 2001; **7**: 583-586
 - 38 **Reche PA**, Glutting JP, Reinherz EL. Prediction of MHC class I binding peptides using profile motifs. *Hum Immunol* 2002; **63**: 701-709
 - 39 **Rammensee H**, Bachmann J, Emmerich NP, Bachor OA, Stevanovic S. SYFPEITHI: database for MHC ligands and peptide motifs. *Immunogenetics* 1999; **50**: 213-219
 - 40 **Guo HC**, Jardetzky TS, Garrett TP, Lane WS, Strominger JL, Wiley DC. Different length peptides bind to HLA-Aw68 similarly at their ends but bulge out in the middle. *Nature* 1992; **360**: 364-366

Edited by Chen WW and Wang XL Proofread by Xu FM

Establishment of *Helicobacter pylori* infection model in Mongolian gerbils

Jie Yan, Yi-Hui Luo, Ya-Fei Mao

Jie Yan, Yi-Hui Luo, Ya-Fei Mao, Department of Medical Microbiology and Parasitology, College of Medical Science, Zhejiang University, Hangzhou 310031, China

Supported by the Excellent Young Teacher Fund of Chinese Education Ministry and the General Research Plan of the Science and Technology Department of Zhejiang Province, No. 001110438

Correspondence to: Jie Yan, Department of Medical Microbiology and Parasitology, College of Medical Science, Zhejiang University, 353 Yan an Road, Hangzhou 310031, Zhejiang Province, China. yanchen@mail.hz.zj.cn

Telephone: +86-571-87217385 **Fax:** +86-571-87217044

Received: 2003-09-15 **Accepted:** 2003-11-13

Abstract

AIM: To establish a stable and reliable model of *Helicobacter pylori* infection model in Mongolian gerbils and to observe pathological changes in gastric mucosa in infected animals.

METHODS: Mongolian gerbils were randomly divided into 18 groups; 6 groups were infected with *H pylori* clinical strain Y06 ($n=6$, groups Y), 6 groups were infected with *H pylori* strain NCTC11637 ($n=6$, groups N), and 6 uninfected groups as negative controls ($n=4$, groups C). *H pylori* suspensions at the concentrations of 2×10^8 and 2×10^9 CFU/mL of strain NCTC11637 and strain Y06 were prepared. The animals in three groups N and in three groups Y were orally challenged once with 0.5 mL of the low concentration of the bacterial suspension. The animals in another three groups N and in another three groups Y were orally challenged with 0.5 mL of the high concentration of the bacterial suspension for 3 times at the intervals of 24 h, respectively. For the negative controls, the animals in six groups C were orally given with the same volume of Brucella broth at the corresponding inoculating time. The animals were killed after 2nd, 4th and 6th week after the last challenge and the gastric mucosal specimens were taken for urease test, bacterial isolation, pathological and immunohistochemical examinations.

RESULTS: Positive isolation rates of *H pylori* in the animals of groups Y at the 2nd, 4th and 6th week after one challenge were 0%, 16.7% and 66.7%, while in the animals of groups N were 0%, 0% and 16.7%, respectively. Positive isolation rates of *H pylori* in the animals of groups Y at the 2nd, 4th and 6th week after three challenges were 66.7%, 100% and 100%, while in the animals of groups N were 66.7%, 66.7% and 100%, respectively. In animals with positive isolation of *H pylori*, the bacterium was found to colonized on the surface of gastric mucosal cells and in the gastric pits, and the gastric mucosal lamina propria was infiltrated with inflammatory cells.

CONCLUSION: By using *H pylori* suspension at high concentration of 2×10^9 CFU/mL for multiple times, the orally challenged Mongolian gerbils can be used as a stable and reliable *H pylori* infection model. The 2 strains of *H pylori* can colonize in gastric mucosa of the infected animals and

cause mild inflammation reaction.

Yan J, Luo YH, Mao YF. Establishment of *Helicobacter pylori* infection model in Mongolian gerbils. *World J Gastroenterol* 2004; 10(6): 852-855

<http://www.wjgnet.com/1007-9327/10/852.asp>

INTRODUCTION

Helicobacter pylori, a microaerophilic, spiral and Gram-negative bacillus, is recognized as an important pathogen causing human gastritis and peptic ulcer and a high risk factor for gastric carcinoma^[1,2]. In China, chronic gastritis and peptic ulcer are two of the most common digestive diseases, and gastric cancer is one of the malignant tumors with high morbidities^[3-34]. An ideal public measure to prevent and control these *H pylori* infection-associated diseases may be a vaccine that could induce strong humoral and cellular immune responses. However, no commercial *H pylori* vaccine is available so far, and the development of *H pylori* vaccine by using genetic engineering techniques is being active^[35-39]. A stable and reliable *H pylori* infection animal model would be necessary for evaluating vaccine efficacy and helpful for understanding the pathological mechanism of the organism. Therapeutic drugs for *H pylori* eradication differ from those for many other bacteria such as using metronidazole^[40,41]. Therefore, *H pylori* infection animal models would contribute to screen new drugs against *H pylori*. In recent published data, Mongolian gerbils have been considered as ideal animals to establish infection model by using internationally collected *H pylori* strains^[42-44]. In this study, we used a clinical *H pylori* isolate named Y06 to establish a stable and reliable infection model in Mongolian gerbils. The colonization sites of *H pylori* and pathological changes in gastric mucosa of the animals were also observed.

MATERIALS AND METHODS

H pylori strains

A clinical strain of *H pylori* named Y06 was isolated from a patient with gastric ulcer. This strain was identified based on their characteristic morphology by Gram staining under microscope, and positive for urease and oxidase activities, further confirmed by slide agglutination test using commercial rabbit antiserum against whole cell of *H pylori* (DAKO). A reference *H pylori* strain, NCTC11637, was used as an infection control. The two strains were subcultured in Columbia agar (bioMérieux) containing 80 mL/L sheep blood under microaerobic conditions containing 100 mL/L CO₂, 50 mL/L O₂ and 850 mL/L N₂.

Animals

Eight-week-old specific pathogen-free male Mongolian gerbils with body mass of 75 ± 5 g were provided by Experimental Animal Center, Zhejiang Academy of Medical Sciences. These gerbils were randomly divided into eighteen groups: six groups infected with the clinical strain Y06 (groups Y, $n=6$ in each group), six groups infected with the reference *H pylori* strain NCTC11637

(groups N, $n=6$ in each group) and six groups as negative controls (groups C, $n=4$ in each group).

Dosages and pathway of inoculation

Bacterial cells grown on the 2 strains on Columbia agar for 3–5 d were collected and diluted to the final concentrations of 2×10^8 CFU/mL and 2×10^9 CFU/mL, respectively, by using Brucella broth (bioMérieux). Each Mongolian gerbils in 3 groups Y and 3 groups N were orally challenged with 0.5 mL of 2×10^8 CFU/mL *H. pylori* suspension, while the animals in another 3 groups Y and 3 groups N were attacked with 0.5 mL of 2×10^9 CFU/mL *H. pylori* suspension through the same pathway. For the negative controls, the animals in 6 groups C were orally given with 0.5 mL of Brucella broth. Each animal in the groups was given with the different concentrations of *H. pylori* suspensions or Brucella broth, respectively, as the described above for 3 times at an interval of 24 h. The animals were deprived of food but offered with water for 12 h before the challenge, and supplied with food and water after 4 h of *H. pylori* inoculation.

Isolation and identification of *H. pylori*

Six animals in group Y, 6 in group N and 4 animals in group C were killed, respectively, at 2, 4 and 6 wk after the last challenge. Two gastric mucosal specimens at the adjacent position were taken from antrum and corpus, respectively. One of the specimens was used for *H. pylori* isolation, and the others were fixed with 40 g/L formaldehyde solution. The colonies on Columbia plates were identified by microscopy after Gram-staining, assays for urease and oxidase activities and slide agglutination test using the commercial *H. pylori*-specific antiserum. The bacterium was defined to be *H. pylori* if it was Gram-negative with arc shape or “seagull-like”, positive for the two enzymes and immune agglutination.

Pathological and immunohistochemical examinations

The gastric mucosal specimens fixed with formaldehyde were pathologically examined after embedding, section and haematoxylin-eosin (HE) staining. *H. pylori* in gastric mucosal specimens were detected by the immunohistochemical method using a commercial rabbit anti-*H. pylori* antibody and goat anti-rabbit HRP-labeled IgG antibody (Jackson ImmunoResearch).

RESULTS

Infection of Mongolian gerbils with *H. pylori* strains

The results of *H. pylori* isolation from gastric mucosal specimens of Mongolian gerbils are shown in Table 1.

Table 1 The detection results of *H. pylori* isolated from gastric mucosa of experimental infected Mongolian gerbils

Group	Detection time (wk)	Infection rate (%) (positive/total cases)	
		1×10^8 CFU (1 challenge)	1×10^9 CFU (3 challenges)
Y	2	0(0/6)	66.7(4/6)
N	2	0(0/6)	66.7(4/6)
C	2	0(0/4)	0(0/4)
Y	4	16.7(1/6)	100(6/6)
N	4	0(0/6)	66.7(4/6)
C	4	0(0/4)	0(0/4)
Y	6	66.7(4/6)	100(6/6)
N	6	16.7(1/6)	100(6/6)
C	6	0(0/4)	0(0/4)

Y, groups infected with strain Y06; N, groups infected with strain NCTC11637; C, negative controls.

Pathological and immunohistochemical findings

In animals with positive *H. pylori* isolation, the organisms were found to colonize the surface of gastric mucosa and the gastric pits (Figure 1). In the presence of *H. pylori* infection, infiltration of chronic inflammatory cells in the lamina propria and erosions on the surface of gastric mucosa were observed (Figure 2).

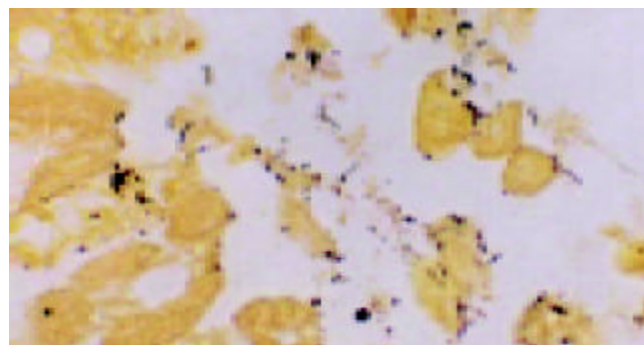


Figure 1 The *H. pylori* bodies located on the surface of gastric mucosal cells and in gastric pits ($\times 1000$).

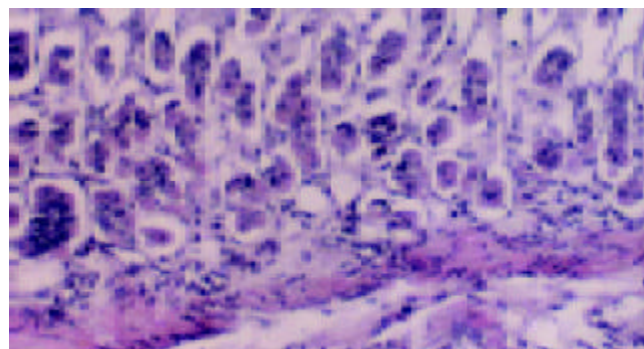


Figure 2 The infiltrated chronic inflammatory cells in the gastric mucosal lamina propria of the specimens with positive *H. pylori* isolation ($\times 400$).

DISCUSSION

In previous published data, animals for establishment of *H. pylori* infection models included guinea pigs, rats, nude mice, chimpanzee *etc.*^[45–48]. These animal models have many disadvantages such as low infection rates, instability, immunodeficiency and high costs. In 1997, Lee *et al* successfully established an animal model infected with a *H. pylori* strain named as SS1 in C₅₇BL/6 and Balb/c mice^[48]. This animal model showed a high frequency and stability for *H. pylori* infection. However, strain SS1 is a mutant of *H. pylori* and its virulence is considerably low. Recently, Mongolian gerbils, which has distinct advantages such as high frequency and stability of infection, large colonization of *H. pylori*, longer living suitable for study with long period of time and pathological changes similar to those observed in human with chronic gastritis, have become the predominant animals for preparing *H. pylori* infection model^[42–44]. In 1999, Chi *et al* established a stable model of *H. pylori* infection in Mongolian gerbils, which was orally pretreated with alcohol^[49]. Therefore, Mongolian gerbils are regarded as an ideal animal for *H. pylori* infection models.

Previous studies have shown that infection model in Mongolian gerbils by oral challenge once with *H. pylori* suspension at the concentration of 1×10^8 CFU of *H. pylori* is stable^[42–44]. In the present study, *H. pylori* was undetectable in the gastric mucosa from Mongolian gerbils at 2 wk after challenge once with 1×10^8 CFU of the bacterium. Furthermore,

the infection rates at 6 wk after one challenge by *H pylori* strain Y06 and strain NCTC11637 were only 66.7% and 16.7%, respectively. On contrast, by using three oral challenges at the dosage of 1×10^9 CFU, *H pylori* colonization rates in the gastric mucosa at 2 and 6 wk after challenge by *H pylori* strain Y06 or strain NCTC11637 were both 66.7% and 100%, respectively, which indicates that multiple challenges with a high concentration of *H pylori* contribute to the increased infection rates.

The infection rates of *H pylori* strain Y06 and strain NCTC11637 in Mongolian gerbils were 100% and 66.7% at 4 wk for 3 challenges using the low concentration of bacterial suspension, and 16.7% and 0% at 4 wk and 66.7% and 16.7% at 6 wk after one challenge using the high concentration. *H pylori* strain Y06, a fresh clinical isolate, seems to be more virulent than strain NCTC11637 and more beneficial for establishing *H pylori* infection model in Mongolian gerbils with a higher infection rate in a shorter period of time.

H pylori was found on the surface of gastric mucosa and in the gastric pits of Mongolian gerbils when infection was established. The observations that there were erosions of mucosal surface and infiltration of chronic inflammatory cells in the lamina propria of gastric mucosa of *H pylori* infected Mongolian gerbils indicates that the two tested *H pylori* strains are able to colonize gastric mucosa of Mongolian gerbils and cause chronic inflammation and gastric erosions.

REFERENCES

- 1 **Freneck RW Jr**, Clemens J. *Helicobacter* in the developing world. *Microbes Infect* 2003; **5**: 705-713
- 2 **Sharma P**, Vakil N. Review article: *Helicobacter pylori* and reflux disease. *Aliment Pharmacol Ther* 2003; **17**: 297-305
- 3 **Zhang Z**, Yuan Y, Gao H, Dong M, Wang L, Gong YH. Apoptosis, proliferation and p53 gene expression of *H pylori* associated gastric epithelial lesions. *World J Gastroenterol* 2001; **7**: 779-782
- 4 **Lu XL**, Qian KD, Tang XQ, Zhu YL, Du Q. Detection of *H pylori* DNA in gastric epithelial cells by in situ hybridization. *World J Gastroenterol* 2002; **8**: 305-307
- 5 **Yao YL**, Xu B, Song YG, Zhang WD. Overexpression of cyclin E in Mongolian gerbil with *Helicobacter pylori*-induced gastric precancerosis. *World J Gastroenterol* 2002; **8**: 60-63
- 6 **Guo DL**, Dong M, Wang L, Sun LP, Yuan Y. Expression of gastric cancer-associated MG7 antigen in gastric cancer, precancerous lesions and *H pylori*-associated gastric diseases. *World J Gastroenterol* 2002; **8**: 1009-1013
- 7 **Peng ZS**, Liang ZC, Liu MC, Ouyang NT. Studies on gastric epithelial cell proliferation and apoptosis in Hp associated gastric ulcer. *Shijie Huaren Xiaohua Zazhi* 1999; **7**: 218-219
- 8 **Hiyama T**, Haruma K, Kitadai Y, Miyamoto M, Tanaka S, Yoshihara M, Sumii K, Shimamoto F, Kajiya G. B-cell monoclonality in *Helicobacter pylori*-associated chronic atrophic gastritis. *Virchows Arch* 2001; **483**: 232-237
- 9 **Xia HHX**. Association between *Helicobacter pylori* and gastric cancer: current knowledge and future research. *World J Gastroenterol* 1998; **4**: 93-96
- 10 **Quan J**, Fan XG. Progress in experimental research of *Helicobacter pylori* infection and gastric carcinoma. *Shijie Huaren Xiaohua Zazhi* 1999; **7**: 1068-1069
- 11 **Liu HF**, Liu WW, Fang DC. Study of the relationship between apoptosis and proliferation in gastric carcinoma and its precancerous lesion. *Shijie Huaren Xiaohua Zazhi* 1999; **7**: 649-651
- 12 **Zhu ZH**, Xia ZS, He SG. The effects of ATRA and 5Fu on telomerase activity and cell growth of gastric cancer cells *in vitro*. *Shijie Huaren Xiaohua Zazhi* 2000; **8**: 669-673
- 13 **Tu SP**, Zhong J, Tan JH, Jiang XH, Qiao MM, Wu YX, Jiang SH. Induction of apoptosis by arsenic trioxide and hydroxy camptothecin in gastric cancer cells *in vitro*. *World J Gastroenterol* 2000; **6**: 532-539
- 14 **Cai L**, Yu SZ, Zhang ZF. *Helicobacter pylori* infection and risk of gastric cancer in Changle County, Fujian Province, China. *World J Gastroenterol* 2000; **6**: 374-376
- 15 **Yao XX**, Yin L, Zhang JY, Bai WY, Li YM, Sun ZC. Htert expression and cellular immunity in gastric cancer and precancerosis. *Shijie Huaren Xiaohua Zazhi* 2001; **9**: 508-512
- 16 **Xu AG**, Li SG, Liu JH, Gan AH. Function of apoptosis and expression of the proteins Bcl-2, p53 and C-myc in the development of gastric cancer. *World J Gastroenterol* 2001; **7**: 403-406
- 17 **Wang X**, Lan M, Shi YQ, Lu J, Zhong YX, Wu HP, Zai HH, Ding J, Wu KC, Pan BR, Jin JP, Fan DM. Differential display of vincristine-resistance-related genes in gastric cancer SGC7901 cell. *World J Gastroenterol* 2002; **8**: 54-59
- 18 **Liu JR**, Li BX, Chen BQ, Han XH, Xue YB, Yang YM, Zheng YM, Liu RH. Effect of cis-9, trans-11-conjugated linoleic acid on cell cycle of gastric adenocarcinoma cell line (SGC-7901). *World J Gastroenterol* 2002; **8**: 224-229
- 19 **Cai L**, Yu SZ. A molecular epidemiologic study on gastric cancer in Changle, Fujian Province. *Shijie Huaren Xiaohua Zazhi* 1999; **7**: 652-655
- 20 **Gao GL**, Yang Y, Yang SF, Ren CW. Relationship between proliferation of vascular and endothelial cells and gastric cancer. *Shijie Huaren Xiaohua Zazhi* 2000; **8**: 282-284
- 21 **Xue XC**, Fang GE, Hua JD. Gastric cancer and apoptosis. *Shijie Huaren Xiaohua Zazhi* 1999; **7**: 359-361
- 22 **Niu WX**, Qin XY, Liu H, Wang CP. Clinicopathological analysis of patients with gastric cancer in 1200 cases. *World J Gastroenterol* 2001; **7**: 281-284
- 23 **Li XY**, Wei PK. Diagnosis of stomach cancer by serum tumor markers. *Shijie Huaren Xiaohua Zazhi* 2001; **9**: 568-570
- 24 **Fang DC**, Yang SM, Zhou XD, Wang DX, Luo YH. Telomere erosion is independent of microsatellite instability but related to loss of heterozygosity in gastric cancer. *World J Gastroenterol* 2001; **7**: 522-526
- 25 **Morgner A**, Miehke S, Stolte M, Neubauer A, Alpen B, Thiede C, Klann H, Hierlmeier FX, Ell C, Ehninger G, Bayerdorffer E. Development of early gastric cancer 4 and 5 years after complete remission of *Helicobacter pylori* associated gastric low-grade marginal zone B-cell lymphoma of MALT type. *World J Gastroenterol* 2001; **7**: 248-253
- 26 **Deng DJ**. Progress of gastric cancer etiology: n-nitrosamides in the 1990s. *World J Gastroenterol* 2000; **6**: 613-618
- 27 **Liu ZM**, Shou NH, Jiang XH. Expression of lung resistance protein in patients with gastric carcinoma and its clinical significance. *World J Gastroenterol* 2000; **6**: 433-434
- 28 **Guo CQ**, Wang YP, Liu GY, Ma SW, Ding GY, Li JC. Study on *Helicobacter pylori* infection and p53, c-erbB-2 gene expression in carcinogenesis of gastric mucosa. *Shijie Huaren Xiaohua Zazhi* 1999; **7**: 313-315
- 29 **Cai L**, Yu SZ, Ye WM, Yi YN. Fish sauce and gastric cancer: an ecological study in Fujian Province, China. *World J Gastroenterol* 2000; **6**: 671-675
- 30 **Xue FB**, Xu YY, Wan Y, Pan BR, Ren J, Fan DM. Association of *H pylori* infection with gastric carcinoma: a Meta analysis. *World J Gastroenterol* 2001; **7**: 801-804
- 31 **Wang RT**, Wang T, Chen K, Wang JY, Zhang JP, Lin SR, Zhu YM, Zhang WM, Cao YX, Zhu CW, Yu H, Cong YJ, Zheng S, Wu BQ. *Helicobacter pylori* infection and gastric cancer: evidence from a retrospective cohort study and nested case-control study in China. *World J Gastroenterol* 2002; **8**: 1103-1107
- 32 **Hua JS**. Effect of Hp: cell proliferation and apoptosis on stomach cancer. *Shijie Huaren Xiaohua Zazhi* 1999; **7**: 647-648
- 33 **Liu DH**, Zhang XY, Fan DM, Huang YX, Zhang JS, Huang WQ, Zhang YQ, Huang QS, Ma WY, Chai YB, Jin M. Expression of vascular endothelial growth factor and its role in oncogenesis of human gastric carcinoma. *World J Gastroenterol* 2001; **7**: 500-505
- 34 **Cao WX**, Ou JM, Fei XF, Zhu ZG, Yin HR, Yan M, Lin YZ. Methionine-dependence and combination chemotherapy on human gastric cancer cells *in vitro*. *World J Gastroenterol* 2002; **8**: 230-232
- 35 **Mao YF**, Yan J, Li LW, Li SP. Construction of *hpaA* gene from a clinical isolate of *Helicobacter pylori* and identification of fusion protein. *World J Gastroenterol* 2003; **9**: 1529-1536
- 36 **Ruggiero P**, Peppoloni S, Rappuoli R, Del Giudice G. The quest for a vaccine against *Helicobacter pylori*: how to move from mouse to man? *Microbes Infect* 2003; **5**: 749-756

- 37 **Garhart CA**, Nedrud JG, Heinzl FP, Sigmund NE, Czinn SJ. Vaccine-induced protection against *Helicobacter pylori* in mice lacking both antibodies and interleukin-4. *Infect Immun* 2003; **71**: 3628-3633
- 38 **Garhart CA**, Heinzl FP, Czinn SJ, Nedrud JG. Vaccine-induced reduction of *Helicobacter pylori* colonization in mice is interleukin-12 dependent but gamma interferon and inducible nitric oxide synthase independent. *Infect Immun* 2003; **71**: 910-921
- 39 **Panthel K**, Faller G, Haas R. Colonization of C57BL/6J and BALB/c wild-type and knockout mice with *Helicobacter pylori*: effect of vaccination and implications for innate and acquired immunity. *Infect Immun* 2003; **71**: 794-800
- 40 **Sheu BS**, Huang JJ, Yang HB, Huang AH, Wu JJ. The selection of triple therapy for *Helicobacter pylori* eradication in chronic renal insufficiency. *Aliment Pharmacol Ther* 2003; **17**: 1283-1290
- 41 **Marais A**, Bilardi C, Cantet F, Mendz GL, Megraud F. Characterization of the genes rdxA and frxA involved in metronidazole resistance in *Helicobacter pylori*. *Res Microbiol* 2003; **154**: 137-144
- 42 **Ohkusa T**, Okayasu I, Miwa H, Ohtaka K, Endo S, Sato N. *Helicobacter pylori* infection induces duodenitis and superficial duodenal ulcer in Mongolian gerbils. *Gut* 2003; **52**: 797-803
- 43 **Sugiyama T**, Hige S, Asaka M. Development of an *H pylori*-infected animal model and gastric cancer: recent progress and issues. *J Gastroenterol* 2002; **37**(Suppl 13): 6-9
- 44 **Wang J**, Court M, Jeremy AH, Aboshkiwa MA, Robinson PA, Crabtree JE. Infection of Mongolian gerbils with Chinese *Helicobacter pylori* strains. *FEMS Immunol Med Microbiol* 2003; **36**: 207-213
- 45 **Fujioka T**, Murakami K, Kodama M, Kagawa J, Okimoto T, Sato R. *Helicobacter pylori* and gastric carcinoma—from the view point of animal model. *Keio J Med* 2002; **51**(Suppl 2): 69-73
- 46 **Eaton KA**, Kersulyte D, Mefford M, Danon SJ, Krakowka S, Berg DE. Role of *Helicobacter pylori* cag region genes in colonization and gastritis in two animal models. *Infect Immun* 2001; **69**: 2902-2908
- 47 **Keenan JI**, Rijpkema SG, Durrani Z, Roake JA. Differences in immunogenicity and protection in mice and guinea pigs following intranasal immunization with *Helicobacter pylori* outer membrane antigens. *FEMS Immunol Med Microbio* 2003; **36**: 199-205
- 48 **Lee A**, O' Rourke J, De Ungria MC, Robertson B, Daskalopoulos G, Dixon MF. A standardized mouse model of *Helicobacter pylori* infection: introducing the Sydney strain. *Gastroenterology* 1997; **112**: 1386-1397
- 49 **Chi J**, Fu BY, Nakajima, Hattori, Kushima. Establishment of Mongolian gerbil animal model infected with *Hp* infection and change of inflammation and proliferation before and after *Hp* eradication. *Shijie Huaren Xiaohua Zazhi* 1999; **7**: 557-560

Edited by Xia HHX and Xu FM

• BASIC RESEARCH •

Effects of non-starch polysaccharides enzymes on pancreatic and small intestinal digestive enzyme activities in piglet fed diets containing high amounts of barley

Wei-Fen Li, Jie Feng, Zi-Rong Xu, Cai-Mei Yang

Wei-Fen Li, Jie Feng, Zi-Rong Xu, Cai-Mei Yang, Animal Science College, Zhejiang University, The Key Laboratory of Molecular Animal Nutrition, Ministry of Education, Hangzhou, 310029, Zhejiang Province, China

Supported by the National Natural Science Foundation of China, No. 30000118

Correspondence to: Jie Feng, Animal Science College, Zhejiang University, 268 Kaixuan Road, Hangzhou, 310029, Zhejiang Province, China. fengj@zju.edu.cn

Telephone: +86-571-86986127 **Fax:** +86-571-86091820

Received: 2003-09-18 **Accepted:** 2003-11-13

Abstract

AIM: To investigate effects of non-starch polysaccharides(NSP) enzymes on pancreatic and small intestinal digestive enzyme activities in piglet fed diets containing high amounts of barley.

METHODS: Sixty crossbred piglets averaging 13.5 kg were randomly assigned to two treatment groups with three replications (pens) based on sex and mass. Each group was fed on the diet based on barley with or without added NSP enzymes (0.15%) for a 40-d period. At the end of the experiment the pigs were weighed. Three piglets of each group were chosen and slaughtered. Pancreas, digesta from the distal end of the duodenum and jejunal mucosa were collected for determination. Activities of the digestive enzymes trypsin, chymotrypsin, amylase and lipase were determined in the small intestinal sections as well as in homogenates of pancreatic tissue. Maltase, sucrase, lactase and γ -glutamyl transpeptidase (γ -GT) activities were analyzed in jejunal mucosa.

RESULTS: Supplementation with NSP enzymes improved growth performance of piglets. It showed that NSP enzymes had no effect on digestive enzyme activities in pancreas, but decreased the activities of proteolytic enzyme, trypsin, amylase and lipase in duodenal contents by 57.56%, 76.08%, 69.03% and 40.22% ($P < 0.05$) compared with control, and increased γ -GT activities in jejunal mucosa by 118.75% ($P < 0.05$).

CONCLUSION: Supplementation with NSP enzymes in barley based diets could improve piglets' growth performance, decrease activities of proteolytic enzyme, trypsin, amylase and lipase in duodenal contents and increase γ -GT activities in jejunal mucosa.

Li WF, Feng J, Xu ZR, Yang CM. Effects of non-starch polysaccharides enzymes on pancreatic and small intestinal digestive enzyme activities in piglet fed diets containing high amounts of barley. *World J Gastroenterol* 2004; 10(6): 856-859
<http://www.wjgnet.com/1007-9327/10/856.asp>

INTRODUCTION

Barley is one of the major energy sources of swine diets in

many parts of the world. But anti-nutritive factors in barley limit its use in feed industry^[1]. The predominant anti-nutritive factor is non-starch polysaccharides (NSP), including β -glucan ((1-3), (1-4)- β -D-glucan)^[2,3] and arabinoxylan^[4]. The β -glucan and pentosan content in whole barley grain was 4.2% and 6.6%, being 1.8% and 1.4% in endosperm^[5]. The major nutrients in barley, starch and protein, are enclosed within endosperm cell walls, which consist mainly of mix-linked β -glucan and arabinoxylan^[6]. Pigs, especially piglets, do not produce enzymes that can degrade the cell wall and NSP in barley. So β -glucan and arabinoxylan in barley may interfere with digestion and absorption of nutrients^[7], even the production of digestive enzymes^[8,9].

Studies have shown that mix-linked β -glucan and arabinoxylan are easily hydrolyzed by β -glucanases and xylanases respectively. Addition of cell wall degrading enzymes *in vitro* increased the release of proteins and non-starch carbohydrate in barley^[10]. Supplementation of exogenous NSP enzymes to piglet diets can increase the digestibility of barley and pigs' growth^[11-13]. This has been attributed mainly to the breakdown of endosperm cell wall components, resulting in more complete digestion of starch and protein in the small intestine. But there is little information on the effect of β -glucanases and xylanases supplementation on digestive enzyme activities in barley-based diets for piglets.

The aim of the present study was to investigate the effect of supplementation of NSP enzymes on pancreatic and small intestine digestive enzyme activities in piglets fed diets containing high amounts of barley.

MATERIALS AND METHODS

Animals, diets and enzyme complex

Sixty crossbred (Duroc \times Landrace \times Jiaying) piglets averaging 13.5 kg were randomly assigned to two treatment groups with three replications (pens) based on sex and mass. Each group was fed on one of the two experimental diets for 40 d. As shown in Table 1, pigs received the same basal diet based on barley-soybean meal and NSP enzymes were added to the basal diet respectively at 0% and 0.15% of the diet at the expense of barley. To accustom pigs to the diets, all pigs were allowed access to the basal diet on alternate days for 7 d prior to commencement of the experiment. The diets and water were offered ad libitum throughout the experiment. Pigs were weighed individually and feed consumption per pen was measured weekly. Growth performance results as average daily gain (ADG), average daily feed intake (ADFI), feed gain ratio (FGR) were collected for all pigs for the experimental period. At the end of feeding trial, three pigs from each treatment (one pig per pen) were slaughtered under general anaesthesia. The pigs were then immediately eviscerated to collect intestinal samples. NSP enzymes complex was supplied by Primal Co. Ltd., BIOTEC, Finland, which contained 10 000 U/g β -glucanase (E.C.3.2.1.6) and 80 000 U/g xylanase (E.C.3.2.1.8).

Table 1 Formula and chemical composition of the basal diet

Ingredients (%)	Percentage
Barley	79.0
Soybean meal (dehulled, solvent)	11.0
Fishmeal	4.0
Yeast meal	2.0
Limestone	1.0
Dicalcium phosphate	1.2
Sodium chloride	0.3
L-Lysine-HCl (78%)	0.2
Vitamin-mineral premix ¹	1.3
Analyzed chemical composition (% as feed)	
Digestible energy(Kcal/kg) ²	2960
Crude protein	18.28
Crude fat	1.70
Crude fiber	5.26
Calcium	1.11
Phosphorus	0.48

¹The vitamin/mineral premix provided (per kg feed): 2 000 IU vitamin A, 200 IU vitamin D₃, 20 mg vitamin E, 1 mg vitamin K, 1 mg thiamine, 3 mg riboflavin, 10 mg d-pantothenic acid, 0.5 mg folic acid, 1 mg pyridoxine, 20 mg niacin, 10 µg cobalamin, 500 mg choline chloride, 0.1 mg biotin, 0.2 mg Se, 0.2 mg I, 80 mg Fe, 5 mg Cu, 2 mg Mn, and 80 mg Zn. ²Digestible energy was based on calculated values.

Sampling procedure

The contents taken from the small intestine were digesta from the distal end of the duodenum to the ileo-cecal junction. Digesta samples were collected by massaging the tract from both ends. The digesta samples were stored immediately at -20 °C until use. Enzyme activity analyses of the samples obtained from the small intestine were performed on freeze-dried material, which was extracted with 1 mmol/L HCl (50 mg lyophilized digesta in 1 mL 1 mmol/L HCl) for 1 h at 4 °C followed by centrifugation (3 000 r/min). The supernatants were then collected for analysis of protease, trypsin, chymotrypsin, amylase and lipase activities.

The pancreas from slaughtered pigs was homogenized in ice-cold 0.2 mol/L Tris-HCl buffer containing 0.05 mol/L NaCl. The homogenate was centrifuged at 3 000 r/min for 15 min at 4 °C and the supernatant was saved. Protease, chymotrypsin, amylase and lipase activities were determined.

Jejunum mucosa was homogenized in 4.0 mL distilled-water and kept at 4 °C for 24 h followed by 10 min centrifugation (3 000 r/min). The supernatants were then collected for analysis of maltase, sucrase, lactase and γ-glutamyl transpeptidase (γ-GT) activities.

Digestive enzyme assay

Protease activity was analyzed using the method of Iwamori *et al.* (1997)^[14] Chymotrypsin (EC 3.4.21.1) was determined according to Erlanger *et al.*^[15] using glutaryl-L-phenylalanine-p-nitroanilid (GPNA) as substrate. Amylase (EC 3.2.1.1) activity was determined using a kit (No.700) from Sigma Chemical Company (Sigma Chemical Co., St. Louis, MO 63178-9916) and lipase (EC 3.1.1.3) by a pH-stat titration method using tributyrin as substrate according to Erlanson-Albertsson *et al.*^[16]. The activities of protease, trypsin, chymotrypsin, amylase, and lipase are expressed as unit (U) which is defined as the amount of enzyme that hydrolyses 1 µmol of substrate per min. Maltase, sucrase, lactase and γ-GT activities were analyzed using the modified method of Dahlqvist^[17]. The activities of maltase, sucrase, lactase and

γ-GT are expressed as unit (U) which is defined as the amount of enzyme that hydrolyses 10 µmol of substrate per min.

Statistical analysis

One way analysis of variance was performed using the General Linear Model (GLM) Procedure of SAS^[18]. Differences among means were tested using Duncan's multiple range test. A significant level of 0.05 was used.

RESULTS

Growth performance

Growth performance of pigs fed NSP enzymes is presented in Table 2. As compared to control, supplementation with 1.5 g/L NSP enzymes significantly improved average daily gain (ADG), average daily feed intake (ADFI) and feed conversion ratio (FCR) by 6.22% ($P<0.01$), 2.14% ($P<0.05$) and 3.69% ($P<0.05$) respectively.

Table 2 Growth performance of piglets fed diets based on barley with and without NSP enzymes

	Dietary NSP enzymes level (%)	
	0	0.15
Initial mass(kg)	13.91±0.25	14.01±0.17
Final mass(kg)	33.95±0.38 ^a	35.35±0.40 ^c
Average daily gain (g)	501.16±16.18 ^a	532.34±6.88 ^c
Average daily feed intake (g)	1 224.00±3.62 ^a	1 250.15±7.27 ^c
Feed/Gain ratio	2.44±0.03 ^a	2.35±0.02 ^c

Values are presented as mean±SD; $n=30$ for average daily gain (ADG), $n=3$ for average daily feed intake (ADFI) and feed/gain ratio per treatment. Means in a row with different letters differ significantly, $P<0.05$.

Pancreatic digestive enzyme activities

The results of the effects of NSP enzymes on the digestive enzyme activities in the pancreas of piglets are shown in Table 3. Supplementation with 1.5 g/L NSP enzymes had no significant effect on the activities of protease, chymotrypsin, amylase and lipase in pancreas.

Table 3 Effects of NSP enzymes on the digestive enzyme activities (U/g pancreas) in the pancreas of piglets

	Dietary NSP enzymes level (%)	
	0	0.15
Protease	160.50±17.49	188.86±63.93
Chymotrypsin	1.09±0.28	0.99±0.19
Trypsin	32.14±21.96	27.25±6.79
Amylase	3 009.40±157.19	2 957.02±302.35
Lipase	89.08±13.86	92.15±13.86

Values are presented as mean±SD; $n=3$ per treatment.

Duodenal digestive enzyme activities

Effects of NSP enzymes on duodenal digestive activities are presented in Table 4. NSP enzymes affected duodenal digestive activities significantly. Compared with the control, protease, trypsin, amylase and lipase activities were decreased by 57.56%, 76.08%, 69.03% and 40.22% ($P<0.05$) respectively.

Jejunal digestive enzyme activities

The activities of digestive enzyme in jejunal mucosa are shown in Table 5. Supplementation with 1.5g/LNSP enzymes had no effect on maltase, sucrase, lactase activities, but increased γ-GT activities by 118.75% ($P<0.05$) compared with the control.

Table 4 Effects of NSP enzymes on the digestive enzyme activities (U/mg protein) in the small intestinal contents of piglets

	Dietary NSP enzymes level (%)	
	0	0.15
Protease	60.04±12.86 ^a	25.48±4.98 ^c
Trypsin	37.21±11.47 ^a	8.90±3.72 ^c
Amylase	3 600.45±155.68 ^a	1 115.16±93.32 ^c
Lipase	68.68±11.93 ^a	41.06±6.81 ^c

Values are presented as mean±SD; *n*=3 per treatment. Means in a row with different letters differ significantly, *P*<0.05.

Table 5 Effects of NSP enzymes on the digestive enzyme activities (U/mg) in jejunal mucosa of piglets

	Dietary NSP enzymes level (%)	
	0	0.15
Maltase	28.49±6.45	29.89±10.017
Sucrase	8.13±0.62	8.92±2.16
Lactase	1.22±0.75	1.72±0.97
γ-Glutamyl transpeptidase	0.16±0.05 ^c	0.35±0.13 ^a

Values are presented as mean±SD; *n*=3 per treatment. Means in a row with different letters differ significantly, *P*<0.05.

DISCUSSION

Numerous researchers have reported increased growth and improved feed conversion ratio as a consequence of NSP enzymes inclusion in animal diets based on barley, especially for poultry^[19-22]. Effects of exogenous enzymes on growth performance for swine have been variable. Inbarr *et al*^[11] reported that barley-based diets supplementation with NSP enzymes increased average daily gain and feed conversion ratio of weaned piglets significantly (*P*<0.05). Yin *et al* (2001)^[23] showed that β-glucanases and xylanase improved growth performance and feed gain ratio when piglets were fed with barley based diets. Lindberg *et al*^[24] found enzymes (including β-glucanases, xylanases and cellulase) could enhance growth performance especially body mass gain of piglets when fed with diets based on barley. However, negative results were also reported. Baas^[25] found there was no effect of β-glucanases on growth performance of finishing swine. But most experiments indicated that NSP had positive effects on growth performance for young pigs. Our study verified this point. Increase of digestibility of nutrients is the main reason for this phenomenon. The inconsistent effects between the experiments may result from different stage of pigs and/or formula of diets used.

Endogenous enzyme is very important for digestibility of nutrients. Increasing gut viscosity due to viscous polysaccharides has been shown to increase the output of pancreatic juice and enzyme activities in rats^[9]. However, Mosenthin *et al*^[26] and Zebrowska and Low^[27] observed no change in the secretion of enzymes from the exocrine pancreas when feeding pigs on diets containing different levels of dietary fibre. Makkink *et al*^[28] showed that trypsin and chymotrypsin activity depended on dietary protein source. However, in the present experiment the protein source was the same as in all other diets which may explain why no differences in enzyme activities were observed. The activities of the pancreatic enzymes in the present study were not changed with the enzyme supplementation. This indicated that the synthesis of pancreatic enzymes was unaffected by these factors.

The present study also showed that NSP enzymes decreased the activities of protease, chymotrypsin, amylase and lipase significantly in digesta from the distal end of the duodenum.

Almirall *et al*^[29] observed that supplementation with β-glucanases increased trypsin, amylase and lipase obviously in chyme of chicken. Jensen^[30] found that when pigs were fed barley based diets supplemented with NSP enzymes, chymotrypsin activity was enhanced sharply. Ikegami *et al* (1990) reported that soluble NSP could increase the activities of lipase, amylase and chymotrypsin in rat gut^[9]. Our results are different from the studies mentioned above, but are consistent with the results reported by Inbarr^[11]. Inbarr found exogenous NSP enzymes decreased the activities of endogenous enzymes and he thought NSP enzymes might provide a situation appropriate for endogenous enzyme action. But this may result from the fact that NSP enzymes degrade β-glucan and arabinoxylan in endosperm cell wall and decrease the viscosity of digesta in small intestine. Viscosity may act as a barrier to prevent contact of digestive enzymes with their substrates, thickening of the unstirred layer of mucosa and prevention of micelle formation required for absorption of lipids^[31]. This process makes the endogenous enzymes to approach substrate easily and work more efficiently.

γ-GT is the key enzyme for amino acids absorption. The present study showed that supplementation with NSP enzymes increased γ-GT activities in jejunal mucosa when piglets were fed barley based diets. The results may indicate that NSP enzymes improves digestibility of the nutrients and supplies more substrates for these endogenous enzymes to act on, which then feedback on the secretion of the enzymes.

REFERENCES

- 1 Bhatti RS. The potential of hull-less Barley - A Review. *Cereal Chem* 1986; **63**: 97-103
- 2 White WB, Bird HR, Sunde ML, Prentice N, Burger WC, Marlett JA. The viscosity interaction of barley beta-glucan with *Trichoderma viride* cellulase in the chick intestine. *Poult Sci* 1981; **60**: 1043-1048
- 3 Hesselman K, Aman P. The effect of β-glucanase on the utilization of starch and nitrogen by broiler chickens fed on barley of low- or high- viscosity. *Anim Feed Sci Technol* 1986; **15**: 83-93
- 4 Fleury MD, Edney MJ, Campbell LD, Crow GH. Total, water-soluble and acid-soluble arabinoxylans in western Canadian barleys. *Can J Plant Sci* 1997; **77**: 191-196
- 5 Henry RJ. A comparison of the non-starch carbohydrates in cereal grains. *J Sci Food Agric* 1985; **36**: 1243-1253
- 6 Chesson A. Feed enzymes. *Anim Feed Sci Technol* 1993; **45**: 65-79
- 7 Campbell GL, Rossnagel BG, Classen HL, Thacker PA. Genotypic and environmental differences in extract viscosity of barley and their relationship to its nutritive value for broiler chickens. *Anim Feed Sci Technol* 1989; **26**: 221-230
- 8 Graham H, Löwgren W, Pettersson D, Åman P. Effect of enzyme supplementation on digestion of a barley/pollard-based pig diet. *Nutr Reports Inter* 1988; **38**: 1073-1079
- 9 Ikegami S, Tsuchihashi F, Harada H, Tsuchihashi N, Nishide E, Innami S. Effect of viscous indigestible polysaccharides on pancreatic-biliary secretion and digestive organs in rats. *J Nutr* 1990; **120**: 353-360
- 10 Boisen S, Fernández JA. Prediction of the total tract digestibility of energy in feedstuffs and pig diets by *in vitro* analyses. *Anim Feed Sci Technol* 1997; **68**: 277-286
- 11 Inbarr J, Schmitz M, Ahrens F. Effect of adding fiber and starch degrading enzymes to a barley/wheat based diet on performance and nutrient digestibility in different segments of the small intestine of early weaned pigs. *Anim Feed Sci Technol* 1993; **44**: 113-127
- 12 Li S, Sauer WC, Mosenthin R, Kerr B. Effect of beta-glucanase supplementation of cereal-based diets for starter pigs on the apparent digestibilities of dry matter, crude protein and energy. *Anim Feed Sci Technol* 1996; **59**: 223-231
- 13 Li S, Sauer WC, Huang SX, Gabert VM. Effect of beta-glucanase supplementation to hullless barley- or wheat-soybean meal diets on the digestibilities of energy, protein, beta- glucans, and amino acids in young pigs. *J Anim Sci* 1996; **74**: 1649-1656
- 14 Iwamori M, Iwamori Y, Ito N. Sulfated lipids as inhibitors of

- pancreatic trypsin and chymotrypsin in epithelium of the mammalian digestive tract. *Biochem Biophys Res Commun* 1997; **237**: 262-265
- 15 **Erlanger BF**, Edel F, Cooper AG. The action of chymotrypsin on two new chromogenic substrates. *Arch Biochem Biophys* 1966; **115**: 206-210
- 16 **Erlanson-Albertsson C**, Larsson A, Duan R. Secretion of pancreatic lipase and colipase from rat pancreas. *Pancreas* 1987; **2**: 531-535
- 17 **Dahlqvist A**. Method for assay of intestinal disaccharides. *Anal Biochem* 1964; **7**: 18-25
- 18 **SAS**, 1991. SAS User's Guide Version 6.03. *SAS Institute, Cary, NC*
- 19 **Krogdahl A**, Sell JL. Influence of age on lipase, amylase and protease activities in pancreatic tissue and intestinal contents of young turkeys. *Poult Sci* 1989; **68**: 1561-1568
- 20 **Almirall M**, Francesch M, Perez-Vendrell AM, Brufau J, Esteve-Garcia E. The differences in intestinal viscosity produced by barley and β -glucanase alter digesta enzyme activities and ileal nutrient digestibilities more in broiler chicks than in cocks. *J Nutr* 1995; **125**: 947-955
- 21 **Yin YL**, Baidoo SK, Boychuk JLL. Effect of enzyme supplementation on the performance of broilers fed maize, wheat, barley or micronized dehulled barley diets. *J Anim Feed Sci* 2000; **9**: 493-504
- 22 **Jamroz D**, Jakobsen K, Bach Knudsen KE, Wiliczkiewicz A, Orda J. Digestibility and energy value of non-starch polysaccharides in young chickens, ducks and geese, fed diets containing high amounts of barley. *Comp Biochem Physiol A Mol Integr Physiol* 2002; **131**: 657-668
- 23 **Yin YL**, Baidoo SK, Schulze H, Simmins PH. Effects of supplementing diets containing hullless barley varieties having different levels of non-starch polysaccharides with β -glucanases and xylanase on the physiological status of the gastrointestinal tract and nutrient digestibility of weaned pigs. *Livestock Prod Sci* 2001; **71**: 97-107
- 24 **Lindberg JE**, Arvidsson A, Wang J. Influence of naked barley cultivar with normal, amylose-rich or amylopectin-rich starch and enzyme supplementation on digestibility and piglet performance. *Anim Feed Sci Technol* 2003; **104**: 121-131
- 25 **Baas TC**, Thacker PA. Impact of gastric pH on dietary enzyme activity and survivability in swine fed β -glucanase supplemented diets. *Can J Anim Sci* 1996; **76**: 245-252
- 26 **Mosenthin R**, Sauer WC, Ahrens F. Dietary pectin's effect on ileal and fecal amino acid digestibility and exocrine pancreatic secretions in growing pigs. *J Nutr* 1994; **124**: 1222-1229
- 27 **Zebrowska T**, Low AG. The influence of diets based on whole wheat, wheat flour and wheat bran on exocrine pancreatic secretion in pigs. *J Nutr* 1987; **117**: 1212-1216
- 28 **Makkink CA**, Negulescu GP, Qin G, Verstegen MW. Effect of dietary protein source on feed intake, growth, pancreatic enzyme activities and jejunal morphology in newly-weaned piglets. *Br J Nutr* 1994; **72**: 353-368
- 29 **Almirall M**, Esteve-Garcia E. *In vitro* stability of a β -glucanase preparation from *Trichoderma longibrachiatum* and its effect in a barley based diet fed to broiler chicks. *Anim Feed Sci Technol* 1995; **54**: 149-158
- 30 **Jensen MS**, Thaela MJ, Pierzynowski SG, Jakobsen K. Exocrine pancreatic secretion in young pigs fed barley-based diets supplemented with β -glucanase. *J Anim Physiol A Anim Nutr* 1996; **75**: 231-241
- 31 **Wang L**, Newman RK, Newman CW, Hofer PJ. Barley beta-glucans alter intestinal viscosity and reduce plasma cholesterol concentrations in chicks. *J Nutr* 1992; **122**: 2292-2297

Edited by Zhu LH and Xu FM

Effects of daidzein on estrogen-receptor-positive and negative pancreatic cancer cells *in vitro*

Jun-Ming Guo, Bing-Xiu Xiao, De-Jian Dai, Qiong Liu, Hong-Hui Ma

Jun-Ming Guo, Bing-Xiu Xiao, Qiong Liu, School of Medicine, Ningbo University, Ningbo 315211, Zhejiang Province, China

De-Jian Dai, Second Affiliated Hospital of Medical College, Zhejiang University, Huangzhou 310009, Zhejiang Province, China

Hong-Hui Ma, School of Life Science and Bioengineering, Ningbo University, Ningbo 315211, Zhejiang Province, China

Supported by Scientific Research Fund of Zhejiang Provincial Education Department, No.20010217

Correspondence to: Dr. Jun-Ming Guo, School of Medicine, Ningbo University, Ningbo 315211, Zhejiang Province, China. junmingguo@yahoo.com

Telephone: +86-574-87600758 **Fax:** +86-574-87608638

Received: 2003-08-26 **Accepted:** 2003-09-18

Abstract

AIM: To study the effects of daidzein on human pancreatic cancer cells *in vitro*.

METHODS: Human estrogen-receptor (ER)-positive pancreatic cancer cells MiaPaCa-2 and ER-negative pancreatic cancer cells PANC-1 were treated by 0.1 $\mu\text{mol/L}$, 1 $\mu\text{mol/L}$, 10 $\mu\text{mol/L}$, 25 $\mu\text{mol/L}$, 50 $\mu\text{mol/L}$, 75 $\mu\text{mol/L}$ and 100 $\mu\text{mol/L}$ of daidzein, respectively. Its antiproliferative effect was studied by MTT assay.

RESULTS: Daidzein inhibited the growth of MiaPaCa-2 and PANC-1 cells at the concentrations from 0.1 $\mu\text{mol/L}$ to 100 $\mu\text{mol/L}$. A dose- and time-dependent manner was found. The IC_{50} of daidzein on MiaPaCa-2 and PANC-1 cells was 45 $\mu\text{mol/L}$ and 75 $\mu\text{mol/L}$, respectively. After MiaPaCa-2 cells were treated by daidzein for 3 d and at the concentrations more than IC_{50} , the inhibitory manner was identical and the inhibition appeared a saturation phenomenon, but the inhibitory manner of daidzein on PANC-1 cells was different from that of MiaPaCa-2 cells.

CONCLUSION: Daidzein has antiproliferative effects on human estrogen-receptor-positive and negative pancreatic cancer cells, but their mechanisms may be different.

Guo JM, Xiao BX, Dai DJ, Liu Q, Ma HH. Effects of daidzein on estrogen-receptor-positive and negative pancreatic cancer cells *in vitro*. *World J Gastroenterol* 2004; 10(6): 860-863
<http://www.wjgnet.com/1007-9327/10/860.asp>

INTRODUCTION

Phytoestrogens are natural compounds, which exhibit estrogen-like activities. They have been thought to have a preventive effect against a wide range of human conditions, including breast cancer, bowel cancer, prostate cancer, colon cancer and other cancers, cardiovascular diseases, brain function, alcohol abuse, osteoporosis and menopausal symptoms^[1-4]. There are three main classes of phytoestrogens, namely isoflavones, coumestans, and lignans^[5]. They are widely distributed in soybeans, oil seeds, and vegetables. Soy contains a number of

isoflavones (such as genistein, genistin, daidzein, and biochanin A), which are found to have potential anticancer properties^[6]. Interestingly, phytoestrogens can not only inhibit the growth of estrogen-receptor (ER)-dependent cancer cells, but also the growth of ER-independent cancer cells^[7]. The mechanisms of their anticancer effects include induction of apoptosis, alterations of cell cycle distribution, *etc.*^[8,9].

The morbidity of pancreatic carcinoma has taken an upward trend all over the world. In Occidental countries, the morbidity of pancreatic carcinoma has increased by 3 to 7 times in nearly thirty years, and pancreatic carcinoma has become one of the ten commonest malignant tumors^[10]. Only 15% of patients with pancreatic cancer could undergo resection and the overall 5-year survival rate was about 10%^[11]. In recent years, many advances in the diagnosis and treatment (including surgical and adjuvant treatment) of pancreatic cancer have been achieved^[12-14].

Estrogen receptor has been found in many cases of pancreatic tumor tissues and antiestrogen therapy has benefit to some patients with pancreatic cancers^[15,16]. There is evidence to support the hypothesis that the increased incidence of pancreatic cancer in Western communities might be related to the relatively low dietary content and protective role of naturally occurring plant hormones and related compounds^[17]. Generally speaking, treatment of pancreatic cancer is still a serious challenge to us^[10]. The key problem is to seek novel diagnostic methods, effective adjunctive therapy and the mechanism of pathogenesis and progression of pancreatic cancer. Pancreatic cancer is often detected in its late stages. As a result, it is very important to develop new potential chemopreventive and anticancer reagents for pancreatic cancer, especially those from nature. The effects of daidzein, one of the rich compounds in Eastern countries' traditional diet, on human pancreatic cancer cells are unclear. In this study, we observed the effects of daidzein on the growth of human pancreatic cancer cells *in vitro*.

MATERIALS AND METHODS

Materials

Daidzein was purchased from Sigma Chemical Co. (St. Louis, MO) and dissolved in dimethylsulfoxide (DMSO). 3-(4,5-dimethylthiazol-2-yl)-2,5-diphenyl tetrazolium bromide (MTT) was from Sigma. RPMI-1640 medium was from Life Technologies (Grand Island, NY). Human pancreatic cancer cell lines MiaPaCa-2 and PANC-1 were obtained from Department of General and Gastroenterological Surgery, Osaka Medical College, Takatsuki City, Japan.

Cell culture and treatment

Cells were cultured in plastic flasks or multi-well plates at 37 °C in a humidified atmosphere of 50 ml/L CO₂ and 950 ml/L air with RPMI-1640 medium containing 100 ml/L fetal calf serum, 50 000 U/L penicillin and 50 mg/L streptomycin. The medium was changed every other day. Exponentially growing cells were used in experiments. For quantitative assays of proliferation, 1×10⁴ MiaPaCa-2 or PANC-1 cells were seeded in 96-well

plates in regular growth medium. Twenty-four hours later, cells were incubated in the medium with test compounds or 1 mL DMSO (as control). There were 7 test groups. Their concentrations of daidzein were 0.1 $\mu\text{mol/L}$, 1 $\mu\text{mol/L}$, 10 $\mu\text{mol/L}$, 25 $\mu\text{mol/L}$, 50 $\mu\text{mol/L}$, 75 $\mu\text{mol/L}$ and 100 $\mu\text{mol/L}$, respectively. After cells were treated for 1 d, 2 d, 3 d, 4 d, 5 d and 6 d, the growth of cells was monitored by MTT assay.

MTT assay

Sets of 12 wells were used for each dose and control in this assay. When the growth time reached, 30 μL MTT solution (2 g/L in PBS) was added into each well of a 96-well plate. After cells were treated for 4 h at 37 $^{\circ}\text{C}$, the medium was removed and then 150 μL DMSO was added into each well to solubilize formazan. After that, the microplate was shaken on a rotary platform for 10 min. Finally, absorbance was measured at 550 nm with a Wellsan (Labsystems, USA). The inhibitive rate (%) = $((A_{\text{control}} - A_{\text{experiment}}) / A_{\text{control}}) \times 100\%$.

Statistics

Statistical analysis was performed using SPSS software 10.0. Student's *t*-test was used to make a statistical comparison between groups. The level of significance was set at $P < 0.05$.

RESULTS

Morphologic change of the cells

The effects of daidzein on the growth of pancreatic cancer MiaPaCa-2 and PANC-1 cells were tested over a range of concentrations from 0.1 $\mu\text{mol/L}$ to 100 $\mu\text{mol/L}$. The changes of configuration and number were observed under a microscope (Figures 1, 2). Both pancreatic cancer cells treated by daidzein grew slower than control (Figures 1, 2). The higher the concentration of daidzein, the less the number of cells.

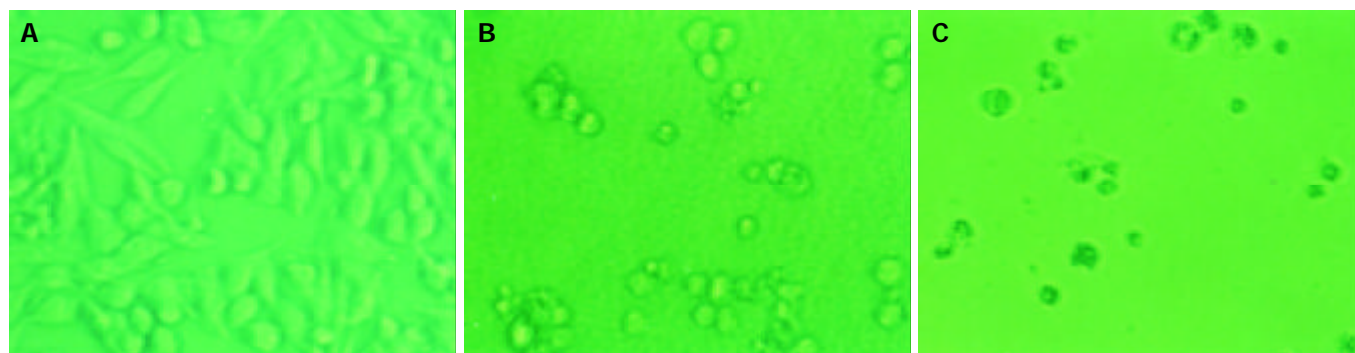


Figure 1 Morphologic changes of MiaPaCa-2 cells treated by daidzein. A: Control, B: Cells treated by 10 $\mu\text{mol/L}$ of daidzein for 3 d, C: Cells treated by 75 $\mu\text{mol/L}$ of daidzein for 3 d ($\times 200$).

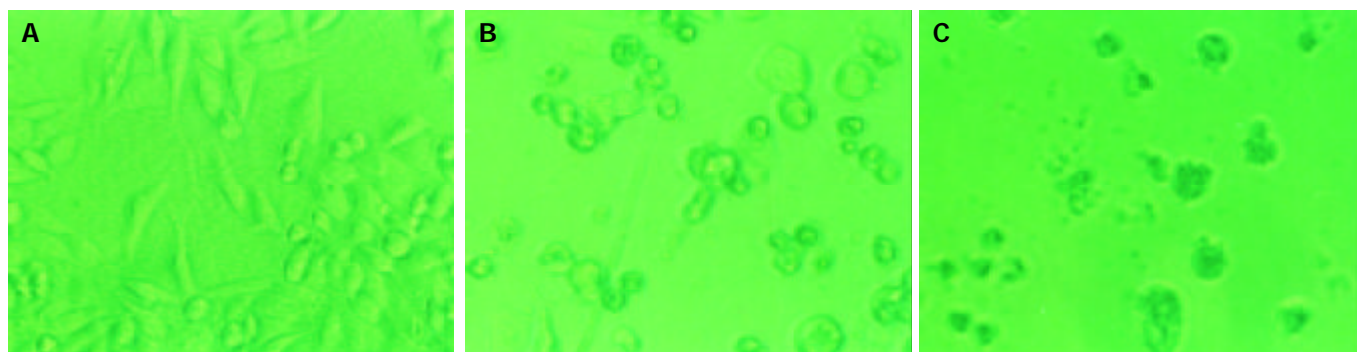


Figure 2 Morphologic changes of PANC-1 cells treated by daidzein. A: Control, B: Cells treated by 10 $\mu\text{mol/L}$ of daidzein for 3 d, C: Cells treated by 75 $\mu\text{mol/L}$ of daidzein for 3 d ($\times 200$).

Inhibitory effect of daidzein on estrogen-receptor-positive pancreatic cancer cells

Estrogen-receptor-positive MiaPaCa-2 cells were treated by various concentrations of daidzein for 1 d to 6 d. At the concentrations from 0.1 $\mu\text{mol/L}$ to 100 $\mu\text{mol/L}$, especially at 50 $\mu\text{mol/L}$, 75 $\mu\text{mol/L}$, and 100 $\mu\text{mol/L}$, daidzein inhibited the growth of cells ($P < 0.01$) in a time-dependent manner (Figure 3). When cells were treated for 3 d, 50% inhibitory rate might be reached. The IC_{50} was 45 $\mu\text{mol/L}$. At the concentrations of more than IC_{50} , the inhibitory patterns were identical ($P > 0.05$, Figure 3).

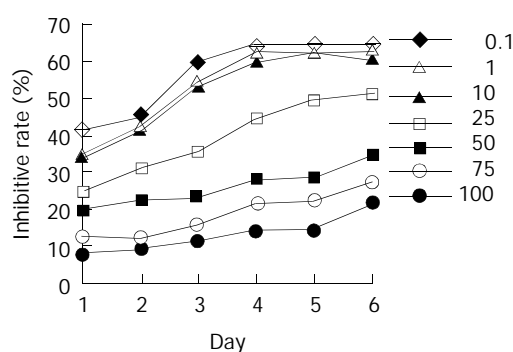


Figure 3 Inhibitory effects of daidzein on growth of estrogen-receptor-positive pancreatic cancer MiaPaCa-2 cells. 0.1 $\mu\text{mol/L}$, 1 $\mu\text{mol/L}$, 10 $\mu\text{mol/L}$, 25 $\mu\text{mol/L}$, 50 $\mu\text{mol/L}$, 75 $\mu\text{mol/L}$ and 100 $\mu\text{mol/L}$ of daidzein were used, respectively.

Inhibitory effect of daidzein on estrogen-receptor-negative pancreatic cancer cells

ER-negative pancreatic cancer PANC-1 cells were treated by daidzein. A dose-dependent effect was observed (Figure 4; 10 $\mu\text{mol/L}$, 25 $\mu\text{mol/L}$, 50 $\mu\text{mol/L}$ and 75 $\mu\text{mol/L}$, $P < 0.05$;

100 $\mu\text{mol/L}$, $P < 0.01$). When cells were treated for 2 d, 50% inhibitory rate might be observed. The IC_{50} was 80 $\mu\text{mol/L}$ on day 2 and 75 $\mu\text{mol/L}$ on day 3.

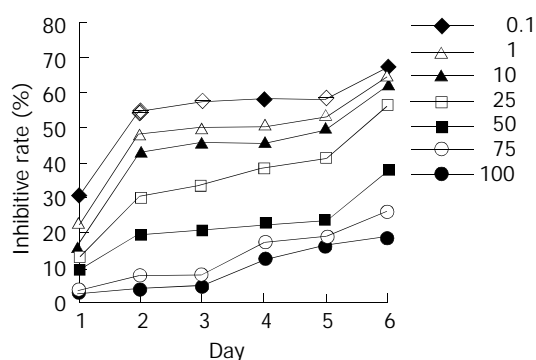


Figure 4 Inhibitory effects of daidzein on growth of estrogen-receptor-negative pancreatic cancer PANC-1 cells. 0.1 $\mu\text{mol/L}$, 1 $\mu\text{mol/L}$, 10 $\mu\text{mol/L}$, 25 $\mu\text{mol/L}$, 50 $\mu\text{mol/L}$, 75 $\mu\text{mol/L}$ and 100 $\mu\text{mol/L}$ of daidzein were used, respectively.

DISCUSSION

There has been an increase in the incidence of pancreatic cancer recent years^[18-21]. The pattern of its increase had some similarities to the high incidence of breast cancer in women and prostate cancer in men in Western communities^[17]. Typical Western diets have a low content of natural plant hormones, phytoestrogens, which are beneficial to our health^[1-6]. They exerted their anticancer effects by their specific bi-effects, estrogenic and antiestrogenic properties^[22-24]. On the one hand, they acted as antiestrogens by competing with endogenous estrogens for receptor binding sites, and decrease the promoting effects of high levels of endogenous estrogens^[25]. On the other hand, they could inhibit the activities of tyrosine protein kinase, DNA topoisomerase, angiogenesis and antioxidant^[26-29].

Hormone products were related to the pathological behaviors of several carcinomas (including colorectal carcinoma, gastric carcinoma, pancreatic carcinoma, etc.) and might help to predict the prognosis and effectiveness of endocrine therapy for some kinds of carcinomas^[30-32]. As to pancreatic carcinoma, there were indications of possible effects of sex hormones^[33]. The pancreatic cell lines, MiaPaCa-2 and PANC-1, used in our study were ER positive and negative cells, respectively^[34,35]. We found that daidzein inhibited the growth of both ER positive and negative pancreatic cancer cells. However, their inhibitory patterns were different. For ER-positive cells, MiaPaCa-2, when the concentrations of daidzein were higher than the level of IC_{50} , the inhibitory effect would not significantly increase. It indicated that its antiproliferative effect was exerted by binding to ER and appeared a saturation phenomenon. For PANC-1, an ER-negative cell, the saturation phenomenon was not found and the inhibition was in a dose-dependent manner. Its IC_{50} was higher than that of MiaPaCa-2, indicating that for the chemoprevention of ER-negative pancreatic cancer, high concentrations of daidzein should be used.

The antiestrogen reagent, tamoxifen was a choice of hormonal therapy for pancreatic cancer^[16,33]. The favorable response to this therapy and survival of patients were dependent on whether the patients' tumor cells were estrogen receptor positive or not^[16]. The presence or absence of estrogen receptors was also important in determining the effects of phytoestrogens on pancreatic cancer cells. A report used four kinds of phytoestrogens to study human pancreatic cancer cells showed that equol and coumestrol had anticarcinogenic effects on human ER positive pancreatic cancer Su86.86 cells. However,

they stimulated the growth of human ER negative pancreatic cancer HPAF-11 cells, genistein stimulated the growth of HPAF-11 cells but had little effect on Su86.86 cells. Another phytoestrogen, biochanin A, inhibited the growth of both Su86.86 cells and HPAF-11 cells^[36]. Our results showed that daidzein, another main phytoestrogen, had inhibitory effects on both ER positive and negative pancreatic cancer cells. As phytoestrogens are a large group of compounds, the possibility of gender differences in response to these reagents may be important in determining their ability to act as chemoprotective reagents for pancreatic cancer.

REFERENCES

- Bingham SA, Atkinson C, Liggins J, Bluck L, Coward A. Phytoestrogens: where are we now? *Br J Nutr* 1998; **79**: 393-406
- Yamamoto S, Sobue T, Kobayashi M, Sasaki S, Tsugane S. Japan Public Health Center-Based Prospective Study on Cancer Cardiovascular Diseases Group. Soy, isoflavones, and breast cancer risk in Japan. *J Natl Cancer Inst* 2003; **95**: 906-913
- Adlercreutz H. Phyto-oestrogens and cancer. *Lancet Oncol* 2002; **3**: 364-373
- Morrissey C, Watson RW. Phytoestrogens and prostate cancer. *Curr Drug Targets* 2003; **4**: 231-241
- Peeters PH, Keinan-Boker L, van der Schouw YT, Grobbee DE. Phytoestrogens and breast cancer risk. Review of the epidemiological evidence. *Breast Cancer Res Treat* 2003; **77**: 171-183
- Zhou JR, Mukherjee P, Gugger ET, Tanaka T, Blackburn GL, Clinton SK. Inhibition of murine bladder tumorigenesis by soy isoflavones via alterations in the cell cycle, apoptosis, and angiogenesis. *Cancer Res* 1998; **58**: 5231-5238
- Maggiolini M, Bonfiglio D, Marsico S, Panno ML, Cenni B, Picard D, Ando S. Estrogen receptor alpha mediates the proliferative but not the cytotoxic dose-dependent effects of two major phytoestrogens on human breast cancer cells. *Mol Pharmacol* 2001; **60**: 595-602
- Yanagihara K, Ito A, Toge T, Numoto M. Antiproliferative effects of isoflavones on human cancer cell lines established from the gastrointestinal tract. *Cancer Res* 1993; **53**: 5815-5821
- Su SJ, Yeh TM, Lei HY, Chow NH. The potential of soybean foods as a chemoprevention approach for human urinary tract cancer. *Clin Cancer Res* 2000; **6**: 230-236
- Tan ZJ, Hu XG, Cao GS, Tang Y. Analysis of gene expression profile of pancreatic carcinoma using cDNA microarray. *World J Gastroenterol* 2003; **9**: 818-823
- Li YJ, Ji XR. Relationship between expression of E-cadherin-catenin complex and clinicopathologic characteristics of pancreatic cancer. *World J Gastroenterol* 2003; **9**: 368-372
- Zheng M, Liu LX, Zhu AL, Qi SY, Jiang HC, Xiao ZY. K-ras gene mutation in the diagnosis of ultrasound guided fine-needle biopsy of pancreatic masses. *World J Gastroenterol* 2003; **9**: 188-191
- Shankar A, Russell RC. Recent advances in the surgical treatment of pancreatic cancer. *World J Gastroenterol* 2001; **7**: 622-626
- Ghaneh P, Slavin J, Sutton R, Hartley M, Neoptolemos JP. Adjuvant therapy in pancreatic cancer. *World J Gastroenterol* 2001; **7**: 482-489
- Singh S, Baker PR, Poulson R, Wright NA, Sheppard MC, Langman MJ, Neoptolemos JP. Expression of oestrogen receptor and oestrogen-inducible genes in pancreatic cancer. *Br J Surg* 1997; **84**: 1085-1089
- Horimi T, Takasaki M, Toki A, Nishimura W, Morita S. The beneficial effect of tamoxifen therapy in patients with resected adenocarcinoma of the pancreas. *Hepatogastroenterology* 1996; **43**: 1225-1229
- Stephens FO. The increased incidence of cancer of the pancreas: is there a missing dietary factor? Can it be reversed? *Aust N Z J Surg* 1999; **69**: 331-335
- Xu HB, Zhang YJ, Wei WJ, Li WM, Tu XQ. Pancreatic tumor: DSA diagnosis and treatment. *World J Gastroenterol* 1998; **4**: 80-81
- Zhao XY, Yu SY, Da SP, Bai L, Guo XZ, Dai XJ, Wang YM. A clinical evaluation of serological diagnosis for pancreatic cancer. *World J Gastroenterol* 1998; **4**: 147-149
- Guo XZ, Friess H, Shao XD, Liu MP, Xia YT, Xu JH, Buchler MW.

- KAI1 gene is differently expressed in papillary and pancreatic cancer: influence on metastasis. *World J Gastroenterol* 2000; **6**: 866-871
- 21 **Yue H**, Na YL, Feng XL, Ma SR, Song FL, Yang B. Expression of p57kip2, Rb protein and PCNA and their relationships with clinicopathology in human pancreatic cancer. *World J Gastroenterol* 2003; **9**: 377-380
 - 22 **So FV**, Guthrie N, Chambers AF, Carroll KK. Inhibition of proliferation of estrogen receptor-positive MCF-7 human breast cancer cells by flavonoids in the presence and absence of excess estrogen. *Cancer Lett* 1997; **112**: 127-133
 - 23 **Shao ZM**, Alpaugh ML, Fontana JA, Barsky SH. Genistein inhibits proliferation similarly in estrogen receptor-positive and negative human breast carcinoma cell lines characterized by P21WAF1/CIP1 induction, G2/M arrest, and apoptosis. *J Cell Biochem* 1998; **69**: 44-54
 - 24 **Hopert AC**, Beyer A, Frank K, Strunck E, Wunsche W, Vollmer G. Characterization of estrogenicity of phytoestrogens in an endometrial-derived experimental model. *Environ Health Perspect* 1998; **106**: 581-586
 - 25 **Scambia G**, Ranelletti FO, Panici PB, Piantelli M, De Vincenzo R, Ferrandina G, Bonanno G, Capelli A, Mancuso S. Quercetin induces type-II estrogen-binding sites in estrogen-receptor-negative (MDA-MB231) and estrogen-receptor-positive (MCF-7) human breast-cancer cell lines. *Int J Cancer* 1993; **54**: 462-466
 - 26 **Robinson MJ**, Corbett AH, Osheroff N. Effects of topoisomerase II-targeted drugs on enzyme-mediated DNA cleavage and ATP hydrolysis: evidence for distinct drug interaction domains on topoisomerase II. *Biochemistry* 1993; **32**: 3638-3643
 - 27 **Spinozzi F**, Pagliacci MC, Migliorati G, Moraca R, Grignani F, Riccardi C, Nicoletti I. The natural tyrosine kinase inhibitor genistein produces cell cycle arrest and apoptosis in Jurkat T-leukemia cells. *Leuk Res* 1994; **18**: 431-439
 - 28 **Fotsis T**, Pepper M, Adlercreutz H, Fleischmann G, Hase T, Montesano R, Schweigerer L. Genistein, a dietary-derived inhibitor of *in vitro* angiogenesis. *Proc Natl Acad Sci U S A* 1993; **90**: 2690-2694
 - 29 **Wei H**, Wei L, Frenkel K, Bowen R, Barnes S. Inhibition of tumor promoter-induced hydrogen peroxide formation *in vitro* and *in vivo* by genistein. *Nutr Cancer* 1993; **20**: 1-12
 - 30 **Xin Y**, Li XL, Wang YP, Zhang SM, Zheng HC, Wu DY, Zhang YC. Relationship between phenotypes of cell-function differentiation and pathobiological behavior of gastric carcinomas. *World J Gastroenterol* 2001; **7**: 53-59
 - 31 **Zhao XH**, Gu SZ, Liu SX, Pan BR. Expression of estrogen receptor and estrogen receptor messenger RNA in gastric carcinoma tissues. *World J Gastroenterol* 2003; **9**: 665-669
 - 32 **Yao GY**, Zhou JL, Lai MD, Chen XQ, Chen PH. Neuroendocrine markers in adenocarcinomas: an investigation of 356 cases. *World J Gastroenterol* 2003; **9**: 858-861
 - 33 **Theve NO**, Pousette A, Carlstrom K. Adenocarcinoma of the pancreas—a hormone sensitive tumor? A preliminary report on Nolvadex treatment. *Clin Oncol* 1983; **9**: 193-197
 - 34 **Kuramoto M**, Yamashita J, Ogawa M. Tissue-type plasminogen activator predicts endocrine responsiveness of human pancreatic carcinoma cells. *Cancer* 1995; **75**: 1263-1272
 - 35 **Abe M**, Yamashita J, Ogawa M. Medroxyprogesterone acetate inhibits human pancreatic carcinoma cell growth by inducing apoptosis in association with Bcl-2 phosphorylation. *Cancer* 2000; **88**: 2000-2009
 - 36 **Lyn-Cook BD**, Stottman HL, Yan Y, Blann E, Kadlubar FF, Hammons GJ. The effects of phytoestrogens on human pancreatic tumor cells *in vitro*. *Cancer Lett* 1999; **142**: 111-119

Edited by Zhang JZ and Wang XL Proofread by Xu FM

• BASIC RESEARCH •

Intravenous administration of glutathione protects parenchymal and non-parenchymal liver cells against reperfusion injury following rat liver transplantation

Rolf J. Schauer, Sinan Kalmuk, Alexander L. Gerbes, Rosemarie Leiderer, Herbert Meissner, Friedrich W. Schildberg, Konrad Messmer, Manfred Bilzer

Rolf J. Schauer, Sinan Kalmuk, Friedrich W. Schildberg, Surgical Department, Klinikum Grosshadern, Ludwig-Maximilians-University of Munich, Germany

Alexander L. Gerbes, Manfred Bilzer, Department of Medicine II, Klinikum Grosshadern, Ludwig-Maximilians-University of Munich, Germany

Rosemarie Leiderer, Konrad Messmer, Institute for Surgical Research, Klinikum Grosshadern, Ludwig-Maximilians-University of Munich, Germany

Herbert Meissner, Institute of Pathology, Klinikum Grosshadern, Ludwig-Maximilians-University of Munich, Germany

Supported in part by a grant from the Friedrich-Baur Stiftung, the Muenchener Medizinische Wochenschrift (MMW) and the Deutsche Forschungsgemeinschaft (DFG Scha 857/1-1; DFG Ge 576/24-1)

Correspondence to: Dr. Rolf J. Schauer, Surgical Department, University Hospital Klinikum Grosshadern, Marchioninistr. 15, 81377 Munich, Germany. schauer@gch.med.uni-muenchen.de

Telephone: +49-89-7095-3560 **Fax:** +49-89-7095-8894

Received: 2004-01-10 **Accepted:** 2004-02-28

Abstract

AIM: To investigate the effects of intravenous administration of the antioxidant glutathione (GSH) on reperfusion injury following liver transplantation.

METHODS: Livers of male Lewis rats were transplanted after 24 h of hypothermic preservation in University of Wisconsin solution in a syngeneic setting. During a 2-h reperfusion period either saline (controls, $n=8$) or GSH (50 or 100 $\mu\text{mol}/(\text{h}\cdot\text{kg})$, $n=5$ each) was continuously administered via the jugular vein.

RESULTS: Two hours after starting reperfusion plasma ALT increased to $1\,457\pm281$ U/L (mean \pm SE) in controls but to only 908 ± 187 U/L ($P<0.05$) in animals treated with 100 μmol GSH/ $(\text{h}\cdot\text{kg})$. No protection was conveyed by 50 μmol GSH/ $(\text{h}\cdot\text{kg})$. Cytoprotection was confirmed by morphological findings on electron microscopy: GSH treatment prevented detachment of sinusoidal endothelial cells (SEC) as well as loss of microvilli and mitochondrial swelling of hepatocytes. Accordingly, postischemic bile flow increased 2-fold. Intravital fluorescence microscopy revealed a nearly complete restoration of sinusoidal blood flow and a significant reduction of leukocyte adherence to sinusoids and postsinusoidal venules. Following infusion of 50 μmol and 100 μmol GSH/ $(\text{h}\cdot\text{kg})$, plasma GSH increased to 65 ± 7 mol/L and 97 ± 18 mol/L, but to only 20 ± 3 mol/L in untreated recipients. Furthermore, plasma glutathione disulfide (GSSG) increased to 7.5 ± 1.0 mol/L in animals treated with 100 $\mu\text{mol}/(\text{h}\cdot\text{kg})$ GSH but did not raise levels of untreated controls (1.8 ± 0.5 mol/L) following infusion of 50 μmol GSH/ $(\text{h}\cdot\text{kg})$ (2.2 ± 0.2 mol/L).

CONCLUSION: Plasma GSH levels above a critical level may act as a "sink" for ROS produced in the hepatic vasculature

during reperfusion of liver grafts. Therefore, GSH can be considered a candidate antioxidant for the prevention of reperfusion injury after liver transplantation, in particular since it has a low toxicity in humans.

Schauer RJ, Kalmuk S, Gerbes AL, Leiderer R, Meissner H, Schildberg FW, Messmer K, Bilzer M. Intravenous administration of glutathione protects parenchymal and non-parenchymal liver cells against reperfusion injury following rat liver transplantation. *World J Gastroenterol* 2004; 10(6): 864-870

<http://www.wjgnet.com/1007-9327/10/864.asp>

INTRODUCTION

A decade after the introduction of the University of Wisconsin (UW) solution for cold preservation of solid organs, hepatic preservation and reperfusion injury is still a serious problem which contributes to primary nonfunction and dysfunction of the liver allograft^[1-3]. Years of research in liver preservation have established the superiority of the UW formulation over other solutions. Although hepatocytes and sinusoidal endothelial cells are injured during cold preservation in UW solution they remain alive even after periods of ischemia well beyond the limit of organ viability^[2-4]. Hepatocyte and SEC death occurs rapidly on oxygenated reperfusion^[2,4] and the extent of SEC death has been shown to be a critical factor influencing graft survival in various animal models^[5-7]. However, therapeutic strategies which reduce reperfusion injury to hepatocytes and SEC during liver transplantation remain to be established.

There is substantial evidence that activation of Kupffer cells (KC), the generation of reactive oxygen species (ROS) and disturbance of the hepatic microcirculation contribute to reperfusion injury^[8-11]. During the reperfusion, activated KC produce mediators of inflammation, including tumor necrosis factor α , interleukins and chemokines, and release ROS into the sinusoidal space^[3,8]. The resulting vascular oxidant stress has been discovered as potential mechanism of vasoconstriction and leukocyte adherence in the liver^[12-16]. This may lead to disturbance of the hepatic microcirculation, ultimately resulting in hypoxic cell injury. Furthermore, KC-derived ROS could activate redox-sensitive transcription factors such as nuclear factor (NF)- κ B and activator protein-1 (AP-1) in endothelial cells and hepatocytes, thereby activating proinflammatory genes and adding to the hepatic damage^[17,18].

Thus, ROS can be considered as signal molecules which trigger several pivotal mechanisms of reperfusion injury. A large number of investigations using antioxidant interventions support this hypothesis^[10]. However, the clinical relevance of many antioxidants is limited by side-effects or high cost which may explain the lack of established antioxidative interventions to prevent hepatic reperfusion injury^[3]. Therefore, recent studies investigated the therapeutic potential of the endogenous

antioxidant *glutathione* (GSH), in particular since it has a low toxicity in humans^[19]. Furthermore, GSH is able to react spontaneously with nearly all oxidants formed during inflammation, which results in the formation of oxidized glutathione (GSSG)^[20-22]. Previous studies demonstrated that GSH released through the GSH transporter of hepatocytes may act as an endogenous defense system against KC – and leukocyte – derived ROS, thus protecting the hepatic vasculature from damage by inflammatory cells^[8]. Therefore, interventions increasing plasma GSH levels should confer protection against reperfusion injury. Accordingly, treatment of cold preserved livers with GSH upon reperfusion prevented damage to hepatocytes in the model of isolated rat liver perfusion^[23]. These *in vitro* findings suggest that GSH, as a candidate drug, could prevent reperfusion injury of the liver allograft. Consequently, future studies need to be directed toward characterization of the protective potential of GSH treatment *in vivo* which may have important implications for an application in the clinical setting.

Therefore, the purpose of this study was to investigate whether intravenous administration of GSH protects the rat liver against reperfusion injury during liver transplantation. In particular, the aims of the current study are: (1) to investigate effects of intravenously applied GSH on hepatocyte and SEC damage; (2) to examine the effect of GSH treatment on disturbances of the hepatic microcirculation, and (3) to determine the functional significance of changes of the extracellular antioxidant capacity.

MATERIALS AND METHODS

Animals and preparation

Syngeneic, male Lewis rats (donors: 207±12 g; recipients: 276±18 g body mass) were purchased from Charles River Wiga, Sulzfeld, Germany and housed in a temperature- and humidity-controlled room under a constant 12-h light/dark cycle. Animals had free access to water and rat chow (standard diet, Altromin, Germany). All experiments were performed with rats fasted 12 h prior to donor and recipient operations. All studies were performed with the permission of the government authorities and in accordance with the German Legislation on Laboratory Animal Experiments.

Donor and recipient operations were performed under spontaneous ether inhalation. The left carotid artery was cannulated with a polyethylene catheter for continuous monitoring of the mean arterial blood pressure and heart rate during the operation. Another catheter was inserted into the jugular vein for substitution of plasma volume and injection of fluorescent compounds as well as for continuous infusion of glutathione during reperfusion. Body temperature was kept between 36.5 °C and 37.5 °C by means of a heating pad. Donor livers were preserved by retrograde aortal flush with 10 mL UW-solution and stored at 4 °C for 24 h. Prior to the implantation procedure, the livers were rinsed with warm Ringer's lactate solution (10 mL) via the portal vein at a hydrostatic pressure of 10 cm H₂O. Orthotopic liver transplantation was performed using a modified cuff technique^[24]. Differing from the original technique, grafted livers were rearterialized and simultaneously reperfused through the portal vein and hepatic artery^[25]. Portal clamping time was less than 20 min in all experiments.

The common bile duct of the graft was cannulated with a PE-tube and bile was collected in Eppendorf cups. Plasma samples (500 µL) were obtained in the recipient before hepatectomy and 60 and 120 min after reperfusion of the transplanted liver. The volume of the blood drawn was replaced by saline. Five minutes after starting reperfusion, all rats received 0.5 mL of albumin (5%) and 0.5 mL sodium bicarbonate in order to maintain blood pressure and physiological pH. To

avoid major fluid loss and drying of the liver, possibly affecting microhemodynamics the abdominal cavity was covered with Saran wrap throughout the operation. After 120 min of reperfusion, experiments were terminated and the liver weight was determined.

Experimental groups

Two intervention groups ($n=5$ each) were compared with the control group ($n=8$). In control animals, saline was infused intravenously (2 mL/h) during reperfusion of the grafted liver, starting 20 min before declamping of the portal vein and hepatic artery. In contrast, intervention groups received GSH via the jugular vein, starting 20 min prior to reperfusion until the end of the two hour reperfusion period (total infusion time 140 min). GSH (Tationil 600®, Roche Pharmaceuticals/Italy) was administered at 50 or 100 µmol/(h·kg) ($n=5$ each) by continuous infusion (2 mL/h) of stock solutions (0.24 mol/L and 0.48 mol/L), using a micro-infusion pump (SP100i, WPI, Aston, UK). Two sham groups underwent laparotomy and intravital microscopy without hepatic ischemia in the absence ($n=6$) or presence of intravenous GSH infusion (100 µmol GSH/(h·kg), $n=5$) for 140 min.

In-vivo fluorescence microscopy (IVM)

In vivo fluorescence microscopic studies were performed 30 min after revascularization under stable hemodynamic conditions, using a modified Leitz-Orthoplan microscope combined with epi-illumination technique^[26,27]. For assessment of microvascular liver perfusion and leukocyte-endothelial interaction the left liver lobe was exteriorized on a stage. For visualization of microcirculatory disturbances, sodium fluorescein (1 µmol/kg; Merck AG, Darmstadt, Germany) and rhodamin 6G (0.1 µmol/kg; Merck AG, Darmstadt, Germany) were injected intravenously for fluorescent staining of hepatocytes (negative contrast for plasma) and leukocytes, respectively. Quantification of microhemodynamic parameters was performed offline by frame-to-frame analysis of the videotaped images in a blinded fashion. Lobular perfusion and leukocyte adherence were analyzed by scanning a region of 10 randomly selected acinar areas and postsinusoidal venules, respectively. *Non – perfused sinusoids* were estimated by counting the number of continuously perfused and non - perfused sinusoids and were expressed as the percentage of all sinusoids visible in a pre-defined area. *Permanent adherence (sticking) of leukocytes to the sinusoidal endothelium* was quantified by counting the number of permanently attached leukocytes (at least for 20 s) within the 3 different segments of sinusoids. *Leukocyte sticking in postsinusoidal venules* was determined by the quantity of leukocytes attached for at least 20 s to the surface of postsinusoidal venules. Furthermore, *temporary adherence of leukocytes (rolling)* was assessed as the number of transiently attached leukocytes along the endothelial surface of postsinusoidal venules during an observation period of 20 s.

Determination of Kupffer cell function

KC function was assessed by determination of their particle phagocytosis as described earlier^[28,29]. At the end of IVM analysis, plain fluorescent latex beads in isotonic saline solution were injected as bolus (3×10^8 /kg) through the carotid catheter (diameter 1.1 µm, Polysciences Inc., Warrington, PA, USA). Phagocytic activity was then analyzed successively during the first 5 min after injection in 10 randomly selected liver lobules in each experiment. Adherence of latex particles was quantified by counting the number of beads moving in sinusoids as a percentage of all beads visible in the field during an observation period of 10 s. Beads in presinusoidal and postsinusoidal venules were not included in analysis.

Analytical methods

Blood samples of 500 μ L were collected for determination of total glutathione (sum of GSH and GSSG) and GSSG. For GSSG analysis, an aliquot (200 μ L) of blood was mixed immediately with 200 μ L of 10 mmol/L N-ethylmaleimide (NEM) in 100 mmol/L phosphate buffer (pH 6.5) containing 17.5 mmol/L EDTA^[30]. The remaining blood was centrifuged at full speed for 1 min. An aliquot (100 μ L) of plasma was pipetted into 100 μ L sulfosalicylic acid (5%) for determination of total glutathione. To separate GSSG from NEM and NEM-GSH adducts, an aliquot of NEM treated plasma was passed through a Sep-Pak_{C18} cartridge (Waters, Framingham, MA, USA) followed by 1 mL of 100 mmol/L phosphate buffer (pH 7.5). GSSG in the eluates and total glutathione in acidified plasma samples was determined by an enzymatic test as described previously^[31]. GSH plasma concentrations were calculated as the difference between total glutathione and GSSG.

Serum aminotransferases

Serum aminotransferases were used as established markers of hepatic injury. Aspartate aminotransferase (AST) and alanine aminotransferase (ALT) were measured 2 h after reperfusion using a serum multiple analyzer (Hitachi 917, Roche Germany).

Transmission electron microscopy

At the end of the experiments, perfusion-fixation of hepatic tissue was performed using a 50 g/L glutaraldehyde/40 g/L paraformaldehyde mixture in phosphate buffer (pH 7.4) via the hepatic artery at a constant pressure of approximately 80 mmHg. Specimens were cut from both the right and left liver lobes and blocks were diced into 1 mm cubes. Samples were stored in fixative for 2 to 3 d prior to further processing. Specimens were postfixed with osmium tetroxide, dehydrated in graded alcohol and embedded in Epon 812. Ultrathin sections were cut and contrasted with uranyl acetate and lead citrate for electron microscopy^[11].

Statistical analysis

All data are expressed as mean \pm SE. Statistical differences between groups were calculated using paired or unpaired Student's *t* test for randomly distributed data and the Mann-Whitney *U* test for nonparametric data following analysis of variance (ANOVA). Differences were considered significant at $P < 0.05$.

RESULTS

Cell injury and liver function after liver transplantation

Injury of parenchymal and non-parenchymal liver cells after liver transplantation was assessed by the release of ALT and AST as well as by electron microscopic analysis at 120 min of reperfusion. Parenchymal cell damage in untreated animals was indicated by a 25- and 40-fold increase of ALT and AST serum levels, respectively, when compared with sham-operated animals (Figure 1). Continuous intravenous administration of 100 μ mol GSH/(h·kg) during reperfusion significantly ($P < 0.05$) reduced ALT and AST levels by almost 40% whereas infusion of 50 μ mol GSH/(h·kg) had no effect (Figure 1).

Transmission electron microphotographs of the untreated liver grafts after 120 min of reperfusion showed alterations of hepatocytes, including cell edema, a substantial loss of microvilli and generalized swelling of mitochondria (Figure 2A,B). Furthermore, non-parenchymal injury was evident by various degrees of SEC-detachment from the perisinusoidal matrix plate or even complete loss of the sinusoidal endothelial lining (Figure 2 A,B). Consequently, the space of Dissé was

enlarged in control livers. In contrast, treatment of animals with 100 μ mol/(h·kg) GSH was effective in protecting hepatocytes with only minimal loss of microvilli of normally shaped parenchymal cells and only sporadic mitochondrial swelling. Moreover, GSH prevented SEC detachment, thus resulting in normal spaces of Dissé (Figure 2 C,D).

Function of liver allografts was estimated by recovery of bile flow. Bile flow of sham-operated animals remained constant during the observation period of 150 min and was comparable to bile flow rates of donor livers before ischemia (Figure 3). After transplantation of control livers, bile flow returned to only 45% of baseline values. Intravenous infusion of 50 μ mol GSH/(h·kg) had no effect on the postischemic bile flow whereas 100 μ mol GSH/(h·kg) significantly ($P < 0.05$) increased bile flow during the complete reperfusion period (Figure 3).

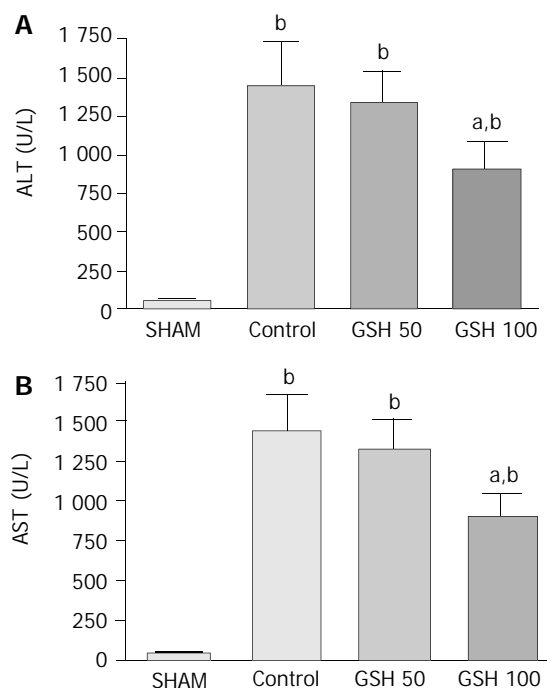


Figure 1 ALT (A) and AST (B) plasma levels after liver transplantation. Livers preserved for 24 h in UW solution at +4 °C before transplantation. Compared to untreated livers ($n=8$) administration of 100 μ mol GSH/(h·kg) ($n=5$), but not of 50 μ mol GSH/(h·kg) ($n=5$), resulted in a significant decrease of plasma ALT and AST levels at 2 h of reperfusion. Results are mean \pm SE. ^b $P < 0.001$ vs sham-operated animals ($n=5$); ^a $P < 0.05$ vs untreated livers.

Kupffer cell function after liver transplantation

Latex particle phagocytosis by KC reflects their function under various conditions. In agreement with earlier observations, rapid clearance of intra-arterially administered fluorescent latex particles was observed in sham-operated animals. Five minutes after injection only $8.1 \pm 2.5\%$ particles were freely movable in the sinusoids. This rate was not influenced by liver transplantation as indicated by $11.2 \pm 1.0\%$ of all visible beads, freely movable in the sinusoids of untreated animals. Neither GSH treatment with 50 μ mol/(h·kg) nor with 100 μ mol/(h·kg) affected phagocytosis of latex particles, resulting in $12.0 \pm 1.1\%$ and $10.5 \pm 2.0\%$ of beads moving in sinusoids at 5 min upon bolus injection, respectively. Since KC represents approximately 90% of the phagocytic capacity in the liver, these results suggest unaltered KC function after reperfusion of untreated and GSH-treated liver grafts.

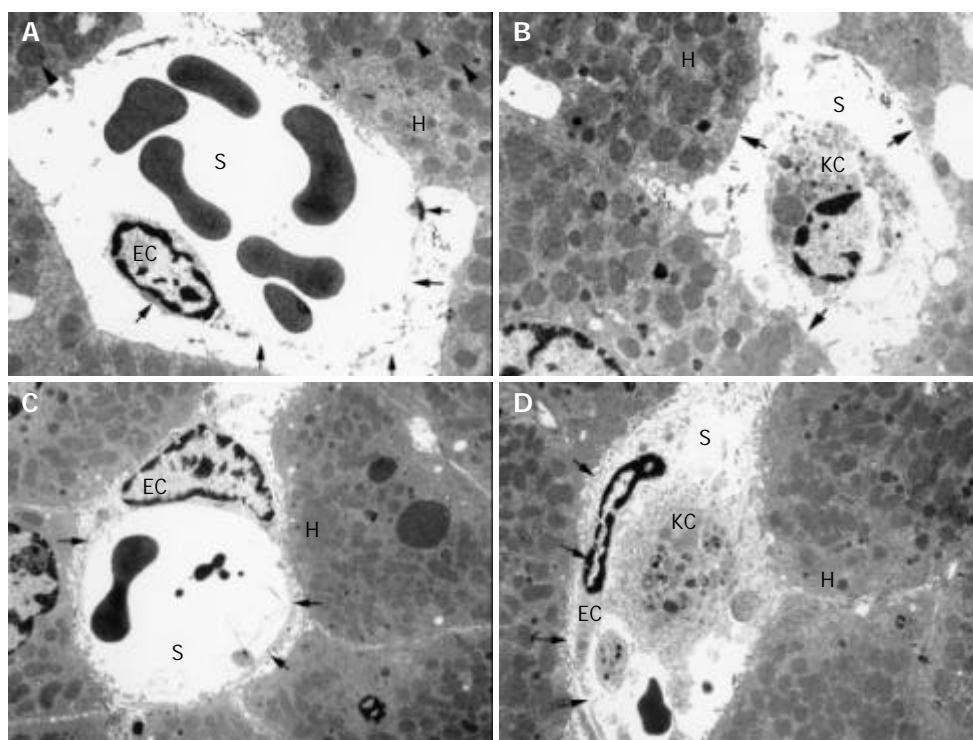


Figure 2 Transmission electron microphotographs of untreated and GSH- treated liver allografts. Arrow-heads indicate mitochondrial swelling of hepatocytes in untreated livers (A) which was almost absent in allografts treated with 100 $\mu\text{mol}/(\text{h} \cdot \text{kg})$ during reperfusion (C). Arrows demonstrate the loss of hepatocyte microvilli in untreated controls (B) whereas GSH administration preserved microvilli in nearly all hepatocyte membranes (D). As indicated by open arrows detachment of SEC (A) as well as its complete loss (B) was evident in untreated livers. GSH- treatment preserved sinusoidal endothelial lining with a normal space of Dissé (C,D). Letters indicate: H, hepatocyte; KC, Kupffer cell; EC, endothelial cell; S, sinusoidal lumen. Bars represent either 1.7 μm (B) or 2.5 μm (A,C,D).

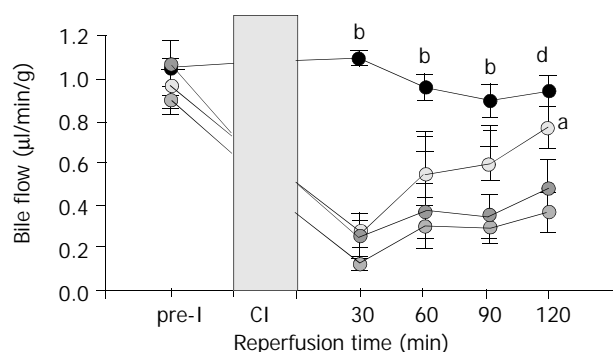


Figure 3 Effect of GSH treatment on bile flow after liver transplantation. Animals were treated with 50 $\mu\text{mol}/(\text{h} \cdot \text{kg})$ GSH (○, $n=5$) or 100 $\mu\text{mol}/(\text{h} \cdot \text{kg})$ GSH (◐, $n=5$) and compared with untreated controls (●, $n=8$) and a sham- operated group (●, $n=5$). Results are mean \pm SE. ^b $P<0.001$ vs untreated or GSH-treated livers; ^d $P<0.01$ vs 100 $\mu\text{mol}/(\text{h} \cdot \text{kg})$ GSH; ^a $P<0.05$ vs untreated controls.

Effect of GSH treatment on the microcirculation of liver allografts

Compared with sham-operated animals, substantial disturbances of the microcirculation were observed in untreated liver allografts (Figure 4). Thirty minutes after starting reperfusion almost 25% of the sinusoids were not perfused. Intravenous infusion of 50 as well as 100 $\mu\text{mol}/(\text{h} \cdot \text{kg})$ prevented this no – reflow phenomenon, thereby improving hepatic perfusion (Figure 4 A).

Furthermore, intravital microscopy revealed considerable leukocyte sticking within sinusoids and postsinusoidal venules in untreated liver allografts (Figure 4 B,C). A significant

reduction ($P<0.001$) of stagnant leukocytes in sinusoids was found in both treatment groups (Figure 4 B). Comparable to acinar leukocyte sticking, permanent adherence of leukocytes to postsinusoidal venules was reduced by 57% and 69% ($P<0.001$) when animals received 50 or 100 $\mu\text{mol}/(\text{h} \cdot \text{kg})$, respectively (Figure 4 C). Temporary adherence of leukocytes (rolling) in postsinusoidal venules is supposed to be the initiating event in the sequence to permanent adherence to the vascular endothelium. However rolling of leukocytes was slightly increased by GSH treatment (Figure 4E).

Effect of intravenous GSH infusion on plasma GSH and GSSG levels

Sixty minutes after starting reperfusion plasma GSH levels of untreated animals increased 2-fold when compared to sham-operated animals (Figure 5). This was accompanied by a 3-fold increase of plasma GSSG (Figure 5). Infusion of 50 $\mu\text{mol}/(\text{h} \cdot \text{kg})$ GSH resulted in a 6-fold increase of plasma GSH whereas GSSG did not exceed levels of untreated controls. In contrast, 100 $\mu\text{mol}/(\text{h} \cdot \text{kg})$ elevated plasma GSH as well as GSSG by up to 9-fold above values obtained in the sham-group (Figure 5). Moreover, plasma GSSG increased to significant higher levels when compared with untreated or GSH – treated (50 $\mu\text{mol}/(\text{h} \cdot \text{kg})$) animals. In order to estimate the role of spontaneous oxidation of intravenously applied GSH a second group of sham-operated animals was treated with 100 $\mu\text{mol}/(\text{h} \cdot \text{kg})$ GSH. This resulted in marked increase of plasma GSH to 93 ± 10 mol/L which was similar to that observed in liver allografts (97 ± 18 mol/L). However, plasma GSSG increased to only 3.0 ± 0.9 in contrast to 7.5 ± 0.9 mol/L in GSH-treated liver allografts. These findings clearly indicate enhanced oxidation of intravenously applied GSH at the cytoprotective dose of 100 $\mu\text{mol}/(\text{h} \cdot \text{kg})$.

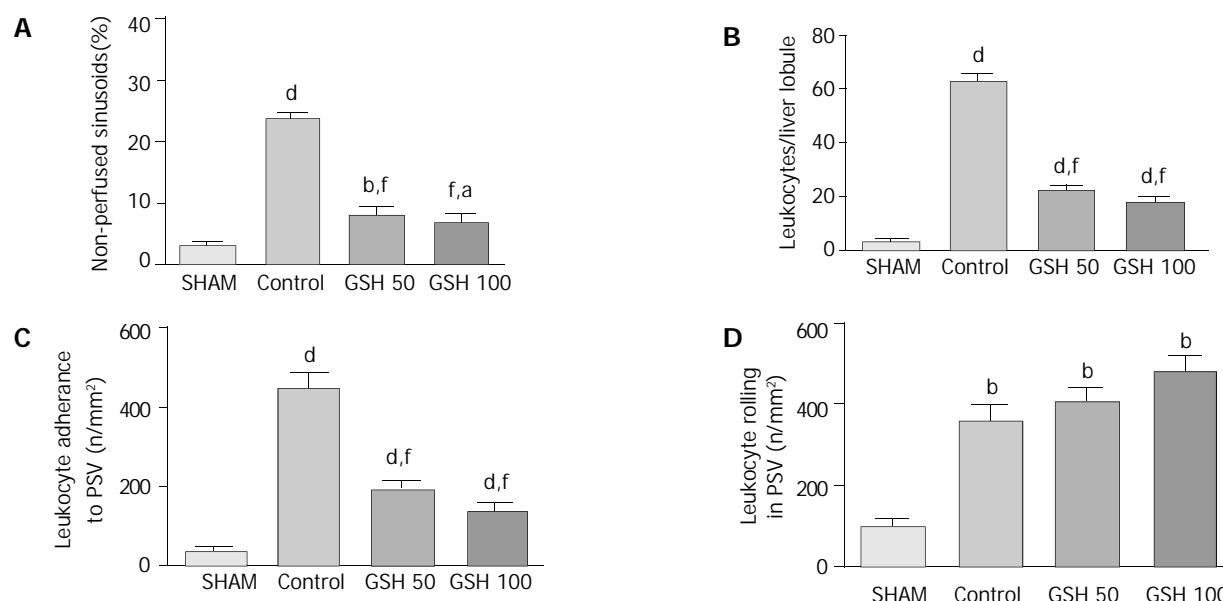


Figure 4 Impact of GSH treatment on the hepatic microcirculation after liver transplantation. Data from *in vivo* microscopy were obtained 30 min after starting reperfusion comparing untreated controls ($n=8$) with GSH- treated allografts (50 $\mu\text{mol}/(\text{h}\cdot\text{kg})$ and 100 $\mu\text{mol}/(\text{h}\cdot\text{kg})$; each $n=5$) as well as to a sham group ($n=5$). (A) Acinar perfusion failure is indicated as the percentage of non-perfused sinusoids (no reflow). (B) Leukocyte-adhesion (sticking) to sinusoids and (C) to postsinusoidal venules. (D) Temporary attachment of leukocytes (rolling) to the endothelium of postsinusoidal venules (PSV). Results are mean \pm SE. ^a $P<0.05$, ^d $P<0.01$ and ^b $P<0.001$ vs sham group. ^f $P<0.001$ vs control group.

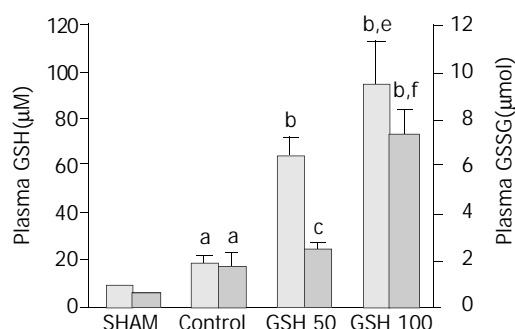


Figure 5 Plasma GSH- and GSSG concentrations following liver transplantation. Compared to sham-operated animals ($n=5$) a significant increase of reduced and oxidized glutathione was determined upon reperfusion of untreated grafts ($n=8$). Intravenous infusion of GSH at rates of 50 $\mu\text{mol}/(\text{h}\cdot\text{kg})$ ($n=5$) and 100 $\mu\text{mol}/(\text{h}\cdot\text{kg})$ ($n=5$) resulted in a dose- dependent increase of plasma GSH concentrations. The corresponding GSSG levels showed only a slight increase after administration of 50 μmol GSH/ $(\text{h}\cdot\text{kg})$, but increased markedly following infusion of 100 μmol GSH/ $(\text{h}\cdot\text{kg})$. Mean \pm SE. ^a $P<0.05$ vs sham; ^b $P<0.001$ and ^c $P<0.05$ vs control group; ^e $P<0.05$ vs GSH 50 and ^f $P<0.01$ vs GSH 50.

DISCUSSION

Recently, we have found that treatment of cold preserved livers with GSH upon reperfusion prevented reperfusion injury in the model of isolated rat liver perfusion^[23]. Due to several limitations of this experimental model, such as the absence of plasma antioxidants and the lack of leukocytes^[32,33], the potential protective effect of GSH treatment during liver transplantation remained to be defined. We also found that intravenous GSH treatment during liver transplantation prevents reperfusion injury of the liver allograft.

We obtained the following main results: (1) increase of the vascular antioxidant capacity by intravenous infusion of GSH causes a significant reduction of injury to hepatocytes and SEC as well as of (2) microcirculatory disturbances in liver allografts, and (3) Administration of GSH does not affect

KC function but enhances detoxification of KC-derived ROS as indicated by a marked increase of plasma GSSG.

Prevention of reperfusion injury to liver allografts by GSH

Intravenous administration of GSH at a dose of 100 $\mu\text{mol}/(\text{h}\cdot\text{kg})$ during the reperfusion phase of liver transplantation significantly reduced ALT and AST release by approximately 40% indicating the protection of the liver allografts. This contention is supported by distinct signs of parenchymal and non-parenchymal cell injury under electron microscopy already after 2 h of re-establishing blood flow. Untreated livers showed a complete detachment of SEC from the perisinusoidal matrix which in part determines graft viability^[4-7]. In contrast, detachment of SEC was dramatically attenuated in GSH-treated livers, indicating preservation of the sinusoidal architecture. Furthermore, GSH treatment markedly reduced mitochondrial swelling and the loss of microvilli in hepatocytes. These cytoprotective effects were accompanied by a marked improvement of postischemic liver function as assessed by a 2.5-fold increase of bile flow. Because postischemic GSH treatment can only protect cells which are not already seriously damaged before the onset of reperfusion, our results clearly demonstrate prevention of reperfusion injury to parenchymal and non-parenchymal liver cells by GSH.

Prevention of reperfusion injury by GSH depended on the GSH dose: 100 $\mu\text{mol}/(\text{h}\cdot\text{kg})$ but not 50 $\mu\text{mol}/(\text{h}\cdot\text{kg})$ showed protection. Based on steady state GSH plasma concentrations following GSH infusion, a concentration of approximately 100 $\mu\text{mol}/\text{L}$ appears to be pivotal for cytoprotection. In view of these findings, GSH seems as ideal and presumably safe candidate drug for prevention of reperfusion injury of the liver allograft since plasma GSH levels up to 500 $\mu\text{mol}/\text{L}$ showed no toxicity in humans^[19].

Mechanisms of GSH – mediated protection

Effect on Kupffer cell function There is extensive experimental evidence for KC activation as a central pathomechanism of reperfusion injury of the liver after warm or cold ischemia^[8,9]. To assess KC function we used the tool of intravital microscopic

analysis of latex particle phagocytosis^[28,29]. In agreement with earlier studies^[29] particle phagocytosis was not affected by cold preservation indicating functionally intact Kupffer cells in liver allografts. Furthermore, clearance of latex particles was not affected by postischemic administration of GSH. These results argue against a suppression of KC function as a potential protective mechanism of GSH action. Thus, potential hazards of other protective approaches interfering with vital host-defense function of KC (e.g. calcium channel blocker, KC-depleting agents,^[8,34,35]) would be avoided by GSH treatment. **Detoxification of ROS in the hepatic vasculature** Intravenous administration of GSH results in the degradation of GSH to its amino acids which are again available for GSH synthesis in various organs including the liver^[36]. However several studies demonstrated no relevant increase of the hepatic GSH content 2 h after starting high-dose GSH infusion^[22,23]. These findings suggest that GSH effects are related rather to the increase in the extracellular antioxidant capacity than to influences on intracellular GSH. In line with this interpretation we obtained evidence for an extracellular mechanism of GSH-mediated cytoprotection.

The increase in plasma GSSG observed during reperfusion of untreated and GSH-treated livers was associated with a marked increase in plasma GSH. This parallel increase in GSH and GSSG suggests that GSSG resulted from extracellular oxidation rather than from intrahepatic generation of GSSG^[37,38]. Accordingly, previous studies with the blood – free perfused rat liver found only a very small release of GSSG into the perfusate during reperfusion^[39]. Furthermore, there was no evidence for a relevant increase of intracellular GSSG formation^[8,39]. Thus, plasma GSSG formation observed during reperfusion of liver allografts is likely to take place extracellularly. This could be due to spontaneous as well as reactive oxygen species-related oxidation of GSH. The results of the present study argue against a predominant role for spontaneous GSH oxidation. First, intravenous infusion of 50 $\mu\text{mol GSH}/(\text{h} \cdot \text{kg})$ during reperfusion of liver allografts resulted in a several fold increase of plasma GSH whereas plasma GSSG did not exceed the levels of untreated controls. Second, a comparable increase of plasma GSH was observed when sham-operated or transplanted animals were treated with 100 $\mu\text{mol GSH}/(\text{h} \cdot \text{kg})$. In contrast, a 2.5-fold higher increase of plasma GSSG was determined in transplanted rats. This difference clearly indicates that spontaneous oxidation of intravenously applied GSH contributes only in part to the increase in plasma GSSG. Based on these findings oxidation of GSH by ROS appears as a major determinant of plasma GSSG formation following liver transplantation. Consequently, the marked increase of plasma GSSG during infusion of the protective GSH dose of 100 $\mu\text{mol}/(\text{h} \cdot \text{kg})$ most likely reflects an enhanced detoxification of ROS in the hepatic vasculature.

Activated KC have been identified as potential source of extracellular ROS formation and GSH oxidation during reperfusion after warm hepatic ischemia^[8,40]. Accordingly, there was no evidence for plasma GSSG formation during reperfusion of KC-depleted liver allografts^[41]. These findings suggest that intravenously applied GSH protects liver allografts against the vascular oxidant stress produced by KC during reperfusion. This interpretation is further substantiated by the observation that externally added GSH and catalase protected leukocyte- free perfused rat livers against oxidant cell injury following selective KC activation^[42,43]. In this experimental model cytoprotection was achieved by vascular GSH concentrations of 100 $\mu\text{mol/L}$, but not by 50 $\mu\text{mol/L}$. The same vascular concentrations of GSH were achieved in the present study. Again, protection of liver allografts was only evident at plasma GSH concentrations of approximately 100 $\mu\text{mol/L}$ and was associated with a considerable extra-formation of plasma GSSG. These findings suggest that plasma GSH above a critical level may act as a “sink”

for ROS produced by KC during reperfusion. This could be due to non-enzymatic reactions between GSH and various ROS which strongly depend on the GSH concentration^[29,44,45].

Prevention of microcirculatory perfusion failure and SEC injury GSH of both doses remarkably improved the hepatic microcirculation. In particular, the number of perfused sinusoids increased to that observed in non-ischemic livers indicating prevention of the no-reflow phenomenon. This could be related to the counteraction of ROS-mediated mechanisms of vasoconstriction and leukocyte adherence to sinusoids and postsinusoidal venules^[12-16]. In accordance with the proposed stepwise process of leukocyte-endothelial interaction from leukocyte rolling as an initial event to permanent attachment of leukocytes as the second step^[46], our results indicate GSH as an inhibitor of the second step: treatment with GSH prevented sticking but slightly increased the rolling of leukocytes. Similar effects can be achieved by the administration of superoxide dismutase^[12,13,16], suggesting superoxide anion ($\text{O}_2^{\cdot -}$) as the contributing mediator of leukocyte adherence. Therefore, it seems likely that GSH prevents leukocyte adherence through reaction with $\text{O}_2^{\cdot -}$ or inhibition of $\text{O}_2^{\cdot -}$ - mediated mechanisms of leukocyte adherence. Protection of leukocyte adherence by 50 $\mu\text{mol GSH}/(\text{h} \cdot \text{kg})$ without evidence for additional GSSG formation does not argue against this concept because the reaction of GSH with $\text{O}_2^{\cdot -}$ can result in the formation of glutathione sulfonate^[44].

However, the antioxidative potential of GSH does not rule out beneficial effects through non-antioxidative properties. Accumulating evidence indicates that detachment of SEC from the perisinusoidal matrix plate represents a critical component of preservation injury and postischemic microcirculatory failure^[5,47,48]. It has been proposed that SEC damage occurs independent of ROS formation because several antioxidants failed to prevent SEC injury in the liver allograft^[6]. SEC detachment is caused by various matrix metalloproteinases (MMPs) released into the extracellular compartment during cold liver preservation. In the present study attachment of SEC to their matrix was impressively preserved by GSH and could contribute to the improvement of the hepatic microcirculation. Recent experiments demonstrated the inhibition of MMPs by GSH *in vitro*. These findings suggest that MMPs were possible targets of GSH in liver allografts but this requires further investigations.

In summary, the present study demonstrates a dose-dependent prevention of reperfusion injury in rat liver allografts by postischemic intravenous administration of GSH. Treatment of recipient animals with GSH prevented reperfusion injury to SEC as well as to hepatocytes, markedly improved the hepatic microcirculation and preserved postischemic liver function. GSH-mediated protection of liver allografts was associated with an increased formation of plasma GSSG providing evidence for an accelerated detoxification of ROS by intravenously applied GSH. Therefore, intravenous administration of GSH appears to be a candidate therapy for the prevention of ROS-related reperfusion injury after liver transplantation, in particular since it has a low toxicity in humans and seems cost-effective.

ACKNOWLEDGMENTS

The excellent technical assistance of Ms I. Liss is gratefully appreciated. Presented in abstract form at the 50th annual meeting of the American Association for the Study of Liver Diseases (AASLD), 1999, Dallas.

REFERENCES

- 1 **Clavien PA**, Harvey PRC, Strasberg SM. Preservation and reperfusion injuries in liver allografts. *Transplantation* 1992; **53**: 957-978
- 2 **Lemasters JJ**, Thurman RG. Reperfusion injury after liver preservation for transplantation. *Annu Rev Pharmacol Toxicol* 1997;

- 37: 327-338
- 3 **Bilzer M**, Gerbes AL. Preservation injury of the liver: mechanisms and novel therapeutic strategies. *J Hepatol* 2000; **32**: 508-515
- 4 **Clavien PA**. Sinusoidal endothelial cell injury during hepatic preservation and reperfusion. *Hepatology* 1998; **28**: 281-285
- 5 **McKeown CMB**, Edwards V, Phillips MJ, Harvey PRC, Petrunka CN, Strasberg SM. Sinusoidal lining cell damage: the critical injury in cold preservation of liver allografts in the rat. *Transplantation* 1988; **46**: 178-191
- 6 **Caldwell-Kenkel JC**, Thurman RG, Lemasters JJ. Selective loss of nonparenchymal cell viability after cold ischemic storage of rat livers. *Transplantation* 1988; **45**: 834-837
- 7 **Gao W**, Bentley R, Madden JF, Clavien PA. Apoptosis of sinusoidal endothelial cells is a critical mechanism of preservation injury in rat liver transplantation. *Hepatology* 1998; **27**: 1652-1660
- 8 **Jaeschke H**, Farhood A. Neutrophil and Kupffer cell-induced oxidant stress and ischemia-reperfusion injury in rat liver. *Am J Physiol* 1991; **260**: G355-G362
- 9 **Brass CA**, Roberts TG. Hepatic free radical production after cold storage: Kupffer cell-dependent and -independent mechanisms in rats. *Gastroenterology* 1995; **108**: 1167-1175
- 10 **Jaeschke H**. Reactive oxygen and ischemia/reperfusion injury of the liver. *Chem Biol Interact* 1991; **79**: 115-136
- 11 **Vollmar B**, Glasz J, Leiderer R, Post S, Menger MD. Hepatic microcirculatory perfusion failure is a determinant of liver dysfunction in warm ischemia-reperfusion. *Am J Pathol* 1994; **145**: 1421-1431
- 12 **Koo A**, Komatsu H, Tao G, Inoue M, Guth PH, Kaplowitz N. Contribution of no-reflow phenomenon to hepatic injury after ischemia-reperfusion: evidence for a role for superoxide anion. *Hepatology* 1992; **15**: 507-514
- 13 **Marzi I**, Knee J, Buhren V, Menger MD, Trentz O. Reduction by superoxide dismutase of leukocyte - endothelial adherence after liver transplantation. *Surgery* 1992; **111**: 90-97
- 14 **Bilzer M**, Gerbes AL. Prolonged modulation of the hepatic circulation by Kupffer cell-derived reactive oxygen species. In Cells of the hepatic sinusoid (eds. E. Wisse, D.L. Knook, C. Balabaud), Vol. 6., Leiden, Netherlands: Kupffer Cell Foundation 1996; pp. 200-201
- 15 **Shibuya H**, Ohkohchi N, Seya K, Satomi S. Kupffer cells generate superoxide anions and modulate reperfusion injury in rat livers after cold preservation. *Hepatology* 1997; **25**: 356-360
- 16 **Kondo T**, Terajima H, Todoroki T, Hirano T, Ito Y, Usia T, Messmer K. Prevention of hepatic ischemia-reperfusion injury by SOD-DIVEMA conjugate. *J Surg Res* 1999; **85**: 26-36
- 17 **Essani NA**, McGuire GM, Manning AM, Jaeschke H. Endotoxin-induced activation of the nuclear transcription factor κ B in in hepatocytes, Kupffer cells and endothelial cells *in vivo*. *J Immunol* 1996; **156**: 2956-2963
- 18 **Essani NA**, Fischer MA, Jaeschke H. Inhibition of NF- κ B activation by dimethyl sulfoxide correlates with suppression of TNF α formation, reduced ICAM-1 gene transcription, and protection against endotoxin-induced liver injury. *Shock* 1997; **7**: 90-96
- 19 **Aebi S**, Assereto R, Lauterburg BH. High-dose intravenous glutathione in man. Pharmacokinetics and effects on cyst(e)ine in plasma and urine. *Eur J Clin Invest* 1991; **21**: 103-110
- 20 **Bilzer M**, Lauterburg BH. Glutathione metabolism in activated human neutrophils: Stimulation of glutathione synthesis and consumption of glutathione by reactive oxygen species. *Eur J Clin Invest* 1991; **21**: 316-322
- 21 **Bilzer M**, Lauterburg BH. Effects of hypochlorous acid and chloramines on vascular resistance, cell integrity, and biliary glutathione disulfide in the perfused rat liver: modulation by glutathione. *J Hepatol* 1991; **13**: 84-89
- 22 **Liu P**, Fisher MA, Farhood A, Smith CY, Jaeschke H. Beneficial effects of extracellular glutathione against endotoxin-induced liver injury during ischemia and reperfusion. *Circ Shock* 1994; **43**: 64-70
- 23 **Bilzer M**, Paumgartner G, Gerbes AL. Glutathione protects the rat liver against reperfusion injury after hypothermic preservation. *Gastroenterology* 1999; **117**: 200-210
- 24 **Kamada N**, Calne RY. Orthotopic liver transplantation in the rat. Technique using cuff for portal vein anastomosis and biliary drainage. *Transplantation* 1979; **28**: 47-56
- 25 **Post S**, Menger MD, Rentsch M, Gonzalez AP, Herfarth C, Messmer K. The impact of arterialization on hepatic microcirculation and leukocyte accumulation after liver transplantation in the rat. *Transplantation* 1992; **54**: 789-794
- 26 **Vollmar B**, Richter S, Menger MD. Leukocyte stasis in hepatic sinusoids. *Am J Physiol* 1996; **270**: G798-G803
- 27 **Menger MD**, Marzi I, Messmer K. *In vivo* fluorescence microscopy for quantitative analysis of the hepatic microcirculation in hamsters and rats. *Eur Surg Res* 1991; **23**: 158-169
- 28 **Bloch EH**, McCuskey RS. Biodynamics of phagocytosis: an analysis of the dynamics of phagocytosis in the liver by *in vivo* microscopy. In Kupffer cells and other liver sinusoidal cells (eds. E. Wisse, D.L. Knook), Amsterdam: Elsevier Science Publishers 1977; pp. 21-32
- 29 **Post S**, Gonzalez AP, Palma P, Rentsch M, Stiehl A, Menger MD. Assessment of hepatic phagocytic activity by *in vivo* microscopy after liver transplantation in the rat. *Hepatology* 1992; **16**: 803-809
- 30 **Jaeschke H**, Mitchell JR. Use of isolated perfused organs in hypoxia and ischemia / reperfusion oxidant stress. *Methods Enzymol* 1990; **186**: 752-759
- 31 **Tietze F**. Enzymatic method for quantitative determination of nanogram amounts of total and oxidized glutathione. *Ann Biochem* 1969; **27**: 502-522
- 32 **Gores GJ**, Kost LJ, LaRusso NF. The isolated perfused rat liver: conceptual and practical considerations. *Hepatology* 1986; **6**: 511-517
- 33 **Halliwell B**, Gutteridge MC. The antioxidants of human extracellular fluids. *Arch Biochem Biophys* 1990; **280**: 1-8
- 34 **Marzi I**, Walcher F, Buehren V. Macrophage activation and leukocyte adhesion after liver transplantation. *Am J Physiol* 1993; **265**: G172-G177
- 35 **Post S**, Palma P, Rentsch M, Gonzalez AP, Menger MD. Differential impact of Carolina Rinse and University of Wisconsin solutions on microcirculation, leukocyte adhesion, Kupffer cell activity and biliary excretion after liver transplantation. *Hepatology* 1993; **18**: 1490-1497
- 36 **Aebi S**, Lauterburg BH. Divergent effects of intravenous GSH and cysteine on renal and hepatic GSH. *Am J Physiol* 1992; **263**: R348-R352
- 37 **Adams JD**, Lauterburg BH, Mitchell JR. Plasma glutathione and glutathione disulfide in the rat: regulation and response to oxidant stress. *J Pharmacol Exp Therapeutics* 1983; **227**: 749-754
- 38 **Lauterburg BH**, Smith CV, Hughes H, Mitchell JR. Biliary excretion of glutathione and glutathione disulfide in the rat. *J Clin Invest* 1984; **73**: 124-133
- 39 **Jaeschke H**, Smith CV, Mitchell JR. Reactive oxygen species and ischemia-reflow injury in isolated perfused rat liver. *J Clin Invest* 1988; **81**: 1240-1246
- 40 **Jaeschke H**, Bautista AP, Spolarics Z, Spitzer JJ. Superoxide generation by Kupffer cells and priming of neutrophils during reperfusion after hepatic ischemia. *Free Radic Res Commun* 1991; **15**: 277-284
- 41 **Schauer R**, Bilzer M, Kalmuk S, Gerbes AL, Leiderer R, Schildberg FW, Messmer K. Microcirculatory failure after rat liver transplantation is related to Kupffer cell- derived oxidant stress but not involved in early graft dysfunction. *Transplantation* 2001; **72**: 1692-1699
- 42 **Baron A**, Gerbes AL, Bilzer M. Prevention of Kupffer cell- induced injury in rat liver by glutathione. *Hepatology* 1999; **30**: 226A
- 43 **Bilzer M**, Jaeschke H, Vollmar AM, Paumgartner G, Gerbes AL. Prevention of Kupffer cell-induced injury in rat liver by atrial natriuretic peptide (ANP): A novel endogenous defense mechanism against oxidant injury. *Am J Physiol* 1999; **276**: G1137-G1144
- 44 **Wefers H**, Sies H. Oxidation of glutathione by the superoxide radical to the disulfide and the sulfonate yielding singlet oxygen. *Eur J Biochem* 1983; **137**: 29-36
- 45 **Winterbourn CC**, Metodieva D. The reaction of superoxide with reduced glutathione. *Arch Biochem Biophys* 1994; **314**: 284-290
- 46 **Hernandez LA**, Grisham MB, Twhig B, Arfors KE, Harlan JM, Granger DN. Role of neutrophils in ischemia-reperfusion-induced microvascular injury. *Am J Physiol* 1987; **253**: H699-H703
- 47 **Clavien PA**, Harvey PRC, Sanabria JR, Cywes R, Levy GA, Strasberg SM. Lymphocyte adherence in the reperfused liver allograft. Mechanisms and effects. *Hepatology* 1993; **17**: 131-142
- 48 **Takey Y**, Marzi I, Gao W, Gores GJ, Lemasters JJ, Thurman RG. Leukocyte adhesion and cell death following orthotopic liver transplantation in the rat. *Transplantation* 1991; **51**: 959-965

Protective effect of exogenous adenosine triphosphate on hypothermically preserved rat liver

Xiao-Dong Tan, Hiroshi Egami, Feng-Shan Wang, Michio Ogawa

Xiao-Dong Tan, Hiroshi Egami, Feng-Shan Wang, Michio Ogawa,
Department of Surgery II, Kumamoto University Medical School,
Kumamoto 860-8556, Japan

Correspondence to: Dr. Xiao-Dong Tan, Department of Surgery II,
Kumamoto University Medical School, Honjo 1-1-1, Kumamoto 860-
8556, Japan. tanxd@hotmail.com

Telephone: +81-96-3735211 **Fax:** +81-96-371-4378

Received: 2003-10-15 **Accepted:** 2003-11-20

Abstract

AIM: To clarify the protective effect of exogenous adenosine triphosphate (ATP) on hypothermically preserved rat livers.

METHODS: Establishment of continuous hypothermic machine perfusion model, detection of nucleotides in hepatocytes with HPLC, measurement of activities of LDH and AST in the perfusate, observation of histopathological changes in different experiment groups, and autoradiography were carried out to reveal the underlying mechanism of the protective effect of ATP.

RESULTS: The intracellular levels of ATP and EC decreased rapidly after hypothermic preservation in control group, while a higher ATP and EC level, and a slower decreasing rate were observed when ATP-MgCl₂ was added to the perfusate ($P < 0.01$). As compared with the control group, the activities of LDH and AST in the ATP-MgCl₂ group were lower ($P < 0.05$). Furthermore, more severe hepatocyte damage and neutrophil infiltration were observed in the control group. Radioactive [α -³²P] ATP entered the hypothermically preserved rat hepatocytes.

CONCLUSION: Exogenous ATP has a protective effect on rat livers during hypothermic preservation. However, Mg²⁺ is indispensable, addition of ATP alone produces no protective effect. The underlying mechanism may be that exogenous ATP enters the hypothermically preserved rat liver cells.

Tan XD, Egami H, Wang FS, Ogawa M. Protective effect of exogenous adenosine triphosphate on hypothermically preserved rat liver. *World J Gastroenterol* 2004; 10(6): 871-874
<http://www.wjgnet.com/1007-9327/10/871.asp>

INTRODUCTION

Improving the quality of cold stored organs and prolonging the effective preservation time are the pivotal contents in the investigation of hypothermic preservation of transplant grafts. Several investigators have reported that the intracellular level of adenosine triphosphate (ATP) in cold stored organs was closely correlated with the viability of transplant grafts^[1-3]. Bowers reported that ATP level in cold stored pretransplant organs was a sensitive parameter for examining the activities of cold stored organs^[4]. Therefore, providing direct energy substrate ATP to cold stored organs^[5], should be a simple and effective method to sustain the high level of intracellular ATP.

However, thus far, whether exogenous ATP could enter cells or not is controversial^[6-9]. Furthermore, there were few reports which elucidated the protective effect of ATP on cold stored transplant grafts. In this study, a continuously hypothermic machine perfusion model of rat liver was applied to reveal the protective effect of ATP on cold stored rat livers and its mechanism.

MATERIALS AND METHODS

Experimental animals

Wistar rats weighing 180-220 g, both male and female, were randomly used.

Experiment groups and protocol

Cold storage study on rat livers The rats mentioned above were divided into 3 groups at random, group A (containing neither ATP nor MgCl₂ in the perfusate), group B (containing 5 mmol/L ATP but no MgCl₂ in the perfusate), group C (containing either ATP or MgCl₂ in the perfusate), respectively. There were 6 rats in each group. The rat liver was weighed immediately after resection by the method described previously^[10-12], then these grafts were put into the modified Hoffmann perfusate^[13] (0-4 °C) for 30 min (Table 1). Finally, the livers were preserved in a hypothermic preservation incubator by continuously hypothermic preservation perfusion model (Figure 1). The perfusate temperature was 6-8 °C^[14], perfusion speed was 0.1 mL/(min.g)^[14], the total volume of perfusate was 120 mL.

Autoradiography study Six rats were chosen randomly, the livers were resected with the same method. One mCi [α -³²P] ATP, 5 mmol/L MgCl₂, 200 μ L and 40 U phenol kinase were added into 1 L perfusate, and the same liver preservation method was applied.

Table 1 Components of perfusate

Composition	Concentration
Hydroxyethyl starch	50 g/L
Calcium gluconate	80 mmol/L
Raffinose	10 mmol/L
KH ₂ PO ₄	25 mmol/L
Hydroxyethyl piperazine	10 mmol/L
Dexamethasone	12 mg/L
Penicillin	2×10 ⁵ units/L
Insulin	100 units/L
¹ MgCl ₂	5 mmol/L
¹ ATP	5 mmol/L

The pH value was modulated to 7.35 with NaOH, and the osmotic pressure was 300-320 mOsm/L; ¹Addition of MgCl₂ and ATP was dependent on the different groups.

Biochemical detection

Detection of energy status in cold stored rat livers The rat liver samples were used to detect the intracellular ATP, ADP, AMP, TAN and EC at 0, 1, 2, 6, 12, 24 and 36 h after

preservation by HPLC method^[15] ($TAN=ATP+ADP+AMP$, $EC=[ATP+0.5ADP]/TAN$)^[16]. One milliliter of perfusate was taken to detect the LDH and AST activities^[17,18] at 6, 12, 24 and 36 h respectively after preservation.

Histological and morphological findings Paraffin sections of HE staining were made after 24 h preservation of the rat livers^[19], and observed by a light microscope.

Autoradiography of [α -³²P] ATP The rat liver samples were made into paraffin sections of HE staining after 4-h preservation. Moreover, whether ATP entered the cells of cold stored rat livers or not was examined by autoradiography of [α -³²P] ATP^[20].

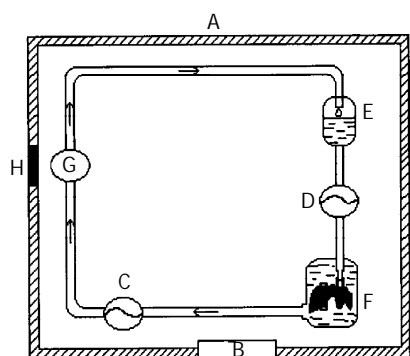


Figure 1 Preservation of continuously hypothermic machine perfusion. A: Organ hypothermic preservation box, B: Temperature displayer, C: Perfusion pump, D: Perfusion pump, (Displaying the perfusion pressure), E: Perfusate container, F: Organ preservation container, G: pH displayer, H: Entry of wire, (Being sealed while preservation).

Statistical analysis

The average values were presented as mean \pm SD, *t*-test was applied and $P<0.05$ was considered to be statistically significant.

RESULTS

Energy status in cold stored rat livers (mmol/g wet liver)

In group A, following the prolongation of preservation time, the ATP and EC levels in rat liver cells were significantly decreased. The ATP and EC levels were also rapidly decreased in group B, there was no statistical difference between these two groups ($P>0.05$). However, the ATP and EC levels were slowly decreased in group C ($P<0.01$, Table 2).

LDH and AST activities in hypothermic preservation perfusate

LDH and AST activities in the perfusate were increased in groups A and B, there was no significant difference between two groups ($P>0.05$). On the other hand, compared with those in groups A and B, the relevant activities were slowly increased in group C ($P<0.05$, Table 3).

Histological and morphological findings after 24-h hypothermic perfusion preservation

In group A (Figure 2), the hepatocytes were obviously swollen, cytosol and part of nucleus were faintly stained. Part of the endothelial cells entered the hepatosinus.

In group B (Figure 3), the hepatocytes were also expanded, cytosol was faintly stained. Some nuclei were strongly stained. Some endothelial cells entering the hepatosinus were also found.

In group C (Figure 4), the hepatocytes were lightly expanded. There was no apparent bubble in cytosol, and the morphology of nucleus was normal. The endothelial cells of hepatosinus were continuous.

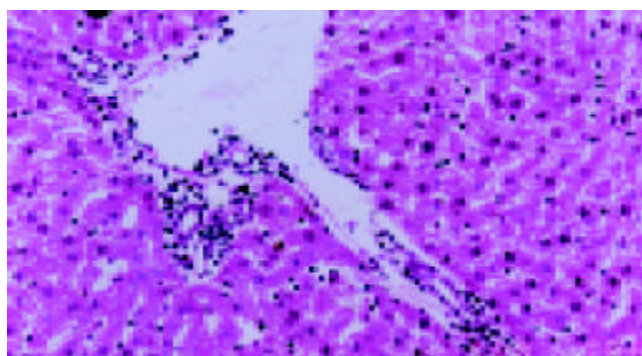


Figure 2 Histological and morphological findings in hypothermically preserved hepatocytes. Group A: 24-h preservation, HE staining 100 \times .

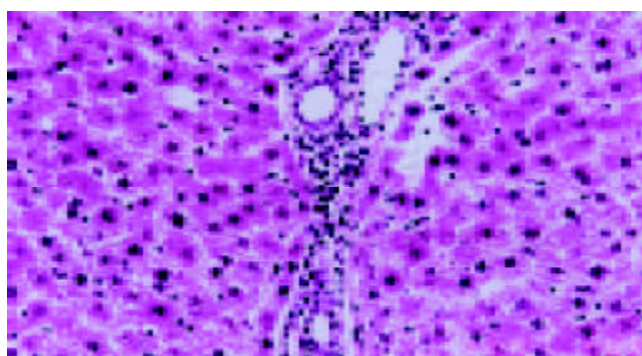


Figure 3 Histological and morphological findings in hypothermically preserved hepatocytes. Group B: 24-h preservation, HE staining 100 \times .

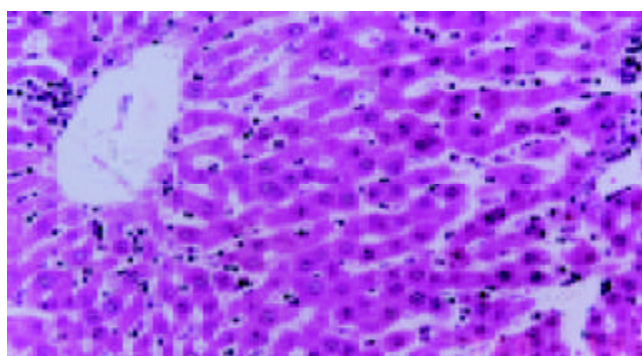


Figure 4 Histological and morphological findings in hypothermically preserved hepatocytes. Group C: 24-h preservation, HE staining 100 \times .

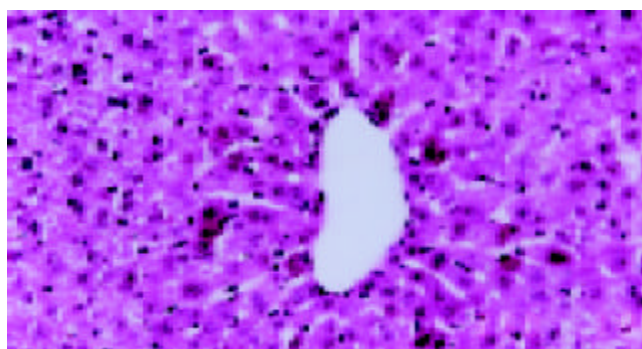


Figure 5 Autoradiography of [α -³²P] ATP in hypothermically preserved hepatocytes. Black spots in hepatocytes are the autoradiographies of [α -³²P] ATP, 4-h preservation, H E staining 100 \times .

Table 2 Energy status in hypothermically preserved rat livers ($n=6$, mean \pm SD)

	ATP ($\mu\text{mol/g}$ wet liver)			EC		
	Group A	Group B	Group C	Group A	Group B	Group C
0 h	2.760 \pm 0.302	2.760 \pm 0.302	2.760 \pm 0.302	0.871 \pm 0.093	0.871 \pm 0.093	0.871 \pm 0.093
1 h	2.337 \pm 0.202	2.263 \pm 0.282	2.514 \pm 0.298	0.803 \pm 0.090	0.789 \pm 0.083	0.791 \pm 0.083
2 h	1.914 \pm 0.209	1.971 \pm 0.205	2.391 \pm 0.276 ^a	0.741 \pm 0.082	0.736 \pm 0.082	0.743 \pm 0.079
6 h	1.509 \pm 0.211	1.506 \pm 0.180	2.523 \pm 0.269 ^b	0.653 \pm 0.071	0.645 \pm 0.068	0.695 \pm 0.071 ^a
12 h	1.145 \pm 0.177	1.136 \pm 0.150	2.715 \pm 0.298 ^b	0.543 \pm 0.063	0.537 \pm 0.060	0.660 \pm 0.070 ^b
24 h	0.755 \pm 0.082	0.842 \pm 0.088	2.547 \pm 0.279 ^b	0.380 \pm 0.045	0.406 \pm 0.045	0.601 \pm 0.068 ^b
36 h	0.603 \pm 0.065	0.706 \pm 0.080	1.782 \pm 0.200 ^b	0.316 \pm 0.040	0.348 \pm 0.042	0.471 \pm 0.051 ^b

^a $P<0.05$, ^b $P<0.01$ vs group A.**Table 3** Activities of AST and LDH in perfusate (IU/L.g liver) ($n=6$, mean \pm SD)

	6 h		12 h		24 h		36 h	
	LDH	AST	LDH	AST	LDH	AST	LDH	AST
Group A	80.2 \pm 3.8	4.6 \pm 0.6	112.7 \pm 4.1	8.9 \pm 0.9	188.4 \pm 5.1	15.6 \pm 1.4	452.2 \pm 7.4	20.1 \pm 1.7
Group B	76.4 \pm 4.2	4.8 \pm 0.5	123.8 \pm 3.6	8.2 \pm 0.8	170.1 \pm 6.2	14.1 \pm 1.7	423.7 \pm 6.5	18.7 \pm 2.2
Group C	9.3 \pm 1.8 ^a	1.2 \pm 0.4 ^a	26.7 \pm 2.3 ^a	2.4 \pm 0.5 ^a	42.6 \pm 3.5 ^a	4.4 \pm 0.6 ^a	90.1 \pm 6.2 ^a	6.3 \pm 0.8 ^a

^a $P<0.05$ vs group A.

Autoradiography of [α -³²P] ATP

Numerous silver spots of [α -³²P] ATP were found to be limited within the rat hepatocytes, while no silver spots were found in the hepatosinus and central vein (Figure 5). This observation demonstrated that [α -³²P] ATP entered the cold stored rat hepatocytes.

DISCUSSION

Protective effects of exogenous ATP on hypothermically preserved rat livers

Up to now, some reports have revealed that ATP-MgCl₂ had a protective effect on the therapy of hemorrhagic shock^[7,21], but reports revealing the protective effect of ATP-MgCl₂ on hypothermically preserved transplant organs were few^[22]. The results of this study demonstrated that the intracellular level of ATP in the group containing no ATP-MgCl₂ or the group containing ATP alone decreased rapidly after hypothermic preservation. Simultaneously, the release of intracellular enzymes was increased, indicating severe damages of the membrane functions. Moreover, significant swelling of the hepatocytes and obvious infiltration of neutrophils were found histologically. On the contrary, the intracellular ATP level in the group containing ATP-MgCl₂ was almost maintained at the normal level for quite a long time, and decreased much slower after hypothermic preservation. Furthermore, because of the protective effect of ATP on cell membranes^[23,24], the metabolic function of hepatocytes was restored, and the release of intracellular enzymes (LDH and AST) was significantly inhibited. The histological observations also showed that the swelling of hepatocytes was milder than that in groups B and C. These results suggested that ATP-MgCl₂ could directly provide the energy or energy substrates for intracellular Na⁺-K⁺ ATPase as well as Ca²⁺-ATPase to remain the extracellular and intracellular ion balance^[25-29], and lighten the intracellular acidosis and cell swelling^[21,23]. In addition, ATP-MgCl₂ also had effects on the amelioration of microcirculation, restoration of membrane voltage, restoration of normal membrane permeability and improvement of cellular functions^[30,31].

Together, ATP showed protective effects on cold stored rat livers, and it might be a synthetical effect of multiple actions.

Mechanism of protective effect of ATP on hypothermically preserved rat livers

ATP had a very strong effect on vascular expansion^[7], but our current study demonstrated that exogenous ATP protected cold stored rat livers not through vascular expansion.

If ATP-MgCl₂ protected the cold stored rat livers through vascular expansion, then addition of ATP alone to the perfusate should also exhibit a protective effect. But no protective effect was observed by the addition of ATP alone in our study (Data not shown). Moreover, addition of MgCl₂ alone to the perfusate also showed no protective effect^[21]. Addition of ADP-MgCl₂ complex, which has a more effective action of vascular expansion, showed no protective effect as ATP-MgCl₂ (Data not shown). An even more important finding was that, ATP-MgCl₂ could enter cold stored rat liver cells in our study. This also directly confirmed that exogenous ATP-MgCl₂ could protect cold stored rat livers through the intracellular mechanism. By our knowledge, no report has revealed that exogenous ATP could enter hepatocytes through the membrane, and the mechanism is still unclear. We suspect that the possible pathway might be considered as followings. First, as ATP is a large biomolecule, the membrane is impermeable to it under normal status. But the permeability is increased to ATP due to the activation of some membrane carrier proteins by hypothermia and anoxia. Second, ATP enters hepatocytes through the disrupted hepatocyte membrane. In addition, how does ATP play the protective effect after entering the cells is still poorly understood.

Taken together, these results indicate that exogenous ATP-MgCl₂ could protect cold stored livers through an intracellular rather than an extracellular mechanism.

Participation of Mg²⁺ in protection of cold stored rat livers by exogenous ATP

As we know, ATP could form chelate with other extracellular bivalent cations (Ca²⁺, Sr²⁺, Mg²⁺, etc.). However, addition of ATP-MgCl₂ complex could inhibit the dephosphorylation and deamino action of ATP, suppress the extracellular hydrolysis of ATP, and prevent the different dynamic effects by interaction of ATP and other extracellular cations^[32]. The other possible reason may be that participation of Mg²⁺ may be required while

ATP goes through the cell membrane. The carrier protein has been found on the intima of mitochondria. The functional mechanism was found to be: $\text{ATP-Mg}^{2+}_{\text{out}} + \text{HPO}_4^{2-}_{\text{in}} \rightleftharpoons \text{ATP-Mg}^{2+}_{\text{in}} + \text{HPO}_4^{2-}_{\text{out}}$ [33]. Further investigation is needed to confirm whether there is such a carrier protein on the outside membrane of hepatocytes or not, and whether ATP enters hepatocytes by interaction with Mg^{2+} or not. In addition, there is also the possibility that, as a co-factor of many intracellular functions, Mg^{2+} could participate in a diverse of ATP dependent intracellular actions, such as $\text{Na}^+ - \text{K}^+$ ATPase, Ca^{2+} -ATPase, and glycolysis [34].

In summary, the results of the current study suggest that exogenous ATP could protect cold stored rat livers by entering hepatocytes. ATP- MgCl_2 should be a pivotal component in the hypothermic preservation solution. Further study is required to clarify the protective mechanism of ATP on cold stored organs, which may contribute to the development of hypothermic preservation solution.

REFERENCES

- 1 **Marubayashi S**, Takenaka M, Dohi K, Ezaki H, Kawasaki T. Adenosine nucleotide metabolism during hepatic ischemia and subsequent blood reflow periods and its relation to organ viability. *Transplantation* 1980; **30**: 294-296
- 2 **Lanir A**, Jenkins RL, Caldwell C, Lee RG, Khettry U, Clouse ME. Hepatic transplantation survival: correlation with adenine nucleotide level in donor liver. *Hepatology* 1988; **8**: 471-475
- 3 **Takesue M**, Maruyama M, Shibata N, Kunieda T, Okitsu T, Sakaguchi M, Totsugawa T, Kosaka Y, Arata A, Ikeda H, Matsuoka J, Oyama T, Kodama M, Ohmoto K, Yamamoto S, Kurabayashi Y, Yamamoto I, Tanaka N, Kobayashi N. Maintenance of cold-preserved porcine hepatocyte function with UW solution and ascorbic acid-2 glucoside. *Cell Transplant* 2003; **12**: 599-606
- 4 **Bowers JL**, Teramoto K, Khettry U, Clouse ME. ³¹P NMR assessment of orthotopic rat liver transplantation viability. The effect of warm ischemia. *Transplantation* 1992; **54**: 604-609
- 5 **Wu XT**, Li JS, Zhao XF, Zhuang W, Feng XL. Modified techniques of heterotopic total small intestinal transplantation in rats. *World J Gastroenterol* 2002; **8**: 758-762
- 6 **Glynn IM**. Membrane adenosine triphosphate and cation transport. *Br Med Bull* 1968; **24**: 165-169
- 7 **Chaudry IH**, Baue AE. Further evidence for ATP uptake by rat tissues. *Biochim Biophys Acta* 1980; **628**: 336-342
- 8 **Chaudry IH**, Sayeed MM, Baue AE. Evidence for enhanced uptake of ATP by liver and kidney in hemorrhagic shock. *Am J Physiol* 1977; **233**: R83-R88
- 9 **Forrester T**. An estimate of adenosine triphosphate release into the venous effluent from exercising human forearm muscle. *J Physiol* 1972; **224**: 611-628
- 10 **Miyata M**, Fischer JH, Fuhs M, Isselhard W, Kasai Y. A simple method for orthotopic liver transplantation in the rat cuff technique for three vascular anastomoses. *Transplantation* 1980; **30**: 335-338
- 11 **Kobayashi E**, Kamada N, Goto S, Miyata M. Protocol for the technique of orthotopic liver transplantation in the rat. *Micorsurgery* 1993; **14**: 541-546
- 12 **Jiang Y**, Gu XP, Qiu YD, Sun XM, Chen LL, Zhang LH, Ding YT. Ischemic preconditioning decreases C-X-C chemokine expression and neutrophil accumulation early after liver transplantation in rats. *World J Gastroenterol* 2003; **9**: 2025-2029
- 13 **Hoffmann RM**, Southard JH, Lutz M, Mackety A, Belzor FO. Synthetic Perfusate for Kidney Preservation. Its use in 72-hour preservation of dog kidneys. *Arch Surg* 1983; **118**: 919-921
- 14 **Tamaki T**, Kamada N, Wight DG, Pegg DE. Successful 48-hour preservation of the rat liver by continuous hypothermic perfusion with haemacel-isotonic citrate solution. *Transplantation* 1987; **43**: 468-471
- 15 **Li YS**, Li JS, Li N, Jiang ZW, Zhao YZ, Li NY, Liu FN. Evaluation of various solutions for small bowel graft preservation. *World J Gastroenterol* 1998; **4**: 140-143
- 16 **Cheng XD**, Jiang XC, Liu YB, Peng CH, Xu B, Peng SY. Effect of ischemic preconditioning on P-selectin expression in hepatocytes of rats with cirrhotic ischemia-reperfusion injury. *World J Gastroenterol* 2003; **9**: 2289-2292
- 17 **Sun B**, Jiang HC, Piao DX, Qian HQ, Zhang L. Effects of cold preservation and warm reperfusion on rat fatty liver. *World J Gastroenterol* 2000; **6**: 271-274
- 18 **Zhu XH**, Qiu YD, Shen H, Shi MK, Ding YT. Effect of matriline on Kupffer cell activation in cold ischemia reperfusion injury of rat liver. *World J Gastroenterol* 2002; **8**: 1112-1116
- 19 **Yang YL**, Dou KF, Li KZ. Influence of intrauterine injection of rat fetal hepatocytes on rejection of rat liver transplantation. *World J Gastroenterol* 2003; **9**: 137-140
- 20 **Pimlott SL**, Piggott M, Owens J, Grealley E, Court JA, Jaros E, Perry RH, Perry EK, Wyper D. Nicotinic Acetylcholine Receptor Distribution in Alzheimer's Disease, Dementia with Lewy Bodies, Parkinson's Disease, and Vascular Dementia: *In Vitro* Binding Study Using 5-[(125)I]-A-85380. *Neuropsychopharmacology* 2004; **29**: 108-116
- 21 **Ohkawa M**, Clemens MG, Chaudry IH. Studies on the mechanism of beneficial effects of ATP- MgCl_2 following hepatic ischemia. *Am J Physiol* 1983; **244**: R695-702
- 22 **Lytton B**, Vaisbort VB, Glazier WB, Chaudry IH, Baue AE. Improved renal function using adenosine triphosphate-magnesium chloride in preservation of canine kidneys subjected to warm ischemia. *Transplantation* 1981; **31**: 187-189
- 23 **Hayashi H**, Chaudry IH, Clemens MG, Hull MJ, Baue AE. Reoxygenation injury in isolated hepatocytes: effect of extracellular ATP on cation homeostasis. *Am J Physiol* 1986; **250** (4 Pt 2): R573-579
- 24 **Stanca C**, Jung D, Meier PJ, Kullak-Ublick GA. Hepatocellular transport proteins and their role in liver disease. *World J Gastroenterol* 2001; **7**: 157-169
- 25 **Tanioka Y**, Kuroda Y, Kim Y, Matsumoto S, Suzuki Y, Ku Y, Fujita H, Saitoh Y. The effect of ouabain (inhibitor of an ATP-dependent Na^+ / K^+ pump) on the pancreas graft during preservation by the two-layer method. *Transplantation* 1996; **62**: 1730-1734
- 26 **Southard JH**, van Gulik TM, Ametani MS, Vreugdenhil PK, Lindell SL, Pienaar BL, Belzer FO. Important components of the UW solution. *Transplantation* 1990; **49**: 251-257
- 27 **Neveux N**, De Bandt JP, Fattal E, Hannoun L, Poupon R, Chaumeil JC, Delattre J, Cynober LA. Cold preservation injury in rat liver: effect of liposomally-entrapped adenosine triphosphate. *J Hepatol* 2000; **33**: 68-75
- 28 **Janicki PK**, Wise PE, Belous AE, Pinson CW. Interspecies differences in hepatic Ca^{2+} -ATPase activity and the effect of cold preservation on porcine liver Ca^{2+} -ATPase function. *Liver Transpl* 2001; **7**: 132-139
- 29 **Belous A**, Knox C, Nicoud IB, Pierce J, Anderson C, Pinson CW, Chari RS. Reversed activity of mitochondrial adenine nucleotide translocator in ischemia-reperfusion. *Transplantation* 2003; **27**: 1717-1723
- 30 **Chaudry IH**. Cellular mechanisms in shock and ischemia and their correction. *Am J Physiol* 1983; **245**: R117-134
- 31 **Mahmoud MS**, Wang P, Chaudry IH. Salutary effects of ATP- MgCl_2 on altered hepatocyte signal transduction after hemorrhagic shock. *Am J Physiol* 1997; **272** (6 Pt 1): G1347-1354
- 32 **Hirasawa H**, Chaudry IH, Baue AE. Improved hepatic function and survival with adenosine triphosphate-magnesium chloride after hepatic ischemia. *Surgery* 1978; **83**: 655-662
- 33 **Joyal J L**, Aprille J R. The ATP-Mg/Pi carrier of rat liver mitochondria catalyzes a divalent electroneutral exchange. *J Biol Chem* 1992; **267**: 19198-19203
- 34 **Zakaria M**, Brown PR. High performance liquid column chromatography of nucleotides, nucleosides and bases. *J Chromatogr* 1981; **226**: 267-290

• BASIC RESEARCH •

Levels of vasoactive intestinal peptide, cholecystokinin and calcitonin gene-related peptide in plasma and jejunum of rats following traumatic brain injury and underlying significance in gastrointestinal dysfunction

Chun-Hua Hang, Ji-Xin Shi, Jie-Shou Li, Wei Wu, Wei-Qin Li, Hong-Xia Yin

Chun-Hua Hang, Ji-Xin Shi, Wei Wu, Hong-Xia Yin, Department of Neurosurgery, Jinling Hospital, School of Medicine, Nanjing University, Nanjing 210002, Jiangsu Province, China

Jie-Shou Li, Wei-Qin Li, Research Institute of General Surgery, Jinling Hospital, School of Medicine, Nanjing University, Nanjing 210002, Jiangsu Province, China

Supported by the Scientific Research Foundation of the Chinese PLA Key Medical Programs during the 10th Five-Year Plan Period, No. 01Z011

Correspondence to: Dr. Chun-Hua Hang, Department of Neurosurgery, Jinling Hospital, 305 East Zhongshan Road, Nanjing 210002, Jiangsu Province, China. hang1965@public1.ptt.js.cn

Telephone: +86-25-80860010 **Fax:** +86-25-84810987

Received: 2003-10-31 **Accepted:** 2003-12-16

Abstract

AIM: To study the alterations of brain-gut peptides following traumatic brain injury (TBI) and to explore the underlying significance of these peptides in the complicated gastrointestinal dysfunction.

METHODS: Rat models of focal traumatic brain injury were established by impact insult method, and divided into 6 groups (6 rats each group) including control group with sham operation and TBI groups at postinjury 3, 12, 24, 72 h, and d 7. Blood and proximal jejunum samples were taken at time point of each group and gross observations of gastrointestinal pathology were recorded simultaneously. The levels of vasoactive intestinal peptide (VIP) in plasma, calcitonin gene-related peptide (CGRP) and cholecystokinin (CCK) in both plasma and jejunum were measured by enzyme immunoassay (EIA). Radioimmunoassay (RIA) was used to determine the levels of VIP in jejunum.

RESULTS: Gastric distension, delayed gastric emptying and intestinal dilatation with a large amount of yellowish effusion and thin edematous wall were found in TBI rats through 12 h and 72 h, which peaked at postinjury 72 h. As compared with that of control group (247.8±29.5 ng/L), plasma VIP levels were significantly decreased at postinjury 3, 12 and 24 h (106.7±34.1 ng/L, 148.7±22.8 ng/L, 132.8±21.6 ng/L, respectively), but significantly increased at 72 h (405.0±29.8 ng/L) and markedly declined on d 7 (130.7±19.3 ng/L). However, Plasma levels CCK and CGRP were significantly increased through 3 h and 7 d following TBI (126-691% increases), with the peak at 72 h. Compared with control (VIP, 13.6±1.4 ng/g; CGRP, 70.6±17.7 ng/g); VIP and CGRP levels in jejunum were significantly increased at 3 h after TBI (VIP, 35.4±5.0 ng/g; CGRP, 103.8±22.1 ng/g), and declined gradually at 12 h and 24 h (VIP, 16.5±1.8 ng/g, 5.5±1.4 ng/g; CGRP, 34.9±9.7 ng/g, 18.5±7.7 ng/g), but were significantly increased again at 72 h (VIP, 48.7±9.5 ng/g; CGRP, 142.1±24.3 ng/g), then declined in various

degrees on d 7 (VIP, 3.8±1.1 ng/g; CGRP, 102.5±18.1 ng/g). The CCK levels in jejunum were found to change in a similar trend as that in plasma with the concentrations of CCK significantly increased following TBI (99-517% increases) and peaked at 72 h.

CONCLUSION: Traumatic brain injury can lead to significant changes of brain-gut peptides in both plasma and small intestine, which may be involved in the pathogenesis of complicated gastrointestinal dysfunction.

Hang CH, Shi JX, Li JS, Wu W, Li WQ, Yin HX. Levels of vasoactive intestinal peptide, cholecystokinin and calcitonin gene-related peptide in plasma and jejunum of rats following traumatic brain injury and underlying significance in gastrointestinal dysfunction. *World J Gastroenterol* 2004; 10(6): 875-880

<http://www.wjgnet.com/1007-9327/10/875.asp>

INTRODUCTION

Gastrointestinal dysfunction occurs frequently in patients with traumatic brain injury (TBI)^[1-3]. More than 50% patients with severe head injuries do not tolerate enteral feedings^[4]. This intolerance is manifested by vomiting, abdominal distention, delayed gastric emptying^[5,6], esophageal reflux^[7] and decreased intestinal peristalsis^[8], indicating that gastrointestinal dysfunction is a common phenomenon following TBI. The association of severity of brain injury with the intolerance of enteral feeding suggests a strong link between the central nervous system and the nonfunctioning gut. However, the precise mechanism of gastrointestinal dysfunction following TBI has not been reported to date and remains to be interpreted.

Gastrointestinal motility is mainly regulated by two factors including humoral hormones and nervous transmitters from both central nervous system and peripheral enteric nervous system^[9]. Brain-gut peptides possess two functions as mentioned above, *e.g.*, exerting action on gastrointestinal motility via both endocrine hormones and peptidergic transmitters. These peptides also play their roles in modulation of the gastrointestinal motility through central nervous system, which is a part of brain-gut interaction^[10]. Recent studies have indicated that some disorders of gastrointestinal motility following sepsis^[11-13], trauma^[14], surgery^[15-17], chronic stress^[18] and experimental spleen deficiency^[19] are related to brain-gut peptides, such as cholecystokinin (CCK), vasoactive intestinal peptide (VIP), calcitonin gene-related peptide (CGRP), neuropeptide Y (NPY) and substance P (SP), suggesting that brain-gut peptides are important mediators in the regulation of gastrointestinal motility^[20-22]. Until now, no study has been made to investigate the relationship between brain-gut peptides and gastrointestinal dysmotility following TBI. Therefore, we hypothesized that TBI could induce marked alterations of

brain-gut peptides in both plasma and gut, which could be involved in the pathogenesis of complicated gastrointestinal dysfunction.

Brain-gut peptides as modulatory mediators appear to be major components of bodily integration and have important regulatory actions on physiological function of gastrointestinal tract. Increasing studies have demonstrated that VIP^[14,17,19,23], CCK^[12,20,21] and CGRP^[11,15,16,24] play important protective role in regulation of blood flow, cell differentiation, immune function and secretion of digestive glands. On the other hand, they have an adverse effect on the gut motility^[11-19]. It is also well known that VIP, CCK and CGRP are located in both central nervous system (CNS) and peripheral enteric nervous system, and mainly exert inhibitory action on gut motility^[16-21,24]. Several kinds of stress, such as trauma, cold, restraint and pain, can induce the release of these brain-gut peptides from CNS and enteric nerve^[14,18], and the alterations of relevant receptors in the gut^[19] to induce the gastrointestinal dysmotility. However, it is unknown how these peptides change and what the underlying significance of these changes is in the gastrointestinal dysmotility following TBI. Further insights into the alterations of brain-gut peptides following TBI may provide new therapeutic opportunities for the gastrointestinal dysfunction complicating head trauma. In current study, rat models of TBI were made to measure the alterations of VIP, CCK and CGRP in both plasma and jejunum and to investigate the underlying role of brain-gut peptides in gastrointestinal dysfunction.

MATERIALS AND METHODS

Rat models of TBI

Male Wistar rats, weighing from 220 to 250 g, were purchased from Animal Center of Chinese Academy of Science, Shanghai, China. The rats were fed rodent chow with free access to tap water and housed in temperature- and humidity-controlled animal quarters with 12 h light/dark cycle. All procedures were approved by the Institutional Animal Care Committee.

The rats were randomly divided into six groups (6 rats/group) including control group with right parietal bone window alone and no brain injury, and TBI groups at h 3, 12, 24 and 72, and day 7, respectively. Following intraperitoneal anesthesia with urethane (1 000 mg/kg), animal head was fixed in the stereotactic device. A right parietal bone window of 5 mm in diameter was made under aseptic conditions with dental drill just behind cranial coronal suture and beside midline. The dura was kept intact. Right parietal brain contusion was adopted from the impact method described by Feeney *et al.*^[25] and severe traumatic brain injury was made by dropping weight with impact diameter of 4 mm, depth of 5 mm and total impact energy of 1 000 g·cm. The control animals were killed for sample collection at 72 h, and TBI group rats were decapitated at corresponding time point. Blood samples were obtained by right ventricle puncture and centrifuged with the plasma stored at -40 °C for further analysis. A segment of the jejunum 15 cm distal to Treitz ligament was taken, rinsed and weighed, then were put into a tube with 1 mL saline water. The tube was plunged into vigorous boiling water and boiled for 3 min, and then all layers of jejunum sample and 0.5 mL of 1 mol/L glacial acetic acid were added to a homogenizer to be homogenized for 10 min. The 0.5 mL of 1 mol/L NaOH was mixed with the homogenized sample. After centrifugation at 3 000 r/min for 5 min at low temperature, the supernatant was collected and stored at -40 °C until assay of brain-gut peptides.

Assay analysis of VIP, CCK and CGRP in plasma

The concentrations of VIP, CCK and CGRP in plasma samples were measured by enzyme immunoassay (EIA) with commercially available kits according to the manufacturer's

instructions. Peptides [VIP (S-80039), CCK (S-80013-B), α -CGRP (S-80011-R)] were purchased from AOR Diagnostics, USA. The minimum detectable concentration for VIP, CCK and α -CGRP was 0.06-0.08 ng/L of sample with intra- and inter-assay variation less than 6% and 15% respectively. There was 25% cross-reaction with β -CGRP.

Assay analysis of VIP, CCK and CGRP in jejunum samples

VIP levels in jejunum were determined by radioimmunoassay (RIA) with the kit purchased from Beijing Huayin Biotechnology Institute, China. The concentrations of CCK and CGRP in all layers of jejunum were measured by EIA as mentioned above. The protein concentration of jejunum samples was determined by using a bicinchoninic acid assay kit with bovine serum albumin as the standard (Pierce Biochemicals, Rockford, IL).

Statistical analysis

Software SPSS 11.0 was used in the statistical analysis. Parameters were expressed as mean \pm SD, and compared using one-way ANOVA analysis of variance, followed by Tukey test. Statistical significance was determined at $P < 0.05$.

RESULTS

Gross observations of gastrointestinal pathology

Gastrointestinal tract was found to be nearly normal in rats of control group and TBI 3 hour group (Figure 1A). In TBI groups at 12, 24 and 72 h postinjury, gastric distention and intestinal dilatation with a large amount of yellowish effusion existing within intestinal cavity were found, and intestinal wall became thinner and edematous (Figures 1B and 1C), suggesting that delayed gastric emptying and paralytic ileus occurred following TBI. The above mentioned pathological changes culminated at 72 h following TBI. On d 7 postinjury, small intestine was found to become thin and slender, suggesting that an atrophy in the gut occurred (Figure 1D).

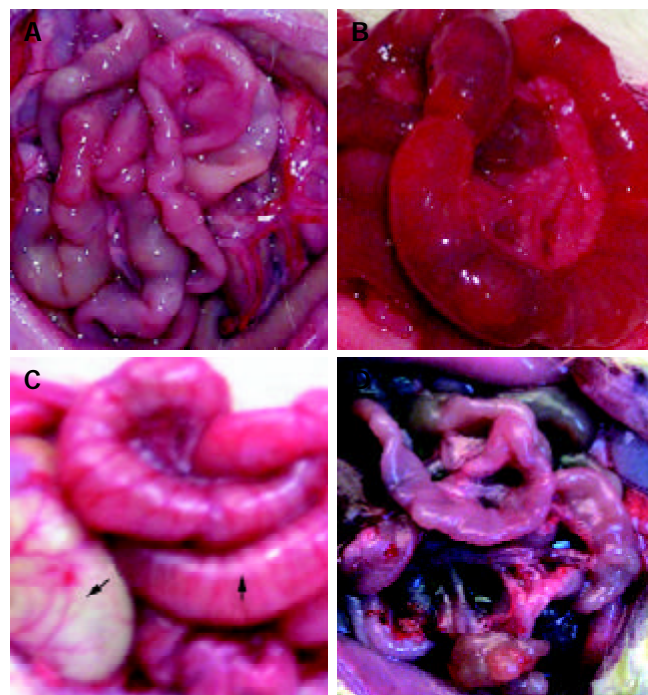


Figure 1 Gross observation of intestinal pathology was shown as A, B, C and D. A: nearly normal morphology at TBI 3 h; B: intestinal dilation with large amount of yellowish effusion and thin edematous wall at 72 h following TBI; C: gastrointestinal distention at 72 h following TBI, stomach indicated by solid arrow and intestine by blank arrow; D: gastrointestinal atrophy on day 7 following TBI.

Levels of VIP, CCK and CGRP in plasma

As compared with that of control group (247.8 ± 29.5 ng/L), plasma VIP levels were significantly decreased at 3, 12 and 24 h postinjury (106.7 ± 34.1 ng/L, 148.7 ± 22.8 ng/L, 132.8 ± 21.6 ng/L, respectively), but significantly increased at 72 h (405.0 ± 29.8 ng/L) and declined markedly on d 7 (130.7 ± 19.3 ng/L) (Figure 2). However, Plasma levels CCK and CGRP were significantly increased through 3 h and 7 d following TBI (126–691% increases), with the peak at 72 h (Figures 3 and 4).

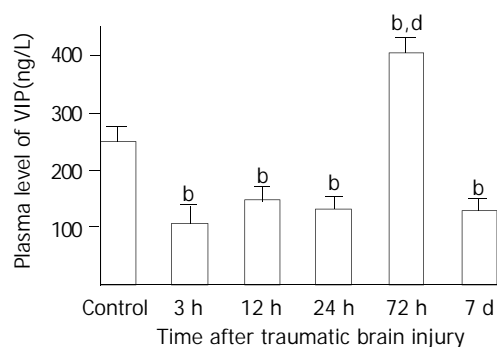


Figure 2 Alteration of VIP in plasma after TBI. Compared with control, plasma level of VIP was significantly decreased at 3, 12 and 24 h postinjury, but was significantly increased at 72 h, then declined to a low level on d 7 with the value similar to that of groups of 3 h, 12 h and 24 h. ^b $P < 0.01$ vs control; ^d $P < 0.01$ vs 3 h, 12 h, 24 h and 7 d.

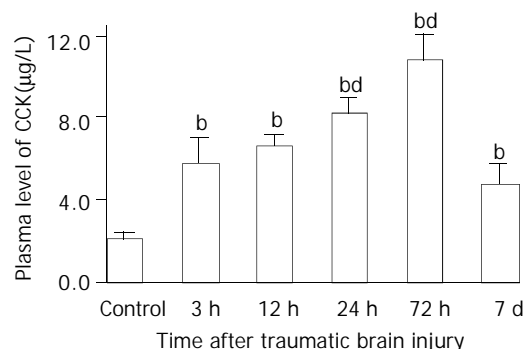


Figure 3 Alteration of CCK in plasma after TBI. Compared with control, plasma level of CCK was significantly increased postinjury, and peaked at 72 h, then declined to some degree on d 7, but was still significantly higher than that of control. ^b $P < 0.01$ vs control; ^d $P < 0.01$ vs 3 h. Mean ± SD of 6 animals, control: 2.1 ± 0.3 μg/L, 3 h: 5.8 ± 1.2 μg/L, 12 h: 6.7 ± 0.5 μg/L, 24 h: 8.3 ± 0.7 μg/L, 72 h: 10.8 ± 1.2 μg/L, 7 d: 4.8 ± 0.9 μg/L.

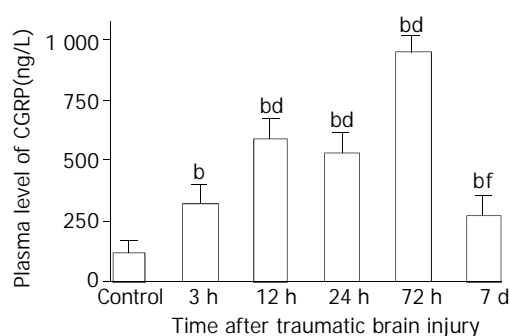


Figure 4 Alteration of CGRP in plasma after TBI. Compared with control, plasma level of CGRP was significantly increased postinjury, and peaked at 72 h, then declined obviously on d 7 with the value still significantly higher than that of control. ^b $P < 0.01$ vs control; ^d $P < 0.01$ vs 3 h; ⁱ $P < 0.01$ vs 12 h, 24 h and 72 h.

Mean ± SD of 6 animals, control: 120.8 ± 47.7 ng/L, 3 h: 323.8 ± 75.9 ng/L, 12 h: 596.7 ± 82.7 ng/L, 24 h: 536.0 ± 77.2 ng/L, 72 h: 955.0 ± 63.0 ng/L, 7 d: 273.3 ± 83.8 ng/L.

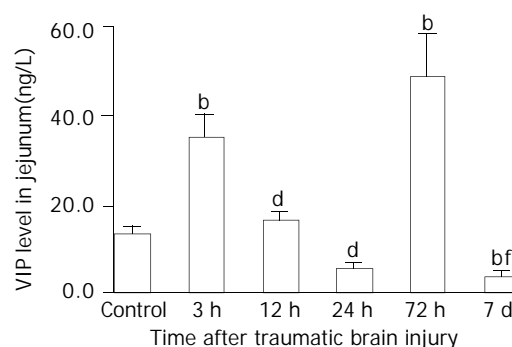


Figure 5 Alteration of VIP levels in all layers of jejunum after TBI. Compared with control, the level of VIP was significantly increased at 3 h following TBI, then declined markedly at 12 h and 24 h, and was significantly increased again at 72 h, but was at its lowest level on day 7 postinjury. ^b $P < 0.01$ vs control; ^d $P < 0.01$ vs 3 h; ⁱ $P < 0.01$ vs 3 h and 12 h.

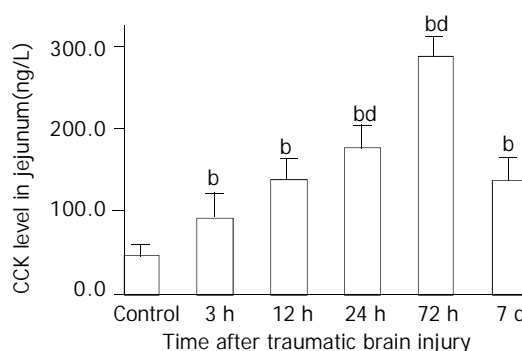


Figure 6 Alteration of CCK levels in all layers of jejunum after TBI. The level of CCK was significantly increased after TBI as compared with that of control, and peaked at 72 h postinjury, then declined to some degree but was still significantly higher than that of control on d 7. ^b $P < 0.01$ vs control; ^d $P < 0.01$ vs 3 h. Mean ± SD of 6 animals, control: 46.5 ± 13.9 ng/g, 3 h: 92.6 ± 28.7 ng/g, 12 h: 139.8 ± 24.7 ng/g, 24 h: 178.5 ± 25.8 ng/g, 72 h: 286.8 ± 25.9 ng/g, 7 d: 137.8 ± 27.3 ng/g.

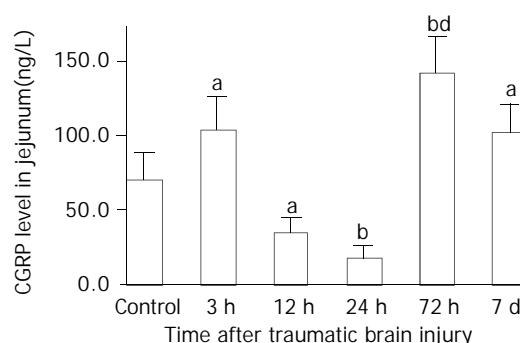


Figure 7 Alteration of CGRP levels in all layers of jejunum after TBI. Compared with control group, the level of CGRP was significantly increased at 3 h, then declined significantly at 12 h and 24 h, and significantly increased again at 72 h postinjury, then declined on d 7, but was still significantly higher than that of control. ^a $P < 0.05$ vs control; ^b $P < 0.01$ vs control; ^d $P < 0.01$ vs 3 h, 12 h, 24 h and 7 d.

Levels of VIP, CCK and CGRP in jejunum

As compared with that of control group (VIP, 13.6 ± 1.4 ng/g;

CGRP, 70.6 ± 17.7 ng/g), VIP and CGRP levels in jejunum were increased significantly at 3 h after TBI (VIP, 35.4 ± 5.0 ng/g; CGRP, 103.8 ± 22.1 ng/g, $P < 0.01$), then declined gradually at 12 h and 24 h (VIP, 16.5 ± 1.8 ng/g, 5.5 ± 1.4 ng/g; CGRP, 34.9 ± 9.7 ng/g, 18.5 ± 7.7 ng/g), but were significantly increased again at 72 h postinjury (VIP, 48.7 ± 9.5 ng/g; CGRP, 142.1 ± 24.3 ng/g, $P < 0.01$). The VIP level declined to a significantly low level on d 7 (3.8 ± 1.1 ng/g) (Figure 5), otherwise, CGRP declined to the level close to that of TBI 3 h group (102.5 ± 18.1 ng/g) (Figure 7). The CCK levels in jejunum were found to change in a similar trend as that in plasma with the concentrations of CCK significantly increased (99-517% increases) from 3 h to 7 d following TBI and peaked at 72 h (Figure 6).

DISCUSSION

TBI is a critically ill condition resulting in metabolic and immune alterations, inflammatory response and disturbance of gastrointestinal peptides via hypothalamo-pituitary-adrenal axis and brain-gut axis^[10,26]. Therefore, TBI can lead to disturbance of peptidergic mediators as a result of systemic stress with the same mechanism as occurred in trauma, sepsis, surgery and burns^[11-17]. Brain-gut peptides possess many biological functions such as dilating vessels, improving focal blood flow perfusion, regulating immune action and relaxing smooth muscle of trachea^[13,27,28]. The present study shows that brain-gut peptides VIP, CCK and CGRP change significantly following TBI in both plasma and jejunum, behave in different manner and partly adapt to the systemic pathophysiological needs. Our data suggest that levels of CCK in plasma and jejunum tissue change in parallel and increase gradually following TBI, with a maximum at 72 h postinjury. By contrast, VIP and CGRP levels in plasma and in jejunum tissue show non-parallel fluctuations. Nevertheless, concentrations of all neurohormonal mediators peak at 72 h postinjury, which coincides with the maximal morphological alterations occurring in the gut following TBI^[29]. High level of VIP, CCK and CGRP in plasma implies a large amount of release of these peptides into circulation from nerve ending due to systemic stress. Decreased VIP and CGRP level in plasma and/or jejunum may be related to the low synthesis, depletion of secretion, more binding to the relevant receptors, reduced tissue perfusion of blood flow and cell edema.

On the other hand, obvious alterations of VIP, CCK and CGRP may play an important role in gastrointestinal dysmotility induced by TBI, mainly because brain-gut peptides involved in the endocrine and enteric nervous systems as well as in the central nervous system are the important factors in the regulation of gastrointestinal motility through pathways of endocrine, paracrine or neurocrine. CCK exerts action mainly via endocrine, otherwise, VIP and CGRP mainly via neurocrine^[9]. Mechanic and chemical stimuli which induce peptide release from the epithelial endocrine cells are the earliest step in the initiation of peristaltic activities. The dorsal vagal complex (DVC), located in the medulla of brainstem, constitutes the basic neural circuit of vago-vagal reflex control of gastrointestinal motility^[9]. Several gut peptides act on the DVC to modify the vagal cholinergic reflexes directly (VIP and CGRP) or indirectly via the afferent fibers in the peripheral (CCK). The DVC is also a primary site of action of many neuropeptides in mediating gastrointestinal motor activities (TRH and NPY). More and more evidences have shown that there is a complicated bidirectional inter-relationship between nervous system and gastrointestinal tract^[30]. Gastrointestinal signals produced during chronic stress and colitis can be transmitted into central nervous system (CNS) and influence the function of the latter. In turn, CNS can modulate the electrical activity of gastrointestinal tract, as occurred in TBI.

VIP is a 28 amino acid neurotransmitter peptide that is widely distributed, particularly in the central and peripheral nervous systems, with a broad spectrum of biological actions mediated by stimulation of parasympathetic nerves coinciding with tissue responses. VIP is one of main inhibitory nervous transmitters located in the gut, which induces relaxation of intestinal smooth muscle and sphincters, dilation of peripheral blood vessels and inhibition of gastric acid secretion. Additionally, *in vivo* studies showed VIP could protect lung, retina, heart, kidney and stomach from the harmful effects of inflammation, ischemia-reperfusion injury and glutamate-induced cell death^[27,31]. It also increases survival rate of animals exposed to severe septic and hemorrhagic shock^[32]. VIP is a nonadrenergic noncholinergic nervous transmitter, and exerts inhibitory action on gastrointestinal motility through its binding to the relevant receptors located in gastrointestinal tract and subsequent activation of cyclic AMP-dependent protein kinase. VIP neurons occupy 40% of submucosal neurons of rat small intestine^[33]. In the intestine, VIP markedly stimulates intestinal secretion of electrolytes and hence of water. The results of this study showed that VIP level in both plasma and jejunum was increased significantly at 72 h following TBI. Increased concentrations of VIP in plasma and jejunum might be responsible for the intestinal dilation and large amounts of intra-intestinal effusion as shown in Figure 1 B and C. From 12 h to 24 h following TBI, VIP concentrations in both plasma and jejunum were decreased significantly due to binding to receptors and low synthesis, which was partially responsible for the acute gastrointestinal mucosal damage induced by ischemia.

CCK is involved in the endocrine cells in the upper small intestine, principally acting to stimulate gallbladder contractions^[34] and pancreatic secretion^[35], and to delay gastric emptying after meals^[26]. Evidence has shown that CCK, stimulated by nutrients, is a physiological mediator which inhibits gastric emptying and subsequently suppresses food intake^[26]. CCK mainly reduces the tone of lower esophageal sphincter, inhibits the peristalsis of proximal duodenum and promotes the peristalsis of distal duodenum and jejunum via activation of Ca^{2+} -dependent protein kinase. Previous studies have demonstrated that CCK could increase the mean contractile amplitude of antral circular muscle, motility index of pyloric circular muscle and the resting tension of fundus^[21,24,36,37]. Therefore, CCK possesses both excitatory and inhibitory action on contractile activity of different regions of stomach. Since systemic administration of CCK increases vagal afferent activity^[27] and this effect is blocked by the disruption of vagal capsaicin-sensitive afferent fibers, it has been suggested that CCK acts on the vagal afferent neurons and induces gastric relaxation^[28] and CCK-A receptor mediates this action^[30,38]. CCK exerts an inhibitory function on the colonic motility, which is mediated by CCK-A receptors^[39]. Besides the effects of CCK on the digestive tract, other biological actions of this peptide have been observed, such as appetite inhibition^[40], prevention of LPS-induced decrease of blood pressure and attenuation of LPS-induced increase of proinflammatory cytokines (TNF- α , IL-1 β and IL-6) *in vivo*^[12]. The current study showed that the levels of CCK in both plasma and jejunum were increased significantly following TBI, suggesting that CCK may play an important role in protection of splanchnic functions. Conversely, increased concentrations of CCK in plasma and jejunum might be highly responsible for the gastric emptying dysfunction^[20, 41-44] and esophageal reflux which usually occur after head trauma^[1,6,7] through the mechanism as mentioned above. Gastric distention was found in rats at 12, 24 and 72 h following TBI, as shown in Figure 1, possibly due to the inhibitory action of persistently high CCK concentrations on the stomach contraction.

CGRP is a 37 amino acid neurotransmitter peptide that is widely distributed in the central and peripheral nervous

systems^[11,28,45], particularly in the viscera and vascular adventitia. It can also be synthesized and released by lymphocytes in rats^[46]. CGRP in blood mainly comes from the gut and vessels. CGRP may be released extensively from the nerve ending around vessels into circulation through organ stimuli such as endotoxin, inflammatory mediators, stress and intestinal ischemia-reperfusion injury in the rat^[11,13,47]. Endotoxemia, inflammatory cytokines and other kinds of stress can also stimulate the synthesis of CGRP in spinal dorsal root ganglia neurons (DRG). Therefore, TBI can also induce the extensive release of CGRP into plasma and synthesis of CGRP in jejunum as demonstrated in this study. CGRP possesses extensive biological functions such as cardiogenic effect, dilating vessels and regulating immune system^[11]. It has been previously shown that CGRP is one of the important mediators involved in the pathogenesis of infection, hemorrhage and trauma, and also is one of the mediators for the interactions of neural-immune systems. Recently, the involvement of CGRP in abdominal surgery-induced inhibition of gastric and colonic motility has been reported^[15]. The postoperative gastric ileus is mediated by CGRP released from spinal afferent neurons in the celiac and superior mesenteric ganglia as part of an extra-spinal gastrointestinal inhibitory reflex pathways^[15,16]. This study demonstrated that the CGRP concentration in plasma was increased persistently after TBI. Increased level of CGRP in plasma following TBI may contribute to the decreased tone of lower esophageal sphincter, delayed gastric emptying and paralytic ileus of small intestine. Decreased concentrations of CGRP in jejunum may be responsible for the ischemic damage of gut mucosa. The mechanism of CGRP inhibiting gastrointestinal motility includes: (1) CGRP is released into local gut tissue or circulation, and then binds to the relevant receptors located on the surface of gastrointestinal smooth muscle to exert inhibitory action; (2) CGRP, acting as a part of inhibitory spinal reflex, is released into local gut induced by all kinds of stress factors to activate spinal afferent nerve fibers, leading to decreased gastrointestinal motility^[15]; (3) CGRP can promote the release of substance P which partly mediate postoperative intestinal ileus^[17]; (4) CGRP interacts with the receptors on surface of D cells to induce the release of somatostatin, inhibiting gastrointestinal motility; (5) CGRP may slow the transmit of cholinergic nerve fibers of enteric nervous system to inhibit gastrointestinal peristalsis.

It is concluded that the concentrations of VIP, CCK and CGRP in both plasma and jejunum change significantly following TBI. All these data imply that alterations of these peptide concentrations in plasma and gut may be involved in the pathogenesis of gastrointestinal dysfunction after traumatic brain injury. Increased CCK level might be responsible for the delayed gastric emptying, otherwise, VIP and CGRP might be responsible for the paralytic dilation of small intestine and large amounts of intra-intestinal effusion.

ACKNOWLEDGEMENT

We would like to thank Dr. Gen-Bao Feng and Zhong-Shu Zhang for their technical assistance.

REFERENCES

- Jackson MD**, Davidoff G. Gastroparesis following traumatic brain injury and response to metoclopramide therapy. *Arch Phys Med Rehabil* 1989; **70**: 553-555
- Pilitsis JG**, Rengachary SS. Complications of head injury. *Neurol Res* 2001; **23**: 227-236
- Brown TH**, Davidson PF, Larson GM. Acute gastritis occurring within 24 hours of severe head injury. *Gastrointest Endosc* 1989; **35**: 37-40
- Norton JA**, Ott LG, McClain C, Adams L, Dempsey RJ, Haack D, Tibbs PA, Young AB. Intolerance to enteral feeding in the brain-injured patient. *J Neurosurg* 1988; **68**: 62-66
- Mackay LE**, Morgan AS, Bernstein BA. Factors affecting oral feeding with severe traumatic brain injury. *J Head Trauma Rehabil* 1999; **14**: 435-447
- Kao CH**, ChangLai SP, Chieng PU, Yen TC. Gastric emptying in head-injured patients. *Am J Gastroenterol* 1998; **93**: 1108-1112
- Saxe JM**, Ledgerwood AM, Lucas CE, Lucas WF. Lower esophageal sphincter dysfunction precludes safe gastric feeding after head injury. *J Trauma* 1994; **37**: 581-584
- Pedoto MJ**, O'Dell MW, Thrun M, Hollifield D. Superior mesenteric artery syndrome in traumatic brain injury: two cases. *Arch Phys Med Rehabil* 1995; **76**: 871-875
- Rogers RC**, McTigue DM, Hermann GE. Vagal control of digestion: modulation by central neural and peripheral endocrine factors. *Neurosci Biobehav Rev* 1996; **20**: 57-66
- Gue M**, Bueno L. Brain-gut interaction. *Semin Neurol* 1996; **16**: 235-243
- Joyce CD**, Fiscus RR, Wang X, Dries DJ, Morris RC, Prinz RA. Calcitonin gene-related peptide levels are elevated in patients with sepsis. *Surgery* 1990; **108**: 1097-1101
- Ling YL**, Meng AH, Zhao XY, Shan BE, Zhang JL, Zhang XP. Effect of cholecystokinin on cytokines during endotoxic shock in rats. *World J Gastroenterol* 2001; **7**: 667-671
- Wang X**, Jones SB, Zhou Z, Han C, Fiscus RR. Calcitonin gene-related peptide (CGRP) and neuropeptide Y (NPY) levels are elevated in plasma and decreased in vena cava during endotoxin shock in the rat. *Circ Shock* 1992; **36**: 21-30
- Onuoha G**, Alpar K, Jones I. Vasoactive intestinal peptide and nitric oxide in the acute phase following burns and trauma. *Burns* 2001; **27**: 17-21
- Zittel TT**, Lloyd KC, Rothenhofer I, Wong H, Walsh JH, Raybould HE. Calcitonin gene-related peptide and spinal afferents partly mediate postoperative colonic ileus in the rat. *Surgery* 1998; **123**: 518-527
- Zittel TT**, Reddy SN, Plourde V, Raybould HE. Role of spinal afferents and calcitonin gene-related peptide in the postoperative gastric ileus in anesthetized rats. *Ann Surg* 1994; **219**: 79-87
- Espat NJ**, Cheng G, Kelley MC, Vogel SB, Sninsky CA, Hocking MP. Vasoactive intestinal peptide and substance P receptor antagonists improve postoperative ileus. *J Surg Res* 1995; **58**: 719-723
- Chen ZY**, Yan MX, Xiang BK, Zhan HW. Alterations of gut hormones of blood and colonic mucosa in rats with chronic stress. *Shijie Huaren Xiaohua Zazhi* 2001; **9**: 59-61
- Li LS**, Qu RY, Wang W, Guo H. Significance of changes of gastrointestinal peptides in blood and ileum of experimental spleen deficiency rats. *World J Gastroenterol* 2003; **9**: 553-556
- Higham A**, Vaillant C, Yegen B, Thompson DG, Dockray GJ. Relation between cholecystokinin and antral innervation in the control of gastric emptying in the rat. *Gut* 1997; **41**: 24-32
- Li W**, Zheng TZ, Qu SY. Effect of cholecystokinin and secretin on contractile activity of isolated gastric muscle strips in guinea pigs. *World J Gastroenterol* 2000; **6**: 93-95
- Yao YL**, Xu B, Zhang WD, Song YG. Gastrin, somatostatin, and experimental disturbance of the gastrointestinal tract in rats. *World J Gastroenterol* 2001; **7**: 399-402
- Pincus DW**, DiCicco-Bloom EM, Black IB. Vasoactive intestinal peptide regulates mitosis, differentiation and survival of cultured sympathetic neuroblasts. *Nature* 1990; **343**: 564-567
- Maggi CA**, Giuliani S, Zagorodnyuk V. Calcitonin gene-related peptide (CGRP) in the circular muscle of guinea-pig colon: role as inhibitory transmitter and mechanisms of relaxation. *Regul Pept* 1996; **61**: 27-36
- Feeney DM**, Boyeson MG, Linn RT, Murray HM, Dail WG. Responses to cortical injury: I. Methodology and local effects of contusions in the rat. *Brain Res* 1981; **211**: 67-77
- Grundy PL**, Harbuz MS, Jessop DS, Lightman SL, Sharples PM. The hypothalamo-pituitary-adrenal axis response to experimental traumatic brain injury. *J Neurotrauma* 2001; **18**: 1373-1381
- Tuncel N**, Erkasap N, Sahinturk V, Ak DD, Tuncel M. The protective effect of vasoactive intestinal peptide (VIP) on stress-induced gastric ulceration in rats. *Ann N Y Acad Sci* 1998; **865**:

- 309-322
- 28 **Melagros L**, Ghatei MA, Bloom SR. Release of vasodilator, but not vasoconstrictor, neuropeptides and of enteroglucagon by intestinal ischemia/reperfusion in the rat. *Gut* 1994; **35**: 1701-1706
- 29 **Hang CH**, Shi JX, Li JS, Wu W, Yin HX. Alterations of intestinal mucosa structure and barrier function following traumatic brain injury in rats. *World J Gastroenterol* 2003; **9**: 2776-2781
- 30 **Wang X**, Wang BR, Zhang XJ, Xu Z, Ding YQ, Ju G. Evidences for vagus nerve in maintenance of immune balance and transmission of immune information from gut to brain in STM-infected rats. *World J Gastroenterol* 2002; **8**: 540-545
- 31 **Said SI**, Dickman KG. Pathways of inflammation and cell death in the lung: modulation by vasoactive intestinal peptide. *Regul Pept* 2000; **93**: 21-29
- 32 **Delgado M**, Martinez C, Pozo D, Calvo JR, Leceta J, Ganea D, Gomariz RP. Vasoactive intestinal peptide (VIP) and pituitary adenylate cyclase-activation polypeptide (PACAP) protect mice from lethal endotoxemia on through the inhibition of TNF-alpha and IL-6. *J Immunol* 1999; **162**: 1200-1205
- 33 **Pataky DM**, Curtis SB, Buchan AM. The co-localization of neuropeptides in the submucosa of the small intestine of normal Wistar and non-diabetic BB rats. *Neuroscience* 1990; **36**: 247-254
- 34 **Pendleton RG**, Bendesky RJ, Schaffer L, Nolan TE, Gould RJ, Clineschmidt BV. Roles of endogenous cholecystokinin in biliary, pancreatic and gastric function: studies with L-364, 718, a specific cholecystokinin receptor antagonist. *J Pharmacol Exp Ther* 1987; **241**: 110-116
- 35 **Li Y**, Owyang C. Vagal afferent pathway mediates physiological action of cholecystokinin on pancreatic enzyme secretion. *J Clin Invest* 1993; **92**: 418-424
- 36 **Grider JR**, Makhoul GM. Regional and cellular heterogeneity of cholecystokinin receptors mediating muscle contraction in the gut. *Gastroenterology* 1987; **92**: 175-180
- 37 **Gerner T**. Pressure responses to OP-CCK compared to CCK-PZ in the antrum and fundus of isolated guinea-pig stomachs. *Scand J Gastroenterol* 1979; **14**: 73-77
- 38 **Xu MY**, Lu HM, Wang SZ, Shi WY, Wang XC, Yang DX, Yang CX, Yang LZ. Effect of devazepide reversed antagonism of CCK-8 against morphine on electrical and mechanical activities of rat duodenum *in vitro*. *World J Gastroenterol* 1998; **4**: 524-526
- 39 **Hayashi K**, Kishimoto S, Kannbe M. Endogenous CCK inhibits colonic contractions in unrestrained conscious rats. *Regul Pept* 1997; **72**: 131-137
- 40 **Du YP**, Zhang YP, Wang SC, Shi J, Wu SH. Function and regulation of cholecystokinin octapeptide, β -endorphin and gastrin in anorexic infantile rats treated with ErBao Granules. *World J Gastroenterol* 2001; **7**: 275-280
- 41 **Forster ER**, Green M, Elliot M, Bremner A, Dockray GJ. Gastric emptying in rats: role of afferent neurons and cholecystokinin. *Am J Physiol* 1990; **258**(4 Pt 1): G552-G556
- 42 **Grundy D**, Bagaev V, Hillsley K. Inhibition of gastric mechanoreceptor discharge by cholecystokinin in the rat. *Am J Physiol* 1995; **268**(2 Pt 1): G355-G360
- 43 **Schwartz GJ**, Moran TH, White WO, Ladenheim EE. Relationships between gastric motility and gastric vagal afferent responses to CCK and GRP in rats differ. *Am J Physiol* 1997; **272**(6 Pt 2): R1726-R1733
- 44 **Shoji E**, Okumura T, Onodera S, Takahashi N, Harada K, Kohgo Y. Gastric emptying in OLETF rats not expressing CCK-A receptor gene. *Dig Dis Sci* 1997; **42**: 915-919
- 45 **Varro A**, Green T, Holmes S, Dockray GJ. Calcitonin gene-related peptide in visceral afferent nerve fibres: quantification by radioimmunoassay and determination of axonal transport rates. *Neuroscience* 1988; **26**: 927-932
- 46 **Wang X**, Xing L, Xing Y, Tang Y, Han C. Identification and characterization of immunoreactive calcitonin gene-related peptide from lymphocytes of the rat. *J Neuroimmunol* 1999; **94**: 95-102
- 47 **Wang X**, Wu Z, Tang Y, Fiscus RR, Han C. Rapid nitric oxide- and prostaglandin-dependent release of calcitonin gene-related peptide (CGRP) triggered by endotoxin in rat mesenteric arterial bed. *Br J Pharmacol* 1996; **118**: 2164-2170

Edited by Zhu LH and Xu FM

Detection of point mutation in K-ras oncogene at codon 12 in pancreatic diseases

Yue-Xin Ren, Guo-Ming Xu, Zhao-Shen Li, Yu-Gang Song

Yue-Xin Ren, Yu-Gang Song, Department of Gastroenterology, Nanfang Hospital, First Military Medical University, Guangzhou 510515, Guangdong Province, China

Guo-Ming Xu, Zhao-Shen Li, Department of Gastroenterology, Changhai Hospital, Second Military Medical University, Shanghai 200433, China

Supported by the Technology Committee of Shanghai, NO.994119044

Correspondence to: Dr Yue-Xin Ren, Department of Gastroenterology, Nanfang Hospital, First Military Medical University, Guangzhou 510515, China. yzxu@fimmu.com

Telephone: +86-21-61641544

Received: 2003-08-26 **Accepted:** 2003-10-22

Abstract

AIM: To investigate frequency and clinical significance of K-ras mutations in pancreatic diseases and to identify its diagnostic values in pancreatic carcinoma.

METHODS: 117 ductal lesions were identified in the available sections from pancreatic resection specimens of pancreatic ductal adenocarcinoma, comprising 24 pancreatic ductal adenocarcinoma, 19 peritumoral ductal atypical hyperplasia, 58 peritumoral ductal hyperplasia and 19 normal duct at the tumor free resection margin. 24 ductal lesions were got from 24 chronic pancreatitis. DNA was extracted. Codon 12 K-ras mutations were examined using the two-step polymerase chain reaction (PCR) combined with restriction enzyme digestion, followed by nonradioisotopic single-strand conformation polymorphism (SSCP) analysis and by means of automated DNA sequencing.

RESULTS: K-ras mutation rate of the pancreatic carcinoma was 79%(19/24) which was significantly higher than that in the chronic pancreatitis 33%(8/24) ($P<0.01$). It was also found that K-ras mutation rate was progressively increased from normal duct at the tumor free resection margin, peritumoral ductal hyperplasia, peritumoral ductal atypical hyperplasia to pancreatic ductal adenocarcinoma. The mutation pattern of K-ras 12 codon of chronic pancreatitis was GGT→GAT, GGT and CGT, which is identical to that in pancreatic carcinoma.

CONCLUSION: K-ras mutation may play a role in the malignant transformation of pancreatic ductal cell. K-ras mutation was not specific enough to diagnose pancreatic carcinoma.

Ren YX, Xu GM, Li ZS, Song YG. Detection of point mutation in K-ras oncogene at codon 12 in pancreatic diseases. *World J Gastroenterol* 2004; 10(6): 881-884

<http://www.wjgnet.com/1007-9327/10/881.asp>

INTRODUCTION

Despite considerable development in sophisticated imaging techniques and cytological examination, an early diagnosis of pancreatic neoplasm is rare. Furthermore, surgical therapy for pancreatic cancer is frequently not curative, most often as a

consequence of this tumor's propensity to metastasize. Only in a minority of cases is the diagnosis made at a very early stage, when curative surgery might significantly ameliorate the 5-year survival rate^[1-3]. Therefore, a better understanding of the molecular basis of transformation into malignant tumor may contribute to the establishment of new criteria for diagnosis, prognosis and treatment of human neoplasms. K-ras mutation at codon 12 is one of the most common mutational events in the carcinogenesis of human malignancies^[4]. It occurs mainly in mucin-producing adenocarcinomas^[5]. The highest incidence of K-ras mutation has been found in ductal adenocarcinoma of the pancreas, in which it ranged from 70% to 100%^[6,7]. Because K-ras has been found in very small incidental carcinomas, which were diagnosed only at autopsy^[8], as well as in intraductal portions of ductal carcinomas, it is considered as an initial event in carcinoma development. This may make it a good tool for detecting pancreatic carcinomas at an early stage^[9,10]. However, Yanagisawa *et al.*^[11] showed that K-ras mutations also occur in hyperplastic ductal lesions in pancreas that do not harbor any malignancy. Therefore the K-ras mutation cannot be used as a marker of pancreatic ductal adenocarcinoma. However, this also suggests that ductal lesions, even without dysplasia, may be the forerunners of ductal adenocarcinoma. This assumption also was fostered by the early observation that some of the described ductal lesions frequently are associated with ductal adenocarcinoma. Several studies generally have confirmed the results of Yanagisawa *et al.*, whereas others failed to detect K-ras mutations in nondysplastic epithelium. To address these issues we analyzed 117 ductal lesions for K-ras mutations.

MATERIALS AND METHODS

Tissue selection

The tissues used in this study were derived from patients who underwent partial duodenopancreatectomy for ductal adenocarcinoma of the pancreas and chronic pancreatitis. The basis for selection was the availability of suitable paraffin blocks (blocks age <5 years). 117 ductal lesions were identified in the available sections from pancreatic resection specimens of 24 pancreatic ductal adenocarcinoma, comprising 24 pancreatic ductal adenocarcinoma, 19 peritumoral ductal atypical hyperplasia, 58 peritumoral ductal hyperplasia and 19 normal duct at the tumor free resection margin. 24 ductal lesions were obtained from 24 patients of chronic pancreatitis. 7 surgical specimens of normal pancreas from patients with widely invasive gastric and colonic carcinoma in whom the tumor had not invaded the pancreas and who did not have pancreatic carcinoma or pancreatitis were examined. Multiple 5- and 10- μ m sections were cut from each block and floated onto glass slides. Hematoxylin and eosin staining was performed on 5- μ m sections from each paraffin block. The blade was replaced after each block was cut to prevent carryover of DNA between sections. Pancreatic carcinoma cell line Patu-8988 was obtained from Doctor Elsasser Philips of University of Germany.

DNA extraction

A boiling method of DNA extraction was employed similar to

that previously described by Shibata^[12]. Tissue sections were deparaffinized and digested with a proteinase K digestion buffer (50 mmol/L Tris-HCL, pH 8.5, with 250 µg/mL proteinase K overnight at 55 °C). The tissue was then boiled for 10 min and centrifuged. DNA was quantitated using a spectrophotometer.

Enriched PCR amplification

The first PCR- mediated amplifications were performed as described previously with minor modifications^[13] and produced a 157-base pair fragment that contain K-ras codon 12. Aliquots of the first PCR product were digested with BstN1 (Biolab) at 60 °C for 2 h under the conditions recommended by the supplier. After boiling the mixture for 5 min to inhibit the enzymatic activity, 1/100 volume of the PCR product was subjected to the second PCR under the same conditions but using a different primer set, which flanked internal sequences of 135 bp DNA fragments. The amplified fragments were directly subjected to SSCP. The oligonucleotide primers were purchased from Sangon Co. (Shanghai, China). The sequences of oligonucleotide primers were as follows: 5' ACT GAA TAT AAA CTT GTG GTA GTT GGA CCT 3' (forward primer for first and second PCR); 5' TCA AAG AAT GGT CCT GGA CC 3' (reverse primer for first PCR); 5' TAA TAT GTC GAC TAA AAC AAG ATT TAC CTC 3' (reverse primer for second PCR).

Nonradioisotopic SSCP analysis

Nonradioisotopic SSCP Analyses were performed as described previously, with minor modification^[13]. After denaturation at 100 °C for 5 min, a 10 µL sample was applied and resolved by 120 g/L polyacrylamide gel electrophoresis at 35 V for 21 h at 4 °C. The gels were silver-stained. Each sample was analyzed by SSCP repeatedly to confirm its accuracy.

Direct sequencing of the amplified PCR product

For sequencing the deviant homoduplex bands were cut out of the gel, the DNA eluted by soaking in TE, reamplified, and TA cloned in the pUCm-T vector. Sequencing was performed on an ABI PRISM 377 automated sequencer.

Statistical analysis

A statistical analysis was performed using the chisquare test, the Fisher's exact test and Student *t* test with SPSS.

RESULTS

Detection of K-ras point mutation by nonradioisotopic SSCP analysis and direct sequencing of PCR product

To estimate the sensitivity of this analysis, 1 µg of the DNA extracted from normal peripheral blood lymphocytes and a pancreatic carcinoma cell line were subjected to PCR. Figure 1 shows the electrophoretic profiles of amplified DNA fragments by SSCP. The positive percentage of K-ras mutation of the pancreatic carcinoma was 79%(19/24) which was significantly higher than that in the chronic pancreatitis 33%(8/24) ($P<0.01$). It was also found that K-ras mutation rate was progressively increased from normal duct at the tumor free resection margin, peritumoral ductal hyperplasia, peritumoral ductal atypical hyperplasia to pancreatic ductal adenocarcinoma (Table 1).

The nucleotide sequences of K-ras mutation showed the following transitions: GGT to GAT, GGT to GTT, and GGT to CGT. (Table 2).

Relationship between K-ras gene mutation and location, histological grade and clinical stage of tumors

The diagnostic accuracy of K-ras mutations in pancreatic

carcinoma relative to the location, histological grade and clinical stage of the tumor is summarized in Table 3. There are no apparent correlation between the location, histological grade, clinical stage of the tumor and the presence of K-ras gene mutations.

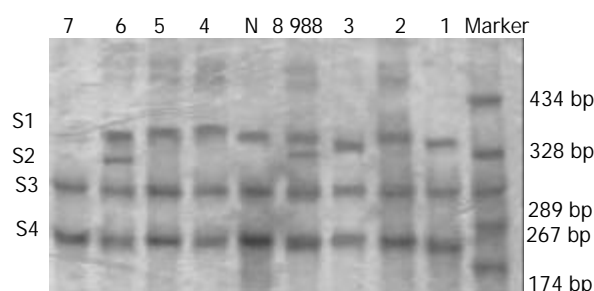


Figure 1 Detection of point mutations of the K-ras oncogene in pancreatic diseases. Lane N, healthy control subject DNA from normal peripheral blood lymphocytes. Lane 988, pancreatic carcinoma cell line Patu-8988 DNA with confirmed mutant K-ras. Lane 6, patients with pancreatic carcinoma with mutant K-ras. Lane 7, normal pancreatic tissue. Lane 1, 3, 4, patients with chronic pancreatitis with mutant K-ras. Lane 2, 5, patients with chronic pancreatitis with wild type K-ras.

Table 1 Relative frequency of K-ras mutation in ductal lesions with pancreatic diseases

Ductal lesion	n	K-ras (-)	K-ras (+)	Positive percentage (%)
Pancreatic ductal adenocarcinoma	24	5	19	79.2
Peritumoral ductal atypical hyperplasia	19	15	14	73.6
Peritumoral ductal hyperplasia	58	38	20	34.5
Normal duct at the tumor free resection margin	16	16	0	0
Chronic pancreatitis	24	16	8	33.3
Normal pancreas	7	7	0	0

Table 2 K-ras mutation pattern of ductal lesions and the corresponding primary pancreatic carcinoma

Ductal lesion	Nucleotide sequence of K-ras12 codon		
	GAT	GTT	CGT
Pancreatic ductal adenocarcinoma	8	4	7
Peritumoral ductal atypical hyperplasia	7	2	3
Peritumoral ductal hyperplasia	10	3	7
Chronic pancreatitis	4	2	2

Table 3 Relationship between K-ras gene mutation and location, histological grade and clinical stage of pancreatic carcinomas

Pathologic factor	n	Positive rate (%)
Tumor location		
Head	18	55.6
Tail/Corpus	6	66.7
Histological grade		
G1	6	66.7
G2	10	50
G3	8	62.5
Clinical stage		
I	1	100
II	3	66.7
III	9	66.7
IV	11	45.5

Clinical and morphologic data on 24 patients with chronic pancreatitis

The occurrence of mutations was unrelated to clinical and morphologic indexes. The difference was not statistically significant (Student *t* test) (Table 4).

Table 4 Clinical and morphologic data on 24 patients with chronic pancreatitis

	K-ras positive cases (n=8)	K-ras negative cases (n=16)
Mean age of patients (yrs)	39.9±15.5(19-68)	51±14.9(23-67)
Gender ratio (M:F)	6:2	10:6
Mean duration of CP (yrs)	6.7±3.2(2-27)	5.7±4.5(3-25)
Mass-CP of pancreatic head	5 cases	10 cases
Weight loss (>10 kg)	3 cases	7 cases
Diabetes (insulin dependent)	4 cases	7 cases
Nicotine(>20 cigarettes/day, >5 yrs)	5 cases	8 cases

CP: chronic pancreatitis.

DISCUSSION

Pancreatic ductal carcinoma is known to have the highest K-ras mutation rate among all tumors. The codon 12 of this gene is affected in 80-100% of the cases. Mutated K-ras also has been found in ductal lesions such as mucinous cell hypertrophy and ductal papillary hyperplasia; therefore these lesions have been regarded as precursor lesions of carcinoma^[11]. However, this assumption is based on rather contradictory results, with K-ras mutation rates in ductal lesions ranging from 0-94%^[14]. The discrepancies between the results of the various studies are based on the wide range of investigated cases, the selection of lesion types, and PCR employed.

Matsubayashi *et al.*^[15] analyzed 317 carcinoma-associated ductal lesions, 39% were positive for K-ras mutations. Moskaluk *et al.*^[14] focused on atypical papillary hyperplasia and found K-ras mutations in 75% of their samples. Both study groups used a detection method (nested PCR-RLFP) with a sensitivity of 5%. But SSCP analysis is one of the simplest and most sensitive methods for detection of mutations based on PCR technology^[16-18]. Since its first report, the SSCP analysis has been widely used to detect mutations in genes responsible for various hereditary diseases and somatic mutations of oncogenes. In an earlier study, Lemoine *et al.*^[19] found no mutations in cases of ductal hyperplasia, but they did find mutation in all severely dysplastic lesions that they regarded as intraductal extensions of the associated ductal adenocarcinoma. It appears that their method, which was based on slot-blot analysis, was not sensitive enough to detect K-ras mutations in nondysplastic ductal lesions.

Chronic pancreatitis, regardless of its etiology, is considered a risk factor for the development of pancreatic ductal adenocarcinoma^[20]. The risk seems to increase with the duration of CP. Some histological studies have searched for possible carcinoma precursor lesions in this disease. Cylwik *et al.*^[21] reported severe dysplasia in 8.6% of 70 resection specimens from patients with CP; advanced fibrosis was associated with dysplasia in 65%. Because of these results, they concluded that surgical removal of the pancreas should be recommended. We cannot confirm these data. We were unable to identify any severe dysplasia carcinoma in situ changes in 24 resection specimens from patients with CP and varying duration of the disease.

K-ras mutation is considered an early event in the tumorigenesis of pancreatic carcinomas. In our study the positive percentage of K-ras mutation of the pancreatic carcinoma was 79%(19/24) which was significantly higher than

that in the chronic pancreatitis 33%(8/24) ($P<0.01$). It was also found that K-ras mutation rate was progressively increased from normal duct at the tumor free resection margin, peritumoral ductal hyperplasia, peritumoral ductal atypical hyperplasia to pancreatic ductal adenocarcinoma. It appeared that the locations, histological grade, clinical stage of pancreatic carcinomas were all not related to the presence of K-ras mutations. The occurrence of K-ras mutations was not associated with the duration of CP and also not with mass-CP of pancreatic head. Rivera *et al.*^[22] reported K-ras mutations in 2 of 11 cases and Yanagisawa *et al.*^[11] even 62.5% mutations in 10 of 16 lesions from 10 cases. K-ras mutations were not detected by Kubrusly *et al.*^[23]. Their negative results probably were due to the comparatively insensitive PCR method and the tissues they selected for investigation. To summarize, when sensitive enough methods are applied, K-ras mutation frequently can be detected in nondysplastic ductal epithelium of patients with CP. Berger *et al.*^[24] reported a clear correlation between K-ras mutations and the nicotine history of their patients. In our study, the relationship was unclear. Therefore, nicotine seems to be a major factor in the induction of the mutation but does not inevitably induce it.

The relation between CP and pancreatic adenocarcinoma remains difficult to explain. Continuous epithelial regeneration and proliferation are thought to promote carcinogenesis in many organs. In our study, the incidence of the ductal lesions and K-ras mutations did not increase with the duration of CP. It therefore seems that hyperplastic ductal changes and K-ras mutations will not inevitably lead to the development of ductal adenocarcinoma.

Future prospective studies should be performed to get a well documented long term follow-up of K-ras positive cases to elucidate the role of K-ras mutations in pancreatic carcinogenesis in CP patients. In addition, other mutations, such as those of the p16, DPC4, and BRCA2 genes or promoter methylation of tumor suppressor, which evidently play role in a linear tumor progression model of pancreatic carcinoma, also should be looked for in lesions that might be responsible for the presumed pancreatic carcinoma sequence in chronic pancreatitis^[25-30].

REFERENCES

- 1 **Postier RG.** Past, present, and future of pancreatic surgery. *Am J Surg* 2001; **182**: 547-551
- 2 **Beger HG,** Gansauge F, Leder G. Pancreatic cancer: who benefits from curative resection? *Can J Gastroenterol* 2002; **16**: 117-120
- 3 **Shankar A,** Russell RC. Recent advances in the surgical treatment of pancreatic cancer. *World J Gastroenterol* 2001; **7**: 622-626
- 4 **Barbacid M.** Ras oncogenes: their role in neoplasia. *Eur J Clin Invest* 1990; **20**: 225-235
- 5 **Bos JL.** Ras oncogenes in human cancer: a review. *Cancer Res* 1989; **49**: 4682-4689
- 6 **Grunewald K,** Lyons J, Frohlich A, Feichtinger H, Weger RA, Schwab G, Janssen JW, Bartram CR. High frequency of Ki-ras codon 12 mutations in pancreatic adenocarcinomas. *Int J Cancer* 1989; **43**: 1037-1041
- 7 **Hruban RH,** van Mansfeld AD, Offerhaus GJ, van Weering DH, Allison DC, Goodman SN, Kensler TW, Bose KK, Cameron JL, Bos JL. K-ras oncogene activation in adenocarcinoma of the human pancreas. A study of 82 carcinomas using a combination of mutant-enriched polymerase chain reaction analysis and allele-specific oligonucleotide hybridization. *Am J Pathol* 1993; **143**: 545-554
- 8 **Kimura W,** Morikane K, Esaki Y, Chan WC, Pour PM. Histologic and biologic patterns of microscopic pancreatic ductal adenocarcinomas detected incidentally at autopsy. *Cancer* 1998; **82**: 1839-1849
- 9 **Miki H,** Matsumoto S, Harada H, Mori S, Haba R, Ochi K, Kobayashi S, Ohmori M. Detection of c-Ki-ras point mutation

- from pancreatic juice. A useful diagnostic approach for pancreatic carcinoma. *Int J Pancreatol* 1993; **14**: 145-148
- 10 **Iguchi H**, Sugano K, Fukayama N, Ohkura H, Sadamoto K, Ohkoshi K, Seo Y, Tomoda H, Funakoshi A, Wakasugi H. Analysis of Ki-ras codon 12 mutations in the duodenal juice of patients with pancreatic cancer. *Gastroenterology* 1996; **110**: 221-226
 - 11 **Yanagisawa A**, Ohtake K, Ohashi K, Hori M, Kitagawa T, Sugano H, Kato Y. Frequent c-Ki-ras oncogene activation in mucous cell hyperplasias of pancreas suffering from chronic inflammation. *Cancer Res* 1993; **53**: 953-956
 - 12 **Shibata D**. Extraction of DNA from paraffin-embedded tissue for analysis by polymerase chain reaction: new tricks from an old friend. *Hum Pathol* 1994; **25**: 561-563
 - 13 **Kahn SM**, Jiang W, Culbertson TA, Weinstein IB, Williams GM, Tomita N, Ronai Z. Rapid and sensitive nonradioactive detection of mutant K-ras genes via 'enriched' PCR amplification. *Oncogene* 1991; **6**: 1079-1083
 - 14 **Moskaluk CA**, Hruban RH, Kern SE. p16 and K-ras gene mutations in the intraductal precursors of human pancreatic adenocarcinoma. *Cancer Res* 1997; **57**: 2140-2143
 - 15 **Matsubayashi H**, Watanabe H, Nishikura K, Ajioka Y, Kijima H, Saito T. Determination of pancreatic ductal carcinoma histogenesis by analysis of mucous quality and K-ras mutation. *Cancer* 1998; **82**: 651-660
 - 16 **Hayashi K**. PCR-SSCP: a method for detection of mutations. *Genet Anal Tech Appl* 1992; **9**: 73-79
 - 17 **Hayashi K**, Yandell DW. How sensitive is PCR-SSCP? *Hum Mutat* 1993; **2**: 338-346
 - 18 **Hayashi K**. Recent enhancements in SSCP. *Genet Anal* 1999; **14**: 193-196
 - 19 **Lemoine NR**, Jain S, Hughes CM, Staddon SL, Maillet B, Hall PA, Kloppel G. Ki-ras oncogene activation in preinvasive pancreatic cancer. *Gastroenterology* 1992; **102**: 230-236
 - 20 **Lowenfels AB**, Maisonneuve P, Cavallini G, Ammann RW, Lankisch PG, Andersen JR, Dimagno EP, Andren-Sandberg A, Domellof L. Pancreatitis and the risk of pancreatic cancer. International Pancreatitis Study Group. *N Engl J Med* 1993; **328**: 1433-1437
 - 21 **Cylwik B**, Nowak HF, Puchalski Z, Barczyk J. Epithelial anomalies in chronic pancreatitis as a risk factor of pancreatic cancer. *Hepatogastroenterology* 1998; **45**: 528-532
 - 22 **Rivera JA**, Rall CJ, Graeme-Cook F, Fernandez-del Castillo C, Shu P, Lakey N, Tepper R, Rattner DW, Warshaw AL, Rustgi AK. Analysis of K-ras oncogene mutations in chronic pancreatitis with ductal hyperplasia. *Surgery* 1997; **121**: 42-49
 - 23 **Kubrusly MS**, Cunha JE, Bacchella T, Abdo EE, Jukemura J, Pentead S, Morioka CY, de Souza LJ, Machado MC. Detection of K-ras point mutation at codon 12 in pancreatic diseases: a study in a Brazilian casuistic. *JOP* 2002; **3**: 144-151
 - 24 **Berger DH**, Chang H, Wood M, Huang L, Heath CW, Lehman T, Ruggeri BA. Mutational activation of K-ras in nonneoplastic exocrine pancreatic lesions in relation to cigarette smoking status. *Cancer* 1999; **85**: 326-332
 - 25 **Moore PS**, Sipos B, Orlandini S, Sorio C, Real FX, Lemoine NR, Gress T, Bassi C, Kloppel G, Kalthoff H, Ungefroren H, Lohr M, Scarpa A. Genetic profile of 22 pancreatic carcinoma cell lines. Analysis of K-ras, p53, p16 and DPC4/Smad4. *Virchows Arch* 2001; **439**: 798-802
 - 26 **Klump B**, Hsieh CJ, Nehls O, Dette S, Holzmann K, Kiesslich R, Jung M, Sinn U, Ortner M, Porschen R, Gregor M. Methylation status of p14ARF and p16INK4a as detected in pancreatic secretions. *Pancreatol* 2002; **2**: 17-25
 - 27 **Fukushima N**, Walter KM, Uek T, Sato N, Matsubayashi H, Cameron JL, Hruban RH, Canto M, Yeo CJ, Goggins M. Diagnosing pancreatic cancer using methylation specific PCR analysis of pancreatic juice. *Cancer Biol Ther* 2003; **2**: 78-83
 - 28 **Fukushima N**, Sato N, Ueki T, Rosty C, Walter KM, Wilentz RE, Yeo CJ, Hruban RH, Goggins M. Aberrant methylation of preproenkephalin and p16 genes in pancreatic intraepithelial neoplasia and pancreatic ductal adenocarcinoma. *Am J Pathol* 2002; **160**: 1573-1581
 - 29 **Ohtsubo K**, Watanabe H, Yamaguchi Y, Hu YX, Motoo Y, Okai T, Sawabu N. Abnormalities of tumor suppressor gene p16 in pancreatic carcinoma: immunohistochemical and genetic findings compared with clinicopathological parameters. *J Gastroenterol* 2003; **38**: 663-671
 - 30 **House MG**, Guo M, Iacobuzio-Donahue C, Herman JG. Molecular progression of promoter methylation in intraductal papillary mucinous neoplasms (IPMN) of the pancreas. *Carcinogenesis* 2003; **24**: 193-198

Edited by Xu JY Proofread by Xu FM

Effect of local CTLA4Ig gene transfection on acute rejection of small bowel allografts in rats

Yi-Fang Wang, Ai-Gang Xu, Yi-Bing Hua, Wen-Xi Wu

Yi-Fang Wang, Ai-Gang Xu, Yi-Bing Hua, Wen-Xi Wu, Department of Gastrointestinal Surgery, the First Affiliated Hospital of Nanjing Medical University, Nanjing 210029, Jiangsu Province, China
Supported by the Innovative Foundation of Nanjing Medical University, N0.200106

Correspondence to: Wen-Xi Wu, Department of Gastrointestinal Surgery, the First Affiliated Hospital of Nanjing Medical University, Nanjing 210029, Jiangsu Province, China. wuwenxi@yahoo.com
Telephone: +86-25-3718836-6828

Received: 2003-10-08 **Accepted:** 2003-12-16

Abstract

AIM: To evaluate the local expression of CTLA4Ig gene in small bowels and its effect on preventing acute rejection of the small bowel allografts.

METHODS: Groups of Wistar rats underwent heterotopic small bowel transplantation from SD rats. The recipients were randomly divided into experimental group (allografts were transfected with CTLA4Ig gene) and control group (non CTLA4Ig gene transfected). In the experimental group, the donor small bowels were perfused *ex vivo* with CTLA4Ig cDNA packaged with lipofectin vector via intra-superior mesenteric artery before transplantation, and the CTLA4Ig expression in the small bowel grafts post-transplantation was assessed by immunohistology. On d 3, 7 and 10 post-transplantation, the allografts in each group were harvested for the examination of histology and detection of apoptosis.

RESULTS: Small bowel allografts treated with CTLA4Ig cDNA showed abundant CTLA4Ig expression after transplantation. Acute rejection of grade I on d 7 and grade II on d 10 after transplantation was noticed in the control allografts, and a dramatically increased number of apoptotic enterocytes in parallel to the progressive rejection could be recognized. In contrast, the allografts treated with CTLA4Ig cDNA showed nonspecific histological changes and only a few apoptotic enterocytes were found after transplantation.

CONCLUSION: Local CTLA4Ig gene transfection of small bowel allograft is feasible, and the local CTLA4Ig expression in the allograft can prevent acute rejection after transplantation.

Wang YF, Xu AG, Hua YB, Wu WX. Effect of local CTLA4Ig gene transfection on acute rejection of small bowel allografts in rats. *World J Gastroenterol* 2004; 10(6): 885-888
<http://www.wjgnet.com/1007-9327/10/885.asp>

INTRODUCTION

CTLA4Ig is a soluble recombinant fusion protein constructed with an extracellular domain of mouse CTLA4 and Fc portion of human IgG. This protein binds to the mouse and rat B7-1/2 molecules, and blocks the co-stimulatory signals from antigen processing cell (APC) to antigen specific T cell. Treatment with CTLA4Ig gene transfection has been shown to prolong

graft survival in mouse and rat heart, liver, pancreatic islet, kidney and lung transplantations and to induce donor-specific tolerance in some of these cases^[1-7].

There are two methods of gene transduction: systemic administration (*ie.* intravenous injection) and local transfection of allograft. Gene transfer of sequences coding for soluble immunosuppressive molecules into transplanted organs aims to create a local microenvironment directly modulating the activation state of immune cells responsible for graft rejection^[8]. Therefore, when compared with systemic administration, local and continuous production of biologically active compounds might increase their bioavailability and allow a more effective treatment. Furthermore, cells not involved in the rejection process could be spared, and side effects or generalized immunosuppression may thus be avoided.

Intra-graft expression of CTLA4Ig by gene transfection at the time of transplantation can successfully prolong survival of several grafts^[9-12]. Nevertheless, study of CTLA4Ig expression within the small bowel allograft has not been reported. In the present study, we transfected gene by *ex vivo* intra-superior mesenteric artery infusion of mCTLA4Ig cDNA packaged with lipofectin vector before transplantation, evaluated the local expression of CTLA4Ig gene and its effect on preventing acute rejection of small bowel allografts in rats.

MATERIALS AND METHODS

Animals and transplantation

Inbred male SD and Wistar rats weighing 250 to 300 g were used as donors and recipients, respectively. All rats were obtained from the Animal Center of Nanjing Medical University.

After fasting for 24 h, donors and recipients were anesthetized with an intraperitoneal injection of pentobarbital (50 mg/kg). The vasculature of the donor small bowel was perfused with 10 mL heparinized saline solution at 4 °C. A segment of 20 cm small bowel with portal vein and superior mesenteric artery attached to a cuff of aorta were removed. The lumen of the donor small bowel perfused with 20 mL pure saline solution at 4 °C. The small bowel graft was transplanted with an end-to-side anastomosis of the cuff of aorta and portal vein of the graft to the infrarenal aorta and infrarenal vena cava (Figure 1). After revascularization of the graft, the oral end and the anal end of the small bowel graft were constructed as a stoma respectively through the right abdominal wall of the recipient. All animals had free access to water within 24 h after transplantation. Starting from postoperative d 1, they received standard rat chow.

Experimental groups

Animals were placed into two groups: One group of recipients did not receive treatment (control group, *n*=21), and the other group of recipients received CTLA4Ig gene transfection (experimental group, *n*=21).

Delivery of mCTLA4Ig to small intestine

The plasmid of AAVmCTLA4Ig was a kind gift of Professor I. Anegón (INSERM U437, Nants, France). DOTAP:Chole (*in vivo* GenSHUTTLE, Qbiogene) was used as the vector.

The AAVmCTLA4Ig was mixed with DOTAP:Chole at room temperature for 15 min to create the DNA-lipid complex. The final concentration of DNA in the complex was 0.5 $\mu\text{g}/\mu\text{L}$. Before cold preservation, the small bowel graft was irrigated with cold saline and then 50 μL lipid (control group) or 50 μL DNA-lipid complex (experimental group) was delivered into the superior mesenteric artery by slow infusion over 5-10 min. After 1.5 h of cold preservation, the superior mesenteric artery of small bowel was reperused with 5 mL cold saline for 10 min before transplantation.



Figure 1 Heterotopic small bowel transplantation in the rat. The vasculature of the graft has been anastomosed. RSB: recipient's small bowel. TSB: transplanted small bowel.

Graft histology, apoptosis detection and immunohistology

Three, seven and ten days after transplantation, 7 rats were killed in each group. Samples of the small bowel allografts were obtained. One half was fixed in paraformaldehyde for histology examination and cell apoptosis detection. Another half was preserved in nitrogen liquid for immunohistology.

For histology, sections from paraffin embedded blocks were stained with hematoxylin-eosin (H&E). Kuusanmaki's protocol^[13] served as basis for the grading of acute graft rejection and determination of diagnostic categories.

Apoptosis was detected on sections from paraffin-embedded blocks by the terminal deoxynucleotidyl transferase (TdTase) mediated d-UTP-biotin nick end labeling (TUNEL) technique^[14-17]. Apoptosis assay with a detection kit from Boehringer (Mannheim, Germany), conformed to the manufacturer's protocol strictly except that the sections were finally counterstained with methylgreen (Vector Laboratories). The nuclei of apoptotic cells were stained brown as detected under light microscope, and the number of apoptotic cells was determined by counting labeled enterocytes in 10 randomly chosen high-power fields^[18].

Immunohistology was performed in cryostat sections. To detect CTLA4Ig in tissues, sections were subsequently incubated (60 min) with hamster anti-murine CTLA4 mAb (UC-4F10-11, BD Biosciences). Tissues probed with the mAb were then incubated with a biotin-conjugated mouse IgG-adsorbed anti-hamster IgG Ab (60 min; G70-204 & G94-56, BD Biosciences), followed by HRP-conjugated streptavidin (45 min; Woburn MA) and DAB substrate, and sections were counterstained with hematoxylin.

Statistical analysis

Data were expressed as mean \pm SD and Student's *t* test was used. Significant difference was assumed when $P < 0.05$.

RESULTS

Immunohistology

The CTLA4Ig expression of implanted small bowels was detected by immunohistology, and the small bowel grafts transduced with CTLA4Ig showed the presence of abundant

labeling in mesenteric vascular walls, muscularis, submucosa and villus. Higher densities of CTLA4Ig were detected in grafts sampled at early time points, and persistent expression of CTLA4Ig was confirmed within 10 d after transplantation (Figure 2: A, B, C). As anticipated, there was no detectable expression of CTLA4Ig in the control small intestines (Figure 2: D).

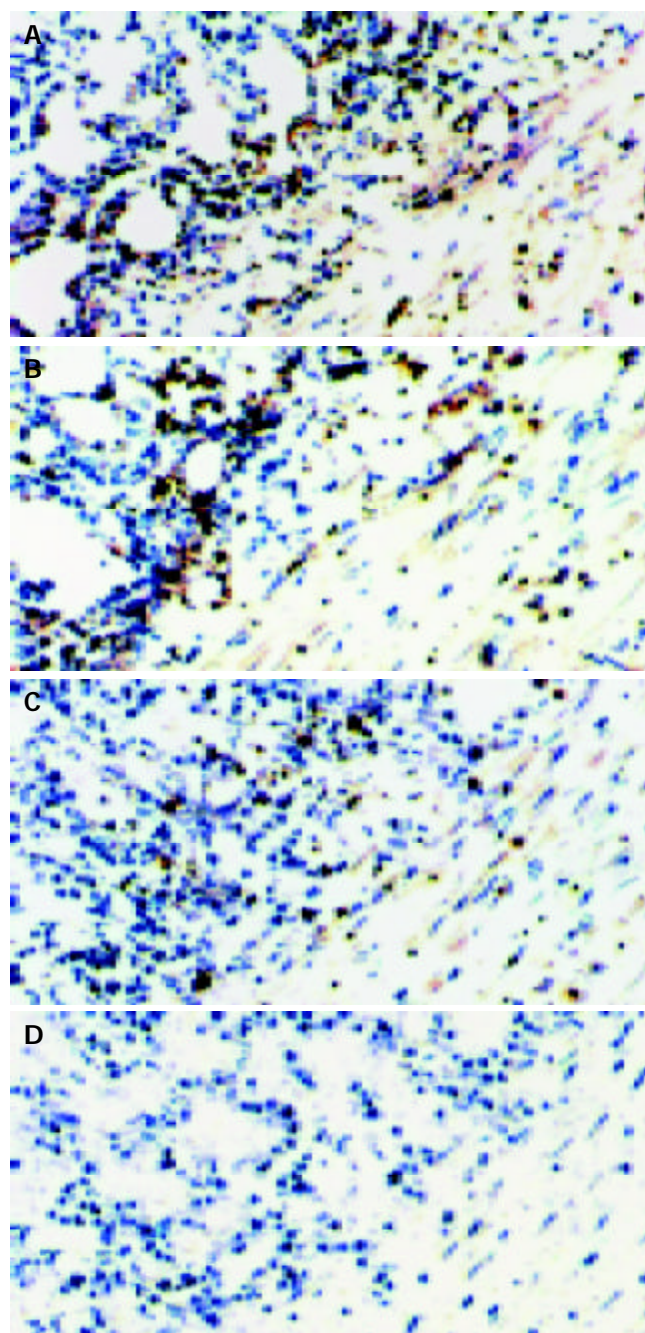


Figure 2 Presence of CTLA4Ig in the small bowel allografts. CTLA4Ig was stained as the brown granules. A, B, C represent the cryostat sections of CTLA4Ig gene transfected grafts on d 3, 7, 10 after transplantation, respectively. D represent the cryostat sections of non-CTLA4Ig gene transfected grafts, expression of CTLA4Ig was not detected. [original magnification $\times 200$].

Morphological findings

In the control group, on d 3 after transplantation, only nonspecific changes were noted. Focal mesenteric inflammation, mild endothelial vacuolization, and minimal swelling and desquamation of enterocytes were observed in allografts, and a relatively normal villiform mucosal structure was retained. On d 7, a widespread inflammatory infiltrate in the mesentery, with moderate invasion of the intestinal wall,

villous blunting and part of the crypt destruction, was noticed in allografts. In addition, endothelial swelling and proliferation with intimal thickening were found in small mesenteric arteries and arterioles. On d 10, a pronounced mesenteric infiltrate with severe invasion of the intestinal wall was found in allografts. Endothelial proliferation with intimal thickening resulted in luminal obliteration. Furthermore, moderate to extreme enterocystic necrosis could be recognized as erosions and focal ulcerations. However, the allografts treated with CTLA4Ig gene transfection showed nearly normal mucosal structure, slight cell infiltration and minimal swelling and desquamation of enterocytes on d 3, 7 and 10 post-transplantation.

Detection of apoptotic enterocytes by TUNEL

Apoptotic cells were detected mainly in the crypts. On d 3 after transplantation, a small number of labeled enterocytes were observed both in control (5.3 ± 1.5 , $n=7$) and experimental (5.8 ± 1.8 , $n=7$) groups. There was no significant difference in the number of apoptotic enterocytes between the two groups. On d 7, the number of labeled enterocytes increased dramatically (61.7 ± 2.8 , $n=7$) and reached a higher level on d 10 (101 ± 6.1 , $n=7$) in control group after transplantation (Figure 3: A1, B1, C1), whereas an increasing number of labeled nuclei could not be recognized in experimental group on d 7 (3.4 ± 1.0 , $n=7$) and on d 10 (3.6 ± 1.3 , $n=7$) after transplantation (Figure 3: A2, B2, C2). The difference in the number of apoptotic enterocytes in allografts between control and experimental groups on d 7 and 10 was extremely significant ($^bP < 0.0005$, $t=41.2876$ on day 7 and $^dP < 0.005$, $t=39.2437$ on d 10).

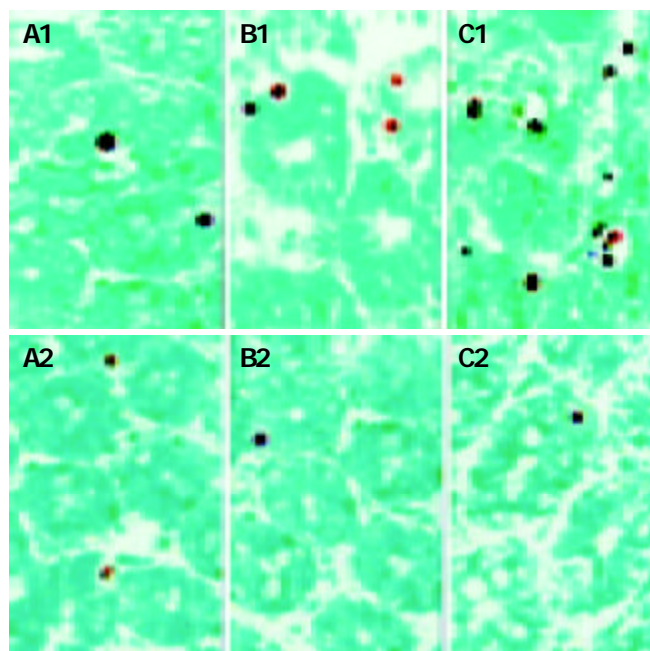


Figure 3 Apoptotic crypt cells in the small bowel allografts. A1, B1, C1 represent the tissue sections of non-CTLA4Ig gene transfected grafts obtained on d 3, 7, 10 after transplantation, respectively. A2, B2, C2 represent the tissue sections of CTLA4Ig gene transfected grafts obtained on d 3, 7, 10 after transplantation, respectively. [original magnification $\times 400$].

DISCUSSION

Small bowel transplantation has emerged as a life-saving therapy for patients with irreversible intestinal failure and is now a routine therapeutic tool at some transplant centers^[19,20]. Nevertheless, graft rejection is still the major obstacle to the transplantation^[21-23]. Blockade of the B7/CD28 co-stimulation signal by systemic transfer of CTLA4Ig gene through

intravenous infusion of AdCTLA4Ig has been shown to prolong small intestinal graft survival^[24]. However, different from heart, liver, kidney and other organs, the small bowel is unique among vascularized organ grafts with rich lymphoid components and large amounts of bacteria, severe infection as well as rejection occurs easier after transplantation. Local CTLA4Ig gene transfection of small bowel allograft could be the ideal therapeutic strategy of anti-rejection. It allows inhibition of the recipient's rejection response, while maintaining the recipient's efficient peripheral immune function (not suppressing the antibacterial response). The local transfection of CTLA4Ig gene has been successfully achieved in rat heart, liver, kidney, islet and lung allografts^[9-12], but it has not been studied in the small bowel transplantation. In the present study, we perfused CTLA4Ig cDNA packaged with lipofectin vector via intra-superior mesenteric artery into the small bowels. By immunohistology, there were a large amount of CTLA4Ig expression in the small bowel allografts on days 3, 7 and 10 after transplantation. The result suggests that local CTLA4Ig gene transfection of small bowel allograft is feasible.

In non-CTLA4Ig gene transfected small bowel allografts, a histological change of progressive acute allograft rejection could be recognized. Although the allografts did not show any specific morphological changes on d 3, acute allograft rejection of grade I on d 7 and grade II on d 10 after transplantation was noticed. In contrast, no evidence of acute rejection was observed in CTLA4Ig gene transfected allografts on d 3, 7 and 10 after transplantation. These data indicate that local CTLA4Ig expression in small bowel allografts can prevent acute rejection after transplantation. The protection of local CTLA4Ig expression in small bowel allografts from acute rejection may be because of the inhibition of expansion of alloantigen-induced T cell priming. The local transfection of CTLA4Ig can block B7 ligand expression on the surface of intra-graft APCs, and thus blocking B7/CD28 co-stimulatory pathway. In the absence of B7/CD28 co-stimulatory signal, the interaction of T cell with the alloantigen commonly produces T cell anergy^[25-29].

Apoptosis is a DNA-dependent cell death mechanism, which occurs under physiological and pathological conditions. In organ transplantation, apoptosis is an important biochemical indicator of allograft rejection^[14-17]. In the process of allograft rejection, the target cells damage is mainly mediated by cytotoxic T lymphocytes through the perforin-dependent granule-exocytosis pathway and the Fas/Fas ligand (FasL) pathway^[30-32]. Both perforin- and Fas-mediated pathways of cytotoxicity can result in target cell apoptosis. Numerous reports have demonstrated up-regulation of transcripts for perforin, granzyme B, and FasL during allograft rejection^[33-36]. In the present study, TUNEL illustrated a few apoptotic enterocytes on d 3 and showed a dramatically increased number of apoptotic enterocytes on d 7 and 10 after transplantation in non-CTLA4Ig gene transfected small bowel allografts. This result demonstrates the existence of acute rejection after transplantation. Nevertheless, in CTLA4Ig gene transfected small bowel allografts, a few apoptotic crypt cells was observed on days 3, but the number of apoptotic enterocytes did not increase on d 7 and 10 after transplantation. It indicates that the apoptosis in small bowel allografts can be prevented by local CTLA4Ig gene transfection, and the cytotoxic roles of infiltrated T lymphocytes and the acute rejection after transplantation can be prevented by CTLA4Ig expression in the allografts. The few apoptosis in allografts on d 3 was likely caused by cold preservation damage and postischemic reperfusion damage^[37-39].

In conclusion, local CTLA4Ig gene transfection of small bowel allograft can be achieved by perfusing CTLA4Ig cDNA packaged with lipofectin vector via intra-superior mesenteric artery into the small bowels, and the local CTLA4Ig expression in the allograft can prevent acute rejection after transplantation.

ACKNOWLEDGMENT

The authors are grateful to Professor I. Anegon (INSERM U437, Nantes, France) for the kind gift of the AAVmCTLA4IgG plasmid, and thank Professor Xirong Guo (Experimental Research Center of Nanjing Medical University) for the experimental help.

REFERENCES

- 1 **Laumonier T**, Potiron N, Boeffard F, Chagneau C, Brouard S, Guillot C, Soullou JP, Anegon I, Le Mauff B. CTLA4Ig adenoviral gene transfer induces long-term islet rat allograft survival, without tolerance, after systemic but not local intragraft expression. *Hum Gene Ther* 2003; **14**: 561-575
- 2 **Kosuge H**, Suzuki J, Gotoh R, Koga N, Ito H, Inobe M, Uede T. Induction of immunologic tolerance to cardiac allograft by simultaneous blockade of inducible co-stimulator and cytotoxic T-lymphocyte antigen 4 pathway. *Transplantation* 2003; **75**: 1374-1379
- 3 **Shiraishi T**, Yasunami Y, Takehara M, Uede T, Kawahara K, Shirakusa T. Prevention of acute lung allograft rejection in rat by CTLA4Ig. *Am J Transplant* 2002; **2**: 223-228
- 4 **Kita Y**, Nogimura H, Ida M, Kageyama Y, Ohi S, Ito Y, Matsushita K, Takahashi T, Suzuki K, Kazui T, Hayashi S, Li XK, Suzuki S. Effects of adenoviral vectors containing CTLA4Ig-gene in rat heterotopic lung implants. *Transplant Proc* 2002; **34**: 1434-1436
- 5 **Yanagida N**, Nomura M, Yamashita K, Takehara M, Murakami M, Echizenya H, Konishi K, Kitagawa N, Furukawa H, Uede T, Todo S. Tolerance induction by a single donor pretreatment with the adenovirus vector encoding CTLA4Ig gene in rat orthotopic liver transplantation. *Transplant Proc* 2001; **33**: 573-574
- 6 **Shindo J**. Effect of CTLA4Ig gene transfer with adenovirus vector on allogeneic renal graft survival in the rat. *Hokkaido Igaku Zasshi* 2001; **76**: 251-256
- 7 **Iwasaki N**, Gohda T, Yoshioka C, Murakami M, Inobe M, Minami A, Uede T. Feasibility of immunosuppression in composite tissue allografts by systemic administration of CTLA4Ig. *Transplantation* 2002; **73**: 334-340
- 8 **Guillot C**, Menoret S, Guillonneau C, Braudeau C, Castro MG, Lowenstein P, Anegon I. Active suppression of allogeneic proliferative responses by dendritic cells after induction of long-term allograft survival by CTLA4Ig. *Blood* 2003; **101**: 3325-3333
- 9 **Kita Y**, Li XK, Nogimura H, Ida M, Kageyama Y, Ohi S, Suzuki K, Kazui T, Suzuki S. Prolonged graft survival induced by CTLA4Ig gene transfection in rat lung allografting. *Transplant Proc* 2003; **35**: 456-457
- 10 **Umeda Y**, Iwata H, Yoshikawa S, Matsuno Y, Marui T, Nitta T, Idia Y, Takagi H, Mori Y, Miyazaki J, Kosugi A, Hirose H. Gene gun-mediated CTLA4Ig-gene transfer for modification of allogeneic cardiac grafts. *Transplant Proc* 2002; **34**: 2622-2623
- 11 **Cheung ST**, Tsui TY, Wang WL, Yang ZF, Wong SY, Ip YC, Luk J, Fan ST. Liver as an ideal target for gene therapy: expression of CTLA4Ig by retroviral gene transfer. *J Gastroenterol Hepatol* 2002; **17**: 1008-1014
- 12 **Benigni A**, Tomasoni S, Remuzzi G. Impediments to successful gene transfer to the kidney in the context of transplantation and how to overcome them. *Kidney Int* 2002; **61**(Suppl 1): 115-119
- 13 **Kuusanmaki P**, Halttunen J, Paavonen T, Pakarinen M, Luukkonen P, Hayry P. Acute rejection of porcine small bowel allograft. An extended histological scoring system. *Transplantation* 1994; **58**: 757-763
- 14 **Wu MY**, Liang YR, Wu XY, Zhuang CX. Relationship between Egr-1 gene expression and apoptosis in esophageal carcinoma and precancerous lesions. *World J Gastroenterol* 2002; **8**: 971-975
- 15 **Sun P**, Ren XD, Zhang HW, Li XH, Cai SH, Ye KH, Li XK. Serum from rabbit orally administered cobra venom inhibits growth of implanted hepatocellular carcinoma cells in mice. *World J Gastroenterol* 2003; **9**: 2441-2444
- 16 **Huang ZH**, Fan YF, Xia H, Feng HM, Tang FX. Effects of TNP-470 on proliferation and apoptosis in human colon cancer xenografts in nude mice. *World J Gastroenterol* 2003; **9**: 281-283
- 17 **Zhao AG**, Zhao HL, Jin XJ, Yang JK, Tang LD. Effects of Chinese Jianpi herbs on cell apoptosis and related gene expression in human gastric cancer grafted onto nude mice. *World J Gastroenterol* 2002; **8**: 792-796
- 18 **Fayyazi A**, Schlemminger R, Gieseler R, Peters JH, Radzun HJ. Apoptosis in the small intestinal allograft of the rat. *Transplantation* 1997; **63**: 947-951
- 19 **Platell CF**, Coster J, McCauley RD, Hall JC. The management of patients with the short bowel syndrome. *World J Gastroenterol* 2002; **8**: 13-20
- 20 **Kato T**, Ruiz P, Thompson JF, Eskind LB, Weppeler D, Khan FA, Pinna AD, Nery JR, Tzakis AG. Intestinal and multivisceral transplantation. *World J Surg* 2002; **26**: 226-237
- 21 **Ding J**, Guo CC, Li CN, Sun AH, Guo XG, Miao JY, Pan BR. Postoperative endoscopic surveillance of human living-donor small bowel transplantation. *World J Gastroenterol* 2003; **9**: 595-598
- 22 **Zhang WJ**, Liu DG, Ye QF, Sha B, Zhen FJ, Guo H, Xia SS. Combined small bowel and reduced auxiliary liver transplantation: case report. *World J Gastroenterol* 2002; **8**: 956-960
- 23 **Ghanekar A**, Grant D. Small bowel transplantation. *Curr Opin Crit Care* 2001; **7**: 133-137
- 24 **Echizenya H**, Yamashita K, Takehara M, Konishi K, Nomura M, Yanagida N, Kitagawa N, Kobayashi T, Furukawa H, Inobe M, Uede T, Todo S. Adenovirus-mediated CTLA4-IgG gene therapy in orthotopic small intestinal transplantation in rats. *Transplant Proc* 2001; **33**: 183-184
- 25 **Vasilevko V**, Ghochikyan A, Sadzikava N, Petrushina I, Tran M, Cohen EP, Kesslak PJ, Cribbs DH, Nicolson GL, Agadjanyan MG. Immunization with a vaccine that combines the expression of MUC1 and B7 co-stimulatory molecules prolongs the survival of mice and delays the appearance of mouse mammary tumors. *Clin Exp Metastasis* 2003; **20**: 489-498
- 26 **Chung JB**, Wells AD, Adler S, Jacob A, Turka LA, Monroe JG. Incomplete activation of CD4 T cells by antigen-presenting transitional immature B cells: implications for peripheral B and T cell responsiveness. *J Immunol* 2003; **171**: 1758-1767
- 27 **Elhalel MD**, Huang JH, Schmidt W, Rachmilewitz J, Tykocinski ML. CTLA-4, FasL induces alloantigen-specific hyporesponsiveness. *J Immunol* 2003; **170**: 5842-5850
- 28 **Arpinati M**, Terragna C, Chirumbolo G, Rizzi S, Urbini B, Re F, Tura S, Baccarani M, Rondelli D. Human CD34(+) blood cells induce T-cell unresponsiveness to specific alloantigens only under costimulatory blockade. *Exp Hematol* 2003; **31**: 31-38
- 29 **Appleman LJ**, Boussiotis VA. T cell anergy and costimulation. *Immunol Rev* 2003; **192**: 161-180
- 30 **Mandrup-Poulsen T**. Beta cell death and protection. *Ann N Y Acad Sci* 2003; **1005**: 32-42
- 31 **Abrahams VM**, Straszewski-Chavez SL, Guller S, Mor G. First trimester trophoblast cells secrete Fas ligand which induces immune cell apoptosis. *Mol Hum Reprod* 2004; **10**: 55-63
- 32 **Catalfamo M**, Henkart PA. Perforin and the granule exocytosis cytotoxicity pathway. *Curr Opin Immunol* 2003; **15**: 522-527
- 33 **D'Errico A**, Corti B, Pinna AD, Altissimi A, Gruppioni E, Gabusi E, Fiorentino M, Bagni A, Grigioni WF. Granzyme B and perforin as predictive markers for acute rejection in human intestinal transplantation. *Transplant Proc* 2003; **35**: 3061-3065
- 34 **Liang LW**, Zhang Q, Gjertson D, Gritsch HA, Reed EF. Non-invasive immune monitoring of perforin/granzyme B in peripheral blood may predict renal allograft rejection. *Hum Immunol* 2003; **64**(10 Suppl): S32
- 35 **Simon T**, Opelz G, Wiesel M, Ott RC, Susal C. Serial peripheral blood perforin and granzyme B gene expression measurements for prediction of acute rejection in kidney graft recipients. *Am J Transplant* 2003; **3**: 1121-1127
- 36 **Zhang SG**, Wu MC, Tan JW, Chen H, Yang JM, Qian QJ. Expression of perforin and granzyme B mRNA in judgement of immunosuppressive effect in rat liver transplantation. *World J Gastroenterol* 1999; **5**: 217-220
- 37 **Wang SF**, Li GW. Early protective effect of ischemic preconditioning on small intestinal graft in rats. *World J Gastroenterol* 2003; **9**: 1866-1870
- 38 **Ma K**, Yu Y, Bu XM, Li YJ, Dai XW, Wang L, Dai Y, Zhao HY, Yang XH. Prevention of grafted liver from reperfusion injury. *World J Gastroenterol* 2001; **7**: 572-574
- 39 **Zhu XH**, Qiu YD, Shen H, Shi MK, Ding YT. Effect of matrine on Kupffer cell activation in cold ischemia reperfusion injury of rat liver. *World J Gastroenterol* 2002; **8**: 1112-1116

Effects of cholesterol on proliferation and functional protein expression in rabbit bile duct fibroblasts

Bao-Ying Chen, Jing-Guo Wei, Yao-Cheng Wang, Jun Yu, Ji-Xian Qian, Yan-Ming Chen, Jing Xu

Bao-Ying Chen, Jing-Guo Wei, Yao-Cheng Wang, Department of Radiology, Tangdu Hospital, Fourth Military Medical University, Xi'an 710038, Shannxi Province, China

Jun Yu, Yan-Ming Chen, Department of Physiology, Fourth Military Medical University, Xi'an 710032, Shannxi Province, China

Ji-Xian Qian, Department of Orthopaedics, Tangdu Hospital, Fourth Military Medical University, Xi'an 710038, Shannxi Province, China

Jing Xu, Cell Engineering Research Center, Fourth Military Medical University, Xi'an 710032, Shannxi Province, China

Correspondence to: Jing-Guo Wei, Department of Radiology, Tangdu Hospital, Fourth Military Medical University, Xi'an 710038, Shannxi Province, China. chenby@fmmu.edu.cn

Telephone: +86-29-3377163 **Fax:** +86-29-3377163

Received: 2003-12-17 **Accepted:** 2004-01-08

Abstract

AIM: To investigate the effect of cholesterol (Ch) on the growth and functional protein expression of rabbit bile duct fibroblasts.

METHODS: The cultured bile duct fibroblasts were divided randomly into two groups: the control group and the experiment group (fibroblasts were incubated respectively with 0.6 g/L Ch for 12, 24, 36 and 48 h). The growth and DNA synthesis of bile duct fibroblasts were measured by the means of ^3H -TdR incorporation. The total protein content of fibroblast was measured by BSA protein assay reagent kit, then the expression of α -actin was analyzed semi-quantitatively by Western blot.

RESULTS: After treatment with 0.6 g/L Ch for 12, 24, 36 and 48 h, the values of ^3H -TdR incorporation of bile duct fibroblasts were respectively 3.1 ± 0.39 , 3.8 ± 0.37 , 4.6 ± 0.48 and 5.2 ± 0.56 mBq/cell, and the values of the corresponding control groups were 3.0 ± 0.33 , 3.2 ± 0.39 , 3.7 ± 0.49 and 4.3 ± 0.43 mBq/cell. After comparing the values of experiment groups and their corresponding control groups, it was found that the ^3H -TdR incorporation of bile duct fibroblasts after treatment with 0.6 g/L Ch for 24, 36 and 48 h were significantly increased ($P < 0.05$, $P < 0.01$, $P < 0.01$), while the ^3H -TdR incorporation of 12-h group was not different statistically from its control group. Ch had no obvious effect on the total protein content of fibroblasts. After incubated with 0.6 g/L Ch for 12, 24, 36 and 48 h, the total protein content of each experiment group was not altered markedly compared with its corresponding control group. The values of experiment groups were 0.246 ± 0.051 , 0.280 ± 0.049 , 0.263 ± 0.044 and 0.275 ± 0.056 ng/cell, and those of corresponding control groups were 0.253 ± 0.048 , 0.270 ± 0.042 , 0.258 ± 0.050 and 0.270 ± 0.045 ng/cell. Western blot analysis revealed that the α -actin expression in fibroblasts affected by Ch for 12 and 24 h was not markedly changed compared with their corresponding control groups ($P > 0.05$), the values of total gray scale of 12- and 24-h groups were $1\,748 \pm 185$ and $1\,756 \pm 173$, respectively. But after stimulation with Ch for 36 h, the total gray scale of fibroblasts ($1\,923 \pm 204$) was significantly higher than that of

control group ($1\,734 \pm 197$). When the time of Ch treatment was lengthened to 48 h, the α -actin expression was markedly elevated, the total gray scale was $2\,189 \pm 231$ ($P < 0.01$ vs control group).

CONCLUSION: Moderately concentrated Ch can promote the proliferation of bile duct fibroblasts at early stage. With the prolongation of Ch treatment, the α -actin expression of fibroblasts was also increased, but the hypertrophy of fibroblasts was not observed.

Chen BY, Wei JG, Wang YC, Yu J, Qian JX, Chen YM, Xu J. Effects of cholesterol on proliferation and functional protein expression in rabbit bile duct fibroblasts. *World J Gastroenterol* 2004; 10(6): 889-893

<http://www.wjgnet.com/1007-9327/10/889.asp>

INTRODUCTION

The disorder of cholesterol metabolism is an important cause of biliary diseases. Previous studies suggest that cholesterol can change the motility of cholecyst^[1,2] and decrease gallbladder contraction^[3-7] in the patients with cholesterol calculus and in the animals with hypercholesterolemia. Weak contraction of gallbladder may be a reason of cholesterol calculus^[8-12]. Researchers consider that cholesterol metabolism disorder has an effect on the structure and function of bile duct and sphincter of bile duct (SBD)^[13-16]. We have found that cholesterol liposome (CL) affected not only the configuration and quantity of cytoskeleton in rabbit SBD smooth muscle cells, but also the proliferation of cells^[17,18]. There are many fibroblasts in biliary system except that SBD is formed mainly with smooth muscle cells^[19-22]. In our previous experiment, we observed that middle concentration Ch could accelerate the proliferation of bile duct fibroblasts and result in the changes of phenotype^[23,24]. Fibroblasts displayed some characteristics of myofibroblasts or smooth muscle cells^[23,24]. In order to lucubrate the reactivity of bile duct fibroblasts to Ch and the role of fibroblasts on the configuration variation of bile duct and SBD, the effects of Ch on bile duct fibroblasts at different time point were studied and the relation between the effects of Ch and time was analyzed in this study.

MATERIALS AND METHODS

Materials

New Zealand rabbits aged 1 month were provided by the Animal Center of the Fourth Military Medical University. Trysin (Gibco, Paisley, Renfrewshire, UK), Dulbecco's modified eagles medium (DMEM) (Gibco, Paisley, Renfrewshire, UK), fetal calf serum (Qinghu Institute of Foetus Bovine Utilization in Jinhua Zhejiang), water soluble cholesterol (Sigma, St. Louis, USA), antibody of vimentin, α -actin and desmin (DakoCytomation, Glostrup, Denmark), ABC immunohistochemical kit (Shaanxi Biotech. Co., Xi'an, China), IMT-2 inverted biological microscope (Olympus

Corporation, Japan), YJ-875 Itra-clean operating boar (Suhang Experimental Animal Technology Development Co), LD4-2 centrifugal machine (Beijing Medical Centrifugal Machine Factory), and BCA protein assay reagent kit (Pierce Chemical Company, Rockford, USA) were commercially obtained.

Dispensing of main reagent

Ch was diluted to 0.6 g/L with DMEM before experiment. DMEM was dispensed according to the description. Fetal calf serum was inactivated for 30 min at 56 °C, and was stored at -20 °C. Trypsin was made into 2.5 g/L solution with PBS (0.01 mol/L, pH 7.4) and stored at 4 °C. TBST was prepared by mixing 10 mL of Tri-Cl, 8.78 g of NaCl, 500 µL of Tween-20, and adding distilled water up to 1L.

Primary culture of rabbit bile duct fibroblasts

Bile ducts of New Zealand rabbits were dissociated by the means of aseptic technique and broken by shears. The tissue was digested to become single cell suspension by trypsin (1.25 g/L). Cells were washed and resuspended with DMEM (containing 100 mL/L fetal calf serum) and incubated at room temperature for 75-90 min. Then the cells were collected and transferred into culture bottles. The cells of 2nd-4th passages were used for experiments.

Identification of rabbit bile duct fibroblasts

Three glass cover slips (18 mm×18 mm) were placed into 6 cm diameter culture dishes, and then cell suspension was added and incubated at room temperature for 48 h. The slips covered with cells were washed twice with PBS (pH 7.4). Some slips were fixed by cold acetone for 15 min at 4 °C and used for HE staining, another three slips were fixed by citomint (40 g/L) for immunohistochemical ABC staining to exam vimentin and desmin expression.

[³H] Thymidine incorporation

Bile duct fibroblasts were planted in 96-well plates. Sub-confluent cells were cultured without serum for 24 h, then treated respectively by 0.6 g/L Ch for 12, 24, 36 and 48 h and pulsed with 18.5 kBq of [³H] thymidine for 4 h. The control group cells were incubated with DMEM containing 20 mL/L fetal calf serum instead of Ch. The radioactivity of each group was counted by Beckman LS6500 counter.

Assay of total protein content

The cells of each group were trypsinized and counted. Cells were centrifuged at 1 000 r/min for 5 min at 4 °C, washed twice with ice-cold PBS and lysed in ice-cold lysis buffer for 30-60 min. The lysates were centrifuged at 12 000 g for 5 min at 4 °C and supernatant was transferred into new Eppendorf tubes. The standard curve was drawn according to the description of BCA protein assay reagent kit, and then the total protein content per cell was measured and converted.

Western blot analysis

Loading buffer was added to each lysate, which was subsequently boiled for 10 min. Equal amounts (10 µg) of cell extracts were separated by 100 g/L SDS-PAGE and transferred to nitrocellulose membrane. The membrane was blocked for one h at room temperature in 50 g/L skim milk and probed with α-actin antibody for one h. The membrane was washed three times with PBS-T and incubated for one h with secondary antibody. After washing the membrane with PBS-T for several times, the protein reactive to the primary antibody were visualized by electrochemiluminescence (ECL) detection, and semi-quantitatively analyzed by Kodak digital science 1D software.

Statistical analyses

Results were presented as mean±SD. Significance was determined by Student's *t* test or one-way ANOVA. *P*<0.05 was considered statistically significant.

RESULTS

Cultured rabbit bile duct fibroblasts

Under phase-contrast microscope, the cultured rabbit bile duct fibroblasts showed shuttle-shaped or multiangular. Their cytoplasm was clear and nucleus was large and ellipse, and their nucleoli were obvious. The isolated bile duct fibroblasts were free of smooth muscle cell contamination because they presented positive staining with vimentin and negative staining with desmin by the means of immunocytochemical ABC staining.

³H-TdR incorporation of bile duct fibroblasts

Following incubation with 0.6 g/L Ch for 12, 24, 36 and 48 h, the values of ³H-TdR incorporation of bile duct fibroblasts were respectively 3.1±0.39, 3.8±0.37, 4.6±0.48 and 5.2±0.56 mBq/cell, and those of the corresponding control groups were 3.0±0.33, 3.2±0.39, 3.7±0.49 and 4.3±0.43 mBq/cell. After comparing the values of experiment groups and their corresponding control groups, we found that the ³H-TdR incorporation of bile duct fibroblasts after treatment with 0.6 g/L Ch for 24, 36 and 48 h were significantly increased (*P*<0.05, *P*<0.01, *P*<0.01), while the ³H-TdR incorporation of the 12 h group was not statistically significant as compared with the control group (Figure 1).

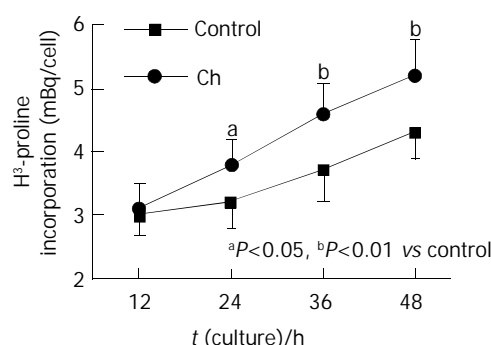


Figure 1 Effects of cholesterol on the H³-TdR incorporation of bile duct fibroblasts.

Total protein content of bile duct fibroblasts

Ch has little effect on the total protein content of fibroblasts. After being incubated with 0.6 g/L Ch for 12, 24, 36 and 48 h, the total protein content of each experiment group was not altered markedly compared with its corresponding control group. The values of experiment groups were 0.246±0.051, 0.280±0.049, 0.263±0.044 and 0.275±0.056 ng/cell, and those of corresponding control groups were 0.253±0.048, 0.270±0.042, 0.258±0.050 and 0.270±0.045 ng/cell (Figure 2).

α-actin expression of bile duct fibroblasts

Western blot analysis revealed that the α-actin expression of fibroblasts affected by Ch for 12 h and 24 h was not markedly changed compared with their corresponding control groups, the values of total gray scale of the 12 h and 24 h groups were 1 748±185 and 1 756±173 respectively, but after stimulation with Ch for 36 h, the total gray scale of fibroblasts (1 923±204) was significantly higher than that of control group (1 734±197). When the time of Ch treatment was lengthened to 48 h, the α-actin expression was markedly elevated, and the total gray

scale was $2\,189 \pm 231$ ($P < 0.01$ vs control group) (Figure 3, Table 1).

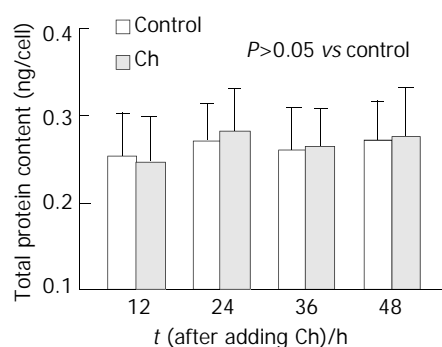
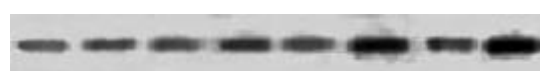


Figure 2 Effects of cholesterol on total protein content of bile duct fibroblasts.



Ch	-	+	-	+	-	+	-	+
t/h	12		24		36		48	

Figure 3 The expression of α -actin in bile duct fibroblasts detected by Western blot.

Table 1 Effects of cholesterol on the expression of α -actin in bile duct fibroblasts (mean \pm SD gray scale)

t/h	Control	Ch
12	1 723 \pm 192	1 748 \pm 185
24	1 719 \pm 138	1 756 \pm 173
36	1 734 \pm 197	1 923 \pm 204 ^a
48	1 746 \pm 164	2 189 \pm 231 ^b

^a $P < 0.05$, ^b $P < 0.01$, vs Control.

DISCUSSION

Fibroblasts are derived from mesenchymal cell of embryo period. During the process of wound healing, fibroblasts can proliferate greatly by mitoses, and also synthesize and excrete collagen fibers and matrix components^[25-29]. With the stimulation of trauma and other agents, some mature fibroblasts could change into infantile fibroblasts and their function could be recovered^[30,31]. Cardiac fibroblasts are able to secrete biological active substances, which facilitate the growth of myocardial cells^[32,33], suggesting that cardiac fibroblasts must play an important role in the normal growth of heart and its pathologic remodeling^[34,35]. Hypoxia could, mediated by pulmonary arterial endothelial cells (PAECs), induce phenotype alteration of human embryonic lung fibroblasts, transforming to smooth muscle cell-like cells, suggesting that the transformation of human embryonic lung fibroblasts might be one of the reasons for nonmuscular lung arteriole to become muscular arteriole^[36-38]. Silent fibroblasts in the border of wound can differentiate to contraction phenotype and have the special expression of α -SM actin. The cells are considered as myofibroblasts which can cause contraction of granulation tissue^[39,40]. It is thus clear that fibroblasts can take part in many kinds of physiological and pathologic responses and they have important effects on the occurrence and development of diseases.

Biliary system is the unique passage of bile ejection,

especially its terminal sphincter, SBD. Biliary system can modulate bile ejection and maintain normal pressure of biliary system^[41,42]. The coordination of its anatomic structure and function makes it not only prevent regurgitation of duodenal fluid but also modulate and stabilize the pressure of bile duct^[42-44]. So the structural remodeling of biliary system, especially the structural change and dysfunction of SBD, might be one of basic reasons of biliary system diseases occurrence. There are a lot of fibroblasts in bile duct system. In previous study, we have found that the middle concentration Ch can promote the proliferation of bile duct fibroblasts and make them present some phenotypic characteristics of muscle cell^[23,24]. But at present, it is still unclear what are the exact effects of cholesterol on bile duct fibroblasts and how fibroblasts are revolved in remodeling of biliary system, especially what roles fibroblasts play in the remodeling of SBD. In order to lucubrate the problem, we observed the effects of Ch on the proliferation and functional protein expression of bile duct fibroblasts at different times and analyzed the relation between the effects of Ch and time.

³H-TdR, prosoma of DNA synthesis, can incorporate into DNA synthesis. So the radioactivity intensity of cells can reflect DNA metabolism and proliferation of cells. It has been demonstrated that middle concentration Ch can accelerate the proliferation of bile duct fibroblasts^[23]. But the relation between Ch effects and time is still unknown. In the present study, our focal point is to observe how the Ch effects on fibroblasts alter with the changes of incubation time. Our results show that the DNA synthesis and proliferation of bile duct fibroblasts are elevated after incubated with moderately concentrated Ch for 24 h, and the effect becomes more significant gradually with the elongation of Ch treatment.

In the research of cardiovascular disease, it has been found that the proliferation and hypertrophy of cardiac fibroblasts participate in the cardiac remodeling^[34,35]. In the process of estrogen-induced uterine enlargement, there are not only the hyperplasia of uterine smooth muscle cell and epithelial cell but also augmentation of size of cells. Chronic enteritis is linked with hypertrophy of intestinal smooth muscle cells^[45-47]. From the phenomena mentioned above, we conjecture whether Ch can not only accelerate the proliferation of bile duct fibroblasts but also cause hypertrophy of fibroblasts. According to our result, the total protein content of bile duct fibroblasts was not altered after fibroblasts were treated with Ch, indicating that Ch might not significantly facilitate the hypertrophy of bile duct fibroblasts although it could promote the proliferation of fibroblasts greatly.

In our previous experiment, we detected that middle concentration Ch could increase α -actin expression of bile duct fibroblasts, and we also observed that bile duct fibroblasts showed some characteristics of muscle cells, which suggested that Ch might lead to the phenotypic variation of fibroblasts^[24]. In present study, we aim to observe the time effects of Ch on fibroblasts by the means of Western blot. It has been demonstrated that α -actin expression in bile duct fibroblasts begins to increase after incubated with Ch for 36 h, and the effect becomes more significant after 48 h. From the results above, we can easily find that the proliferation of bile duct fibroblasts is enhanced after Ch treatment for 24 h, however, it is not until Ch incubation for 36 h that the α -actin expression in bile duct fibroblasts begins to ascend. It indicates that the short-term effects of Ch are mainly to promote the proliferation of bile duct fibroblasts, and by the prolongation of Ch treatment time, Ch can also alter the functional protein expression of fibroblasts. Ch has no obvious effect on the total protein content of bile duct fibroblasts, nevertheless, it can enhance α -actin expression in fibroblasts. It suggests that Ch can only result in the changes of some special protein

expression instead of causing the hypertrophy of bile duct fibroblasts. The protein, α -actin, is an important functional protein existing in myofibroblasts and smooth muscle cells^[48,49]. So we can realize that Ch accelerates the proliferation of bile duct fibroblasts, and what is most important is that Ch can induce bile duct fibroblasts to possess some phenotypic characteristics of muscle cell.

By studying the anatomy of SBD, people found that the length of SBD is 5-15 mm without accordant result and the data fluctuates in a wide range. It has not been lucubrated whether it is only attributed to the congenital diversity of individual or it is the result of SBD remodeling induced by some postnatal factors. Wei *et al.*^[21] have found that gallbladder-derived abdominal pain after cholecystectomy, recurrent bile calculus and cholangiectasis have significant correlation with too lengthy of SBD (≥ 10 mm). It has also been manifested that most of the patients whose SBD length exceeds 10 mm are often accompanied by SBD motor dysfunction^[50]. Combining our present outcome, we suspect that some postnatal factors may result in constitution alteration of SBD, including the changes of length. The proliferation of fibroblasts, especially their phenotype transformation, may play an important role during the constitution changes of bile duct and SBD.

In conclusion, cholesterol does activate bile duct fibroblasts at the early stage, facilitating the proliferation of fibroblasts, and it can also induce the phenotype transformation of fibroblasts following the elongation of Ch treatment time. The alteration of fibroblasts might participate in the configuration remodeling of biliary system, especially the reconstitution of SBD. Gradually the function of bile duct system becomes abnormal and ultimately biliary system diseases occur. But the change *in vivo* is affected by multiple factors and is a multistage procedure. *In vitro* experiments can not absolutely reflect the conditions *in vivo*. So our experiment provides a clue to research the occurrence, development and treatment of biliary system diseases, but the certain role of bile duct fibroblasts and the certain mechanisms are still open to be elucidated.

REFERENCES

- 1 Li XP, Ouyang KQ, Cai SX. The regulation of bile secretion and education. *Shijie Huaren Xiaohua Zazhi* 2001; **9**: 1066-1070
- 2 Wei JG, Wang YC, Du F, Yu HJ. Dynamic and ultrastructural study of sphincter of Oddi in early-stage cholelithiasis in rabbits with hypercholesterolemia. *World J Gastroenterol* 2000; **6**: 102-106
- 3 Lammert F, Sudfeld S, Busch N, Matern S. Cholesterol crystal binding of biliary immunoglobulin A: visualization by fluorescence light microscopy. *World J Gastroenterol* 2001; **7**: 198-202
- 4 Lui P, Chen DF. The separation and primary culture of canine gallbladder epithelium. *Shijie Huaren Xiaohua Zazhi* 2001; **9**: 99-100
- 5 Zapata R, Severin C, Manriquez M, Valdivieso V. Gallbladder motility and lithogenesis in obese patients during diet-induced weight loss. *Dig Dis Sci* 2000; **45**: 421-428
- 6 Greaves RR, O'Donnell LJ, Farthing MJ. Differential effect of prostaglandins on gallstone-free and gallstone-containing human gallbladder. *Dig Dis Sci* 2000; **45**: 2376-2381
- 7 Buhman KK, Accad M, Novak S, Choi RS, Wong JS, Hamilton RL, Turley S, Farese RV Jr. Resistance to diet-induced hypercholesterolemia and gallstone formation in ACAT2-deficient mice. *Nat Med* 2000; **6**: 1341-1347
- 8 Gustafsson U, Sahlin S, Einarsson C. High level of deoxycholic acid in human bile does not promote cholesterol gallstone formation. *World J Gastroenterol* 2003; **9**: 1576-1579
- 9 Bogdarian IuA, Kozlov DV. Correction of lipid metabolism in rabbits with experimental cholelithiasis. *Vopr Med Khim* 2002; **48**: 368-372
- 10 Quallich LG, Stern MA, Rich M, Chey WD, Barnett JL, Elta GH. Bile duct crystals do not contribute to sphincter of Oddi dysfunction. *Gastrointest Endosc* 2002; **55**: 163-166
- 11 Masclee AA, Vu MK. Gallbladder motility in inflammatory bowel diseases. *Dig Liver Dis* 2003; **35**(Suppl 3): S35-S38
- 12 Pallotta N. Ultrasonography in the assessment of gallbladder motor activity. *Dig Liver Dis* 2003; **35**(Suppl 3): S67-S69
- 13 Rhee JY, Elta GH. The relationship of bile duct crystals to sphincter of Oddi dysfunction. *Curr Gastroenterol Rep* 2003; **5**: 160-163
- 14 Kohut M, Nowak A, Nowakowska-Duiawa E, Marek T. Presence and density of common bile duct microlithiasis in acute biliary pancreatitis. *World J Gastroenterol* 2002; **8**: 558-561
- 15 Zanolungo S, Nervi F. The molecular and metabolic basis of biliary cholesterol secretion and gallstone disease. *Front Biosci* 2003; **8**: S1166-S1174
- 16 Toouli J. Biliary dyskinesia. *Curr Treat Options Gastroenterol* 2002; **5**: 285-291
- 17 Wang XJ, Wei JG, Wang CM, Wang YC, Wu QZ, Xu JK, Yang XX. Effect of cholesterol liposomes on calcium mobilization in muscle cells from the rabbit sphincter of Oddi. *World J Gastroenterol* 2002; **8**: 144-149
- 18 Wang XJ, Wei JG, Wang YC, Xu JK, Wu QZ, Wu DC, Yang XX. Effect of cholesterol liposome on contractility of rabbit Oddi's sphincter smooth muscle cells. *Shijie Huaren Xiaohua Zazhi* 2000; **8**: 633-637
- 19 Corazziari E. Sphincter of Oddi dysfunction. *Dig Liver Dis* 2003; **35**(Suppl 3): S26-S29
- 20 Avisse C, Flament JB, Delattre JF. Ampulla of Vater. Anatomic, embryologic, and surgical aspects. *Surg Clin North Am* 2000; **80**: 201-212
- 21 Wei JG, Wang YC, Liang GM, Wang W, Chen BY, Xu JK, Song LJ. The study between the dynamics and the X-ray anatomy and regularizing effect of gallbladder on bile duct sphincter of the dog. *World J Gastroenterol* 2003; **9**: 1014-1019
- 22 Savrasov VM. Functional radiographic anatomy of the terminal sphincter duct of the biliary pancreatic system. *Eksp Klin Gastroenterol* 2002; **6**: 81-82
- 23 Chen BY, Wei JG, Wang YC, Yang XX, Qian JX, Yu J, Chen ZN, Xu J, Wu DC. Effects of cholesterol on the proliferation of cultured rabbit bile duct fibroblasts. *Shijie Huaren Xiaohua Zazhi* 2002; **10**: 566-570
- 24 Chen BY, Wei JG, Wang YC, Wang CM, Yu J, Yang XX. Effects of cholesterol on the phenotype of rabbit bile duct fibroblasts. *World J Gastroenterol* 2003; **9**: 351-355
- 25 Laplante AF, Germain L, Auger FA, Moulin V. Mechanisms of wound reepithelialization: hints from a tissue-engineered reconstructed skin to long-standing questions. *FASEB J* 2001; **15**: 2377-2389
- 26 Jun JB, Kuechle M, Harlan JM, Elkon KB. Fibroblast and endothelial apoptosis in systemic sclerosis. *Curr Opin Rheumatol* 2003; **15**: 756-760
- 27 Gabbiani G. The myofibroblast in wound healing and fibrocontractive diseases. *J Pathol* 2003; **200**: 500-503
- 28 Phan SH. Fibroblast phenotypes in pulmonary fibrosis. *Am J Respir Cell Mol Biol* 2003; **29**(3 Suppl): S87-92
- 29 Tejedo-Trujillo R. How do fibroblasts interact with the extracellular matrix in wound contraction? *J Wound Care* 2001; **10**: 237-242
- 30 Hinz B, Gabbiani G. Cell-matrix and cell-cell contacts of myofibroblasts: role in connective tissue remodeling. *Thromb Haemost* 2003; **90**: 993-1002
- 31 Bisson MA, McGrouther DA, Mudera V, Grobbelaar AO. The different characteristics of Dupuytren's disease fibroblasts derived from either nodule or cord: expression of alpha-smooth muscle actin and the response to stimulation by TGF-beta1. *J Hand Surg* 2003; **28**: 351-356
- 32 Piper C, Schultheiss HP, Akdemir D, Rudolf J, Horstkotte D, Pauschinger M. Remodeling of the cardiac extracellular matrix differs between volume- and pressure-overloaded ventricles and is specific for each heart valve lesion. *J Heart Valve Dis* 2003; **12**: 592-600
- 33 Jugdutt BI. Remodeling of the myocardium and potential targets in the collagen degradation and synthesis pathways. *Curr Drug Targets Cardiovasc Haematol Disord* 2003; **3**: 1-30
- 34 Yang F, Liu YH, Yang XP, Xu J, Kapke A, Carretero OA. Myocardial infarction and cardiac remodeling in mice. *Exp Physiol* 2002; **87**: 547-555
- 35 Manabe I, Shindo T, Nagai R. Gene expression in fibroblasts and fibrosis: involvement in cardiac hypertrophy. *Circ Res* 2002; **91**: 1103-1113

- 36 **Papakonstantinou E**, Aletras AJ, Roth M, Tamm M, Karakiulakis G. Hypoxia modulates the effects of transforming growth factor-beta isoforms on matrix-formation by primary human lung fibroblasts. *Cytokine* 2003; **24**: 25-35
- 37 **Das M**, Dempsey EC, Reeves JT, Stenmark KR. Selective expansion of fibroblast subpopulations from pulmonary artery adventitia in response to hypoxia. *Am J Physiol Lung Cell Mol Physiol* 2002; **282**: L976-986
- 38 **Bogatkevich GS**, Tourkina E, Abrams CS, Harley RA, Silver RM, Ludwicka-Bradley A. Contractile activity and smooth muscle alpha-actin organization in thrombin-induced human lung myofibroblasts. *Am J Physiol Lung Cell Mol Physiol* 2003; **285**: L334-343
- 39 **Eyden B**. Electron microscopy in the study of myofibroblastic lesions. *Semin Diagn Pathol* 2003; **20**: 13-24
- 40 **Ehrlich HP**, Diez T. Role for gap junctional intercellular communications in wound repair. *Wound Repair Regen* 2003; **11**: 481-489
- 41 **Li XP**, Mao XZ. Effect of estrogen, cholic acid loading and bile draining on hepatobiliary functions in rats. *Shijie Huaren Xiaohua Zazhi* 2000; **8**: 1009-1012
- 42 **Zhu XF**, Chen GH, He XS, Lu MQ, Wang GD, Cai CJ, Yang Y, Huang JF. Liver transplantation and artificial liver support in fulminant hepatic failure. *World J Gastroenterol* 2001; **7**: 566-568
- 43 **He XS**, Huang JF, Liang LJ, Lu MD, Cao XH. Surgical resection for hepato portal bile duct cancer. *World J Gastroenterol* 1999; **5**: 128-131
- 44 **Yang HM**, Wu J, Li JY, Zhou JL, He LJ, Xu XF. Optic properties of bile liquid crystals in human body. *World J Gastroenterol* 2000; **6**: 248-251
- 45 **Diana A**, Pietra M, Guglielmini C, Boari A, Bettini G, Cipone M. Ultrasonographic and pathologic features of intestinal smooth muscle hypertrophy in four cats. *Vet Radiol Ultrasound* 2003; **44**: 566-569
- 46 **Cheng AC**, Wang MS, Chen XY, Guo YF, Liu ZY, Fang PF. Pathogenic and pathological characteristic of new type gosling viral enteritis first observed in China. *World J Gastroenterol* 2001; **7**: 678-684
- 47 **Bettini G**, Muracchini M, Della Salda L, Preziosi R, Morini M, Guglielmini C, Sanguinetti V, Marcato PS. Hypertrophy of intestinal smooth muscle in cats. *Res Vet Sci* 2003; **75**: 43-53
- 48 **Gunst SJ**, Tang DD, Opazo Saez A. Cytoskeletal remodeling of the airway smooth muscle cell: a mechanism for adaptation to mechanical forces in the lung. *Respir Physiol Neurobiol* 2003; **137**: 151-168
- 49 **Schelling JR**, Sinha S, Konieczkowski M, Sedor JR. Myofibroblast differentiation: plasma membrane microdomains and cell phenotype. *Exp Nephrol* 2002; **10**: 313-319
- 50 **Prajapati DN**, Hogan WJ. Sphincter of Oddi dysfunction and other functional biliary disorders: evaluation and treatment. *Gastroenterol Clin North Am* 2003; **32**: 601-618

Edited by Gupta MK and Xu FM

• CLINICAL RESEARCH •

Fenofibrate for patients with asymptomatic primary biliary cirrhosis

Kazufumi Dohmen, Toshihiko Mizuta, Makoto Nakamuta, Naoya Shimohashi, Hiromi Ishibashi, Kyosuke Yamamoto

Kazufumi Dohmen, Department of Internal Medicine, Okabe Hospital, Japan

Hiromi Ishibashi, Department of Clinical Research Center, National Nagasaki Medical Center, Japan

Toshihiko Mizuta, Kyosuke Yamamoto, Department of Internal Medicine, Saga Medical School, Japan

Makoto Nakamuta, Department of Medicine and Bioregulatory Science, Graduate School of Medical Sciences, Kyushu University, Japan

Naoya Shimohashi, Department of Internal Medicine, Fukuoka City Hospital, Japan

Correspondence to: Dr. Kazufumi Dohmen, Department of Internal Medicine, Okabe Hospital, 1-2-1 Myojinzaka Umi-machi Kasuyagun Fukuoka 811-2122 Japan. dohmenk@par.odn.ne.jp

Telephone: +81-92-932-0025 **Fax:** +81-92-933-7253

Received: 2003-11-17 **Accepted:** 2004-01-18

Abstract

AIM: Primary biliary cirrhosis (PBC) is a chronic, cholestatic disease of autoimmune etiology, the histology of which shows a destruction of the intrahepatic bile duct and portal inflammation. Ursodeoxycholic acid (UDCA) is now used as a first-line drug for asymptomatic PBC (aPBC) because it is reported that UDCA decreases mortality and prolongs the time of liver transplantation. However, only 20-30% of patients respond fully to UDCA. Recently, lipoprotein-lowering agents have been found to be effective for PBC. The aim of this study was to examine the safety and efficacy of fenofibrate, a member of the fibrate class of hypolipidemic and anti-inflammatory agent via peroxysome proliferator-activated receptor α , in patients with aPBC.

METHODS: Fenofibrate was administered for twelve weeks in nine patients with aPBC who failed to respond to UDCA. UDCA was used along with fenofibrate during the study. The data from aPBC patients were analyzed to assess the biochemical effect of fenofibrate during the study.

RESULTS: The serum levels of alkaline phosphatase (ALP) (285 ± 114.8 IU/L) and immunoglobulin M (IgM) (255.8 ± 85.9 mg/dl) significantly decreased to 186.9 ± 76.2 IU/L and 192.9 ± 67.5 mg/dL respectively, after fenofibrate treatment in patients with aPBC ($P < 0.05$). Moreover, the titer of antimitochondrial antibody (AMA) also decreased in 4 of 9 patients with aPBC. No adverse reactions were observed in any patients.

CONCLUSION: Fenofibrate appears to be significantly effective in treating patients with aPBC who respond incompletely to UDCA alone. Although the mechanism of fenofibrate on aPBC has not yet been fully clarified, combination therapy using fenofibrate and UDCA might be related to the anti-immunological effects, such as the suppression of AMA production as well as its anti-inflammatory effect.

Dohmen K, Mizuta T, Nakamuta M, Shimohashi N, Ishibashi H, Yamamoto K. Fenofibrate for patients with asymptomatic primary biliary cirrhosis. *World J Gastroenterol* 2004; 10(6): 894-898 <http://www.wjgnet.com/1007-9327/10/894.asp>

INTRODUCTION

Primary biliary cirrhosis (PBC) is a chronic, cholestatic liver disease characterized by inflammation and progressive destruction of interlobular bile ducts, eventually leading to cholestasis, biliary cirrhosis and finally hepatic failure. The etiology of PBC is attributed to autoimmunity mainly due to the association with autoantibodies such as antimitochondrial antibodies (AMA), which present in 95% of PBC patients, and an increased level of immunoglobulin M (IgM). Regarding this therapy, orthotopic liver transplantation is selected for PBC patients with liver failure and intractable pruritus, while ursodeoxycholic acid (UDCA) has been widely used as a first-line drug for asymptomatic PBC (aPBC) to slow the disease progression^[1-3]. Although the biochemical data of the liver functions tend to normalize in 20-30% of patients with aPBC who are administered UDCA, the rest of the patients often progress to cirrhosis^[4,5]. Therefore, there is a need for a more effective treatment^[6].

PBC is often associated with lipoprotein abnormalities such as an elevation of serum cholesterol concentration^[7]. Recently, several studies focusing on lipoprotein-lowering drugs for PBC have been reported^[8-15]. Simvastatin, an HMG-CoA reductase inhibitor, was proven to be useful as a modulator of cholestasis and an immune response in PBC^[8]. Bezafibrate, a hypolipidemic agent, was also effective in PBC patients who failed to respond to UDCA^[9-15]. The mechanism of action of bezafibrate is believed to be the anti-inflammatory effects via peroxysome proliferator-activated receptor α (PPAR α), a member of the nuclear hormone receptor superfamily, and the expression of multiple drug resistance gene-3, both of which ameliorate hepatobiliary inflammation in PBC^[11,16-18]. Fenofibrate is a member of fibrate class agents as bezafibrate and works as a ligand of PPAR α , showing a potent triglyceride-lowering effect. Fenofibrate treatment for PBC has been addressed in very few studies^[19], including our previous abstracts which we presented at conferences^[20,21]. The effect of fenofibrate on PBC therefore has to be clarified and is currently being evaluated.

For this purpose, we studied the efficacy of fenofibrate on nine patients with aPBC who responded insufficiently to monotherapy of UDCA.

MATERIALS AND METHODS

Patients and regimen

Nine patients with aPBC consisting of 2 males and 7 females were included in the prospective study. Ages were 50.3 ± 11.7 (mean \pm SD) yr ranging from 34 to 69 yr, and mean body mass 57.9 ± 5.6 (mean \pm SD) kg ranging from 50.0 to 64.6 kg. They were diagnosed to have aPBC according to laboratory and/or histological findings. All patients were negative both for anti-hepatitis C virus antibody and for hepatitis B surface antigen. All 9 patients with aPBC exhibited a poor therapeutic response to UDCA of 600 mg/d for 6 mo or more. Fenofibrate of 100 mg/d was administered for 4 patients (less than 60 kg in body mass) and of 150 mg for 5 patients (60 kg or more in body mass) for at least 12 wk. The study was approved by the local ethics committee, and informed consent was obtained from each patient included in the study.

Laboratory examination

During the study, any changes in dietary therapy were prohibited. In order to determine the drug compliance and safety, all patients were required to visit the hospital every 2 wk, and the serum blood chemistry including apolipoprotein was examined every 4 wk. Serum concentrations of total bilirubin, immunoglobulins G and M (IgG, IgM) as well as aspartate aminotransferase (AST), alanine aminotransferase (ALT), alkaline phosphatase (ALP) and gamma-glutamyltransferase (γ GTP) were determined before the fenofibrate treatment as well after the treatment of 12 wk by routine laboratory procedures. AMA titers were measured using indirect immunofluorescence based on stomach/kidney frozen sections. Blood was sampled early in the morning during fasting, and a medical laboratory (SRL Co., Tokyo) centrally controlled the measurements up to 12 wk after the start of administration.

Statistical analysis

Differences in the means and proportions were evaluated by Chi-square test and Student's *t*-test. Baseline variables were assessed in the study, including AST, ALT, ALP, γ GTP, apolipoproteins, IgG, IgM and AMA titers. *P* value less than 0.05 was considered statistically significant.

RESULTS

Effect of fenofibrate on laboratory findings for hepatobiliary system and serum lipids

Table 1 and Figure 1 show the enzymatic changes in the hepatobiliary system identified up to 12 wk after the start of the combination therapy of fenofibrate and UDCA. The mean ALP value of 285.0 IU/L prior to fenofibrate therapy decreased to 186.9 IU/L at wk 12 after the initiation of the therapy, thus showing a statistically significant difference. The serum γ -GTP concentration also decreased after 12 wk of fenofibrate and UDCA treatment compared to that at initiation, although the difference was not statistically significant. The serum concentrations of AST and ALT did not change statistically regarding those obtained prior to and after 12 wk of treatment. The serum concentration of IgM of 255.8 mg/dL prior to the treatment was significantly reduced to 192.9 mg/dL at wk 12, whereas the concentration of IgG did not decrease. Regarding the titer of AMA, a reduction was identified in 4 of the 9 patients based on that obtained prior to and after 12 wk of treatment. As shown in Figure 2, the AMA titer of 320 decreased to 40, 320 to 80, 80 to 20 and 40 to 20 in 4 of 9 patients, respectively. The titers of AMA in the rest 5 patients remained unchanged. The serum levels of ALP of 571 IU/L and IgM of 236 mg/dL decreased to 306 IU/L and 154 mg/dL, respectively, in a patient whose AMA titer decreased from more than 320 to 40. Likewise, those of 276 and 159 decreased to 285 and 102 in a patient whose AMA titer decreased from more than 320 to 80, those of 215 and 375 decreased to 107 and 241 in a patient whose AMA titer decreased from 80 to 20, and those of 191 and 240 decreased to 114 and 180 in a patient whose AMA titer decreased from 80 to 20, respectively. Interestingly, all the four cases who showed a reduction of the AMA titer were females.

Table 2 shows the changes in serum lipids and apoprotein levels in all 9 patients. The concentrations of apo A-II (median value: 31.6 mg/dL) and apo C-II (median value: 3.9 mg/dL) increased statistically to 44.1 mg/dL and 4.5 mg/dL during fenofibrate therapy ($P < 0.005$), respectively. The concentrations of total cholesterol (TC), triglyceride (TG), low density lipoprotein-cholesterol (LDL-C) and Apo B lipoprotein tended to decrease while the high density lipoprotein-cholesterol (HDL-C), apo A-I and apo E levels tended to increase. However, the difference was not statistically significant.

Table 1 Change in concentrations of laboratory data (mean \pm SD)

Laboratory Variable	Before therapy	4 wk	8 wk	12 wk
AST (IU/L)	29.9 \pm 8.1	50.0 \pm 36.3	46.6 \pm 24.9	46.9 \pm 28.3
ALT (IU/L)	31.1 \pm 13.2	48.6 \pm 35.2	57.0 \pm 38.9	48.4 \pm 42.5
ALP (IU/L)	285.0 \pm 114.8	238.5 \pm 88.4	200.6 \pm 76.7 ^a	186.9 \pm 76.2 ^a
γ -GTP (IU/L)	149.6 \pm 143.0	147.0 \pm 178.6	128.8 \pm 128.1	125.2 \pm 110.3
LDH (IU/L)	311.2 \pm 46.7	318.4 \pm 44.8	320.1 \pm 59.9	324.6 \pm 59.2
TB (mg/dl)	0.7 \pm 0.7	0.4 \pm 0.2	0.6 \pm 0.4	0.6 \pm 0.5
IgG (mg/dl)	1 431.4 \pm 285.3	-	-	1 415.0 \pm 316.1
IgM (mg/dl)	255.8 \pm 85.9	-	-	192.9 \pm 67.5 ^a

^a $P < 0.05$ (baseline-matched *t*-test) vs the serum concentrations prior to the treatment.

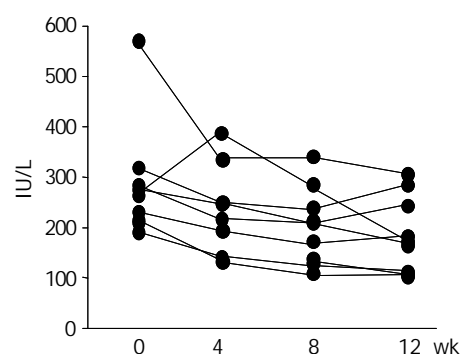


Figure 1 Change in the serum alkaline phosphatase levels during fenofibrate treatment.

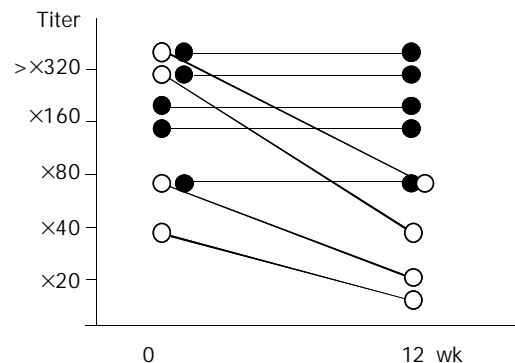


Figure 2 Change in antimitochondria antibody titers before and after fenofibrate treatment.

Table 2 Change in concentrations of serum lipids and apoproteins

Variables	Before	4 wk	8 wk	12 wk
TC (mg/dL)	206.3 \pm 26.5	186.3 \pm 22.9	189.9 \pm 27.7 ^a	192.1 \pm 30.1
TG (mg/dL)	126.0 \pm 50.1	119.5 \pm 76.2	102.8 \pm 52.3	103.6 \pm 53.0
HDL-C (mg/dL)	63.6 \pm 11.3	63.8 \pm 14.0	68.8 \pm 12.6	69.3 \pm 13.1
LDL-C (mg/dL)	115.7 \pm 22.1	99.3 \pm 29.3	105.6 \pm 28.0	105.2 \pm 25.1
Apo A-I (mg/dL)	159.0 \pm 17.9	154.7 \pm 19.4	158.3 \pm 17.9	172.1 \pm 24.3
Apo A-II (mg/dL)	31.6 \pm 6.5	39.5 \pm 7.0 ^a	40.7 \pm 4.6 ^a	44.1 \pm 4.9 ^a
Apo B (mg/dL)	95.1 \pm 22.9	84.1 \pm 31.4	81.0 \pm 26.5	84.1 \pm 23.1
Apo C-II (mg/dL)	3.9 \pm 1.7	4.6 \pm 2.0 ^a	4.2 \pm 1.6	4.5 \pm 1.5 ^a
Apo C-III (mg/dL)	9.7 \pm 3.8	9.5 \pm 4.2	8.9 \pm 2.9	9.8 \pm 3.6
Apo E (mg/dL)	4.3 \pm 1.0	4.3 \pm 0.8	4.4 \pm 0.8	4.6 \pm 0.9

TC: total cholesterol, TG: triglyceride, HDL-C: HDL-cholesterol, LDL-C: LDL-cholesterol, Apo: apoprotein. ^a $P < 0.05$ (baseline-matched *t*-test) vs the serum concentrations prior to the treatment.

Rate of change of each variable between AMA-reduced group and AMA-unchanged group

The rate of change of each variable between the AMA-reduced group and the AMA-unchanged group was compared before and after the combination therapy of fenofibrate and UDCA. As shown in Table 3, the IgM concentrations dropped to $35.4 \pm 0.6\%$ in the AMA-reduced group and $7.1 \pm 1.8\%$ in the AMA-unchanged group, showing a statistically significance between the two groups. Interestingly, however, the values of ALP, γ -GTP and apo A-II dropped at a similar rate in two groups.

Table 3 Rate of change in the valuables between AMA-reduced group and AMA-unchanged group

Factors	AMA-reduced group	AMA-unchanged group	t-test
ALT (IU/L)	61.6 ± 124.8^1	52.0 ± 109.2	0.905
ALP (IU/L)	-33.4 ± 24.8	-33.8 ± 16.0	0.978
γ -GTP (IU/L)	-2.8 ± 73.4	-5.3 ± 39.8	0.950
IgM (mg/dL)	-35.4 ± 0.6	-7.1 ± 11.8	0.010
Apo A-II (mg/dL)	52.0 ± 17.3	37.4 ± 38.6	0.573
Apo C-II (mg/dL)	29.5 ± 13.8	10.6 ± 10.1	0.089

¹Changing rate (%) (mean \pm SD).

Adverse effects

In all the nine patients, no subjective symptoms such as systemic malaise, anoxia, were observed. No deterioration of the liver function tests was identified in any cases as shown in Table 1. The blood urea nitrogen and creatinine levels did not change either after fenofibrate administration.

DISCUSSION

Primary biliary cirrhosis presents as a chronic cholestatic disease involving predominantly middle-aged women with a very frequent association with AMA. In addition, PBC has been found to be often associated with other autoimmune diseases^[22-27]. Therefore, PBC is thought to be an autoimmune disease and most therapies have thus been directed at altering the immune response. So far, the use of corticosteroid, azathioprine, cyclosporine^[28], D-penicillamine^[29], methotrexate^[30,31], colchicines^[31,32] has been studied for patients with PBC.

However, none of these drugs appeared to offer any significant benefits while they tended to induce adverse effects such as osteoporosis, or pulmonary toxicity^[24]. Recently UDCA appeared to be a drug which most effectively treated patients with PBC^[1-3] through cytoprotective and choleric effects and alterations in the bile pool by competition for uptake by ileal bile acid receptors. However, a considerable number of patients with PBC still clinically respond insufficiently to UDCA alone, and now a new problem has emerged concerning which agent should be used for these patients.

Several clinical studies on lipoprotein-lowering agents such as simvastatin^[8] and bezafibrate^[9-15] for PBC patients who failed to respond to UDCA have so far been conducted, and the results have been found to be of value. In addition, fenofibrate, a member of such fibrate class agents as bezafibrate, has recently been found to be an expected agent for PBC because of its stronger activity of an anti-inflammatory effect via PPAR α ^[33], and more potentiality in reducing TG and LDL-C levels^[34] than that of bezafibrate. Early attempts of the apoprotein-lowering agents focused on treating concomitant conditions of hypertriglyceremia or hypercholesterolemia. Therefore, we conducted a study on the efficacy of fenofibrate in nine patients with aPBC.

Indeed, serum concentrations of TC and TG decreased and the concentration of HDL-C increased in all the 9 patients with aPBC, however, these changes were not statistically significant. As for apoprotein, apo AII and apo C II, which are major protein constituents of HDL, were significantly increased in the study. As a result, lipoprotein, an indicator for the risk of developing atherosclerotic disease was improved after fenofibrate treatment in PBC patients in our study^[7,35].

Fenofibrate has been shown to regulate the expression of various kinds of lipids and proteins, and cell proliferation through the activation of PPAR α ^[36,37]. However, apart from the lipoprotein-lowering effect, its pleiotropic effects have recently received much attention ranging from inhibited production of interleukin (IL)-1, IL-6, IL-1- and IL-6-induced prostaglandin E2 as well as cyclooxygenase (COX)-2 expression to the induction of apo A-II through the inhibition of the nuclear factor (NF)- κ B signalling by activation of PPAR α ^[38,39]. Furthermore, fenofibrate could inhibit the expression of intercellular adhesion molecule (ICAM)-1 and vascular cell adhesion molecule (VCAM)-1, which play a role in the adhesion of monocytes through apo A-II induction or NF- κ B inhibition

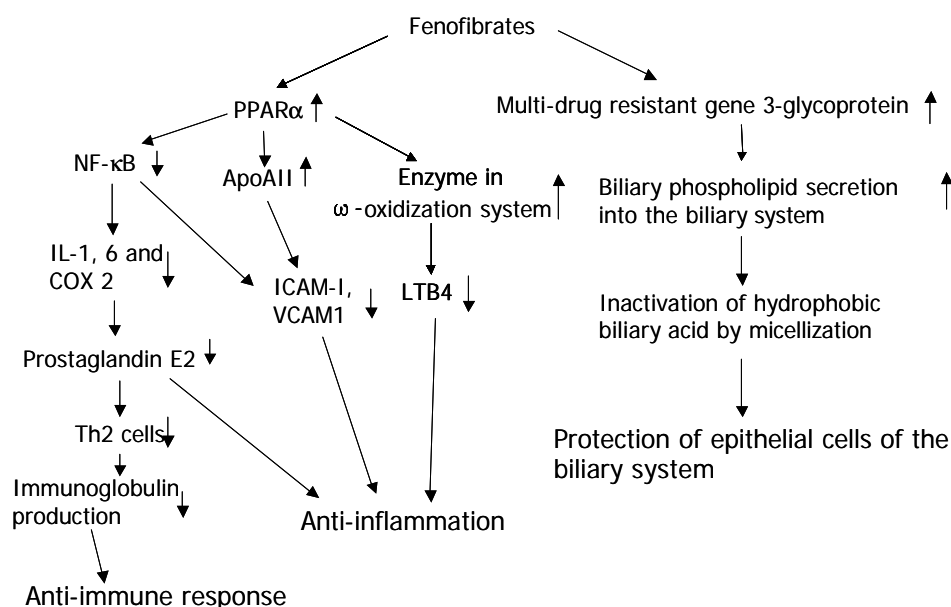


Figure 3 Possible mechanisms of action for fibrates on PBC.

[40]. These findings suggest that fenofibrate can inhibit not only the lipid metabolism but also the inflammatory reaction through PPAR α . It is therefore likely that the PPAR α activation-mediated anti-inflammatory effects of fenofibrate, such as the inhibited expression of NF- κ B, IL-1, IL-6, COX-2 and prostaglandin E2 might contribute to an improvement of PBC. Apo A-II could inhibit the expression of such adhesion molecules as ICAM-1 and VCAM-1 which are believed to be progression factors in cases of PBC, because adhesion molecules induce lymphocytes into epithelial cells of hepatobiliary ducts. From another point of view, as reported by Iwasaki *et al* [11], improvement of PBC might also occur because the canalicular phospholipid translocator, encoded by multi-drug resistant gene-3 (MDR3) expressed by bezafibrate administration, was exclusively present on the canalicular membrane, increases the secretion of biliary phospholipids and inactivating hydrophobic bile acid by micellization to protect hepatocytes and epithelial cells of bile ducts [18] (Figure 3). Thus, MDR3 messenger RNA and the canalicular phospholipid translocator (MDR3-P glycoprotein) of fibrates are strictly PPAR α dependent. Although the different sensitivities to PPAR α between fenofibrate and bezafibrate have not yet been clarified, a possible reason is that fenofibrate could selectively act on PPAR α only, while bezafibrate could act on PPAR α , γ as well as δ [33].

The emerging question is whether fenofibrate's anti-immunological effect is truly mediated via PPAR α or its receptor-independent anti-inflammatory effects. Our results demonstrated that fenofibrate did not only improve dyslipoproteinemia but also significantly reduce serum ALP and IgM levels. It was of great interest that a reduction of AMA titer was also observed in 4 of 9 patients. The immunological response of PBC patients to fenofibrate therapy thus raises another question, namely, how is the AMA production regulated by PPAR α in PBC? Is the AMA production interrelated in the inflammation or lipid synthesis? Kurihara *et al* reported 5 cases of aPBC who responded to the combination therapy of bezafibrate and UDCA [9], however, the AMA titer remained unchanged in all cases. Nevertheless, there was a reduction of IgM as well as ALP, γ GTP and TC. Similarly, Iwasaki *et al* described that IgM decreased significantly, but the AMA titers were not affected in all 5 PBC patients treated with bezafibrate [11]. In contrast, Fukuo *et al* showed 6 cases of aPBC who responded to bezafibrate with a decreased AMA titer [10]. Nakai *et al* did not analyze the AMA titer among 23 patients with PBC treated with a combination therapy of bezafibrate and UDCA, while they confirmed a decrease in the IgM concentration [12]. Although no relationship between IgM concentration and AMA titer was observed in these papers, our study demonstrated that IgM concentration closely correlated with the reduction of AMA titer, whereas the decrease of ALP and γ -GTP levels was not correlated with the AMA reduction. Interestingly, immunoglobulins, the secretory products of stimulated B lymphocytes, were characteristically elevated, with a distinct focus on IgM in PBC. One possibility to explain the reduction of IgM by fenofibrate treatment for PBC is that the decreased production of prostaglandin E2 via PPAR α suppressed the Th2 lymphocytes that induce B cells, thus leading to the reduced production of immunoglobulin [41]. However, our study showed that fenofibrate treatment for PBC resulted in a decrease in IgM level, while IgG level was unchanged. Fenofibrate may also possess an additional or synergistic potential for lowering IgM levels as observed in the ALP and γ GTP levels. The exact cause of hyperglobulinemia in PBC, however, remains to be elucidated.

Regarding the adverse effect of fenofibrate, diabetes arteriosclerosis intervention study (DAIS) showed that micronized fenofibrate at 200 mg (equivalent to 300 mg of the

standard formulation) was administered for 3 yr to type 2 diabetic patients in order to observe its inhibitory effect on the progression of coronary arterial stenosis. As a result, no difference in the safety between fenofibrate and placebo was observed [42]. In addition, studies of human first-generation cultured cells and HepG2 cells suggested that serum aminotransferase levels were transiently elevated and then normalized or returned to pretreatment levels [43]. The increase in the aminotransferase level after treatment with fenofibrate was not considered to be clinically significant. As fenofibrate could activate the aminotransferase gene expression, thus leading to a mild and transient elevation of aminotransferase through mechanisms of PPAR α involving increased levels of reactive oxygen species and intracellular glutathion depletion, thus leading to mitochondrial dysfunction and perturbation of intracellular Ca⁺⁺ homeostasis and also to cell death [43,44]. A dosage of 100 mg or 150 mg per day of fenofibrate in the 9 patients studied, which is half the commonly administered dose, was thus administered to poor responders to UDCA, and a blood examination was performed every 2 wk. No adverse effect was observed either clinically or biochemically in all the 9 patients in our study.

Administration of fenofibrate in combination with UDCA was safe and useful for patients with aPBC. This finding confirms our belief that fenofibrate's beneficial effects are mediated only through its lipoprotein-lowering effect. The mechanism underlying the long term efficacy of fenofibrate for symptomatic PBC remains to be elucidated [15]. The expansive array of ligands, target genes, and metabolic processes regulated by nuclear receptors such as PPAR α , β , γ within hepatocytes, and ever-changing internal milieu, has made a completely comprehensive regulatory scheme virtually impossible to depict graphically [44]. Nuclear receptors-regulated gene products may create or disable a protein ligand or regulate the import or export of another nuclear receptor, which might be related to the production of IgM or AMA. There are likely many more mechanisms of action for fenofibrate on PBC still awaiting further discovery.

In conclusion, fenofibrate can be well tolerated by all patients with aPBC, while it has no remarkable side effects. This agent is beneficial for the treatment of aPBC. However, further studies are needed to elucidate the effect of fenofibrate on PBC and to determine its long-term biochemical and histological efficacy.

REFERENCES

- 1 **Poupon RE**, Poupon R, Balkau B. Ursodiol for the long-term treatment of primary biliary cirrhosis. *N Eng J Med* 1994; **330**: 1342-1347
- 2 **Poupon R**, Poupon RE. Treatment of primary biliary cirrhosis. *Bailliere's Clin Gastroenterol* 2000; **14**: 615-628
- 3 **Combes B**, Carithers RL, Maddrey WC, Lin D, McDonald MF, Wheeler DE, Eigenbrodt EH, Munoz SJ, Rubin R, Garcia-Tsao G, Bonner GF, West AB, Boyer J, Luketic VA, Shiffman ML, Mills AS, Peters MG, White HM, Zetterman RK, Rossi SS, Hofman AF, Markin RS. A randomized, double-blind, placebo-controlled trial of ursodeoxycholic acid in primary biliary cirrhosis. *Hepatology* 1995; **22**: 759-766
- 4 **Jorgensen RA**, Dickson ER, Hofmann AF, Rossi SS, Lindor KD. Characterisation of patients with a complete biochemical response to ursodeoxycholic acid. *Gut* 1995; **36**: 935-938
- 5 **Leuschner M**, Dietrich CF, You T, Seidl C, Raedle J, Herrmann G, Ackermann H, Leuschner U. Characterization of patients with primary biliary cirrhosis responding to long term ursodeoxycholic acid treatment. *Gut* 2000; **46**: 121-126
- 6 **Levy C**, Lindor KD. Current management of primary biliary cirrhosis and primary sclerosing cholangitis. *J Hepatol* 2003; **38**: S24-S37
- 7 **Jahn CE**, Schaefer EJ, Taam LA, Hoofnagle JH, Lindgren FT,

- Albers JJ, Jones EA, Brewer Jr B. Lipoprotein abnormalities in primary biliary cirrhosis. Association with hepatic lipase inhibition as well as altered cholesterol esterification. *Gastroenterology* 1985; **89**: 1266-1278
- 8 **Ritzel U**, Leonhardt U, Nather M, Schafer G, Armstrong VW, Ramadori G. Simvastatin in primary biliary cirrhosis: effects on serum lipids and distinct disease markers. *J Hepatol* 2002; **36**: 454-458
- 9 **Kurihara T**, Yanagisawa A, Kitamura Y, Itabashi K, Arita Y, Tsuchiya M, Akimoto M, Ishiguro H, Hashimoto H, Maeda A, Shigemoto M, Yamashita K, Yokoyama I. Effect of bezafibrate in patients with PBC. *Rhinsho Iyaku* 1997; **13**: 4255-4258
- 10 **Fukuo Y**, Tada N, Yamamoto K. Study of efficacy of bezafibrate for PBC. *Rinsho Seijinkyō* 1999; **29**: 1367-1372
- 11 **Iwasaki S**, Tsuda K, Ueta H, Aono R, Ono M, Saibara T, Maeda T, Onishi S. Bezafibrate may have a beneficial effect in pre-cirrhotic primary biliary cirrhosis. *Hepatol Res* 1999; **16**: 12-18
- 12 **Nakai S**, Masaki T, Kurokohchi K, Deguchi A, Nishioka M. Combination therapy of bezafibrate and ursodeoxycholic acid in primary biliary cirrhosis: a preliminary study. *Am J Gastroenterol* 2000; **95**: 326-327
- 13 **Miyaguchi S**, Ebinuma H, Imaeda H, Nitta Y, Watanabe T, Saito H, Ishii H. A novel treatment for refractory primary biliary cirrhosis? *Hepatogastroenterology* 2000; **47**: 1518-1521
- 14 **Kurihara T**, Niimi A, Maeda A, Shigemoto M, Yamashita K. Bezafibrate in the treatment of primary biliary cirrhosis: Comparison with ursodeoxycholic acid. *Am J Gastroenterol* 2000; **95**: 2990-2992
- 15 **Yano K**, Kato H, Morita S, Takahara O, Ishibashi H, Furukawa R. Is bezafibrate histologically effective for primary biliary cirrhosis? *Am J Gastroenterol* 2002; **97**: 1075-1077
- 16 **Krey G**, Braissant O, L'Horset F, Kalkhoven E, Perroud M, Parker MG, Wahli W. Fatty acid, eicosanoids, and hypolipidemic agents identified as ligands of peroxisome proliferator-activated receptors by coactivator-dependent receptor ligand assay. *Mol Endocrinol* 1997; **11**: 779-791
- 17 **Devchand PR**, Keller H, Peters JM, Vazquez M, Gonzalez FJ, Wahli W. The PPAR α -leukotriene B $_4$ pathway to inflammation control. *Nature* 1996; **384**: 39-43
- 18 **Chianale J**, Vollrath V, Wieland AM, Amigo L, Rigotti A, Nervi F, Gonzalez S, Andrade L, Pizarro M, Accatino L. Fibrates induce *mdr2* gene expression and biliary phospholipid secretion in the mouse. *Biochem J* 1996; **314**: 781-786
- 19 **Ohira H**, Sato Y, Ueno T, Sata M. Fenofibrate treatment in patients with primary biliary cirrhosis. *Am J Gastroenterol* 2002; **97**: 2147-2149
- 20 **Mizuta T**, Dohmen K, Nakamuta M, Shimohashi N, Yamamoto K. Study of efficacy of fenofibrate on primary biliary cirrhosis poorly responded to ursodeoxycholic acid. *Acta Hepatol Jpn* 2001; **42** (Suppl 1): A294
- 21 **Dohmen K**, Mizuta T, Nakamuta M, Shimohashi N, Ishibashi H, Yamamoto K. Fenofibrate for patients with asymptomatic primary biliary cirrhosis. *Hepatology* 2003; **38**(Suppl 1): 518A
- 22 **Culp KS**, Fleming CR, Duffy J, Baldus WP, Dickson ER. Autoimmune associations in primary biliary cirrhosis. *Mayo Clin Proc* 1982; **57**: 365-370
- 23 **Harada N**, Dohmen K, Itoh H, Ohshima T, Yamamoto H, Nagano M, Iwata Y, Hachisuka K, Ishibashi H. Sibling cases of primary biliary cirrhosis associated with polymyositis, vasculitis and Hashimoto's thyroiditis. *Internal Med* 1992; **31**: 289-293
- 24 **Lindor KD**, Dickson ER. Primary biliary cirrhosis. In Schiff's Diseases of the Liver, Eighth ed. *Lippin Cott Raevan Publishers, Philadelphia* 1999: 679-692
- 25 **Shimoda S**, Nakamura M, Shigematsu H, Tanimoto H, Gushima H, Gershwin ME, Ishibashi H. Mimicry peptides of human PDC-E2, 163-176, the immunodominant T-cell epitope of primary biliary cirrhosis. *Hepatology* 2000; **31**: 1212-1216
- 26 **Dohmen K**. Primary biliary cirrhosis and pernicious anemia. *J Gastroenterol Hepatol* 2001; **16**: 1316-1318
- 27 **Dohmen K**, Shigematsu H, Miyamoto Y, Yamasaki F, Irie K, Ishibashi H. Atrophic corpus gastritis and *Helicobacter pylori* infection in primary biliary cirrhosis. *Dig Dig Sci* 2002; **47**: 162-169
- 28 **Wiesner RH**, Ludwig J, Lindor KD, Jorgensen RA, Baldus WP, Hombueger HA, Dickson ER. A controlled trial of cyclosporine in the treatment of primary biliary cirrhosis. *N Engl J Med* 1990; **322**: 1419-1424
- 29 **Dickson ER**, Fleming TR, Wiesner RH, Baldus WP, Fleming CR, Ludwig J, McCall JT. Trial of penicillamine in advanced primary biliary cirrhosis. *N Engl J Med* 1985; **312**: 1011-1015
- 30 **Bach N**, Bodian C, Bodenheimer H, Croen E, Berk PD, Thung SN, Lindor KD, Therneau T, Schaffner F. Methotrexate therapy for primary biliary cirrhosis. *Am J Gastroenterol* 2003; **98**: 187-193
- 31 **Kaplan MM**, Schmid C, Provenzale D, Sharma A, Dickstein G, McKusick A. A prospective trial of colchicines and methotrexate in the treatment of primary biliary cirrhosis. *Gastroenterology* 1999; **117**: 1173-1180
- 32 **Lee YM**, Kaplan MM. Efficacy of colchicine in patients with primary biliary cirrhosis poorly responsive to ursodiol and methotrexate. *Am J Gastroenterol* 2003; **98**: 205-208
- 33 **Willson TM**, Brown PJ, Sternbach DD, Henke BR. The PPARs: From orphan receptors to drug discovery. *J Med Chem* 2000; **43**: 527-550
- 34 **Hata Y**, Goto Y, Itakura H, Nakaya N, Saito Y. Clinical evaluation of fenofibrate (GRS-001) on hyperlipidemia -Double-blind study with bezafibrate. *Ronen Igaku* 1995; **33**: 765-822
- 35 **Longo M**, Crosignani A, Battezzati PM, Squarcia Giussani C, Invernizzi P, Zuin IM, Podda M. Hyperlipidaemic state and cardiovascular risk in primary biliary cirrhosis. *Gut* 2002; **51**: 265-269
- 36 **Gebel T**, Arand M, Oesch F. Induction of the peroxisome proliferator activated receptor by fenofibrate in rat liver. *FEBS Lett* 1992; **309**: 37-40
- 37 **Schoonjans K**, Staels B, Auwerx J. Role of the peroxisome proliferator-activated receptor (PPAR) in mediating the effects of fibrates and fatty acids on gene expression. *J Lipid Res* 1996; **37**: 907-925
- 38 **Vu-Dac N**, Schoonjans K, Kosykh V, Dallongeville J, Fruchart JC, Staels B, Auwerx J. Fibrates increase human apolipoprotein A-II expression through activation of the peroxisome proliferator-activated receptor. *J Clin Invest* 1995; **96**: 741-750
- 39 **Staels B**, Koenig W, Habib A, Merval R, Lebreton M, Torra IP, Delerive P, Fadel A, Chinetti G, Fruchart JC, Najib J, Maclout J, Tedgui A. Activation of human aortic smooth-muscle cells is inhibited by PPAR α but not by PPAR γ activators. *Nature* 1998; **393**: 790-793
- 40 **Marx N**, Sukhova GK, Collins T, Libby P, Plutzky J. PPAR α activators inhibit cytokine-induced vascular cell adhesion molecule-1 expression in human endothelial cells. *Circulation* 1999; **99**: 3125-3131
- 41 **Betz M**, Fox BS. Prostaglandin E2 inhibits production of Th1 lymphokines but not of Th2 lymphokines. *J Immunol* 1991; **146**: 108-113
- 42 **Diabetes Arteriosclerosis Intervention Study Investigators**. Effect of fenofibrate on progression of coronary-artery disease in type 2 diabetes: the Diabetes Arteriosclerosis Intervention Study, a randomized study. *Lancet* 2001; **357**: 905-910
- 43 **Edgar AD**, Tomkiewicz C, Costet P, Legendre C, Aggerbeck M, Bouguet J, Staels B, Guyomard C, Pneau T, Barouki R. Fenofibrate modifies transaminase gene expression via a peroxisome proliferator activated receptor α -dependent pathway. *Toxicol Lett* 1998; **98**: 13-23
- 44 **Jiao HL**, Zhao BL. Cytotoxic effect of peroxisome proliferator fenofibrate on human HepG2 hepatoma cell line and relevant mechanisms. *Toxicol Appl Pharmacol* 2002; **185**: 172-179
- 45 **Karpen SJ**. Nuclear receptor regulation of hepatic function. *J Hepatol* 2002; **36**: 832-850

• CLINICAL RESEARCH •

Clinical features and risk factors of patients with fatty liver in Guangzhou area

Qi-Kui Chen, Hai-Ying Chen, Kai-Hong Huang, Ying-Qiang Zhong, Ji-Ao Han, Zhao-Hua Zhu, Xiao-Dong Zhou

Qi-Kui Chen, Kai-Hong Huang, Ying-Qiang Zhong, Ji-Ao Han, Zhao-Hua Zhu, Department of Gastroenterology, The Second Affiliated Hospital, Sun Yat-Sen University, Guangzhou 510120, Guangdong Province, China

Hai-Ying Chen, Department of Gastroenterology, The People's Hospital of Zhongshan City, Zhongshan, 528400, Guangdong Province, China
Xiao-Dong Zhou, The Medical Research Center, The Second Affiliated Hospital, Sun Yat-Sen University, Guangzhou 510120, Guangdong Province, China

Supported by the National Natural Science Foundation of China, No.30270371

Correspondence to: Dr. Qi-Kui Chen, Department of Gastroenterology, The Second Affiliated Hospital, Sun Yat-Sen University, 107 West Yanjiang Road, Guangzhou 510120, Guangdong Province, China. qkchen@21cn.com

Telephone: +86-20-81332598 **Fax:** +86-20-81332244

Received: 2003-10-31 **Accepted:** 2003-12-22

Abstract

AIM: There is still no accepted conclusion regarding the clinical features and related risk factors of patients with fatty liver. The large-scale clinical studies have not carried out yet in Guangzhou area. The aim of the present study was to investigate the clinical features and related risk factors of patients with fatty liver in Guangzhou area.

METHODS: A total of 413 cases with fatty liver were enrolled in the study from January 1998 to May 2002. Retrospective case-control study was used to evaluate the clinical features and related risk factors of fatty liver with logistic regression.

RESULTS: Obesity (*OR*: 21.204), alcohol abuse (*OR*: 18.601), type 2 diabetes mellitus (*OR*: 4.461), serum triglyceride (TG) (*OR*: 3.916), serum low-density lipoprotein cholesterol (LDL-C) (*OR*: 1.840) and fasting plasma glucose (FPG) (*OR*: 1.535) were positively correlated to the formation of the fatty liver. The levels of serum alanine aminotransferase (ALT) and gamma-glutamyltransferase (GGT) increased mildly in the patients with fatty liver and were often less than 2-fold of the normal limit. The higher abnormalities of aspartate aminotransferase (AST) levels (42.9%) with AST/ALT more than 2 (17.9%) were found in patients with alcoholic fatty liver (AFL) than those with nonalcoholic fatty liver (NAFL) (16.9% and 5.0% respectively). The elevation of serum TG, cholesterol (CHOL), LDL-C was more common in patients with NAFL than with AFL.

CONCLUSION: Obesity, alcohol abuse, type 2 diabetes mellitus and hyperlipidemia may be independent risk factors of fatty liver. The mildly abnormal hepatic functions can be found in patients with fatty liver. More obvious damages of liver function with AST/ALT usually more than 2 were noted in patients with AFL.

Chen QK, Chen HY, Huang KH, Zhong YQ, Han JA, Zhu ZH, Zhou XD. Clinical features and risk factors of patients with fatty liver in Guangzhou area. *World J Gastroenterol* 2004; 10(6): 899-902
<http://www.wjgnet.com/1007-9327/10/899.asp>

INTRODUCTION

Fatty liver is a condition of hepatic steatosis caused by many risk factors and may progress to liver fibrosis and cirrhosis. Generally, the diagnosis of fatty liver should be based on the history, clinical manifestation, laboratory investigation and medical imaging. Liver biopsy should be taken if necessary. After to know the possible related risk factors of fatty liver existed in the history, the abnormal degree of the biochemical and imaging features can provide a clue for early diagnosis. Although the related risk factors and laboratory features have already been reported, there is still no well-accepted conclusion^[1-3]. The large-scale clinical studies have not carried yet in Guangzhou area, southern China^[4].

Retrospective case-control study was used to analyze fatty liver. The age, gender, obesity, type 2 diabetes mellitus, hyperlipidemia, alcohol abuse, smoking, and history of drugs or toxins and so on were recorded to evaluate the effects of these variables on fatty liver and investigate the related risk factors. The liver function and other serum biochemical levels were compared to find out the difference of laboratory abnormalities, so that they could provide a scientific foundation for the diagnosis, prevention and treatment of fatty liver.

MATERIALS AND METHODS

Clinical data

The data of 413 cases of fatty liver in this hospital from January 1998 to May 2002 were collected. Fatty liver was diagnosed according as the standard by Chinese Association of Medicine and Sherlock^[5-7]. The 200 cases without fatty liver during the same period were selected randomly as control. Age, gender, serum lipids, fasting plasma glucose (FPG), obesity (body mass index, BMI ≥ 25), alcohol abuse, smoking, type 2 diabetes mellitus, history of drugs and toxins, hepatitis virus infection (HCV and HBV), pregnancy, jejuno-ileal bypass surgery and total parenteral nutrition were recorded in fatty liver group and non fatty liver group respectively.

The laboratory data of serum triglyceride (TG), cholesterol (CHOL), high-density lipoprotein cholesterol (HDL-C), low-density lipoprotein cholesterol (LDL-C), apolipoprotein AI (Apo AI), apolipoprotein B (Apo B), uric acid (UA), aspartate aminotransferase (AST), alanine aminotransferase (ALT), the ratio of AST/ALT, albumin (ALB), globin (GLB), ratio of A/G, gamma-glutamyltransferase (GGT) and total bilirubin were collected in two groups respectively. The serum biochemical indexes were examined by an autoanalyzer based on a standard protocol.

Statistical analysis

All data analysis was performed with EXCEL 97 and SPSS 10.0/PC statistical package. A *P* value less than 0.05 (2-tailed) was considered to be statistically significant. The frequency was compared using Chi-squared (χ^2) test. The univariate and multivariate stepwise logistic regression was used to select the independent variables. Data with normal distribution were expressed as mean \pm SD. The differences between groups were analyzed for statistical significance using Student's *t* test. Data

with abnormal distribution were expressed as median and interquartile range.

RESULTS

General condition

Among 413 fatty liver cases, the gender ratio (M/F) was 1.02:1. The age ranged from 8 to 83 years. The median age was 57 years. No significant differences in age and gender were found between the fatty liver group and non-fatty liver group. The possible causes of fatty liver are showed in Table 1.

Table 1 Possible causes of fatty liver and its comparison with non-fatty liver group (%)

Factors	Fatty liver group (n=413)	Non-fatty liver group (n=200)
Alcohol abuse	51(12.4) ^b	7(3.5)
Obesity	244(59.1) ^b	17(8.5)
Type 2 diabetes mellitus	206(49.9) ^b	15(7.5)
Hyperlipidemia	276(66.8) ^b	63(31.5)
Hypertriglyceridemia	92(22.3) ^b	17(8.5)
Hypercholesterolemia	64(15.5)	35(17.5)
Mixed Hyperlipidemia	120(29.1) ^b	11(5.5)
HBV infection	50(12.1)	31(15.5)
HCV infection	34(8.2)	10(5.0)
History of drugs and toxins	6(1.5)	2(1.0)

^bP<0.001, vs Non-fatty liver group.

Analysis of independent risk factors of patients with fatty liver

Analysis of univariate logistic regression was performed among 20 variables, such as age, gender, obesity, alcohol abuse, smoking, type 2 diabetes mellitus, TG, CHOL, HDL-C, LDL-C, Apo AI, Apo B, FPG, HCV and HBV infection, history of drugs and toxins, pregnancy, jejunio-ileal bypass surgery and total parenteral nutrition. TG, CHOL, HDL-C, LDL-C, Apo B, FPG, obesity, alcohol abuse, smoking, type2 diabetes mellitus were positively correlated to fatty liver respectively (odds rate, $OR>1$, $P<0.05$), while Apo AI was negatively correlated to it ($OR<1$, $P<0.05$). Multivariate stepwise logistic regression was used to select the variables independently associated with fatty liver. Obesity, alcohol abuse, type 2 diabetes mellitus, TG, LDL-C and FPG were entered the model of logistic regression as the independent risk factors of fatty liver. In contrast, Apo B was negatively correlated to it (Table 2).

Table 2 Multivariate stepwise logistic regression

Variables	β	SE	OR	95%CI	P-value
Obesity	3.054	0.354	21.204	10.539-42.429	0.000
Alcohol abuse	2.923	0.509	18.601	6.585-50.432	0.000
Type 2 diabetes mellitus	1.495	0.354	4.461	2.228-8.952	0.022
TG	1.365	0.268	3.916	2.316-6.621	0.000
LDL-C	0.610	0.184	1.840	1.283-2.640	0.001
FPG	0.429	0.094	1.535	1.278-1.846	0.000
Apo B	-1.590	0.530	0.204	0.072-0.576	0.003

β : partial regression coefficient; SE: standard error of partial regression coefficient; OR: odds ratio; CI: confidence interval.

Abnormal liver function in patients with fatty liver

Using χ^2 test, the abnormal frequencies of ALT, AST/ALT and GGT showed significant differences between the patients with and without fatty liver (Table 3).

Comparison of serum biochemical features between alcoholic fatty liver (AFL) group and nonalcoholic fatty liver (NAFL) group

The abnormal frequencies of serum TG, CHOL, LDL-C and ApoB were higher in NAFL group than those in AFL group. The proportion of HDL-C \leq 1.0, AST \geq 40 and AST/ALT \geq 2 were higher in patients with AFL than with NAFL (Table 4).

Table 3 Abnormal liver function in the patients with fatty liver and non-fatty liver (%)

Liver function	Fatty liver group (n=413)	Non-fatty liver group (n=200)
AST (\geq 40 U)	85(20.6)	38(19.0)
(40-80 U)	65(15.7)	26(13.0)
(\geq 80 U)	20(4.8)	12(6.0)
ALT (\geq 40 U)	129(31.2) ^a	37(18.5)
(40-80 U)	84(20.3) ^a	26(13.0)
(\geq 80 U)	45(10.9) ^a	11(5.5)
AST/ALT (<1)	161(39.0) ^a	28(14.0)
(≥ 2)	23(5.6) ^a	54(27.0)
ALB (\leq 35 g/L)	16(3.9)	15(7.5)
GLB (\geq 30 g/L)	42(10.2)	29(14.5)
A/G (\leq 1.5)	84(20.3)	47(23.5)
GGT (\geq 50 U/L)	145(35.1) ^a	46(23.0)
TBIL (\geq 17.1 μ mol/L)	75(18.2)	39(19.5)

^aP<0.05, vs Non-fatty liver group.

Table 4 Comparison of laboratory abnormalities among AFL, NAFL and control groups (%)

Biochemical Index	AFL group (n=28)	NAFL group (n=301)	Control group (n=163)
TG (\geq 1.7 mmol/L)	2(7.1) ^a	169(56.2) ^c	27(17.7)
CHOL (\geq 5.2 mmol/L)	2(7.1) ^a	148(49.2) ^c	35(22.9)
HDL-C (\leq 1.0 mmol/L)	9(32.1) ^a	35(11.6)	27(17.7)
LDL-C (\geq 2.6 mmol/L)	12(42.9) ^a	214(71.1)	97(63.4)
Apo AI (\leq 1.2 mmol/L)	13(46.4)	118(39.2)	45(29.4)
Apo B (\geq 1.1 mmol/L)	4(14.3) ^{ac}	149(49.5) ^e	53(34.6)
UA (\geq 452 mg/dL)	5(17.9)	89(29.6) ^e	18(11.8)
AST (\geq 40 U)	12(42.9) ^{ac}	51(16.9)	24(15.7)
ALT (\geq 40 U)	10(35.7) ^c	87(28.9) ^e	26(17.0)
AST/ALT (<1)	11(39.3) ^c	168(55.8) ^e	31(20.3)
(≥ 2)	5(17.9) ^a	15(5.0) ^e	40(26.1)
ALB (\leq 35 g/L)	3(10.7)	9(3.0)	7(4.6)
GLB (\geq 30 g/L)	3(10.7)	32(10.6)	20(13.1)
A/G (\leq 1.5)	7(25.0)	64(21.3)	31(20.3)
GGT (\geq 50 U/L)	10(35.7)	95(31.6) ^e	30(19.6)
TBIL (\geq 17.1 μ mol/L)	6(21.4)	50(16.6)	30(19.6)

^aP<0.05, vs NAFL group; ^cP<0.05, vs control group; ^eP<0.05, vs control group.

DISCUSSION

In recent years, the prevalence of fatty liver is constantly increasing along with the improvement of life-style, the change of dietetic structure, the aged population and the application of new diagnostic technique. The incidence of fatty liver in 3432 Japanese adults thorough medical examination was 21.8%^[2]. In China, fatty liver affected 10.2% of cadres in Nanjing^[8] with 11.4% of male and 6.8% of female. There were no data to show the prevalence of fatty liver in the southern China. Because of distinct life-style and climate feature in Guangzhou, the pattern

of fatty liver could be different from other area. Among 413 patients with fatty liver, the gender ratio (M/F) was 1.02:1. The age ranged widely. The median age was 57 years.

Fatty liver may be an independent disease, but more generally, it is a lesion of the liver in certain systemic diseases. Fatty liver may be caused by many diseases and risk factors, and can progress from mild steatohepatitis to severe fibrosis and cirrhosis^[9]. The etiological prevention is very important because of the lack of effective therapy. Although the etiology of hepatic steatosis is explored extensively, the complicated and multi-factor pathogenesis make it remain poorly understood. The possible related risk factors include: alcohol abuse, diabetes mellitus, obesity, hyperlipidemia, drugs and toxins, hepatitis virus infection (especially HCV), rapid weight loss, jejuno-ileal bypass surgery, total parenteral nutrition, pregnancy and so on^[10-16].

413 patients with fatty liver were diagnosed mainly according to the history, clinical manifestations, laboratory and ultrasound examination. Liver biopsy was the best method of diagnosing fatty liver. But it was difficult to carry out in large sample of populations. This was the possible limitations of the study.

Our data from 413 patients with fatty liver showed that obesity, alcohol abuse, type 2 diabetes mellitus, hyperlipidemia and elevation of fasting plasma were independent risk factors confirmed by a multivariate logistic analysis. These correlations were similar to the researches at home and abroad^[3,4]. It suggested that the pathogenesis of fatty liver in southern China might have a similar pattern to other area in China and abroad.

Obesity was easily accompanied with fatty liver^[17]. The percentage of the obese patients with fatty liver (59.1%) was significantly higher than controls (8.5%). Obesity is a very common phenomenon in the developed countries. 60-100% patients of non-alcoholic steatohepatitis (NASH) were proved to have obesity^[18]. This situation was also found in developing country, especially in China. According to the data in 11 provinces/autonomous regions/municipalities of China from July 1995 to July 1997, the prevalence rate of overweight and obesity among 42 751 Chinese adults aged 20-74 years were 21.51% and 2.92% respectively^[19]. There were about 200-300 million of overweight and 30-40 million of obese populations in China. With the odds ratio of 21.204, obesity was a predictor of fatty liver. The practice of prevention for overweight and obesity was very important for control of fatty liver.

Alcohol liver disease was the major medical complications of alcohol abuse. Alcohol abuse was one of the major causes of fatty liver and cirrhosis in the Western countries. At least 80% of heavy drinkers developed fatty liver, 10-35% of alcoholic hepatitis, and approximately 10% cirrhosis^[20]. Alcohol drinkers were not as common in southern China as in northern China^[19]. Based on our data, there were only 12.4% patients with alcohol abuse and 6.8% of them with alcoholic fatty liver among 413 patients with fatty liver according to diagnostic standard of China in 2002. But, the proportion of alcoholic abuse was still higher in patients with fatty liver than those without fatty liver. Alcoholic abuse contributed to a risk factor of fatty liver.

Type 2 diabetes mellitus usually accompanied insulin resistance^[12,21]. Both peripheral and hepatic insulin resistance were present in almost all patients with nonalcoholic fatty liver disease, irrespective of the coexistence of related risk factors^[21]. Above findings, together with the associated hyperlipidemia, obesity, hypertension and hyperuricemia, were considered as the manifestations of the metabolic syndrome that was associated with insulin resistance^[22,23]. In this study, either type 2 diabetes or elevation of fasting plasma glucose was related to fatty liver. It suggested that insulin resistance might be a risk factor of fatty liver.

The role of serum lipids in fatty liver remained controversial^[16,24]. Some researches showed that the effects of hyperlipidemia on fatty liver were complicated and difficult to be disassociated with obesity and type 2 diabetes mellitus. Among the 413 patients with fatty liver, the total incidence of hyperlipidemia was 66.8%, which consisted of 22.3% of hypertriglyceridemia, 15.5% of hypercholesterolemia and 29.1% of mixed hyperlipidemia. TG and LDL-C were independent risk factors and ApoB was a protective factor confirmed by multivariate logistic analysis. TG and LDL-C stimulated the proliferation and collagen synthesis of hepatic stellate (HSC) and increased deposition of extracellular matrix (ECM) in the liver by means of lipid peroxidation^[25,26]. This process was relative to hepatic fibrosis and effected prognosis of patients with fatty liver.

The correlation between hepatitis virus infection (especially HCV) and hepatic steatosis was found^[27]. Although the incidence of chronic HBV and HCV infection in China remained the highest proportion in the world, there was no significant difference in the incidence of HBV or HCV infection between patients with and without fatty liver. The infection of HBV and HCV was excluded from the model of multivariate stepwise logistic regression.

The clinical and laboratory features varied greatly with different causes and degree of hepatic steatosis in patients with fatty liver^[28]. The elevation of serum TG, CHOL and LDL-C was more common in patients with NAFL than those with AFL. Most patients with fatty liver had no obvious symptoms and signs of liver disease at the time of diagnosis. But a higher proportion of patients with cryptogenic cirrhosis shared many of the clinical and demographic features of patients with fatty liver. NASH played an under-recognized role in many patients with cryptogenic cirrhosis^[29]. Mild elevation usually less than 2 folds of the normal limit of serum ALT and GGT was showed in this investigation. The mitochondria was the most likely source of the reactive oxygen species (ROS) leading to lipid peroxidation in patients with fatty liver^[30]. AST, a mitochondrial enzyme, was more easily affected by ethanol^[31]. Among the abnormal hepatic functions, the higher AST levels with AST/ALT more than 2 were found in those with AFL. The increases of serum lipids and AST/ALT ratio might be useful in differentiating NAFL from AFL.

ACKNOWLEDGMENTS

We greatly thank Dr. Jie Yan from the Department of Medical Statistics of Sun Yat-Sen University for statistical analysis.

REFERENCES

- 1 **Angulo P.** Nonalcoholic fatty liver disease. *N Engl J Med* 2002; **346**: 1221-1231
- 2 **Omagari K,** Kadokawa Y, Masuda J, Egawa I, Sawa T, Hazama H, Ohba K, Isomoto H, Mizuta Y, Hayashida K, Murase K, Kadota T, Murata I, Kohno S. Fatty liver in non-alcoholic non-overweight Japanese adults: incidence and clinical characteristics. *J Gastroenterol Hepatol* 2002; **17**: 1098-1105
- 3 **Angulo P,** Lindor KD. Non-alcoholic fatty liver disease. *J Gastroenterol Hepatol* 2002; **17**: S187-190
- 4 **Fan JG.** Studies on fatty liver in China. *Shijie Huaren Xiaohua Zazhi* 2001; **9**: 6-10
- 5 **Sherlock S,** Dooley J. Diseases of the liver and biliary system. 10ed. Oxford: Blackwell Sci Pub 1997: 427-433
- 6 **Fatty Liver and Alcoholic Liver Disease Study Group of Chinese Liver Disease Association.** Diagnostic criteria of nonalcoholic fatty liver disease. *Zhonghua Ganzangbing Zazhi* 2003; **11**: 71
- 7 **Fatty Liver and Alcoholic Liver Disease Study Group of Chinese Liver Disease Association.** Diagnostic criteria of alcoholic fatty liver disease. *Zhonghua Ganzangbing Zazhi* 2003; **11**: 72
- 8 **Wang H,** Chen J. Epidemiological studies of fatty livers. *Xin*

- Xiaohuabingxue Zazhi* 1997; **5**: 100-101
- 9 **Bacon BR**, Farahvash MJ, Janney CG, Neuschwander-Tetri BA. Nonalcoholic steatohepatitis: An expanded clinical entity. *Gastroenterology* 1994; **107**: 1103-1109
 - 10 **James O**, Day C. Non-alcoholic steatohepatitis: another disease of affluence. *Lancet* 1999; **353**: 1634-1636
 - 11 **Pares A**, Tresserras R, Nurez L, Cerralbo M, Plana P, Pujol FJ, Massip J, Caballeria L, Bru C, Caballeria J, Vidal J, Salleras L, Rodes J. Prevalence and factors associated to the presence of fatty liver in apparently healthy adult men. *Med Clin* 2000; **114**: 561-565
 - 12 **Marchesini G**, Brizi M, Morselli-Labate AM, Bianchi G, Bugianesi E, McCullough AJ, Forlani G, Melchionda N. Association of non-alcoholic fatty liver disease with insulin resistance. *Am J Med* 1999; **107**: 450-455
 - 13 **Falchuk KR**, Fiske SC, Haggitt RC, Federman M, Trey C. Pericentral hepatic fibrosis and intracellular hyaline in diabetes mellitus. *Gastroenterology* 1980; **78**: 535-541
 - 14 **Rinella ME**, Alonso E, Rao S, Whittington P, Fryer J, Abecassis M, Superina R, Flamm SL, Blei AT. Body mass index as a predictor of hepatic steatosis in living liver donors. *Liver Transpl* 2001; **7**: 409-414
 - 15 **Powell EE**, Cooksley WG, Hanson R, Searle J, Halliday JW, Powell LW. The natural history of nonalcoholic steatohepatitis: a follow-up study of forty-two patients for up to 21 years. *Hepatology* 1990; **11**: 74-80
 - 16 **Assy N**, Kaita K, Mymin D, Levy C, Rosser B, Minuk G. Fatty infiltration of liver in hyperlipidemic patients. *Dig Dis Sci* 2000; **45**: 1929-1934
 - 17 **Gray DS**. Diagnosis and prevalence of obesity. *Med Clin North Am* 1989; **73**: 1-13
 - 18 **Sheth SG**, Gordon FD, Chopra S. Nonalcoholic steatohepatitis. *Ann Intern Med* 1997; **126**: 137-145
 - 19 **Wang WJ**, Wang KA, Li TL, Xiang HD, Ma LM, Fu ZY, Chen JS, Liu ZY, Bai J, Fong JG, Jin SX, Li YQ, Qing NL, Chen H. A study on the epidemiological characteristics of obesity in Chinese Adults. *Zhonghua Liuxingbingxue Zazhi* 2001; **22**: 129-132
 - 20 **Walsh K**, Alexander G. Alcoholic liver disease. *Postgrad Med J* 2000; **76**: 280-286
 - 21 **Marceau P**, Biron S, Hould FS, Marceau S, Simard S, Thung SN, Kral JG. Liver pathology and the metabolic syndrome X in severe obesity. *J Clin Endocrinol Metab* 1999; **84**: 1513-1517
 - 22 **Marchesini G**, Brizi M, Bianchi G, Tomassetti S, Bugianesi E, Lenzi M, McCullough AJ, Natale S, Forlani G, Melchionda N. Nonalcoholic fatty liver disease: a feature of the metabolic syndrome. *Diabetes* 2001; **50**: 1844-1850
 - 23 **Luyckx FH**, Lefebvre PJ, Scheen AJ. Non-alcoholic steatohepatitis: association with obesity and insulin resistance, and influence of weight loss. *Diabetes Metab* 2000; **26**: 98-106
 - 24 **Neuschwander-Tetri BA**, Bacon BR. Nonalcoholic steatohepatitis. *Med Clin North Am* 1996; **80**: 1147-1166
 - 25 **Lu LG**, Zeng MD, Li JQ, Hua J, Fan JG, Fan ZP, Oiu DK. Effect of lipid on proliferation and activation of rat hepatic stellate cells (I). *World J Gastroenterol* 1998; **4**: 497-499
 - 26 **Lu LG**, Zeng MD, Li JQ, Hua J, Fan JG, Oiu DK. Study on the role of free fatty acids in proliferation of rat hepatic stellate cells (II). *World J Gastroenterol* 1998; **4**: 500-502
 - 27 **Rubbia-Brandt L**, Leandro G, Spahr L, Giostra E, Quadri R, Male PJ, Negro F. Liver steatosis in chronic hepatitis C: a morphological sign suggesting infection with HCV genotype 3. *Histopathology* 2001; **39**: 119-124
 - 28 **Itoh S**, Yougel T, Kawagoe K. Comparison between nonalcoholic steatohepatitis and alcoholic hepatitis. *Am J Gastroenterol* 1987; **82**: 650-654
 - 29 **Caldwell SH**, Oelsner DH, Iezzoni JC, Hespenheide EE, Battle EH, Driscoll CJ. Cryptogenic cirrhosis: clinical characterization and risk factors for underlying disease. *Hepatology* 1999; **29**: 664-669
 - 30 **Day CP**. Non-alcoholic steatohepatitis (NASH): where are we now and where are we going? *Gut* 2002; **50**: 585-588
 - 31 **French SW**. Mechanisms of alcoholic liver injury. *Can J Gastroenterol* 2000; **14**: 327-332

Edited by Zhang JZ Proofread by Xu FM

Disseminated tumor cells homing into rats' liver: A new possible mechanism of HCC recurrence

Qi-Gen Li, Guang-Shun Yang, Qing Yang, Li-Xin Wei, Ning Yang, Xue-Ping Zhou, Feng-Qi Jia

Qi-Gen Li, Guang-Shun Yang, Qing Yang, Li-Xin Wei, Ning Yang, Xue-Ping Zhou, Feng-Qi Jia, Eastern Hepatobiliary Surgery Hospital, Second Military Medical University, Shanghai 200438, China
Supported by the National Natural Science Foundation of China, No. 39870752

Correspondence to: Dr. Guang-Shun Yang, Eastern Hepatobiliary Surgery Hospital, Second Military Medical University, Shanghai 200438, China. guangshun@smmu.edu.cn

Telephone: +86-21-25070803

Received: 2003-03-02 **Accepted:** 2003-05-21

Abstract

AIM: To detect the origin of hepatocellular carcinoma (HCC) recurring and attempt to propose a new recurrent mechanism.

METHODS: Orthotopic liver allotransplantation was performed on male rats with HCC- induced by diethylnitrosamine using female donors. Metastatic tumors in transplanted livers were obtained. A DNA probe that exhibits specificity for the rat Y chromosome was generated by using a set of primers specific to murine *sry* gene. *In situ* hybridization (ISH) for Y chromosome was used to detected the origin of HCC recurring. Male HCC tissue was designed to be positive control. ISH on female tissue and using non-labeled with DIG probe was thought to be negative control.

RESULTS: Positive marks were seen through ISH for Y chromosome in recurrent tumor tissue and positive control. No signal was detected in both negative controls.

CONCLUSION: Recurrent HCC after liver transplantation originated from disseminated tumor cells in recipients. Extrahepatic cells homing into liver may be a new HCC recurrence mechanism. Likewise, it implicates that this mechanism is responsible for HCC recurring after hepatectomy.

Li QG, Yang GS, Yang Q, Wei LX, Yang N, Zhou XP, Jia FQ. Disseminated tumor cells homing into rats' liver: A new possible mechanism of HCC recurrence. *World J Gastroenterol* 2004; 10(6): 903-905

<http://www.wjgnet.com/1007-9327/10/903.asp>

INTRODUCTION

The poor outcomes of patients with hepatocellular carcinoma (HCC) are mainly resulted from high postoperative recurrence rate with 65% after radical resection versus 58% after liver transplantation^[1,2]. Over the past decades, many investigations using clinicopathological and molecular biological methods have showed that there existed two HCC recurrent mechanisms of intrahepatic metastasis (IM) and multicentric occurrence (MO)^[3-5]. However, the both mechanisms are very reluctant to elucidate the HCC recurrence following liver transplantation in rigidly selected patients. Therefore, we refer a hypothesis that recurrent HCC in transplanted liver is likely to originate from extrahepatic tumor cells in recipient if de novo

carcinogenesis is excluded. Likewise, disseminated tumor cells possibly go back to remnant liver after hepatectomy.

We have established an animal model of liver transplantation for HCC in rats. Male rat liver with HCC induced by diethylnitrosamine (DENa) was replaced by allograft from normal syngenic female animal. Recurrent tumors from male recipient of female liver were analyzed using *in situ* hybridization (ISH) for the Y chromosome to indicate cells origins. On the basis of our investigation and other supportive literatures, we make an attempt to propose a new possible mechanism of HCC recurrence.

MATERIALS AND METHODS

Orthotopic liver transplantation (OLT) for HCC-induced in gender discordant rats

Ninety-eight inbred seven-week-old male SD rats, weight ranged from 100 g to 120 g, were purchased from PEAK Company in Shanghai with the approval of Shanghai Animal Committee. HCC was induced by oral administration of 100 ppm DENa (Sigma Company, USA) water solution. OLT for HCC was performed according to Kamada cuff techniques^[6] on male rats with HCC and donor livers were from normal syngenic female SD rats with weight ranged from 250 g to 300 g. No immunosuppressant was postoperatively administered. Explanted livers were examined pathologically. The recurrent tumors in the transplants may be explored through laparotomy before the recipients' death. Harvested specimens were preserved at -70 °C.

Using ISH to detect the Y chromosomes in recurrent HCC cells^[7,8]

Male rat genomic DNA was purified from 300 µL blood sample using Wizard Genomic DNA Purification Kit (Promega). *sry* gene specific primer, of which the sequences are 5'-CAGAGATCAGCAAGCAGCTG-3' and 5'-TGCAGCTCTACTCCAGTCTTG-3', was synthesized by Shengong Biochemical Incorporation in Shanghai. 0.1 µg of the genomic DNA as template, *sry* gene was amplified by PCR. The reaction was comprised of 35 cycles of 5 min at 94 °C, 0.5 min at 60 °C, 1 min at 72 °C. PCR products were analyzed on 15 g/L agarose gel and then purified with QIAquick Gel Extraction Kit (Qiagen). Target gene was labeled according to the instruction of DIG High Prime DNA Labeling and Detection Starter Kit II (Roche).

Male SD rat HCC tissue confirmed by pathology was designed to be positive control. ISH on female SD rat liver tissue and using non-labeled with DIG probe was thought to be negative control. ISH efficacy would be verified by the both controls.

Frozen tissue sections (5 µm in thickness) were fixed on the slides treated by 40g/L polyformaldehyde. Slides were washed in PBS (PH7.4) for 5 min (2 times), 3g/L Triton X-100/PBS for 10 min, and PBS (PH7.4) for 5 min (2 times). Tissue was digested with pepsin 2 µg/mL for 15 min at 37 °C, and then washed in PBS for 5 min and rinsed in 4×sodium saline citrate (SSC) for 2 min at room temperature. Slides were

denatured with 50% formamide in 2×SSC for 15 min at room temperature, then dehydrated and air dried. Probe for Y chromosome (10 ng/μL) was denatured for 5 min at 75 °C, added to the denatured tissue, coverslipped and incubated in a humid chamber overnight at 42 °C. Slides were then washed in 2×SSC for 10 min (2 times), 1×SSC for 10 min (2 times), 0.1×SSC 10 min (3 times), and in buffer1 (Tris-HCl, PH7.5, 100 mmol/L; NaCl 150 mmol/L) for 5 min. Anti-DiG-Ap (1:500 dilution) was added to tissues and incubated for 2 h at 43 °C. Slides were washed in buffer1 for 5 min (2 times) and buffer 2 (Tris-HCl, PH9.5, 100 mmol/L; NaCl 100 mmol/L, MgCl₂ 50 mmol/L) for 10 min. And then slides were transferred to NBT/BCIP solution to be stained for more than 2 h, and rinsed with distilled water. Tissue sections were mounted and evaluated by light microscopy.

RESULTS

HCC recurrence was found in 6 transplants from 98 transplanted rats. Of them, 3 grafts were discarded because the recipients have been dead when laparotomy. Thirteen lesions were obtained in other three available transplants, confirmed to HCC by pathological examination. These specimens were preserved at -70 °C as a bank for further utilization.

HCC cells carrying a positive reaction product (blue staining) were seen in control male rats. No signal was detected in the controls of female liver and system using non-labeled probe. Control trials showed that the *sry* gene specific probe was efficient.

Positive staining was seen in frozen sections of the 3 recurrent transplants. Typically, the probe was successfully hybridized with target gene on tumor cells, whereas failed to on para-tumor tissues. The capsule, aimed at by arrow, definitely parts the recurrent tumor from the recipient liver parenchyma under 10×10 magnification (Figure 1).

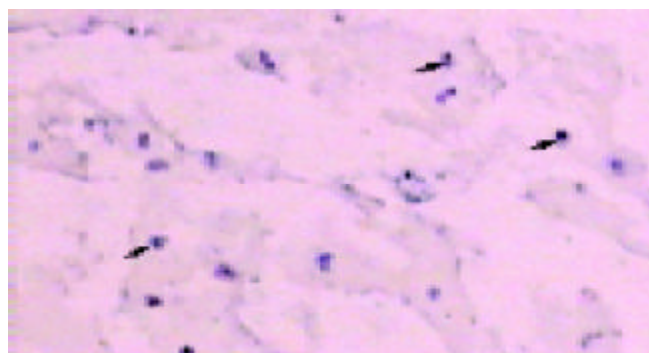


Figure 1 The blue blots under the purple background indicated Y chromosomes in these nuclei of recurrent tumor cells with 10×10 magnification microscope. The capsule definitely parted the recurrent tumor tissue from the recipient liver parenchyma. No positive signals were found out in the para-tumor tissue.

DISCUSSION

Liver transplantation for HCC in rats provides an excellent animal model to carcinogenesis investigation^[9]. Intrahepatic tumors and underlying lesions are removed completely, and then some interventional trials could be executed etiologically. In our experiments, no immunosuppressants were administered because rejective reaction was weak in allotransplantation on syngenic SD rats. The promotion of immunosuppressants to tumor growth can be excluded. However, it remains indefinite that induction of HCC existed in recipients after the withdrawal of DENA^[10]. There were two possible mechanisms of tumor recurring with the inclusion of disseminated tumor cells homing

into implanted liver and sequential contribution of DENA. Therefore, a marker is a key to discriminate between the two possibilities.

Cellular markers have been obtained through varieties of strategies such as transgenic animal, retroviral transduction. But these strategies are very complicated and low efficient. Discordant gender transplants offer the benefit of having 100% of the cells marked, as opposed to retroviral transduction, where at best only 5-10% of the cells are marked^[11]. In our experience, Y chromosome, uniquely existed in male cell, was initially acted as a marker with which male and female tissues were differentiated. Y chromosome-specific probe was successfully hybridized with *sry* gene of which multiple copies facilitated this hybridization^[7]. This *in situ* hybridization system was proved to be reliable by positive and negative control we designed. Our results therefore indicated that the origin of recurrent HCC in female liver was from disseminated tumor cells in male recipient. We personally define this phenomenon that extrahepatic tumor cells go back to liver as “homing”.

Other studies could support the homing hypothesis we proposed. (1). Alpha-fetoprotein (AFP) messenger RNA (mRNA) has been proposed as a marker of HCC cells disseminated into the circulation. Multiple molecular methods, such as nested and semi-quantitative retro-transcription polymerase chains reaction (RT-PCR), have been utilized to detect AFP mRNA in order to confirm the presence of hematogenous HCC cells. This marker expression in peripheral blood of patients with HCC indicates the existence of tumor cells, although it remains controversial that AFP mRNA is taken as an evidence of HCC recurrence^[12-14]. (2). The homing of both lymphocytes and malignant hematic cells has been acknowledged^[15,16]. Involved adhesion molecules that mediate their migration also contribute to invasiveness of liver cancer^[16]. (3). Metastasis is the result of multiple sequential steps and is a highly organized, nonrandom, and organ-selective process^[17]. A group of biological molecules is collectively responsible for determining whether tumor cells can progress from a single malignant cell to a metastatic disease^[17]. But metastatic cells eventually colonize a particular organ that provides an optimal microenvironment^[18,19]. It therefore is warranted that transplanted liver or regenerating liver after resection may be a particularly fertile ground for extrahepatic HCC cells to proliferate.

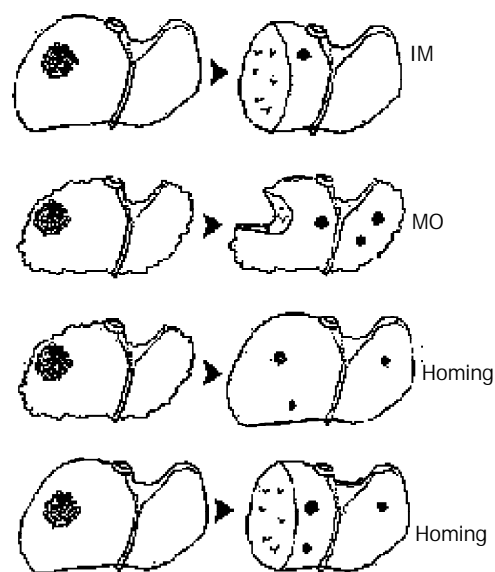


Figure 2 It is acknowledged that there exist two HCC recurring mechanisms of intrahepatic metastasis through portal venous system and multicentric occurrence from cirrhotic nodules. These extrahepatic cells homing into liver may be a

new mechanism after liver transplantation. Likewise, it implicates that this mechanism is responsible for HCC recurrence after hepatectomy.

On the basis of this experiment, we concluded that recurrent HCC after liver transplantation originated from the disseminated tumor cells. These extrahepatic cells homing into liver may be a new HCC recurrence mechanism. Likewise, it implicates that this new mechanism is responsible for HCC recurrence after hepatectomy besides MO and IM (Figure 2). But our experiment, to some extent, was to describe a homing phenomenon. Its real mechanism needs to be further investigated by molecular biology.

REFERENCES

- Schlitt HJ**, Neipp M, Weimann A, Oldhafer KJ, Schmoll E, Boeker K, Nashan B, Kubicka S, Maschek H, Tusch G, Raab R, Ringe B, Manns MP, Pichlmayr R. Survival and recurrence after hepatic resection of 386 consecutive patients with hepatocellular carcinoma. *J Am Coll Surg* 2000; **191**: 381-388
- Schlitt HJ**, Neipp M, Weimann A. Recurrence patterns of hepatocellular and fibrolamellar carcinoma after liver transplantation. *J Clin Oncol* 1999; **17**: 324-331
- Nakashima O**, Kojiro M. Recurrence of hepatocellular carcinoma: multicentric occurrence or intrahepatic metastasis? A viewpoint in terms of pathology. *J Hepatobiliary Pancreat Surg* 2001; **8**: 404-409
- Poon RT**, Fan ST, Ng IO, Lo CM, Liu CL, Wong J. Different risk factors and prognosis for early and late intrahepatic recurrence after resection of hepatocellular carcinoma. *Cancer* 2000; **89**: 500-507
- Kumada T**, Nakano S, Takeda I, Sugiyama K, Osada T, Kiriyaama S, Sone Y, Toyoda H, Shimada S, Takahashi M, Sassa T. Patterns of recurrence after initial treatment in patients with small hepatocellular carcinoma. *Hepatology* 1997; **25**: 87-92
- Goto S**, Kamada N, Delriviere L, Kobayashi E, Lord R, Ware F, Hara Y, Edwards-Smith C, Shimizu Y, Vari F. Orthotopic liver retransplantation in rats. *Microsurgery* 1995; **16**: 167-170
- An J**, Beauchemin N, Albanese J, Abney TO, Sullivan AK. Use of a rat cDNA probe specific for the Y chromosome to detect male-derived cells. *J Androl* 1997; **18**: 289-293
- Theise ND**, Nimmakayalu M, Gardner R, Illei PB, Morgan G, Teperman L, Henegariu O, Krause DS. Liver from bone marrow in humans. *Hepatology* 2000; **32**: 11-15
- Schotman SN**, Schraa EO, Marquet RL, Zondervan PE, Ijzermans JN. Hepatocellular carcinoma and liver transplantation: an animal model. *Transpl Int* 1998; **11**: 201-205
- Curtis C**, Terry W, Pamela D. Diethylnitrosamine-induced hepatocarcinogenesis in rats: a theoretical study. *Toxicol Appl Pharmacol* 1991; **109**: 289-304
- Eckert JW**, Buerkle CJ, Major AM, Finegold MJ, Brandt ML. *In situ* hybridization utilizing a Y chromosome DNA probe. *Transplantation* 1995; **59**: 109-111
- Gross-Goupil M**, Saffroy R, Azoulay D, Precetti S, Emile JF, Delvart V, Tindiliere F, Laurent A, Bellin MF, Bismuth H, Debuire B, Lemoine A. Real-time quantification of AFP mRNA to assess hematogenous dissemination after transarterial chemoembolization of hepatocellular carcinoma. *Ann Surg* 2003; **238**: 241-248
- Ijichi M**, Takayama T, Matsumura M, Shiratori Y, Omata M, Makuuchi M. alpha-Fetoprotein mRNA in the circulation as a predictor of postsurgical recurrence of hepatocellular carcinoma: a prospective study. *Hepatology* 2002; **35**: 853-860
- Wong IH**, Yeo W, Leung T, Lau WY, Johnson PJ. Hematogenous dissemination of hepatocytes and tumor cells after surgical resection of hepatocellular carcinoma: a quantitative analysis. *Clin Cancer Res* 1999; **5**: 4021-4027
- Wiedle G**, Dunon D, Imhof BA. Current concepts in lymphocyte homing and recirculation. *Crit Rev Clin Lab Sci* 2001; **38**: 1-31
- Aziz KA**, Till KJ, Zuzel M, Cawley JC. Involvement of CD44-hyaluronan interaction in malignant cell homing and fibronectin synthesis in hairy cell leukemia. *Blood* 2000; **96**: 3161-3167
- Sun JJ**, Zhou XD, Liu YK, Tang ZY, Feng JX, Zhou G, Xue Q, Chen J. Invasion and metastasis of liver cancer: expression of intercellular adhesion molecule 1. *J Cancer Res Clin Oncol* 1999; **125**: 28-34
- Ji XN**, Ye SL, Li Y, Tian B, Chen J, Gao DM, Chen J, Bao WH, Liu YK, Tang ZY. Contributions of lung tissue extracts to invasion and migration of human hepatocellular carcinoma cells with various metastatic potentials. *J Cancer Res Clin Oncol* 2003; **129**: 556-564
- Fidler IJ**. Seed and soil revisited: contribution of the organ microenvironment to cancer metastasis. *Surg Oncol Clin N Am* 2001; **10**: 257-269

Edited by Ma JY and Xu FM

Risk factors influencing recurrence following resection of pancreatic head cancer

De-Qing Mu, Shu-You Peng, Guo-Feng Wang

De-Qing Mu, Shu-You Peng, Department of Surgery, the Second Affiliated Hospital, Medical College of Zhejiang University, Hangzhou 310009, Zhejiang Province, China

Guo-Feng Wang, Department of Pathology, the Second Affiliated Hospital, Medical College of Zhejiang University, Hangzhou 310009, Zhejiang Province, China

Correspondence to: Dr De-Qing Mu, Department of Surgery, the Second Affiliated Hospital, Medical College of Zhejiang University, Hangzhou 310009 Zhejiang Province, China. samier-1969@163.com
Telephone: +86-571-87783762

Received: 2003-06-10 **Accepted:** 2003-09-01

Abstract

AIM: Whether operative procedure is a risk factor influencing recurrence following resection of carcinoma in the head of pancreas or not remains controversies. In this text we compared the recurrence rate of two operative procedure: the Whipple procedure and extended radical operation, and inquired into the factors influencing recurrence after radical resection.

METHODS: From January 1995 to December 1998, 35 cases of carcinoma of pancreas underwent the Whipple operadure, 21 patients received the Extended radical operation. All patients were followed up for more than 3 years. Prognostic factors included operative procedure, size of tumor, lymph node, interstitial invasion.

RESULTS: Deaths duo to recurrence within 3 years after operation were studied. The death rate was 51.4% in the Whipple procedure and 42.9% in the Extended radical operative procedure. There was a significant difference between the two groups. Recurrence occurred in 75% patients with tumor large than 4 cm, in 87.5% patients with lymph node involvement, and in 50% patients with the presence of interstitial invasion.

CONCLUSION: Tumor exceeding 4 cm, lymph node involvement, and presence of interstitial invasion are high risk factors of recurrence after Whipple's procedure and extended radical operation.

Mu DQ, Peng SY, Wang GF. Risk factors influencing recurrence following resection of pancreatic head cancer. *World J Gastroenterol* 2004; 10(6): 906-909
<http://www.wjgnet.com/1007-9327/10/906.asp>

INTRODUCTION

Recurrence of pancreatic cancer is common after operation. Intraabdominal recurrence ranged 38% to 86%^[1-3]. Factors influencing recurrence in some studies included lymph node metastasis^[4,5], tumor size^[5,6], and tumor in surgical resection^[5-7]. In the present study we retrospectively analysis 56 patients with carcinoma located in pancreatic head after operation in our department of surgery, The aim was to find the factors

influencing recurrence following surgical resection for patients with pancreatic cancer hoping to improve the therapeutic results of carcinoma in the head of pancreas.

MATERIALS AND METHODS

Materials

Fifty six curative surgical resections were performed for pancreatic cancer in our department of surgery between January 1995 and December 1998. The patients did not receive any anticancer therapy before or after surgery.

Methods

Our radical procedures employed for carcinoma of pancreas was the Whipple operation in 35 cases, male/female ratio was 2.2:1(24/11), patients with an average of age were (57.3±4.6) years. According to the General Rules for Cancer of the Pancreas (4th edition, 1996), lymphatic clearance was limited to the regional lymph nodes immediately adjacent to the pancreatic head (D1⁻). In the pancreas, the line of resection was on the left border of the superior mesenteric vein. Extended radical operation (D2⁺) was performed in the other 21 cases, the male/female ratio was 2.5:1(15/6) with an average of age 58.9±5.1 years (Figure 1A and B). On the basis of n1 and n2 group and neighboring connective tissue clearance, the n3 group lymph nodes and soft tissues were properly cleared, nerve-plexus dissection around the retroperitoneum in 13 cases. Resection and reconstruction of the portal -vein system were performed in 6 cases, the line of resection of the pancreas was 1-2 cm outside the left border of the aorta.

The resected specimens were fixed in 40g/L formaldehyde solution, and sliced into 5 µm sections. Histologic sections were stained with hematoxylin and eoxin. We measure the maximum size of the tumor, metastasis in lymph nodes, and determined whether tumors extended directly beyond the posterior confines of the pancreas. The maximum tumor sizes were classified into four grades: 0<t1≤2 cm, 2.0<t2≤4.0 cm (t2), 4.0<t3≤6.0 cm, and t4>6.0 cm. The lymph node involvement were graded into n0, n1, n2, and n3 accoding to the General Rules for Pancreatic Cancer Study (4th edition, 1996) proposed by the Japanese Pancreatic Society. The primary group included N₀₆: infrapyloric, N₀₈: anterosuperior nodes along the common hepatic artery, N_{012inferior}: inferior nodes along the proper hepatic artery, along the bile duct, and along the posterior to the portal vein, N₀₁₃: posterior surface of the head of pancreas, N₀₁: origins of the superior mesenteric artery, the inferior pancreaticoduodenal artery, and the middle colic artery along the first jejunal branch, and the the superior mesenteric vein, N₀₁₇: on the anterior surface of the head of pancreas. The second group included (N2): N₀₉: around the celiac artery, N₀₁₁: along the splenic artery, N_{012superior}: superior nodes along the proper hepatic artery, the bile duct, superior to the portal vein, around the cystic duct, N₀₁₆: paraabdominal aorta. The third group (N3) included N₀₃: lessur curvature, N₀₄: greater curvature, N₀₅: suprapyloric, N₀₇: left gastric artery. Retroperitoneal invasion was classified into two grades Rp (+) and Rp(-) on the basis of whether the tumors extended directly beyond the posterior confines of the pancreas.

After surgery, all patients were followed up by serial determinations of plasma carcinoembryonic antigen (CEA), CA19-9, ultrasonograms and computed tomograms (CT) to determine whether and where cancer recurrence developed. The mode of clinical recurrence was classified into four types: hepatic metastasis (H), retroperitoneal recurrence (R), peritoneal dissemination (P), and distant metastasis (M). Retroperitoneal recurrence was divided into two subtypes: (1) local retroperitoneal recurrence was defined as infiltration of nerves, lymphatic vessels, and connective soft tissue, and (2) lymph node metastasis (LN).

The cumulative recurrence rate was analysed by using a χ^2 test. *P* value less than 0.05 was considered statistically significant.

RESULTS

No operative death occurred within 1 mo after excision. The follow-up period was more than 3 years for all patients of the two groups. In D1⁻ group, 6 cases were lost to be followed, 7 cases died of other diseases unrelated to cancer within three years, the remaining 22 patients died of recurrence, of which 18 patients was dead within 3 years. In D2⁺ group, 2 patients were lost to be followed, 3 patients died of other diseases within

3 years, the remaining 9 patients died of recurrence within 3 years. The 3 years cumulative rate of death due to recurrence was 51.4% in D1⁻ group and 42.9% in D2⁺ group, there was a significant difference between the 2 groups ($P < 0.05$). The histopathological backgrounds in patients who died of recurrence are showed in Table 1.

Recurrent styles

In D1⁻ group at least more than 2 recurrent sites could be found. Eighteen patients had retroperitoneal recurrence, among them 7 patients were complicated with peritoneal dissemination, 2 patients were complicated with liver metastasis, and 1 patient was complicated with extroabdomen metastasis. In D2⁺ group, the major recurrent styles of were as fellows: hepatic metastasis alone or in combination with retroperitoneal recurrence ($n=5$), peritoneal dissemination alone or combined with abdomen lymph node enlargement ($n=4$), or combined with other organ out of abdomen cavity metastasis ($n=1$).

Histopathological diagnosis

The distribution of cases was histopathologically (Figure 2) based on 3 factors: maximum tumor size, lymph node involvement, and interstitial invasion (Table 2).

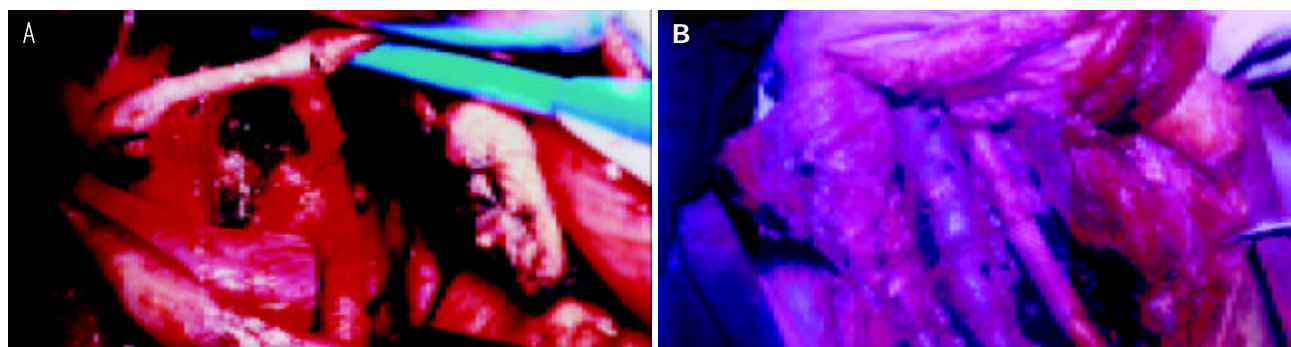


Figure 1 A: Ranges of lymphatic and neighboring connective tissue dissection n1, n2, and part of n3 group nodes were cleared with neighboring connective tissue, B: lymph node dissection around aorta, inferior vein, resection and reconstruction portal vein.

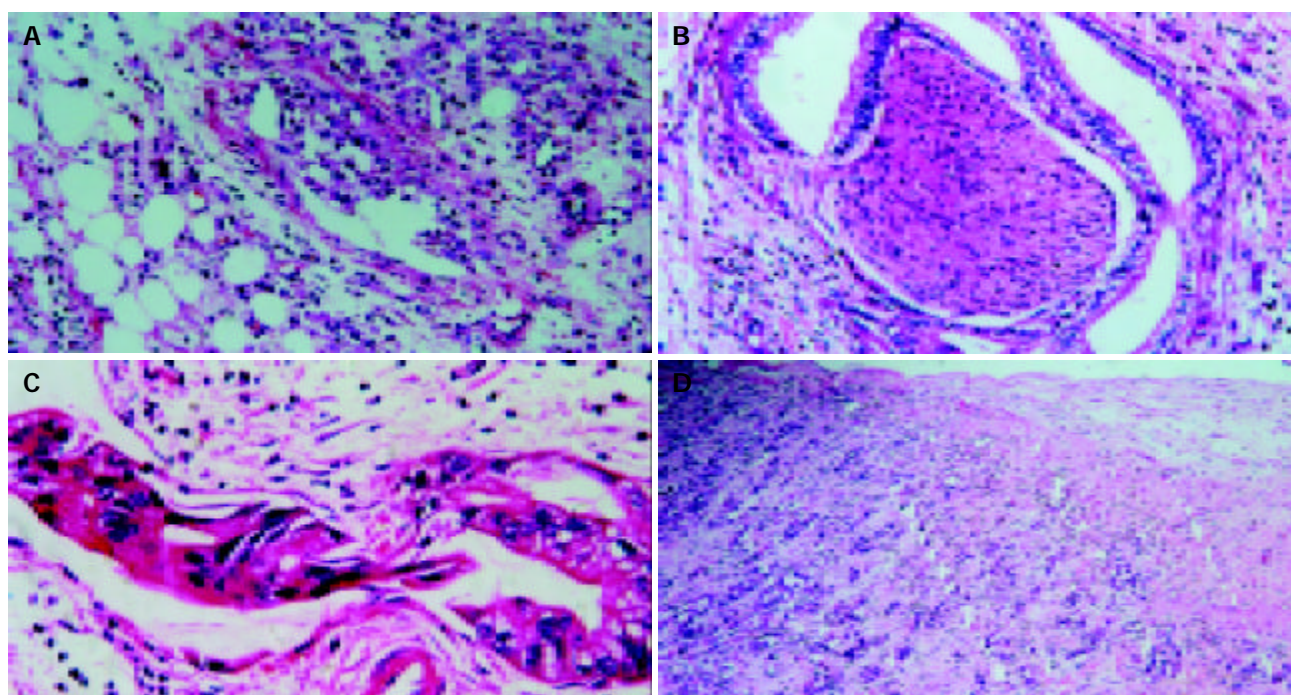


Figure 2 A: peritoneal dissemination, B: nerve invasion, C: cancer thrombus in lymphatic vessel, D: portal venous wall invasion. (HE original magnification $\times 200$).

Table 1 Histopathological findings in patients died of Recurrence

Operative procedure (No. of patients)	Maximum size				Nodal involvement				Interstitial invasion	
	t1	t2	t3	t4	n0	n1	n2	n3	Ii (-)	Ii (+)
D1 ⁻	1/5	7/16	10/14	-	3/9	15/26	-	-	6/13	12/22
D2 ⁺	0/4	3/9	3/5	3/3	0/6	2/7	4/5	3/3	1/5	8/16

Table 2 Comparision of tumor Size, nodal involvement and interstitial invasion between two groups

Operative procedure (No. of patients)	Maximum size				Nodal involvement				Interstitial invasion	
	t1	t2	t3	t4	n0	n1	n2	n3	Ii (-)	Ii (+)
D1 ⁻	5	16	14	-	9	26			13	22
D2 ⁺	4	9	5	3	6	7	5*	3**	2	19

*5 is positive also in n1, **3 is also positive in n1, and n2.

In D2⁺ group, tumors were less than 2 cm in diameter (4 cases), one case had lymph-node metastasis, and 2 lymph node vessels and perineural invasion respectively. In t2 group, 77.8%(7/9) of cases was associated with lymph-vessel invasion. Perineural invasion was present in 88.9%(8/9) of the tumor, and loose connective tissue invasion occurred in 55.6%(5/9). Tumors larger than 4.1 cm were all associated with lymph-vessel, perineural, and loose connective tissue invasion. Metastatic rate of lymph node was 69.2% (n=15). Lymph node metastatic rate was 69.2% (n=15). Rates of histologically proved metastasis to individual lymph nodes observed in our series were as follows: N1: N₀₆: 23.8%(n=5), N₀₈: 14.4%(n=3), N_{012inferior}: 33.3%(n=7), N₀₁₃: 33.3%(n=7), N₀₁₄: 28.6%(n=6), N₀₁₇: 33.3%(n=7); N2: N₀₉: 14.4%(n=3), N₀₁₁: 19.1%(n=4), N_{012superior}: 23.8%(n=5), N₀₁₆: 23.8%(n=5); N3: N₀₃: 0%, N₀₄: 0%, N₀₅: 14.4%(n=3), N₀₇: 13.3%(n=2). In tumors with negative lymph nodes, 5/6 had lymph-vessel invasion, and 4/6 had perineural invasion. The tumors with nodal involvement were all associated with lymph-vessel, perineural, and loose connective tissue invasion.

DISCUSSION

Argument existed about whether operative procedure on the risk factors influencing recurrence or not^[8-11]. Factors that influence the recurrent rate after resection were the absence of lymph node involvement^[12,13], and retroperitoneal invasion^[14], and microscopic curative resection^[12,14]. Such a procedure is also called Ro surgery. In our current study we confirmed that D2⁺ procedure could decrease recurrence in comparison with D1⁻. In D2⁺ group we found there exists wide extension of nodal involvement, and 'interstitial invasion' required careful dissection. D1⁻ procedure only provided simple lymphadenectomy limited to the region of the head of pancreas without resection of surrounding connective tissues, and dissection of the second and tertiary group lymph node was inadequate for the purpose of lymphatic clearance. Theoretically D2⁺ procedure could achieve a microscopic curative resection^[15,16]. Macroscopic curative resection has been proven to be microscopic noncurative resection by precise serial section analysis. Even the patients with microscopic curative resection had a surgical margin of only a few millimeters away from tumor^[17], that could not assure avoidance of future metastasis. Only in those with small (t1/t2), noninvasive lesions or slight retroperitoneal invasion, could D2⁺ actually decrease recurrence. In those with t3/t4 tumors, even after extended lymphatic and soft tissue dissection that goes beyond the regional lymph-node stations, D2⁺ procedure still has a higher recurrence.

The rate of recurrence in patients with t1 and t2 tumors generally was lower than that in those with t3 and t4 tumors

after D2⁺ procedure. The collective recurrence rate in t3 and t4 tumors was 75%(6 of 8). Tumors larger than 4.1 cm were all associated with lymph-vessel and perineural invasions. Therefore, our conclusion is that the larger the tumor the more extensive infiltration within interstitial invasion and nodal involvement, or the higher the recurrent risk, this is in accord with that reported in the literature^[18-21].

In comparison with D1⁻, D2⁺ procedure decreased recurrence in no and n1 group. There was a close relation between lymph node involvement and 'interstitial invasion'. Positive lymph node was often accompanied by lymph vessels invasion. Even if in pNo stage, lymph vessels invasion was present in 64% of the cases^[19]. Lymph vessel invasion might imply lymphatic metastasis before cancer cells flowed into lymph nodes. If nodal involvement was found in n1 region, microinvasion had already occurred in the n2 region^[22]. If n2 and n3 groups were invaded, the chance of distant recurrence was much increased.

Our study confirmed that pancreatic cancer tended to be accompanied by 'interstitial invasion' and positive of 'interstitial invasion' was a factor influencing recurrence. The so-called 'interstitial invasion' includes lymph vessel, nerves, and loose connective tissue invasions. The recurrence rate in patients with or without 'interstitial invasion' was 50% and 20%, respectively. The significance of nerve invasion has been annotated by other researchers^[23-25]. Peritoneal dissemination after excision could not be treated by surgery alone, because cancer cells either as single cells or cell clumps were randomly allocated on the large area of loose connective tissue of the peritoneum^[26]. About 40% of patients had small distant metastases. Such metastases were typical 1-2 mm nodules located on the surface of the peritoneum^[27]. So far as peritoneal dissemination concerned, there is no effective treatment. Even extensive lymph node dissection and resection of surrounding connective tissues and major vessels combined with radiotherapy and chemotherapy could not assure avoidance of recurrence up to now^[28-30].

In summary, the long term survival following resection depends on decrease of recurrence. Therefore rationally standardized operative procedure with due attention to factors of recurrence may help improve the long term survival of pancreatic cancer patients.

REFERENCES

- 1 Nitecki SS, Sarr MG, Colby TV, van Heerden JA. Long-term survival after resection for ductal adenocarcinoma of the pancreas. Is it really improving? *Ann Surg* 1995; **221**: 59-66
- 2 Griffin JF, Smalley SR, Jewell W, Paradelo JC, Raymond RD, Hassanein RE, Evans RG. Patterns of failure after curative

- resection of pancreatic carcinoma. *Cancer* 1990; **66**: 56-61
- 3 **Westerdahl J**, Andren-Sandberg A, Ihse I. Recurrence of exocrine pancreatic cancer- local or hepatic? *Hepatogastroenterology* 1993; **40**: 384-387
 - 4 **Meyer W**, Jurowich C, Reichel M, Steinhauser B, Wunsch PH, Gebhardt C. Pathomorphological and histological prognostic factors in curatively resected ductal adenocarcinoma of the pancreas. *Surg Today* 2000; **30**: 582-587
 - 5 **Benassai G**, Mastroiilli M, Quarto G, Gappiello A, Giani U, Mosella G. Survival after pancreaticoduodenectomy for ductal adenocarcinoma of the head of the pancreas. *Chir Ital* 2000; **52**: 263-270
 - 6 **Yamaguchi K**, Mizumoto K, Noshiro H, Sugitani A, Shimizu S, Chijiwa K, Tanaka M. Pancreatic carcinoma: <or = 2 cm versus> 2 cm in size. *Int Surg* 1999; **84**: 213-219
 - 7 **van Geenen RC**, van Gulik TM, Offerhaus GJ, de Wit LT, Busch OR, Obertop H, Gouma DJ. Survival after pancreaticoduodenectomy for periampullary adenocarcinoma: an update. *Eur J Surg Oncol* 2001; **27**: 549-557
 - 8 **Iacono C**, Facci E, Bortolasi L, Zamboni G, Scarpa A, Talamini G, Prati G, Nifosi F, Serio G. Intermediate results of extended pancreaticoduodenectomy. Verona experience. *J Hepatobiliary Pancreat Surg* 1999; **6**: 74-78
 - 9 **Tsiotos GG**, Farnell MB, Sarr MG. Are the results of pancreatectomy for pancreatic cancer improving? *World J Surg* 1999; **23**: 913-919
 - 10 **Pedrazzoli S**, Pasquali C, Sperti C. General aspects of surgical treatment of pancreatic cancer. *Dig Surg* 1999; **16**: 265-275
 - 11 **Benassai G**, Mastroiilli M, Mosella F, Mosella G. Significance of lymph node metastases in the surgical management of pancreatic head carcinoma. *J Exp Clin Cancer Res* 1999; **18**: 23-28
 - 12 **Yeo CJ**, Cameron JL, Sohn TA, Lillemoe KD, Pitt HA, Talamini MA, Hruban RH, Ord SE, Sauter PK, Coleman J, Zahurak ML, Grochow LB, Abrams RA. Six hundred fifty consecutive pancreaticoduodenectomies in the 1990s: Pathology, complications, and outcomes. *Ann Surg* 1997; **226**: 248-257
 - 13 **Nagakawa T**, Nagamori M, Futakami F, Tsukioka Y, Kayahara M, Ohta T, Uen K, Miyazaki I. Results of extensive surgery for pancreatic carcinoma. *Cancer* 1996; **77**: 640-645
 - 14 **Nakao A**, Harada A, Nonami T, Kaneko T, Takagi H. Clinical significance of carcinoma invasion of the extrapancreatic nerve plexus in pancreatic cancer. *Pancreas* 1996; **12**: 357-361
 - 15 **Nakao A**, Kaneko T, Takeda S, Inoue S, Harada A, Nomoto S, Ekmel T, Yamashita K, Hatsuno T. The role of extended radical operation for pancreatic cancer. *Hepatogastroenterology* 2001; **48**: 949-952
 - 16 **Imamura M**, Hosotani R, Kogire M. Rationale of the so-called extended resection for pancreatic invasive ductal carcinoma. *Digestion* 1999; **60** (Suppl 1): 126-129
 - 17 **Kayahara M**, Nagakawa T, Ueno K, Ohta T, Takeda T, Miyazaki I. An evaluation of radical resection for pancreatic cancer based on the mode of recurrence as determined by autopsy and diagnostic imaging. *Cancer* 1993; **172**: 2118-2123
 - 18 **Nagai H**, Kuroda A, Morioka Y. Lymphatic and local spread of T1 and T2 pancreatic cancer. A study of autopsy material. *Ann Surg* 1986; **204**: 65-71
 - 19 **Gebhardt C**, Meyer W, Reichel M, Wunsch PH. Prognostic factors in the operative treatment of ductal pancreatic carcinoma. *Langenbecks Arch Surg* 2000; **385**: 14-20
 - 20 **Takao S**, Shinci H, Sha K, Natsugoe S, Maenohara S, Suenaga T, Nishimata Y, Aikou T. Clinical and biological features of T1 ductal adenocarcinoma of the pancreas. *Hepatogastroenterology* 1999; **46**: 498-503
 - 21 **Benassai G**, Mastroiilli M, Quarto G, Gappiello A, Giani U, Forestieri P, Mazzeo F. Factors influencing survival after resection for ductal adenocarcinoma of the head of the pancreas. *J Surg Oncol* 2000; **73**: 212-218
 - 22 **Ishikawa O**, Ohhigashi H, Sasaki Y, Kabuto T, Fukuda I, Furukawa H, Imaoka S, Iwanaga T. Practical usefulness of lymphatic and connective tissue clearance for the carcinoma of the pancreas head. *Ann Surg* 1998; **208**: 215-220
 - 23 **Ozaki H**, Hiraoka T, Mizumoto R, Matsuno S, Matsumoto Y, Nakayama T, Tsunoda T, Suzuki T, Monden M, Saitoh Y, Yamauchi H, Ogata Y. The prognostic significance of lymph node metastasis and intrapancreatic perineural invasion in pancreatic cancer after curative resection. *Surg Today* 1999; **29**: 16-22
 - 24 **Dang C**, Qin Z, Ji Z, Li Y, Zhao J, Takashi E, Naito Z, Yokoyama M, Asono G. Morphological characteristics and clinical significance of nerve distribution in pancreatic cancers. *Nippon Ika Daigaku Zasshi* 1997; **64**: 526-531
 - 25 **Takahashi S**, Hasebe T, Oda T, Sasaki S, Kinoshita T, Konishi M, Ueda T, Ochiai T, Ochiai A. Extra-tumor perineural invasion predicts postoperative development of peritoneal dissemination in pancreatic ductal adenocarcinoma. *Anticancer Res* 2001; **21**(2B): 1407-1412
 - 26 **Hiraoka T**, Uchino R, Kanemitsu K, Toyonaga M, Saitoh N, Nakamura I, Tashiro S, Miyauchi Y. Combination of intraoperative radiation with resection of cancer of the pancreas. *Int J Pancreatol* 1990; **7**: 201-207
 - 27 **Warshaw AL**, Tepper JE, Shipley WU. Laparoscopy in the staging and planning of therapy for pancreatic cancer. *Am J Surg* 1986; **151**: 76-80
 - 28 **Cellini N**, Trodella L, Valentini V, Doglietto GB, Morganti AG, Ziccarelli P, Alfieri S, Bossola M, Brizi MG, Crucitti F. Radiotherapy, local control and survival in carcinomas of the exocrine pancreas. *Rays* 1998; **23**: 528-534
 - 29 **Alfieri S**, Morganti AG, Di Giorgio A, Valentini V, Bossola M, Trodella L, Cellini N, Doglietto GB. Improved survival and local control after intraoperative radiation therapy and post-operative radiotherapy: a multivariate analysis of 46 patients undergoing surgery for pancreatic head cancer. *Arch Surg* 2001; **136**: 343-347
 - 30 **Foo ML**, Gunderson LL, Nagorney DM, McIlrath DC, van Heerden JA, Robinow JS, Kvols LK, Garton GR, Martenson JA, Cha SS. Patterns of failure in grossly resected pancreatic ductal adenocarcinoma treated with adjuvant irradiation +/- 5 fluorouracil. *Int J Radiat Oncol Biol Phys* 1993; **26**: 483-489

Edited by Wang XL Proofread by Xu FM

Efficacy and safety of lamivudine treatment for chronic hepatitis B in pregnancy

Guan-Guan Su, Kong-Han Pan, Nian-Feng Zhao, Su-Hua Fang, Dan-Hong Yang, Yong Zhou

Guan-Guan Su, Kong-Han Pan, Su-Hua Fang, Dan-Hong Yang, Yong Zhou, Department of Infection, Sir Run Run Shaw Hospital affiliated to Zhejiang University, Hangzhou, 310016, Zhejiang Province, China

Nian-Feng Zhao, First Hospital affiliated to Zhejiang University, Hangzhou, 310007, Zhejiang Province, China

Correspondence to: Dr. Guan-Guan Su, Department of Infection, Sir Run Run Shaw Hospital Affiliated to Zhejiang University, Hangzhou, 310016, Zhejiang Province, China. pankonghan@medmail.com.cn

Telephone: +86-571-86090073-6013 **Fax:** +86-571-86032877

Received: 2003-08-02 **Accepted:** 2003-09-24

Abstract

AIM: To evaluate the efficacy and safety of lamivudine treatment of chronic hepatitis B disease in pregnancy.

METHODS: The study group was comprised of 38 chronic HBV patients who were diagnosed pregnant during lamivudine treatment and voluntary to continue the same therapy. The control group was from documented patient data in the literatures. We compared the following parameters with those of a control group: anti-HBV efficacy, complications of pregnancy (abortion, preterm birth, neonatal asphyxia, fetal death, and congenital anomaly), incidence of HBV-positive babies and developmental anomalies in pregnant women treated with lamivudine.

RESULTS: The blocking rate of lamivudine treatment was significantly higher than that of active vaccine immunization for babies with double-positive (HBsAg/HBeAg) mothers with 30-30-10 µg doses of vaccine (74.07%) and with 30-20-10 µg (64.87%). The natural vertical HBV transmission from mother to infant of "double-positive" mothers was 100% (10/10). No pregnancy complication was noted during the observation period, but in the control group the incidences of pregnancy complication were 16.67% (abortion), 43.02% (preterm), 15.62% (neonatal asphyxia), and 4.49% (fetal death), 10.0% (congenital anomaly). No HBV-positive newborn was detected and no developmental anomaly was found in the study group.

CONCLUSION: Lamivudine is helpful to prevent maternal-infant HBV transmission and may reduce the complications of HBV-infected pregnant patients.

Su GG, Pan KH, Zhao NF, Fang SH, Yang DH, Zhou Y. Efficacy and safety of lamivudine treatment for chronic hepatitis B in pregnancy. *World J Gastroenterol* 2004; 10(6): 910-912
<http://www.wjgnet.com/1007-9327/10/910.asp>

INTRODUCTION

Throughout the world, over 300 million people have chronic hepatitis B virus (HBV) infection, and more than 75 percent of those affected are of Asian origin^[1]. Chronic HBV infection causes cirrhosis, liver cancer, and death^[2,3]. The disease is

endemic in Africa and Asia, where the virus is transmitted from mother to newborn or between close contacts in early childhood^[4-6].

Chronically infected persons with viral replication are at the highest risk for progressive liver disease^[7]. In China, chronic HBV infection is a common clinical occurrence in pregnancy as well as a potentially serious condition^[8]. In pregnant patients the complications of HBV occur more frequently and with a higher mortality^[9]. Also vertical transmission of HBV to the infant is common^[4,5]. Perinatal transmission of HBV is the most important cause of chronic HBV infection and remains one serious problem despite passive immunization (hepatitis B immune globulin at birth) and active immunization (hepatitis B vaccination according to the standard 3-dose schedule). In different studies high maternal HBV DNA levels were associated with a vaccination breakthrough^[10,11]. Recently nucleoside analogues have been used to prevent mother-to-infant transmission of HIV-1^[12]. In that setting, lamivudine given during the last weeks of pregnancy in HIV-1 and HBV positive women appeared to be safe^[12-15]. Following a similar rationale, there was a clinical trial about the use of lamivudine, a potent inhibitor of HBV replication, in pregnant women with high HBV viral loads in highly endemic countries^[16].

However, few data are available regarding the efficacy and safety of lamivudine treatment for chronic HBV from the early phase of pregnancy. Pharmaceutical inserts regarding lamivudine indicate it is of "uncertain safety" during pregnancy. In this retrospective analysis, we evaluated 38 cases of chronic HBV pregnant patients treated with lamivudine from the early phase of pregnancy for pregnancy-related complications and congenital anomalies.

MATERIALS AND METHODS

Patients

Forty-two chronic HBV-infected women were found to be pregnant during lamivudine treatment and presented to the physician between 2-3 mo of gestation. Then they were enrolled in the study. During the study, one patient chose to terminate her pregnancy, two stopped lamivudine therapy, and one was lost to follow-up. Thus the final study consisted of 38 pregnant patients who continued lamivudine therapy. The pretreatment diagnosis of HBV was based on National Prevention and Treatment Profiles of Viral Hepatitis (2000)^[17] criteria with the following criteria: detectable HBsAg and HBeAg/HBeAb in serum, detectable serum HBV DNA, and elevated alanine aminotransferase (ALT) levels (more than 3-4 times normal level). Patients were excluded if they had hepatitis C or D infection. Patients had not received any other antiviral drugs in the preceding 6 mo. All patients were warned about that studies in rabbits had demonstrated lamivudine to result in fetal demise. However, it was also explained that the dosages used in animal studies were nearly 60 times higher than those used in humans (private communication).

Currently there is a clinical trial in Asia evaluating lamivudine use perinatally in mothers with high HBV viral

loads with the goal to reduce vertical HBV transmission to the infants^[13]. The patients who earlier stopped lamivudine often experienced significant clinical deterioration. Thus overall we felt it appropriate to consider continuing lamivudine therapy. HBV infection in pregnant women was more serious than in non-pregnant women^[9]. All the above were informed to any pregnant patients with HBV infection. Decision was made by patient herself on whether to terminate lamivudine treatment or not.

The data of complications of HBV hepatitis and HBV-positive babies were based on Prevention and Treatment of Viral Hepatitis study edited by Gao^[19]. Lamivudine safety profile was obtained from international studies^[13-15,18].

Regimen and parameters

Pregnant women with chronic HBV infection were treated with lamivudine. The dosage, course, efficacy evaluation, follow-up, measures to deal with resistant mutation were based on the Guideline for Lamivudine Clinical Use (2000)^[20] and Expert Consensus on Lamivudine Clinical Use (2001)^[21]. Complications of pregnancy included abortion, preterm birth, neonatal asphyxia, fetal death, and congenital anomaly^[19]. Regular ultrasonic examination was carried out to monitor the safety of the fetus. All newborns were given the standard passive-active immunization or actively immunized at birth. Twelve babies were tested of HVB DNA (PCR), HBsAg, HBeAg, anti-HBs, anti-HBe, anti-HBc at birth before HBIG administration (T_0) and at the 6th mo (T_6) and the 12th mo (T_{12}) after birth. The percentage of HBV-positive babies was calculated. The health status and development of babies were assessed by the local children healthcare institution. All children were followed-up and documented.

RESULTS

Antiviral efficacy

HBV-DNA was converted to negative in 35 patients (92.11%) of the study group. HBeAg was converted to negative in 12 patients (31.58%). The rate of HBeAg seroconversion (loss of HBeAg or development of antibody to HBeAg) was 26.32% (10/38). The normalization rate of ALT was 73.68% (28/38). The rate of resistant mutation was 11.43% (4/35). Lamivudine efficacy was similar to other reports in the international medical literatures^[13-15]. ALT normalization may have been confounded by hepatic injury of pregnancy. Thus the complete efficacy of lamivudine was difficult to assess.

Incidence of HBV-positive baby (Table 1)

Twelve maternal-baby pairs were evaluated for HBV markers (HBsAg, HBeAg, anti-HBs, and anti-HBe, anti-HBc) before and after delivery. All 12 mothers were double positive (HBsAg/HBeAg) before lamivudine treatment. Although the HBV-DNA parameters of all 12 mothers were converted to negative prepartum, 8 mothers remained HBeAg-positive, 1 HBeAg negative, and 3 reached seroconversion. Of the 8 mothers who were HBeAg-positive at childbirth, 3 babies were HBsAg-positive at birth (T_0), but turned negative at T_6 and T_{12} postpartum. The other babies were all HBsAg-negative during 12 months of follow-up. Thus after one year, 100% of the babies were HBsAg-negative. But in control group, the blocking rates of active vaccine immunization for babies with double-positive (HBsAg/HBeAg) mothers were 74.07% with 30-30-10 µg doses of vaccine and 64.87% with 30-20-10 µg. The natural vertical HBV transmission from mother (double-positive) to infant was 100% (10/10)^[19]. The prevention of HBV maternal-infant transmission was very significant in lamivudine-treated mothers.

Table 1 Blocking of maternal transmission in HBsAg and HBeAg double-positive mothers^[19]

	<i>n</i>	HBsAg(+)			HBV-DNA(+)	Blocking rate
		T_0	T_6	T_{12}		
Lamivudine treatment	12	3	0	0	0	100.00
Vaccine 30-30-10 µg	81		21	21	21	74.07
Vaccine 30-20-10 µg	37		13	13	13	64.87
Natural transmission	10		10	10	10	0.00

Complications of pregnancy (Table 2)

The infants of lamivudine-treated mothers were delivered at full term without any complication. The incidence of pregnancy complication was lower in the study group than in the control group of pregnant mothers with chronic HBV^[19].

Table 2 Complications of pregnancy in different groups^[19]

	Abortion (%)	Preterm (%)	Neonatal asphyxia (%)	Fetal death (%)	Congenital anomaly (%)
Lamivudin	0/38	0/38	0/38	0/38	0/38
Control	16.67 (1/6)	43.02 (37/86)	15.62 (14/89)	4.49 (4/89)	10 (1/10)

Control of viral hepatitis activity (Table 3)

Although three out of 38 patients in the study group did not convert to HBV-DNA-negative within one year, ALT normalized in all three patients. Ten patients in the study group converted to HBV-DNA-negative, but their ALT remained abnormal. They were included in the pregnancy liver injury group. Six patients were HBeAg-negative, and four patients had seroconversion for HBeAb. A resistant HBV mutant emerged in four cases though their ALT remained normal. Thus overall hepatitis activity was controlled in all the study patients (100%). In the two patients who quitted lamivudine after the consultation, active hepatitis recurred within 6 months. Honkoop *et al* reported that the incidence of "lamivudine withdrawal hepatitis" was 17% (7/41)^[22]. Hepatitis activity was better controlled in lamivudine treatment group than in the group who quitted lamivudine therapy (Table 3).

Table 3 Control of hepatitis activity^[22]

	<i>n</i>	Active hepatitis (%)
Lamivudine treatment during pregnancy	38	0 (0.00)
Stop lamivudine while pregnant	2	2 (100.00)
Stop lamivudine	41	7 (17.07)

Infant development and health

Community maternal-child health clinics failed to detect any unfavorable outcome related to the infant's health and development.

DISCUSSION

It has been well-known that the pregnant women chronically infected with HBV have more complications and a higher mortality during pregnancy^[5,8,9]. Lamivudine has been found to be an effective treatment strategy for chronic HBV^[15]. However, its use is not recommended during pregnancy especially during the first trimester because animal studies have demonstrated lethal effects on the rabbit fetus (private communication). In our study 38 pregnant women with chronic HBV infection continued lamivudine therapy during the entire pregnancy. Their decision to continue its therapy was voluntary

after informed consent. They were all provided with information about the drug benefits and risks. Our results indicated lamivudine therapy not only provided a protective effect against maternal-infant HBV transmission, but decreased the likelihood of active HBV infection in the mother. Further complications were minimal compared with the control group. These results should be presented to a mother contemplating continuation of lamivudine therapy during pregnancy.

Pregnancy complications are likely caused by the activity of hepatitis B virus in mothers with chronic HBV infections. The rate of vertical maternal-infant HBV transmission was 90-100% in mothers who were double positive for both HBsAg and HBeAg^[19]. It is probable that such a high transmission rate has been led by the high viral load^[10,11]. The data in our study indicated lamivudine was able to neutralize hepatitis activity and reduction in the viral load might result in fewer pregnancy complications and prevent maternal-infant HBV transmission. This benefit may well outweigh the risk of lamivudine's early toxic effects on the infant during the first trimester. Lamivudine has been found belonging to the L-form enantiomorph nucleotide analogue which is negatively selective for the human nucleotide^[15]. Toxicity was detected only at very high dosages of 1 000 times higher than the recommended human dosages. The dosage used in animals was 60 times greater than that used in human (private communication). Thus currently recommended lamivudine dosages for human may represent little risk to the pregnant mother.

However, there are several concerns about our current study. First, our study was not designed as a randomized-placebo-controlled study, thus any improvement in the study group could be due to such confounding factors as "self-selection" bias, or observer bias. Second, the study group was small and thus might lack power to distinguish a true difference between the treated group and the control group. However, we do consider the study to be of value in raising the question of benefit of lamivudine treatment of chronic HBV in pregnancy. Further studies, especially larger well-designed placebo-controlled studies are needed to confirm a true beneficial effect of lamivudine therapy for chronic HBV infection in pregnancy.

REFERENCES

- 1 **Maynard JE**. Hepatitis B: global importance and need for control. *Vaccine* 1990; **8**: S18-20
- 2 **Liaw YF**, Tai DI, Chu CM, Chen TJ. The development of cirrhosis in patients with chronic type B hepatitis: a prospective study. *Hepatology* 1988; **8**: 493-496
- 3 **Chang MH**, Chen CJ, Lai MS, Hsu HM, Wu TC, Kong MS, Liang DC, Shau WY, Chen DS. Universal hepatitis B vaccination in Taiwan and the incidence of hepatocellular carcinoma in children. Taiwan Childhood Hepatoma Study Group. *N Engl J Med* 1997; **336**: 1855-1859
- 4 **Stevens CE**, Neurath RA, Beasley RP, Szmunn W. HBeAg and anti-HBe detection by radioimmunoassay: correlation with vertical transmission of hepatitis B virus in Taiwan. *J Med Virol* 1979; **3**: 237-241
- 5 **Xu ZY**, Liu CB, Francis DP, Purcell RH, Gun ZL, Duan SC, Chen RJ, Margolis HS, Huang CH, Maynard JE. Prevention of perinatal acquisition of hepatitis B virus carriage using vaccine: preliminary report of a randomized, double-blind placebo-controlled and comparative trial. *Pediatrics* 1985; **76**: 13-18
- 6 **Beasley RP**, Hwang LY. Postnatal infectivity of hepatitis B surface antigen-carrier mothers. *J Infect Dis* 1983; **147**: 185-190
- 7 **de Jongh FE**, Janssen HL, de Man RA, Hop WC, Schalm SW, van Blankenstein M. Survival and prognostic indicators in hepatitis B surface antigen-positive cirrhosis of the liver. *Gastroenterology* 1992; **103**: 1630-1635
- 8 **Yang H**, Chen R, Li Z, Zhou G, Zhao Y, Cui D, Li S, Han C, Yang L. Analysis of fetal distress in pregnancy with hepatitis B virus infection. *Zhonghua Fuchanke Zazhi* 2002; **37**: 211-213
- 9 **Khuroo MS**, Kamili S. Aetiology, clinical course and outcome of sporadic acute viral hepatitis in pregnancy. *J Viral Hepat* 2003; **10**: 61-69
- 10 **Ip HM**, Lelie PN, Wong VC, Kuhns MC, Reesink HW. Prevention of hepatitis B virus carrier state in infants according to maternal serum levels of HBV DNA. *Lancet* 1989; **1**: 406-410
- 11 **del Canho R**, Grosheide PM, Mazel JA, Heijtkink RA, Hop WC, Gerards LJ, de Gast GC, Fetter WP, Zwijsen J, Schalm SW. Ten-year neonatal hepatitis B vaccination program, The Netherlands, 1982-1992: Protective efficacy and long-term immunogenicity. *Vaccine* 1997; **15**: 1624-1630
- 12 **Faucher P**, Batallan A, Bastian H, Matheron S, Morau G, Madelenat P, Benifla JL. Management of pregnant women infected with HIV at Bichat Hospital between 1990 and 1998: analysis of 202 pregnancies. *Gynecol Obstet Fertil* 2001; **29**: 211-225
- 13 **van Zonneveld M**, van Nunen AB, Niesters HG, de Man RA, Schalm SW, Janssen HL. Lamivudine treatment during pregnancy to prevent perinatal transmission of hepatitis B virus infection. *J Viral Hepat* 2003; **10**: 294-297
- 14 **Moodley J**, Moodley D, Pillay K, Coovadia H, Saba J, van Leeuwen R, Goodwin C, Harrigan PR, Moore KH, Stone C, Plumb R, Johnson MA. Pharmacokinetics and antiretroviral activity of lamivudine alone or when coadministered with zidovudine in human immunodeficiency virus type 1-infected pregnant women and their offspring. *J Infect Dis* 1998; **178**: 1327-1333
- 15 **Johnson MA**, Moore KH, Yuen GJ, Bye A, Pakes GE. Clinical pharmacokinetics of lamivudine. *Clin Pharmacokinet* 1999; **36**: 41-66
- 16 **Van Nunen AB**, de Man RA, Heijtkink RA, Niesters HG, Schalm SW. Lamivudine in the last 4 weeks of pregnancy to prevent perinatal transmission in highly viremic chronic hepatitis B patients. *J Hepatol* 2000; **32**: 1040-1041
- 17 **Branch society of Infectious Disease and Parasitology and Branch society of Hepatology of Chinese Medical Association**. National Prevention and Treatment Profiles of Viral Hepatitis (2000). *Zhonghua Chuanranbing Zazhi* 2001; **19**: 56-62
- 18 **Lai CL**, Chien RN, Leung NW, Chang TT, Guan R, Tai DI, Ng KY, Wu PC, Dent JC, Barber J, Stephenson SL, Gray DF. A one-year trial of lamivudine for chronic hepatitis B. Asia Hepatitis Lamivudine Study Group. *N Engl J Med* 1998; **339**: 61-68
- 19 **Gao SZ**. Research on prevention and treatment of viral hepatitis. *Beijing: Beijing pub* 1993: 38-46, 286-291
- 20 **Expert team for lamivudine clinical use**. The year 2000 guideline for lamivudine clinical use. *Zhonghua Ganzangbing Zazhi* 2000; **8**: 249-250
- 21 **Expert team for lamivudine clinical use**. Expert consensus on lamivudine clinical use (2001). *Zhonghua Ganzangbing Zazhi* 2002; **10**: 157-158
- 22 **Honkoop P**, de Man RA, Niesters HG, Zondervan PE, Schalm SW. Acute exacerbation of chronic hepatitis B virus infection after withdrawal of lamivudine therapy. *Hepatology* 2000; **32**: 635-639

Edited by Gupta MK and Wang XL Proofread by Xu FM

Clinical value of *Helicobacter pylori* stool antigen test, ImmunoCard STAT HpSA, for detecting *H pylori* infection

Yi-Hui Li, Hong Guo, Peng-Bin Zhang, Xiao-Yan Zhao, Si-Ping Da

Yi-Hui Li, Hong Guo, Peng-Bin Zhang, Xiao-Yan Zhao, Si-Ping Da, Department of Gastroenterology, Xinqiao Hospital, Third Military Medical University, Chongqing 400037, China

Correspondence to: Hong Guo, Department of Gastroenterology, Xinqiao Hospital, Third Military Medical University, Chongqing 400037, China. haoguo11@yahoo.com

Telephone: +86-23-68755604

Received: 2003-08-23 **Accepted:** 2003-10-12

Abstract

AIM: To evaluate the reliability of the *Helicobacter pylori* stool antigen test, ImmunoCard STAT HpSA, for detecting *H pylori* infection.

METHODS: Stool specimens were collected from 53 patients who received upper endoscopy examination due to gastrointestinal symptoms. ImmunoCard STAT HpSA was used to detect *H pylori* stool antigens. *H pylori* infection was detected based on three different tests: the urease test, Warthin-Starry staining and culture. *H pylori* status was defined as positive when both the urease test and histology or culture alone was positive.

RESULTS: Sensitivity, specificity, positive predictive and negative predictive values and the total accuracy of ImmunoCard STAT HpSA for the diagnosis of *H pylori* infection were 92.6% (25/27), 88.5% (23/26), 89.3% (25/28), 92% (23/25) and 90.6% (48/53), respectively.

CONCLUSION: The stool antigen test, ImmunoCard STAT HpSA, is a simple noninvasive and accurate test for the diagnosis of *H pylori* infection.

Li YH, Guo H, Zhang PB, Zhao XY, Da SP. Clinical value of *Helicobacter pylori* stool antigen test, ImmunoCard STAT HpSA, for detecting *H pylori* infection. *World J Gastroenterol* 2004; 10(6): 913-914

<http://www.wjgnet.com/1007-9327/10/913.asp>

INTRODUCTION

Helicobacter pylori infection is a major cause of chronic gastritis and peptic ulcer, and is associated with gastric cancer and gastric MALT lymphoma^[1-4]. There are several methods of diagnosing *H pylori* infection including invasive procedures using mucosa biopsies taken during endoscopy (mainly culture, histology and the rapid urease test) and noninvasive procedures (mainly ¹³C or ¹⁴C urea breath tests (UBTs) and serological tests). But invasive procedures suffer from biopsies and endoscopy, and the UBTs require expensive equipment or is harmful to patients. Because *H pylori* antibody titers fall very slowly even after successful eradication, tests lack of specificity and sensitivity^[5-9]. Recently, the *H pylori* stool antigen (HpSA) test has been put in the market as another noninvasive technique^[10-13], but has rarely validated in China^[14]. The aim of this study is to evaluate the

clinical value of a new test, ImmunoCard STAT HpSA, for the diagnosis of *H pylori* infection.

MATERIALS AND METHODS

Patients

A total of 56 patients (33 males and 23 females, average age 43.7 years old) participated in this study. Chronic gastritis and peptic ulcer were endoscopically diagnosed in 47 and 9 patients, respectively. Patients treated with antibiotics, bismuth, or proton pump inhibitors within 4 weeks preceding the study were excluded.

Methods

Invasive tests using mucosal biopsies including culture, histology (Warthin-Starry staining) and the rapid urease test (RUT) were used to establish the "gold standard", in order to evaluate the accuracy of the new stool antigen test, ImmunoCard STAT HpSA.

Mucosal biopsies for detecting Hp

During upper endoscopy, three gastric biopsies were taken. One biopsy was used for RUT and the remaining two were used for Warthin-Starry staining and culture. The gold standard for the presence of *H pylori* infection was defined when both RUT and Warthin-Starry staining or culture alone was positive. The absence of *H pylori* infection required all three tests to be negative.

ImmunoCard STAT HpSA

On the same day of endoscopy, patients collected stool into an air tight container. The stool assay was performed using the same test series of the ImmunoCard STAT HpSA (Meridian Diagnostics, Inc, USA). A small portion (5-6 mm diameter) of stool specimen was transferred into the sample diluent vial using the applicator stick, vortexed for 15 s, and then 4 drops were dispensed into the round window at the lower end of the device. The results were read 5 min later. Positive and negative results were judged as recommended by the manufactures. The endoscopy-based tests and HpSA test were carried out by different people with double blind procedures.

Statistical analysis

Sensitivity, specificity, PPV, NPV and accuracy of the kit were calculated according to the gold standard.

RESULTS

Altogether, 53 patients were enrolled and tested by ImmunoCard STAT HpSA and the endoscopy-based tests. *H pylori* infection was present in 27 patients as determined by the gold standard. The HpSA test produced positive and negative results in 28 and 25 patients, respectively. Compared with the gold standard, the HpSA was inaccurate in five patients (three false positive, and two false negative), giving a sensitivity, specificity, positive predictive and negative predictive values and total accuracy of the ImmunoCard STAT HpSA of 92.6% (25/27), 88.5% (23/26), 89.3% (25/28), 92% (23/25) and 90.6% (48/53), respectively (Table 1).

Table 1 Performance of the ImmunoCard STAT HpSA test in the detection of *H pylori* infection, according to the biopsy-based gold standard

ImmunoCard STAT HpSA	Gold standard		Total
	Positive	Negative	
Positive	25	3	28
Negative	2	23	25
Total	27	26	53

DISCUSSION

A variety of highly sensitive and specific tests are available to diagnose *H pylori* infection. Invasive tests using mucosal biopsies taken during endoscopy might lead to cross infection. In addition, some patients refuse to undergo endoscopy, especially after eradication therapy, due to its invasive nature. Fortunately, there are several noninvasive tests including ^{13}C or ^{14}C urea breath tests (UBT) and serological tests. The UBT tests are currently proven to have high sensitivity and specificity, and considered to be the optimal test for monitoring *H pylori* eradication therapy. However, ^{13}C -UBT needs special equipment and is expensive, and ^{14}C -UBT requires a radioactive isotope, and cannot be used for children and pregnant women. As a result, UBTs are not widely available. Therefore, it is necessary to find a new, easy, cheaper and accurate noninvasive test.

Gastric epithelial cells renew once in one to three days, and are output in feces with *H pylori*, which can be detected by polyclonal capture anti-*H pylori* antibodies. The HpSA was reported in America Gastroenterology Week in 1997, and put in the market by Meridian Company in the same year, with the name Premier Platinum HpSA. Premier Platinum HpSA is a microplate enzyme-immunoassay for the qualitative detection of *H pylori* antigens in human stool, and was approved by FDA to be used in clinic in 1998. The HpSA test has been widely evaluated around the world, with a weighted mean sensitivity and specificity of 90-98%, respectively^[13,15,16]. The HpSA test is a cheap and useful method for the diagnosis of *H pylori* infection before and after eradication therapy^[17,18]. It is an accurate test in all age groups of children too^[19]. However, Peitz *et al* reported that the diagnostic accuracy, in particular the sensitivity, of the HpSA stool test was reduced by upper gastrointestinal bleeding, and a negative test result should be confirmed by a further diagnostic method^[20,21]. Although the HpSA test seems to be less accurate than the UBT, both UBT and stool antigen tests are reliable noninvasive tests for monitoring the efficacy of *H pylori* eradication therapy.

A novel easier stool antigen test named ImmunoCard STAT HpSA has recently been put in the market by Meridian Company. This test was first reported to have a sensitivity of 96.1% and specificity of 90.6% at Gastrointestinal Pathology and *Helicobacter* Conference in 2002 in Athens, but have not been reported since. In the present study, we conclude that the ImmunoCard STAT HpSA test has a diagnostic value comparable to the gold standard in detecting *H pylori*. The sensitivity and specificity of the ImmunoCard STAT HpSA for the diagnosis of *H pylori* infection were 92.6% and 88.5%, respectively, with an accuracy of 90.6%. Because it is easy and convenient to perform, the ImmunoCard STAT HpSA could be used at many situations, especially for children, pregnant women, old people and others who are not suitable for endoscopy. The ImmunoCard STAT HpSA is an ideal test for the diagnosis of *H pylori* infection in clinical practice.

REFERENCES

1 **Hobsley M**, Tovey FI. *Helicobacter pylori*: the primary cause of

duodenal ulceration or a secondary infection? *World J Gastroenterol* 2001; **7**: 149-151

2 **Xia HHX**. Association between *Helicobacter pylori* and gastric cancer: current knowledge and future research. *World J Gastroenterol* 1998; **4**: 93-96

3 **Wang KX**, Wang XF, Peng JL, Cui YB, Wang J, Li CP. Detection of serum anti-*Helicobacter pylori* immunoglobulin G in patients with different digestive malignant tumors. *World J Gastroenterol* 2003; **9**: 2501-2504

4 **Wang RT**, Wang T, Chen K, Wang JY, Zhang JP, Lin SR, Zhu YM, Zhang WM, Cao YX, Zhu CW, Yu H, Cong YJ, Zheng S, Wu BQ. *Helicobacter pylori* infection and gastric cancer: evidence from a retrospective cohort study and nested case-control study in China. *World J Gastroenterol* 2002; **8**: 1103-1107

5 **Wang XZ**, Li D. The serodiagnosis of *Helicobacter pylori*. *Shijie Huaren Xiaohua Zazhi* 2000; **8**: 550-551

6 **Sun T**, Ye JX, Ma GX, Cui LH, Liu CQ, Pu J, Fu SF, Jiang Y. Using ^{13}C -urea breath test to diagnose *Helicobacter pylori* infection. *Shijie Huaren Xiaohua Zazhi* 2000; **8**: 270

7 **Li ZJ**, Jiang T, Zhou WM. The value of detecting *Helicobacter pylori* antibody in saliva by enzyme-linked immuno-sorbent assay. *Shijie Huaren Xiaohua Zazhi* 2000; **8**: 241-242

8 **Wang CD**, Lu XQ. Clinical application of *Helicobacter pylori* urea breath test. *Shijie Huaren Xiaohua Zazhi* 2000; **8**: 789-792

9 **Huang Y**, Xu LN. The dependent test of *Helicobacter pylori* urea enzyme. *Shijie Huaren Xiaohua Zazhi* 2000; **8**: 549-550

10 **Makristathis A**, Pasching E, Schutze K, Wimmer M, Rotter ML, Hirschl AM. Detection of *Helicobacter pylori* in stool specimens by PCR and antigen enzyme immunoassay. *J Clin Microbiol* 1998; **36**: 2772-2774

11 **Vaira D**, Malfertheiner P, Megraud F, Axon AT, Deltenre M, Hirschl AM, Gasbarrini G, O' Morain C, Garcia JM, Quina M, Tytgat GN. Diagnosis of *Helicobacter pylori* infection with a new non-invasive antigen-based assay. HpSA European study group. *Lancet* 1999; **354**: 30-33

12 **Fanti L**, Mezzi G, Cavallero A, Gesu G, Bonato C, Masci E. A new simple immunoassay for detecting *Helicobacter pylori* infection: antigen in stool specimens. *Digestion* 1999; **60**: 456-460

13 **Metz DC**. Stool testing for *Helicobacter pylori* infection: yet another noninvasive alternation. *Am J Gastroenterol* 2000; **95**: 546-548

14 **Liu X**, Zhi M, Dong L, Chang BX. The evaluation of *Helicobacter pylori* stool antigen test. *Shijie Huaren Xiaohua Zazhi* 2002; **10**: 726-728

15 **Monteiro L**, de Mascarel A, Sarrasqueta AM, Bergey B, Barberis C, Talby P, Roux D, Shouler L, Goldfain D, Lamouliatte H, Megraud F. Diagnosis of *Helicobacter pylori* infection: noninvasive methods compared to invasive methods and evaluation of two new tests. *Am J Gastroenterol* 2001; **96**: 353-358

16 **Manes G**, Balzano A, Iaquinto G, Ricci C, Piccirillo MM, Giardullo N, Todisco A, Lioniello M, Vaira D. Accuracy of the stool antigen test in the diagnosis of *Helicobacter pylori* infection before treatment and in patients on omeprazole therapy. *Aliment Pharmacol Ther* 2001; **15**: 73-79

17 **Aksoy DY**, Aybar M, Ozaslan E, Kav T, Engin D, Ercis S, Altinok G, Hascelik G, Uzunalimoglu B, Arslan S. Evaluation of the *Helicobacter pylori* stool antigen test (HpSA) for the detection of *Helicobacter pylori* infection and comparison with other methods. *Hepatogastroenterology* 2003; **50**: 1047-1049

18 **Tanaka A**, Watanabe K, Tokunaga K, Hoshiya S, Imase K, Sugano H, Shingaki M, Kai A, Itoh T, Ishida H, Takahashi S. Evaluation of *Helicobacter pylori* stool antigen test before and after eradication therapy. *J Gastroenterol Hepatol* 2003; **18**: 732-738

19 **Kato S**, Ozawa K, Okuda M, Fujisawa T, Kagimoto S, Konno M, Maisawa S, Iinuma K. Accuracy of the stool antigen test for the diagnosis of childhood *Helicobacter pylori* infection: a multicenter Japanese study. *Am J Gastroenterol* 2003; **98**: 296-300

20 **Peitz U**, Leodolter A, Kahl S, Agha-Amiri K, Wex T, Wolle K, Gunther T, Steinbrink B, Malfertheiner P. Antigen stool test for assessment of *Helicobacter pylori* infection in patients with upper gastrointestinal bleeding. *Aliment Pharmacol Ther* 2003; **17**: 1075-1084

21 **van Leerdam ME**, van der Ende A, ten Kate FJ, Rauws EA, Tytgat GN. Lack of accuracy of the noninvasive *Helicobacter pylori* stool antigen test in patients with gastroduodenal ulcer bleeding. *Am J Gastroenterol* 2003; **98**: 798-801

Functional hepatic flow in patients with liver cirrhosis

Zheng Pan, Xing-Jiang Wu, Jie-Shou Li, Fang-Nan Liu, Wei-Su Li, Jian-Ming Han

Zheng Pan, Xing-Jiang Wu, Jie-Shou Li, Fang-Nan Liu, Wei-Su Li, Jian-Ming Han, Research Institute of General Surgery, Nanjing General Hospital of Nanjing Command/Clinical School of Medical College of Nanjing University, Nanjing 210002, Jiangsu Province, China

Correspondence to: Zheng Pan, Research Institute of General Surgery, Nanjing General Hospital of Nanjing Command, No.305, Eastern Road of Zhongshan, Nanjing 210002, Jiangsu Province, China. pz2233@sina.com

Telephone: +86-25-80860065 **Fax:** +86-25-84803956

Received: 2003-07-12 **Accepted:** 2003-10-07

Abstract

AIM: To evaluate hepatic reserve function by investigating the change of functional hepatic flow and total hepatic flow in cirrhotic patients with portal hypertension.

METHODS: HPLC method was employed for the determination of concentration of D-sorbitol in human plasma and urine. The functional hepatic flow (FHF) and total hepatic flow (THF) were determined by means of modified hepatic clearance of D-sorbitol combined with duplex doppler color sonography in 20 patients with cirrhosis and 10 healthy volunteers.

RESULTS: FHF, evaluated by means of the D-sorbitol clearance, was significantly reduced in patients with cirrhosis in comparison to controls (764.74 ± 167.91 vs $1\ 195.04 \pm 242.97$ mL/min, $P < 0.01$). While THF was significantly increased in patients with cirrhosis in comparison to controls ($1\ 605.23 \pm 279.99$ vs $1\ 256.12 \pm 198.34$ mL/min, $P < 0.01$). Portal blood flow and hepatic artery flow all were increased in cirrhosis compared to controls ($P < 0.05$ and $P < 0.01$). D-sorbitol total clearance was significantly reduced in cirrhosis compared to control ($P < 0.01$), while D-sorbitol renal clearance was significantly increased in cirrhosis ($P < 0.05$). In controls FHF was similar to THF ($1\ 195.05 \pm 242.97$ vs $1\ 256.12 \pm 198.34$ mL/min, $P = 0.636$), while FHF was significantly reduced compared with THF in cirrhosis (764.74 ± 167.91 vs $1\ 605.23 \pm 279.99$ mL/min, $P < 0.01$).

CONCLUSION: Our method that combined modified hepatic clearance of D-sorbitol with duplex doppler color sonography is effective in the measurement of FHF and THF. FHF can be used to estimate hepatic reserve function.

Pan Z, Wu XJ, Li JS, Liu FN, Li WS, Han JM. Functional hepatic flow in patients with liver cirrhosis. *World J Gastroenterol* 2004; 10(6): 915-918
<http://www.wjgnet.com/1007-9327/10/915.asp>

INTRODUCTION

The management of portal hypertension in patients with liver cirrhosis is still a therapeutic challenge^[1]. Liver failure and variceal bleeding are the chiefly causes that lead to death in cirrhosis. Now surgical devascularization and shunting play an important role in treatment of portal hypertension. Though operation is useful in controlling variceal bleeding, the mortality of operation is very high. Some cirrhotic patients

can not bear the strike of operation and anaesthesia because of inadequate hepatic reserve function. So the evaluation of hepatic reserve function preoperatively is very important, in addition to proper perioperative management. At present the evaluation of clinical severity of cirrhosis is mostly based on the Child-Pugh score. However, such an approach can not directly provide reliable quantitative evaluations of the integrity and functional reserve of the hepatic parenchyma because the parameters are not very specific and test sensitivity is sometimes too low to detect mild liver alteration^[2]. Recently several studies^[3-10] have considered that hepatic clearance of D-sorbitol was a valid procedure in determination of FHF, by which hepatic reserve function could be estimated. The aim of this study was to measure THF and FHF of control subjects and patients with cirrhosis by means of duplex doppler color sonography combined with modified hepatic clearance of D-sorbitol and then to evaluate the hepatic reserve function.

MATERIALS AND METHODS

Patients

This study was carried out on 20 patients with cirrhosis and portal hypertension. The diagnosis of cirrhosis was established by liver biopsy intraoperatively. Fourteen patients with cirrhosis were males and six were females. They ranged in age from 35 to 73 years. The etiology of the disease was virus-related in 19 cases and drug-induced in the remaining one. The exclusion criteria were: patients with a variceal bleeding in the previous four weeks; those on portal-pressure-lowering drugs; those with portal and splenic vein thrombosis; those with severe ascites.

Ten subjects that without any clinical or laboratory evidence of liver disease served as controls. They were matched with the patients with cirrhosis for sex, age and body surface area. All patients gave their informed consent before participation in this study, which was performed according to the Helsinki Declaration.

Measurement of THF

Duplex doppler measurements of the portal vein and common hepatic artery were obtained using a real-time electronic sector scanner and a pulsed doppler unit.

All the patients and controls were kept fasting overnight prior to the procedure. They were examined in the supine position and were asked to hold their breath during the doppler recording. The portal vein was scanned longitudinally, and the sample volume was positioned in the middle of the portal trunk. The hepatic artery measurements were taken where a straight stretch ran parallel to the portal vein, some centimeters away from the coeliac axis. Care was taken to maintain the angle at below 55°. Portal vein and hepatic artery flow were determined by multiplying the mean blood velocity (V mean) by the sectional area (πr^2). Total hepatic flow was calculated as the sum of portal flow and hepatic artery flow.

Measurement of FHF

All tests were carried out at rest after an overnight fast. The sterile pyrogen-free 5% water solution of D-sorbitol (Fluka,

US) was intravenously infused at a constant rate of 50 mg/min. The steady-state regimen would be achieved after 2-h of continuous infusion^[11]. Three blood samples were taken from peripheral vein at about 15-min intervals between 135 and 165 min after the start of the infusion. Urine samples were spontaneously collected for a 1-h period between 120 and 180 min during the infusion. FHF was determined on the basis of the hepatic clearance of SOR, as previously described by Molino^[8].

Analyses

Blood and urine samples were centrifuged at 2 500 r/min for 15 min and the supernatants were stored at -40 °C until analysis. All samples were thawed before concentration measurement, then deproteinized by means of super-filter.

HPLC method was employed for the determination of concentration of D-sorbitol in human plasma and urine. The HPLC system (Waters) consisted of a pump, an injector and a fluorescence-detection (4210). The extracts of samples were chromatographed on a CORGEL-87P column that was kept at 85 °C and monitored by fluorescence-detection. The mobile phase was H₂O at a flow-rate of 1.0 mL/min. All data were treated according to the formula described by Molino^[8].

Statistical analysis

All the data are expressed as mean±SD. The statistical analyses were performed by means of two-sample *t*-test and paired *t*-test.

RESULTS

The results are shown in the Table 1. All the tests were performed on 20 patients with cirrhosis and 10 healthy controls and all subjects tolerated the procedure without complications or side effects. As expected, FHF, evaluated by means of the D-sorbitol clearance, was significantly reduced in patients with cirrhosis in comparison to controls (764.74±167.91 vs 1 195.05±242.97 mL/min, *P*<0.01). While THF was significantly increased in patients with cirrhosis in comparison to controls (1 605.23±279.99 vs 1 256.12±198.34 mL/min, *P*<0.01).

Portal blood flow and hepatic artery flow were increased in cirrhosis compared to controls (*P*<0.05 and *P*<0.01). D-sorbitol total clearance was significantly reduced in cirrhosis compared to control, while D-sorbitol renal clearance was significantly increased in cirrhosis (*P*<0.01).

In controls FHF and THF were similar (1 195.05±242.97 vs 1 256.12±198.34 mL/min, *P*=0.636), while FHF was significantly reduced compared to THF in cirrhosis (764.74±167.91 vs 1 605.23±279.99 mL/min, *P*<0.01).

DISCUSSION

Liver cirrhosis is the final pathologic and clinical expression of a wide variety of chronic liver diseases. The commonest causes of cirrhosis are chronic hepatitis B or C virus infection (nearly 90% of the total cases of cirrhosis in China). Pathophysiologically, the clinical manifestation of liver cirrhosis arises from the occurrence of two major events: hepatocellular insufficiency and portal hypertension^[12]. In cirrhosis, portal hypertension develops as a result of an increased sinusoidal or post-sinusoidal portal resistance to blood flow, due to the loss of normal hepatic architecture and collagenization of the space of Disse^[13,14]. The major pathophysiologic consequences of portal hypertension include portal-systemic collaterals formation, ascites and splenomegaly. The gastric and esophageal varices constitute the major cause of life-threatening digestive tract bleeding in cirrhosis. Now surgical devascularization and shunting play an important role in management of the complications of portal hypertension. Though operation is effective in controlling bleeding, the mortality of operation is still higher as some patients can not bear the strike of operation and anaesthesia due to inadequate hepatic reserve function. Recently some study discovered that the patients whose liver volume was decreased by 40% and the hepatic clearance of D-sorbitol was below 600 mL/min would have a higher incidence of postoperative complication^[15]. Therefore it is of much importance to evaluate the hepatic reserve function preoperatively for the selection of operation approaches and the timing of operation.

FHF may be defined as the blood perfusing the liver that makes contact with functioning hepatocytes. The most widely used procedures to assess FHF are based on the clearance technique. But the test compound must not be eliminated by any organ other than the liver, must not re-enter the circulation once it has been eliminated, and has relatively high hepatic intrinsic clearance. To date, no compound has fulfilled these requirements completely. D-sorbitol, a naturally occurring polyol with prevailing hepatic metabolism, is almost completely extracted by the liver during the first-pass, and extrahepatic elimination is negligible^[16]. Reproducible first-order kinetics and flow-dependent principle were demonstrated for D-sorbitol in previous studies^[2,10,11,17]. D-sorbitol had an exceptionally high extraction ratio in the normal liver (approaching 100%)^[16,17], even in the presence of a severely impaired liver function, so we might consider that hepatic clearance of D-sorbitol very closely approximates total hepatic flow. While in cirrhosis, the hepatic clearance of D-sorbitol is less than total hepatic flow due to intrahepatic shunting. The

Table 1 Results of Duplex doppler and D-sorbitol clearance in 20 patients with liver cirrhosis and 10 healthy controls

	Controls	Cirrhosis	<i>P</i>
Portal blood flow (mL/min)	960.35±220.86	1 181.10±279.79	<0.05
Hepatic artery flow (mL/min)	295.77±82.59	424.13±116.89	<0.01
Total hepatic flow (THF) (mL/min)	1 256.12±198.34	1 605.23±279.99	<0.01
THF per kg b.w. (mL/min)	20.14±3.51	25.12±4.40	<0.01
D-sorbitol concentration in blood (mg/dL)	4.15±0.81	6.05±1.22	<0.01
D-sorbitol total clearance (mL/min)	1 246.72±242.59	857.22±167.61	<0.01
D-sorbitol urinary elimination rate (mg/min)	2.16±1.0	5.58±2.76	<0.01
D-sorbitol renal clearance (mL/min)	51.67±19.96	92.48±48.66	<0.05
Functional hepatic flow(FHF) (mL/min)	1 195.05±242.97	764.74±167.91	<0.01
FHF per kg b.w. (mL/min)	19.18±4.28	12.07±2.40	<0.01

The data are expressed as mean±SD.

difference between THF and FHF can be assumed to be a parameter reflecting intrahepatic shunting.

Generally THF was measured by means of the hepatic extraction of D-sorbitol and indocyanine green, according to the Fick's principle^[4,10]. But the procedure, which needs hepatic vein catheterization is invasive and difficult to popularize. In addition, direct measurements of total hepatic flow through the hepatic artery and the portal vein have been achieved with electromagnetic flow probes or laser doppler flow meter^[18]. But the technique is applicable only during surgical procedures, which severely limits its usefulness. Recently the technique of duplex doppler color sonography has been gaining increasing popularity in the measurement of hepatic blood flow and found to be a safe, reproducible, noninvasive and fairly accurate method^[19-22].

There are still large variabilities in determination of FHF and THF by means of hepatic clearance of D-sorbitol and duplex doppler color sonography because of limitation of techniques and operations. To the former, the measurement of concentration of D-sorbitol is difficult. A small error of D-sorbitol concentration will lead to a large variability of final outcome. The concentration of D-sorbitol in plasma and urine used to be determined by an enzymatic-spectrophotometric method. It needs an enzymatic oxidation and deoxidization reaction since there is no absorption of ultraviolet for D-sorbitol. The concentration of D-sorbitol is determined indirectly following the measurement of fluorescence intensity of NADH1 that produced in reaction. While the attenuation of fluorescence and the incompleteness of reaction will result in certainty errors. To minimize these errors, we first established the method that measured the concentration of D-sorbitol by the use of HPLC and made the standard concentration curve. The data obtained in our study are in agreement with previous observations^[2,3,9]. Moreover, there is smaller standard error than that of other studies due to absence of extremely big or small data. In the latter, the errors stem from uncertainty in the measurement of blood velocity, vessel caliber and the possible non-circular shape of the cross-sectional area of the vessel. To minimize these errors, the examination was always performed by the same investigator, who had more than 5 years' experience in doppler examination of deep vessels and was unaware of the clinical diagnosis of the subject, and following strict guidelines during the operation.

The results of our study showed that THF was similar to FHF in controls ($1\,256.12 \pm 198.34$ vs $1\,195.05 \pm 242.97$ mL/min, $P=0.636$), which support the measurement of FHF and THF by non-invasive techniques. However, since D-sorbitol hepatic extraction was never completed, the FHF slightly underestimated THF in controls. In cirrhosis, the FHF was significantly decreased, while doppler-assessed THF was increased, indicating that a part of the portal flow was diverted through intrahepatic shunts or a substantial impairment of the functional integrity of hepatocytes^[23]. In this case simultaneous assessment of these two non-invasive parameters could be useful to quantify functional shunting in cirrhosis. As expected, portal vein and hepatic artery blood flow were increased in cirrhosis in comparison to controls respectively, suggesting a hyperkinetic systemic circulation with a high cardiac output and decreased total peripheral vascular resistance. Though the THF was preserved or increased, the FHF was still reduced. This is thought to be due to reduced FHF and a compensatory increase in THF to maintain hepatic perfusion. In addition, we measured the FHF and THF in six patients with liver cirrhosis before and after transjugular intrahepatic portosystemic shunt (TIPS). We discovered that the THF measured one week after TIPS was more than that of before TIPS, while FHF was reduced significantly in all subjects. It may be considered that the reduction of portal vein pressure and increase in

portosystemic shunting caused by TIPS are associated with the reduction of hepatic perfusion, which can partly explain the high incidence of hepatic encephalopathy in patients with liver cirrhosis^[24-26].

REFERENCES

- 1 **Seewald S**, Seitz U, Yang AM, Soehendra N. Variceal bleeding and portal hypertension: still a therapeutic challenge? *Endoscopy* 2001; **33**: 126-139
- 2 **Garello E**, Battista S, Bar F, Niro GA, Cappello N, Rizzetto M, Molino G. Evaluation of hepatic function in liver cirrhosis: clinical utility of galactose elimination capacity, hepatic clearance of D-sorbitol, and laboratory investigations. *Dig Dis Sci* 1999; **44**: 782-788
- 3 **Zoli M**, Magalotti D, Bianchi G, Ghigi G, Orlandini C, Grimaldi M, Marchesini G, Pisi E. Functional hepatic flow and Doppler-assessed total hepatic flow in control subjects and in patients with cirrhosis. *J Hepatol* 1995; **23**: 129-134
- 4 **Molino G**, Avagnina P, Ballare M, Torchio M, Niro AG, Aurucci PE, Grosso M, Fava C. Combined evaluation of total and functional liver plasma flows and intrahepatic shunting. *Dig Dis Sci* 1991; **36**: 1189-1196
- 5 **Molino G**, Battista S, Bar F, Garello E, Avagnina P, Grosso M, Spalluto E. Determination of functional portal-systemic shunting in patients submitted to hepatic angiography. *Liver* 1996; **16**: 347-352
- 6 **Ott P**, Clemmesen O, Keiding S. Interpretation of simultaneous measurements of hepatic extraction fractions of indocyanine green and sorbitol: evidence of hepatic shunts and capillarization? *Dig Dis Sci* 2000; **45**: 359-365
- 7 **Bar F**, Battista S, Garello E, Grosso M, Spalluto F, Zanon E, Torchio M, Molino G. Short-term effects of transjugular intrahepatic portosystemic shunt (TIPS) on functional liver plasma flow in patients with advanced cirrhosis. *Liver* 1998; **18**: 245-250
- 8 **Molino G**, Avagnina P, Belforte G, Bircher J. Assessment of the hepatic circulation in humans: new concepts based on evidence derived from a D-sorbitol clearance method. *J Lab Clin Med* 1998; **131**: 393-405
- 9 **Fabbri A**, Magalotti D, Brizi M, Bianchi G, Zoli M, Marchesini G. Prostaglandin E1 infusion and functional hepatic flow in control subjects and in patients with cirrhosis. *Dig Dis Sci* 1999; **44**: 377-384
- 10 **Clemmesen JO**, Tygstrup N, Ott P. Hepatic plasma flow estimated according to Fick's principle in patients with hepatic encephalopathy: evaluation of indocyanine green and D-sorbitol as test substances. *Hepatology* 1998; **27**: 666-673
- 11 **Molino G**, Avagnina P, Garrone C, Sansoe G, Degerfeld MM, Peretti P, Tinivella M, Bianco S. Time-dependent modifications of splanchnic circulation in female pigs submitted to end-to-side portacaval anastomosis. *Dig Dis Sci* 2001; **46**: 489-494
- 12 **Bilbao JI**, Quiroga J, Herrero JJ, Benito A. Transjugular intrahepatic portosystemic shunt (TIPS): current status and future possibilities. *Cardiovasc Intervent Radiol* 2002; **25**: 251-269
- 13 **Liu YK**, Shen W. Inhibitive effect of cordyceps sinensis on experimental hepatic fibrosis and its possible mechanism. *World J Gastroenterol* 2003; **9**: 529-533
- 14 **Wang XB**, Liu P, Lu X, Liu CH, Hu YY, Gu HT, Liu C. Dynamic changes of pressure of portal vein in development of liver fibrosis induced by dimethylnitrosamine in rats. *Shijie Huaren Xiaohua Zazhi* 2002; **10**: 401-405
- 15 **Li YM**, Lv F, Xu X, Ji H, Gao WT, Lei TJ, Ren GB, Bai ZL, Li Q. Evaluation of liver functional reserve by combining D-sorbitol clearance rate and CT measured liver volume. *World J Gastroenterol* 2003; **9**: 2092-2095
- 16 **Burggraaf J**, Schoemaker RC, Lentjes EG, Cohen AF. Sorbitol as a marker for drug-induced decreases of variable duration in liver blood flow in healthy volunteers. *Eur J Pharm Sci* 2000; **12**: 133-139
- 17 **Bar F**, Battista S, Bucchi MC, Zanon C, Grosso M, Alabiso O, Miraglia S, Cappello N, Gariboldi A, Molino G. Sorbitol removal by the metastatic liver: a predictor of systemic toxicity of intra-arterial chemotherapy in patients with liver metastases. *J Hepatol*

- 1999; **30**: 1112-1118
- 18 **Tomoda F**, Yamanaka N, Furukawa K, Kawamura E, Tanaka T, Ichikawa N, Kuroda N, Okamoto E. Contribution of the portal flow on hepatic tissue perfusion increases in reduced hepatic vascular bed. *Hepatol Res* 2000; **17**: 212-222
- 19 **Chawla Y**, Santa N, Dhiman RK, Dilawari JB. Portal hemodynamics by duplex Doppler sonography in different grades of cirrhosis. *Dig Dis Sci* 1998; **43**: 354-357
- 20 **Walsh KM**, Leen E, MacSween RN, Morris AJ. Hepatic blood flow changes in chronic hepatitis C measured by duplex Doppler color sonography: relationship to histological features. *Dig Dis Sci* 1998; **43**: 2584-2590
- 21 **Merkel C**, Sacerdoti D, Bolognesi M, Bombonato G, Gatta A. Doppler sonography and hepatic vein catheterization in portal hypertension: assessment of agreement in evaluating severity and response to treatment. *J Hepatol* 1998; **28**: 622-630
- 22 **Bolognesi M**, Sacerdoti D, Merkel C, Bombonato G, Gatta A. Noninvasive grading of the severity of portal hypertension in cirrhotic patients by echo-color-Doppler. *Ultrasound Med Biol* 2001; **27**: 901-907
- 23 **Molino G**, Bar F, Battista S, Torchio M, Niro AG, Garelo E, Avagnina P, Fava C, Grosso M, Spalluto F. Arterial-venous shunting in liver cirrhosis. *Dig Dis Sci* 1998; **43**: 51-55
- 24 **Riggio O**, Merli M, Pedretti G, Servi R, Meddi P, Lionetti R, Rossi P, Bezzi M, Salvatori F, Ugolotti U, Fiaccadori F, Capocaccia L. Hepatic encephalopathy after transjugular intrahepatic portosystemic shunt. Incidence and risk factors. *Dig Dis Sci* 1996; **41**: 578-584
- 25 **Sanyal AJ**, Freedman AM, Shiffman ML, Purdum PP 3rd, Luketic VA, Cheatham AK. Portosystemic encephalopathy after transjugular intrahepatic portosystemic shunt: results of a prospective controlled study. *Hepatology* 1994; **20**(1 Pt 1): 46-55
- 26 **Jalan R**, Gooday R, O'Carroll R, Redhead DN, Elton RA, Hayes PC. A prospective evaluation of changes in neuropsychological and liver function tests following transjugular intrahepatic portosystemic stent-shunt. *J Hepatol* 1995; **23**: 697-705

Edited by Zhu LH Proofread by Xu FM

Clinical characteristics and management of patients with early acute severe pancreatitis: Experience from a medical center in China

Hou-Quan Tao, Jing-Xia Zhang, Shou-Chun Zou

Hou-Quan Tao, Jing-Xia Zhang, Shou-Chun Zou, Department of Surgery, Zhejiang Provincial Peoples' Hospital, Hangzhou 310014, Zhejiang Province, China

Correspondence to: Dr. Hou-Quan Tao, Department of Surgery, Zhejiang Provincial Peoples' Hospital, Hangzhou 310014, Zhejiang Province, China. houquantao@yahoo.com

Telephone: +86-571-85239988

Received: 2003-10-10 **Accepted:** 2003-11-13

Abstract

AIM: To study clinical characteristics and management of patients with early severe acute pancreatitis (ESAP).

METHODS: Data of 297 patients with severe acute pancreatitis (SAP) admitted to our hospital within 72 h after onset of symptoms from January 1991 to June 2003 were reviewed for the occurrence and development of early severe acute pancreatitis (ESAP). ESAP was defined as presence of organ dysfunction within 72 h after onset of symptoms. Sixty-nine patients had ESAP, 228 patients without organ dysfunction within 72 h after onset of symptoms had SAP. The clinical characteristics, incidence of organ dysfunction during hospitalization and prognosis between ESAP and SAP were compared.

RESULTS: Impairment degree of pancreas (Balthazar CT class) in ESAP was more serious than that in SAP (5.31 ± 0.68 vs 3.68 ± 0.29 , $P < 0.01$). ESAP had a higher mortality than SAP (43.4% vs 2.6%, $P < 0.01$), and a higher incidence of hypoxemia (85.5% vs 25%, $P < 0.01$), pancreas infection (15.9% vs 7.5%, $P < 0.05$), abdominal compartment syndrome (ACS) (78.3% vs 23.2%, $P < 0.01$) and multiple organ dysfunction syndrome (MODS) (78.3% vs 10.1%, $P < 0.01$). In multiple logistic regression analysis, the main predisposing factors to ESAP were higher APACHE II score, Balthazar CT class, MODS and hypoxemia.

CONCLUSION: ESAP is characterised by MODS, severe pathological changes of pancreas, early hypoxemia and abdominal compartment syndrome. Given the poor prognosis of ESAP, these patients should be treated in specialized intensive care units with special measures such as close supervision, fluid resuscitation, improvement of hypoxemia, reduction of pancreatic secretion, elimination of inflammatory mediators, prevention and treatment of pancreatic infections.

Tao HQ, Zhang JX, Zou SC. Clinical characteristics and management of patients with early acute severe pancreatitis: Experience from a medical center in China. *World J Gastroenterol* 2004; 10(6): 919-921

<http://www.wjgnet.com/1007-9327/10/919.asp>

INTRODUCTION

Despite considerable improvement in the treatment of severe acute pancreatitis (SAP), the mortality of the disease still ranges

between 15-25%^[1-3]. Multiple organ dysfunction syndrome (MODS)^[4-7], the extent of necrotic pancreatic parenchyma and the presence of bacterial infection have been identified as major determinants for death^[8,9]. A number of such patients developed pancreatitis-associated intractable organ failure during the early course of SAP, and no effective treatment methods were available, the mortality was up to 40-60%^[3,10,11]. For the purpose of assessing the clinical course and management of these specific severe pancreatitis, we defined these severe acute pancreatitis with presence of organ dysfunction within 72 h after onset of symptoms as early severe acute pancreatitis (ESAP)^[12]. In this paper, we analyzed the clinical features of 69 cases of ESAP and discussed the key of ESAP management.

MATERIALS AND METHODS

Clinical data

From January 1991 to June 2003, a total of 297 patients with SAP were treated in our hospital, including 140 males and 157 females (average age 58.53, from 15 to 79 years). Among them 69 cases were with organ dysfunction within 72 h after onset of symptoms, and 228 cases without organ dysfunction.

SAP and organ dysfunction definitions were adopted from the Atlanta Classification System for SAP^[13]. All patients received standardized intensive care treatment as the following: (1) Supportive care including maintaining circulation volume, nutritional supplements, prophylactic antibiotics for pancreatic infection, oxygen supplementation, and mechanical ventilation, as well as monitoring for respiratory, cardiovascular and renal insufficiency and correcting them early. (2) To 'rest the pancreas' by fasting with nasogastric drainage to remove gastric secretions and by using anticholinergic agents or H₂-blocking agents and somatostatin to inhibit pancreatic secretion. (3) Multiple measures were taken early for accelerating the recovery of gastrointestinal function. (4) Infectious necrosis of pancreas was identified by dynamic contrast-enhanced CT. (5) Oddi's sphincterotomy and nasobile drainage were performed for biliary pancreatitis accompanied by bile duct obstruction. (6) Surgical treatment (necrosectomy with drainage and continuous postoperative lavage of the lesser sac) was performed if infected pancreatic necrosis was identified or if the patient did not respond to maximal intensive care treatment over a period of more than 72 h.

Patients were divided into two sub-groups: ESAP with organ dysfunction and SAP without organ dysfunction within 72 h after onset of symptoms. APACHEII score, Balthazar CT class, number of organ dysfunction and rate of pancreatic infection in both groups were analyzed retrospectively.

Statistical analysis

Measurement data was expressed as mean \pm SD, the difference between the groups was analyzed with Student's *t* test. Quantitative data was analyzed with Chi-square test. To identify the risk factors for ESAP, multiple logistic regression analysis with backward elimination was used. The level of significance was $P < 0.05$.

RESULTS

ESAP characteristic

Data of 297 SAP are given in Table 1. The mean time between onset of symptoms and hospital admission was 25.64 h. Mortality of ESAP was higher than that of SAP, early death rate (within 1 wk) was 53.3%(16/30) in ESAP and 33.3%(2/6) in SAP respectively. Pulmonary failure was the most frequent organ dysfunction in ESAP. Compared with SAP group, the different types of organ dysfunction were observed more frequently in the ESAP group. The hospital course of patients with ESAP was characterized by a high incidence of progressive MODS (Table 2).

Table 1 Comparison of clinical characteristics between ESAP and SAP

Factor	ESAP group	SAP group
Age (year)	58.95±5.51 ^a	60.12±5.16
Sex (M/F)	38/31 ^a	102/126
Hours between onset and admission	24.72±5.21 ^a	26.04±4.03
APACHE II at admission	16.6±0.72 ^b	9.4±0.45
Impairment degree of pancreas (Balthazar CT class)	5.31±0.68 ^b	3.68±0.29
Hypoxemia (%)	59(85.5) ^b	57(25)
ACS (%)	54(78.3) ^b	53(23.2)
Fever (T>38.5 °C)(%)	38(55.1) ^b	55(24.1)
Pancreas infection (%)	11(15.9) ^a	17(7.5)
Other infections (%)	40(57.9) ^b	41(17.9)
Non-effective after 48 h	42(60.8) ^b	27(11.8)
ICU treatment (%)		
Surgical treatment (%)	18(26.1) ^b	15(6.5)
Death (%)	30(43.4) ^b	6(2.6)
Death within 3 d	7	1
Death within 1 wk	16	2
Death after 1 wk	14	4
Mean hospitalization (d)	44.72±42.15 ¹	21.26±23.66

¹P>0.05, ^aP<0.05, ^bP<0.01, vs SAP group, ACS: abdominal compartment syndrome.

Table 2 Incidence of organ dysfunction during hospitalization in patients with ESAP and SAP (%)

Factor	ESAP group	SAP group
Single organ dysfunction	15(21.7) ^a	25(10.9)
MODS	54(78.3) ^b	20(10.1)
Pulmonary insufficiency	59(85.5) ^b	27(11.8)
Hepatic dysfunction	14(20.3) ^b	17(7.5)
Renal insufficiency	28(40.6) ^b	9(3.9)
GI dysfunction	24(34.8) ^b	16(7.0)
Shock	29(42.0) ^b	10(4.4)

^aP<0.05, ^bP<0.01, vs SAP group.

Table 3 Features of victim in ESAP group

Factor	Death group (n=30)	Cure group (n=39)
Numbers of organ dysfunction	3.33±0.25 ^b	2.27±0.21
APACHE II score	16.1±1.12 ^b	14.2±1.09
Balthazar CT class	5.69±0.62 ^b	4.47±0.43
Hypoxemia (%)	30(100) ^b	27(69.2)
Abdominal compartment syndrome (%)	27(90) ^b	22(56.4)
Pancreas infection (%)	8(26.7) ¹	4(10.3)
Other infections (%)	16(53.3) ¹	24(61.5)

¹P>0.05, ^bP<0.01, vs cure group.

Features of victim in ESAP

Table 3 shows the features of death cases of ESAP. Multiple logistic regression analysis with backward elimination revealed that hypoxemia, higher APACHE II score, MODS and the extent of pancreatic necrosis were high risks for ESAP death.

DISCUSSION

With the advance in SAP study over the years, that the occurrence of early organ dysfunction is correlated with cascade response which gives rise to inflammatory mediators such as cytokine has been recognized gradually^[14-16]. The effect of cytokine on the early stage of SAP should be emphasized. In fact, ESAP, a special critical type of SAP, is manifested as sharp changes during the early stage of SAP of non-stable vital signs and early organ dysfunction. Isenmann and Beger reported a group of SAP cases admitted to hospital within 72 h after onset of abdominal pain with organ dysfunction, which was defined as ESAP, and the mortality rate was up to 42%^[12]. According to McKay's data^[11], 40% of all death occurred within 3 d in SAP. In our data, the mortality rate was 23.3% (7/30) in ESAP group within 3 d and 53.3% (16/30) within 1 week. This indicated that ESAP was the higher risk group of acute pancreatitis death. Therefore it is very important to understand the characteristics of ESAP, which were mainly summarized as: a short disease course with progressive multiple organ dysfunction; early hypoxemia; a higher incidence of abdominal compartment syndrome; a higher incidence of infected pancreatic necrosis; and higher CT score of pancreatic changes. ESAP is a critical type of SAP with a high early mortality rate and poor prognosis. High-risk factors of mortality in ESAP group are early hypoxemia and multiple organs dysfunction.

Because there is an extremely high risk of progressive MODS, as well as an extremely high mortality rate in ESAP, ESAP patients should receive maximal intensive care treatment for organ dysfunction. First of all, our data showed that hypoxemia occurred in 85.5% ESAP. For correcting hypoxemia, all patients were given positive end-expiratory pressure (PEEP) early. Respirator respiration through tracheal intubation should be used if hypoxemia can not be improved after 4-6 h. The principle of respirator use is 'to use early and to stop early', the oxygen concentration should be lower than 40%. The most important change of respiration system is ARDS. Pulmonary infection may be present due to ARDS, and even pulmonary infection may become the main reason for deterioration in ESAP. Monitoring of occurrence and progression of ARDS should be emphasized. Secondly, abdominal compartment syndrome (ACS) will be established if intra-abdominal pressure is higher than 15 mmHg (2kPa) with low cardiac output and progressive oliguria, and hypoxia occurred even if the airway peak value is normal or higher. Our result showed that higher pressure of abdominal cavity was presented in 78.3% ESAP. Higher pressure of abdominal cavity may damage the function of lung, heart, kidney and liver, inducing or exacerbating organ dysfunction. Abdominal decompression is the only way treating ACS. ACS can be divided into two types: one is present as ascites, peritoneal lavage or drainage can not only reduce the higher intra-abdominal pressure by using laparoscope but can also reduce systemic inflammation by diluting and draining abdominal exudates which contained pancreatic juice and cytokines. Another type of ACS is the result of enteroparalysis and gastrointestinal (GI) pneumatosis. Recovery of GI function is very important. We usually use purgative agents such as magnesium sulfate or Dahuang decoction (TCM) for accelerating GI function. These agents can promote GI peristalsis, decrease the intra-abdominal pressure, combat bacteria infection, protect the barrier function of GI tract, decrease translocation of bacterial and endotoxin and accelerate

the ascites absorption. Also, magnesium sulfate can reduce the opportunity of bacterial infection by promoting bile excretion and pancreatic juice excretion. Additionally, Pixiao can draw ascites out of peritoneal cavity. Our results indicated that the earlier the ACS was relived, the better the prognosis was. Thirdly, most ESAP cases had systemic inflammatory response syndrome (SIRS), which is the result of interaction of multiple inflammatory cytokines and has no specific therapeutic treatment modality. Hemofiltration has the effect of stabilizing hemodynamic and homeostasis, cleaning excess inflammatory factors such as cytokines, improving the function of heart, lung and kidney, and reducing the degree of illness^[17-20]. We treated 25 ESAP patients with SIRS by hemofiltration at the early stage and obtained satisfactory (Data not shown). Fourthly, our data showed that the prognosis of early non-organ dysfunction group was satisfactory based on the same treatment principle and the mortality rate was just 2.6%. In the absence of evidence for pancreatic necrosis, SAP should be treated by non-surgical treatment if the condition is stable^[21-25]. Owing to the unstable condition in ESAP, the mortality rate may increase because of operation^[26]. Surgical treatment would be considered when: (1) Higher intra-abdominal pressure is not resolved or ascites is increased after 8-12 h' therapy. (2) Dynamic CT examination indicates the evidence of severe pancreatic lesion or inflammatory necrosis. As conventional operation may make patient's condition worse at this stage, we proposed the method with minimal interruptions on body function such as peritoneal lavage under laparoscope, posterior peritoneal or paracolic sulci drainage to avoid systemic circulation or metabolism disturbances. The emphasis of surgery is peritoneal drainage and relief of intraabdominal pressure. Our data indicated that the outcome was better than simple conservation group and the mortality rate was reduced. Fifthly, prophylactic antibiotic was used early. All patients were given antibiotics once SAP was diagnosed. Antibiotics which can pass the blood-pancreas barrier and have effect on normal gut bacteria were first of choice. In general, Tienam or third generation cephalosporin with flagyl was applied. Sometimes, antibiotic was given by using arterial catheterization so that the pancreas could encounter higher drug concentration. Sixthly, low molecular weight heparin and Alprostadil can improve the microcirculation in pancreas^[27,28]. We usually used these agents early. Lastly, nutritional support should be applied under the circumstance of stable systemic condition^[29,30]. In general, we used parenteral nutrition (PN) at early stage. Enteral nutrition (EN) was used through jejunum once gut function recovered. EN can maintain gut mucosa barrier function, prevent or reverse the damage of gut mucosa barrier.

As our knowledge about the pathogenesis of systemic complications of ESAP is limited, patients with early organ dysfunction still remain a serious problem. The mechanism of ESAP and effective therapy still pose a challenge for future study.

REFERENCES

- Bradley EL 3rd. A fifteen year experience with open drainage for infected pancreatic necrosis. *Surg Gynecol Obstet* 1993; **177**: 215-222
- Tsiotos GG, Luque-de Leon E, Soreide JA, Bannon MP, Zietlow SP, Baerga-Varela Y, Sarr MG. Management of necrotizing pancreatitis by repeated operative necrosectomy using a zipper technique. *Am J Surg* 1998; **175**: 91-98
- Beger HG, Isenmann R. Surgical management of necrotizing pancreatitis. *Surg Clin North Am* 1999; **79**: 783-800
- de Beaux AC, Palmer KR, Carter DC. Factors influencing morbidity and mortality in acute pancreatitis; an analysis of 279 cases. *Gut* 1995; **37**: 121-126
- Tenner S, Sica G, Hughes M, Noordhoek E, Feng S, Zinner M, Banks PA. Relationship of necrosis to organ failure in severe acute pancreatitis. *Gastroenterology* 1997; **113**: 899-903
- Neoptolemos JP, Raraty M, Finch M, Sutton R. Acute pancreatitis: the substantial human and financial costs. *Gut* 1998; **42**: 886-891
- Buter A, Imrie CW, Carter CR, Evans S, McKay CJ. Dynamic nature of early organ dysfunction determines outcome in acute pancreatitis. *Br J Surg* 2002; **89**: 298-302
- Isenmann R, Rau B, Beger HG. Bacterial infection and extent of necrosis are determinants of organ failure in patients with acute necrotizing pancreatitis. *Br J Surg* 1999; **86**: 1020-1024
- Takeda K, Matsuno S, Sunamura M, Kobari M. Surgical aspects and management of acute necrotizing pancreatitis: recent results of a cooperative national survey in Japan. *Pancreas* 1998; **16**: 316-322
- Bosscha K, Hulstaert PF, Hennipman A, Visser MR, Gooszen HG, van Vroonhoven TJ, vd Werken C. Fulminant acute pancreatitis and infected necrosis: results of open management of the abdomen and "planned" reoperations. *J Am Coll Surg* 1998; **18**: 255-262
- McKay CJ, Evans S, Sinclair M, Carter CR, Imrie CW. High early mortality rate from acute pancreatitis in Scotland, 1984-1995. *Br J Surg* 1999; **86**: 1302-1305
- Isenmann R, Rau B, Beger HG. Early severe acute pancreatitis: characteristics of a new subgroup. *Pancreas* 2001; **22**: 274-278
- Bradley EL 3rd. A clinically based classification system for acute pancreatitis. *Ann Chir* 1993; **47**: 537-541
- Norman J. The role of cytokines in the pathogenesis of acute pancreatitis. *Am J Surg* 1998; **17**: 76-83
- Osman MO, Gesser B, Mortensen JT, Matsushima K, Jensen SL, Larsen CG. Profiles of pro-inflammatory cytokines in the serum of rabbits after experimentally induced acute pancreatitis. *Cytokine* 2002; **17**: 53-59
- Frossard JL. Pathophysiology of acute pancreatitis: a multistep disease. *Acta Gastroenterol Belg* 2003; **66**: 166-173
- Oda S, Hirasawa H, Shiga H, Nakanishi K, Matsuda K. Continuous hemofiltration/hemodiafiltration in critical care. *Ther Apher* 2002; **6**: 193-198
- Pupelis G, Austrums E, Snippe K. Blood purification methods for treatment of organ failure in patients with severe pancreatitis. *Zentralbl Chir* 2001; **126**: 780-784
- Xie HL, Ji DX, Gong DH, Liu Y, Xu B, Zhou H, Liu ZH, Li LS, Li WQ, Quan ZF, Li JS. Continuous veno venous hemofiltration in treatment of acute necrotizing pancreatitis. *Chin Med J* 2003; **116**: 549-553
- Wang H, Li WQ, Zhou W, Li N, Li JS. Clinical effects of continuous high volume hemofiltration in severe acute pancreatitis complicated with multiple organ dysfunction syndrome. *World J Gastroenterol* 2003; **9**: 2096-2099
- Mier J, Leon EL, Castillo A, Robledo F, Blanco R. Early versus late necrosectomy in severe necrotizing pancreatitis. *Am J Surg* 1997; **173**: 71-75
- Hartwig W, Maksan SM, Foitzik T, Schmidt J, Herfarth C, Klar E. Reduction in mortality with delayed surgical therapy of severe pancreatitis. *J Gastrointest Surg* 2002; **6**: 481-487
- Silverman WB. Medical and endoscopic treatment of acute pancreatitis. *Curr Treat Options Gastroenterol* 2003; **6**: 381-387
- Werner J, Uhl W, Buchler MW. Surgical treatment of acute pancreatitis. *Curr Treat Options Gastroenterol* 2003; **6**: 359-367
- Slavin J, Ghaneh P, Sutton R, Hartley M, Rowlands P, Garvey C, Hughes M, Neoptolemos J. Management of necrotizing pancreatitis. *World J Gastroenterol* 2001; **7**: 476-481
- Dugernier T, Reynaert M, Laterre PF. Early multi-system organ failure associated with acute pancreatitis: a plea for a conservative therapeutic strategy. *Acta Gastroenterol Belg* 2003; **66**: 177-183
- Sunamura M, Yamauchi J, Shibuya K, Chen HM, Ding L, Takeda K, Kodari M, Matsuno S. Pancreatic microcirculation in acute pancreatitis. *J Hepatobil Pancreat Surg* 1998; **5**: 62-68
- Zhou ZG, Chen YD. Influencing factors of pancreatic microcirculatory impairment in acute pancreatitis. *World J Gastroenterol* 2002; **8**: 406-412
- Zhao G, Wang CY, Wang F, Xiong JX. Clinical study on nutrition support in patients with severe acute pancreatitis. *World J Gastroenterol* 2003; **9**: 2105-2108
- Tu WF, Li JS, Zhu WM, Li ZD, Liu FN, Chen YM, Xu JG, Shao HF, Xiao GX, Li A. Influence of Glutamine and caecostomy/colonic irrigation on gut bacterial/endotoxin translocation in acute severe pancreatitis in pigs. *Shijie Huaren Xiaohua Zazhi* 1999; **7**: 135-138

Relationship between plasma D-dimer levels and clinicopathologic parameters in resectable colorectal cancer patients

Gang Xu, Ya-Li Zhang, Wen Huang

Gang Xu, Ya-Li Zhang, Wen Huang, Institute of Gastroenterology, First Military Medical University, Guangzhou 510515, Guangdong Province, China

Correspondence to: Gang Xu, Institute of Gastroenterology, First Military Medical University, Guangzhou 510515, Guangdong Province, China. tianzr@sdu.edu.cn

Telephone: +86-20-85141544

Received: 2001-10-12 **Accepted:** 2001-11-27

Abstract

AIM: To assess the clinical significance of the D-dimer levels and the relationship between plasma D-dimer levels and clinicopathologic parameters in operable colorectal cancer patients.

METHODS: The plasma levels of D-dimer were measured pre- and postoperatively in 35 patients with colorectal cancer, and 30 healthy subjects served as controls by the method of quantitative enzyme-linked immunosorbent assay (ELISA).

RESULTS: The mean preoperative plasma levels of D-dimer in the patients with colorectal cancer (1.06 ± 0.24 mg/L) were significantly higher than those of controls (0.33 ± 0.12 mg/L, $P < 0.01$). The D-dimer levels were remarkably elevated on the 1st day after operation (1.22 ± 0.55 mg/L, $P < 0.01$). On the 3rd day the level of D-dimer began to stepwise descend and on the 14th day nearly returned to control level. The preoperative levels of D-dimer were significantly correlated with the lymph node metastasis and Dukes stage but had no association with tumor location and the degree of differentiation. A stepwise increase in the mean D-dimer levels was found with increase of the tumor stage.

CONCLUSION: Hypercoagulation and higher fibrinolytic activities occur in patients with colorectal cancer. The operative trauma could enhance the fibrinolysis in the patients with colorectal cancer. The measurement of preoperative D-dimer levels is considered to be useful for predicting lymph node metastasis and stage of colorectal cancer.

Xu G, Zhang YL, Huang W. Relationship between plasma D-dimer levels and clinicopathologic parameters in resectable colorectal cancer patients. *World J Gastroenterol* 2004; 10 (6): 922-923

<http://www.wjgnet.com/1007-9327/10/922.asp>

INTRODUCTION

Activation of coagulation and fibrinolysis is known to be frequently associated with malignancy, although the mechanism involved has not been fully clarified. The extent of such activation has been reported to correlate with tumor stage and prognosis in some malignancies, including

colorectal cancer^[1-3]. D-dimer is a stable end-product of fibrin degradation and levels of D-dimer are elevated by enhanced fibrin formation and fibrinolysis. It is a marker of hypercoagulable stage. D-dimer levels are elevated in the plasma of various solid tumor patients^[4,5]. The present study was to assess the clinical significance of the D-dimer levels and the relationship between plasma D-dimer levels and clinicopathologic findings in pre and post operative patients with colorectal cancer.

MATERIALS AND METHODS

Patients

Thirty-five patients with colorectal cancer were investigated. There were 21 males and 14 females, with a median age of 52 years, ranging from 32 to 75 years. Patients with cerebrovascular and diabetes were excluded. Meanwhile, 30 healthy subjects served as controls (17 males and 13 females, median age 56 years, ranging from 33 to 86 years).

Measurement of plasma D-dimer

Five milliliter of whole blood was drawn from antecubital vein of patients on the day prior to operation and on the 1st, 3rd, 7th, 14th postoperative days, using 3.8g sodium citrate collection tube. All samples were centrifuged within 4 h of veinpuncture, the plasma components were pipetted off and placed in plastic tubes. Centrifuged plasma was stored at -80°C until assay. Meanwhile 30 samples of healthy subjects served as controls. Plasma D-dimer levels were determined by quantitative enzyme-linked immunosorbent assay (ELISA).

Statistical analysis

Statistical analysis of mean value of D-dimer levels was made by Student's *t* test and Student Newman-keuls' *s* test. $P < 0.05$ was considered to be significant.

RESULTS

Relationship between plasma D-dimer levels and clinicopathologic parameters

The D-dimer levels of colorectal cancer patients with positive lymph nodes were significantly higher than that of negative lymph nodes (0.94 ± 0.26 vs 1.15 ± 0.12 , $P < 0.01$, Table 1). A stepwise increase in the mean D-dimer levels was found with the increase of tumor clinical stage. There was no association between D-dimer levels and tumor location or degree of the differentiation.

Pre- and postoperative plasma D-dimer levels in colorectal cancer patients

The mean plasma levels of D-dimer in the patients with colorectal cancer were significantly higher than that of the controls ($P < 0.01$, Table 1). It was also observed that D-dimer levels were remarkably elevated on the 1st day after the operation ($P < 0.01$). On the 3rd day after operation the D-dimer levels began to stepwise descend and on the 14th day almost returned to control ($P > 0.05$).

Table 1 Relationship between plasma D-dimer levels (mean±SD) and clinicopathology variables

Course (d)	Clinicopathology	n	D-dimer (mg/L)
Preoperation	Location	Colon	14
		Rectum	21
	Differentiation	Well	13
		Moderate	16
		Poor	6
	Lymph node	Negative	15
	Metastasis	Positive	20
	Dukes stage	A + B	15
		C	15
		D	5
Postoperation	1	35	1.06±0.24 ^b
	3	35	1.11±0.16
	7	30	1.03±0.25
	14	17	1.01±0.28
Control		30	1.02±0.31
			1.08±0.14
			0.94±0.26
			1.15±0.12 ^a
			0.94±0.26
			1.12±0.11 ^c
			1.29±0.11 ^d
			1.22±0.55 ^b
			0.82±0.49 ^{be}
			0.67±0.41 ^{bf}
			0.46±0.17 ^f
			0.33±0.12

^b*P*<0.01 vs control; ^a*P*<0.05 vs negative; ^c*P*<0.05, ^d*P*<0.01 vs Dukes A+B; ^e*P*<0.05, ^f*P*<0.01 vs preoperation.

DISCUSSION

Both experimental and clinical data have shown that coagulation disorders are common in patients with cancer although clinical symptoms may occur rarely. Recent reports showed hypercoagulable state in cancer patients and the plasma D-dimer levels were increased in these patients^[4,5]. The process of metastasis involves multiple tumor-host interactions. To survive, metastatic cancer cells must leave the primary tumor, migrate into the lymphovascular system and establish a new blood supply at their metastatic site^[6-8]. Fibrin remodeling is almost certainly involved in all steps of metastasis and has been proved to play a crucial role in new vessel formation^[9-11]. Our study showed that the preoperative D-dimer levels were higher and correlated with the tumor lymph node metastasis. It confirmed that unregulated fibrinolytic activities in colorectal cancer and increased levels of fibrinolytic activities in metastasis of colorectal cancer. The reason may be that cancer cells appear to be capable of both thrombin formation and induction of fibrin degradation because cancer cells tend to adhere to, aggregate, necrose, which could induce monocytes and endothelioid cells to release many clotting factors^[12,13]. Studies suggested that higher D-dimer levels could induce the secretion of interleukin-1, urokinase-type plasminogen activator (u-PA) and plasminogen activator inhibitor-2 in a human promonocytic leukemia cell line. u-PA is the predictive marker in many malignant tumors and may play an important role in the invasive cancer^[14-16]. The prethrombotic state (depicted by a prolongation of PT and increase of D-dimer) is confirmed to be an aggravating condition in cancers. Studies suggesting an attempt to reverse possible haemostatic abnormalities with the use of anticoagulants have been justified. Thus anticoagulant treatment may have a positive influence on colorectal cancer therapy.

We found that D-dimer levels were remarkably elevated on the 1st day after the operation. On the 3rd day after operation the D-dimer levels began to stepwise descend and on the 14th day returned to control. The remarkable increase in D-dimer levels occurring in patients indicated that patients undergoing surgery were at high risks for the occurrence of a thromboembolic event. Thus D-dimer could be used for estimating individual risk of thromboembolism and prophylactic treatment in these patients. Oya *et al* had obtained the same results. In addition,

we found the D-dimer levels of colorectal cancer patients with positive lymph nodes were significantly higher than that of negative lymph nodes. A stepwise increase in the mean D-dimer levels was found with the increase of tumor clinical stage. The measurement of preoperative D-dimer levels is considered to be useful for predicting lymph node metastasis and clinical stage of colorectal cancer.

REFERENCES

- 1 **Kalweit GA**, Feindt P, Micek M, Gams E, Hellstern P. Markers of activated hemostasis and fibrinolysis in patients with pulmonary malignancies: comparison of plasma levels in central venous and pulmonary venous blood. *Thromb Res* 2000; **97**: 105-111
- 2 **Tanabe K**, Terada Y, Shibutani T, Kunitada S, Kondo T. A specific inhibitor of factor Xa, DX-9065a, exerts effective protection against experimental tumor induced disseminated intravascular coagulation in rats. *Thromb Res* 1999; **96**: 135-143
- 3 **Oya M**, Akiyama Y, Okuyama T, Ishikawa H. High preoperative plasma D-dimer level is associated with advanced tumor stage and short survival after curative resection in patients with colorectal cancer. *Jpn J Clin Oncol* 2001; **31**: 388-394
- 4 **Blackwell K**, Haroon Z, Broadwater G, Berry D, Harris L, Iglehart JD, Dewhurst M, Greenberg C. Plasma D-dimer levels in operable breast cancer patients correlate with clinical stage and axillary lymph node status. *J Clin Oncol* 2000; **18**: 600-608
- 5 **Kobayashi T**, Gabazza EC, Taguchi O, Risteli J, Risteli L, Kobayashi H, Yasui H, Yuda H, Sakai T, Kaneda M, Adachi Y. Type I collagen metabolites as tumor markers in patients with lung carcinoma. *Cancer* 1999; **85**: 1951-1957
- 6 **Hou L**, Li Y, Jia YH, Wang B, Xin Y, Ling MY, Lü S. Molecular mechanism about lymphogenous metastasis of hepatocarcinoma cells in mice. *World J Gastroenterol* 2001; **7**: 532-536
- 7 **Takes RP**, Baatenburg-de Jong RJ, Wijffels K, Schuurin E, Litvinov SV, Hermans J, van-Krieken JH. Expression of genetic markers in lymph node metastases compared with their primary tumours in head and neck cancer. *J Pathol* 2001; **194**: 298-302
- 8 **Sun HC**, Li XM, Xue Q, Chen J, Gao DM, Tang ZY. Study of angiogenesis induced by metastatic and non-metastatic liver cancer by corneal micropocket model in nude mice. *World J Gastroenterol* 1999; **5**: 116-118
- 9 **Xu G**, Tian KL, Liu GP, Zhong XJ, Tang SL, Sun YP. Clinical significance of plasma D-dimer and von Willebrand factor levels in patients with ulcer colitis. *World J Gastroenterol* 2002; **8**: 575-576
- 10 **Simpson-Haidaris PJ**, Rybarczyk B. Tumors and fibrinogen. The role of fibrinogen as an extracellular matrix protein. *Ann N Y Acad Sci* 2001; **936**: 406-425
- 11 **Shoji M**, Hancock WW, Abe K, Micko C, Casper KA, Baine RM, Wilcox JN, Danave I, Dillehay DL, Matthews E, Contrino J, Morrissey JH, Gordon S, Edgington TS, Kudryk B, Kreutzer DL, Rickles FR. Activation of coagulation and angiogenesis in cancer: immunohistochemical localization in situ of clotting proteins and vascular endothelial growth factor in human cancer. *Am J Pathol* 1998; **152**: 399-411
- 12 **Ornstein DL**, Zacharski LR. Treatment of cancer with anticoagulants: rationale in the treatment of melanoma. *Int J Hematol* 2001; **73**: 157-161
- 13 **Chiarugi V**, Ruggiero M, Magnelli L. Molecular polarity in endothelial cells and tumor-induced angiogenesis. *Oncol Res* 2000; **12**: 1-4
- 14 **Delebecq TJ**, Porte H, Zerimech F, Copin MC, Gouyer V, Dacquembonne E, Balduyck M, Wurtz A, Huet G. Overexpression level of stromelysin 3 is related to the lymph node involvement in non-small cell lung cancer. *Clin Cancer Res* 2000; **6**: 1086-1092
- 15 **Vasse M**, Thibout D, Paysant J, Legrand E, Soria C, Crepin M. Decrease of breast cancer cell invasiveness by sodium phenylacetate (NaPa) is associated with an increased expression of adhesive molecules. *Br J Cancer* 2001; **84**: 802-807
- 16 **Kitange G**, Tsunoda K, Anda T, Nakamura S, Yasunaga A, Naito S, Shibata S. Immunohistochemical expression of Ets-1 transcription factor and the urokinase-type plasminogen activator is correlated with the malignant and invasive potential in meningiomas. *Cancer* 2000; **89**: 2292-2300